Czech Technical University in Prague
Faculty of Nuclear Sciences and Physical Engineering

Dissertation Thesis

2009

Tomáš Oberhuber

Czech Technical University in Prague
Faculty of Nuclear Sciences and Physical Engineering

Dissertation Thesis

Numerical Solution of Willmore Flow

Tomáš Oberhuber

A thesis submitted to the Faculty of Nuclear Sciences and Physical Engineering, Czech Technical University in Prague, in partial fulfilment of the requirements for the degree Doctor of Philosophy (Ph. D.) in Mathematical Engineering.

Název práce: **Numerické řešení pro Willmorův tok**

Autor: Tomáš Oberhuber

Obor: Matematické inženýrství

Druh práce: Disertační práce

Vedoucí práce: Michal Beneš. Katedra matematiky, Fakulta jaderná a fyzikálně inženýrská, České vysoké učení technické v Praze

Abstrakt: Cílem této práce je nalezení vhodného numerického schématu pro aproximaci evoluce rovinných křivek podle Willmorova toku. Willmorův tok je silně nelineární problém parabolického typu čtvrtého řádu. Je uvažována úloha izotropní, ale i anizotropní. Postupně jsou navrženy tři typy schémat založených na metodách konečných diferencí a konečných objemů. Je uvažována jak explicitní, tak semi-implicitní diskretizace v čase. Nejprve je studována jednodušší grafová formulace, poté je přikročeno k vrstevnicové metodě. Výsledky získané touto metodou jsou porovnány s metodou parametrického popisu. Na vhodně vybraných počátečních podmínkách je napočítán experimentální řád konvergence. Je provedena celá řada výpočtů i s různými anizotropiemi ukazující rozdílný vývoj křivek řízený buď střední křivostí nebo Willmorovým tokem.
Klíčová slova: diferenciální geometrie, střední křivost, Willmorův tok, variační počet, anizotropie, grafová formulace, vrstevnicová formulace, parametrická formulace, metoda konečných diferencí, metoda konečných objemů

Title: **Numerical Solution of Willmore Flow**

Author: Tomáš Oberhuber

Abstract: The aim of this thesis is to find appropriate numerical scheme for the approximation of the evolution of plannar curves driven by the Willmore flow. The Willmore flow is strongly non-linear parabolic problem of the fourth order. Both isotropic and anisotropic problems are considered. Three types of numerical schemes are presented - they are based on the finite difference and the finite volume methods. For the discretisation in time, both explicit and semi-implicit approaches are studied. Firstly simpler graph formulation is presented and then we proceed to the level-set formulation. Results obtained by the latter one are compared with those achieved by the parametric method. On appropriately chosen initial conditions the experimental order of convergence is evaluated. A serie of numerical experiments with different anisotropies is also presented. We show differences in evolution of curves driven either by the mean-curvature or the Willmore flow.
Keywords: differential geometry, mean curvature, Willmore flow, calculus of variations, anisotropies graph formulation, level-set formulation, parametric formulation, finite difference method, finite volume method.

I confirm having prepared the thesis by my own and having listed all used sources of information in the bibliography.

Tomáš Oberhuber

Prague, June 25, 2010

This thesis would never exists without help of the following people – Prof. Charles M. Elliott who introduced me to the Willmore flow, Prof. Masato Kimura who spent many hours explaining me theory of differential geometry, Prof. Karol Mikula and Prof. Daniel Ševčovič who helped me with design of numerical schemes and my supervisor Doc. Dr. Ing. Michal Beneš for many beneficial advices. I also would like to thank my parents for supporting me during my PhD. study.

State of Art

Willmore flow is a problem defined in differential geometry. It finds many real applications in physics of elasticity e.g. modelling of bio-membranes. In image processing the Willmore flow was successfully applied to a problem called image inpainting. Even though the Willmore functional has been defined almost one hundred years ago it has not been studied from the numerical point of view for long time. Evolutionary law for finding a minimum of the Willmore functional is a fourth-order parabolic partial differential equation. It is highly non-linear problem. It is challenging problem from theoretical point of view but also for a numerical approximation. Anisotropic Willmore flow has not been studied yet. Also for the isotropic level-set formulation, new numerical schemes need to be investigated.

Research Goals

The main goals of this thesis are to derive graph and level-set formulations for anisotropic Willmore flow and to design reliable numerical scheme for the level-set formulation of the (anisotropic) Willmore flow of planar curves. First we test proposed schemes on the graph formulation which is easier to approximate. We find experimental order of convergence. Approximate solutions obtained by the isotropic level-set method are compared with the parametric approach. As a reference problem we also solve mean-curvature flow and we demonstrate differences in evolutions of both problems. We consider explicit and semi-implicit discretisation in time and investigate efficiency, accuracy and reliability of both approaches. We do not study numerical analysis of the schemes. We only show simple energy equality for the graph formulation.

Methods Used

We present numerical schemes based on the finite-difference method and complementary finite-volume method. For planar curves, level-set method and parametric approach (discretised by flowing finite-volume method with asymptotically uniform redistribution) are both implemented. For the explicit time discretisation, the Merson alternative of the Runge-Kutta method is used. Linear systems coming from the semi-implicit time discretisation are solved by restarted GMRES method with ILUT preconditioning.

Research Results

The thesis describes isotropic and anisotropic Willmore flow of surfaces given as graphs or curves given as a zero level-set of an auxiliary function. Three classes of numerical schemes are studied. They are compared on several qualitative numerical experiments and by evaluating the experimental order of convergence. For all of them energy equality is proven. The most reliable scheme (the one based on the finite-volume method) is then tested more extensively on the level-set formulation but also on anisotropic problems.

Contents

1. Notation

Notation	Meaning	Definition
$\nabla_\Gamma f$	the surfacial gradient of function $f \in C^1(\Gamma)$	D: 4.2.7
$\nabla_\Gamma \cdot \mathbf{h}$	the surfacial divergence of vector field $\mathbf{h} \in C^1(\Gamma, \mathbb{R}^n)$	D: 4.2.8
$\partial_i u$	denotes $\frac{\partial u}{\partial x_i}$ for $i = 1, \cdots n$ and $u \in C^1(\mathbb{R}^n)$	
$\partial_{\mathbf{n}} f$	denotes $\nabla f \cdot \mathbf{n}$	
$\partial^2_{\mathbf{n}} f$	denotes $\mathbf{n}^T D^2 f \mathbf{n}$	
$\mathcal{A}$	surface area functional	(5.1)
$\mathcal{A}_\gamma$	surface area functional	(5.20)
α	tangential velocity for parametric curves	(5.117)
β	normal velocity for parametric curves	(5.117)
$\gamma(u)$	parametrisation of Γ	D: 4.1.1
$\gamma(s)$	arclength parametrisation of Γ	D: 4.1.1
γ	anisotropy function	D: 5.1.9
Γ	hypersurface or curve in $\mathbb{R}^n$	D: 4.2.1
Γ_{ext}	exterior of hypersurface Γ	
Γ_{int}	interior of hypersurface Γ	
$\Gamma(t)$	moving hypersurface	D:4.3.1
$D^2 f$	the Hessian matrix of f i.e. $D^2_{ij} = \partial_i \partial_j f$	
d_Γ	signed distance function to Γ	D: 4.4.1
$d\mathcal{H}^n$	Hausdorff measure of $\mathbb{R}^n$	D: A.0.4
$\mathbf{d}_i$	principal directions	D:4.2.6
$D_t f$	normal time derivative	D:4.38
EOC	experimental order of convergence	(7.13)
g	local length	D: 5.118
h	space step for numerical discretisation	
H	mean curvature of Γ	D: 4.9
K	Gauss curvature of Γ	D: 4.10
κ	curvature of a curve Γ	D: 4.1.11
κ_i	principal curvatures	D: 4.2.6
L	length of a curve	
$\mathbf{n}(\mathbf{x})$	outward normal unit vector of Γ at point $\mathbf{x}$	(4.7)
ν	normal of the boundary of finite volume Ω_{ij} resp. domain Ω	
$\mathcal{P}_h$	projection operator on ω_h	(6.2)
$\mathbb{P}$	projection to the tangential space	(5.38)
φ	function expressing Γ given as a graph	
s	parameter of arclength parametrisation	
$\tau_{\mathbf{x}}$	tangential vector of Γ at point $\mathbf{x}$	D: 4.2.2
$\mathbf{t}(\mathbf{x})$	oriented tangential unit vector of Γ at point $\mathbf{x}$	D: 4.1.7
$\mathbf{T}(\mathbf{x})$	tangential space at $\mathbf{x}$	D: 4.2.3
$\{\mathbf{t}_1, \cdots, \mathbf{t}_{n-1}\}$	orthonormal basis of $\mathbf{T}(\mathbf{x})$	
τ	time step for numerical discretisation	
$\mathrm{Tr}\ A$	trace of matrix $A \in \mathbb{R}^{n \times n}$	

Notation	Meaning	Definition
U	neighbourhood of $\mathbf{x}$	
u	function expressing Γ by the level-set method	
$\mathbf{u} \otimes \mathbf{v}$	tensor product of vectors $\mathbf{u}$ and $\mathbf{v}$	
v	parameter of general parametrisation of a curve	
V	normal velocity	D: 4.3.2
V_h	dual mesh to the grid ω_h	(6.54)
W	Weingarten map or shape operator	D: 4.2.10
Ω	domain in $\mathbb{R}^n$	
ω_h	numerical grid	(6.1)

2. Introduction

2.0.1. Willmore flow and related topics

In this thesis we present several numerical schemes for a numerical approximation of the Willmore flow. This problem was introduced by an English geometer **Thomas James Willmore** (see the Figure 2.1) in his well-known book [100]. In differential geometry the Willmore surface (curve) is understood as a minimiser of mean curvature square. The Willmore flow also finds its applications in the physics of elasticity. However, our main interest is in applications to image processing. By minimising the elastic energy of the image lines (for example the edges of some object), we can get a continuation of some missing parts which will look very natural to the human eye. We would like to note that the Willmore flow belongs to a much wider class of problems. They are usually referred to as (mean) curvature dependent flows. We begin by introducing these both interesting and important mathematical problems.

We consider a curve in $\mathbb{R}^2$ or surface in $\mathbb{R}^3$. Such a curve or surface may represent an interface between two different phases of some substance (for example melting ice in water), a growing crystal, a soap bubble in the air, a water drop, the boundary of advancing water in nature, an advancing fire in a forest, elastic membranes or the boundary of an object in image resp. segmented organ in some medical data. In most of these problems the curve or surface represents an interface or boundary which is moving. We are interested in the evolutionary laws describing the motion.

Let us go back to the problem of the bubble floating in the air. To simulate this phenomenon we first note that the bubble moves in the direction of wind. Denoting this direction as $\mathbf{d}$ we move all particles of the bubble in the direction of vector $\mathbf{d}$. In terms of the partial differential equation we use the term "**advection**". Let us assume that the bubble goes to a region with a higher air pressure. It will shrink a little bit. In this case all particles move in the **inner normal** direction. Denoting by $\mathbf{n}$ the **outer normal** we get a motion in the direction of $-\mathbf{n}$. If the bubble gets into a stronger wind it may be deformed. However, it will restore its original shape when the wind disappears. The motion of each particle depends on the bubble shape.

Figure 2.1.: T. J. Willmore in 1979 at the Oberwolfach mathematical research institute (by Wikipedia).

Therefore a quantity to express the shape is needed. Considering the normal vector need not to be enough. Differential geometry provides the notion of **shape operator** which describes a change of normal vector along a curve or surface respectively. In this sense, the normal vector can be understood as the first derivative of the shape and the shape operator as the second derivative of the shape. In many situations its trace is enough to work with.This is precisely how we get the **mean curvature** H of a surface. The motion of the surface inward in the normal direction proportionally to the mean curvature will shrink the bubble. The smaller the bubble is the larger the mean curvature will be. It would lead, however, to a complete disappearance of the bubble. It is not realistic. We know that the bubble preserves the air inside. This constraint is related to the interior volume. If we have a balloon instead of the bubble which is made of some textile material it can change the shape but it preserves its total surface area S. Finally if it is a rubber ball, the change of shape depends on its elasticity which can be expressed in terms of fourth derivatives of the shape.

We can summarise that the change of the surface shape Γ given by the motion of particles creating the surface can be expressed as

$$\partial_t \mathbf{x} = f\left(\mathbf{x}, \mathbf{F}, \mathbf{n}, \partial^2\mathbf{x}, \partial^4\mathbf{x}, \int_{Int\Gamma} g_1\left(\mathbf{x}\right) \mathrm{d}\mathbf{x}, \int_{\Gamma} g_2\left(\mathbf{p}, \mathbf{n}, \partial^2\mathbf{x}, \partial^4\mathbf{x}\right) \mathrm{d}S\right)$$

where

- $\mathbf{x}$ is the position of the surface point
- $\mathbf{F}$ is exterior force which does not depend on the shape of Γ
- $\mathbf{n}$ is the normal vector of Γ
- $\partial^2\mathbf{x}$ is the second derivative of the shape related to the mean curvature
- $\partial^4\mathbf{x}$ is the fourth derivative of the shape related to elasticity
- $\int_{\mathrm{Int}\Gamma} g_1\left(\mathbf{p}\right) \mathrm{d}\mathbf{x}$ expresses dependency on the interior of Γ
- $\int_{\Gamma} g_2\left(\mathbf{x}, \mathbf{n}, \partial^2\mathbf{x}, \partial^4\mathbf{x}\right) \mathrm{d}S$ expresses dependency on some global quantity g_2 defined on Γ

If f does not depend on the integrals, its value at a certain point $\mathbf{x}_0$ is given by the knowledge of some small neighbourhood of $\mathbf{x}_0$. We speak of **local law**. Otherwise, it is a **non-local law**. When we are interested in the change of shape, we do not identify motion of particular points along the curve or surface Γ. Such **tangential motion** is important in some applications – for example in medical data processing, where we would like to trace motion of tissues. In cardiac MRI, the complete reconstruction of the heart motion, not only the change of shape, is of the main interest. Such applications, however, usually need some special techniques. To our knowledge there is no general approach to solve these problems. Therefore we only consider the motion in the normal direction. Most of the laws then might be given as a formula for the **normal velocity** prescribing velocity of Γ in the normal direction.

In this text we consider **the mean-curvature flow** given by

$$V = H \text{ on } \Gamma, \tag{2.1}$$

as supporting issue of the main topic given by the **Willmore flow**

$$V = -\Delta_\Gamma H - \frac{1}{2}H^3 + 2KH \text{ on } \Gamma. \tag{2.2}$$

Another well known problem is **the surface-diffusion flow** (often referred only as the surface diffusion)

$$V = -\Delta_\Gamma H \text{ on } \Gamma, \tag{2.3}$$

which, however, is not studied in this text. These problems belong to the class of **geometrical partial differential equations** or, to be more specific, **curvature-driven flows** . We show that they can be formulated as variational problems. They also can be understood as examples of **gradient flow** i.e. processes of functional relaxations. In this view, the system state moves ("flows") towards a minimum-energy state.

The mean-curvature flow has been studied extensively in recent years. On the other hand, the surface-diffusion flow and the Willmore flow are problems with limited knowledge. The results obtained for the mean-curvature flow are good motivation for solving more difficult problems. For example we show that with the complementary finite volume method we may obtain nice numerical convergence in the case of the mean-curvature flow. This is more difficult in case of the surface-diffusion flow and the Willmore flow. This is supported by numerical experiments showing the difference between particular laws under the same initial condition.

Numerical solution of given problems is possible by several approaches as discussed by Elliott in [45]. These methods can be divided into **parametric** and **implicit** ones. The parametric methods parametrise the curve (or surface). The curve is given as an image of some mapping. Quantities like outer normal or curvature can be expressed in a straightforward way. The evolution law becomes an equation for the parametrisation. On the other hand, some stabilising methods are often necessary to obtain robust algorithm - see e.g. Mikula and Ševčovič [77]. This stabilisation makes the final scheme more complicated. Nevertheless, it is still efficient method. Main disadvantage is its incapability to handle changes of topology (situations when two curves merge together or one curve splits into two). One way to solve this problem is using re-parametrisation from time to time (see e.g. **topological snakes** or T-snakes by McInerney and Terzopoulos [73]). T-snakes were applied to image processing. To our best knowledge, their mathematical properties have not yet been studied.

Sethian and Osher [90, 85] proposed an elegant approach which is known as a **level-set method**. It is an implicit method. The curve is given as a zero level set of some mapping referred as a **level-set function**. Such approach increases the dimension of the problem by one which makes this method less efficient then the parametric approach. On the other hand, the changes in topology are handled automatically. The main difficulty of the level-set method is related to the behaviour of other level sets. They can evolve in agreement with the same law imposed on the zero level set. This can lead to a deformation of the level-set function. The **signed distance function** [85], for which the gradient size equals to 1, is usually said to be the best choice for the level-set method. Here the mean curvature simplifies to the Laplace operator. Consider the signed distance function to a unit circle. Its graph is a cone in $\mathbb{R}^3$ – see the Figure 2.2. Level sets for negative real numbers are smaller circles then the one given by the zero level set. In case of the mean curvature flow each level set shrinks with velocity proportional to the curvature. It means that smaller circles shrink faster and at certain time they disappear. It makes the vertex of the level-set function graph to rise up and the gradient size to decrease. The level-set function is deformed and the property of the signed distance functions is lost. This can negatively affect accuracy of the numerical approximation. It happens especially in case of the Willmore flow. The level-set formulation of the surface-diffusion flow was studied in [83]. To restore the signed distance function one can employ **redistancing**. It, however, brings in some errors too.

The remedy of this problem can be found either in highly reliable re-distancing method or in different normal velocity prescribed to the non-zero level sets. The first approach has been proposed by Sussman and Fatemi [94]. Their method is explained later in this thesis. For the

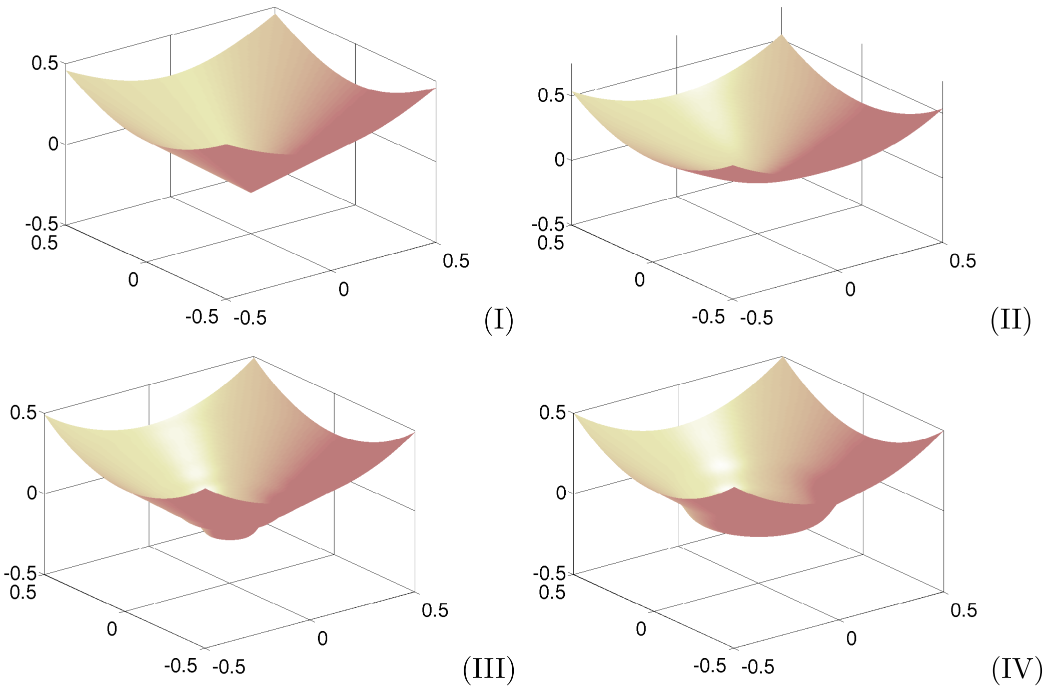

Figure 2.2.: Evolution of a level-set function. The initial function (I) has been evolved by the mean-curvature flow (II), the surface-diffusion flow (III) and the Willmore flow (IV) until the time $t = 0.001$.

second approach, the extension of the normal velocity might be promising. Sethian [1] gives examples of several problems where it is not possible to define the normal velocity in the same way for all the level sets. He applied the fast marching method to extend the normal velocity from some narrow neighbourhood of the zero level set to the rest of the computational domain. He also shows that this method preserves the signed distance function. A similar method was described by Smereka [92]. He employed it for the surface-diffusion flow. Its application to the Willmore flow might be promising.

Another method is the **phase-field** approach originally introduced by Allen and Cahn [2]. The spatial domain is split into a part with, for example a liquid phase, another part with a solid phase and a narrow interface between them. We consider a function u which is zero at the solid part, one at the liquid part and it continuously changes from zero to one at the interface. The interface is usually narrow but with finite thickness. The level set corresponding to the value $1/2$ is related to the interface. An advantage in comparison with the level-set method is in the fact that the function u preserves well its property to stay between zero and one. On the other hand, the phase-field models are often sensitive with respect to the parameter which controls the thickness of the interface. It is known that the Allen-Cahn equation approximates the mean curvature flow [2], the Cahn-Hilliard equation approximates the surface-diffusion flow [17] and recently Du, Liu, Ryham and Wang [42, 41] derived a phase-field model for the Willmore flow.

Some comparisons between different approaches have been done by Beneš and Mikula [8], Beneš, Mikula, Oberhuber, Ševčovič [13] and Elliott and Styles [46].

3. Physical background

Goal of this chapter is to provide a motivation to the effort of finding a numerical approximation of the mentioned evolutionary laws. We show that these laws find many important applications in physics.

3.1. Physical problems related to the curvature-driven flow

3.1.1. Capillary surfaces

Consider unusual phenomena allowing water drops hanging on a spider web or water strider walking on water. We speak of **surface tension**. It appears in situations when two different fluids or fluid and solid material are in contact. If these fluids do not diffuse one into each other they remain separate. Small water drop diffuses in contact with sand or textiles. On the other hand, on plastic or in the air it remains as a water drop. In 1805, Thomas Young [104] introduced a notion of the mean curvature H by showing **the Young-Laplace equation**

$$\Delta p = 2\sigma H, \tag{3.1}$$

where Δp is the pressure drop across the interface separating the fluids, σ is **the surface tension** and H is the mean curvature. When equilibrium $\Delta p = 0$ is attained, it means that $H = 0$ and we arrive to so called **minimal surface**. Trivial solution for $H = 0$ is a plane. However, if we set up some non-trivial boundary conditions we may get more complex shapes. Soap film in non-planar wire loop is one example (height of the wire loop represents the Dirichlet boundary conditions). A water drop on plastic plate with prescribed **contact angle** (it depends only on the materials) represented by the Neumann boundary conditions is another example of this phenomenon.

The mentioned phenomenon is related with an interesting domain of physics. Even though the Young-Laplace equation is now older than 200 years, this domain is a living source of problems to be solved. Readers more interested in this topic may read for example a survey text by Finn [51]. For a derivation of the equation (3.1) together with its applications in nanoscaled solids, we refer to Chen, Chiu and Weng [19].

3.1.2. Stefan problem

The Stefan problem arises in phase transitions – see Gurtin [54]. Consider a homogeneous and isotropic material which can exist in two phases – liquid and solid. We denote by Ω a bounded domain in $\mathbb{R}^3$, by $\Omega_l(t)$ the liquid subdomain and by $\Omega_s(t)$ the solid subdomain for $t \in [0, T]$ – see the Figure 3.1. Let $\Gamma(t) = \partial\Omega_l(t) \cap \partial\Omega_s(t)$ be an interface between the phases, $u(\mathbf{x}, t)$ space dependent temperature of the system, c **heat capacity** per unit volume at constant pressure, λ_l, λ_s **thermal conductivity** of given phases and L the **latent heat** which is the heat exchanged by the phase transition of a unit volume.

Assuming that both phases are incompressible, from the classical Fourier conduction law and energy balance in each phase (see. Visintin [96] for details) we get **the heat equations** in

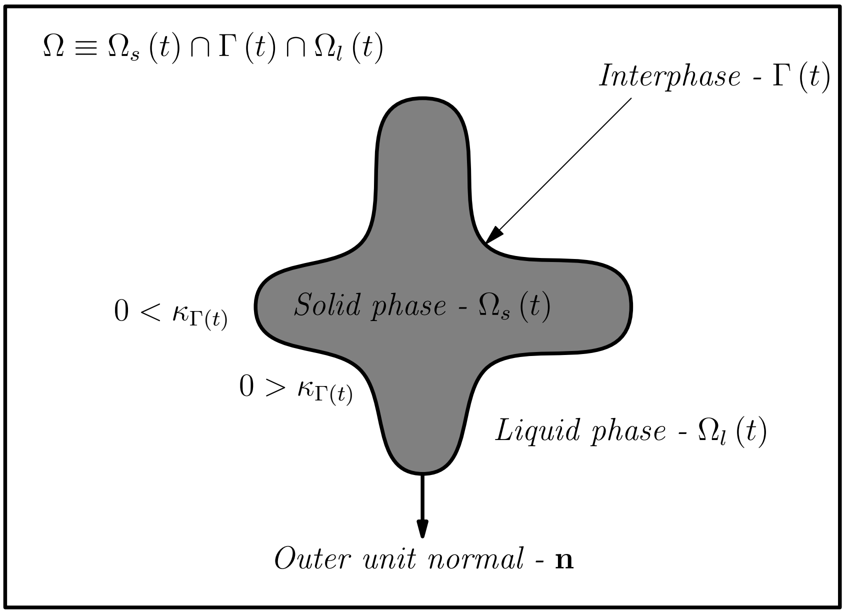

Figure 3.1.: Setting of the Stefan problem.

both phases as

$$c\partial_t u = \nabla \cdot (\lambda_l \nabla u) \text{ in } \Omega_l(t), \tag{3.2}$$

$$c\partial_t u = \nabla \cdot (\lambda_s \nabla u) \text{ in } \Omega_s(t). \tag{3.3}$$

Denote by V the normal velocity of the interface $\Gamma(t)$ (i.e. the speed in what $\Gamma(t)$ is moving in its unit interface normal $\mathbf{n}$ direction at each point). Consider a small element $\mathrm{d}S$ of the interface moving with the velocity V. Denoting $\mathbf{q}_l$, $\mathbf{q}_s$ **the heat flux** of the liquid resp. solid phase (both are given as $\mathbf{q}_l = -\lambda_l \nabla u$, resp. $\mathbf{q}_s = -\lambda_s \nabla u$). Then the latent heat L is absorbed resp. released according to the following formula

$$\mathbf{q}_l \cdot \mathbf{n} - \mathbf{q}_s \cdot \mathbf{n} = LV \text{ on } \Gamma(t).$$

It yields **Stefan condition** of the heat-flux jump

$$\lambda_s \partial_{\mathbf{n}} u \mid_s - \lambda_l \partial_{\mathbf{n}} u \mid_l = -LV \text{ on } \Gamma(t), \tag{3.4}$$

where we denoted $\partial_{\mathbf{n}} u \mid_s$ normal derivative of u relative to $\Omega_s(t)$ (similarly for $\partial_{\mathbf{n}} u \mid_l$). If the phase transitions are studied at the microscopic scale, we incorporate effect of the **surface tension** . It is described by **the Gibbs-Thomson law**

$$u - u^* = -\frac{\sigma}{\Delta s}\kappa_{\Gamma(t)} - \alpha\frac{\sigma}{\Delta s}V, \tag{3.5}$$

where u^* denotes temperature at what the phase change occurs in equilibrium, σ is **the surface tension coefficient** , $\Delta s = S_l \mid_l - S_s \mid_s$ denotes the difference in **the unit volume entropy density** across the interface and $\kappa_{\Gamma(t)}$ is the (mean) curvature of the interface $\Gamma(t)$. Clearly we observe a similarity between equations (3.1) and (3.5).

3.1.3. Grain boundary motion

Phase transition is a phenomenon where one phase turns into another one. Solid volume may consist of grains - domains of the same crystallographic orientation. The phase change need not

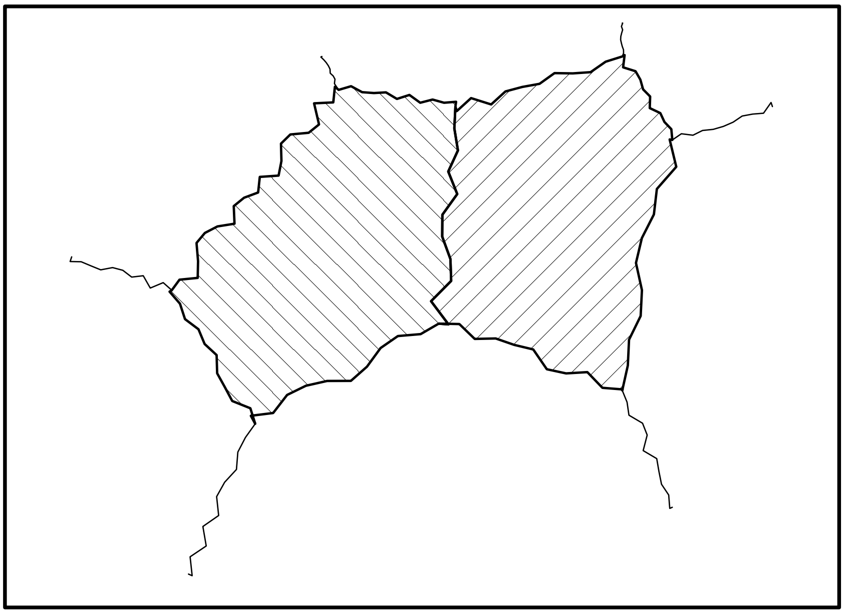

Figure 3.2.: Example of two grains with different orientation.

occur simultaneously in whole volume. Crystal growth is initiated at impurity. Under special conditions, only one grain is formed creating a **monocrystal**. However, usually many impurities cause formation of many crystals forming the grain structure of a **polycrystal** – see the Figure 3.2. The boundaries between particular crystals or **grains** are called **grain boundaries** .

The **grain boundary motion** is a phenomenon which may occur under many different circumstances. Some of them are described in Beck [5]. Mullins [78] describes situation when a metal crystal, after not very strong deformation, recrystallise back to strain-free state while it is annealed. During this process the grain boundary moves "toward its centre of curvature with a speed proportional to the curvature". Moreover, the motion is induced by pressure $p = \kappa\sigma$ where κ is the curvature and σ stands for free energy per unit area. This is the Young-Laplace equation again.

Another example might be the **diffusion-induced grain-boundary motion**. Assuming a thin metallic polycrystalline film which is inserted in a vapour consisting of another metal. The film has grain boundaries. Since these boundaries are gaps in atomic structure, they are good places where the metallic atoms from the vapour can diffuse in. An interesting thing is that these atoms do not fill the grain boundaries but the grain boundaries start to move. The deposition of vapour atoms changes the chemical composition. This phenomenon has been studied mathematically e.g. by Styles and Elliott [46].

3.2. Willmore flow

Let us now turn from the physics of materials to physics of elasticity resp. to biology of the **red blood cells** . They have been discovered in the seventeenth century and since then, many scientists tried to find explanation of their biconcave shape. In 1960's, it has been shown that after deformation, the red blood cells can quickly restore their shape again. It seemed that this shape is a minimiser of some energy. In 1970 Canham [18] proposed an explanation of the shape by minimising the **bending energy** of the membrane. Such energy is given by

$$\mathcal{E} = \frac{D}{2}\int_{\Gamma(t)} \frac{1}{R_1^2} + \frac{1}{R_2^2}\mathrm{d}\mathcal{H}^{n-1} = \frac{D}{2}\int_{\Gamma(t)} H^2 - 2K\mathrm{d}\mathcal{H}^{n-1}, \tag{3.6}$$

where R_1, R_2 are radii of the principal curvatures, H is the mean curvature, K is the Gauss curvature and D is the **bending rigidity** given by

$$D = \frac{Eh^3}{12\left(1-\nu^2\right)},$$

for E denoting the **Young modulus of elasticity**, h denotes the **membrane thickness** and ν is the **Poisson ratio**. Applying the global Gauss-Bonnet theorem (A.0.12) together with the fact that the **Euler-Poincaré characteristic** $\chi\left(\Gamma\right)=2$ for all surfaces obtained from a sphere in $\mathbb{R}^3$ by a **diffeomorphism** (i.e. it does not change the topology of the surface) we get that the minimum of $\mathcal{E}$ is the same as for

$$\mathcal{W}^* = \frac{D}{2}\int_{\Gamma(t)} H^2 \mathrm{d}\mathcal{H}^{n-1}, \tag{3.7}$$

which is the **Willmore functional** . In the same article [18], Canham achieved correspondence between observed and predicted shapes. His method consists of evaluation of (3.6) for **Cassini ovals** and taking those with minimal values. It is surprising that using such a simple technique, he was able to get reliable results. For readers interested in the red-blood cells shapes we also refer to Helfrich [57] or Svetina and Žekš [95].

4. Evolving hypersurfaces

In this chapter we introduce some tools of differential geometry and explain the theory of evolving surfaces. Introduction to the planar curves is brief and for more details we refer to Oprea [84] or Ševčovič [98]. The theory of evolving surfaces is explained more deeply. The importance of some theorems for this text is crucial because they make the derivation of the later presented evolutionary laws easier. Even though they can be found in a very similar form in Kimura [65], some of our definitions are slightly different (less general, designed for the purpose of this text).

4.1. Planar curves

Definition of planar curves

The planar curves can represent e.g. boundaries of objects in images, interfaces in phase transitions etc. Suitable definition of a curve, that would be general enough and would not allow any spurious objects to be the curves, is difficult to find. It was not solved completely yet - see Lomtatidze [68]. In this section we define important properties of curves corresponding to the scope of the text.

Definition 4.1.1. *A* **curve** $\Gamma \in \mathbb{R}^n$ *is an image of a continuous mapping* $\gamma : I \to \mathbb{R}^n$*, where* I *is an interval in* $\mathbb{R}$ *consisting of more than one point.*

For the previous definition we refer to Jöst [64]. However, for our purposes we have changed the meaning of the curve to be an image of a mapping rather then the mapping itself. The mapping γ will be referred to a **parametrisation** of the curve $\Gamma \equiv \gamma(I)$ (in this text we always assume that the parametrisation γ is defined on interval $I \subset \mathbb{R}$ having more then one point). The parametrisation choice is not unique. Having bijective continuous mapping $\varphi : I_1 \to I$ for some nonempty interval $I_1 \subset \mathbb{R}$ the mapping $\gamma \circ \varphi : I_1 \to \mathbb{R}^n$ provides another parametrisation. It means, that two different parametrisations can define the same curve. (On the other hand, Jöst [64] defines *an arc* for a class of parametrisations describing the same curve in our sense - we will not use this terminology).

Let $\gamma = \gamma(v)$ for $v \in I$. The theory of curves uses the **arclength parametrisation** for which $|\partial_v \gamma(v)| = 1$ for all $v \in I$, where $\partial_v \gamma$ denotes the derivative of γ with respect to v. The arclength parameter is denoted by s.

Definition 4.1.2. *Assume that* $I \equiv [a, b]$*, and* $\gamma : I \to \mathbb{R}^n$ *is a parametrisation of a curve* $\Gamma \equiv \gamma(I)$*.* Γ *is called the* **closed curve** *iff* $\gamma(a) = \gamma(b)$*.*

In case of closed curves, the parameter v can belong to the unit circle S^1 instead of the interval I. Then $\gamma : S^1 \to \mathbb{R}^n$. The following definition and theorem on the Jordan curves were adopted from Jöst [64].

Definition 4.1.3. *A* **planar curve** Γ *is defined by the Definition 4.1.1 where* $n = 2$*.*

Definition 4.1.4. *A curve* Γ *is called the* **Jordan curve** *iff it is represented by an injective parametrisation* $\gamma : I \to \mathbb{R}^n$ *.*

If the mapping γ is injective it means that for each $v_1, v_2 \in I$, $v_1 \neq v_2 \Rightarrow \gamma(v_1) \neq \gamma(v_2)$ holds. We say that **the curve** $\gamma(I)$ **is non-selfintersecting**.

Theorem 4.1.5. *A closed planar Jordan curve* Γ *partitions* $\mathbb{R}^2$ *into exactly two open and connected sets, that is,* $\mathbb{R}^2 \setminus \Gamma = \Omega_1 \cup \Omega_2$*,* $\partial\Omega_1 = \Gamma = \partial\Omega_2$*,* $\Omega_1 \cap \Omega_2 = 0$*,* Ω_1*,* Ω_2 *are open and connected. Only one of these two sets is bounded. It is called the* **interior of** Γ *denoted as* $Int(\Gamma)$*. The other one is unbounded and is called the* **exterior of** Γ*, denoted as* $Ext(\Gamma)$*.*

The property of the Theorem 4.1.5 is important for many applications. For example in image segmentation the interior of Γ usually corresponds to the segmented object. Unfortunately, this definition can not be applied when we need to segment more then one object. In this case we have to consider more then one Jordan curve i.e. curves $\Gamma_1, \cdots, \Gamma_m$ with interiors $\mathrm{Int}(\Gamma_1), \cdots \mathrm{Int}(\Gamma_m)$ corresponding to the segmented objects and with one exterior $\mathrm{Ext}(\Gamma_1, \cdots \Gamma_m) = \bigcap_{i=1}^n \mathrm{Ext}(\Gamma_i)$.

Normal and tangential vector of planar curve

Definition of a curve by the mapping γ allows to employ the differential calculus. We observe that the differentiation of γ could indicate many important properties of the curve $\gamma(I)$. Corresponding domain of mathematics is called the *differential geometry* [38, 63, 84, 100]. It studies qualitative aspects of curves expressed by derivatives or partial derivatives. We start with a definition establishing important condition for the curve parametrisation.

Definition 4.1.6. *Let* $\gamma = \gamma(v)$ *be a parametrisation of a curve* $\Gamma \equiv \gamma(I)$*. We say that the* **parametrisation** γ **is regular** *iff* $|\partial_v \gamma(v)| \neq 0$ for all $v \in I$.

The arclength parametrisation is regular. Therefore the class of regular parametrisations is not empty. We proceed by defining the tangential space and the normal vector:

Definition 4.1.7. *Let* Γ *be a closed, planar, Jordan curve parametrised by a regular parametrisation* $\gamma : I \to \mathbb{R}^2$ *and* $\gamma = \gamma(v)$*. The* **tangential space** $\mathbf{T}(\mathbf{x})$ *at a point* $\mathbf{x} \in \Gamma$ *is a linear vector space* $\mathbf{T}(\mathbf{x}) = [\partial_v \gamma]_\lambda$*, where* $[\mathbf{v}]_\lambda$ *denotes the linear span of the vector* $\mathbf{v}$*. The* **normal unit vector** $\mathbf{n}(\mathbf{x})$ *at a point* $\mathbf{x} \in \Gamma$ *is given by* $\mathbf{n}(\mathbf{x}) \in \mathbf{T}(\mathbf{x})^\perp$ *and* $|\mathbf{n}(\mathbf{x})| = 1$*. We say that* $\mathbf{n}(\mathbf{x})$ *is an* **inward normal vector** *iff there exists* $\epsilon > 0$ *such that* $\mathbf{x} + \epsilon\mathbf{n}(\mathbf{x}) \in Int(\Gamma)$*. Otherwise it is an* **outward normal vector***. The* **tangential unit vector** *at a point* $\mathbf{x} \in \Gamma$ *is any vector* $\tau(\mathbf{x}) \in \mathbf{T}(\mathbf{x})$ *such that* $|\tau(\mathbf{x})| = 1$*. The* **oriented tangential unit vector** $\mathbf{t}(\mathbf{x})$ *at a point* $\mathbf{x} \in \Gamma$ *is given by the conditions* $\mathbf{t}(\mathbf{x}) = \mathbf{n}(\mathbf{x})^\perp$*,* $|\mathbf{t}(\mathbf{x})| = 1$ *and* $\det[\mathbf{n}(\mathbf{x}), \mathbf{t}(\mathbf{x})] = 1$*, where* $\mathbf{n}(\mathbf{x})$ *is the outward normal unit vector, the matrix* $[\mathbf{n}(\mathbf{x}), \mathbf{t}(\mathbf{x})]$ *consists of the rows given by the vectors* $\mathbf{t}(\mathbf{x})$ *and* $\mathbf{n}(\mathbf{x})$*.*

In this text, if we do not say explicitly, we always mean by $\mathbf{n}(\mathbf{x})$ the outward normal unit vector. The definition of $\mathbf{t}(\mathbf{x})$ is such that if we stand on Γ looking in the $\mathbf{t}(\mathbf{x})$ direction we have the interior of Γ on the left-hand side and $\mathbf{n}(\mathbf{x})$ points to the right. For the following two definitions we refer to Yazaki [103].

Definition 4.1.8. *The parametrisation* γ *is the* **immersion** *iff* $\partial_v \gamma \neq 0$ *for all* $v \in I$*.*

Definition 4.1.9. *The parametrisation* γ *is the* **embedding** *iff it is the immersion and injection.*

Remark: As already mentioned, the parametrisation γ is identified with Γ in some texts. Then the notion of **immersed curve** is used often. One should, however, keep in mind that it is a property of the mapping describing the curve. On the other hand, if γ is embedding, the curve $\gamma(I)$ is not self-intersecting and it is a property of the image of the mapping γ as well. The notion **embedded curve** is frequent too. In textbooks on differential geometry one can find more general definitions of immersion and embedding - see e.g. do Carmo [38]. For our purposes such formalism is not necessary.

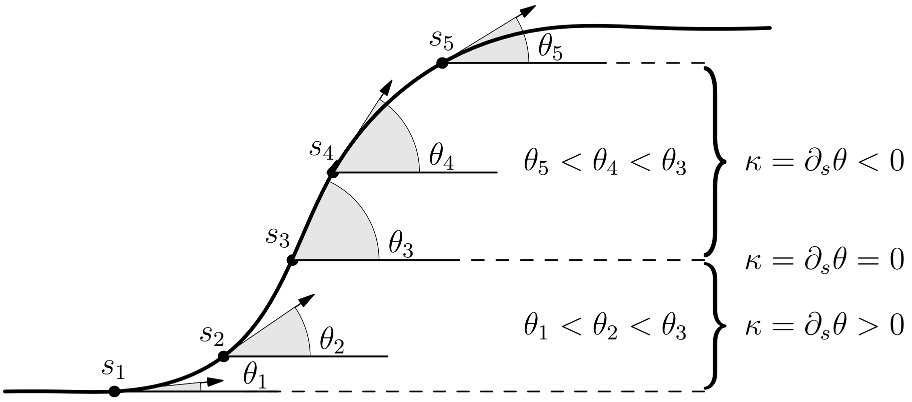

Figure 4.1.: Meaning of κ.

Frenet formulae for planar curves

The Frenet formulae for planar curves show an important relationship between the derivatives of the tangential and the normal vector.

Theorem 4.1.10. The Frenet formulae: *Let* Γ *be a closed, planar, Jordan curve,* $\gamma : I \to \mathbb{R}^2$*,* $\gamma = \gamma(s)$ *the arclength parametrisation of* Γ*, let* $\mathbf{t}(s) = \mathbf{t}_{\gamma(s)}$ *is the tangential vector at a point* $\gamma(s) \in \Gamma$ *and* $\mathbf{n}(s) = \mathbf{n}_{\gamma(s)}$ *is the outer normal vector at the same point. Then there exists function* $\kappa : I \to \mathbb{R}$ *such that:*

$$\partial_s \mathbf{n} = \kappa \mathbf{t} \text{ on } I, \tag{4.1}$$

$$\partial_s \mathbf{t} = -\kappa \mathbf{n} \text{ on } I. \tag{4.2}$$

Proof. Take fixed $s \in I$. Since we have that $(\mathbf{n}(s), \mathbf{n}(s)) = 1$ (here $(\cdot,\cdot)$ denotes the Euclidean scalar product in $\mathbb{R}^2$) and $0 = \partial_s (\mathbf{n}(s), \mathbf{n}(s)) = 2(\partial_s \mathbf{n}(s), \mathbf{n}(s))$ we see that $\partial_s \mathbf{n}(s)$ is orthogonal to $\mathbf{n}(s)$. It means that it is proportional to $\mathbf{t}(s)$ and (4.1) holds. Now from $(\mathbf{n}(s), \mathbf{t}(s)) = 0$ and since $(\partial_s \mathbf{t}(s), \mathbf{t}(s)) = 0$ we have that $\mathbf{n}(s)$ is proportional to $\partial_s \mathbf{t}(s)$. Also $0 = \partial_s (\mathbf{n}(s), \mathbf{t}(s)) = (\partial_s \mathbf{n}(s), \mathbf{t}(s)) + (\mathbf{n}(s), \partial_s \mathbf{t}(s))$. Therefore

$$(\mathbf{n}(s), \partial_s \mathbf{t}(s)) = -(\partial_s \mathbf{n}(s), \mathbf{t}(s)) = -(\kappa \mathbf{t}(s), \mathbf{t}(s)) = -\kappa.$$

□

The meaning of the quantity κ is discussed below. Writing $\mathbf{t} = (\cos\theta(s), \sin\theta(s))$ and differentiating with respect to s we obtain $\partial_s \mathbf{t} = \partial_s \theta (-\sin\theta(s), \cos\theta(s)) = -\partial_s \theta \mathbf{n}$ and so

$$\kappa = \partial_s \theta. \tag{4.3}$$

In convex parts $\theta(s)$ is increasing and $\kappa \geq 0$. In concave parts $\theta(s)$ is decreasing and $\kappa \leq 0$. This tells us that κ has a meaning of the rate of change of $\mathbf{t}$ and so we say that:

Definition 4.1.11. *Function* κ *defined on* I *by (4.1) and (4.2) is the* **curvature** *of* Γ.

From (4.2) we also see that

$$\kappa = -(\partial_s \mathbf{t}, \mathbf{n}) = -(\partial_s^2 \gamma, \mathbf{t}^\perp) = -(\partial_s^2 \gamma, \partial_s \gamma^\perp) = -\det\left[\partial_s^2 \gamma, \partial_s \gamma\right] = \det\left[\partial_s \gamma, \partial_s^2 \gamma\right], \tag{4.4}$$

where $\det[\mathbf{a}, \mathbf{b}]$ denotes determinant of matrix, columns of which are vectors $\mathbf{a}$ and $\mathbf{b}$.

Implicit curves

So far we studied the curves described by a parametrisation γ. The implicit description of curves represents an alternative in case of closed curves. The approaches like the level-set method or the phase-field method are based on the implicit curves.

Definition 4.1.12. *We say that* **the curve Γ is implicit** *iff there exists a domain $\Omega \subset \mathbb{R}^2$ such that $\Gamma \subset \Omega$ and there is a function $u \in C(\Omega;\mathbb{R})$ such that*

$$\Gamma \equiv \{\mathbf{x} \in \Omega \mid u(\mathbf{x}) = 0\}. \tag{4.5}$$

If $u \in C^q(\Omega)$ in (4.5) then the implicit function theorem (A.0.2) implies that each implicit curve given by (4.5), can by locally parametrised by a mapping $\gamma_{\mathbf{x}} \in C^q\left(I;\mathbb{R}^2\right)$ on the neighbourhood of an arbitrary point $\mathbf{x} \in \Gamma$ where $\gamma_{\mathbf{x}}$ is defined on some interval $I \subset S^1$. As a consequence we can fully parametrise each compact curve Γ. Then it is enough, in mathematical theory, to study the curves given by some parametrisation.

4.2. Hypersurfaces

In this section hypersurfaces are discussed. The approach of the previous section can be extended to higher dimensions. A definition and evaluation of the mean curvature and the Laplace-Beltrami operator are the main results. Major part of this section is adopted from Kimura [65].

Hypersurfaces in $\mathbb{R}^n$, tangential vector and normal vector field

Definition 4.2.1. *$\Gamma \subset \mathbb{R}^n$ is called* **C^m-hypersurface $(m \geq 1)$ in $\mathbb{R}^n$** *iff there is a function $u \in C^m(\mathbb{R}^n)$ such that*

$$\Gamma \equiv \{\mathbf{x} \in \mathbb{R}^n \mid u(\mathbf{x}) = 0\}, \tag{4.6}$$

and ∇u does not vanish on Γ. Moreover, if there exists a bounded set Γ_{int} and a set Γ_{ext} such that Γ, Γ_{int} and Γ_{ext} are disjoint, $\mathbb{R}^n \equiv \Gamma \cup \Gamma_{\mathrm{int}} \cup \Gamma_{\mathrm{ext}}$, $u(\mathbf{x}) < 0$ on Γ_{int} and $u(\mathbf{x}) > 0$ on Γ_{ext}, we call u **the level-set function of Γ***.*

Definition 4.2.2. *Let Γ be a C^m-hypersurface. We say that vector $\tau(\mathbf{x})$ is the* **tangential vector** *of Γ at point $\mathbf{x}$ iff there exists a curve $\gamma(I) \subset \Gamma$ with parametrisation $\gamma = \gamma(v)$, $\gamma \in C^m(I;\mathbb{R}^n)$ defined on interval $I \subset \mathbb{R}$, $0 \in I$ such that $\gamma(0) = \mathbf{x}$ and $(\partial_v\gamma)(0) = \tau(\mathbf{x})$.*

Fixing some $\mathbf{x} \in \Gamma$, taking the curve $\gamma(I)$ from the previous definition and inserting it to a function u from (4.2.1) we have that $u(\gamma(v)) = 0$ and so $\frac{\mathrm{d}u}{\mathrm{d}v} = \nabla u \cdot \partial_v \gamma = 0$ which holds for all $\tau(\mathbf{x})$. It means that ∇u is orthogonal to all the tangential vectors $\tau(\mathbf{x})$. If u is the level-set function then ∇u points to Γ_{ext} and we have that the **outer normal unit vector field** is given by

$$\mathbf{n}(\mathbf{x}) = \frac{\nabla u(\mathbf{x})}{|\nabla u(\mathbf{x})|}. \tag{4.7}$$

It is clear that for any $\mathbf{x} \in \Gamma$ all the tangential vectors $\tau(\mathbf{x})$ create vector space $\mathbf{T}(\mathbf{x})$ given by $\mathbf{T}(\mathbf{x}) \equiv \{\tau(\mathbf{x}) \in \mathbb{R}^n \mid (\mathbf{n}(\mathbf{x}), \tau(\mathbf{x})) = 0\}$. Its dimension is $n-1$. Let $\{\mathbf{t}_1, \cdots \mathbf{t}_{n-1}\}$ be the orthonormal basis of $\mathbf{T}(\mathbf{x})$.

Definition 4.2.3. *The vector space $\mathbf{T}(\mathbf{x})$ is called the* **tangential space at the point $\mathbf{x} \in \Gamma$.**

Definition 4.2.4. *A C^m-hypersurface $\Gamma \in \mathbb{R}^n$ is called* **oriented** *iff there exists a vector field $\mathbf{n}(\mathbf{x}) \in C^1\left(\Gamma, \mathbb{R}^{n+1}\right)$ such that $\mathbf{n}(\mathbf{x}) \perp \mathbf{T}(\mathbf{x})$ and $|\mathbf{n}(\mathbf{x})| = 1$ for all $\mathbf{x} \in \Gamma$.*

Remark 4.2.5. Let $\mathbf{x} \in \Gamma$ be an arbitrary point. Without loss of generality we may assume that $\mathbf{x} = \mathbf{0}$, $\mathbf{t}_i = \mathbf{e}_i$ for $i = 1, \cdots n-1$ and $\mathbf{n}(\mathbf{x}) = \mathbf{e}_n$ where $\{\mathbf{e}_1, \cdots, \mathbf{e}_n\}$ is the standard basis of $\mathbb{R}^n$. By the implicit function theorem we know that for a neighbourhood O of $\mathbf{0}$ there exists a function $\varphi \in C^m(O)$ such that Γ is given as a graph of $\varphi = \varphi(\xi)$ on O i.e. $\Gamma \cap O \equiv \{(\xi, \varphi(\xi)) \mid \xi \in O\}$. In other words, for any $\mathbf{x} \in \Gamma$ there exists a neighbourhood U of $\mathbf{x} \in \Gamma$ such that

$$\Gamma \cap U \equiv \{\mathbf{x} + \mathbb{T}\xi + \varphi(\xi)\mathbf{n}(\mathbf{x}) \mid \xi \in O\}$$

where rows of the matrix $\mathbb{T}$ consists of vectors $\mathbf{t}_1, \cdots, \mathbf{t}_{n-1}$. We say that Γ **is given as a graph of φ on U**.

Mean curvature and Gauss curvature

One of the most important local quantity for the curve is the curvature. Its counterparts in case of hypersurfaces are the mean curvature and the Gauss curvature . We will define them using an auxiliary curve defined on Γ. Consider now a unit tangential vector $\tau(\mathbf{x}) \in \mathbf{T}(\mathbf{x})$ and define a plane curve $\gamma(s) = \mathbf{x} + s\tau(\mathbf{x}) + \varphi(s\tau(\mathbf{x}))\mathbf{n}(\mathbf{x})$, where $\varphi(\xi)$ is the function from the Remark 4.2.5 and $s \in (-\epsilon, \epsilon)$ for ϵ small enough. Then $\gamma(s) \subset \Gamma$ and $\gamma(0) = \mathbf{x}$,

$$\partial_s\gamma(s) = \tau(\mathbf{x}) + (\nabla\varphi(s\tau(\mathbf{x}))\tau(\mathbf{x}))\mathbf{n}(\mathbf{x})$$

and

$$\partial_s^2\gamma(s) = \left(\left(D^2\varphi(s\tau(\mathbf{x}))\tau(\mathbf{x})\right)\tau(\mathbf{x})\right)\mathbf{n}(\mathbf{x}) = \left(\tau(\mathbf{x})^T D^2\varphi(s\tau(\mathbf{x}))\tau(\mathbf{x})\right)\mathbf{n}(\mathbf{x}),$$

where

$$\left(D^2\varphi(\xi)\right)_{ij} := \frac{\partial^2\varphi}{\partial\xi_i\partial\xi_j}(\xi),$$

is a **Hessian matrix** of $\varphi(\xi)$. If Γ is C^2-hypersurface then $\varphi \in C^2\left(\mathbb{R}^{n-1}\right)$ and $D^2\varphi$ is symmetric. Since from (4.4) $\kappa = -\left(\partial_s^2\gamma, \mathbf{n}(\mathbf{x})\right)$ we have

$$\kappa_{\tau(\mathbf{x})} = -\tau(\mathbf{x})^T D^2\varphi\tau(\mathbf{x}), \tag{4.8}$$

which is the curvature of Γ at the point $\mathbf{x}$ in the direction of the tangential vector $\tau(\mathbf{x})$.

Definition 4.2.6. *Denote the eigenvalues and the eigenvectors of the symmetric matrix $D^2\varphi(\mathbf{x})$ by κ_i and $\mathbf{d}'_i \in \mathbb{R}^{n-1}$ for $i = 1, \cdots, n-1$. Then κ_i are called the* **principal curvatures** *of Γ at the point $\mathbf{x}$ and $\mathbf{d}_i \in \mathbf{T}(\mathbf{x})(\Gamma)$ given by $\mathbf{d}_i = \mathbb{T}\mathbf{d}'_i$ are called the* **principal directions** *. Here the columns of the matrix $\mathbb{T}$ consist of vectors $\mathbf{t}_1, \cdots, \mathbf{t}_{n-1}$. We define the* **mean curvature** *as*

$$H = \sum_{i=1}^{n-1} \kappa_i, \tag{4.9}$$

and **the Gauss curvature** *as*

$$K = \prod_{i=1}^{n-1} \kappa_i. \tag{4.10}$$

Differential calculus on Γ

In the following we are interested in the differential calculus restricted on Γ. Assume having a function $f \in C^1(\mathbb{R}^n)$ and a curve $\gamma(s)$ such that $\gamma(0) = \mathbf{x} \in \Gamma$. Assume that there exists $\epsilon > 0$ such that $\gamma(s) \subset \Gamma$ for all $s \in (-\epsilon, \epsilon)$. We want to study the change of f along γ. We get that $\frac{\mathrm{d}}{\mathrm{d}s}f(\gamma(s)) = \nabla f \cdot \partial_s\gamma(s)$. Since $\partial_s\gamma(s) \in \mathbf{T}(\mathbf{x})$ we can project ∇f to $\mathbf{T}(\mathbf{x})$ without affecting the correct result. It follows that $\nabla f \cdot \partial_s\gamma(s) = [\nabla f - (\nabla f, \mathbf{n}(\mathbf{x}))\mathbf{n}(\mathbf{x})] = [(\mathbb{I} - \mathbf{n}(\mathbf{x}) \otimes \mathbf{n}(\mathbf{x}))]\nabla f$.

Definition 4.2.7. *For a function $f \in C^1(\Gamma)$ we define the* **surfacial gradient of f on Γ** *as*

$$\nabla_\Gamma f(\mathbf{x}) := \mathbb{P}(\mathbf{x}) \nabla \tilde{f}(\mathbf{x}) \text{ for } \mathbf{x} \in \Gamma, \tag{4.11}$$

where

$$\mathbb{P}(\mathbf{x}) := \mathbb{I} - \mathbf{n}(\mathbf{x}) \otimes \mathbf{n}(\mathbf{x}) = \mathbb{I} - \mathbf{n}(\mathbf{x})\mathbf{n}(\mathbf{x})^T, \tag{4.12}$$

is orthogonal projection from $\mathbb{R}^n$ to $\mathbf{T}(\mathbf{x})$ and $\tilde{f} \in C^1(\mathbb{R}^n)$ is an arbitrary extension of f to $\mathbb{R}^n$.

One has to show that the previous definition does not depend on the choice of $\tilde{f}$. Assume having two different extensions $\tilde{f}_1$ and $\tilde{f}_2$. Then $\tilde{f}_1 - \tilde{f}_2 = 0$ on Γ. $\tilde{f}_1 - \tilde{f}_2$ can become a level-set function of Γ on $\mathbb{R}^n$ up to the sign of $\tilde{f}_1 - \tilde{f}_2$ in Γ_{int} and Γ_{ext}. Its gradient is therefore orthogonal to $\mathbf{T}(\mathbf{x})$. It means that $\mathbb{P}(\mathbf{x}) \nabla \left(\tilde{f}_1 - \tilde{f}_2\right) = 0$ and so $\mathbb{P}(\mathbf{x}) \nabla \tilde{f}_1 = \mathbb{P}(\mathbf{x}) \nabla \tilde{f}_2$.

Definition 4.2.8. *For the vector field $\mathbf{h} \in C^1(\Gamma, \mathbb{R}^n)$ we define the* **surfacial divergence of $\mathbf{h}$ on Γ** *as*

$$\nabla_\Gamma \cdot \mathbf{h} := \mathrm{tr} \nabla_\Gamma \mathbf{h}^T. \tag{4.13}$$

Definition 4.2.9. *For the function $f \in C^2(\Gamma)$ we define the* **Laplace-Beltrami operator of f on Γ** *as*

$$\Delta_\Gamma f := \nabla_\Gamma \cdot \nabla_\Gamma f. \tag{4.14}$$

Weingarten map (shape operator)

Definition 4.2.10. The Weingarten map *or* **the shape operator** $W \in C^0(\Gamma, \mathbb{R}^{n \times n})$ *is defined as*

$$W(\mathbf{x}) := -\nabla_\Gamma \mathbf{n}^T(\mathbf{x}), \text{ for } \mathbf{x} \in \Gamma. \tag{4.15}$$

Theorem 4.2.11. *$W(\mathbf{x})$ is symmetric, $W(\mathbf{x})\mathbf{n}(\mathbf{x}) = \mathbf{0}$ and $W(\mathbf{x})\mathbf{d}_i = \kappa_i \mathbf{d}_i$ for $i = 1, \cdots, n-1$ where $\mathbf{d}_i$ are the principal directions from the Definition 4.2.6.*

Proof. Let $\mathbf{x} \in \Gamma$ be a fixed point. Clearly $W(\mathbf{x}) : \Gamma \to \mathbf{T}(\mathbf{x})(\Gamma)$ and $W(\mathbf{x})\mathbf{n}(\mathbf{x}) = \mathbf{0}$ (all columns of the matrix $W(\mathbf{x})$ are from $\mathbf{T}(\mathbf{x})$). Without loss of generality we may assume that $\mathbf{x} = \mathbf{0}$, $\mathbf{t}_i = \mathbf{e}_i$ for $i = 1, \cdots, n-1$ and $\mathbf{n}(\mathbf{x}) = \mathbf{e}_n$ where $\{\mathbf{e}_1, \cdots, \mathbf{e}_n\}$ is the standard basis of $\mathbb{R}^n$. Let O be a neighbourhood of $\mathbf{0}$. Let φ be a function such that Γ is given as a graph of φ on O. Writing $\mathbf{n}(\mathbf{x}) = (n_1(\mathbf{x}), \cdots, n_n(\mathbf{x}))$ we get

$$\mathbf{n}(\mathbf{x}) = \frac{1}{\sqrt{1 + |\nabla\varphi(\mathbf{x})|^2}} \begin{pmatrix} -\nabla\varphi(\mathbf{x}) \\ 1 \end{pmatrix} = n_n(\mathbf{x}) \begin{pmatrix} -\nabla\varphi(\mathbf{x}) \\ 1 \end{pmatrix}.$$

Let $\mathbf{d}_i$ be a principal direction and $\mathbf{d}'_i$ related eigenvector of $D^2\varphi(\xi)$. Define a plane curve $\gamma(v) = \mathbf{x} + v\mathbf{d}_i + \varphi(v\mathbf{d}'_i)\mathbf{n}(\mathbf{x})$.

Now we see that

$$\frac{\mathrm{d}}{\mathrm{d}v}\mathbf{n}(\gamma(v))\,|_{v=0} = \frac{\mathrm{d}}{\mathrm{d}v} n_n\left[\mathbf{x} + v\mathbf{d}_i + \varphi\left(v\mathbf{d}'_i\right)\mathbf{n}(\mathbf{x})\right] \begin{pmatrix} -\nabla\varphi(\mathbf{0}) \\ 1 \end{pmatrix} + n_n(\mathbf{0}) \begin{pmatrix} -D^2\varphi(\mathbf{0})\,\mathbf{d}'_i \\ 0 \end{pmatrix} \tag{4.16}$$

We will show that

$$\frac{\mathrm{d}}{\mathrm{d}v} n_n\left[\mathbf{x} + v\mathbf{d}_i + \varphi\left(v\mathbf{d}'_i\right)\mathbf{n}(\mathbf{x})\right] = 0. \tag{4.17}$$

Indeed

$$\begin{aligned} 0 &= \frac{\mathrm{d}}{\mathrm{d}v}\left|\mathbf{n}\left(\mathbf{x}+v\mathbf{d}_i+\varphi\left(v\mathbf{d}_i'\right)\mathbf{n}\left(\mathbf{x}\right)\right)\right|^2 |_{v=0}= 2\mathbf{n}\left(\mathbf{0}\right)\begin{pmatrix} \frac{\mathrm{d}}{\mathrm{d}v}n_1\left(\mathbf{x}+v\mathbf{d}_i+\varphi\left(v\mathbf{d}_i'\right)\mathbf{n}\left(\mathbf{x}\right)\right) \\ \vdots \\ \frac{\mathrm{d}}{\mathrm{d}v}n_n\left(\mathbf{x}+v\mathbf{d}_i+\varphi\left(v\mathbf{d}_i'\right)\mathbf{n}\left(\mathbf{x}\right)\right)\end{pmatrix}|_{v=0} \\ &= 2\frac{\mathrm{d}}{\mathrm{d}v}n_n\left(\mathbf{x}+v\mathbf{d}_i+\varphi\left(v\mathbf{d}_i'\right)\mathbf{n}\left(\mathbf{x}\right)\right), \end{aligned}$$

where the last equality follows from $\mathbf{n}\left(\mathbf{0}\right) = \left(0,\cdots,1\right)^T$. It is a proof of (4.17). Together with $n_n\left(\mathbf{0}\right) = 1$ we have from (4.16)

$$\frac{\mathrm{d}}{\mathrm{d}v}\mathbf{n}\left(\gamma\left(v\right)\right)|_{v=0}= \begin{pmatrix} -D^2\varphi\left(0\right)\mathbf{d}_i' \\ 0 \end{pmatrix} = -\kappa_i\mathbf{d}_i.$$

Now we see that

$$\partial_v\gamma\left(v\right) = \mathbf{d}_i + \mathbf{d}_i'\nabla\varphi\left(v\mathbf{d}_i'\right)\mathbf{n}\left(\mathbf{x}\right).$$

By our assumptions we have that $\mathbf{n}\left(\mathbf{0}\right) = \left(0,\cdots,0,1\right)^T = \left(-\nabla\varphi\left(\mathbf{0}\right),1\right)^T$. It means that $\nabla\varphi\left(\mathbf{0}\right) = \mathbf{0}$. It follows that

$$\partial_v\gamma\left(0\right) = \mathbf{d}_i,$$

and

$$\kappa_i\mathbf{d}_i = -\frac{\mathrm{d}}{\mathrm{d}v}\mathbf{n}\left(\gamma\left(0\right)\right) = -\left(\nabla_\Gamma\mathbf{n}^T\left(\gamma\left(0\right)\right)\right)\partial_v\gamma\left(0\right) = W\left(\mathbf{x}\right)\mathbf{d}_i.$$

It means that the vectors $\{\mathbf{d}_1,\cdots,\mathbf{d}_{n-1},\mathbf{n}\left(\mathbf{x}\right)\}$ are orthonormal eigenvectors with the corresponding eigenvalues $\{\kappa_1,\cdots,\kappa_{n-1},0\}$ and that $W\left(\mathbf{x}\right)$ is symmetric. □

Some useful expressions for H and the Laplace-Beltrami operator

The theorem (4.2.11) allows us to express the mean curvature as

$$H = \mathrm{Tr}\ W = -\nabla_\Gamma\cdot\mathbf{n}. \tag{4.18}$$

We might be tempted to say that $K = \det W$ but we know that the eigenvalue corresponding to $\mathbf{n}$ is 0. To make it 1 we add the matrix $\mathbf{n}\mathbf{n}^T$ to W. Then

$$K = \det\left(W + \mathbf{n}\mathbf{n}^T\right). \tag{4.19}$$

Our interest is to express the mean curvature H efficiently. The following theorem contributes to this effort.

Theorem 4.2.12. *Let $\tilde{\mathbf{n}}$ be a C^1-extension of $\mathbf{n}$ i.e. $\tilde{\mathbf{n}} \in C^1\left(\mathbb{R}^n\right)$, $|\tilde{\mathbf{n}}\left(\mathbf{x}\right)| = 1$ in some neighbourhood of Γ and $\tilde{\mathbf{n}}\left(\mathbf{x}\right) = \mathbf{n}\left(\mathbf{x}\right)$ on Γ. Then*

$$H = \nabla\cdot\tilde{\mathbf{n}} \tag{4.20}$$

holds.

Proof. For $\mathbf{x}\in\Gamma$ fixed and small $\epsilon > 0$, we have $|\tilde{\mathbf{n}}\left(\mathbf{x}+\epsilon\mathbf{n}\right)|^2 = 1$. Now

$$0 = \frac{\mathrm{d}}{\mathrm{d}\epsilon}|\tilde{\mathbf{n}}\left(\mathbf{x}+\epsilon\mathbf{n}\right)|^2|_{\epsilon=0}= 2\tilde{\mathbf{n}}\left(\mathbf{x}+\epsilon\mathbf{n}\right)^T\left[\nabla\tilde{\mathbf{n}}\left(\mathbf{x}+\epsilon\mathbf{n}\right)^T\right]\mathbf{n}|_{\epsilon=0}= 2\mathbf{n}^T\left(\nabla\tilde{\mathbf{n}}^T\right)\mathbf{n} \tag{4.21}$$

and

$$H = -\nabla_\Gamma\cdot\tilde{\mathbf{n}} = \mathrm{Tr}\ \nabla_\Gamma\tilde{\mathbf{n}}^T = \mathrm{Tr}\ \left[\left(\mathbb{I}-\mathbf{n}\mathbf{n}^T\right)\nabla\tilde{\mathbf{n}}^T\right] = \nabla\cdot\tilde{\mathbf{n}} - \mathbf{n}^T\left(\nabla\tilde{\mathbf{n}}^T\right)\mathbf{n} = \nabla\cdot\tilde{\mathbf{n}},$$

where the last equality follows from (4.21). □

If Γ is given as a zero level-set of some level-set function $u \in C^2(\mathbb{R}^n)$ (i.e. $u < 0$ in Γ_{int}) then $\tilde{\mathbf{n}}(\mathbf{x}) = \frac{\nabla u}{|\nabla u|}$ and $H = \nabla \cdot \frac{\nabla u}{|\nabla u|}$. In the definition of the hypersurface Γ, we assume that $\nabla u \neq \mathbf{0}$ on Γ. At the points where $\nabla u = \mathbf{0}$, $\tilde{\mathbf{n}}$ would not be defined. Since we assume $u \in C^m(\mathbb{R}^n)$ for $m \geq 1$, we observe that $\nabla u \neq \mathbf{0}$ in some neighbourhood of Γ as well. This is enough for the application of the theorem (4.2.12). In the other parts of $\mathbb{R}^n$ we may introduce regularisation by a non-zero function $\epsilon(\mathbf{x})$ vanishing in some neighbourhood of Γ where ∇u is non-zero. Then we define

$$\tilde{\mathbf{n}}_\epsilon = \frac{\nabla u}{\sqrt{\epsilon(\mathbf{x})^2 + |\nabla u|^2}}. \tag{4.22}$$

and

$$H = \nabla \cdot \tilde{\mathbf{n}}_\epsilon = \nabla \cdot \left(\frac{\nabla u}{\sqrt{\epsilon(\mathbf{x})^2 + |\nabla u|^2}} \right). \tag{4.23}$$

Later, in the numerical computations, we assume that $\epsilon(\mathbf{x}) = \epsilon$ is constant.

If Γ is given as a graph of a function $\varphi \in C^2(\mathbb{R}^{n-1})$, $\varphi = \varphi(\xi)$ then we have

$$\mathbf{n} = \frac{1}{\sqrt{1 + |\nabla\varphi|^2}} \begin{pmatrix} -\nabla\varphi \\ 1 \end{pmatrix}, \tag{4.24}$$

for $\mathbf{x} \in \Gamma$ expressed as $\mathbf{x} = (\xi, \varphi(\xi))^T$. However, (4.24) can be easily extended on $\mathbb{R}^n$ and we can define $\tilde{\mathbf{n}}$ as

$$\tilde{\mathbf{n}} = \frac{1}{\sqrt{1 + |\nabla\varphi|^2}} \begin{pmatrix} -\nabla\varphi \\ 1 \end{pmatrix} \text{ on } \mathbb{R}^n. \tag{4.25}$$

It follows that

$$\begin{aligned} H &= \nabla \cdot \tilde{\mathbf{n}} = \partial_{x_1} \frac{\partial_{x_1}\varphi}{\sqrt{1 + |\nabla\varphi|^2}} + \cdots + \partial_{x_{n-1}} \frac{\partial_{x_{n-1}}\varphi}{\sqrt{1 + |\nabla\varphi|^2}} + \partial_{x_n} \frac{1}{\sqrt{1 + |\nabla\varphi|^2}} \\ &= \partial_{x_1} \frac{\partial_{x_1}\varphi}{\sqrt{1 + |\nabla\varphi|^2}} + \cdots + \partial_{x_{n-1}} \frac{\partial_{x_{n-1}}\varphi}{\sqrt{1 + |\nabla\varphi|^2}} \\ &= -\nabla \cdot \left(\frac{\nabla\varphi}{\sqrt{1 + |\nabla\varphi|^2}} \right), \end{aligned}$$

because $\partial_{x_n} \frac{1}{\sqrt{1+|\nabla\varphi|^2}} = 0$. Therefore we often simplify the normal of Γ given as a graph of φ to $\mathbf{n} = \nabla\varphi / \sqrt{1 + |\nabla\varphi|^2}$. The same holds even for the normal unit vector field extension $\tilde{\mathbf{n}}$. For better consistency of the notation, we will consider inner normal unit vector in the case of the graph formulation and write

$$H = \nabla \cdot \left(\frac{\nabla\varphi}{\sqrt{1 + |\nabla\varphi|^2}} \right). \tag{4.26}$$

Denote $Q = |\nabla u|$ for the level-set formulation resp. $Q = \sqrt{1 + |\nabla\varphi|^2}$ for the graph formulation. It allows us to express the unit normal vector and the mean curvature as

$$\mathbf{n} = \frac{\nabla u}{Q} \text{ and } H = \nabla \cdot \left(\frac{\nabla u}{Q} \right),$$

for the level-set formulation resp.

$$\mathbf{n} = \frac{\nabla\varphi}{Q} \text{ and } H = \nabla\cdot\left(\frac{\nabla\varphi}{Q}\right),$$

Then we get (what follows holds even for the graph formulation - we would write φ instead of u)

$$\begin{aligned}
\nabla\mathbf{n}^T &= \nabla\left(\frac{\nabla u}{Q}\right)^T = \frac{1}{Q}\left[D^2u - \frac{1}{Q}\left(\nabla u\,(\nabla Q)^T\right)\right] = \frac{1}{Q}\left[D^2u - \frac{1}{Q}\left(\nabla u\frac{(\nabla u)^T D^2u}{Q}\right)\right] \\
&= \frac{1}{Q}\left(\mathbb{I} - \frac{\nabla u}{Q}\left(\frac{\nabla u}{Q}\right)^T\right)D^2u = \frac{1}{Q}\left(\mathbb{I} - \mathbf{n}\mathbf{n}^T\right)D^2u = \frac{1}{Q}\mathbb{P}D^2u
\end{aligned}$$

and

$$W = \nabla_\Gamma^T\mathbf{n} = \mathbb{P}\left(\frac{1}{Q}\mathbb{P}D^2u\right) = \frac{1}{Q}\mathbb{P}D^2u. \tag{4.27}$$

Using (4.27) we get

$$\begin{aligned}
H &= \mathrm{Tr}W = \frac{1}{Q}\mathrm{Tr}\left(\mathbb{P}D^2u\right) = \frac{1}{Q}\mathrm{Tr}\left(\left(\mathbb{I} - \frac{\nabla u\otimes\nabla u}{Q^2}\right)D^2u\right) \\
&= \frac{1}{Q}\left(\Delta u - \sum_{1\le i,j\le N}\frac{\partial_i u\partial_j u}{Q^2}\partial_i\partial_j u\right).
\end{aligned} \tag{4.28}$$

We will also find useful to consider the Frobenius norm of the Weingarten map matrix defined as

$$\|W\|_F^2 := \sum_{i,j=1}^n W_{ij}^2 = \mathrm{Tr}\big(W^TW\big)$$

for which we have

$$\|W\|_F^2 = \mathrm{Tr}\big(W^TW\big) = \frac{1}{Q^2}\mathrm{Tr}\big(\mathbb{P}D^2u\mathbb{P}D^2u\big) = \mathrm{Tr}\big(\nabla\mathbf{n}^T\nabla\mathbf{n}^T\big). \tag{4.29}$$

It follows from

$$\begin{aligned}
\nabla\mathbf{n}^T &= \nabla\left(\frac{(\nabla u)^T}{Q}\right) = \frac{\nabla\,(\nabla u)^T}{Q} - \frac{\nabla Q\,(\nabla u)^T}{Q^2} \\
&= \frac{1}{Q}\left(D^2u - \frac{\nabla u D^2 u}{Q}\frac{(\nabla u)^T}{Q}\right) = \frac{1}{Q}\left(\mathbb{I} - \frac{\nabla u}{Q}\frac{(\nabla u)^T}{Q}\right)D^2u = \frac{1}{Q}\mathbb{P}D^2u,
\end{aligned}$$

where we used $\nabla Q = \big(\nabla u D^2 u\big)/Q$. Concerning the Laplace-Beltrami operator, the following identity is important:

Lemma 4.2.13. *Let $\mathcal{O}$ be an open set in $\mathbb{R}^n$ such that $\Gamma\subset\mathcal{O}\subset\mathbb{R}^n$ and $f\in C^2(\mathcal{O})$. Then we have*

$$\Delta_\Gamma f = \Delta f - H\partial_{\mathbf{n}}f - \partial_{\mathbf{n}}^2 f, \tag{4.30}$$

on Γ, where we denoted $\partial_{\mathbf{n}}f = \nabla f\mathbf{n}$ and $\partial_{\mathbf{n}}^2 = \mathbf{n}^T D^2 f\mathbf{n}$.

Proof. Since

$$\nabla_\Gamma \cdot \nabla f = \mathrm{Tr}\Big(\nabla_\Gamma (\nabla f)^T\Big) = \mathrm{Tr}\big(\left(\mathbb{I} - \mathbf{n}\mathbf{n}^T\right) D^2 f\big) = \Delta f - \mathbf{n}^T D^2 u \mathbf{n} = \Delta f - \partial^2_{\mathbf{n}} f,$$

we have

$$\begin{aligned} \Delta f &= \nabla_\Gamma \cdot \nabla f + \partial^2_{\mathbf{n}} f = \nabla_\Gamma \cdot (\nabla_\Gamma f + \partial_{\mathbf{n}} f \mathbf{n}) + \partial^2_{\mathbf{n}} f \\ &= \Delta_\Gamma f + (\nabla_\Gamma \cdot \mathbf{n})\, \partial_{\mathbf{n}} f + \mathbf{n}^T \nabla_\Gamma \partial_{\mathbf{n}} f + \partial^2_{\mathbf{n}} f \\ &= \Delta_\Gamma f - H \partial_{\mathbf{n}} f + \partial^2_{\mathbf{n}} f, \end{aligned}$$

where it is easy to see that $\mathbf{n}^T \nabla_\Gamma g = 0$ for any $g \in C^1(\mathbb{R}^n)$. $\square$

The following was adopted from Deckelnick, Dziuk and Eliott [36]. Let Γ be given as graph of function $\varphi \in C^2(\Omega)$ for $\Omega \subset \mathbb{R}^{n-1}$ i.e. $\Gamma \equiv \{(\mathbf{x}, \varphi(\mathbf{x})) \mid \mathbf{x} \in \Omega\}$ and we seek for an expression of $\Delta_\Gamma f$ for $f \in C^2(\Gamma)$. Let $\tilde{f}$ be an C^2-extension of f to $\mathbb{R}^n$, let $\xi \in C^\infty(\Gamma)$ be a test function and $\tilde{\xi}$ its C^∞-extension to $\mathbb{R}^n$ such that ξ is vanishing on $\partial\Gamma$ and $\tilde{\xi}$ is vanishing on $\partial\Omega$. Then we have

$$\begin{aligned} (\nabla_\Gamma f, \nabla_\Gamma \xi) &= \Big(\nabla \tilde{f} - \Big(\nabla \tilde{f}, \mathbf{n}\Big)\mathbf{n}, \nabla\tilde{\xi} - \Big(\nabla\tilde{\xi}, \mathbf{n}\Big)\mathbf{n}\Big) \\ &= \Big(\nabla \tilde{f}, \nabla\tilde{\xi}\Big) - \Big(\nabla \tilde{f}, \mathbf{n}\Big)\Big(\mathbf{n}, \nabla\tilde{\xi}\Big) - \Big(\nabla\tilde{\xi}, \mathbf{n}\Big)\Big(\mathbf{n}, \nabla\tilde{f}\Big) + \Big(\nabla\tilde{f}, \mathbf{n}\Big)\Big(\nabla\tilde{\xi}, \mathbf{n}\Big) \\ &= \Big(\nabla \tilde{f}, \nabla\tilde{\xi}\Big) - \frac{1}{Q^2}\Big(\nabla\tilde{f} \cdot \nabla\varphi\Big)\Big(\nabla\tilde{\xi} \cdot \nabla\varphi\Big) \\ &= \Big(\nabla \tilde{f}, \nabla\tilde{\xi}\Big) - \frac{1}{Q^2}\Big(\nabla\tilde{\xi}\Big)^T (\nabla\varphi \otimes \nabla\varphi)\, \nabla\tilde{f} \\ &= \frac{1}{Q}\Big(\nabla\tilde{\xi}\Big)^T \mathbb{E}\nabla\tilde{f} \end{aligned}$$

for

$$\mathbb{E} := Q\mathbb{I} - \frac{\nabla\varphi \otimes \nabla\varphi}{Q}.$$

Integrating over Γ we get

$$\int_\Gamma (\nabla_\Gamma f, \nabla_\Gamma \xi)\, \mathrm{d}\mathcal{H}^{n-1} = \int_\Omega (\nabla_\Gamma f, \nabla_\Gamma \xi)\, Q \mathrm{dx} = \int_\Omega \Big(\nabla\tilde{\xi}\Big)^T \mathbb{E}\nabla\tilde{f}\mathrm{dx}.$$

and the Gauss-Green theorem on Γ (A.0.8) we obtain

$$\begin{aligned} \int_\Gamma \xi \Delta_\Gamma f \mathrm{d}\mathcal{H}^{n-1} &= -\int_\Gamma \nabla_\Gamma \xi \nabla_\Gamma f \mathrm{d}\mathcal{H}^{n-1} = -\int_\Omega \Big(\mathbb{E}\nabla\tilde{f}\Big) \cdot \nabla\tilde{\xi}\mathrm{dx} \\ &= \int_\Omega \tilde{\xi}\nabla \cdot \mathbb{E}\nabla\tilde{f}\mathrm{dx} = \int_\Gamma \xi \frac{1}{Q} \nabla \cdot \mathbb{E}\nabla\tilde{f}\mathrm{d}\mathcal{H}^{n-1}. \end{aligned}$$

Since the last is true for all testing functions ξ and their extensions $\tilde{\xi}$ we can conclude in the following Lemma:

Lemma 4.2.14. *Let Γ be given as $\Gamma \equiv \{(\mathbf{x}, \varphi(\mathbf{x})) \mid \mathbf{x} \in \Omega\}$ for $\varphi \in C^2(\Omega)$ and $\Omega \subset \mathbb{R}^{n-1}$, let $f \in C^2(\Gamma)$ and $\tilde{f}$ is an extension of f into $\mathbb{R}^n$. Then we have*

$$\Delta_\Gamma f = \frac{1}{Q}\nabla \cdot \left(\left(Q\mathbb{I} - \frac{\nabla\varphi \otimes \nabla\varphi}{Q}\right)\nabla\tilde{f}\right). \tag{4.31}$$

Remark 4.2.15. The previous lemma can be proved in the same way even for Γ given as a zero level set of a function $u \in C^2(\Omega)$.

4.3. Moving hypersurfaces

Following Kimura [65] we present several tools necessary for studying moving hypersurfaces.

Definition 4.3.1. *Let $\Gamma(t)$ for $t \in \mathcal{I}$ be a time dependent class of oriented hypersurfaces in $\mathbb{R}^n$. Let $\Gamma(t)$ be nonempty for all $t \in \mathcal{I}$. Then $\Gamma(t)$ is called* **oriented moving hypersurface** *iff*

$$\mathcal{M} = \bigcup_{t\in\mathcal{I}} \{\Gamma(t) \times \{t\}\} \subset \mathbb{R}^{n+1} \tag{4.32}$$

is C^1-hypersurface in $\mathbb{R}^{n+1}$ and for its normal vector field $\mathbf{n} \in C^1(\mathcal{M}, \mathbb{R}^n)$ holds.

Definition 4.3.2. *Let $(\mathbf{x}_0, t_0) \in \mathcal{M}$, $\varphi \in C^1\left(\mathbb{R}^{n-1} \times \mathcal{I}_0, \mathbb{R}\right)$, $\mathcal{I}_0 \subset \mathcal{I}$, $\mathcal{I}_0$ is open in $\mathcal{I}$ and φ is such that $\mathcal{M}$ is given as a graph of φ on some neighbourhood U of $(\mathbf{x}_0, t_0)$. Then if we write the normal vector $\mathbf{n}$ as $\mathbf{n} = (n_1, \cdots, n_n)$ we define* **the normal velocity of** $\Gamma(t)$ **at** $(\mathbf{x}_0, t_0)$ *as*

$$V(\mathbf{x}_0, t_0) := \partial_t \varphi(\mathbf{x}_0, t_0) \cdot n_n(\mathbf{x}_0, t_0). \tag{4.33}$$

Remark 4.3.3. To explain the meaning of (4.3.2) we assume that $\Omega \subset \mathbb{R}^{n-1}$, $\varphi \in C^1(\Omega; [0, T])$ and $\Gamma(t)$ is given as

$$\Gamma(t) \equiv \{(\xi, \varphi(\xi, t)) \mid \xi \in \Omega\}.$$

Then the velocity of a point $\mathbf{x}(t) \in \Gamma(t)$ such that

$$\mathbf{x}(t) = (\xi, \varphi(\xi, t)),$$

is

$$\frac{\mathrm{d}}{\mathrm{d}t}\mathbf{x}(t) = (\mathbf{0}, \partial_t \varphi(\xi, t)).$$

If $\mathbf{n}$ is the normal vector and $\mathbf{n} = (n_1, \cdots n_n)$ then the normal velocity reads as

$$V(\mathbf{x}, t) = \frac{\mathrm{d}}{\mathrm{d}t}\mathbf{x}(t) \cdot \mathbf{n} = \partial_t \varphi(\xi, t) \cdot n_n.$$

Since $\mathbf{n}$ is given by (up to the sign) (4.24) we get that

$$n_n = \pm \frac{1}{\sqrt{1 + |\nabla \varphi|}}.$$

If $\mathbf{n}$ is the inner normal then

$$n_n = \frac{-1}{\sqrt{1 + |\nabla_\xi \varphi|^2}}$$

and we have that

$$V(\mathbf{x}_0, t_0) = \frac{-\partial_t \varphi(\mathbf{x}_0, t_0)}{\sqrt{1 + |\nabla_\xi \varphi(\mathbf{x}_0, t_0)|^2}}. \tag{4.34}$$

Remark 4.3.4. Note that the definition of V does not depend on the choice of φ. Indeed, consider another neighbourhood U' of $(\mathbf{x}_0, t_0)$ and $\varphi' \in C^1\left(\mathbb{R}^{n-1} \times \mathcal{I}_0, \mathbb{R}\right)$ such that $\mathcal{M}$ is given as a graph of φ' on U' and $(\mathbf{x}_0, t_0) \in U \cap U'$. Then $\varphi(\mathbf{x}, t) = \varphi'(\mathbf{x}, t)$ on $U \cap U'$ must hold and so $\partial_t \varphi(\mathbf{x}_0, t_0) = \partial_t \varphi'(\mathbf{x}_0, t_0)$ holds as well.

Definition 4.3.5. *A curve γ is called* **C^1-trajectory on** $\mathcal{M}$ *iff $\gamma \in C^1(\mathcal{I}_0, \mathbb{R}^n)$, $\gamma(t) \in \Gamma(t)$ for $t \in \mathcal{I}_0$ and $\mathcal{I}_0$ is some open subinterval of $\mathcal{I}$.*

Theorem 4.3.6. *Let* $(\mathbf{x}_0, t_0) \in \mathcal{M}$ *and let* γ *be a* C^1*-trajectory such that* $\gamma(t_0) = (\mathbf{x}_0, t_0)$*. Then*

$$V(\mathbf{x}_0, t_0) = \partial_t \gamma(t_0) \cdot \mathbf{n}(\mathbf{x}_0, t_0). \tag{4.35}$$

Proof. Let $\varphi \in C^1(U, \mathbb{R}^n)$ be such that $\mathcal{M}$ is given as a graph of φ on some neighbourhood U of $(\mathbf{x}_0, t_0)$. Without loss of generality we may assume that $\mathbf{x}_0 = \mathbf{0}$ and $\mathbf{n}(\mathbf{x}_0)(0, \cdots, 0, 1)$. Let γ be defined for $t \in \mathcal{I}_0 \subset \mathcal{I}$, $\mathcal{I}_0$ open in $\mathcal{I}$ and $t_0 \in \mathcal{I}_0$. Then there exists $\zeta(t) : \mathcal{I}_0 \to \mathbb{R}^{n-1}$ such that $\gamma(t) = (\zeta(t), \varphi(\zeta(t), t))$ for $t \in \mathcal{I}_0$. Then

$$\partial_t \gamma(t) = (\partial_t \zeta(t), \partial_t \varphi(\zeta(t), t))^T \text{ for } t \in \mathcal{I}_0$$

and

$$\partial_t \gamma(t_0) \cdot \mathbf{n}(\mathbf{x}_0, t_0) = \partial_t \varphi(\mathbf{x}_0, t_0) \cdot n_n(\mathbf{x}_0, t_0) = V(\mathbf{x}_0, t_0).$$

□

Remark 4.3.7. If $\Gamma(t) \subset \Omega \subset \mathbb{R}^n$ is described by a level-set function $u(\mathbf{x}, t)$ as

$$\Gamma(t) \equiv \{\mathbf{x} \in \Omega \mid u(\mathbf{x}, t) = 0\},$$

then for C^1-trajectory $\gamma(t)$ defined on some $\mathcal{I}_0 \subset \mathcal{I}$ such that for some $t_0 \in \mathcal{I}_0$ and $\gamma(t_0) = (\mathbf{x}_0, t_0)$ we have that $u(\gamma(t), t) = 0$ for all $t \in \mathcal{I}_0$. Then we see that

$$\frac{\mathrm{d}}{\mathrm{d}t} u(\gamma(t), t) \mid_{t=t_0} = \partial_t u(\mathbf{x}_0, t_0) + \nabla u(\mathbf{x}_0, t_0) \cdot \partial_t \gamma(\mathbf{x}_0, t_0) = 0. \tag{4.36}$$

Since

$$V(\mathbf{x}_0, t_0) = \partial_t \gamma(t_0) \cdot \mathbf{n}(\mathbf{x}_0, t_0) = \partial_t \gamma(t) \cdot \frac{\nabla u(\mathbf{x}_0, t_0)}{|\nabla u(\mathbf{x}_0, t_0)|},$$

we have that

$$V(\mathbf{x}_0, t_0) = \frac{-\partial_t u(\mathbf{x}_0, t_0)}{|\nabla u(\mathbf{x}_0, t_0)|}. \tag{4.37}$$

Definition 4.3.8. *A* C^1*-trajectory* $\gamma(t)$ *defined on* $\mathcal{I}_0$ *is called* **normal trajectory on** $\mathcal{M}$ *iff* $\partial_t \gamma(t) \in \mathbf{T}_{\gamma(t)}(\Gamma(t))^{\perp}$ *for all* $t \in \mathcal{I}_0$.

Definition 4.3.9. *Let* $f \in C^1(\mathcal{M}, \mathbb{R}^m)$*,* $(\mathbf{x}_0, t_0) \in \mathcal{M}$ *and* $\gamma(t)$ *is the normal trajectory on* $\mathcal{M}$ *through the point* $(\mathbf{x}_0, t_0)$*. Then the* **normal time derivative of** f **on** $\mathcal{M}$ *is defined as*

$$D_t f(\mathbf{x}_0, t_0) := \frac{\mathrm{d}}{\mathrm{d}t} [f(\gamma(t))] \mid_{t=t_0}. \tag{4.38}$$

Lemma 4.3.10. *For an open neighbourhood* U *of* $\mathcal{M}$ *in* $\mathbb{R}^{n+1}$*,* $f \in C^1(U)$ *we have*

$$D_t f(\mathbf{x}, t) = f_t(\mathbf{x}, t) + V(\mathbf{x}, t) \partial_{\mathbf{n}} f(\mathbf{x}, t), \tag{4.39}$$

where $\partial_{\mathbf{n}} f(\mathbf{x}, t) = \nabla f(\mathbf{x}, t) \cdot \mathbf{n}(\mathbf{x}, t)$.

Proof. From $V(\mathbf{x}_0, t_0) = \partial_t \gamma(t_0) \cdot \mathbf{n}(\mathbf{x}_0, t_0)$ we get that $V(\mathbf{x}_0, t_0) \cdot \mathbf{n}(\mathbf{x}_0, t_0) = \partial_t \gamma(t_0)$. Simple calculation shows

$$\begin{aligned} D_t f(\mathbf{x}, t) &= \frac{\mathrm{d}}{\mathrm{d}t} f(\gamma(t), t) \\ &= \nabla f(\mathbf{x}, y)^T \partial_t \gamma(t) + f_t(\mathbf{x}, t) \\ &= V(\mathbf{x}, t) \nabla f(\mathbf{x}, t)^T \mathbf{n}(\mathbf{x}, t) + f_t(\mathbf{x}, t). \end{aligned}$$

□

Lemma 4.3.11. *For $f \in C^1(\mathcal{M})$ and a C^1-trajectory $\gamma(t)$ on $\mathcal{M}$ (not necessarily the normal trajectory) we have*

$$\frac{\mathrm{d}}{\mathrm{d}t} f(\gamma(t), t) = D_t f(\gamma(t), t) + \nabla_\Gamma f(\gamma(t), t)^T \partial_t \gamma(t).$$

Proof. Let $\tilde{f} \in C^1(U)$ be a C^1-extension of f and $\mathbf{x} = \gamma(t) \in \Gamma(t)$. Then we have

$$\begin{aligned}
\frac{\mathrm{d}}{\mathrm{d}t} f(\gamma(t), t) &= \frac{\mathrm{d}}{\mathrm{d}t} \tilde{f}(\gamma(t), t) \\
&= \nabla \tilde{f}(\mathbf{x}, t)^T \partial_t \gamma(t) + \partial_t \tilde{f}(\mathbf{x}, t) \\
&= \left(\nabla_\Gamma f(\mathbf{x}, t) + \partial_{\mathbf{n}} \tilde{f}(\mathbf{x}, t)\, \mathbf{n}(\mathbf{x}, t)\right)^T \partial_t \gamma(t) + \partial_t \tilde{f}(\mathbf{x}, t) \\
&= \nabla_\Gamma f(\mathbf{x}, t)^T \partial_t \gamma(t) + \left(\partial_{\mathbf{n}} \tilde{f}(\mathbf{x}, t)\, \mathbf{n}(\mathbf{x}, t)^T \partial_t \gamma(t) + \partial_t \tilde{f}(\mathbf{x}, t)\right) \\
&= \nabla_\Gamma f(\mathbf{x}, t)^T \partial_t \gamma(t) + \left(\partial_{\mathbf{n}} \tilde{f}(\mathbf{x}, t)\, V(\mathbf{x}, t) + \partial_t \tilde{f}(\mathbf{x}, t)\right) \\
&= \nabla_\Gamma f(\mathbf{x}, t)^T \partial_t \gamma(t) + \left(\nabla \tilde{f}(\mathbf{x}, t) \cdot \mathbf{n}(\mathbf{x}, t)^T V(\mathbf{x}, t) + \partial_t \tilde{f}(\mathbf{x}, t)\right) \\
&= \nabla_\Gamma^T f(\mathbf{x}, t)\, \partial_t \gamma(t) + D_t f(\mathbf{x}, t).
\end{aligned}$$

$\square$

Remark: If $\gamma(t)$ is a normal trajectory we have that $\nabla_\Gamma^T f(\mathbf{x}, t)\, \partial_t \gamma(t) = 0$ which is in good agreement with (4.38).

Theorem 4.3.12. *Let $\Gamma(t)$ be a moving hypersurface, $f \in C^1(\mathcal{M})$ with compact* $\operatorname{supp}(f)$. *Then*

$$\frac{\mathrm{d}}{\mathrm{d}t} \int_{\Gamma(t)} f(\mathbf{x}, t)\, d\mathcal{H}^{n-1} = \int_{\Gamma(t)} (D_t f - f H V)\, d\mathcal{H}^{n-1}, \tag{4.40}$$

where $d\mathcal{H}^{n-1}$ denotes the Hausdorff measure of $\mathbb{R}^{n-1}$.

Proof. Let $\mathbf{x} \in \Gamma(t)$. Without loss of generality we assume that $\mathbf{x} = \mathbf{0}$, $\mathbf{t}_i(\vec{x}) = \mathbf{e}_i$ for $i = 1, \cdots, n-1$ and $\mathbf{n}(\mathbf{x}) = \mathbf{e}_n$. Then there exists a neighbourhood U of $\mathbf{x}$ and a function $\varphi(\mathbf{x}, t)$ defined on $O \times \mathcal{I}_0$ with $O \subset \mathbb{R}^{n-1}$ such that $\Gamma(t)$ is given as a graph of φ for $t \in \mathcal{I}_0 \subset \mathcal{I}$ i.e.

$$\Gamma(t) \equiv \left\{\varphi(\xi, t) \mid \xi \in O \subset \mathbb{R}^{n-1}\right\},$$

Suppose now that $\operatorname{supp} f \subset U$. Denoting $A(\xi, t) := \left(\nabla^T \varphi(\xi, t), \mathbf{n}(\varphi(\xi, t))\right) \in \mathbb{R}^{n \times n}$ we may write

$$\int_{\Gamma(t)} f(\mathbf{x}, t)\, d\mathcal{H}^{n-1} = \int_O f(\varphi(\xi, t), t) \det A(\xi, t)\, d\xi.$$

Defining the inverse mapping $\mathbf{\Psi} = \mathbf{\Psi}(\mathbf{x}, t)$ such that $\mathbf{x} = \varphi(\xi, t) = \varphi(\mathbf{\Psi}(\mathbf{x}, t), t)$ for $\mathbf{x} \in U \subset \Gamma(t)$ i.e. $\mathbf{\Psi} : (U \times \mathcal{I}_0) \to O \times \mathcal{I}_0$ we have that

$$A(\xi, t)^{-1} = \begin{pmatrix} \nabla_\Gamma^T \mathbf{\Psi}(\mathbf{x}, t) \\ \mathbf{n}^T(\mathbf{x}, t) \end{pmatrix}.$$

Differentiating the determinant of A w.r. to t and using the Jocabi's formula (A.0.13) we get

$$\partial_t \det A(\xi, t) = \det A(\xi, t) \operatorname{Tr}\left(A(\xi, t)^{-1} A_t(\xi, t)\right)$$

and

$$\begin{aligned}
\operatorname{Tr}\left(A\left(\boldsymbol{\Psi}\left(\mathbf{x},t\right),t\right)^{-1}A_t\left(\xi,t\right)\right) &= \operatorname{Tr}\left[\begin{pmatrix} \nabla_\Gamma^T\boldsymbol{\Psi}\left(\mathbf{x},t\right) \\ \mathbf{n}^T \end{pmatrix}\left(\nabla^T\partial_t\varphi\left(\xi,t\right),\partial_t\mathbf{n}\left(\varphi\left(\xi,t\right)\right)\right)\right] \\
&= \operatorname{Tr}\begin{bmatrix} \left(\nabla_\Gamma^T\boldsymbol{\Psi}\left(\mathbf{x},t\right)\right)\left(\nabla^T\partial_t\varphi\left(\xi,t\right)\right) & \left(\nabla_\Gamma^T\boldsymbol{\Psi}\left(\mathbf{x},t\right)\right)\partial_t\mathbf{n}\left(\varphi\left(\xi,t\right)\right) \\ \mathbf{n}^T\left(\nabla^T\partial_t\varphi\left(\xi,t\right)\right) & \frac{1}{2}\partial_t\left|\mathbf{n}\right|^2 \end{bmatrix} \\
&= \operatorname{Tr}\left[\left(\nabla_\Gamma^T\boldsymbol{\Psi}\left(\mathbf{x},t\right)\right)\left(\nabla^T\partial_t\varphi\left(\xi,t\right)\right)\right] \\
&= \operatorname{Tr}\left[\nabla_\Gamma\left(\partial_t\varphi^T\left(\boldsymbol{\Psi}\left(\mathbf{x},t\right),t\right)\right)\right] \\
&= \nabla_\Gamma\cdot\partial_t\varphi\left(\xi,t\right).
\end{aligned}$$

We obtain

$$\begin{aligned}
\frac{\mathrm{d}}{\mathrm{d}t}\int_{\Gamma(t)} f\left(\mathbf{x},t\right)d\mathcal{H}^{n-1} &= \frac{\mathrm{d}}{\mathrm{d}t}\int_{\mathcal{O}} f\left(\varphi\left(\xi,t\right),t\right)\det A\left(\xi,t\right)d\xi \\
&= \int_{\mathcal{O}}\left\{\left(\left(\nabla_\Gamma^T f\right)\partial_t\varphi + D_t f\right)\det A + f\partial_t\det A\right\}d\xi \\
&= \int_{\mathcal{O}}\left\{\left(\left(\nabla_\Gamma^T f\right)\partial_t\varphi + D_t f\right) + f\operatorname{Tr}\left(A^{-1}A_t\right)\right\}\det A d\xi \\
&= \int_{\Gamma(t)}\left\{\left(\nabla_\Gamma^T f\right)\partial_t\varphi + D_t f + f\nabla_{\Gamma(t)}\cdot\partial_t\varphi\left(\xi,t\right)\right\}d\mathcal{H}^{n-1}.
\end{aligned}$$

The Gauss-Green formula on $\Gamma\left(t\right)$ (A.0.8) gives

$$\int_{\Gamma(t)}\partial_t\varphi\nabla_{\Gamma(t)}^T f d\mathcal{H}^{n-1} = -\int_{\Gamma(t)}\left(\nabla_\Gamma\cdot\partial_t\varphi + H\mathbf{n}\cdot\partial_t\varphi\right)f d\mathcal{H}^{n-1},$$

and finally we get the result

$$\frac{\mathrm{d}}{\mathrm{d}t}\int_{\Gamma(t)} f\left(\mathbf{x},t\right)d\mathcal{H}^{n-1} = \int_{\Gamma(t)} D_t f - H\mathbf{n}\cdot\partial_t\varphi f d\mathcal{H}^{n-1} = \int_{\Gamma(t)} D_t f - HVf d\mathcal{H}^{n-1}.$$

If $\mathrm{supp}f \not\subset U$ we apply the above result with a partition of unity (see Evans [47]) of $\mathcal{M}$. □

Remark 4.3.13. The Theorem 4.3.12 simplifies evaluation of evolutionary laws for minimising functionals defined as

$$\mathcal{F}\left(\Gamma\left(t\right)\right) = \int_{\Gamma(t)} f\left(\mathbf{x},t\right)d\mathcal{H}^{n-1},$$

for $f \in C^1\left(\mathcal{M}\right)$. The right-hand side of (4.40) contains the normal time derivative $D_t f$. In the case of mean-curvature dependent flows f often depends on H. Therefore we would like to know $D_t H$. The Theorem 4.5.1 gives answer to this question. To be able to prove it, we need to define the signed distance function and establish some results concerning it.

4.4. Signed distance function

In this section we define the signed distance function and briefly explain some basic properties which we will need in the next section for the proof of the Theorem 4.5.1. In later parts, we will also study calculation of the signed distance function. It is important for the level-set method.

Definition 4.4.1. *Let Γ be a C^m-hypersurface in $\mathbb{R}^n$ for which Γ_{int} and Γ_{ext} is defined. We define* **the signed distance function to the hypersurface** Γ *as*

$$d_\Gamma\left(\mathbf{x}\right) := \begin{cases} \operatorname{dist}\left(\mathbf{x},\Gamma\right) & \mathbf{x}\in\Gamma_{\text{ext}}, \\ 0 & \mathbf{x}\in\Gamma, \\ -\operatorname{dist}\left(\mathbf{x},\Gamma\right) & \mathbf{x}\in\Gamma_{\text{int}}, \end{cases} \tag{4.41}$$

where

$$\operatorname{dist}(\mathbf{x},\Gamma) := \inf_{\mathbf{y}\in\Gamma} |\mathbf{x}-\mathbf{y}|\,.$$

It is easy to see that if Γ is closed (in the topological sense) then for each $\mathbf{x}\in\mathbb{R}^n$ there exists $\overline{\mathbf{x}}\in\Gamma$ such that $|\mathbf{x}-\overline{\mathbf{x}}| = \min_{\mathbf{y}\in\Gamma}|\mathbf{x}-\mathbf{y}| = \operatorname{dist}(\mathbf{x},\Gamma)$. We would like to know under which conditions there exists unique minimiser $\overline{\mathbf{x}}$. For this purpose let us define

$$X(\mathbf{y},\rho) := \mathbf{y}+\rho\mathbf{n}(\mathbf{y})\,, \text{ for } \mathbf{y}\in\Gamma, \rho>0,$$

$$\mathcal{N}^{\epsilon}(\Gamma) := \{X(\mathbf{y},\rho) \mid \mathbf{y}\in\Gamma, |\rho|<\epsilon\}\,,$$

$$\mathcal{N}^{\epsilon}_{\pm}(\Gamma) := \{X(\mathbf{y},\rho) \mid \mathbf{y}\in\Gamma, 0<\pm\rho<\epsilon\}\,,$$

where $\mathbf{n}(\mathbf{y})$ denotes the outer unit normal vector at $\mathbf{y}$.

Theorem 4.4.2. *Let Γ be a C^m-hypersurface for which Γ_{int} and Γ_{ext} is defined. Then there exists $\epsilon>0$ and mapping $X:\Gamma\times(-\epsilon,\epsilon)\to\mathcal{N}^{\epsilon}(\Gamma)$ such that X is C^{m-1} diffeomorphism.*

Proof. For the proof of this theorem we refer to Kimura [65]. □

This theorem says that there exists an inverse mapping such that $X^{-1}(\mathbf{x})$ is defined for all $\mathbf{x}\in\mathcal{N}^{\epsilon}(\Gamma)$. It allows us to define mapping $\zeta\in C^{m-1}(\mathcal{N}^{\epsilon}(\Gamma),\Gamma)$ such that $X(\zeta(\mathbf{x}),d_{\Gamma}(\mathbf{x}))=\mathbf{x}$. The meaning of the mapping ζ is that for each $\mathbf{x}\in\mathcal{N}^{\epsilon}(\Gamma)$ it gives the closest point on Γ in the distance $|d_{\Gamma}(\mathbf{x})|$ and in fact $\zeta(\mathbf{x})=\overline{\mathbf{x}}$. This point is unique and $\overline{\mathbf{x}}=\mathbf{x}-d_{\Gamma}(\mathbf{x})\,\mathbf{n}(\overline{\mathbf{x}})$.

Theorem 4.4.3. *Let Γ be an oriented C^m-hypersurface for which Γ_{int} and Γ_{ext} is defined and let d_{Γ} is its signed distance function. Then there exists ϵ such that $d_{\Gamma}\in C^m(\mathcal{N}^{\epsilon}(\Gamma))$ and for all $\mathbf{x}\in\mathcal{N}^{\epsilon}(\Gamma)$*

$$\begin{aligned} \nabla d_{\Gamma}(\mathbf{x}) &= \mathbf{n}(\overline{\mathbf{x}})\,, && (4.42)\\ D^2 d_{\Gamma}(\mathbf{x}) &= (\mathbb{I}+d_{\Gamma}(\mathbf{x})W(\overline{\mathbf{x}}))^{-1}\,W(\overline{\mathbf{x}})\,, && (4.43) \end{aligned}$$

hold.

Proof. The proof can be found in Kimura [65] too.

□

Theorem 4.4.4. *Let $\Gamma(t)$ be an oriented moving C^m-hypersurface such that for each t $\Gamma_{\text{int}}(t)$ and $\Gamma_{\text{ext}}(t)$ is defined and let $d_{\Gamma}(\mathbf{x},t)$ is its signed distance function. For $(\mathbf{x},t)\in\mathcal{N}^{\epsilon}(\mathcal{M})$*

$$\begin{aligned} \partial_t d_{\Gamma}(\mathbf{x},t) &= -V(\overline{\mathbf{x}},t)\,, && (4.44)\\ \partial_t \nabla d_{\Gamma}(\mathbf{x},t) &= (\mathbb{I}+d_{\Gamma}(\mathbf{x},t)W(\mathbf{x},t))^{-1}\,\nabla_{\Gamma}V(\mathbf{x},t) && (4.45) \end{aligned}$$

hold. If $(\mathbf{x},t)\in\mathcal{M}$ then

$$\partial_t D^2 d_{\Gamma}(\mathbf{x},t) = \nabla^2_{\Gamma}V(\mathbf{x},t) - \mathbf{n}(\mathbf{x},t)\,\nabla^T_{\Gamma}V(\mathbf{x},t)\,W(\mathbf{x},t)\,, \tag{4.46}$$

is true.

Proof. The proof comes from Kimura [65] as well.

□

4.5. Normal time derivatives of some geometric quantities

In this section, we compute the normal time derivatives (see the definition 4.38)) of some basic geometric quantities which we will employ later using the Theorem 4.3.12 in the gradient flows of given energies depending on Γ.

Theorem 4.5.1. *Let $\Gamma(t)$ be a moving hypersurface in $\mathbb{R}^n$ such that its interior and exterior is defined. Let $\mathbf{n}$ be the outer unit normal vector, V the normal velocity and W the Weingarten map. Then the following equalities hold for any $(\mathbf{x}, t) \in \mathcal{M}$.*

$$
\begin{aligned}
D_t \mathbf{n} &= \nabla_\Gamma V, && (4.47)\\
D_t W &= -V W^2 + \nabla_\Gamma^2 V - \mathbf{n}\left(\nabla_\Gamma^T V\right) W, && (4.48)\\
D_t H &= V \sum_{i=1}^{n-1} \kappa_i^2 + \Delta_\Gamma V. && (4.49)
\end{aligned}
$$

Proof. The proof was adopted from Kimura [65]. Let $\gamma(t)$ be a normal trajectory on $\mathcal{M}$ passing through $\mathbf{x} = \gamma(t) \in \Gamma(t)$ and $d_\Gamma(\mathbf{x}, t)$ the signed distance function to $\Gamma(t)$. Then

$$
\begin{aligned}
D_t \mathbf{n}(\mathbf{x}, t) &= \frac{\mathrm{d}}{\mathrm{d}t}\left(\mathbf{n}(\gamma(t), t)\right)\\
&= \nabla_\Gamma \mathbf{n}(\gamma(t), t)^T \cdot \partial_t \gamma(t) + \partial_t \mathbf{n}(\gamma(t), t)\\
&= W(\mathbf{x}, t)\, \mathbf{n}(\mathbf{x}, t)\, V(\mathbf{x}, t) + \partial_t \nabla_\Gamma d_\Gamma(\mathbf{x}, t),
\end{aligned}
$$

and since $W(\mathbf{x}, t)\, \mathbf{n}(\mathbf{x}, t) = \mathbf{0}$ we have that $D_t \mathbf{n}(\mathbf{x}, t) = \nabla_{\Gamma(t)} \partial_t d(\mathbf{x}, t)$. It shows that (4.47) is true. For (4.48) we have

$$
\begin{aligned}
D_t W(\mathbf{x}, t) &= \frac{\mathrm{d}}{\mathrm{d}t}\left(\nabla \mathbf{n}(\gamma(\mathbf{x}, t))^T\right) = \frac{\mathrm{d}}{\mathrm{d}t}\left(\nabla\left(\nabla^T d_\Gamma(\gamma(\mathbf{x}, t))\right)\right) = \frac{\mathrm{d}}{\mathrm{d}t}\left(D^2 d_\Gamma(\gamma(\mathbf{x}, t))\right)\\
&= D^3 d_\Gamma(\mathbf{x}) \partial_t \gamma(\mathbf{x}, t) + \partial_t D^2 d_\Gamma(\mathbf{x}, t)\\
&= D^3 d_\Gamma(\mathbf{x}, t) V(\mathbf{x}, t)\, \mathbf{n}(\mathbf{x}, t) + \partial_t D^2 d_\Gamma(\mathbf{x}, t)\\
&= V(\mathbf{x}, t)\, \partial_{\mathbf{n}} D^2 d_\Gamma(\mathbf{x}, t) + \partial_t D^2 d_\Gamma(\mathbf{x}, t).
\end{aligned}
$$

For the first term we have (using (4.43) on $D^2 d(\mathbf{x}, t)$ with $r = d_\Gamma(\mathbf{x})$)

$$
\begin{aligned}
\partial_{\mathbf{n}} D^2 d_\Gamma(\mathbf{x}, t) &= \frac{\mathrm{d}}{\mathrm{d}r}\left(D^2 d(\mathbf{x} + r\mathbf{n}(\mathbf{x}, t), t)\right)|_{r=0}\\
&= \frac{\mathrm{d}}{\mathrm{d}r}\left((\mathbb{I} + rW(\mathbf{x}, t))^{-1} W(\mathbf{x}, t)\right)|_{r=0}\\
&= -\left((\mathbb{I} + rW(\mathbf{x}, t))^{-2} W^2(\mathbf{x}, t)\right)|_{r=0} = -W^2(\mathbf{x}, t)
\end{aligned}
$$

Employing (4.46) gives (4.48). (4.49) follows easily from (4.48) using $D_t H = D_t \mathrm{Tr}(W) = \mathrm{Tr}(D_t W)$. ☐

4.6. Gradient flow structure

In this section, we define **gradient flows**. They serve as a mathematical framework for a class of geometric evolution problems.

Let us start with a simple problem. Assume that we have a smooth strictly convex function F in $\mathbb{R}^n$ and we want to find its minimum. From calculus, we know that the change of F at a point $\mathbf{x}$ in a direction $\mathbf{d}$ is given by

$$\delta F(\mathbf{x}, \mathbf{d}) = (\nabla F(\mathbf{x}), \mathbf{d}), \tag{4.50}$$

where $(\cdot,\cdot)$ denotes standard scalar product. From all directions $\mathbf{d}$ such that $|\mathbf{d}| = |\nabla F(\mathbf{x})|$, the function F decreases the most in the direction

$$\mathbf{d}^* = \arg\min_{|\mathbf{d}|=|\nabla F|} (\nabla F(\mathbf{x}), \mathbf{d}) = -\nabla F(\mathbf{x}),$$

We start with some initial guess $\mathbf{x}_0$ and we apply the following iterative formula

$$\mathbf{x}^{n+1} = \mathbf{x}^n - \tau \nabla F(\mathbf{x}^n). \tag{4.51}$$

If τ is small enough then $\{\mathbf{x}^n\}_{n=0}^{\infty}$ is monotonically decreasing and bounded from bellow by the minimum of F. Therefore it must converge to some $\mathbf{x}^* \in \mathbb{R}^n$. But then $\lim_{n\to\infty}\left(\mathbf{x}^{n+1} - \mathbf{x}^n\right) = \mathbf{0}$ and so $-\nabla F(\mathbf{x}^*) = \mathbf{0}$. We see that F attains its minimum at $\mathbf{x}^*$.

We may rewrite the formula (4.51) as

$$\frac{\mathbf{x}^{n+1} - \mathbf{x}^n}{\tau} = -\nabla F(\mathbf{x}^n),$$

and we denote $\mathbf{x}(t)\,|_{n\tau} = \mathbf{x}^n$. Passing $\tau \to 0$ we get a differential formula

$$\partial_t \mathbf{x}(t) := -\nabla F(\mathbf{x}(t)). \tag{4.52}$$

As before, as t goes to infinity, $\mathbf{x}(t)$ converges to $\mathbf{x}^*$ which is the minimum of F.

Another way how to look at the equation (4.52) is that it defines an evolutionary law for motion of $\mathbf{x}(t)$ and the convergence to minimum of F is a secondary effect. To define another evolutionary laws for the motion of $\mathbf{x}$ we may replace the standard scalar product $(\cdot,\cdot)$ in (4.50) by another scalar product or even a scalar product. This is the idea of the gradient flows. From now we can classify certain motions of vectors in $\mathbb{R}^n$ by taking appropriate function F and scalar product $g(\cdot,\cdot)$.

Proceeding to Banach spaces we may arrive to evolutionary laws using **gradient flows** of certain real valued functionals $\mathcal{E}$ and given bilinear forms g. For the following definition we adopt the concept from Droske [39].

Definition 4.6.1. *Let Ω be a domain in $\mathbb{R}^n$, let X be a Banach space of functions defined on Ω, let g be scalar product defined on X, $g : X \times X \to \mathbb{R}$ and let $\mathcal{E}$ be a real valued functional $\mathcal{E} : X \to \mathbb{R}$ having the Fréchet derivative. The g-**gradient flow** for the functional $\mathcal{E}$ is defined as*

$$\begin{aligned} \partial_t u &= -\nabla_g \mathcal{E}(u) \quad \text{in } \mathbb{R}^+ \times \Omega, \\ u(0,\cdot) &= u_{ini} \qquad\quad \text{on } \Omega, \end{aligned}$$

with appropriate boundary conditions where $\nabla_g \mathcal{E}(u)$ is a representation of the Fréchet derivative $\mathcal{E}'(u)$ in a product induced by g, i.e.

$$g(\nabla_g \mathcal{E}(u), v) = \left(\mathcal{E}'(u), v\right) \text{ for all } v \in C_0^\infty(\Omega) \text{ resp. } v \in C^\infty(\Omega).$$

Remark: If the scalar product g can be represented as

$$g(u,v) = (A_g u, v)_{X' \times X},$$

then the g-gradient flow can be written as

$$\partial_t u = -A_g^{-1} \mathcal{E}'(u)$$

and we have the uniqueness and the solution existence. The following theorem was also taken from Droske [39]:

Theorem 4.6.2. *Suppose that X is a Banach space and there exists a Banach space Y such that $X \subset Y$ and Y is continuously embedded to X'. Let A_g be a linear isomorphism from X onto Y. Suppose that $\mathcal{E}'$ is Lipschitz continuous mapping from X to Y. Then there exists a unique solution of the evolution problem of finding a solution $u : \mathbb{R}_0^+ \to X$, such that*

$$\begin{aligned} \partial_t u &= -A_g^{-1} \mathcal{E}'(u), \\ u(0) &= u_{ini}. \end{aligned}$$

Sometimes we want to define general evolutionary law for $\Gamma(t)$ without any assumptions on the form of $\Gamma(t)$. In this case we may operate only with the normal velocity and quantities which do not depend on the way we express $\Gamma(t)$. The gradient flow for the normal velocities can be defined as follows:

Definition 4.6.3. *Let $\Gamma(t)$ be a moving hypersurface in $\mathbb{R}^n$, let X be a Banach space of functions defined on $\Gamma(t)$, let g be scalar product defined on X, $g : X \times X \to \mathbb{R}$ and let $\mathcal{E}$ be a real valued functional $\mathcal{E} : X \to \mathbb{R}$ having a Fréchet derivative. The g-**gradient flow** for the functional $\mathcal{E}$ is defined as*

$$\begin{aligned} V &= -\nabla_g \mathcal{E}(\Gamma) \quad \text{on } \Gamma(t), \\ \Gamma(0) &= \Gamma_{ini}, \end{aligned}$$

where $\nabla_g \mathcal{E}(\Gamma)$ is a representation of the Fréchet derivative $\mathcal{E}'(\Gamma)$ in a product induced by g, i.e.

$$g(\nabla_g \mathcal{E}(\Gamma), v) = \big(\mathcal{E}'(\Gamma), v\big) \text{ for all } v \in C^\infty(\Gamma(t)).$$

5. Mathematical formulation

The aim of this chapter is to give a mathematical formulation for the Willmore flow. It is a variational problem which can be understood as a L_2-gradient flow of a functional $\mathcal{W}$ defined as

$$\mathcal{W}(\Gamma) = \int_\Gamma H^2 \mathrm{d}\mathcal{H}^{n-1},$$

where Γ is a C^m-hypersurface in $\mathbb{R}^n$ and $\mathcal{H}^{n-1}$ is $(n-1)$-dimensional Haussdorf measure. There is another geometrical problem closely related to the Willmore flow. It is a **mean-curvature flow** which is a L_2-gradient flow of a functional $\mathcal{A}$ given by

$$\mathcal{A}(\Gamma) = \int_\Gamma 1 \mathrm{d}\mathcal{H}^{n-1}. \tag{5.1}$$

The mean-curvature flow is a second order problem whilst the Willmore flow is the fourth order problems. Both of them can be studied in more general anisotropic form.

To be more educative we start with the simplest problem which is the isotropic mean-curvature flow. Then we insert the anisotropy and finally we proceed to the fourth order problem i.e. the Willmore flow. We restrict ourselves only to graph, parametric and the level-set formulation.

Remark 5.0.4. We remind that for the graph formulation we assume that $\Gamma(t)$ is a graph of a function $\varphi : \Omega \times [0,T] \to \mathbb{R}$ where Ω is a domain in $\mathbb{R}^{n-1}$:

$$\Gamma(t) \equiv \{[\mathbf{x}, \varphi(\mathbf{x},t)] \mid \mathbf{x} \in \Omega\}, \tag{5.2}$$

We denote

$$Q = \sqrt{1 + |\nabla\varphi|^2}, \quad H = \nabla \cdot \left(\frac{\nabla\varphi}{Q}\right). \tag{5.3}$$

In the case of the level-set method $\Gamma(t)$ is given by a field $u : \Omega \times [0,T] \to \mathbb{R}$ where Ω is a domain in $\mathbb{R}^n$:

$$\Gamma(t) \equiv \{\mathbf{x} \in \Omega \mid u(\mathbf{x},t) = 0\}, \tag{5.4}$$

and we denote

$$Q_\epsilon = \sqrt{\epsilon^2 + |\nabla u|^2}, \quad H = \nabla \cdot \left(\frac{\nabla u}{Q_\epsilon}\right). \tag{5.5}$$

By $\partial\Omega$ we mean boundary of Ω. In fact, $\partial\Omega$ is an oriented C^m-hypersurface in $\mathbb{R}^{n-1}$ in the case of the graph formulation resp. oriented C^m-hypersurface in $\mathbb{R}^n$ in the case of the level-set formulation. If it is a C^1-hypersurface then the outer unit normal vector ν exists at each point $\mathbf{x} \in \partial\Omega$.

Remark 5.0.5. Evolving planar curve $\Gamma(t)$ can be parametrised either by $\gamma : [0,1] \times [0,T] \to \mathbb{R}^2$ such that

$$\Gamma(t) \equiv \{\gamma(v,t) \mid v \in [0,1]\}, \tag{5.6}$$

or by the arclength parametrisation $\gamma : \mathcal{I} \times [0,T] \to \mathbb{R}^2$ for which

$$\Gamma(t) \equiv \{\gamma(s,t) \mid s \in \mathcal{I} \subset \mathbb{R}\} \text{ and } |\partial_s \gamma(s,t)| = 1, \tag{5.7}$$

5.1. Mean-curvature flow

5.1.1. Brief introduction

In the Chapter 3, the Young-Laplace equation was introduced. It concerns the pressure jump across an interface separating two domains with for example different fluids. It depends on the mean-curvature H of the interface. The equilibrium is reached when the mean-curvature H equals zero. In this section we will show that $H = 0$ holds for **minimal surfaces**. It will be also a proof of fact that the surface tension minimises the surface resp. interface area [14].

The mean-curvature flow is a minimisation of the surface area resp. curve length. It reads as

$$V = H, \tag{5.8}$$

where V is the normal velocity, H is the mean curvature In dependence on how we express $\Gamma(t)$ we can get several formulations of this problem:

- the graph formulation of the mean-curvature flow defined in the Definition 5.1.4,
- the level-set formulation of the mean-curvature flow defined in the Definition 5.1.6,
- parametric approach of the mean-curvature flow defined in the Definition 5.1.8.

Then we proceed to the anisotropic formulations of the mean-curvature flow:

- the anisotropic graph formulation of the mean-curvature flow defined in the Definition 5.1.11
- the anisotropic level-set formulation of the mean-curvature flow defined in the Definition 5.1.12

At the end of this section we give brief overview of some results obtained for the mean curvature and mean-curvature flow.

5.1.2. Isotropic formulation for graphs

We start with the graph formulation of (5.8). Having Γ given by (5.2) for $n = 3$ then the surface area is

$$\mathcal{A}(\varphi) = \mathcal{A}(\Gamma) = \int_\Gamma 1 \mathrm{d}\mathcal{H}^{n-1} = \int_\Omega \left|\partial_x f \times \partial_y f\right| \mathrm{dx} = \int_\Omega \left|\left(1, -\partial_x\varphi, -\partial_y\varphi\right)\right| \mathrm{dx} = \int_\Omega Q \mathrm{dx}, \tag{5.9}$$

where we defined function $f : \mathbb{R}^2 \to \mathbb{R}^3$ as $f(x, y) = (x, y, \varphi(x, y))$.

First of all we should ask whether there exists some minimiser.

Lemma 5.1.1. *(Johnson, Thomeé - [62]) The area functional (5.9) is convex .*

Proof. If we denote $Q(\mathbf{p}) = \sqrt{1 + |\mathbf{p}|^2}$ we get

$$\begin{aligned}
\partial_{p_i}\partial_{p_j} Q(\mathbf{p})\, \xi_i \xi_j &= \left(1 + |\mathbf{p}|^2\right)^{-\frac{3}{2}} \left[\left(1 + p_1^2\right)\xi_1^2 - 2p_1p_2\xi_1\xi_2 + \left(1 + p_2^2\right)\xi_2^2\right] \\
&= \left(1 + |\mathbf{p}|^2\right)^{-\frac{3}{2}} \left[\xi_1^2 + \xi_2^2 + \left(p_1\xi_2 - p_2\xi_1\right)^2\right] \geq \left(1 + |\mathbf{p}|^2\right)^{-\frac{3}{2}} |\xi|^2 .
\end{aligned}$$

Thus

$$\sum_{i,j=1}^{n} \partial_{p_i}\partial_{p_j} Q(\mathbf{p})\, \xi_i\xi_j \geq 0 \text{ for all } \xi, \mathbf{p} \in \mathbb{R}^n$$

and from [52] page. 178, the functional $\mathcal{A}(\varphi) = \int_\Omega Q(\nabla\varphi)\, dx$ is convex. $\square$

From the previous lemma we see that it makes good sense looking for the minimiser of (5.9). Let $\delta\varphi \in C_0^\infty(\Omega)$ be small variation of φ vanishing on $\partial\Omega$ and let us define function G as

$$G_{\delta\varphi}(s) = \mathcal{A}(\varphi + s\delta\varphi) = \int_\Omega \sqrt{1 + |\nabla(\varphi + s\delta\varphi)|^2}.$$

This function indicates us what is the change of $\mathcal{A}$ when we perturb the graph of φ by $\delta\varphi$. Assume $\delta\varphi = 0$ on $\partial\Omega$ i.e. φ is fixed at the boundaries of the domain Ω. By differentiating this function w.r. to s we obtain

$$\begin{aligned}
\lim_{s\to 0} \partial_s G_{\delta\varphi}(s) &= \lim_{s\to 0} \int_\Omega \frac{\nabla\varphi \cdot \nabla\delta\varphi + s|\nabla\delta\varphi|^2}{\sqrt{1 + |\nabla(\varphi + s\delta\varphi)|^2}} dx = \int_\Omega \frac{\nabla\varphi}{Q} \cdot \nabla\delta\varphi dx \\
&= \int_{\partial\Omega} \frac{\delta\varphi}{Q} \partial_\nu \varphi \mathrm{d}S - \int_\Omega \nabla \cdot \frac{\nabla\varphi}{Q} \delta\varphi dx \\
&= -\int_\Omega H\delta\varphi dx = (\delta\mathcal{A}(\varphi), \delta\varphi)_{L_2(\Omega)},
\end{aligned}$$

were we applied the Green formula (A.0.6) and the integral $\int_{\partial\Omega} \frac{\delta\varphi}{Q} \partial_\nu \varphi \mathrm{d}S$ vanishes because $\delta\varphi\mid_{\partial\Omega} \equiv 0$.

Remark 5.1.2. The **minimal surface problem** is the second order elliptic problem with the boundary condition g defined as:

$$\begin{aligned}
H &= 0 \quad \text{on } \Omega \\
\varphi &= g \quad \text{on } \partial\Omega.
\end{aligned}$$

To get a parabolic problem we employ $L_2(\Omega)$-gradient flow. If we look at the Definition 4.6.1 we see that $\mathcal{E} = \mathcal{A}$, $g(\varphi, \delta\varphi) = (\varphi, \delta\varphi)_{L_2(\Omega)}$ and we want

$$\int_\Omega \nabla_g \mathcal{A}(\varphi)\, \delta\varphi \mathrm{d}\mathbf{x} = \int_\Omega H(\varphi)\, \delta\varphi \mathrm{d}\mathbf{x} \text{ for all } \delta\varphi \in C_0^\infty(\Omega) \text{ resp. } \delta\varphi \in C^\infty(\Omega).$$

It means that $\nabla_g \mathcal{A} = H$.
Remark: Notice that to obtain the Euler-Lagrange equations for $\mathcal{A}$ we might also assume $\partial_\nu\varphi\mid_{\partial\Omega} \equiv 0$ to eliminate the integral $\int_{\partial\Omega} \frac{\delta\varphi}{Q} \partial_\nu \varphi \mathrm{d}S$ and we may drop the assumption on $\delta\varphi$. This assumption then defines the Neumann boundary condition for φ. We did not consider it in the case of the problem (5.1.2) because such a problem may not have unique solution (it is given up to an arbitrary constant).

Resulting problem is a parabolic second order equation:

Remark 5.1.3. The **parabolic minimal surface problem with the Dirichlet boundary conditions** is the second order parabolic problem and the initial condition φ_{ini} which satisfies

$$\begin{aligned}
\partial_t\varphi - H &= 0 \quad \text{on } (0, \mathrm{T}\rangle \times \Omega && (5.10) \\
\varphi\mid_{t=0} &= \varphi_{ini} \quad \text{on } \Omega, \\
\varphi &= g \quad \text{on } \partial\Omega. && (5.11)
\end{aligned}$$

The **parabolic minimal surface problem with the Neumann boundary conditions** is the second order parabolic problem and the initial condition φ_{ini} which satisfies (5.10)–(5.11) and

$$\partial_\nu\varphi = 0 \quad \text{on } \partial\Omega.$$

The disadvantage of the equation (5.10) is that the evolution of $\Gamma(t)$ depends on the choice of coordinates and not only on $\Gamma(t)$ itself. To avoid this, we need to express the change of $\Gamma(t)$ in terms of the normal velocity V. It can be done by considering a scalar product of normal velocities defined on Γ

$$(V_1, V_2)_{L_2(\Gamma)} = \int_\Gamma \frac{\partial_t \varphi_1}{Q} \frac{\partial_t \varphi_2}{Q} \mathrm{d}\mathcal{H}^{n-1} = \int_\Omega \frac{\partial_t \varphi_1}{Q} \frac{\partial_t \varphi_2}{Q} Q \mathrm{dx} = \int_\Omega \partial_t \varphi_1 \partial_t \varphi_2 Q^{-1} \mathrm{dx}.$$

Since the space $L_2(\Gamma)$ is used, we speak of the L_2-gradient flow. In general, for two functions $\varphi_1, \varphi_2 \in L_2(\Omega)$ we have

$$g(\varphi_1, \varphi_2) = \int_\Omega \varphi_1 \varphi_2 Q^{-1} \mathrm{dx}. \tag{5.12}$$

From the Definition 4.6.1 we get that

$$g(\nabla_g \mathcal{A}(\varphi), \delta\varphi) = \int_\Omega \nabla_g \mathcal{A}(\varphi) \delta\varphi Q^{-1} \mathrm{d}\mathbf{x} = \int_\Omega H(\varphi) \delta\varphi \mathrm{d}\mathbf{x} \text{ for all } \delta\varphi \in C_0^\infty(\Omega) \text{ resp. } \delta\varphi \in C^\infty(\Omega),$$

which gives that $\nabla_g \mathcal{A} = QH$. The gradient flow reads as

$$\partial_t \varphi = QH.$$

Definition 5.1.4. *Let Ω be a domain on $\mathbb{R}^{n-1}$. The* **graph formulation of the mean-curvature flow with the Dirichlet boundary conditions** *and the initial condition φ_{ini} is a second order parabolic problem given by*

$$\begin{aligned} \partial_t \varphi &= Q \nabla \cdot \left(\frac{\nabla \varphi}{Q} \right) \quad \text{on } (0, \mathrm{T}\rangle \times \Omega, \\ \varphi\,|_{t=0} &= \varphi_{ini} \quad \text{on } \Omega, \\ \varphi &= g \quad \text{on } \partial\Omega. \end{aligned}$$

The **graph formulation of the mean-curvature flow with the Neumann boundary conditions** *and the initial condition φ_{ini} is a second order parabolic problem given by (5.13)–(5.13) and*

$$\partial_\nu \varphi = 0 \quad \text{on } \partial\Omega. \tag{5.13}$$

To complete the definition of the mean-curvature flow of graphs we will also show its weak formulation. As we said before we may either consider $\delta\varphi$ vanishing on $\partial\Omega$ leading to the Dirichlet boundary conditions for φ or $\partial_\nu \varphi = 0$ on $\partial\Omega$ which gives the Neumann boundary conditions for φ.

Multiplying (5.13) by a testing function $\varphi \in H_0^1(\Omega)$ resp. $\varphi \in H^1(\Omega)$, integrating over Ω and applying the Green formula we have:

$$\int_\Omega \frac{\partial_t \varphi}{Q} \varphi - H\varphi \mathrm{dx} = \int_\Omega \frac{\partial_t \varphi}{Q} \varphi \mathrm{dx} - \int_{\partial\Omega} \frac{\varphi}{Q} \partial_\nu \varphi \mathrm{d}\mathcal{H}^{n-1} + \int_\Omega \frac{\nabla \varphi}{Q} \cdot \nabla \varphi \mathrm{dx}.$$

The integral over $\partial\Omega$ is zero since φ resp. $\partial_\nu \varphi$ is vanishing at the boundaries. We conclude in the following definition.

Definition 5.1.5. *The weak solution for the graph formulation of the mean-curvature flow with the Dirichlet boundary conditions is a function* $\varphi : (0, T) \to H^1(\Omega)$ *satisfying a.e. in* $(0, T)$ *for all test functions* $\varphi \in H_0^1(\Omega)$ *:*

$$\int_\Omega \frac{\partial_t \varphi}{Q}\varphi + \frac{\nabla\varphi}{Q}\nabla\varphi \mathrm{dx} = 0 \quad \text{a.e. in } (0, T), \tag{5.14}$$

with the initial condition

$$\varphi\,|_{t=0} = \varphi_{ini} \quad \text{on } \Omega. \tag{5.15}$$

Weak solution for the homogeneous Neumann boundary condition is a function $\varphi : (0, T) \to H^1(\Omega)$ *which satisfies (5.14) a.e. in* $(0, T)$ *for all test functions* $\varphi \in H^1(\Omega)$*.*

5.1.3. Isotropic level-set formulation

Now we assume that $\Gamma(t)$ is given as a zero level set by (5.4). We remind that we want to minimise

$$\mathcal{A}_{ls}(\Gamma) := \int_{\Gamma(t)} 1\mathrm{d}\mathcal{H}^{n-1} = \int_{\{u(t)=0\}} 1\mathrm{d}\mathcal{H}^{n-1},$$

where u is the level-set function of $\Gamma(t)$. If u is smooth enough each level set defines some hypersurface in Ω (some of them might be disconnected since Ω is bounded). It allows us to define $\mathcal{A}$ even for all non-zero level sets of u. Integrating over all the level sets of u and using the co-area formula (A.0.5) restricted on Ω we get

$$\int_{\min_\Omega u(\cdot,t)}^{\max_\Omega u(\cdot,t)} \left(\int_{u(\cdot,t)=r} \gamma \mathrm{d}\mathcal{H}^{n-1} \right) \mathrm{d}r = \int_\Omega \gamma \left|\nabla u\right| \mathrm{d}x.$$

In the next step, we minimise the length of all level sets appearing in the graph of u on Ω. In fact, we minimise

$$\mathcal{A}_{ls} = \int_\Omega \left|\nabla u\right| \mathrm{d}x.$$

It is the same functional which we had for the mean-curvature flow of graphs (5.9), just $|\nabla u|$ replaces Q. We can repeat the same process to compute

$$\delta\mathcal{A}_{ls} = -H \;= -\nabla \cdot \left(\frac{\nabla u}{|\nabla u|} \right) \text{ on } \Omega.$$

To find a proper scalar product for the gradient flow we take again two normal velocities $V_1 = \partial_t u_1 / \left|\nabla u\right|$ and $V_2 = \partial_t u_2 / \left|\nabla u\right|$ and integrate them over all level-lines of u in Ω

$$\int_{\mathbb{R}} (V_1, V_2)_{L_2(\Gamma(s))} \mathrm{d}s = \int_{\mathbb{R}} \int_{\Gamma(s)} \frac{\partial_t u_1}{|\nabla u|}\frac{\partial_t u_2}{|\nabla u|} \mathrm{d}\mathcal{H}^{n-1}\mathrm{d}s = \int_\Omega \frac{\partial_t u_1}{|\nabla u|}\frac{\partial_t u_2}{|\nabla u|} \left|\nabla u\right| \mathrm{dx} = \int_\Omega \partial_t u_1 \partial_t u_2 \left|\nabla u\right|^{-1} \mathrm{dx},$$

where we again applied the co-area formula and denoted $\Gamma(s) \equiv \{\mathbf{x} \in \Omega \mid u(\mathbf{x}) = s\}$. Thus we define the scalar product

$$g(u_1, u_2) := \int_\Omega u_1 u_2 \left|\nabla u\right|^{-1} \mathrm{dx}. \tag{5.16}$$

Since it is very similar to the one for the gradient flow of graphs (5.12) it is now easy to see that the L_2-gradient flow reads as

$$\partial_t u = H \left|\nabla u\right|.$$

Taking regularising parameter $\epsilon > 0$ and replacing $|\nabla u|$ by $Q_\epsilon = \sqrt{\epsilon^2 + |\nabla u|^2}$, we may define the level-set formulation for the mean-curvature flow.

Definition 5.1.6. *Let Ω be a domain in $\mathbb{R}^n$. The* **level-set formulation of the mean-curvature flow with the Dirichlet boundary conditions** *and the initial condition u_{ini} is a second order parabolic problem given by*

$$\begin{aligned} \frac{\partial_t u}{Q_\epsilon} &= \nabla \cdot \left(\frac{\nabla u}{Q_\epsilon} \right) \quad \text{on } (0, \mathrm{T}\rangle \times \Omega, && (5.17) \\ u\,|_{t=0} &= u_{ini} \quad \text{on } \Omega, && (5.18) \\ u &= g \quad \text{on } \partial\Omega. \end{aligned}$$

The **level-set formulation of the mean-curvature flow with the Neumann boundary conditions** *and the initial condition u_{ini} is a second order parabolic problem given by (5.17)–(5.18) and*

$$\partial_\nu u = 0 \quad \text{on } \partial\Omega.$$

Remark 5.1.7. Here u_{ini} is usually the signed distance function of Γ_0 (but it is not necessary) and we set the Neumann boundary conditions $\partial_\nu u = 1$ because they better fit to the signed distance function.

5.1.4. Evolution of interface

In the preceding text we showed how to derive the level-set and the graph formulation for the mean-curvature flow. We used a simple approach when we only needed very fundamental knowledge of the calculus of variations. We have found it more educative and easier to follow for readers who are not familiar with the theory of the normal time derivatives on the hypersurfaces. However, once we know this theory, it is more efficient for the computation of the gradient flows and its main advantage is that it is not dependent on representation of the hypersurface. In this section we derive general law for the mean-curvature flow which will be also necessary for the parametric method for the mean-curvature flow. Note, however, that the theorem (4.5.1) which we will employ does not allow any anisotropy. Such generalisation would be very nice but we do not study it in this text. Since only the isotropic problems will be sufficient for us concerning the parametric method, it is not a big problem.

Consider now a hypersurface $\Gamma(t)$ which we perturb by an arbitrary normal velocity V. Each such normal velocity corresponds to some moving hypersurface. The change of $\mathcal{A}$ is given by the theorem (4.5.1) with $f(\mathbf{x}, t) = 1$ which gives

$$\frac{\mathrm{d}}{\mathrm{d}t}\mathcal{A} = \frac{\mathrm{d}}{\mathrm{d}t} \int_{\Gamma(t)} 1 \mathrm{d}\mathcal{H}^{n-1} = \int_{\Gamma(t)} -HV \mathrm{d}\mathcal{H}^{n-1} = (-H, V)_{L_2(\Gamma(t))}.$$

The scalar product for the gradient flow now takes the form

$$g(V_1, V_2) = (V_1, V_2)_{L_2(\Gamma(t))}$$

and we require an equality

$$(\nabla_g \mathcal{A}, v)_{L_2(\Omega)} = (-H, v) \text{ for all } v \in C^\infty(\Gamma(t)).$$

It is trivial to see that $\nabla_g \mathcal{A} = -H$ and by the Definition 4.6.3 we have:

Definition 5.1.8. *The* **normal velocity for the mean-curvature flow** *is defined as*

$$V = H. \tag{5.19}$$

5.1.5. Anisotropic mean-curvature flow of graphs

Introducing an anisotropy is very important generalisation of the mean-curvature flow. Instead of the surface area we will now consider a weighted surface area given by a function of the surface normal $\gamma_{\mathbf{n}} : \mathbb{S}^n \to \mathbb{R}^+$ where $\mathbb{S}^n$ denotes the unit ball in $\mathbb{R}^n$. Rather than the surface area we speak of the anisotropic surface energy

$$\mathcal{A}_\gamma = \int_\Gamma \gamma_{\mathbf{n}}(\mathbf{n})\, \mathrm{d}\mathcal{H}^{n-1}. \tag{5.20}$$

Since for the graph formulation $\mathbf{n} = (\nabla\varphi, -1)/Q(\nabla\varphi)$ holds, we usually extend the definition of $\gamma_{\mathbf{n}}$ from $\mathbb{S}^n$ to $\mathbb{R}^n$ as follows

$$\gamma(\nabla\varphi, -1) := |\nabla\varphi|\, \gamma_{\mathbf{n}}\left(\frac{(\nabla\varphi, -1)}{Q}\right) \quad \text{for } \nabla\varphi \in \mathbb{R}^n, \tag{5.21}$$

and we get

$$\mathcal{A}_\gamma = \int_\Omega \gamma_{\mathbf{n}} Q \mathrm{dx} = \int_\Omega \gamma_{\mathbf{n}}\left(\frac{\nabla\varphi}{Q}, \frac{-1}{Q}\right) Q \mathrm{dx} = \int_\Omega \gamma(\nabla\varphi, -1)\, Q \mathrm{dx}. \tag{5.22}$$

To emphasise the dependence of γ on $\nabla\varphi$ we will write

$$\gamma(\nabla\varphi, -1) = \gamma(\mathbf{p}, -1) \ \text{ for } \mathbf{p} = \nabla\varphi \in \mathbb{R}^{n-1}.$$

We are now interested in the first variation of $\mathcal{A}_\gamma$ which will define the anisotropic mean-curvature

$$H_\gamma := -\delta\mathcal{A}_\gamma, \tag{5.23}$$

as it was in the isotropic case. For $\delta\varphi \in C_0^\infty(\Omega)$ we have

$$\begin{aligned}
(\delta\mathcal{A}_\gamma, \delta\varphi)_{L_2(\Omega)} &= \lim_{s\to 0} \partial_s \mathcal{A}_\gamma(\varphi + s\delta\varphi) = \int_\Omega \sum_{i=1}^n \partial_{p_i}\gamma(\nabla\varphi, -1)\, \partial_{x_i}\delta\varphi \mathrm{dx} \\
&= \int_{\partial\Omega} \sum_{i=1}^n \partial_{p_i}\gamma(\nabla\varphi, -1)\, \nu_i \delta\varphi \mathrm{d}\mathcal{H}^{n-1} - \int_\Omega \sum_{i=1}^n \partial_{x_i}\left(\partial_{p_i}\gamma(\nabla\varphi, -1)\right) \delta\varphi \mathrm{dx} \\
&= -\int_\Omega \nabla\cdot\left(\nabla_{\mathbf{p}}\gamma(\nabla\varphi, -1)\right) \delta\varphi \mathrm{dx},
\end{aligned}$$

where we again used the Green formula (A.0.6) and we denoted

$$\nabla_{\mathbf{p}}\gamma := \left(\partial_{p_1}\gamma, \cdots, \partial_{p_{n-1}}\right)^T.$$

We also see that the form of the Neumann boundary conditions is strongly dependent on the anisotropic function γ. If $\delta\varphi \neq 0$ on $\partial\Omega$ then $\nabla_{\mathbf{p}}\gamma(\nabla u, -1)\,\nu = 0$ must hold on $\partial\Omega$ to eliminate the integral $\int_{\partial\Omega} \nabla_{\mathbf{p}}\gamma(\nabla u, -1)\,\nu\delta u \mathrm{d}\mathcal{H}^{n-1}$.

Remark: Before we give the definition of the anisotropic mean curvature we need to conclude the assumptions on the function γ. From (5.21) we see that γ is positively homogeneous of degree one which means

$$\gamma(\lambda\mathbf{P}) = \lambda\gamma(\mathbf{P}) \quad \text{for } \mathbf{P} \in \mathbb{R}^n \setminus \{0\}, \lambda > 0.$$

Important assumption for the existence of the minimiser of the surface area functional $\mathcal{A}$ in (5.9) was convexity of Q. Putting this assumption even on γ gives us the definition of an **admissible anisotropy** function - see Deckelnick, Dziuk and Elliott [32, 35].

Definition 5.1.9. *Admissible anisotropy function* $\gamma : \mathbb{R}^{n+1} \setminus \{0\} \to \mathbb{R}^+$, $\gamma \in C^3\left(\mathbb{R}^{n+1} \setminus \{0\}\right)$ *which is positively homogeneous of degree one and which is convex in the sense that there exists a constant* $c_0 > 0$ *such that*

$$\mathbf{Q}^T D^2(\gamma(\mathbf{P}))\mathbf{Q} \geq c_0 |\mathbf{Q}|^2 \quad \text{for all } \mathbf{P}, \mathbf{Q} \in \mathbb{R}^n \text{ with } \mathbf{P}\cdot\mathbf{Q} = 0, |\mathbf{P}| = 1. \tag{5.24}$$

Remark: If we substitute $\mathbf{n}$ for $\mathbf{P}$ in the previous definition the condition $\mathbf{Q}\cdot\mathbf{P}$ means that $\mathbf{Q} \in \mathbf{T}$. The condition (5.24) therefore means that γ is convex with respect to the tangential space $\mathbf{T}$.

Definition 5.1.10. *For admissible anisotropy function* γ *the anisotropic mean curvature is defined as*

$$H_\gamma := \nabla \cdot (\nabla_{\mathbf{p}}\gamma(\nabla\varphi, -1)). \tag{5.25}$$

The gradient flow with $g(\varphi_1, \varphi_2) = \int_\Omega \varphi_1\varphi_2 Q^{-1}\mathrm{dx}$ leads in the same way as for the isotropic problem to the following definition:

Definition 5.1.11. *Let* Ω *be a domain in* $\mathbb{R}^{n-1}$, *let* γ *be an admissible anisotropy function. Then the* **anisotropic graph formulation of the mean-curvature flow with the Dirichlet boundary conditions** *and the initial condition* φ_{ini} *is a second order parabolic problem given by*

$$\begin{aligned} \partial_t\varphi &= Q\nabla\cdot(\nabla_{\mathbf{p}}\gamma(\nabla\varphi,-1)) \quad \text{on } (0,\mathrm{T}\rangle \times \Omega & (5.26)\\ \varphi\,|_{t=0} &= \varphi_{ini} \quad \text{on } \Omega & (5.27)\\ \varphi &= g \quad \text{on } \partial\Omega. \end{aligned}$$

The **anisotropic graph formulation of the mean-curvature flow with the Neumann boundary conditions** *and the initial condition* φ_{ini} *is a second order parabolic problem given by (5.26)–(5.27) and*

$$\nabla_{\mathbf{p}}\gamma(\nabla\varphi,-1)\cdot\nu = 0 \quad \text{on } \partial\Omega. \tag{5.28}$$

5.1.6. Anisotropic level-set formulation

As before for the isotropic level-set formulation, we assume that $\Gamma(t)$ is given as a level set by (5.4). We want to minimise

$$\mathcal{A}_{ls}(\Gamma) := \int_{\Gamma(t)} \gamma \mathrm{d}\mathcal{H}^{n-1} = \int_{\{u(t)=0\}} \gamma \mathrm{d}\mathcal{H}^{n-1},$$

where γ is the admissible anisotropic function and u is the level set function of $\Gamma(t)$. We define $\mathcal{A}$ even for all non-zero level sets of $u(t)$. We integrate over all the level-sets of $u(t)$ and apply the co-area formula (A.0.5) restricted on Ω to get

$$\int_{\min_\Omega u(t)}^{\max_\Omega u(t)} \left(\int_{u(t)=r} \gamma \mathrm{d}\mathcal{H}^{n-1} \right) \mathrm{d}r = \int_\Omega \gamma \left|\nabla u\right| \mathrm{d}x.$$

Hence, we minimise the surface energy of all level sets appearing in the graph of u on Ω i.e. we minimise the following functional

$$\mathcal{A}_{ls} = \int_\Omega \gamma \left|\nabla u\right| \mathrm{d}x.$$

It is very similar to the functional for the anisotropic graph formulation (5.22), just $|\nabla u|$ replaces Q. We can repeat the same process to get

$$\delta\mathcal{A}_{ls} = -H_\gamma \ = -\nabla \cdot \left(\nabla_{\mathbf{p}} \gamma\left(\nabla u\right)\right) \ \text{ on } \Omega.$$

In the same way we obtained the scalar product g for the isotropic level-set formulation (5.16) we get

$$g\left(u_1, u_2\right) := \int_\Omega u_1 u_2 \left|\nabla u\right|^{-1} \mathrm{dx}, \tag{5.29}$$

and the L_2-gradient flow reads as

$$\partial_t u = -\nabla_g \mathcal{A}_{ls} = -\delta\mathcal{A}_{ls} \left|\nabla u\right| = H_\gamma \left|\nabla u\right|.$$

We may now define the anisotropic level-set formulation for the mean-curvature flow.

Definition 5.1.12. *Let Ω be a domain in $\mathbb{R}^n$. The* **anisotropic level-set formulation of the mean-curvature flow with the Dirichlet boundary condition** *and the initial condition u_{ini} is a second order parabolic problem given by*

$$\frac{\partial_t u}{Q_\epsilon} = \nabla \cdot \left(\nabla_{\mathbf{p}} \gamma\left(\nabla u\right)\right) \quad \text{on } (0, \mathrm{T}\rangle \times \Omega, \tag{5.30}$$

$$u\,|_{t=0} = u_{ini} \quad \text{on } \Omega, \tag{5.31}$$

$$u = g \quad \text{on } \partial\Omega.$$

The **anisotropic level-set formulation of the mean-curvature flow with the Neumann boundary condition** *and the initial condition u_{ini} is a second order parabolic problem given by (5.30)–(5.31) and*

$$\nabla_{\mathbf{p}} \gamma\left(\nabla u\right) \cdot \nu = 0 \quad \text{on } \partial\Omega. \tag{5.32}$$

5.1.7. Some results from the mathematical analysis of the minimal surfaces and the mean-curvature flow

Now we would like to present brief overview of results concerning the minimal surfaces problem as well as the mean-curvature flow.

The readers interested in the minimal surfaces problem should read a good survey text by Nietsche [79].

In [59] Huisken studies evolution by the mean-curvature flow of convex surfaces into spheres. He shows what evolutions hold for the unit normal, the Weingarten map (the second fundamental form) as well as the evolution of the mean-curvature. He also shows that the convex surface preserves its convexity and approach the shape of sphere very rapidly. He gives proof for a bound of $|\nabla H|$ and existence of solution of the mean-curvature flow until final time T. In [60] he shows that in the case of the graph formulation "surfaces with vertical contact angle at the boundary asymptotically converge to a constant function". In the case of the Dirichlet boundary conditions he proves the following theorem:

Theorem 5.1.13. *Assume that $\Omega \subset \mathbb{R}^n$, ϕ and u_0 are functions in $C^{2,\alpha}\left(\overline{\Omega}\right)$ and $u_0 = \phi$ on $\partial\Omega$. If $\partial\Omega$ has non-negative mean-curvature, then the boundary value problem (5.1.4) with the Dirichlet boundary conditions has a smooth solution $u(\cdot, t)$ which converges to the solution of the minimal surface problem (5.1.2) with the boundary data ϕ.*

Deckelnick and Dziuk study the mean-curvature flow of graphs and level-set in [33]. It is very nice introductory text to the mean-curvature flow. The authors also show some simple mathematical analysis of the problem. Here we just cite an energy equality for (5.1.4):

Theorem 5.1.14. *For the solution of the problem (5.1.4) one has an energy equation*

$$\int_\Omega \frac{u_t^2}{Q} \mathrm{d}\mathbf{x} + \frac{\mathrm{d}}{\mathrm{d}t} \int_\Omega Q \mathrm{d}\mathbf{x} = 0. \tag{5.33}$$

In this text we will study in more details very similar equality for the Willmore flow of graphs. Applied to the numerical analysis it can prove stability of our schemes. In the same way we could prove stability even for the mean-curvature flow.

Evans and Spruck [49] give proof of short time existence for the level-set formulation. The global existence and uniqueness have been proved by Chen, Giga and Goto [101]. In the case of the level-set formulation we especially refer to Giga [53].

Bellettini and Paolini [6] study motion by mean curvature in context of the Finsler geometry. They show that if the anisotropy function γ is convex and smooth, the evolution law then reads $V = H_\gamma$ where H_γ has a meaning of anisotropic mean curvature.

5.2. Willmore flow

5.2.1. Brief introduction to the Willmore flow

The Willmore flow is a minimiser of the **Willmore functional** defined as

$$\mathcal{W}(\Gamma) = \frac{1}{2} \int_\Gamma H^2 \mathrm{d}\mathcal{H}^{n-1}. \tag{5.34}$$

This functional has name after **Thomas James Willmore** who introduced a problem of so called **Willmore surface** in his book [100] published 1993. Willmore gave the first talk about the Willmore surfaces in 1960. However, in his book we can read that the origin of the Euler-Lagrange equation for this functional goes back to 1923 when it was first studied by Thomsen and Schadow.

The Willmore flow minimises an elastic energy given by

$$\mathcal{W}(\Gamma) = \frac{1}{2} \int_\Gamma H^2 \mathrm{d}\mathcal{H}^{n-1}, \tag{5.35}$$

where Γ is C^2-hypersurface in $\mathbb{R}^n$ and H is the mean curvature. The normal velocity is given by

$$V = -\Delta_\Gamma H - \frac{1}{2} H^3 + 2KH, \tag{5.36}$$

where Δ_Γ is the Laplace-Beltrami operator and K is the Gauss curvature. As well as for the mean-curvature flow we will define the following problems:

- the graph formulation of the Willmore flow defined in the Definition 5.2.2,
- the level-set formulation of the Willmore flow defined in the Definition 5.2.4,
- parametric approach of the Willmore flow defined in the Definition 5.2.5,

and their anisotropic counterparts (except of the parametric approach)

- the anisotropic graph formulation of the Willmore flow defined in the Definition 5.2.6
- the anisotropic level-set formulation of the Willmore flow defined in the Definition 5.2.8

5.2.2. Formulation for graphs

If Γ is given as graph of function φ by (5.2) then the Willmore functional reads as

$$\mathcal{W}\left(\varphi\right) = \int_\Omega H^2 Q \mathrm{d}\mathbf{x}. \tag{5.37}$$

Taking small variation $\delta\varphi \in C_0^\infty\left(\Omega\right)$ of φ vanishing on $\partial\Omega$, defining function G as

$$G_{\delta\varphi}\left(s\right) = \mathcal{W}\left(\varphi + s\delta\varphi\right) = \int_\Omega \left[\nabla \cdot \left(\frac{\nabla\varphi}{\sqrt{1+|\nabla\varphi|}}\right)\right]^2 \sqrt{1+|\nabla\left(\varphi+s\delta\varphi\right)|^2}\mathrm{d}\mathbf{x}.$$

and differentiate it w.r. to s we get

$$\begin{aligned}
\lim_{s\to 0}\partial_s G_{\delta\varphi}\left(s\right) &= \lim_{s\to 0}\frac{1}{2}\int_\Omega \partial_s\left\{\left[\nabla\cdot\left(\frac{\nabla\left(\varphi+s\delta\varphi\right)}{\sqrt{1+|\nabla\left(\varphi+s\delta\varphi\right)|^2}}\right)\right]^2\sqrt{1+|\nabla\left(\varphi+s\delta\varphi\right)|^2}\right\}\mathrm{dx} \\
&= \lim_{s\to 0}\int_\Omega \frac{1}{2}\left[\nabla\cdot\left(\frac{\nabla\left(\varphi+s\delta\varphi\right)}{\sqrt{1+|\nabla\left(\varphi+s\delta\varphi\right)|^2}}\right)\right]^2\frac{\nabla\varphi\cdot\nabla\delta\varphi+s\left|\nabla\delta\varphi\right|^2}{\sqrt{1+|\nabla\left(\varphi+s\delta\varphi\right)|^2}} \\
&+ \nabla\cdot\left(\frac{\nabla\left(\varphi+s\delta\varphi\right)}{\sqrt{1+|\nabla\left(\varphi+s\delta\varphi\right)|^2}}\right)\nabla\cdot\left(\partial_s\left(\frac{\nabla\left(\varphi+s\delta\varphi\right)}{\sqrt{1+|\nabla\left(\varphi+s\delta\varphi\right)|^2}}\right)\right) \\
&\cdot \sqrt{1+|\nabla\left(\varphi+s\delta\varphi\right)|^2}\mathrm{dx},
\end{aligned}$$

and since

$$\begin{aligned}
&\nabla\cdot\left(\partial_s\left(\frac{\nabla\left(\varphi+s\delta\varphi\right)}{\sqrt{1+|\nabla\left(\varphi+s\delta\varphi\right)|^2}}\right)\right) = \\
&\nabla\cdot\left(\frac{\left(1+|\varphi+s\delta\varphi|^2\right)\nabla\delta\varphi - \left(\nabla\varphi\cdot\nabla\delta\varphi+s\left|\nabla\delta\varphi\right|^2\right)\nabla\left(\varphi+s\delta\varphi\right)}{\sqrt{1+|\nabla\left(\varphi+s\delta\varphi\right)|^2}^3}\right),
\end{aligned}$$

we get

$$\begin{aligned}
\lim_{s\to 0}\partial_s G_{\delta\varphi}(s) &= \int_\Omega \frac{1}{2}\left[\nabla\cdot\left(\frac{\nabla\varphi}{\sqrt{1+|\nabla\varphi|^2}}\right)\right]^2 \frac{\nabla\varphi\cdot\nabla\delta\varphi}{\sqrt{1+|\nabla\varphi|^2}} \\
&+ \nabla\cdot\left(\frac{\nabla\varphi}{\sqrt{1+|\nabla\varphi|^2}}\right)\nabla\cdot\left(\frac{\nabla\delta\varphi}{\sqrt{1+|\nabla\varphi|^2}} - \frac{(\nabla\varphi\cdot\nabla\delta\varphi)\nabla\varphi}{\sqrt{1+|\nabla\varphi|^2}^3}\right) \\
&= \int_\Omega \frac{1}{2}\frac{H^2}{Q}\nabla\varphi\cdot\nabla\delta\varphi + H\nabla\cdot\left(\frac{\nabla\delta\varphi}{Q} - \frac{(\nabla\varphi\cdot\nabla\delta\varphi)\nabla\varphi}{Q^3}\right)Q\mathrm{dx}
\end{aligned}$$

Writing

$$(\nabla\varphi\cdot\nabla\delta\varphi)\nabla\varphi = (\nabla\varphi\otimes\nabla\varphi)\nabla\delta\varphi,$$

where in general $(\mathbf{u}\otimes\mathbf{v})_{ij} = u_i v_j$ for $i = 1,\cdots n$ and denoting

$$\mathbb{P} = \mathbb{I} - \frac{\nabla\varphi}{Q}\otimes\frac{\nabla\varphi}{Q} \tag{5.38}$$

we have

$$\lim_{s\to 0}\partial_s G_{\delta\varphi}(s) = \int_\Omega \frac{1}{2}\frac{H^2}{Q}\nabla\varphi\cdot\nabla\delta\varphi + HQ\nabla\cdot\left(\frac{1}{Q}\mathbb{P}\nabla\delta\varphi\right)\mathrm{dx}. \tag{5.39}$$

The Green formula gives

$$\int_\Omega \frac{1}{2}\frac{H^2}{Q}\nabla\varphi\cdot\nabla\delta\varphi\mathrm{dx} = \int_{\partial\Omega}\frac{1}{2}\frac{H^2}{Q}\partial_\nu\varphi\delta\varphi\mathrm{d}\mathcal{H}^{n-1} - \int_\Omega \frac{1}{2}\nabla\cdot\left(\frac{H^2}{Q}\nabla\varphi\right)\delta\varphi\mathrm{dx}. \tag{5.40}$$

The first term on the right hand side is zero because of $\delta\varphi$ vanishing on $\partial\Omega$. Now we need to apply the Green formula twice on the second term in (5.39).

$$\begin{aligned}
\int_\Omega QH\nabla\cdot\left(\frac{1}{Q}\mathbb{P}\nabla\delta\varphi\right)\mathrm{dx} &= \int_{\partial\Omega} QH\mathbb{P}\nabla\delta\varphi\nu\mathrm{d}\mathcal{H}^{n-1} \\
&- \int_\Omega \nabla(QH)\cdot\left(\frac{1}{Q}\mathbb{P}\nabla\delta\varphi\right)\mathrm{dx}
\end{aligned} \tag{5.41}$$

Assuming $H = 0$ on $\partial\Omega$ and using the symmetry of $\frac{1}{Q}\mathbb{P}$ we can write

$$\int_\Omega \nabla(QH)\nabla\cdot\left(\frac{1}{Q}\mathbb{P}\nabla\delta\varphi\right)\mathrm{dx} = -\int_\Omega \nabla\delta\varphi\cdot\left(\frac{1}{Q}\mathbb{P}\nabla(QH)\right)\mathrm{dx} =$$
$$-\int_{\partial\Omega}\delta\varphi\cdot\left(\frac{1}{Q}\mathbb{P}\nabla(QH)\right)\nu + \int_\Omega \nabla\cdot\left(\frac{1}{Q}\mathbb{P}\nabla(QH)\right)\delta\varphi\mathrm{dx},$$

where we applied the Green formula again. The integral over $\partial\Omega$ is equal to zero because of $\delta\varphi$ vanishing on $\partial\Omega$. Finally we see that

$$(\mathcal{W}(\varphi),\delta\varphi)_{L_2(\Omega)} = \int_\Omega \nabla\cdot\left(\frac{1}{Q}\mathbb{P}\nabla(QH) - \frac{1}{2}\frac{H^2}{Q}\nabla\varphi\right)\delta\varphi\mathrm{dx}, \tag{5.42}$$

and the Euler-Lagrange equation reads

$$\nabla\cdot\left(\frac{1}{Q}\mathbb{P}\nabla w - \frac{1}{2}\frac{w^2}{Q^3}\nabla\varphi\right) = 0, \tag{5.43}$$

where we denoted

$$w = QH.$$

In the differential geometry, every surface for which the isotropic version of (5.43) holds is called the Willmore surface .

Remark 5.2.1. To get the graph formulation with the Neumann boundary conditions we take $\delta\varphi \in C^{\infty}(\Omega)$. We multiply (5.43) by $\delta\varphi$ and integrate over Ω

$$\int_{\Omega} \nabla \cdot \left(\frac{1}{Q}\mathbb{P}\nabla w - \frac{1}{2}\frac{w^2}{Q^3}\nabla\varphi \right) \delta\varphi \mathrm{d}\mathbf{x} = 0. \tag{5.44}$$

we apply the Green formula on the left-hand side of (5.44) to obtain

$$\begin{aligned} \int_{\Omega} \nabla \cdot \left(\frac{1}{Q}\mathbb{P}\nabla w - \frac{1}{2}\frac{w^2}{Q^3}\nabla\varphi \right) \delta\varphi \mathrm{d}\mathbf{x} &= \int_{\partial\Omega} \frac{1}{Q}\left(\mathbb{P}\nabla w\right)\nu - \frac{1}{2}\frac{w^2}{Q^3}\nabla\varphi\delta\varphi\nu \mathrm{d}\mathcal{H}^{n-1} \\ &+ \int_{\Omega} \frac{1}{Q}\mathbb{P}\nabla w - \frac{1}{2}\frac{w^2}{Q^3}\nabla\varphi\nabla\delta\varphi \mathrm{d}\mathbf{x}. \end{aligned}$$

If we set $\nabla\varphi \cdot \nu = \partial_\nu \varphi = 0$ on $\partial\Omega$ we have

$$\int_{\partial\Omega} \frac{1}{2}\frac{w^2}{Q^3}\delta\varphi\nabla\varphi\nu \mathrm{d}\mathcal{H}^{n-1} = 0,$$

and since

$$\left(\mathbb{P}\nabla w\right)\cdot\nu = \left(\mathbb{I} - \frac{\nabla\varphi}{Q}\otimes\frac{\nabla\varphi}{Q}\right)\nabla w\cdot\nu = \partial_\nu w - \frac{1}{Q^2}\left(\left(\nabla\varphi\otimes\nabla\varphi\right)\nabla w\right)\cdot\nu = \partial_\nu w - \frac{\nabla\varphi\cdot\nabla w}{Q^2}\partial_\nu\varphi,$$

setting $\partial_\nu w = 0$ on $\partial\Omega$ together with $\partial_\nu \varphi = 0$ on $\partial\Omega$ gives

$$\int_{\partial\Omega} \frac{1}{Q}\left(\mathbb{P}\nabla w\right)\nu \mathrm{d}\mathcal{H}^{n-1} = 0.$$

Therefore the Neumann boundary conditions read $\partial_\nu u = \partial_\nu w = 0$ on $\partial\Omega$.

Taking again the scalar product g (5.12) having the form

$$g\left(\varphi_1, \varphi_2\right) = \int_{\Omega} \varphi_1\varphi_2 Q^{-1} \mathrm{dx},$$

we get the L_2-gradient flow for the Willmore functional.

Definition 5.2.2. *Let Ω be a domain in $\mathbb{R}^{n-1}$. The* **graph formulation of the Willmore flow with the Dirichlet boundary conditions** *and the initial condition φ_{ini} is a fourth order parabolic problem given by*

$$\begin{aligned} \partial_t\varphi &= -Q\nabla\cdot\left(\frac{1}{Q}\mathbb{P}\nabla w - \frac{1}{2}\frac{w^2}{Q^3}\nabla\varphi\right) \text{ on } \Omega\times(0,T], & (5.45) \\ w &= Q\nabla\cdot\left(\frac{\nabla\varphi}{Q}\right) \text{ on } \Omega\times[0,T], & (5.46) \\ \varphi\mid_{t=0} &= \varphi_{ini} \text{ on } \Omega, & (5.47) \\ \varphi &= g, w = 0 \text{ on } \partial\Omega. & (5.48) \end{aligned}$$

The **the graph formulation of the Willmore flow with the Neumann boundary conditions** *and the initial condition φ_{ini} is a fourth order parabolic problem given by (5.45)–(5.47) and*

$$\partial_\nu\varphi = 0, \partial_\nu w = 0 \text{ on } \partial\Omega. \tag{5.49}$$

5.2.3. Isotropic level-set formulation for the Willmore flow

Let $\Gamma(t)$ be given as a zero level set by (5.4). We want to minimise

$$\mathcal{W}(\Gamma) := \int_{\Gamma(t)} H^2 \mathrm{d}\mathcal{H}^{n-1} = \int_{\{u(t)=0\}} H^2 \mathrm{d}\mathcal{H}^{n-1},$$

where u is the level-set function of $\Gamma(t)$. Assuming that u is smooth enough we see that each level-set defines some hypersurface in Ω. This way we extend definition of $\mathcal{W}$ even for all non-zero level sets of u. We integrate over all the level sets of u and using the co-area formula (A.0.5) restricted on Ω we get

$$\int_{\min_\Omega u(\cdot,t)}^{\max_\Omega u(\cdot,t)} \left(\int_{u(\cdot,t)=r} H^2 \mathrm{d}\mathcal{H}^{n-1} \right) \mathrm{d}r = \int_\Omega H^2 |\nabla u| \, \mathrm{d}x,$$

and hence we want to minimise a functional

$$\mathcal{W}_{ls}(u) := \int_\Omega H^2 |\nabla u| \, \mathrm{d}\mathcal{H}^{n-1}, \tag{5.50}$$

resp. its regularised counterpart

$$\mathcal{W}_{ls}(u) := \int_\Omega H^2 Q_\epsilon \mathrm{d}\mathcal{H}^{n-1}, \tag{5.51}$$

Again we see, that formally (5.51) is the same as (5.37) where we just replace Q by Q_ϵ. Therefore the Euler-Lagrange equation has the same form as (5.43) and we write Q_ϵ instead of Q i.e.

$$\nabla \cdot \left(\frac{1}{|\nabla u|} \mathbb{P} \nabla w - \frac{1}{2} \frac{w^2}{|\nabla u|^3} \nabla \varphi \right) = 0, \tag{5.52}$$

where we denoted

$$w = |\nabla u| \, H.$$

Remark 5.2.3. It is easy to see from the Remark 5.2.1 that the Neumann boundary conditions are $\partial_\nu u = \partial_\nu w = 0$ on $\partial\Omega$.

Following (5.16) and taking

$$g(u_1, u_2) := \int_\Omega u_1 u_2 |\nabla u|^{-1} \, \mathrm{dx}.$$

we get the level-set formulation for the L_2-gradient flow of the Willmore functional:

Definition 5.2.4. *Let Ω be a domain in $\mathbb{R}^n$. The* **level-set formulation for the Willmore flow with the Dirichlet boundary conditions** *and the initial condition u_{ini} is a fourth order parabolic problem given by*

$$\partial_t u = -Q\nabla \cdot \left(\frac{1}{Q}\mathbb{P}\nabla w - \frac{1}{2}\frac{w^2}{Q^3}\nabla u\right) \text{ on } \Omega \times (0,T], \quad (5.53)$$

$$w = Q\nabla \cdot \left(\frac{\nabla u}{Q}\right) \text{ on } \Omega \times [0,T], \quad (5.54)$$

$$u\mid_{t=0} = u_{ini} \text{ on } \Omega, \quad (5.55)$$

$$u = g, w = 0 \text{ on } \partial\Omega. \quad (5.56)$$

The **level-set formulation for the Willmore flow with the Dirichlet boundary conditions** *and the initial condition u_{ini} is a fourth order parabolic problem given by (5.53)–(5.55) and*

$$\partial_\nu u = 0, \partial_\nu w = 0 \text{ on } \partial\Omega.$$

5.2.4. Evolution of interface

Let us now consider arbitrary normal velocity V. We know that it generates the moving hypersurface for which the change of $\mathcal{W}$ defined by (5.34) is given by the Theorem (4.3.12) where $f(\mathbf{x},t) = H^2$. From the definition of the normal time derivative (4.38) we have that

$$\begin{aligned} D_t H^2(\mathbf{x}_0,t_0) &= \frac{\mathrm{d}}{\mathrm{d}t}\left[H^2(\gamma(t))\right]\mid_{t=t_0} = 2H\frac{\mathrm{d}}{\mathrm{d}t}\left[H^2(\gamma(t))\right]\mid_{t=t_0} \\ &= 2H(\mathbf{x}_0,t_0)\, D_t H(\mathbf{x}_0,t_0), \end{aligned}$$

where $\gamma(t)$ is the normal trajectory passing through the point $(\mathbf{x}_0,t_0)$. Together with (4.40) and (4.49) we obtain

$$\begin{aligned} \frac{\mathrm{d}}{\mathrm{d}t}\frac{1}{2}\int_{\Gamma(t)} H^2 \mathrm{d}\mathcal{H}^{n-1} &= \frac{1}{2}\int_{\Gamma(t)} D_t H^2 - H^3 V \mathrm{d}\mathcal{H}^{n-1} \\ &= \int_{\Gamma(t)} H D_t H - \frac{1}{2}H^3 V \mathrm{d}\mathcal{H}^{n-1} \\ &= \int_{\Gamma(t)} H\left(V\sum_{i=1}^{n-1}\kappa_i^2 + \Delta_\Gamma V\right) - \frac{1}{2}H^3 V \mathrm{d}\mathcal{H}^{n-1}. \end{aligned}$$

We apply the Gauss-Green formula on $\Gamma(t)$ (A.0.8) on the term $\int_{\Gamma(t)} H\Delta_\Gamma V \mathrm{d}\mathcal{H}^{n-1}$ to get

$$\int_{\Gamma(t)} H\Delta_\Gamma V \mathrm{d}\mathcal{H}^{n-1} = -\int_{\Gamma(t)} \nabla_\Gamma H \cdot \nabla_\Gamma V \mathrm{d}\mathcal{H}^{n-1} = \int_{\Gamma(t)} \Delta_\Gamma H V \mathrm{d}\mathcal{H}^{n-1}.$$

It allows us to write

$$\begin{aligned} \frac{\mathrm{d}}{\mathrm{d}t}\frac{1}{2}\int_{\Gamma(t)} H^2 \mathrm{d}\mathcal{H}^{n-1} &= \int_{\Gamma(t)} \left(H\sum_{i=1}^{n-1}\kappa_i^2 + \Delta_\Gamma H - \frac{1}{2}H^3\right) V \mathrm{d}\mathcal{H}^{n-1} \\ &= \left(\Delta_\Gamma H + H\sum_{i=1}^{n-1}\kappa_i^2 - \frac{1}{2}H^3, V\right)_{L_2(\Gamma)}, \end{aligned}$$

and so the L_2-gradient flow for the Willmore flow w.r. to the Definition 4.6.3 with $g(u,v) = (u,v)_{L_2(\Omega)}$ is

$$V = -\Delta_\Gamma H - H \sum_{i=1}^{n-1} \kappa_i^2 + \frac{1}{2} H^3. \tag{5.57}$$

To avoid the dependency on m we use the fact that $\sum_{i=1}^{n-1} \kappa_i^2 = \|W\|_F^2$ (we remind that the last eigenvalue of W is zero) and so we may define:

Definition 5.2.5. *The* **normal velocity for the isotropic Willmore flow** *is defined as*

$$V = -\Delta_\Gamma H - H \|W\|_F^2 + \frac{1}{2} H^3, \tag{5.58}$$

resp.

$$V = -\Delta_\Gamma H - H \sum_{i=1}^{n-1} \kappa_i^2 + \frac{1}{2} H^3.$$

Remark: In the case of the surfaces in $\mathbb{R}^3$ we have that $n = 3$ and

$$H \sum_{i=1}^{n-1} \kappa_i^2 = (\kappa_1 + \kappa_2) \left(\kappa_1^2 + \kappa_2^2\right) = H^3 - 2KH.$$

The normal velocity then reads as

$$V = -\Delta_\Gamma H - \frac{1}{2} H^3 + 2KH.$$

In the rest of this section we will show how to get back to the graph and the level-set formulation for the Willmore flow knowing only the normal velocity (5.58). First of all we apply (4.30) on $\Delta_\Gamma H$ to obtain

$$\Delta_\Gamma H = \Delta H - H \nabla H \cdot \mathbf{n} - \mathbf{n}^T D^2 H \mathbf{n} = \Delta H - \frac{1}{2} \nabla \left(H^2\right) \cdot \mathbf{n} - \mathbf{n}^T D^2 H \mathbf{n}. \tag{5.59}$$

Clearly

$$\sum_{i,j=1}^{n} \partial_j \left(\partial_i H \mathbf{n}_i \mathbf{n}_j\right) = \sum_{i,j=1}^{n} \partial_j \partial_i H \mathbf{n}_i \mathbf{n}_j + \sum_{i,j=1}^{n} \partial_i H \partial_j \mathbf{n}_i \mathbf{n}_j + \sum_{i,j=1}^{n} \partial_i H \mathbf{n}_i \partial_j \mathbf{n}_j,$$

which we may write as

$$\nabla \cdot \left(\left(\mathbf{n} \otimes \mathbf{n}\right) \nabla H\right) = \mathbf{n}^T D^2 H \mathbf{n} + \left(\nabla H\right)^T \left(\nabla^T \mathbf{n}\right) \mathbf{n} + \nabla H \cdot \mathbf{n} H. \tag{5.60}$$

Inserting into (5.59) we get

$$\begin{aligned} \Delta_\Gamma H &= \Delta H - \frac{1}{2} \nabla \left(H^2\right) \cdot \mathbf{n} - \nabla \cdot \left(\left(\mathbf{n} \otimes \mathbf{n}\right) \nabla H\right) + \left(\nabla H\right)^T \left(\nabla^T \mathbf{n}\right) \mathbf{n} + \frac{1}{2} \nabla \left(H^2\right) \cdot \mathbf{n} \\ &= \nabla \cdot \left(\left(\mathbb{I} - \mathbf{n} \otimes \mathbf{n}\right) \nabla H\right) + \left(\nabla H\right)^T \left(\nabla^T \mathbf{n}\right) \mathbf{n}. \end{aligned} \tag{5.61}$$

From (4.29) we have

$$H \|W\|_F^2 = H \mathrm{Tr}\left(\nabla^T \mathbf{n} \nabla^T \mathbf{n}\right). \tag{5.62}$$

Writing

$$\sum_{i,j=1}^{n} \partial_i \left(H\mathbf{n}_j \partial_j \mathbf{n}_i\right) = \sum_{i,j=1}^{n} \partial_i H\mathbf{n}_j \partial_j \mathbf{n}_i + \sum_{i,j=1}^{n} H\partial_i \mathbf{n}_j \partial_j \mathbf{n}_i + \sum_{i,j=1}^{n} H\mathbf{n}_j \partial_j \partial_i \mathbf{n}_i,$$

we see that

$$\nabla \cdot \left(H\mathbf{n}^T \nabla^T \mathbf{n}\right) = \left(\nabla H\right)^T \nabla^T \mathbf{n} + H\mathrm{Tr}\left(\nabla^T \mathbf{n} \nabla^T \mathbf{n}\right) + H\nabla H \cdot \mathbf{n},$$

and so

$$H \left\|W\right\|_F^2 = \nabla \cdot \left(H\mathbf{n}^T \nabla^T \mathbf{n}\right) - \left(\nabla H\right)^T \nabla^T \mathbf{n} - \frac{1}{2} \nabla \left(H^2\right) \cdot \mathbf{n}. \tag{5.63}$$

For the last term in (5.2.5) we get

$$\frac{1}{2} H^2 H = \frac{1}{2} H^2 \nabla \cdot \mathbf{n} = \frac{1}{2} \nabla \left(H^2 \mathbf{n}\right) - \frac{1}{2} \nabla \left(H^2\right) \mathbf{n}. \tag{5.64}$$

Putting this all together gives

$$\begin{aligned} \Delta_\Gamma H + H \left\|W\right\|_F^2 - \frac{1}{2} H^3 &= \nabla \cdot \left(\left(\mathbb{I} - \mathbf{n} \otimes \mathbf{n}\right) \nabla H\right) \\ &+ \nabla \cdot \left(H\mathbf{n}^T \nabla^T \mathbf{n}\right) - \frac{1}{2} \nabla \left(H^2\right) \cdot \mathbf{n} - \frac{1}{2} \nabla \left(H^2 \mathbf{n}\right). \end{aligned}$$

From (4.27) we have

$$\left(\nabla^T \mathbf{n}\right) \mathbf{n} = \frac{1}{Q} \mathbb{P}\left(\mathbf{x}\right) D^2 u \mathbf{n} = \frac{1}{Q} \mathbb{P}\left(\mathbf{x}\right) \nabla Q,$$

where we used $\nabla Q = D^2 u \frac{\nabla u}{Q}$. Therefore

$$\begin{aligned} \nabla \cdot \left(\left(\mathbb{I} - \mathbf{n} \otimes \mathbf{n}\right) \nabla H\right) + \nabla \cdot \left(H\mathbf{n}^T \nabla^T \mathbf{n}\right) &= \nabla \cdot \left(\mathbb{P}\left(\mathbf{x}\right) \nabla H + \frac{H}{Q} \mathbb{P}\left(\mathbf{x}\right) \nabla Q\right) \\ &= \nabla \cdot \left(\frac{1}{Q} \mathbb{P}\left(\mathbf{x}\right) \left(Q\nabla H + H\nabla Q\right)\right) \\ &= \nabla \cdot \left(\frac{1}{Q} \mathbb{P}\left(\mathbf{x}\right) \nabla \left(QH\right)\right). \end{aligned}$$

The final equation then reads

$$V = \nabla \cdot \left(\frac{1}{Q} \mathbb{P}\left(\mathbf{x}\right) \nabla \left(QH\right) - \frac{1}{2} \frac{H^2}{Q} \nabla u\right),$$

which can be splitted into two PDEs of the form

$$\frac{\partial_t u}{Q} = -\nabla \cdot \left(\frac{1}{Q} \mathbb{P}\left(\mathbf{x}\right) \nabla W - \frac{1}{2} \frac{W^2}{Q^3} \nabla u\right), \tag{5.65}$$

$$W = QH. \tag{5.66}$$

5.2.5. Anisotropic Willmore flow of graphs

We start again with the graph formulation where $\Gamma\left(t\right)$ is determined by (5.2). The anisotropic Willmore functional then reads as

$$\mathcal{W}_\gamma\left(\varphi\right) = \frac{1}{2} \int_\Omega H_\gamma^2 Q \mathrm{dx}. \tag{5.67}$$

We will now derive the Euler-Lagrange equation for (5.67). We consider small variation $\delta\varphi$ of φ vanishing at the boundaries of Ω. Then we define function $G_{\delta\varphi} : \mathbb{R} \to \mathbb{R}$ as $G(s) = \mathcal{W}_\gamma(\varphi + s\delta\varphi)$ and we differentiate it with respect to s

$$\begin{aligned}\lim_{s\to0} \partial_s \mathcal{W}_\gamma(\varphi + s\delta\varphi) &= \lim_{s\to0} \int_\Omega \frac{1}{2}\partial_s \left[H_\gamma^2(\varphi + s\delta\varphi) Q(\varphi + s\delta\varphi)\right] \mathrm{dx} \\ &= \lim_{s\to0} \int_\Omega H_\gamma(\varphi + s\delta\varphi) Q(\varphi + s\delta\varphi) \partial_s H_\gamma(\varphi + s\delta\varphi) \\ &+ \frac{1}{2} H_\gamma^2(\varphi + s\delta\varphi) \partial_s Q(\varphi + s\delta\varphi) \mathrm{dx}. \end{aligned} \tag{5.68}$$

Since

$$\partial_s Q(\varphi + s\delta\varphi) = \partial_s \sqrt{1 + |\nabla(\varphi + s\delta\varphi)|^2} = \frac{\nabla\varphi\nabla\delta\varphi + s|\nabla\delta\varphi|^2}{Q(\varphi + s\delta\varphi)} \tag{5.69}$$

and

$$\begin{aligned}\partial_s H_\gamma(\varphi + s\delta\varphi) &= \partial_s \nabla\cdot\left(\nabla_{\mathbf{p}}\gamma(\nabla(\varphi + s\delta\varphi), -1)\right) \\ &= \partial_s \sum_{i=1}^n \partial_{x_i}\partial_{p_i}\gamma(\nabla(\varphi + s\delta\varphi), -1) \\ &= \sum_{i=1}^n \partial_{x_i}\partial_{p_i}\left[\partial_s\gamma(\nabla(\varphi + s\delta\varphi), -1)\right] \\ &= \sum_{i=1}^n \partial_{x_i}\partial_{p_i}\left[\sum_{j=1}^n \partial_{p_j}\gamma(\nabla(\varphi + s\delta\varphi), -1)\partial_{x_j}\delta\varphi\right] \\ &= \sum_{i,j=1}^n \partial_{x_i}\partial_{p_i}\partial_{p_j}\gamma(\nabla(\varphi + s\delta\varphi), -1)\partial_{x_j}\delta\varphi \\ &= \nabla\cdot\left(\mathbb{E}_\gamma(\varphi + s\delta\varphi)\nabla\delta\varphi\right), \end{aligned} \tag{5.70}$$

where we denoted

$$\mathbb{E}_\gamma(\varphi) := \partial_{p_i}\partial_{p_j}\gamma(\nabla\varphi, -1) = (\nabla_{\mathbf{p}} \otimes \nabla_{\mathbf{p}})\gamma(\nabla\varphi, -1), \tag{5.71}$$

the substitution of (5.69) and (5.70) to (5.68) gives

$$\begin{aligned}(\delta\mathcal{W}_\gamma, \delta\varphi)_{L_2(\Omega)} &= \lim_{s\to0} \partial_s \mathcal{W}_\gamma(\varphi + s\delta\varphi) \\ &= \int_\Omega H_\gamma Q \nabla\cdot(\mathbb{E}_\gamma\nabla\delta\varphi) + \frac{1}{2}H_\gamma^2 \frac{\nabla\varphi\nabla\delta\varphi}{Q}\mathrm{dx} \\ &= \int_\Omega w_\gamma \nabla\cdot(\mathbb{E}_\gamma\nabla\delta\varphi) + \frac{1}{2}\frac{w_\gamma^2}{Q^3}\nabla\varphi\cdot\nabla\delta\varphi\mathrm{dx} \qquad (5.72) \\ &= \int_{\partial\Omega} w_\gamma\mathbb{E}_\gamma\nabla\delta\varphi\cdot\nu\mathrm{d}\mathcal{H}^{n-1} - \int_\Omega \nabla w_\gamma\cdot(\mathbb{E}_\gamma\nabla\delta\varphi) \qquad (5.73) \\ &+ \frac{1}{2}\int_{\partial\Omega}\frac{w_\gamma^2}{Q^3}\nabla\varphi\cdot\nu\delta\varphi\mathrm{d}\mathcal{H}^{n-1} - \frac{1}{2}\int_\Omega \nabla\cdot\left(\frac{w_\gamma^2}{Q^3}\nabla\varphi\right)\delta\varphi\mathrm{dx} \qquad (5.74) \\ &= -\int_{\partial\Omega}\mathbb{E}_\gamma\nabla w_\gamma\cdot\nu\delta\varphi\mathrm{d}\mathcal{H}^{n-1} + \int_\Omega \nabla\cdot(\mathbb{E}_\gamma\nabla w_\gamma)\delta\varphi - \frac{1}{2}\nabla\cdot\left(\frac{w_\gamma^2}{Q^3}\nabla\varphi\right)\delta\varphi\mathrm{dx} \\ &\qquad (5.75) \\ &= \int_\Omega \nabla\cdot\left(\mathbb{E}_\gamma\nabla w_\gamma - \frac{1}{2}\frac{w_\gamma^2}{Q^3}\nabla\varphi\right)\delta\varphi\mathrm{dx}, \end{aligned}$$

where in (5.72) we denoted

$$w_\gamma := QH_\gamma.$$

To eliminate the first integral in (5.73) we assumed that $w_\gamma \mid_{\partial\Omega} \equiv 0$(which is equivalent to $H_\gamma \mid_{\partial\Omega} \equiv 0$) and the first integral in (5.74) is zero since $\delta\varphi \in C_0^\infty(\Omega)$. In (5.75) $\nabla w_\gamma \cdot (\mathbb{E}_\gamma \nabla \delta) = \nabla\delta\varphi\,(\mathbb{E}_\gamma \nabla w_\gamma)$ because $\mathbb{E}_\gamma$ is symmetric, it follows directly from the definition. The first integral in (5.75) is zero because of the choice of $\delta\varphi$. What we obtained is the Euler-Lagrange equation for the Willmore functional :

$$\nabla \cdot \left(\mathbb{E}_\gamma \nabla w_\gamma - \frac{1}{2}\frac{w_\gamma^2}{Q^3}\nabla\varphi \right) = 0. \tag{5.76}$$

Remark: The Neumann boundary conditions Let us now drop the assumption $\delta\varphi \in C_0^\infty(\Omega)$ and consider only $\delta\varphi \in C^\infty(\Omega)$ which will allow us to define the Neumann boundary conditions. We need to eliminate the integrals

$$\frac{1}{2}\int_{\partial\Omega} \frac{w_\gamma^2}{Q^3}\nabla\varphi \cdot \nu\delta\varphi \mathrm{d}\mathcal{H}^{n-1} \tag{5.77}$$

in (5.74) and

$$\int_{\partial\Omega} \mathbb{E}_\gamma \nabla w_\gamma \cdot \nu\delta\varphi \mathrm{d}\mathcal{H}^{n-1} \tag{5.78}$$

in (5.75). (5.77) is zero if

$$\nabla\varphi \cdot \nu = \partial_\nu \varphi = 0 \text{ on } \partial\Omega, \tag{5.79}$$

which is usual Neumann boundary condition for φ. The situation is more complicated for the integral (5.78) where we would like to have

$$\mathbb{E}_\gamma \nabla w_\gamma \cdot \nu = 0 \text{ on } \partial\Omega. \tag{5.80}$$

We now turn our attention to the L_2-gradient flow. As we already mentioned, we do not have any definition of the geometric equation for the fourth order partial differential equations and so we cannot affirm that we will get such an equation as we did for the mean-curvature flow. However, majority of the texts concerning the Willmore flow deal only with the variations of $\Gamma(t)$ in the normal direction. Therefore we do not show the counterpart of (5.10) for the Willmore functional. Instead of it we define the Willmore flow of graphs given as the gradient flow for the Willmore functional (5.67) with the scalar product (5.12)

$$g(\varphi, v) = \int_\Omega uvQ^{-1}$$

and as before we want

$$g(\nabla_g \mathcal{W}_\gamma, v) = (\delta\mathcal{W}_\gamma, v)_{L_2(\Omega)}, \text{ for all } v \in C^\infty(\Omega), \text{ resp. } v \in C_0^\infty(\Omega).$$

It means that

$$\nabla_g \mathcal{W}_\gamma = Q\delta\mathcal{W}_\gamma,$$

and we may define:

Definition 5.2.6. *Let Ω be a domain in $\mathbb{R}^{n-1}$. The* **anisotropic Willmore flow of graphs with the Dirichlet boundary conditions** *and the initial condition φ_{ini} is a fourth order parabolic problem given by*

$$\partial_t \varphi = -Q\nabla \cdot \left(\mathbb{E}_\gamma \nabla w_\gamma - \frac{1}{2}\frac{w_\gamma^2}{Q^3}\nabla\varphi \right) \quad \text{on } (0,T)\times\Omega, \tag{5.81}$$

$$w_\gamma = QH_\gamma \quad \text{on } (0,T)\times\Omega, \tag{5.82}$$

$$\varphi\,|_{t=0} = \varphi_{ini} \quad \text{on } \Omega, \tag{5.83}$$

$$\varphi = g,\ w_\gamma = 0 \quad \text{on } \partial\Omega. \tag{5.84}$$

The **anisotropic Willmore flow of graphs with the Neumann boundary conditions** *and the initial condition φ_{ini} is a fourth order parabolic problem given by (5.81)–(5.83) and*

$$\partial_\nu \varphi = 0,\ \mathbb{E}_\gamma \nabla w_\gamma \cdot \nu = 0 \quad \text{on } \partial\Omega. \tag{5.85}$$

For the weak solution, we first multiply the equation (5.81) by a test function $\varphi \in H_0^1(\Omega)$ resp. $\varphi \in H^1(\Omega)$ and integrate over Ω. Then we have

$$\begin{aligned}
\int_\Omega \frac{\partial_t \varphi}{Q}\varphi \mathrm{dx} &= -\int_\Omega \nabla \cdot \left(\mathbb{E}_\gamma \nabla w_\gamma - \frac{1}{2}\frac{w_\gamma^2}{Q^3}\nabla\varphi \right)\varphi \mathrm{dx} \\
&= -\int_{\partial\Omega} (\mathbb{E}_\gamma \nabla w_\gamma)\cdot\nu\varphi - \frac{1}{2}\frac{w_\gamma^2}{Q^3}\partial_\nu\varphi\varphi \mathrm{d}\mathcal{H}^{n-1} \\
&+ \int_\Omega \left(\mathbb{E}_\gamma \nabla w_\gamma - \frac{1}{2}\frac{w_\gamma^2}{Q^3}\nabla\varphi \right)\cdot\nabla\varphi \mathrm{dx}.
\end{aligned}$$

When $\varphi \in H_0^1(\Omega)$ it is easy to see that the integral over $\partial\Omega$ is zero. In the case $\varphi \in H^1(\Omega)$ we set the Neumann boundary conditions (5.85).

Definition 5.2.7. *Let Ω be a domain in $\mathbb{R}^{n-1}$. The weak solution of the graph formulation for the Willmore flow with the Dirichlet boundary conditions*

$$\begin{aligned} \varphi &= g \quad \text{on } \partial\Omega, \\ w_\gamma &= 0 \quad \text{on } \partial\Omega, \end{aligned}$$

is a couple $\varphi, w : (0,T) \to H_0^1(\Omega)$ which for each test function $\varphi, \xi \in H_0^1(\Omega)$ and a.e in $(0,T)$ satisfies,

$$\int_\Omega \frac{\varphi_t}{Q}\varphi \mathrm{dx} = \int_\Omega (\mathbb{E}_\gamma \nabla w_\gamma) \cdot \nabla\varphi - \frac{1}{2}\frac{w_\gamma^2}{Q^3}\nabla\varphi \cdot \nabla\varphi \mathrm{dx} \text{ a.e. in } (0,T) \tag{5.86}$$

$$\int_\Omega \frac{w_\gamma}{Q}\xi \mathrm{dx} = -\int_\Omega \nabla_{\mathbf{p}}\gamma \cdot \nabla\xi \mathrm{dx}. \tag{5.87}$$

with the initial condition

$$\varphi \mid_{t=0} = \varphi_{ini}. \tag{5.88}$$

The weak solution for the problem with homogeneous Neumann boundary conditions

$$\begin{aligned} \partial_\nu \varphi &= 0 \quad \text{on } \partial\Omega, \\ \mathbb{E}_\gamma \nabla w \cdot \nu &= 0 \quad \text{on } \partial\Omega, \end{aligned}$$

is a couple $\varphi, w : (0,T) \to H^1(\Omega)$ which for each test function $\varphi, \xi \in H^1(\Omega)$ and a.e. in $(0,T)$ satisfies (5.86)-(5.87) and the initial condition (5.88).

5.2.6. Anisotropic level-set formulation

In the same way we derived the level-set formulation for the mean-curvature flow, we will proceed even for the Willmore flow. Taking the Willmore functional (5.34) and the scalar product (5.16) we get that the gradient flow for the level-set formulation of the Willmore flow reads as

$$\partial_t u = -\nabla_g \mathcal{W}_\gamma = -\delta \mathcal{W}_\gamma \left|\nabla u\right|,$$

and we may define:

Definition 5.2.8. *Let Ω be a domain in $\mathbb{R}^n$. The* **anisotropic level-set formulation of the Willmore flow with the Dirichlet boundary conditions** *and the initial condition φ_{ini} is a fourth order parabolic problem*

$$\begin{aligned}
\partial_t u &= -Q_\epsilon \nabla \cdot \left(\mathbb{E}_\gamma \nabla w_\gamma - \frac{1}{2}\frac{w_\gamma^2}{Q^3}\nabla u \right) \quad \text{on } (0,T)\times\Omega, && (5.89)\\
w_\gamma &= Q_\epsilon \nabla \cdot \left(\nabla_{\mathbf{p}} \gamma \left(\nabla \varphi, -1 \right) \right) \quad \text{on } (0,T)\times\Omega, && (5.90)\\
u\mid_{t=0} &= u_{ini} \quad \text{on } \Omega, && (5.91)\\
u &= g,\ w_\gamma = 0 \quad \text{on } \partial\Omega. && (5.92)
\end{aligned}$$

The **anisotropic level-set formulation of the Willmore flow with the Dirichlet boundary conditions** *and the initial condition φ_{ini} is a fourth order parabolic problem given by (5.89)–(5.91) and*

$$\partial_\nu u = 0,\ \mathbb{E}_\gamma \nabla w_\gamma \cdot \nu = 0 \quad \text{on } \partial\Omega. \tag{5.93}$$

To get the weak formulation for the level-set formulation of the (anisotropic) Willmore flow we proceed in the same way we did for the graph formulation:

Definition 5.2.9. *Let Ω be a domain in $\mathbb{R}^n$. The weak solution of the anisotropic level-set formulation for the Willmore flow with the Dirichlet boundary conditions*

$$\begin{aligned}
u &= g \quad \text{on } \partial\Omega,\\
w_\gamma &= 0 \quad \text{on } \partial\Omega,
\end{aligned}$$

is a couple $u, w : (0,T) \to H_0^1(\Omega)$ which for each test function $\varphi, \xi \in H_0^1(\Omega)$ and a.e in $(0,T)$ satisfies,

$$\begin{aligned}
\int_\Omega \frac{\partial_t u}{Q_\epsilon}\varphi \mathrm{dx} &= \int_\Omega (\mathbb{E}_\gamma \nabla w_\gamma)\cdot\nabla\varphi - \frac{1}{2}\frac{w_\gamma^2}{Q^3}\nabla u\cdot\nabla\varphi \mathrm{dx} \text{ a.e. in } (0,T) && (5.94)\\
\int_\Omega \frac{w_\gamma}{Q_\epsilon}\xi \mathrm{dx} &= -\int_\Omega \nabla_{\mathbf{p}}\gamma\cdot\nabla\xi \mathrm{dx}. && (5.95)
\end{aligned}$$

with the initial condition

$$u\mid_{t=0} = u_{ini}. \tag{5.96}$$

The weak solution for the problem with homogeneous Neumann boundary conditions

$$\begin{aligned}
\partial_\nu u &= 0 \quad \text{on } \partial\Omega,\\
\mathbb{E}_\gamma \nabla w_\gamma \cdot \nu &= 0 \quad \text{on } \partial\Omega,
\end{aligned}$$

is a couple $u, w : (0,T) \to H^1(\Omega)$ which for each test function $\varphi, \xi \in H^1(\Omega)$ and a.e. in $(0,T)$ satisfies (5.94)-(5.95) and the initial condition (5.96).

5.2.7. Integral equality for the graph formulation

For the numerical analysis we will need the following theorem, proof of which can be found in Deckelnick and Dziuk [34]. We incorporate the proof into this text for better understanding of a more general modification we will show later.

Theorem 5.2.10. *For the solution φ, w of the isotropic problem (5.45)-(5.46) the Dirichlet boundary conditions the following equality holds:*

$$\int_\Omega \frac{(\partial_t\varphi)^2}{Q}\mathrm{dx} + \frac{1}{2}\frac{\mathrm{d}}{\mathrm{d}t}\int_\Omega H^2 Q\mathrm{dx} = 0. \tag{5.97}$$

Proof. Differentiating (5.46) with respect to t gives

$$\int_\Omega \frac{\partial_t w\xi}{Q}\mathrm{dx} - \int_\Omega \frac{w\xi\partial_t Q}{Q^2}\mathrm{dx} + \int_\Omega \mathbb{E}\nabla\partial_t\varphi\cdot\nabla\xi = 0 \quad \text{for all } \xi \in H_0^1(\Omega) \tag{5.98}$$

where we used the fact that

$$\frac{\mathrm{d}}{\mathrm{d}t}\left(\frac{\nabla\varphi}{Q}\right) = \frac{Q\nabla\partial_t\varphi - \partial_t Q\nabla\varphi}{Q^2} \tag{5.99}$$

and

$$\partial_t Q = \frac{\nabla\partial_t\varphi\cdot\nabla\varphi}{Q}. \tag{5.100}$$

Inserting (5.100) to (5.99) we have

$$\frac{\mathrm{d}}{\mathrm{d}t}\left(\frac{\nabla\varphi}{Q}\right) = \frac{\partial_t\nabla\varphi}{Q} - \frac{(\nabla\partial_t\varphi\cdot\nabla\varphi)\nabla\varphi}{Q^2} = \frac{1}{Q}\left(\mathbb{I} - \left(\frac{\nabla\varphi}{Q}\otimes\frac{\nabla\varphi}{Q}\right)\right)\nabla\partial_t\varphi = \mathbb{E}\nabla\partial_t\varphi.$$

Substituting $\xi = w$ in (5.98) and $\varphi = \partial_t\varphi$ in (5.45) we have

$$\begin{aligned}
\int_\Omega \frac{(\partial_t\varphi)^2}{Q}\mathrm{dx} - \int_\Omega (\mathbb{E}\nabla w)\cdot\nabla\partial_t\varphi\mathrm{dx} + \int_\Omega \frac{1}{2}\frac{w^2}{Q^3}\nabla\varphi\cdot\nabla\partial_t\varphi\mathrm{dx} &= 0, &(5.101)\\
\int_\Omega \frac{\partial_t ww}{Q}\mathrm{dx} - \int_\Omega \frac{w^2\partial_t Q}{Q^2}\mathrm{dx} + \int_\Omega \mathbb{E}\nabla\partial_t\varphi\cdot\nabla w &= 0 &(5.102)
\end{aligned}$$

The sum of (5.101) and (5.102) gives

$$\int_\Omega \frac{\partial_t\varphi^2}{Q} + \frac{\partial_t ww}{Q} - \frac{w^2\partial_t Q}{Q^2} + \frac{1}{2}\frac{w^2}{Q^3}\nabla\varphi\cdot\nabla\partial_t\varphi\mathrm{dx} = 0. \tag{5.103}$$

Since $\nabla\partial_t\varphi\cdot\nabla\varphi = \partial_t QQ$ (5.103) turns to

$$\int_\Omega \frac{(\partial_t\varphi)^2}{Q} + \frac{\partial_t ww}{Q} - \frac{1}{2}\frac{w^2\partial_t Q}{Q^2}\mathrm{dx} = 0,$$

which is indeed what we wanted to show because

$$\frac{1}{2}\frac{\mathrm{d}}{\mathrm{d}t}H^2 Q = \frac{1}{2}\frac{\mathrm{d}}{\mathrm{d}t}\frac{w^2}{Q} = \frac{\partial_t ww}{Q} - \frac{1}{2}\frac{w^2\partial_t Q}{Q^2}.$$

□

In the following theorem we extend the equality (5.2.10) even for the anisotropic problem:

Theorem 5.2.11. *For the solution φ, w of (5.81)-(5.82) with the Dirichlet boundary conditions the following equality holds:*

$$\int_\Omega \frac{(\partial_t\varphi)^2}{Q}\mathrm{dx} + \frac{1}{2}\frac{\mathrm{d}}{\mathrm{d}t}\int_\Omega H_\gamma^2 Q\mathrm{dx} = 0. \tag{5.104}$$

Proof. As well as in the case of the isotropic problem we differentiate (5.87) with respect to t

$$\int_\Omega \frac{\partial_t w_\gamma \xi}{Q}\mathrm{dx} - \int_\Omega \frac{w_\gamma \xi \partial_t Q}{Q^2}\mathrm{dx} + \int_\Omega \mathbb{E}_\gamma \nabla \partial_t \varphi \cdot \nabla \xi = 0 \quad \text{for all } \xi \in H_0^1(\Omega) \tag{5.105}$$

which follows from

$$\begin{aligned} \frac{\mathrm{d}}{\mathrm{d}t}\nabla_{\mathbf{p}}\gamma(\nabla\varphi,-1)\cdot\nabla\xi &= \frac{\mathrm{d}}{\mathrm{d}t}\sum_{i=1}^{n}\partial_{p_i}\gamma(\nabla\varphi,-1)\,\partial_{p_i}\xi \\ &= \sum_{i,j=1}^{n}\partial_{p_i}\partial_{p_j}\gamma(\nabla\varphi,-1)\,\partial_t\partial_{x_j}\varphi\partial_{p_i}\xi \\ &= \mathbb{E}_\gamma\nabla\partial_t\varphi\cdot\nabla\xi. \end{aligned}$$

The rest of the proof remains the same as in the isotropic case. □

5.2.8. Some results from the mathematical analysis of the elastic energy and the Willmore flow

Dziuk, Kuwert and Schätzle [44] showed long time solution existence for the curves in $\mathbb{R}^n$ where the evolution is driven by elastic energy (the Willmore functional) possibly with some additional constraints on the curve length. Kuwert and Schätzle [67] show lower bound on the lifespan of smooth solution for compact immersed surfaces in $\mathbb{R}^n$. Under assumption that the initial surface is close to a sphere, Simonett [91] shows the global solution existence, uniqueness and regularity. He also proves that the solution converges exponentially fast to a sphere. Very similar result obtained also Kuwert and Schätzle [66]. Mayer and Simonett [72] prove "that the Willmore flow can drive embedded surfaces to self-intersections in finite time". In the case of anisotropy, Clarenz [21] gives proof that "Wulff-shapes are the only minimisers (of the Willmore functional)". It is important result for the surface restoration problem.

5.3. Examples of anisotropies

In this section we show some examples of the anisotropy functions γ. To visualise them, we define the Wulff shape - see Giga [53]:

Definition 5.3.1. *Let γ be an admissible anisotropy function. We say that*

$$W = \bigcap_{|\mathbf{q}|=1}\{\mathbf{x}\in\mathbb{R}^n \mid (\mathbf{x},\mathbf{q}) \le \gamma(\mathbf{q})\}, \tag{5.106}$$

is the **Wulff shape** *associated with γ.*

We start with γ for the isotropic problem. It takes a form

$$\gamma_{iso}(\mathbf{p},-1) = \sqrt{1+|\mathbf{p}|^2}, \tag{5.107}$$

for the graph formulation resp.

$$\gamma_{iso}(\mathbf{p}) = \sqrt{\epsilon^2+|\mathbf{p}|^2}. \tag{5.108}$$

for the level-set formulation. Note that in both cases (if we set $\epsilon = 0$) $\gamma_{iso}(\mathbf{n}) = \|\mathbf{n}\|_2 = 1$ and in fact for the isotropic problem γ_{iso} is the Euclidean norm of normal. For the derivatives w.r.t to p_i for $i = \{1,2\}$ we have

$$\partial_{p_i}\gamma_{iso} = \frac{p_i}{\gamma_{iso}}, \tag{5.109}$$

and substituting $\mathbf{p} = \nabla u$ we have

$$H_{\gamma_{iso}} = \nabla \cdot \left(\frac{\nabla u}{\sqrt{1 + |\nabla u|^2}} \right), \text{ resp. } H_{\gamma_{iso}} = \nabla \cdot \left(\frac{\nabla u}{\sqrt{\epsilon^2 + |\nabla u|^2}} \right).$$

The second derivatives w.r.t. to p_i are

$$\partial^2_{p_i} \gamma_{iso} = \frac{1}{\gamma_{iso}} \left(1 - \frac{p_i^2}{\gamma_{iso}^2} \right) \text{ and } \partial_{p_i} \partial_{p_j} \gamma_{iso} = -\frac{p_i p_j}{\gamma_{iso}^2}, \text{ for } i \neq j.$$

The substitution $\mathbf{p} = \nabla u$ gives

$$\mathbb{E} = \frac{1}{Q} \left(\mathbb{I} - \frac{\nabla u}{Q} \otimes \frac{\nabla u}{Q} \right). \tag{5.110}$$

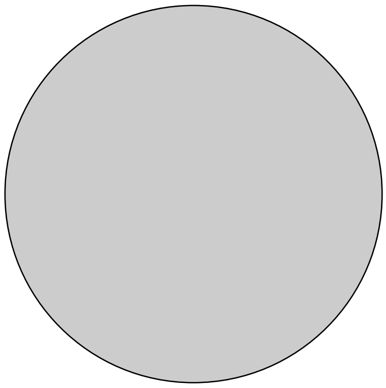

Figure 5.1.: The Wulff shape of γ_{iso} given by (5.108) and (5.109).

Slightly more general is an anisotropy induced by a quadratic form $G : \mathbb{R}^2 \times \mathbb{R}^2 \to \mathbb{R}$, $G(\mathbf{p}_1, \mathbf{p}_2) = \mathbf{p}_1^T \mathbb{G} \mathbf{p}_2$ given by positive definite matrix $\mathbb{G} \in \mathbb{R}^{2,2}$. The anisotropy, which might be understood as a weighted Euclidean norm, is defined as

$$\gamma_{\mathbb{G}}(\mathbf{p}, -1) := \sqrt{1 + \mathbf{p}^T \mathbb{G} \mathbf{p}}, \text{ resp. } \gamma_{\mathbb{G}}(\mathbf{p}) := \sqrt{\epsilon^2 + \mathbf{p}^T \mathbb{G} \mathbf{p}}, \tag{5.111}$$

and since ($\mathbb{G}_{.i}$ denotes the i-th column of $\mathbb{G}$)

$$\begin{aligned}
\partial_i \gamma_{\mathbb{G}} &= \frac{\mathbf{p}^T \mathbb{G}_{.i}}{\gamma_{\mathbb{G}}}, \text{ for } i = 1, 2, \\
\partial_i^2 \gamma_{\mathbb{G}} &= \frac{1}{\gamma_{\mathbb{G}}} \left(G_{ii} - \frac{\mathbf{p}^T \mathbb{G}_{.i}}{\gamma_{\mathbb{G}}} \frac{\mathbb{G}_{i.} \mathbf{p}}{\gamma_{\mathbb{G}}} \right), \text{ for } i = 1, 2, \\
\partial_i \partial_j \gamma_{\mathbb{G}} &= \frac{1}{\gamma_{\mathbb{G}}} \left(G_{ij} - \frac{\mathbf{p}^T \mathbb{G}_{.i}}{\gamma_{\mathbb{G}}} \frac{\mathbb{G}_{j.} \mathbf{p}}{\gamma_{\mathbb{G}}} \right), \text{ for } i, j = 1, 2, i \neq j,
\end{aligned}$$

we have

$$H_{\gamma_{\mathbb{G}}} = \nabla \cdot \left(\frac{\mathbb{G} \nabla u}{\gamma_{\mathbb{G}}} \right), \text{ and } \mathbb{E}_{\gamma_{\mathbb{G}}} = \frac{1}{\gamma_{\mathbb{G}}} \left(\mathbb{G} - \frac{\mathbb{G} \nabla u}{\gamma_{\mathbb{G}}} \otimes \frac{\mathbb{G} \nabla u}{\gamma_{\mathbb{G}}} \right). \tag{5.112}$$

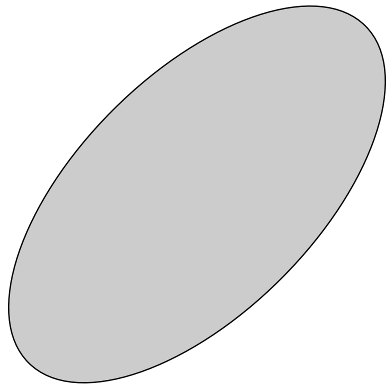

Figure 5.2.: The Wulff shape of $\gamma_{\mathbb{G}}$ given by (5.111).

Another (stronger) anisotropy is given by formula

$$\gamma_{abs}\left(\mathbf{P}\right) = \sum_{i=1}^{3} \sqrt{P_i^2 + \epsilon_{abs} \sum_{j=1}^{3} P_j^2}, \tag{5.113}$$

where the vector $\mathbf{P}$ is defined as $\mathbf{P} = (\mathbf{p}, -1)$ for graphs and $\mathbf{P} = (\mathbf{p}, \epsilon)$ for the level-set formulation. If we set $\epsilon_{abs} = 0$ we have a sum of absolute values of the coordinates of $\mathbf{P}$. The term $\epsilon_{abs} \sum_{j=1}^{3} P_j^2$ is therefore only regularisation in the case when $\mathbf{p} = 0$. It is difficult to express $H_{\gamma_{abs}}$ and $\mathbb{E}_{\gamma_{abs}}$ in some compact form and so we only show partial derivatives of γ_{abs} with respect to p_i and p_j for $i, j = 1, 2$.

$$\begin{aligned}
\gamma_{abs,p_i} &= \sum_{j=1}^{3} \frac{\epsilon_{abs} p_i}{\sqrt{P_j^2 + \epsilon_{abs} \sum_{k=1}^{3} P_k^2}} + \frac{p_i}{\sqrt{p_i^2 + \epsilon_{abs} \sum_{j=1}^{3} P_j^2}} \quad \text{for} \quad i = 1, 2, \\
\gamma_{abs,p_i p_i} &= \sum_{j=1}^{3} \left(\frac{\epsilon_{abs}}{\sqrt{P_j^2 + \epsilon_{abs} \sum_{k=1}^{3} P_k^2}} - \frac{\epsilon_{abs}^2 p_i^2}{\left(P_j^2 + \epsilon_{abs} \sum_{k=1}^{3} P_k^2\right)^{\frac{3}{2}}} \right) \\
&+ \frac{1}{\sqrt{p_i^2 + \epsilon_{abs} \sum_{j=1}^{3} P_j^2}} - \frac{p_i^2}{\left(p_i^2 + \epsilon_{abs} \sum_{j=1}^{3} P_j^2\right)^{\frac{3}{2}}} \quad \text{for} \quad i = 1, 2, \\
\gamma_{abs,p_i p_j} &= -\sum_{k=1}^{3} \frac{\epsilon_{abs}^2 p_i p_j}{\left(P_k^2 + \epsilon_{abs} \sum_{l=1}^{3} P_l^2\right)^{\frac{3}{2}}} - \sum_{k=1}^{2} \frac{\epsilon_{abs} p_i p_j}{\left(P_k^2 + \epsilon_{abs} \sum_{l=1}^{3} P_l^2\right)^{\frac{3}{2}}}.
\end{aligned}$$

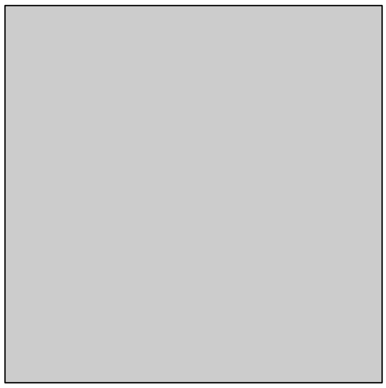

Figure 5.3.: The Wulff shape of γ_{abs} given by (5.113).

Another anisotropy is the discrete l^m-norm for $1 \leq m \leq \infty$

$$\gamma_{l^m}(\mathbf{P}) = \left(\sum_{i=1}^{3} |P_i|^m\right)^{\frac{1}{m}}. \tag{5.114}$$

The partial derivatives then read as

$$\begin{aligned}
\gamma_{l^m,p_i} &= \gamma_{l^m}^{1-m} |p_i|^{m-2} p_i, \\
\gamma_{l^m,p_ip_i} &= \gamma_{l^m}^{1-m} |p_i|^{m-2} \left((1-m)\gamma_{l^m}^{-m} |p_i|^m + m - 1\right), \\
\gamma_{l^m,p_ip_j} &= (1-m)\gamma_{l^m}^{1-2m} p_i p_j |p_i p_j|^{n-2}.
\end{aligned}$$

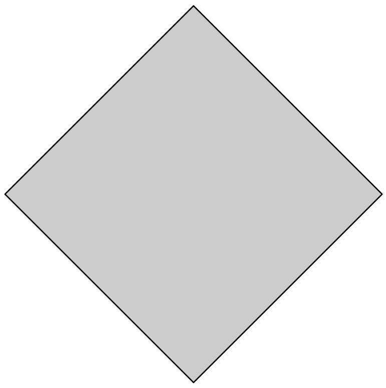

Figure 5.4.: The Wulff shape of γ_{l^m} given by (5.114).

5.4. Parametric approach

In this section, we mention another method of interface description based on parametrisation. In the Chapter 7 we will compare the results obtained by the level-set method and this approach (sometimes called Lagrangian).

Assume that for fixed $t \geq 0$, $\Gamma(t)$ is described by $\gamma : \langle 0, 1\rangle \to \mathbb{R}^2$

$$\Gamma(t) \equiv \{\gamma(\sigma, t) \mid \sigma \in [0,1]\}, \tag{5.115}$$

or by the arclength parametrisation $\gamma : \mathcal{I} \times [0, T] \to \mathbb{R}^2$ for which

$$\Gamma(t) \equiv \{\gamma(s, t) \mid s \in \mathcal{I} \subset \mathbb{R}\} \text{ and } |\partial_s \gamma(s, t)| = 1, \tag{5.116}$$

holds for all $t \geq 0$. Of course $\Gamma(t)$ is evolving in time as t grows. Since $\Gamma(t)$ should remain closed for all $t > 0$ we set periodic boundary conditions on any function f related to the evolution of $\Gamma(t)$ i.e $f(0,t) = f(1,t)$ for $t > 0$. It is easy to see that the movement of each point can be decomposed into the shift in the tangential and the normal direction and so we may write

$$\partial_t \gamma(s,t) = \alpha \mathbf{t} + \beta \mathbf{n}, \tag{5.117}$$

where α and β depend on given evolution. $\Gamma(t)$ will change only when $\beta \neq 0$ for some $\mathbf{x} \in \Gamma(t)$. On the other hand $\alpha \neq 0$ will never change the shape of $\Gamma(t)$ and so theoretically we might omit the tangential direction of the movement. However, some works [75, 76, 77] show that suitable choice of α can significantly improve the accuracy of numerical schemes and even more. in some cases it can prevent from the brake down of the numerical simulation. In the rest of this section we will show how to choose α if we have only β in hand.

In the numerical simulations, we may not assume that if $\Gamma(0)$ is given by the arclength parametrisation then also all $\Gamma(t)$ for $t > 0$ will remain implicitly parametrised by the arclength. Therefore we assume general parametrisation $\gamma(\sigma,t)$ and denote

$$g = |\partial_\sigma \gamma| > 0, \tag{5.118}$$

which is not necessarily equal to 1. After a discretisation in space, g has a meaning of the distance between two successive points x_{i-1} and x_i (all details concerning the discretisation will be described in the next chapter). In [77], the authors study so called relative local length g/L where L stands for the length of Γ. In agreement with Ševčovič [98], we now show what is the change of g. First of all we denote $\mathbf{p} = \partial_\sigma \gamma$. We have

$$\begin{aligned}
\partial_t \mathbf{p} &= \partial_t \partial_\sigma \gamma = \partial_\sigma \partial_t \gamma = \partial_\sigma (\alpha \mathbf{t} + \beta \mathbf{n}) = g \partial_s (\alpha \mathbf{t} + \beta \mathbf{n}) \\
&= g (\partial_s \alpha \mathbf{t} + \alpha \partial_s \mathbf{t} + \partial_s \beta \mathbf{n} + \beta \partial_s \mathbf{n}) \\
&= g (\partial_s \alpha \mathbf{t} + \alpha \kappa \mathbf{n} + \partial_s \beta \mathbf{n} - \beta \kappa \mathbf{t}) \\
&= g ((\partial_s \alpha - \beta \kappa) \mathbf{t} + (\alpha \kappa + \partial_s \beta) \mathbf{n})
\end{aligned}$$

where we used the fact that $\partial_\sigma \partial_t = \partial_t \partial_\sigma$. Also for $\gamma = \gamma(s(\sigma), t)$ we have $\partial_\sigma \gamma = \partial_s \gamma \frac{\mathrm{d}s}{\mathrm{d}\sigma}$ and so $\frac{\mathrm{d}s}{\mathrm{d}\sigma} = g$. Finally we also applied the Frenet formulas (4.1) and (4.2). Multiplying the last equality by $\mathbf{p}$ we have

$$\mathbf{p} \cdot \partial_t \mathbf{p} = g \mathbf{t} \cdot \partial_t \mathbf{p} = g^2 (\partial_s \alpha - \beta \kappa),$$

and finally we obtain

$$\partial_t g = \partial_t |\partial_\sigma \gamma| = \frac{\partial_\sigma \gamma \cdot \partial_t \partial_\sigma \gamma}{|\partial_\sigma \gamma|} = \frac{\mathbf{p} \cdot \partial_t \mathbf{p}}{g},$$

and so

$$\partial_t g = g (\partial_s \alpha - \beta \kappa). \tag{5.119}$$

Of course, the same periodic boundary conditions, we set for α and β, must hold even for g. We denote $L(t)$ the length of $\Gamma(t)$ for which we have $L(t) = \int_0^1 g(\sigma,t)\,\mathrm{d}\sigma$. Differentiating this equality w.r. to t gives

$$\frac{\mathrm{d}}{\mathrm{d}t} L(t) = \int_0^1 \partial_t g(\sigma,t)\,\mathrm{d}\sigma = \int_0^1 g(\partial_s \alpha - \beta \kappa)\,\mathrm{d}\sigma = \int_{\Gamma(t)} \partial_s \alpha - \beta \kappa \mathrm{d}s.$$

Taking into account the periodicity of α we get

$$\frac{\mathrm{d}}{\mathrm{d}t} L(t) + \int_{\Gamma(t)} \beta \kappa \mathrm{d}s = 0. \tag{5.120}$$

Let us introduce a nonlocal quantity $\langle \kappa\beta \rangle = \frac{1}{L}\int_\Gamma \kappa\beta \mathrm{d}s$ and $\theta = \ln\left(\frac{g}{L}\right)$. Then we may write

$$\frac{\mathrm{d}}{\mathrm{d}t}L\left(t\right) + \langle \kappa\beta \rangle_{\Gamma(t)} L = 0.$$

and

$$\partial_t \theta = \partial_t \left(\ln \frac{g}{L}\right) = \frac{\partial_t g}{g} - \frac{\partial_t L}{L} = -\kappa\beta + \partial_s \alpha + \langle \kappa\beta \rangle_\Gamma .$$

Writing the last equation as

$$\partial_s \alpha = \partial_t \theta + \kappa\beta - \langle \kappa\beta \rangle_\Gamma \tag{5.121}$$

we see that appropriate choice of $\partial_s \alpha$ allows us to control θ. Choosing $\partial_s \alpha$ as

$$\partial_s \alpha = \left(e^{-\theta} - 1\right)\omega\left(t\right) + \kappa\beta - \langle \kappa\beta \rangle_\Gamma ,$$

gives $\partial_t \theta = \left(e^{-\theta} - 1\right)\omega\left(t\right)$. Setting $\omega\left(t\right) = 0$ yields $\partial_t \theta = 0$ which means that θ as well as the relative local length will be preserved for all $\sigma \in [0,1]$ and all $t \in [0, T_{max})$ where T_{max} denotes maximal time of the existence of the evolving curve (it is finite for the mean-curvature flow and infinite for the surface diffusion flow and the Willmore flow). Such strategy is called **redistribution preserving relative local length** [77].

Another strategy is to suppose that

$$\int_0^{T_{max}} \omega\left(\tau\right) \mathrm{d}\tau = +\infty, \tag{5.122}$$

and solving the ODE $\partial_t \theta = \left(e^{-\theta} - 1\right)\omega\left(t\right)$ which gives $\ln\left(1 - e^{\theta(t)}\right) = -\int_0^t \omega\left(\tau\right) \mathrm{d}\tau$. It means that $\theta\left(\sigma, t\right) \to 0$ when $t \to T_{max}$ uniformly on $[0,1]$ which yields

$$\frac{g\left(\sigma, t\right)}{L\left(t\right)} \to 1 \text{ as } t \to T_{max} \text{ uniformly on } [0,1] .$$

This strategy is called **asymptotically uniform redistribution** . To fulfil the assumption (5.122) we might set $\omega = \delta_1 > 0$ when $T_{max} = +\infty$ or $\omega = \delta_2 \langle \kappa\beta \rangle_{\Gamma(t)}$ if T_{max} is finite. Indeed, in this case $\Gamma\left(t\right)$ shrinks to a single point which means that $L\left(t\right) \to 0$ as $t \to T_{max}$. From (5.120) we have $\delta_2 \frac{\mathrm{d}}{\mathrm{d}t} L = -\delta_2 L \langle \kappa\beta \rangle_{\Gamma(t)} = -\delta_2 L\omega$ and

$$\int_0^t \omega\left(\tau\right) \mathrm{d}\tau = -\delta_2 \int_0^{L(t)} \frac{1}{L} \mathrm{d}L = \delta_2 \left(\ln L\left(0\right) - \ln L\left(t\right)\right) \to +\infty \text{ as } t \to T_{max}.$$

Finally we obtain ODE for α in a form

$$\partial_s \alpha = \kappa\beta - \langle \kappa\beta \rangle_{\Gamma(t)} + \left(\frac{L\left(t\right)}{g\left(\sigma, t\right)} - 1\right)\omega\left(t\right), \tag{5.123}$$

$$\omega\left(t\right) = \delta_1 + \delta_2 \langle \kappa\beta \rangle_{\Gamma(t)} , \tag{5.124}$$

$$\alpha\left(0, t\right) = 0. \tag{5.125}$$

To complete our explanation of the Lagrangian method we only need to show the expressions for the normal velocity β. We consider only the isotropic problems. For the mean-curvature flow it is given by (5.1.8). The plane curves have only one principal curvature which is just the curvature and therefore $H = \kappa$. It means that:

Remark 5.4.1. The normal velocity for the parametric mean-curvature flow of the planar curves has a form

$$\beta = \kappa. \tag{5.126}$$

The general normal velocity for the Willmore flow is (5.2.5). For the plane curves we have $n = 2$ and so

Remark 5.4.2. The normal velocity for the parametric Willmore flow of the planar curves has a form

$$\beta = -\partial_s^2 \kappa - \frac{1}{2}\kappa^3. \tag{5.127}$$

5.5. Signed distance function as a viscosity solution of the eikonal equation

The signed distance function is important for most of the methods based on the level-set formulation. Evaluation based on the definition (4.4.1) is not efficient. In this section we provide another approach based on the eikonal partial differential equation.

In the Theorem 4.4.3 we showed that for given hypersurface Γ_0 there exists ϵ and certain "secure" neighbourhood $\mathcal{N}^\epsilon(\Gamma_0)$ of Γ_0 where the equality $\nabla d(\mathbf{x}) = \mathbf{n}(\overline{\mathbf{x}})$ holds. It also means that

$$|\nabla d| = 1 \text{ for all } \mathbf{x} \in \mathcal{N}^\epsilon(\Gamma).$$

By "secure" we mean that there are no singular points of d in $\mathcal{N}^\epsilon(\Gamma)$. For the signed distance function to a unit circle in $\mathbb{R}^2$

$$d_{S^1}(\mathbf{x}) = |\mathbf{x}| - 1$$

we see that

$$\nabla d_{S^1}(\mathbf{x}) = \frac{1}{|\mathbf{x}|}\mathbf{x}^T,$$

which does not make sense at the origin where $x = y = 0$. For a function given by

$$d'(x, y) = \begin{cases} |\mathbf{x}| - 1 & \text{for } |\mathbf{x}| > 0.25 \\ -|\mathbf{x}| - 0.5 & \text{for } |\mathbf{x}| \leq 0.25 \end{cases}$$

However, it is not the signed distance function for the unit circle because it contains redundant local minima at points where $|\mathbf{x}| = 0.25$. One can also see simpler example in $\mathbb{R}^1$ on the Figure 5.5.

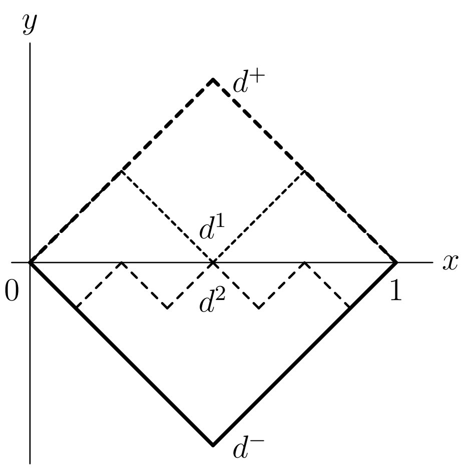

Figure 5.5.: Examples of functions for which $|d'| = 1$ a.e. on $[0, 1]$ but only d^+ and d^- are the viscosity solutions to the equations $\pm|d'| = \pm 1$ on $(0, 1)$ when $u(0) = u(1) = 0$.

We seek for a mechanism of minimising number of singularities of d. for avoiding this and get the simplest (in meaning with the less singularities as possible) function.

Consider now simple example in $\mathbb{R}^1$. Assume that $\Gamma \equiv \{-1, 1\}$ and $\mathrm{Int}\Gamma \equiv (-1, 1)$. The signed distance function to Γ is then given by $d_\Gamma = |x| - 1$. It has one local minimum at $x = 0$ and no local maxima. Let $u \in C^2((-1, 1))$ be an arbitrary smooth function for which $u(-1) = u(1) = 0$ and $u < 0$ on $(-1, 1)$. If it has more then one local minimum it must also have at least one local maximum. From the basic calculus we know that local maxima might be detected by $u''(x) < 0$. So if we somehow ensure that $u'' \geq 0$ for all $x \in (-1, 1)$ there will be no local maxima of u and therefore only one local minimum. Now take a look at the following equation:

$$\left|u'(x)\right| - 1 = -\epsilon u''(x) .$$

For any critical point where $u'(x) = 0$ we have $u''(x) = \frac{1}{\epsilon} > 0$ which can be only local minimum. On the other hand any solution of equation

$$\left|u'(x)\right| - 1 = \epsilon u''(x) ,$$

can have only one local maximum and is positive everywhere in $(-1, 1)$.

Going back to the general space $\mathbb{R}^n$ we will solve a problem:

$$H(\mathbf{x}, u^\epsilon, \nabla u^\epsilon) - \epsilon \Delta u = 0 \quad \text{in } \mathbb{R}^n, \tag{5.128}$$

where we denoted $H(\mathbf{x}, u, \nabla u) = \pm(|\nabla u| - 1)$. Equation (5.128) is in fact regularised **Hamilton-Jacobi equation** of a form:

$$H(\mathbf{x}, u, \nabla u) = 0 \quad \text{in } \mathbb{R}^n, \tag{5.129}$$

where we only assume that $H : \mathbb{R}^n \times \mathbb{R}^n \to R$ is continuous. When we pass $\epsilon \to 0$ we talk about the method of **the vanishing viscosity** for the Hamilton-Jacobi equation - see Evans [47]. If we assume that the class of functions $\{u^\epsilon\}_{\epsilon > 0}$ is bounded and equicontinuous on compact subset of $\mathbb{R}^n \times \langle 0, \infty)$ then from the Arzela-Ascoli compactness criterion (A.0.3) we get that there exists a sequence $\{u^{\epsilon_j}\}$

$$u^{\epsilon_j} \to u \text{ locally uniformly in } \mathbb{R}^n \times \langle 0, \infty) .$$

Our aim now is to find some formulation for the weak solution of (5.129). We cannot apply the Green formula because (5.129) is not in a divergence form. We need to find another approach how to avoid evaluation of ∇u and shift the derivatives on some testing function $v \in C^\infty(\mathbb{R}^n)$. Fix now any such function v and suppose that

$$u - v \text{ has a strict local maximum at some point } \mathbf{x}_0. \tag{5.130}$$

It means that

$$(u - v)(\mathbf{x}_0) > (u - v)(\mathbf{x}) \text{ for } \mathbf{x} \in B(\vec{x}_0, r) ,$$

where $B(\vec{x}_0, r)$ denotes a closed ball in $\mathbb{R}^n$ with centre in $\mathbf{x}_0$ and radius r. Now we see that for each sufficiently small $r > 0$

$$\max_{\partial B}(u - v) < (u - v)(\mathbf{x}_0) ,$$

holds. From the locally uniform convergence of u^{ϵ_j} we get uniform convergence $u^{\epsilon_j} \to u$ on B and so

$$\max_{\partial B}(u^{\epsilon_j} - v) < (u^{\epsilon_j} - v)(\mathbf{x}_0) ,$$

provided ϵ_j is small enough. Consequently

$$u^{\epsilon_j} - v \text{ attains a local maximum at some point } \mathbf{x}_j \in B(r, \mathbf{x}_0) . \tag{5.131}$$

Replacing now r by some subsequence $r_j \to 0$ we get $\mathbf{x}_j \to \mathbf{x}_0$ as $j \to \infty$. From (5.131) we have

$$\begin{aligned} \nabla u^{\epsilon_j}(\mathbf{x}_j) &= \nabla v(\mathbf{x}_j), \\ -\Delta u^{\epsilon_j}(\mathbf{x}_j) &\geq -\Delta v(\mathbf{x}_j), \end{aligned}$$

and directly from (5.128) we get

$$\begin{aligned} H(\nabla v(\mathbf{x}_j), \mathbf{x}_j) &= H(\nabla u^{\epsilon_j}(\mathbf{x}_j), \mathbf{x}_j) \qquad (5.132) \\ &= \epsilon_j \Delta u^{\epsilon_j}(\mathbf{x}_j) \leq \epsilon_j \Delta v(\mathbf{x}_j), \qquad (5.133) \end{aligned}$$

and letting $j \to \infty$ we end with

$$H(\nabla v(\mathbf{x}_0), \mathbf{x}_0) \leq 0.$$

Assume now only

$$u - v \text{ has a local maximum at some point } \mathbf{x}_0,$$

where we dropped the assumption of strictness. Then we define function

$$\tilde{v}(\mathbf{x}) := v(\mathbf{x}) + \delta\left(|\mathbf{x} - \mathbf{x}_0|^2\right), \ \delta > 0.$$

for which $u - \tilde{v}$ has strict local maximum at $\mathbf{x}_0$ and

$$H(\nabla v(\mathbf{x}_0), \mathbf{x}_0) = H(\nabla \tilde{v}(\mathbf{x}_0), \mathbf{x}_0) \leq 0. \qquad (5.134)$$

In the same way we might show that

$$H(\nabla v(\mathbf{x}_0), \mathbf{x}_0) \geq 0,$$

provided that

$$u - v \text{ has a local minimum at some point } \mathbf{x}_0.$$

We see that we have reached what we were looking for i.e. putting the derivatives of u on v. This allows us to define a weak solution of (5.129).

Definition 5.5.1. *Let H be a continuous function $H : \mathbb{R}^n \times \mathbb{R} \times \mathbb{R}^n \to R$. Then:*

1. *function $u = u(\mathbf{x})$ is called the* **viscosity subsolution** *of (5.129) if for each function $v \in C^1(\mathbb{R}^n)$ if $u - v$ has a local maximum at $\mathbf{x}_0 \in \mathbb{R}^n$ then*

$$H(\mathbf{x}_0, u(\mathbf{x}_0), \nabla v(\mathbf{x}_0)) \leq 0,$$

2. *function $u = u(\mathbf{x})$ is called the* **viscosity supersolution** *of (5.129) if for each function $v \in C^1(\mathbb{R}^n)$ if $u - v$ has a local minimum at $\mathbf{x}_0 \in \mathbb{R}^n$ then*

$$H(\mathbf{x}_0, u(\mathbf{x}_0), \nabla v(\mathbf{x}_0)) \geq 0.$$

Function u is called the **viscosity solution** *of (5.129) if it is both viscosity subsolution and supersolution of (5.129).*

The existence and uniqueness of the viscosity solution of Hamilton-Jacobi equation $H(\mathbf{x}, u^\epsilon, \nabla u^\epsilon) = f$ for convex H and discontinuous f has been proved by Deckelnick and Elliott [37].

In the same way we may define the viscosity solution for the initial-value problem of the Hamilton-Jacobi equation

$$\begin{aligned} u_t + H(\mathbf{x}, u, \nabla u) &= 0 \text{ in } \mathbb{R}^n \times (0, \infty), \\ u\,|_{t=0} &= u_0 \text{ on } \mathbb{R}^n \end{aligned} \tag{5.135}$$

as Evans [47]:

Definition 5.5.2. *Let H be a continuous function $H : \mathbb{R}^n \times \mathbb{R} \times \mathbb{R}^n \to R$. Then:*

1. *function $u = u(\mathbf{x}, t)$ is called* **viscosity subsolution** *of (5.135) if $u\,|_{t=0} = u_0$ on $\mathbb{R}^n$ and for each function $v \in C^1(\mathbb{R}^n \times (0, \infty))$ if $u-v$ has a local maximum at $(\mathbf{x}_0, t_0) \in \mathbb{R} \times (0, \infty)$ then $H(\mathbf{x}_0, u(\mathbf{x}_0, t_0), \nabla v(\mathbf{x}_0, t_0)) \le 0$,*
2. *function $u = u(\mathbf{x}, t)$ is called* **viscosity supersolution** *of (5.135) if $u\,|_{t=0} = u_0$ on $\mathbb{R}^n$ and for each function $v \in C^1(\mathbb{R}^n \times (0, \infty))$ if $u-v$ has a local minimum at $(\mathbf{x}_0, t_0) \in \mathbb{R} \times (0, \infty)$ then $H(\mathbf{x}_0, u(\mathbf{x}_0, t_0), \nabla v(\mathbf{x}_0, t_0)) \ge 0$.*

Function u is called **viscosity solution** *of (5.135) if it is both viscosity subsolution and supersolution of (5.135).*

To demonstrate the consistency with the classical solution u^* of (5.135) we choose $v \in C^1(\mathbb{R}^n \times (0, \infty))$ such that $u^* - v$ has local maximum at $(\mathbf{x}_0, t_0)$. Then $\nabla u^*(\mathbf{x}_0, t_0) = \nabla(\mathbf{x}_0, t_0)$, $u_t^*(\mathbf{x}_0, t_0) = v_t(x_0, t_0)$ and

$$\begin{aligned} & v_t(\mathbf{x}_0, t_0) + H(\mathbf{x}_0, u^*(\mathbf{x}_0, t_0), \nabla v(\mathbf{x}_0, t_0)) \\ & = u_t^*(\mathbf{x}_0, t_0) + H(\mathbf{x}_0, u^*(\mathbf{x}_0, t_0), \nabla u^*(\mathbf{x}_0, t_0)) = 0. \end{aligned}$$

The same equality holds for any $(\mathbf{x} + 0, t_0)$ where $u^* - v$ has its local minimum and so u is the viscosity solution of (5.135).

For $H \in C(\mathbb{R}^n)$ and uniformly Lipschitz u_0 the equation (5.135) has been studied in Bardi and Osher [4].

Remark: Viscosity solution for bounded Ω If $\Omega \subset \mathbb{R}^n$ is bounded the definition (5.5.2) is still valid, we only consider the local extremes $\mathbf{x}_0 \in \Omega$. However, some authors impose explicit conditions on v at $\partial\Omega$ - see. Briggs [16] or Claisse [20].

Let us now return to the signed distance function d_Γ of Γ. If Γ is given as a level-set of some continuous function u_0 we want d to have the same signum as u_0 everywhere in Ω. It means that we require

$$\begin{aligned} d_\Gamma \text{ is a viscosity solution of } & -|\nabla d_\Gamma| = -1 \text{ where } \operatorname{sign}(u_0) < 0, \\ d_\Gamma \text{ is a viscosity solution of } & |\nabla d_\Gamma| = 1 \text{ where } \operatorname{sign}(u_0) > 0, \end{aligned}$$

or

$$d_\Gamma \text{ is a viscosity solution of } \operatorname{sign}(u_0)(|\nabla d_\Gamma| - 1) = 0. \tag{5.136}$$

Note however, that in the last equality $H(\mathbf{x}, d_\Gamma(\mathbf{x}, t), \nabla d_\Gamma(\mathbf{x}, t)) = \operatorname{sign}(u_0)(|\nabla d_\Gamma| - 1)$ is not continuous. This fact brings many difficulties into the analysis of such equation.

Similar, but evolutionary equation is (see Sethian [90])

$$u_t - \operatorname{sign}(u_0)(1 - |\nabla u|) = 0 \text{ on } \Omega \times (0, T), \tag{5.137}$$

$$u\,|_{t=0} = u_0, \tag{5.138}$$

the steady state of which should correspond with the solution of (5.136).

The notion of the viscosity solution was proposed by Crandall and Lions in [25]. Even though the existence has been proved already before the viscosity solution allowed the authors to show the uniqueness. Introductory texts are by Crandall [26] and Crandall, Ishii and Lions [24] or a book by Giga [53].

6. Numerical approximation

In this chapter, we present methods for space discretisation of the graph and the level-set formulation of the Willmore flow . Explicit and semi-implicit schemes are used for the time discretisation. Fully implicit schemes are not considered in this thesis.

Finite element approximation of the minimal surfaces problem together with the error estimates been have studied by Johnson and Thomeé in [62].

Numerical approximation of the mean-curvature flow has been studied by Deckelnick and Dziuk. In [28, 29] they study the finite element approximation, convergence and the error estimates. The anisotropic problem was studied in [31, 32]. A finite difference scheme approximating the viscosity solution of the level-set formulation for the mean-curvature flow together with L_∞ error bound can be found in [27]. A finite element scheme and proof of the convergence appeared in [30, 33]. Dziuk [43] also studied the parametric formulation of the anisotropic mean-curvature flow. Methods by Mikula [74] will be explained in details later in this chapter.

The finite elements approximation of the Willmore flow of graphs has been studied by Deckelnick and Dziuk [34] and the finite element approximation for the surface restoration by Clarenz, Diewald, Dziuk, Rumpf and Rusu [22].

Droske and Rumpf [40] used the finite element method for the approximation of the level-set formulation of the Willmore flow.

Numerical schemes for the parametric formulation of the elastic curves hes been proposed by Dziuk, Kuwert and Schätzle [44].

Numerical scheme for axisymmetric surfaces with applications to the mean-curvature flow, surface diffusion flow and the Willmore flow propose Mayer and Simonett [71].

In this text we extend the results obtained in the works of Beneš where he applied the finite difference method for the approximation of the mean-curvature flow [9, 10, 11, 7] and the surface diffusion flow in [12]. We also adopt complementary volume method introduced by Handlovičová, Mikula and Sgallari [55] and we show relation of this class of schemes with schemes based on the finite difference method. For the graph formulation we show stability of the scheme for the Willmore flow.

Finite element method based scheme for the surface diffusion of graphs together with the error analysis can be found in Baënsch, Morin and Nochetto [3], the anisotropic problem has been studied by Deckelnick, Dziuk and Elliott [36]. Finite element numerical scheme for the level-set formulation of the surface diffusion flow was presented by Smereka [92], scheme for the anisotropic problem was proposed by Clarenz, Hausser, Rumpf, Voigt and Weikard [23]. Tangentially stabilised scheme for parametric curves was developed by Mikula and Ševčovič [77].

We will discus the schemes only for two dimensional problems, however the extension to three dimension is very straightforward.

6.1. Notation

We assume having the domain $\Omega \equiv (0, L_1) \times (0, L_2)$. Let h_1, h_2 be space steps such that $h_1 = \frac{L_1}{N_1}$ and $h_2 = \frac{L_2}{N_2}$ for some $N_1, N_2 \in \mathbb{N}^+$. We define a numerical grid, its closure and its boundary as

$$\begin{aligned} \omega_h &= \{(ih_1, jh_2) \mid i = 1 \cdots N_1 - 1, j = 1 \cdots N_2 - 1\}, \\ \overline{\omega}_h &= \{(ih_1, jh_2) \mid i = 0 \cdots N_1, j = 0 \cdots N_2\}, \\ \partial\omega_h &= \overline{\omega_h} \setminus \omega_h, \end{aligned} \tag{6.1}$$

for $u \in C\left(\overline{\Omega}\right)$ we define the projection operator $\mathcal{P}_h : C\left(\overline{\Omega}_h\right) \to \overline{\omega}$ as

$$\mathcal{P}_h\left(u\right)_{ij} := u^h_{ij} := u\left(ih_1, jh_2\right). \tag{6.2}$$

6.2. Space discretisation

6.2.1. Semidiscrete scheme based on one-sided finite differences

The finite difference approximation introduced in [81] combines forward and backward differences. Similar schemes were already successfully applied to other problems [7, 9, 10, 11, 12]. In agreement with Samarskij [89] we define the forward and backward finite differences as follows:

$$u^h_{f.,ij} := \frac{u^h_{i+1,j} - u^j_{ij}}{h_1}, \qquad u^h_{.f,ij} := \frac{u^h_{i,j+1} - u^h_{ij}}{h_2}, \tag{6.3}$$

$$u^h_{b.,ij} := \frac{u^h_{i,j} - u^j_{i-1,j}}{h_1}, \qquad u^h_{.b,ij} := \frac{u^h_{i,j} - u^h_{i,j-1}}{h_2}, \tag{6.4}$$

$$\nabla_f u_{ij} := \left(u^h_{f.,ij}, u^h_{.f,ij}\right), \qquad \nabla_b u_{ij} := \left(u^h_{b.,ij}, u^h_{.b,ij}\right), \tag{6.5}$$

The discrete operator of divergence is approximated in the same manner as the discrete gradient. We define the grid boundary normal difference $\partial^h_\nu u^h_{ij}$.

$$\partial^h_\nu u^h_{0,j} = u_{b.,1,j} \quad \text{for } j = 0, \ldots, N_2, \tag{6.6}$$

$$\partial^h_\nu u^h_{N_1,j} = u_{b.,N_1,j} \quad \text{for } j = 0, \ldots, N_2, \tag{6.7}$$

$$\partial^h_\nu u^h_{i,0} = u_{.b,i,1} \quad \text{for } i = 0, \ldots, N_1, \tag{6.8}$$

$$\partial^h_\nu u^h_{i,N_2} = u_{.b,i,N_2} \quad \text{for } i = 0, \ldots, N_1. \tag{6.9}$$

Remark 6.2.1. Numerical experiments 7.2.2 and 7.2.4 show that this kind of scheme fails in some cases even for the isotropic Willmore flow of graphs. Therefore we do not consider neither the anisotropic problems in this section nor the level-set formulation.

Denoting

$$\begin{aligned} \bar{Q}^h_{ij} &= \sqrt{1 + \frac{1}{2}\left(u^2_{f.,ij} + u^2_{b.,ij} + u^2_{.f,ij} + u^2_{.b,ij}\right)}, \\ & \quad i = 1, \cdots, N_1 - 1, \quad j = 1, \cdots, N_2 - 1, \\ Q^h_{ij} &= \sqrt{1 + u^2_{f.,ij} + u^2_{.f,ij}}, \\ & \quad i = 0, \cdots, N_1 - 1, \quad j = 0, \cdots, N_2 - 1, \end{aligned}$$

we may introduce the following schemes:

Scheme 6.2.2. The **one-sided finite difference** semi-discrete approximation of the **mean-curvature flow of graphs with the Dirichlet boundary conditions** reads as

$$\frac{du_{ij}^h}{dt} = \bar{Q}_{ij}^h \nabla_b \cdot \left(\frac{\nabla_f u_{ij}^h}{Q_{ij}^h} \right) \text{ on } \omega_h, \tag{6.10}$$

$$u_{ij}^h \mid_{t=0} = \mathcal{P}\left(u_{ini}\right)_{ij} \text{ on } \overline{\omega}_h, \tag{6.11}$$

$$u_{ij}^h = g_{ij} \text{ on } \partial\omega_h.$$

The **one-sided finite difference** semi-discrete approximation of the **mean-curvature flow of graphs with the Neumann boundary conditions** is given by (6.10)–(6.11) and

$$\partial_\nu^h u_{ij}^h = 0 \text{ on } \partial\omega_h. \tag{6.12}$$

Scheme 6.2.3. The **one-sided finite difference** semidiscrete approximation of the **Willmore flow of graphs with the Dirichlet boundary conditions** is given by

$$\frac{du_{ij}^h}{dt} = -\bar{Q}_{ij}^h \nabla_b \cdot \left(\frac{1}{Q_{ij}^h} \begin{pmatrix} 1 - \frac{u_{f.,ij}^2}{\left(Q_{ij}^h\right)^2} & -\frac{u_{f.,ij} u_{.f,ij}}{\left(Q_{ij}^h\right)^2}, \\ -\frac{u_{f.,ij} u_{.f,ij}}{\left(Q_{ij}^h\right)^2} & 1 - \frac{u_{.f,ij}^2}{\left(Q_{ij}^h\right)^2} \end{pmatrix} \nabla_f w_{ij}^h - \frac{1}{2} \frac{\left(w_{ij}^h\right)^2}{\left(Q_{ij}^h\right)^3} \nabla_f u_{ij}^h \right) \text{ on } \omega_h, \tag{6.13}$$

$$w_{ij}^h = Q_{ij}^h \nabla_b \cdot \left(\frac{\nabla_f u_{ij}^h}{Q_{ij}^h} \right) \text{ on } \omega_h, \tag{6.14}$$

$$u_{ij}^h \mid_{t=0} = \mathcal{P}\left(u_{ini}\right)_{ij} \text{ on } \overline{\omega}_h, \tag{6.15}$$

$$u_{ij}^h = g_{ij} \text{ and } w_{ij}^h = 0 \text{ on } \partial\omega_h. \tag{6.16}$$

The **one-sided finite difference** semidiscrete approximation of the **Willmore flow of graphs with the Neumann boundary conditions** is given by (6.13)–(6.15) and

$$\partial_\nu^h u_{ij}^h = 0 \text{ and } \partial_\nu^h w_{ij}^h = 0 \text{ on } \partial\omega_h. \tag{6.17}$$

Remark: The level set counterparts of the schemes (6.2.2) and (6.2.3) differs only in the quantities $\bar{Q}_{ij}^h$ and Q_{ij}^h. For the level-set formulation they take the form:

$$\begin{aligned} \bar{Q}_{ij}^h &= \sqrt{\epsilon^2 + \frac{1}{2}\left(u_{f.,ij}^2 + u_{b.,ij}^2 + u_{.f,ij}^2 + u_{.b,ij}^2\right)}, \\ & \qquad i = 1, \cdots, N_1 - 1, \quad j = 1, \cdots, N_2 - 1, \\ Q_{ij}^h &= \sqrt{\epsilon^2 + u_{f.,ij}^2 + u_{.f,ij}^2}. \end{aligned}$$

Stability for the approximation of the Willmore flow of graphs with the one-sided differences

Now we aim to prove the discrete version of the theorem (5.2.11). Let us first of all introduce some necessary notation. For $f, g : \overline{\omega}_h \to \mathbb{R}$, $\mathbf{f}, \mathbf{g} : \overline{\omega}_h \to \mathbb{R}^2$, $\mathbf{f} = \left(f^1, f^2\right)$, $\mathbf{g} = \left(g^1, g^2\right)$ and denoting

$$[f, g]_{pq}^{PQ} = \sum_{i=p,j=q}^{P,Q} h_1 h_2 f_{ij} g_{ij}, \tag{6.18}$$

we define

$$\begin{array}{rclrcl} (f,g)_h & = & [f,g]_{1,1}^{N_1-1,N_2-1}, & \|f\|_h^2 & = & (f,f)_h\,, \\ (\mathbf{f},\mathbf{g})_h & = & \left(f^1,g^1\right)_h + \left(f^2,g^2\right)_h, & \left(f,g^1+g^2\right)_h & = & \left(f,g^1\right)_h + \left(f,g^2\right)_h, \\ \left(f^1,g^1\right)_{f.} & = & \left[f^1,g^1\right]_{1,1}^{N_1,N_2-1}, & \left(f^2,g^2\right)_{.f} & = & \left[f^2,g^2\right]_{1,1}^{N_1-1,N_2}, \\ (\mathbf{f},\mathbf{g})_f & = & \left(f^1,g^1\right)_{f.} + \left(f^2,g^2\right)_{.f}, & \left(f,g^1+g^2\right)_f & = & \left(f,g^1\right)_{f.} + \left(f,g^2\right)_{.f}, \\ \left(f^1,g^1\right)_{b.} & = & \left[f^1,g^1\right]_{0,1}^{N_1-1,N_2-1}, & \left(f^2,g^2\right)_{.b} & = & \left[f^2,g^2\right]_{1,0}^{N_1-1,N_2-1}, \\ (\mathbf{f},\mathbf{g})_b & = & \left(f^1,g^1\right)_{b.} + \left(f^2,g^2\right)_{.b}, & \left(f,g^1+g^2\right)_b & = & \left(f,g^1\right)_{b.} + \left(f,g^2\right)_{.b}, \end{array} \tag{6.19}$$

Now we may proceed to some supporting lemmas.

Lemma 6.2.4. *Let $u : \overline{\omega}_h \to \mathbb{R}$, $\mathbf{v} : \overline{\omega}_h \to \mathbb{R}^2$. Then the following Green formulas are valid*

$$\begin{aligned} (\nabla_f u, \mathbf{v})_h &= -(u, \nabla_b \cdot \mathbf{v})_f + \sum_{l=1}^{N_2-1} h_2 \left(u_{N_1,l} v^1_{N_1,l} - u_{1l} v^1_{0l}\right) \\ &\quad + \sum_{k=1}^{N_1-1} h_1 \left(u_{k,N_2} v^2_{k,N_2} - u_{k1} v^2_{k0}\right), \end{aligned} \tag{6.20}$$

$$\begin{aligned} (\nabla_b u, \mathbf{v})_h &= -(u, \nabla_f \cdot \mathbf{v})_b + \sum_{l=1}^{N_2-1} h_2 \left(u_{N_1-1,l} v^1_{N_1,l} - u_{0l} v^1_{0l}\right) \\ &\quad + \sum_{k=1}^{N_1-1} h_1 \left(u_{k,N_2-1} v^2_{k,N_2} - u_{k0} v^2_{k0}\right). \end{aligned} \tag{6.21}$$

Proof. It is quite straightforward to show that for fixed $k = 0, \cdots N_1$, $l = 0, \cdots, N_2$ the following relations hold:

$$\left[u_{f.}, v^1\right]_{1,l}^{N_1-1,l} = -\left[u, v^1_{b.}\right]_{1,l}^{N_1,l} + h_2 \left(u_{N_1,l} v^1_{N_1,l} - u_{1l} v^1_{0l}\right), \tag{6.22}$$

$$\left[u_{b.}, v^1\right]_{1,l}^{N_1-1,l} = -\left[u, v^1_{f.}\right]_{0,l}^{N-1,l} + h_2 \left(u_{N_1-1,l} v^1_{N_1,l} - u_{0l} v^1_{0l}\right), \tag{6.23}$$

$$\left[u_{.f}, v^2\right]_{k,1}^{k,N_2-1} = -\left[u, v^2_{.b}\right]_{k,1}^{k,N_2} + h_1 \left(u_{k,N_2} v^2_{k,N_2} - u_{k1} v^2_{k0}\right), \tag{6.24}$$

$$\left[u_{.b}, v^2\right]_{k,1}^{k,N_1-1} = -\left[u, v^2_{.f}\right]_{k,0}^{k,N_2-1} + h_1 \left(u_{k,N_2-1} v^2_{k,N_2} - u_{k0} v^2_{k0}\right). \tag{6.25}$$

For example for (6.22) we have (see also [89])

$$
\begin{aligned}
&\left[u_{f.}, v^1\right]_{1,l}^{N_1-1,l} = \sum_{i=1}^{N_1-1} \frac{u_{i+1,l}-u_{i,l}}{h_1} v_{i,l}^1 h_1 h_2 = \sum_{i=1}^{N_1-1} u_{i,l} v_{i+1,l}^1 h_2 - \sum_{i=1}^{N_1-1} u_{i,l} v_{i,l}^1 h_2 \\
&= \sum_{i=2}^{N_1} u_{i,l} v_{i-1,l}^1 h_2 - \sum_{i=1}^{N_1-1} u_{i,l} v_{i,l}^1 h_2 = \sum_{i=2}^{N_1-1} u_{i,l}\left(v_{i-1,l}^1 - v_{i,l}^1\right) h_2 + \left(u_{N_1,l} v_{N_1-1,l}^1 - u_{1,l} v_{1,l}^1\right) h_2 \\
&= \sum_{i=2}^{N-1} u_{i,l}\left(v_{i-1,l}^1 - v_{i,l}^1\right) h_2 + \left[u_{N_1,l} v_{N_1,l} + u_{N_1,l}\left(v_{N_1-1,l}^1 - v_{N_1,l}^1\right) - u_{1,l} v_{0,l}^1 + u_{1,l}\left(v_{0,l}^1 - v_{1,l}^1\right)\right] h_2 \\
&= \left(u_{N_1,l} v_{N_1,l}^1 - u_{1,l} v_{0,l}^1\right) h_2 - \left[u, v_{b.}^1\right]_{1,l}^{N_1,l}.
\end{aligned}
$$

Now we have

$$
\begin{aligned}
&\left(\nabla_f u, \mathbf{v}\right)_h = \left(u_{f.}, v^1\right)_h + \left(u_{.f}, v^2\right) = \left[u_{f.}, v^1\right]_{1,1}^{N_1-1,N_2-1} + \left[u_{.f}, v^2\right]_{1,1}^{N_1-1,N_2-1} \\
&= \sum_{l=1}^{N_2-1} \left[u_{f.}, v^1\right]_{1,l}^{N_1-1,l} + \sum_{k=1}^{N_1-1} \left[u_{.f}, v^2\right]_{k,1}^{k,N_2-1} = -\sum_{l=1}^{N_2-1} \left(\left[u, v_{b.}^1\right]_{1,l}^{N_1,l} + h_2\left(u_{N_1,l} v_{N_1,l}^1 - u_{1l} v_{0l}^1\right)\right) \\
&- \sum_{k=1}^{N_1-1} \left(\left[u, v_{.b}^2\right]_{k,1}^{k,N_2} + h_1\left(u_{k,N_2} v_{k,N_2}^2 - u_{k1} v_{k0}^2\right)\right) = -\left[u, v_{b.}^1\right]_{1,1}^{N_1,N_2-1} \\
+ &\sum_{l=1}^{N_2-1} \left(h_2\left(u_{N_1,l} v_{N_1,l}^1 - u_{1l} v_{0l}^1\right)\right) - \left[u, v_{.b}^2\right]_{1,1}^{N_1-1,N_2} + \sum_{k=1}^{N_1-1} \left(h_1\left(u_{k,N_2} v_{k,N_2}^2 - u_{k1} v_{k0}^2\right)\right) \\
&= -\left(u, v_{b.}^1\right)_{f.} - \left(u, v_{.b}^2\right)_{.f} + \sum_{l=1}^{N_2-1} \left(h_2\left(u_{N_1,l} v_{N_1,l}^1 - u_{1l} v_{0l}^1\right)\right) + \sum_{k=1}^{N_1-1} \left(h_1\left(u_{k,N_2} v_{k,N_2}^2 - u_{k1} v_{k0}^2\right)\right) \\
&= -\left(u, \nabla_b \cdot \mathbf{v}\right)_f + \sum_{l=1}^{N_2-1} \left(h_2\left(u_{N_1,l} v_{N_1,l}^1 - u_{1l} v_{0l}^1\right)\right) + \sum_{k=1}^{N_1-1} \left(h_1\left(u_{k,N_2} v_{k,N_2}^2 - u_{k1} v_{k0}^2\right)\right),
\end{aligned}
$$

which is a proof of (6.20). The proof of (6.21) is analogous. □

Corollary 6.2.5. *Let $p, u, v : \overline{\omega}_h \to \mathbb{R}$ and assume $v \mid_{\partial\omega_h} \equiv 0$. Then the following equalities hold:*

$$
\left(\nabla_b \cdot \left(p \nabla_f u\right), v\right)_h = -\left(p \nabla_f u, \nabla_f v\right)_b, \tag{6.26}
$$

$$
\left(\nabla_f \cdot \left(p \nabla_b u\right), v\right)_h = -\left(p \nabla_b u, \nabla_b v\right)_f. \tag{6.27}
$$

Proof. The proof is trivial application of (6.20) and (6.21). □

Theorem 6.2.6. *For the solution of (6.13)-(6.14) u^h, w^h and $w^h \mid_{\partial\omega_h} \equiv 0$ the following equality holds:*

$$
\left(\left(u_t^h\right)^2, \frac{1}{Q^h}\right)_h + \frac{\mathrm{d}}{\mathrm{d}t}\left(\left(H^h\right)^2, Q^h\right)_h = 0. \tag{6.28}
$$

Proof. We start with the equation for w_{ij}^h (6.14), divide by Q_{ij}^h, multiply by ξ_{ij} vanishing on $\partial\omega_h$ and sum over ω.

$$
\left(\frac{w^h}{Q^h}, \xi\right)_h = \left(\nabla_b \cdot \left(\frac{\nabla_f u^h}{Q^h}\right), \xi\right)_h.
$$

The Green theorem (6.26) gives

$$\left(\frac{w^h}{Q^h}, \xi\right)_h = -\left(\left(\frac{\nabla_f u_{ij}^h}{Q_{ij}^h}\right), \nabla_f \xi\right)_f. \tag{6.29}$$

Now consider the right hand side of (6.13), multiply it by the test function φ vanishing at $\partial\omega_h$, summing over ω_h and applying again the Green theorem (6.26) to obtain

$$\left(-\nabla_b \cdot \left(\mathbb{E}^h \nabla_f w^h - \frac{1}{2}\frac{\left(w^h\right)^2}{\left(Q^h\right)^3}\nabla_f u^h\right), \varphi\right)_h = \left(\mathbb{E}^h \nabla_f w^h - \frac{1}{2}\frac{\left(w^h\right)^2}{\left(Q^h\right)^3}\nabla_f u^h, \nabla_f \varphi\right)_f. \tag{6.30}$$

Differentiating (6.29) with respect to t we obtain

$$\begin{aligned}
&\frac{d}{dt}\left(\frac{w^h}{Q^h}, \xi\right)_h + \frac{d}{dt}\left(\left(\frac{\nabla_f u^h}{Q^h}\right), \nabla_f \xi\right)_f \\
= \;&\frac{d}{dt}\left(\frac{w^h}{Q^h}, \xi\right)_h + \left(\frac{Q^h \nabla_f \partial_t u^h - \partial_t Q^h \nabla_f u^h}{\left(Q^h\right)^2}, \nabla_f \xi\right)_f \\
= \;&\left(\frac{w_t^h}{Q^h}, \xi\right)_h - \left(\frac{Q_t^h \cdot w^h}{\left(Q^h\right)^2}, \xi\right)_h + \left(\mathbb{E}^h \nabla_f u_t^h, \nabla_f \xi\right)_f = 0,
\end{aligned}$$

where we used

$$\partial_t Q^h = \frac{\nabla_f \partial_t u^h \cdot \nabla_f u^h}{Q^h},$$

and so

$$\frac{Q^h \nabla_f \partial_t u^h - \partial_t Q^h \nabla_f u^h}{\left(Q^h\right)^2} = \frac{\partial_t \nabla_f u^h}{Q^h} - \frac{\left(\partial_t \nabla_f u^h \cdot \nabla_f u^h\right)\nabla_f u^h}{\left(Q^h\right)^2} = \frac{1}{Q^h}\left(\mathbb{I} - \left(\frac{\nabla_f u^h}{Q^h} \otimes \frac{\nabla_f u^h}{Q^h}\right)\right) = \mathbb{E}^h$$

Substitution $\xi = w^h$ gives

$$\left(\frac{w_t^h}{Q^h}, w^h\right)_h - \left(\frac{Q_t^h}{\left(Q^h\right)^2}, \left(w^h\right)^2\right)_h + \left(\mathbb{E}^h \nabla_f u_t^h, \nabla_f w^h\right)_f = 0, \tag{6.31}$$

and a substitution $\varphi = u_t^h$ in (6.30) gives

$$\left(\left(u_t^h\right)^2, \frac{1}{Q^h}\right)_h - \left(\mathbb{E}^h \nabla_f w^h - \frac{1}{2}\frac{\left(w^h\right)^2}{\left(Q^h\right)^3}\nabla_f u^h, \nabla_f u_t^h\right)_f = 0. \tag{6.32}$$

Adding (6.31) to (6.32) and using the symmetry of $\mathbb{E}^h$ we have

$$\left(\left(u_t^h\right)^2, \frac{1}{Q^h}\right)_h + \left(\frac{w_t^h}{Q^h}, w^h\right)_h - \left(\frac{Q_t^h}{\left(Q^h\right)^2}, \left(w^h\right)^2\right)_h + \frac{1}{2}\left(\frac{\left(w^h\right)^2}{\left(Q^h\right)^3}, \nabla_f u^h \cdot \nabla_f u_t^h\right)_f = 0. \tag{6.33}$$

Since $\nabla_f u^h \cdot \nabla_f u_t^h = Q^h \cdot Q_t^h$ we get

$$\left(\left(u_t^h\right)^2, \frac{1}{Q^h}\right)_h + \left(\frac{w_t^h}{Q^h}, w^h\right)_h - \left(\frac{Q_t^h}{\left(Q^h\right)^2}, \left(w^h\right)^2\right)_h + \frac{1}{2}\left(\frac{\left(w^h\right)^2}{\left(Q^h\right)^2}, Q_t^h\right)_f = 0, \tag{6.34}$$

which is equivalent to

$$\left(\left(u_t^h\right)^2, \frac{1}{Q^h}\right)_h + \left(\frac{w_t^h}{\left(Q^h\right)^2}, w^h\right)_h - \frac{1}{2}\left(\frac{Q_t^h}{\left(Q^h\right)^2}, \left(w^h\right)^2\right)_h = 0, \tag{6.35}$$

because for $w^h \mid_{\partial\omega} \equiv 0$

$$\left(\frac{\left(w^h\right)^2}{\left(Q^h\right)^2}, Q_t^h\right)_f = \left(\frac{\left(w^h\right)^2}{\left(Q^h\right)^2}, Q_t^h\right)_h .$$

Finally from (6.35) we have

$$\left(\left(u_t^h\right)^2, \frac{1}{Q^h}\right)_h + \frac{1}{2}\frac{d}{dt}\left(\left(H_\gamma^h\right)^2, Q^h\right)_h = 0.$$

□

Remark: Numerical experiments (7.2.1)-(7.2.4) demonstrate that the schemes based on the forward and the backward differences is sufficient for the mean-curvature flow and the surface diffusion flow of graphs (at least for the isotropic problems). However, in the case of the Willmore flow one can see very strong deformation of the solution. It is caused by a non-symmetric stencil of the numerical scheme - see Figure 6.1. In what follows we will try to solve this problem by use of the central differences.

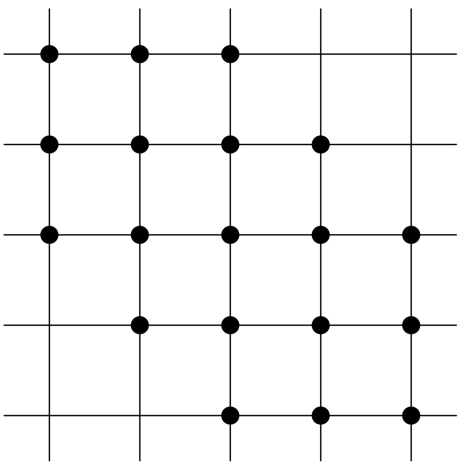

Figure 6.1.: Non-symmetric stencil of the numerical scheme (6.2.3)

6.2.2. Semidiscrete scheme based on central finite differences

The central-difference approach yields a symmetric scheme (see Oberhuber [82]). The central differences are defined as:

$$u^h_{c.,ij} := \frac{u^h_{i+1,j} - u^j_{i-1,j}}{2h_1}, \qquad u^h_{.c,ij} := \frac{u^h_{i,j+1} - u^h_{i,j-1}}{2h_2}, \tag{6.36}$$

$$\nabla_c u_{ij} := \left(u^h_{c.,ij}, u^h_{.c,ij}\right). \tag{6.37}$$

As well as in case of the one-sided differences, the discrete operator is approximated in the same way as the discrete gradient. We have

$$u^h_{c.,ij} = \frac{1}{2}\left(u^h_{f.,ij} + u^h_{b.,ij}\right) \text{ and } u^h_{.c,ij} = \frac{1}{2}\left(u^h_{.f,ij} + u^h_{.b,ij}\right). \tag{6.38}$$

We denote

$$
\begin{aligned}
\bar{Q}^h_{ij} &= \sqrt{1+\frac{1}{2}\left(u^2_{\bar{f}.,ij}+u^2_{\bar{b}.,ij}+u^2_{.f,ij}+u^2_{.\bar{b},ij}\right)},\\
Q^h_{ij} &= \sqrt{1+u^2_{c.,ij}+u^2_{.c,ij}},\\
R_{visc} &= C_{visc}\bar{Q}^h_{ij}\left(h_1^2\left(u^h_{\bar{b}.ij}\right)_{f.,ij}+h_2^2\left(u^h_{.\bar{b},ij}\right)_{.f,ij}\right),
\end{aligned}
$$

for $i=1,\cdots,N_1-1,\quad j=0,\cdots,N_2-1$

Remark 6.2.7. It is known that the approximation by the central differences requires functions of higher regularity at least $u\in C^2(\Omega)$. If this condition is not fulfilled oscillations may appear as Figure 6.2 demonstrates. It is the reason why we introduce the artificial viscosity term (6.39) to keep the approximate grid function u^h_{ij} smooth enough.

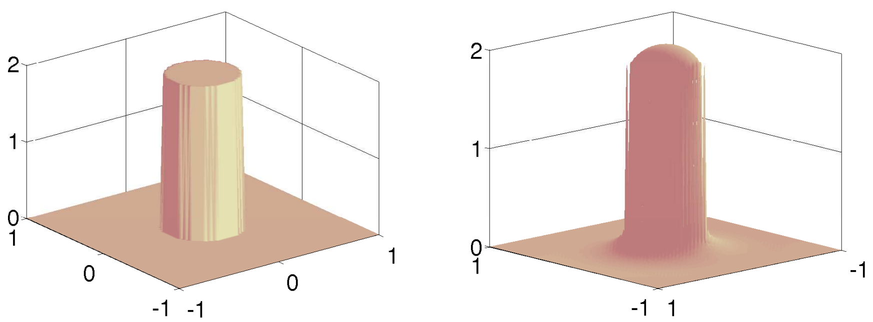

Figure 6.2.: Oscilations which may appear when the explicit central finite difference numerical scheme (6.3.5) is applied. The figure shows initial condition (on the left) and the evolution of the graph by the mean of the Willmore flow. On the right, there is a state of the evolution at time $t=0.0006$.

The necessity of setting the parameter R_{visc} is a disadvantage of the central-difference schemes. Numerical schemes based on complementary finite volumes avoid this. It is a reason why we do not study the anisotropic and the level-set formulation in this section.

The central schemes have the following forms:

Scheme 6.2.8. The **central finite difference** semi-discrete approximation of the **mean-curvature flow of graphs with the Dirichlet boundary conditions** is given by

$$
\begin{aligned}
\frac{du^h_{ij}}{dt} &= Q^h_{ij}\nabla_c\cdot\left(\frac{\nabla_c u^h_{ij}}{Q^h_{ij}}\right)+R_{visc}\text{ on }\omega_h, && (6.39)\\
u^h_{ij}\,|_{t=0} &= \mathcal{P}\left(u_{ini}\right)_{ij}\ \text{ on }\overline{\omega}_h && (6.40)\\
u^h_{ij} &= g_{ij}\text{ on }\partial\omega_h.
\end{aligned}
$$

The **central finite difference** semi-discrete approximation of the **mean-curvature flow of graphs with the Neumann boundary conditions** is given by (6.39)–(6.40) and

$$\partial^h_\nu u^h_{ij}=0\text{ on }\partial\omega_h.$$

Scheme 6.2.9. The **central finite difference** semi-discrete approximation of the **Willmore flow of graphs with the Dirichlet boundary conditions** is given by

$$
\begin{aligned}
\frac{du_{ij}^h}{dt} &= -\bar{Q}_{ij}^h \nabla_c \cdot \left(\frac{1}{Q_{ij}^h} \begin{pmatrix} 1 - \frac{u_{c.,ij}^2}{\left(Q_{ij}^h\right)^2} & -\frac{u_{c.,ij}u_{.c,ij}}{\left(Q_{ij}^h\right)^2}, \\ -\frac{u_{c.,ij}u_{.c,ij}}{\left(Q_{ij}^h\right)^2} & 1 - \frac{u_{.c,ij}^2}{\left(Q_{ij}^h\right)^2} \end{pmatrix} \nabla_c w_{ij}^h - \frac{1}{2} \frac{\left(w_{ij}^h\right)^2}{\left(Q_{ij}^h\right)^3} \nabla_c u_{ij}^h \right) \\
&+ R_{visc} \text{ on } \omega_h, &(6.41) \\
w_{ij}^h &= Q_{ij}^h \nabla_c \cdot \left(\frac{\nabla_c u_{ij}^h}{Q_{ij}^h} \right), \text{ on } \omega_h, &(6.42) \\
u_{ij}^h \mid_{t=0} &= \mathcal{P}\left(u_{ini}\right)_{ij} \text{ on } \overline{\omega}_h, &(6.43) \\
u_{ij}^h &= g_{ij} \text{ and } w_{ij}^h = 0 \text{ on } \partial\omega_h. &(6.44)
\end{aligned}
$$

The **central finite difference** semi-discrete approximation of the **Willmore flow of graphs with the Neumann boundary conditions** is given by (6.41)–(6.43) and

$$\partial_\nu^h u_{ij}^h = 0 \text{ and } \partial_\nu^h w_{ij}^h = 0 \text{ on } \partial\omega_h.$$

Remark 6.2.10. Since the stencil of the schemes (6.2.8) and (6.2.9) is larger then in case of the one-sided schemes, we need to evaluate the first derivatives on $\overline{\omega}_h$ to be able to approximate the second derivatives on ω_h (and the same is true also for the third and the fourth derivatives). For this purpose, we replace central differences for the approximation of the first and the third derivatives at the boundaries of ω_h by forward resp. backward differences depending on which ones are appropriate.

Energy equality for the Willmore flow of graphs with central differences

As in the previous section, we would like to gain an equality similar to (5.2.11). Once we become aware of (6.38) the proof is straightforward.

Lemma 6.2.11. *Let $u : \overline{\omega}_h \to \mathbb{R}$, $\mathbf{v} : \overline{\omega}_h \to \mathbb{R}^2$. Then the Green formula is valid*

$$
\begin{aligned}
(\nabla_c u, \mathbf{v})_h &= -\frac{1}{2}\left[(u, \nabla_b \cdot \mathbf{v})_f + (u, \nabla_f \cdot \mathbf{v})_b \right] &(6.45) \\
&+ \sum_{l=1}^{N_2-1} \frac{h_2}{2} \left(u_{N_1,l} v_{N_1,l}^1 - u_{1l} v_{0l}^1 + u_{N_1-1,l} v_{N_1,l}^1 - u_{0l} v_{0l}^1 \right) \\
&+ \sum_{k=1}^{N_1-1} \frac{h_1}{2} \left(u_{k,N_2} v_{k,N_2}^2 - u_{k1} v_{k0}^2 + u_{k,N_2-1} v_{k,N_2}^2 - u_{k0} v_{k0}^2 \right). &(6.46)
\end{aligned}
$$

Proof. The proof follows directly from (6.20) and (6.21) by writing

$$(\nabla_c u, \mathbf{v})_h = \left(\frac{1}{2} \left(\nabla_f u + \nabla_b u \right), \mathbf{v} \right)_h.$$

□

Corollary 6.2.12. *Let $p, u, v : \overline{\omega}_h \to \mathbb{R}$ and assume $v \mid_{\partial\omega_h} \equiv 0$. Then the following equality holds:*

$$(\nabla_c u, \mathbf{v})_h = -\frac{1}{2}\left[(u, \nabla_b \cdot \mathbf{v})_f + (u, \nabla_f \cdot \mathbf{v})_b \right]. \tag{6.47}$$

Theorem 6.2.13. *For the solution of (6.41)-(6.42) u^h, w^h and $w^h \mid_{\partial\omega_h} \equiv 0$, the following equality holds:*

$$\left(\left(u_t^h\right)^2, \frac{1}{Q^h}\right)_h + \frac{\mathrm{d}}{\mathrm{d}t}\left[\left(\left(H^h\right)^2, Q^h\right)_h - C_{visc}\frac{h^2}{2}\left(\nabla_b^h u^h, \nabla_b^h u^h\right)_h\right] = 0, \tag{6.48}$$

where for simplicity we assume $h = h_1 = h_2$.

Proof. To proof is very similar to (6.2.6). Taking (6.42), divide by Q_{ij}^h, multiply by ξ_{ij} vanishing on $\partial\omega_h$, summing over ω and applying (6.47 gives

$$\left(\frac{w^h}{Q^h}, \xi\right)_h = -\frac{1}{2}\left[\left(\left(\frac{\nabla_c u_{ij}^h}{Q_{ij}^h}\right), \nabla_f \xi\right)_f + \left(\left(\frac{\nabla_c u_{ij}^h}{Q_{ij}^h}\right), \nabla_b \xi\right)_b\right] \tag{6.49}$$

Repeating the same with the right hand side of (6.41) and the test function φ vanishing at $\partial\omega_h$ leads to

$$\begin{aligned}\left(-\nabla_c \cdot \left(\mathbb{E}^h \nabla_c w^h - \frac{1}{2}\frac{\left(w^h\right)^2}{\left(Q^h\right)^3}\nabla_c u^h\right), \varphi\right)_h &= \frac{1}{2}\left[\left(\mathbb{E}^h \nabla_c w^h - \frac{1}{2}\frac{\left(w^h\right)^2}{\left(Q^h\right)^3}\nabla_c u^h, \nabla_f \varphi\right)_f\right.\\ &\left.+\left(\mathbb{E}^h \nabla_c w^h - \frac{1}{2}\frac{\left(w^h\right)^2}{\left(Q^h\right)^3}\nabla_c u^h, \nabla_b \varphi\right)_b\right],\end{aligned} \tag{6.50}$$

where

$$\mathbb{E}^h = \frac{1}{Q_{ij}^h}\begin{pmatrix} 1 - u_{c.,ij}^2 & -u_{c.,ij}u_{.c,ij} \\ -u_{c.,ij}u_{.c,ij} & 1 - u_{.c,ij}^2 \end{pmatrix}.$$

Differentiating (6.49) with respect to t we have

$$\left(\frac{w_t^h}{Q^h}, \xi\right)_h - \left(\frac{Q_t^h \cdot w^h}{\left(Q^h\right)^2}, \xi\right)_h + \frac{1}{2}\left[\left(\mathbb{E}^h \nabla_c u_t^h, \nabla_f \xi\right)_f + \left(\mathbb{E}^h \nabla_c u_t^h, \nabla_b \xi\right)_b\right] = 0.$$

Substituting $\xi = w^h$ and applying $w^h \mid_{\partial\omega_h}$ gives

$$\left(\frac{w_t^h}{Q^h}, w^h\right)_h - \left(\frac{Q_t^h}{\left(Q^h\right)^2}, \left(w^h\right)^2\right)_h + \left(\mathbb{E}^h \nabla_c u_t^h, \nabla_c w^h\right)_h = 0, \tag{6.51}$$

and a substitution $\varphi = u_t^h$ in (6.30) together with $u_t^h \mid_{\partial\omega_h} \equiv 0$ (we assume the Dirichlet boundary conditions) gives

$$\left(\left(u_t^h\right)^2, \frac{1}{Q^h}\right)_h - \left(\mathbb{E}^h \nabla_c w^h - \frac{1}{2}\frac{\left(w^h\right)^2}{\left(Q^h\right)^3}\nabla_c u^h, \nabla_c u_t^h\right)_h = 0. \tag{6.52}$$

Adding (6.51) to (6.52), using the symmetry of $\mathbb{E}^h$ and the fact that $\nabla_c u^h \cdot \nabla_c u_t^h = Q^h \cdot Q_t^h$ we have

$$\left(\left(u_t^h\right)^2, \frac{1}{Q^h}\right)_h + \left(\frac{w_t^h}{\left(Q^h\right)^2}, w^h\right)_h - \frac{1}{2}\left(\frac{Q_t^h}{\left(Q^h\right)^2}, \left(w^h\right)^2\right)_h = 0, \tag{6.53}$$

and

$$\left(\left(u_t^h\right)^2, \frac{1}{Q^h}\right)_h + \frac{1}{2}\frac{d}{dt}\left(\left(H^h\right)^2, Q^h\right)_h = 0.$$

For the viscose term R_{visc} we have $R_{visc} = C_{visc} h^2 \nabla_f^h \nabla_b^h u^h$. Multiplying by φ vanishing on $\partial\omega^h$ we get

$$\left(C_{visc} h^2 \nabla_f^h \nabla_b^h u^h, \varphi\right)_h = -C_{visc} h^2 \left(\nabla_b^h u^h, \nabla_b^h \varphi\right)_f = -C_{visc} h^2 \left(\nabla_b^h u^h, \nabla_b^h \varphi\right)_h .$$

The last equality holds since $\varphi\,|_{\partial\omega^h} = 0$. Setting $\varphi = u_t^h$ we obtain

$$-C_{visc} h^2 \left(\nabla_b^h u^h, \nabla_b^h u_t^h\right)_h = -C_{visc} \frac{h^2}{2} \frac{d}{dt} \left(\nabla_b^h u^h, \nabla_b^h u^h\right)_h .$$

□

Remark: Unfortunately, from (6.48) we can not claim that $\left(H^h\right)^2 Q^h$ is decreasing when C_{visc} is non-zero. The viscosity term is main problem of this scheme. In the next section, we will try to avoid it. The Figure 6.3 shows the stencil for the central schemes applied to the fourth order problems. For the isotropic problem it is a 41 point stencil. Another disadvantage of the scheme is the fact that the matrix arising in a semi-implicit scheme would have many non-zero elements.

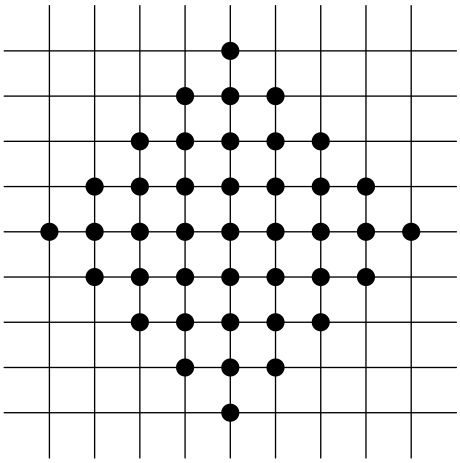

Figure 6.3.: Stencil of the numerical scheme (6.2.9) is symmetric, however it is very large.

6.2.3. Semidiscrete scheme based on the finite volume method

The third class of the numerical schemes is based on the method of the finite volumes. More precisely, we follow complementary volume concept introduced by Walkington [99] who combined the complementary volumes with the finite elements . Handlovičová, Mikula and Sgallari [55] applied similar scheme in image processing. For the level-set formulation of the Willmore flow, we introduced the complementary finite volume scheme in [13]. We restrict ourselves only to $\Omega \subset \mathbb{R}^2$. First we demonstrate the finite volume principles of the scheme. Later in this section we derive the same scheme with the finite difference approach which will allow to prove the energy equality (5.2.11).

Complementary finite volumes

For the purpose of this section we define the dual mesh V_h as

$$\begin{aligned} V_h \equiv & \left\{ v_{ij} = \left\langle \left(i - \frac{1}{2}\right) h_1, \left(i + \frac{1}{2}\right) h_1 \right\rangle \times \left\langle \left(j - \frac{1}{2}\right) h_2, \left(j + \frac{1}{2}\right) h_2 \right\rangle \mid \right. \\ & \left. i = 1 \cdots N_1 - 1, j = 1 \cdots N_2 - 1 \right\}. \end{aligned} \tag{6.54}$$

For $0 < i < N_1$, $0 < j < N_2$, i and j fixed, consider a volume v_{ij} of the dual mesh V_h, denote its interior as Ω_{ij}, its boundary as Γ_{ij} and let $\mu(\Omega_{ij})$ be the volume of Ω_{ij}. We also denote all the neighbouring volumes of the volume v_{ij} as $\mathcal{N}_{ij}$. For all finite volumes v_{ij} of the dual mesh V_h, the boundary Γ_{ij} consists of four linear segments. We denote them as $\Gamma_{ij,\bar{i}\bar{j}}$. It means that $\Gamma_{ij,\bar{i}\bar{j}}$ is a boundary of the finite volume v_{ij} between nodes (i,j) and $(\bar{i},\bar{j})$. By $l_{ij,\bar{i}\bar{j}}$ we denote the length of this part of Γ_{ij}.

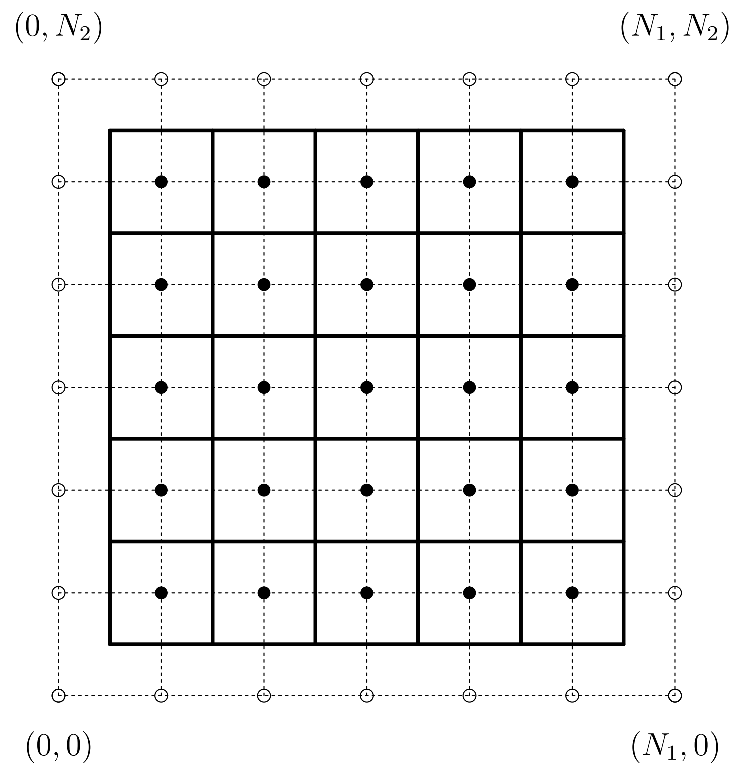

Figure 6.4.: Dual mesh (6.54) for the complementary finite volumes method - circles denote $\partial\omega_h$, dots denote ω_h and solid lines stand for V_h.

Evaluation of isotropic mean curvature of graphs We start with the equation for the isotropic mean curvature

$$H = \nabla \cdot \left(\frac{\nabla \varphi}{Q} \right)$$

which we integrate over the finite volume v_{ij} and apply the Stokes theorem (A.0.7)

$$\int_{\Omega_{ij}} H \mathrm{dx} = \int_{\Omega_{ij}} \nabla \cdot \left(\frac{\nabla \varphi}{Q} \right) \mathrm{dx} = \int_{\Gamma_{ij}} \frac{\nabla \varphi}{Q} \cdot \nu \mathrm{d}\mathcal{H}^{n-1}, \tag{6.55}$$

where ν denotes the outer unit normal vector to the finite volume boundary Γ_{ij}. If Γ_{ij} is a part of the boundary of V_h we set in agreement with (5.28) $\nabla\varphi \cdot \nu = 0$. We approximate the term on the left as

$$\int_{\Omega_{ij}} H \mathrm{dx} \approx \mu(\Omega_{ij}) H^h_{ij} \tag{6.56}$$

and the term on the right as

$$\int_{\Gamma_{ij}} \frac{\nabla \varphi}{Q} \cdot \nu \mathrm{d}\mathcal{H}^{n-1} = \sum_{v_{\bar{i}\bar{j}} \in \mathcal{N}_{ij}} \int_{\Gamma_{ij,\bar{i}\bar{j}}} \frac{\nabla \varphi}{Q} \cdot \nu \mathrm{d}\mathcal{H}^{n-1} \tag{6.57}$$

For the inner finite volume $v_{ij} \in V_h$, there are four different neighbours $v_{\bar{i}\bar{j}} \in \mathcal{N}_{ij}$. All the boundaries $\Gamma_{ij,\bar{i}\bar{j}}$ are linear segments and so $\nu = \nu_{ij,\bar{i}\bar{j}}$ is constant there. Moreover we assume that $\nabla\varphi$ and Q are constant along $\Gamma_{ij,\bar{i}\bar{j}}$ too. It gives

$$\sum_{v_{\bar{i}\bar{j}} \in \mathcal{N}_{ij}} \int_{\Gamma_{ij,\bar{i}\bar{j}}} \frac{\nabla\varphi}{Q} \cdot \nu \mathrm{d}\mathcal{H}^{n-1} \approx \sum_{v_{\bar{i}\bar{j}} \in \mathcal{N}_{ij}} l_{ij,\bar{i}\bar{j}} \frac{\nabla\varphi^h_{ij,\bar{i}\bar{j}}}{Q^h_{ij,\bar{i}\bar{j}}} \cdot \nu_{ij,\bar{i}\bar{j}} \tag{6.58}$$

Putting (6.56) and (6.58) together we get

$$H^h_{ij} \approx \frac{1}{\mu(\Omega_{ij})} \sum_{v_{\bar{i}\bar{j}} \in \mathcal{N}_{ij}} l_{ij,\bar{i}\bar{j}} \frac{\nabla\varphi^h_{ij,\bar{i}\bar{j}}}{Q^h_{ij,\bar{i}\bar{j}}} \cdot \nu_{ij,\bar{i}\bar{j}}. \tag{6.59}$$

For the dual mesh V_h given by (6.54), we may substitute $\mu(\Omega_{ij}) = h_1 h_2$. For v_{ij}, $v_{\bar{i}\bar{j}}$ such that $\nu_{ij,\bar{i}\bar{j}} = (\pm 1, 0)$ we have $l_{ij,\bar{i}\bar{j}} = h_2$ and if $\nu_{ij,\bar{i}\bar{j}} = (0, \pm 1)$ then $l_{ij,\bar{i}\bar{j}} = h_1$. We also see that for fixed finite volume v_{ij} one of its neighbours is determined by the form of the normal $\nu_{ij,\bar{i}\bar{j}}$ of the boundary $\Gamma_{ij,\bar{i}\bar{j}}$. There are four possibilities for the normal $\nu_{ij,\bar{i}\bar{j}}$. For $r, s \in \{-1, 1\}$ and $|r| + |s| = 1$ the unit outer normal $\nu_{ij,\bar{i}\bar{j}}$ can take the values $\nu_{ij,\bar{i}\bar{j}} = (r, s)$ when $\bar{i} = i + r$ and $\bar{j} = j + s$ - see Figure 6.5. The complementary finite volume isotropic mean curvature approximation from (6.59) then reads

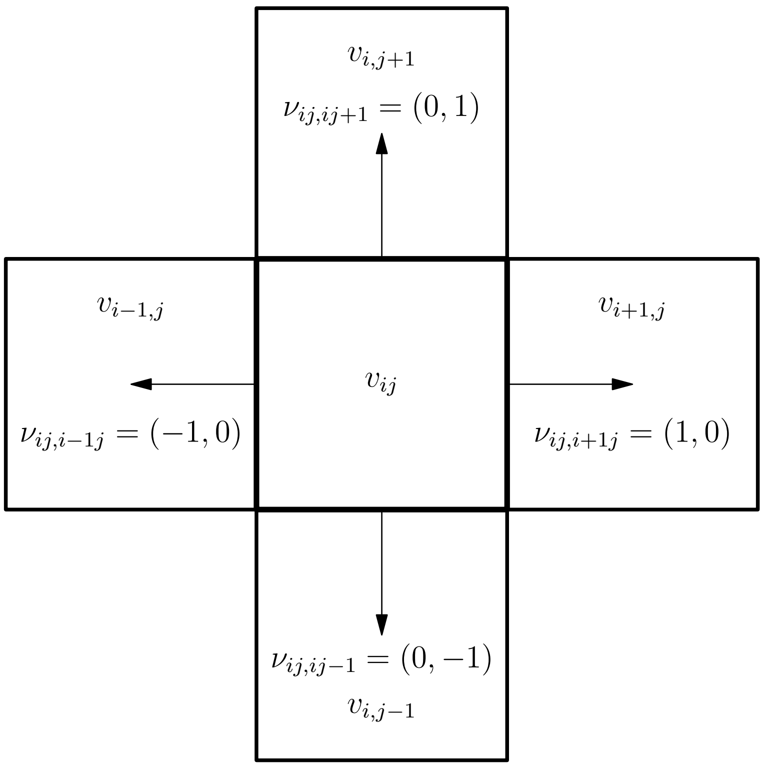

Figure 6.5.: Notation $\nu_{ij,\bar{i}\bar{j}}$.

$$
\begin{aligned}
H_{ij}^h &\approx \frac{1}{h_1 h_2}\Bigg(l_{ij,i+1j}\frac{\nabla\varphi_{ij,i+1j}^h}{Q_{ij,i+1j}^h}\cdot\nu_{ij,i+1j} + l_{ij,ij+1}\frac{\nabla\varphi_{ij,ij+1}^h}{Q_{ij,ij+1}^h}\cdot\nu_{ij,ij+1} \\
&+ l_{ij,i-1j}\frac{\nabla\varphi_{ij,i-1j}^h}{Q_{ij,i-1j}^h}\cdot\nu_{ij,i-1j} + l_{ij,ij-1}\frac{\nabla\varphi_{ij,ij-1}^h}{Q_{ij,ij-1}^h}\cdot\nu_{ij,ij-1}\Bigg) \\
&= \frac{1}{h_1 h_2}\Bigg(h_2\frac{\nabla\varphi_{ij,i+1j}^h}{Q_{ij,i+1j}^h}\cdot(1,0)^T + h_1\frac{\nabla\varphi_{ij,ij+1}^h}{Q_{ij,ij+1}^h}\cdot(0,1)^T \\
&+ h_2\frac{\nabla\varphi_{ij,i-1j}^h}{Q_{ij,i-1j}^h}\cdot(-1,0)^T + h_1\frac{\nabla\varphi_{ij,ij-1}^h}{Q_{ij,ij-1}^h}\cdot(0,-1)^T\Bigg) \\
&= \left(\frac{\partial_{x_1}^h\varphi_{ij,i+1j}^h}{h_1 Q_{ij,i+1j}^h} + \frac{\partial_{x_2}^h\varphi_{ij,ij+1}^h}{h_2 Q_{ij,ij+1}^h} - \frac{\partial_{x_1}^h\varphi_{ij,i-1j}^h}{h_1 Q_{ij,i-1j}^h} - \frac{\partial_{x_2}^h\varphi_{ij,ij-1}^h}{h_2 Q_{ij,ij-1}^h}\right) \\
&= \left(\frac{\varphi_{i+1j}^h - \varphi_{ij}^h}{h_1^2 Q_{ij,i+1j}^h} + \frac{\varphi_{ij+1}^h - \varphi_{ij}^h}{h_2^2 Q_{ij,ij+1}^h} - \frac{\varphi_{ij}^h - \varphi_{i-1j}^h}{h_1^2 Q_{ij,i-1j}^h} - \frac{\varphi_{ij}^h - \varphi_{ij-1}^h}{h_2^2 Q_{ij,ij-1}^h}\right).
\end{aligned}
\tag{6.60}
$$

We set

$$Q_{ij,i+1j}^h = \sqrt{1 + \left(\partial_{x_1}^h\varphi_{ij,i+1j}^h\right)^2 + \left(\partial_{x_2}^h\varphi_{ij,i+1j}^h\right)^2}, \tag{6.61}$$

$$Q_{ij,ij+1}^h = \sqrt{1 + \left(\partial_{x_1}^h\varphi_{ij,ij+1}^h\right)^2 + \left(\partial_{x_2}^h\varphi_{ij,ij+1}^h\right)^2}, \tag{6.62}$$

$$Q_{ij,i-1j}^h = \sqrt{1 + \left(\partial_{x_1}^h\varphi_{ij,i-1j}^h\right)^2 + \left(\partial_{x_2}^h\varphi_{ij,i-1j}^h\right)^2}, \tag{6.63}$$

$$Q_{ij,ij-1}^h = \sqrt{1 + \left(\partial_{x_1}^h\varphi_{ij,ij-1}^h\right)^2 + \left(\partial_{x_2}^h\varphi_{ij,ij-1}^h\right)^2}, \tag{6.64}$$

for

$$\partial_{x_1}^h\varphi_{ij,i+1j}^h = \frac{\varphi_{i+1j}^h - \varphi_{ij}^h}{h_1} \quad , \quad \partial_{x_1}^h\varphi_{ij,i-1j}^h = \frac{\varphi_{ij}^h - \varphi_{i-1j}^h}{h_1}, \tag{6.65}$$

$$\partial_{x_2}^h\varphi_{ij,ij+1}^h = \frac{\varphi_{ij+1}^h - \varphi_{ij}^h}{h_2} \quad , \quad \partial_{x_2}^h\varphi_{ij,ij-1}^h = \frac{\varphi_{ij}^h - \varphi_{ij-1}^h}{h_2}, \tag{6.66}$$

and

$$\partial_{x_2}^h\varphi_{ij,i+1j}^h = \frac{\varphi_{ij,i+1j+1}^h - \varphi_{ij,i+1j-1}^h}{h_2} \quad , \quad \partial_{x_2}^h\varphi_{ij,i-1j}^h = \frac{\varphi_{ij,i-1j+1}^h - \varphi_{ij,i-1j-1}^h}{h_2}, \tag{6.67}$$

$$\partial_{x_1}^h\varphi_{ij,ij+1}^h = \frac{\varphi_{ij,i+1j+1}^h - \varphi_{ij,i-1j+1}^h}{h_1} \quad , \quad \partial_{x_1}^h\varphi_{ij,ij-1} = \frac{\varphi_{ij,i+1j-1} - \varphi_{ij,i-1j-1}}{h_1}, \tag{6.68}$$

where we denote (see Figure 6.6).

$$\varphi_{ij,i+1j+1}^h = \frac{1}{4}\left(\varphi_{ij}^h + \varphi_{i+1j}^h + \varphi_{ij+1}^h + \varphi_{i+1j+1}^h\right) \tag{6.69}$$

$$\varphi_{ij,i+1j-1}^h = \frac{1}{4}\left(\varphi_{ij}^h + \varphi_{i+1j}^h + \varphi_{ij-1}^h + \varphi_{i+1j-1}^h\right) \tag{6.70}$$

$$\varphi_{ij,i-1j+1}^h = \frac{1}{4}\left(\varphi_{ij}^h + \varphi_{i-1j}^h + \varphi_{ij+1}^h + \varphi_{i-1j+1}^h\right) \tag{6.71}$$

$$\varphi_{ij,i-1j-1}^h = \frac{1}{4}\left(\varphi_{ij}^h + \varphi_{i-1j}^h + \varphi_{ij-1}^h + \varphi_{i-1j-1}^h\right). \tag{6.72}$$

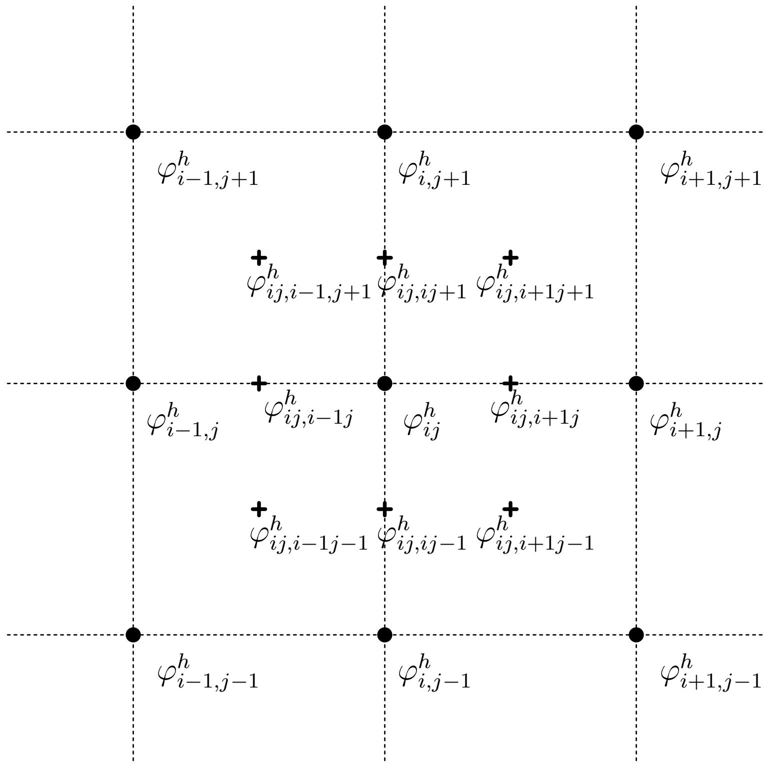

Figure 6.6.: Notation $\varphi^h_{ij,\overline{ij}}$ on the dual mesh.

In the case of the Neumann boundary conditions from (5.13) or (5.49) we set:

$$\text{if } i=1 \text{ then } \nu=(-1,0) \quad \Rightarrow \quad \frac{\varphi^h_{1j}-\varphi^h_{0j}}{h_1}=0 \Rightarrow \varphi^h_{0j}=\varphi^h_{1j}, \tag{6.73}$$

$$\text{if } i=N_1-1 \text{ then } \nu=(1,0) \quad \Rightarrow \quad \frac{\varphi^h_{N_1j}-\varphi^h_{N_1-1j}}{h_1}=0 \Rightarrow \varphi^h_{N_1j}=\varphi^h_{N_1-1j}, \tag{6.74}$$

$$\text{if } j=1 \text{ then } \nu=(0,-1) \quad \Rightarrow \quad \frac{\varphi^h_{i1}-\varphi^h_{i0}}{h_2}=0 \Rightarrow \varphi^h_{i0}=\varphi^h_{i1}, \tag{6.75}$$

$$\text{if } j=N_2-1 \text{ then } \nu=(0,1) \quad \Rightarrow \quad \frac{\varphi^h_{iN_2}-\varphi^h_{iN_2-1}}{h_2}=0 \Rightarrow \varphi^h_{iN_2}=\varphi^h_{iN_2-1}. \tag{6.76}$$

Approximation of isotropic Willmore flow of graphs We first need to approximate

$$w^h_{ij}=Q^h_{ij}H^h_{ij}. \tag{6.77}$$

H^h_{ij} is given by (6.60). For Q^h_{ij} we set

$$Q^h_{ij}=\frac{1}{4}\left(Q^h_{ij,i+1j}+Q^h_{ij,ij+1}+Q^h_{ij,i-1j}+Q^h_{ij,ij-1}\right). \tag{6.78}$$

Integrating (5.45) over Ω_{ij} and applying the Stokes theorem we get

$$\int_{\Omega_{ij}}\frac{1}{Q}\partial_t\varphi \mathrm{dx} \quad = \quad -\int_{\Gamma_{ij}}\mathbb{E}\nabla w\nu-\frac{1}{2}\frac{w^2}{Q^3}\partial_\nu\varphi \mathrm{d}\mathcal{H}^{n-1} \tag{6.79}$$

where ν is the unit outer normal of the boundary Γ_{ij}. The integral on the left hand side is approximated as follows:

$$\int_{\Omega_{ij}}\frac{1}{Q}\partial_t\varphi \mathrm{dx}\approx\frac{\mu\left(\Omega_{ij}\right)}{Q_{ij}}\frac{\mathrm{d}}{\mathrm{d}t}\varphi^h_{ij} \tag{6.80}$$

where we again assumed that φ_{ij}^h and Q_{ij}^h are constant on the element v_{ij}. For the integral on the right hand side of (6.79) we have

$$-\int_{\Gamma_{ij}} \mathbb{E}\nabla w\nu - \frac{1}{2}\frac{w^2}{Q^3}\partial_\nu u \mathrm{d}\mathcal{H}^{n-1} \approx -\sum_{v_{\overline{ij}}\in\mathcal{N}_{ij}} l_{ij,\overline{ij}}\left(\mathbb{E}^h_{ij,\overline{ij}}\nabla w^h_{ij,\overline{ij}}\nu_{ij,\overline{ij}} - \frac{1}{2}\frac{\left(w^h_{ij,\overline{ij}}\right)^2}{\left(Q^h_{ij,\overline{ij}}\right)^3}\nabla\varphi^h_{ij,\overline{ij}}\nu_{ij,\overline{ij}}\right). \tag{6.81}$$

(6.80) together with (6.81) gives

$$\begin{aligned}
\frac{\mathrm{d}}{\mathrm{d}t}\varphi_{ij}^h \approx \frac{Q_{ij}^h}{\mu\left(\Omega_{ij}\right)}\Bigg[& l_{ij,i+1j}\left(\mathbb{E}^h_{ij,i+1j}\nabla w^h_{ij,i+1j}\nu_{ij,i+1j} - \frac{1}{2}\frac{\left(w^h_{ij,i+1j}\right)^2}{\left(Q^h_{ij,i+1j}\right)^3}\nabla\varphi^h_{ij,i+1j}\nu_{ij,i+1j}\right) \\
+ & l_{ij,ij+1}\left(\mathbb{E}^h_{ij,ij+1}\nabla w^h_{ij,ij+1}\nu_{ij,ij+1} - \frac{1}{2}\frac{\left(w^h_{ij,ij+1}\right)^2}{\left(Q^h_{ij,ij+1}\right)^3}\nabla\varphi^h_{ij,ij+1}\nu_{ij,ij+1}\right) \\
+ & l_{ij,i-1j}\left(\mathbb{E}^h_{ij,i-1j}\nabla w^h_{ij,i-1j}\nu_{ij,i-1j} - \frac{1}{2}\frac{\left(w^h_{ij,i-1j}\right)^2}{\left(Q^h_{ij,i-1j}\right)^3}\nabla\varphi^h_{ij,i-1j}\nu_{ij,i-1j}\right) \\
+ & l_{ij,ij-1}\left(\mathbb{E}^h_{ij,ij-1}\nabla w^h_{ij,ij-1}\nu_{ij,ij-1} - \frac{1}{2}\frac{\left(w^h_{ij,ij-1}\right)^2}{\left(Q^h_{ij,ij-1}\right)^3}\nabla\varphi^h_{ij,ij-1}\nu_{ij,ij-1}\right)\Bigg].
\end{aligned}$$

In the terms of the regular dual mesh (6.54) it means that

$$\begin{aligned}
\frac{\mathrm{d}}{\mathrm{d}t}\varphi_{ij}^h \approx \frac{Q_{ij}^h}{h_1 h_2}\Bigg[& h_2\left(\mathbb{E}^h_{ij,i+1j}\nabla w^h_{ij,i+1j}\left(1,0\right)^T - \frac{1}{2}\frac{\left(w^h_{ij,i+1j}\right)^2}{\left(Q^h_{ij,i+1j}\right)^3}\nabla\varphi^h_{ij,i+1j}\left(1,0\right)^T\right) \\
+ & h_1\left(\mathbb{E}^h_{ij,ij+1}\nabla w^h_{ij,ij+1}\left(0,1\right)^T - \frac{1}{2}\frac{\left(w^h_{ij,ij+1}\right)^2}{\left(Q^h_{ij,ij+1}\right)^3}\nabla\varphi^h_{ij,ij+1}\left(0,1\right)^T\right) \\
+ & h_2\left(\mathbb{E}^h_{ij,i-1j}\nabla w^h_{ij,i-1j}\left(-1,0\right)^T - \frac{1}{2}\frac{\left(w^h_{ij,i-1j}\right)^2}{\left(Q^h_{ij,i-1j}\right)^3}\nabla\varphi^h_{ij,i-1j}\left(-1,0\right)^T\right) \\
+ & h_1\left(\mathbb{E}^h_{ij,ij-1}\nabla w^h_{ij,ij-1}\left(0,-1\right)^T - \frac{1}{2}\frac{\left(w^h_{ij,ij-1}\right)^2}{\left(Q^h_{ij,ij-1}\right)^3}\nabla\varphi^h_{ij,ij-1}\left(0,-1\right)^T\right)\Bigg],
\end{aligned}$$

and

$$
\begin{aligned}
\frac{\mathrm{d}}{\mathrm{d}t}\varphi_{ij}^h \quad &\approx \quad Q_{ij}^h \left[\frac{1}{h_1} \left(\mathbb{E}_{ij,i+1j}^h \nabla w_{ij,i+1j}^h \,(1,0)^T - \frac{1}{2} \frac{\left(w_{ij,i+1j}^h\right)^2}{\left(Q_{ij,i+1j}^h\right)^3} \nabla \varphi_{ij,i+1j}^h \,(1,0)^T \right) \right. \\
&+ \quad \frac{1}{h_2} \left(\mathbb{E}_{ij,ij+1}^h \nabla w_{ij,ij+1}^h \,(0,1)^T - \frac{1}{2} \frac{\left(w_{ij,ij+1}^h\right)^2}{\left(Q_{ij,ij+1}^h\right)^3} \nabla \varphi_{ij,ij+1}^h \,(0,1)^T \right) \\
&+ \quad \frac{1}{h_1} \left(\mathbb{E}_{ij,i-1j}^h \nabla w_{ij,i-1j}^h \,(-1,0)^T - \frac{1}{2} \frac{\left(w_{ij,i-1j}^h\right)^2}{\left(Q_{ij,i-1j}^h\right)^3} \nabla \varphi_{ij,i-1j}^h \,(-1,0)^T \right) \\
&+ \quad \left. \frac{1}{h_2} \left(\mathbb{E}_{ij,ij-1}^h \nabla w_{ij,ij-1}^h \,(0,-1)^T - \frac{1}{2} \frac{\left(w_{ij,ij-1}^h\right)^2}{\left(Q_{ij,ij-1}^h\right)^3} \nabla \varphi_{ij,ij-1}^h \,(0,-1)^T \right) \right],
\end{aligned}
$$

which gives

$$
\begin{aligned}
\frac{\mathrm{d}}{\mathrm{d}t}\varphi_{ij}^h \quad &= \quad Q_{ij}^h \left[\frac{1}{h_1} \left(\mathbb{E}_{11,ij,i+1j}^h \partial_{x_1}^h w_{ij,i+1j}^h + \mathbb{E}_{12,ij,i+1j}^h \partial_{x_2}^h w_{ij,i+1j}^h - \frac{1}{2} \frac{\left(w_{ij,i+1j}^h\right)^2}{\left(Q_{ij,i+1j}^h\right)^3} \partial_{x_1}^h \varphi_{ij,i+1j}^h \right) \right. \\
&+ \quad \frac{1}{h_2} \left(\mathbb{E}_{21,ij,ij+1}^h \partial_{x_1}^h w_{ij,ij+1}^h + \mathbb{E}_{22,ij,ij+1}^h \partial_{x_2}^h w_{ij,ij+1}^h - \frac{1}{2} \frac{\left(w_{ij,ij+1}^h\right)^2}{\left(Q_{ij,ij+1}^h\right)^3} \partial_{x_2}^h \varphi_{ij,ij+1}^h \right) \\
&- \quad \frac{1}{h_1} \left(\mathbb{E}_{11,ij,i-1j}^h \partial_{x_1}^h w_{ij,i-1j}^h + \mathbb{E}_{12,ij,i-1j}^h \partial_{x_2}^h w_{ij,i-1j}^h - \frac{1}{2} \frac{\left(w_{ij,i-1j}^h\right)^2}{\left(Q_{ij,i-1j}^h\right)^3} \partial_{x_1}^h \varphi_{ij,i-1j}^h \right) \\
&- \quad \left. \frac{1}{h_2} \left(\mathbb{E}_{21,ij,ij-1}^h \partial_{x_1}^h w_{ij,ij-1}^h + \mathbb{E}_{22,ij,ij-1}^h \partial_{x_2}^h w_{ij,ij-1}^h - \frac{1}{2} \frac{\left(w_{ij,ij-1}^h\right)^2}{\left(Q_{ij,ij-1}^h\right)^3} \partial_{x_2}^h \varphi_{ij,ij-1}^h \right) \right].
\end{aligned}
$$

We approximate $\partial_{x_1}\varphi_{ij,\overline{ij}}^h$ and $\partial_{x_2}\varphi_{ij,\overline{ij}}^h$ by (6.65)–(6.68) and the same holds for $\partial_{x_1} w_{ij,\overline{ij}}^h$ and $\partial_{x_2} w_{ij,\overline{ij}}^h$ with

$$
w_{ij,i+1j}^h = \frac{1}{2}\left(w_{ij}^h + w_{i+1j}^h\right) \quad , \quad w_{ij,ij+1}^h = \frac{1}{2}\left(w_{ij}^h + w_{ij+1}^h\right), \tag{6.82}
$$

$$
w_{ij,i-1j}^h = \frac{1}{2}\left(w_{ij}^h + w_{i-1j}^h\right) \quad , \quad w_{ij,ij-1}^h = \frac{1}{2}\left(w_{ij}^h + w_{ij-1}^h\right), \tag{6.83}
$$

and $w_{ij,i+1j+1}^h$, $w_{ij,i+1j-1}^h$, $w_{ij,i-1j+1}^h$ and $w_{ij,i-1j-1}^h$ are approximated in the same way as (6.69)–(6.72). $Q_{ij,\overline{ij}}^h$ are given by (6.61)–(6.64), Q_{ij}^h as

$$
Q_{ij}^h = \frac{1}{4}\left(Q_{ij,i+1j}^h + Q_{ij,ij+1}^h + Q_{ij,i-1j}^h + Q_{ij,ij-1}^h\right). \tag{6.84}
$$

For

$$
\mathbb{E}_{ij,\overline{ij}}^h = \begin{pmatrix} \mathbb{E}_{11,ij,\overline{ij}}^h & \mathbb{E}_{12,ij,\overline{ij}}^h \\ \mathbb{E}_{21,ij,\overline{ij}}^h & \mathbb{E}_{22,ij,\overline{ij}}^h \end{pmatrix}, \tag{6.85}
$$

the following holds

$$\mathbb{E}^h_{ij,i+1j} \approx \frac{1}{Q_{ij,i+1j}} \begin{pmatrix} 1-\left(\partial_{x_1}\varphi^h_{ij,i+1j}\right)^2 & -\partial_{x_1}\varphi^h_{ij,i+1j}\partial_{x_2}\varphi^h_{ij,i+1j} \\ -\partial_{x_1}\varphi^h_{ij,i+1j}\partial_{x_2}\varphi^h_{ij,i+1j} & 1-\left(\partial_{x_2}\varphi^h_{ij,i+1j}\right)^2 \end{pmatrix},$$

$$\mathbb{E}^h_{ij,ij+1} \approx \frac{1}{Q_{ij,ij+1}} \begin{pmatrix} 1-\left(\partial_{x_1}\varphi^h_{ij,ij+1}\right)^2 & -\partial_{x_1}\varphi^h_{ij,ij+1}\partial_{x_2}\varphi^h_{ij,ij+1} \\ -\partial_{x_1}\varphi^h_{ij,ij+1}\partial_{x_2}\varphi^h_{ij,ij+1} & 1-\left(\partial_{x_2}\varphi^h_{ij,ij+1}\right)^2 \end{pmatrix},$$

$$\mathbb{E}^h_{ij,i-1j} \approx \frac{1}{Q_{ij,i-1j}} \begin{pmatrix} 1-\left(\partial_{x_1}\varphi^h_{ij,i-1j}\right)^2 & -\partial_{x_1}\varphi^h_{ij,i-1j}\partial_{x_2}\varphi^h_{ij,i-1j} \\ -\partial_{x_1}\varphi^h_{ij,i-1j}\partial_{x_2}\varphi^h_{ij,i-1j} & 1-\left(\partial_{x_2}\varphi^h_{ij,i-1j}\right)^2 \end{pmatrix},$$

$$\mathbb{E}^h_{ij,ij-1} \approx \frac{1}{Q_{ij,ij-1}} \begin{pmatrix} 1-\left(\partial_{x_1}\varphi^h_{ij,ij-1}\right)^2 & -\partial_{x_1}\varphi^h_{ij,ij-1}\partial_{x_2}\varphi^h_{ij,ij-1} \\ -\partial_{x_1}\varphi^h_{ij,ij-1}\partial_{x_2}\varphi^h_{ij,ij-1} & 1-\left(\partial_{x_2}\varphi^h_{ij,ij-1}\right)^2 \end{pmatrix}$$

The Neumann boundary conditions $\partial_\nu \varphi = 0$ on $\partial\Omega$ take the form (6.73)–(6.76). The same is true even for the Neumann boundary conditions $\partial_\nu w = 0$

$$\text{if } i=1 \text{ then } \nu=(-1,0) \;\Rightarrow\; \frac{1}{h_1}\left(w^h_{1,j}-w^h_{0,j}\right)=0 \Rightarrow w^h_{1,j}=w^h_{0,j}, \tag{6.86}$$

$$\text{if } i=N_1-1 \text{ then } \nu=(1,0) \;\Rightarrow\; \frac{1}{h_1}\left(w^h_{N_1,j}-w^h_{N_1-1,j}\right)=0 \Rightarrow w^h_{N_1,j}=w^h_{N_1-1,j}, \tag{6.87}$$

$$\text{if } j=1 \text{ then } \nu=(0,-1) \;\Rightarrow\; \frac{1}{h_2}\left(w^h_{i,1}-w^h_{i,0}\right)=0 \Rightarrow w^h_{i,1}=w^h_{i,0}, \tag{6.88}$$

$$\text{if } j=N_2-1 \text{ then } \nu=(0,1) \;\Rightarrow\; \frac{1}{h_2}\left(w^h_{i,N_2}-w^h_{i,N_2-1}\right)=0 \Rightarrow w^h_{i,N_2}=w^h_{i,N_2-1}. \tag{6.89}$$

Numerical schemes for the isotropic graph formulations We conclude with the following schemes:

Scheme 6.2.14. The **complementary finite volume** semi-discrete numerical scheme for the **isotropic mean-curvature flow of graphs with the Dirichlet boundary conditions** takes the following form

$$\frac{\mathrm{d}}{\mathrm{dt}}\varphi^h_{ij} = Q^h_{ij}\left(\frac{\varphi^h_{i+1j}-\varphi^h_{ij}}{h_1^2 Q^h_{ij,i+1j}} + \frac{\varphi^h_{ij+1}-\varphi^h_{ij}}{h_2^2 Q^h_{ij,ij+1}} - \frac{\varphi^h_{ij}-\varphi^h_{i-1j}}{h_1^2 Q^h_{ij,i-1j}} - \frac{\varphi^h_{ij}-\varphi^h_{ij-1}}{h_2^2 Q^h_{ij,ij-1}}\right) \tag{6.90}$$

$$\text{on } \omega_h, \tag{6.91}$$

$$\varphi^h_{ij}\,|_{t=0} = \mathcal{P}\left(\varphi^h_{ini}\right)_{ij} \text{ on } \overline{\omega}_h, \tag{6.92}$$

$$\varphi^h_{ij} = g_{ij} \text{ on } \partial\omega_h,$$

where Q^h_{ij} is given by (6.78) and $Q^h_{ij,i+1j}$, $Q^h_{ij,ij+1}$, $Q^h_{ij,i-1j}$ and $Q^h_{ij,ij-1}$ are given by (6.61)–(6.64).
The **complementary finite volume** semi-discrete numerical scheme for the **isotropic mean-curvature flow of graphs with the Neumann boundary conditions** is given by (6.91)–(6.92) and (6.73)–(6.76).

Scheme 6.2.15. The **complementary finite volume** semi-discrete numerical scheme for the **isotropic Willmore flow of graphs with the Dirichlet boundary conditions** takes the following form

$$
\begin{aligned}
\frac{\mathrm{d}}{\mathrm{d}t}\varphi_{ij}^h &= Q_{ij}^h \left[\frac{1}{h_1} \left(\mathbb{E}_{11,ij,i+1j}^h \partial_{x_1}^h w_{ij,i+1j}^h + \mathbb{E}_{12,ij,i+1j}^h \partial_{x_2}^h w_{ij,i+1j}^h - \frac{1}{2} \frac{\left(w_{ij,i+1j}^h\right)^2}{\left(Q_{ij,i+1j}^h\right)^3} \partial_{x_1}^h \varphi_{ij,i+1j}^h \right) \right. \\
&+ \frac{1}{h_2} \left(\mathbb{E}_{21,ij,ij+1}^h \partial_{x_1}^h w_{ij,ij+1}^h + \mathbb{E}_{22,ij,ij+1}^h \partial_{x_2}^h w_{ij,ij+1}^h - \frac{1}{2} \frac{\left(w_{ij,ij+1}^h\right)^2}{\left(Q_{ij,ij+1}^h\right)^3} \partial_{x_2}^h \varphi_{ij,ij+1} \right) \\
&- \frac{1}{h_1} \left(\mathbb{E}_{11,ij,i-1j}^h \partial_{x_1}^h w_{ij,i-1j}^h + \mathbb{E}_{12,ij,i-1j}^h \partial_{x_2}^h w_{ij,i-1j}^h - \frac{1}{2} \frac{\left(w_{ij,i-1j}^h\right)^2}{\left(Q_{ij,i-1j}^h\right)^3} \partial_{x_1}^h \varphi_{ij,i-1j} \right) \\
&\left. - \frac{1}{h_2} \left(\mathbb{E}_{21,ij,ij-1}^h \partial_{x_1}^h w_{ij,ij-1}^h + \mathbb{E}_{22,ij,ij-1}^h \partial_{x_2}^h w_{ij,ij-1}^h - \frac{1}{2} \frac{\left(w_{ij,ij-1}^h\right)^2}{\left(Q_{ij,ij-1}^h\right)^3} \partial_{x_2}^h \varphi_{ij,ij-1} \right) \right],
\end{aligned} \tag{6.93}
$$

$$
w_{ij}^h = Q_{ij}^h \left(\frac{\varphi_{i+1j}^h - \varphi_{ij}^h}{h_1^2 Q_{ij,i+1j}^h} + \frac{\varphi_{ij+1}^h - \varphi_{ij}^h}{h_2^2 Q_{ij,ij+1}^h} - \frac{\varphi_{ij}^h - \varphi_{i-1j}^h}{h_1^2 Q_{ij,i-1j}^h} - \frac{\varphi_{ij}^h - \varphi_{ij-1}^h}{h_2^2 Q_{ij,ij-1}^h} \right) \text{ on } \omega_h, \tag{6.94}
$$

$$
\begin{aligned}
\varphi_{ij}^h \,|_{t=0} &= \mathcal{P}\left(u_{ini}\right)_{ij} \text{ on } \overline{\omega}_h, \\
\varphi_{ij}^h &= g_{ij} \text{ and } w_{ij}^h = 0 \text{ on } \partial\omega_h,
\end{aligned} \tag{6.95}
$$

where Q_{ij}^h is given by (6.78) and $Q_{ij,i+1j}^h$, $Q_{ij,ij+1}^h$, $Q_{ij,i-1j}^h$ and $Q_{ij,ij-1}^h$ are given by (6.61)–(6.64), $\mathbb{E}_{ij,\bar{i}\bar{j}}^h$ is given by (6.85), $w_{ij,\bar{i}\bar{j}}^h$ by (6.82)–(6.83) and as (6.69)–(6.72). $\partial_{x_1}^h \varphi_{ij,\bar{i}\bar{j}}^h$ and $\partial_{x_2}^h \varphi_{ij,\bar{i}\bar{j}}^h$ is approximated by (6.65)–(6.68).
The **complementary finite volume** semi-discrete numerical scheme for the **isotropic Willmore flow of graphs with the Neumann boundary conditions** is given by (6.93)–(6.95) and (6.73)–(6.76) and (6.86)–(6.89).

Evaluation of isotropic mean curvature for the level-set formulation We take the right-hand side of the equation (5.17) and integrate it over a finite volume Ω_{ij}

$$
\int_{\Omega_{ij}} H \mathrm{d}x = \int_{\Omega_{ij}} \nabla \cdot \left(\frac{\nabla u}{Q_\epsilon} \right). \tag{6.96}
$$

As for the graph formulation we get

$$
\begin{aligned}
H_{ij}^h &\approx \frac{1}{\mu(\Omega_{ij})} \sum_{v_{\overline{ij}} \in \mathcal{N}_{ij}} l_{ij,\overline{ij}} \frac{\nabla u_{ij,\overline{ij}}^h}{Q_{\epsilon,ij,\overline{ij}}^h} \cdot \nu_{ij,\overline{ij}} \\
&= \frac{1}{h_1 h_2} \left(h_2 \frac{\nabla u_{ij,i+1j}^h}{Q_{\epsilon,ij,i+1j}^h} \cdot (1,0)^T + h_1 \frac{\nabla u_{ij,ij+1}^h}{Q_{\epsilon,ij,ij+1}^h} \cdot (0,1)^T \right. \\
&+ \left. h_2 \frac{\nabla u_{ij,i-1j}^h}{Q_{\epsilon,ij,i-1j}^h} \cdot (-1,0)^T + h_1 \frac{\nabla u_{ij,ij-1}^h}{Q_{\epsilon,ij,ij-1}^h} \cdot (0,-1)^T \right),
\end{aligned}
$$

which gives

$$
H_{ij}^h \approx \left(\frac{u_{i+1j}^h - u_{ij}^h}{h_1^2 Q_{\epsilon,ij,i+1j}^h} + \frac{u_{ij+1}^h - u_{ij}^h}{h_2^2 Q_{\epsilon,ij,ij+1}^h} - \frac{u_{ij}^h - u_{i-1j}^h}{h_1^2 Q_{\epsilon,ij,i-1j}^h} - \frac{u_{ij}^h - u_{ij-1}^h}{h_2^2 Q_{\epsilon,ij,ij-1}^h} \right),
$$

where

$$
Q_{\epsilon,ij,i+1j}^h = \sqrt{\epsilon^2 + \left(\partial_{x_1}^h u_{ij,i+1j}^h\right)^2 + \left(\partial_{x_2}^h u_{ij,i+1j}^h\right)^2}, \tag{6.97}
$$

$$
Q_{\epsilon,ij,ij+1}^h = \sqrt{\epsilon^2 + \left(\partial_{x_1}^h u_{ij,ij+1}^h\right)^2 + \left(\partial_{x_2}^h u_{ij,ij+1}^h\right)^2}, \tag{6.98}
$$

$$
Q_{\epsilon,ij,i-1j}^h = \sqrt{\epsilon^2 + \left(\partial_{x_1}^h u_{ij,i-1j}^h\right)^2 + \left(\partial_{x_2}^h u_{ij,i-1j}^h\right)^2}, \tag{6.99}
$$

$$
Q_{\epsilon,ij,ij-1}^h = \sqrt{\epsilon^2 + \left(\partial_{x_1}^h u_{ij,ij-1}^h\right)^2 + \left(\partial_{x_2}^h u_{ij,ij-1}^h\right)^2}. \tag{6.100}
$$

Evaluation of isotropic level-set formulation of the Willmore flow We integrate the equation (5.53) over the finite volume Ω_{ij} and we apply the Stokes theorem to get

$$
\int_{\Omega_{ij}} \frac{1}{Q_\epsilon} \partial_t u \mathrm{dx} = -\int_{\Gamma_{ij}} \mathbb{E} \nabla w \nu - \frac{1}{2} \frac{w^2}{Q_\epsilon^3} \partial_\nu u \mathrm{d}\mathcal{H}^{n-1}, \tag{6.101}
$$

which gives

$$
\frac{\mu(\Omega_{ij})}{Q_{\epsilon,ij}^h} \frac{\mathrm{d}}{\mathrm{d}t} u_{ij}^h = -\sum_{v_{\overline{ij}} \in \mathcal{N}_{ij}} l_{ij,\overline{ij}} \left(\mathbb{E}_{ij,\overline{ij}}^h \nabla w_{ij,\overline{ij}}^h \nu_{ij,\overline{ij}} - \frac{1}{2} \frac{\left(w_{ij,\overline{ij}}^h\right)^2}{\left(Q_{\epsilon,ij,\overline{ij}}^h\right)^3} \nabla u_{ij,\overline{ij}}^h \nu_{ij,\overline{ij}} \right), \tag{6.102}
$$

where

$$
Q_{\epsilon,ij}^h = \frac{1}{4} \left(Q_{\epsilon,ij,i+1j}^h + Q_{\epsilon,ij,ij+1}^h + Q_{\epsilon,ij,i-1j}^h + Q_{\epsilon,ij,ij-1}^h \right). \tag{6.103}
$$

and

$$
w_{ij}^h = Q_{\epsilon,ij}^h H_{ij}^h, \tag{6.104}
$$

$$
w_{ij,i+1j}^h = \frac{1}{2}\left(w_{ij}^h + w_{i+1j}^h\right) \quad , \quad w_{ij,ij+1}^h = \frac{1}{2}\left(w_{ij}^h + w_{ij+1}^h\right), \tag{6.105}
$$

$$
w_{ij,i-1j}^h = \frac{1}{2}\left(w_{ij}^h + w_{i-1j}^h\right) \quad , \quad w_{ij,ij-1}^h = \frac{1}{2}\left(w_{ij}^h + w_{ij-1}^h\right). \tag{6.106}
$$

In terms of the regular dual mesh (6.54) it reads

$$
\begin{aligned}
\frac{\mathrm{d}}{\mathrm{d}t} u^h_{ij} &= Q^h_{\epsilon,ij} \left[\frac{1}{h_1} \left(\mathbb{E}^h_{11,ij,i+1j} \partial^h_{x_1} w^h_{ij,i+1j} + \mathbb{E}^h_{12,ij,i+1j} \partial^h_{x_2} w^h_{ij,i+1j} - \frac{1}{2} \frac{\left(w^h_{ij,i+1j}\right)^2}{\left(Q^h_{\epsilon,ij,i+1j}\right)^3} \partial^h_{x_1} u^h_{ij,i+1j} \right) \right. \\
&+ \frac{1}{h_2} \left(\mathbb{E}^h_{21,ij,ij+1} \partial^h_{x_1} w^h_{ij,ij+1} + \mathbb{E}^h_{22,ij,ij+1} \partial^h_{x_2} w^h_{ij,ij+1} - \frac{1}{2} \frac{\left(w^h_{ij,ij+1}\right)^2}{\left(Q^h_{\epsilon,ij,ij+1}\right)^3} \partial^h_{x_2} u^h_{ij,ij+1} \right) \\
&- \frac{1}{h_1} \left(\mathbb{E}^h_{11,ij,i-1j} \partial^h_{x_1} w^h_{ij,i-1j} + \mathbb{E}^h_{12,ij,i-1j} \partial^h_{x_2} w^h_{ij,i-1j} - \frac{1}{2} \frac{\left(w^h_{ij,i-1j}\right)^2}{\left(Q^h_{\epsilon,ij,i-1j}\right)^3} \partial^h_{x_1} u^h_{ij,i-1j} \right) \\
&- \left. \frac{1}{h_2} \left(\mathbb{E}^h_{21,ij,ij-1} \partial^h_{x_1} w^h_{ij,ij-1} + \mathbb{E}^h_{22,ij,ij-1} \partial^h_{x_2} w^h_{ij,ij-1} - \frac{1}{2} \frac{\left(w^h_{ij,ij-1}\right)^2}{\left(Q^h_{\epsilon,ij,ij-1}\right)^3} \partial^h_{x_2} u^h_{ij,ij-1} \right) \right],
\end{aligned}
$$

Numerical schemes for the isotropic level-set formulations We conclude with the following schemes:

Scheme 6.2.16. The **complementary finite volume** semi-discrete numerical scheme for the **level-set formulation of the isotropic mean-curvature flow with the Dirichlet boundary conditions** takes the form

$$
\frac{\mathrm{d}}{\mathrm{d}t} u^h_{ij} = Q^h_{\epsilon,ij} \left(\frac{u^h_{i+1j} - u^h_{ij}}{h_1^2 Q^h_{\epsilon,ij,i+1j}} + \frac{u^h_{ij+1} - u^h_{ij}}{h_2^2 Q^h_{\epsilon,ij,ij+1}} - \frac{u^h_{ij} - u^h_{i-1j}}{h_1^2 Q^h_{\epsilon,ij,i-1j}} - \frac{u^h_{ij} - u^h_{ij-1}}{h_2^2 Q^h_{\epsilon,ij,ij-1}} \right) \text{ on } \omega_h, \tag{6.107}
$$

$$
u^h_{ij} \mid_{t=0} = \mathcal{P}\left(u_{ini}\right)_{ij} \text{ on } \overline{\omega}_h, \varphi^h_{ij} = g_{ij} \text{ on } \partial\omega_h, \tag{6.108}
$$

where $Q^h_{\epsilon,ij}$ is given by (6.103) and $Q^h_{\epsilon,ij,i+1j}$, $Q^h_{\epsilon,ij,ij+1}$, $Q^h_{\epsilon,ij,i-1j}$ and $Q^h_{\epsilon,ij,ij-1}$ are given by (6.61)–(6.64).

The **complementary finite volume** semi-discrete numerical scheme for the **level-set formulation of the isotropic mean-curvature flow with the Neumann boundary conditions** is given by (6.73)–(6.76).

Scheme 6.2.17. The **complementary finite volume** semi-discrete numerical scheme for the **level-set formulation of the isotropic Willmore flow with the Dirichlet boundary conditions** takes the form

$$
\begin{aligned}
\frac{\mathrm{d}}{\mathrm{d}t} u_{ij}^{h} &= Q_{\epsilon,ij} \left[\frac{\mathbb{E}^{h}_{11,ij,i+1j} \partial^{h}_{x_1} w^{h}_{ij,i+1j} + \mathbb{E}^{h}_{12,ij,i+1j} \partial^{h}_{x_2} w^{h}_{ij,i+1j} - \frac{1}{2} \frac{\left(w^{h}_{ij,i+1j}\right)^2}{\left(Q^{h}_{\epsilon,ij,i+1j}\right)^3} \partial^{h}_{x_1} u^{h}_{ij,i+1j}}{h_1} \right. \\
&+ \frac{\mathbb{E}^{h}_{21,ij,ij+1} \partial^{h}_{x_1} w^{h}_{ij,ij+1} + \mathbb{E}^{h}_{22,ij,ij+1} \partial^{h}_{x_2} w^{h}_{ij,ij+1} - \frac{1}{2} \frac{\left(w^{h}_{ij,ij+1}\right)^2}{\left(Q^{h}_{\epsilon,ij,ij+1}\right)^3} \partial^{h}_{x_2} u^{h}_{ij,ij+1}}{h_2} \\
&- \frac{\mathbb{E}^{h}_{11,ij,i-1j} \partial^{h}_{x_1} w^{h}_{ij,i-1j} + \mathbb{E}^{h}_{12,ij,i-1j} \partial^{h}_{x_2} w^{h}_{ij,i-1j} - \frac{1}{2} \frac{\left(w^{h}_{ij,i-1j}\right)^2}{\left(Q^{h}_{\epsilon,ij,i-1j}\right)^3} \partial^{h}_{x_1} u^{h}_{ij,i-1j}}{h_1} \\
&- \left. \frac{\mathbb{E}^{h}_{21,ij,ij-1} \partial^{h}_{x_1} w^{h}_{ij,ij-1} + \mathbb{E}^{h}_{22,ij,ij-1} \partial^{h}_{x_2} w^{h}_{ij,ij-1} - \frac{1}{2} \frac{\left(w^{h}_{ij,ij-1}\right)^2}{\left(Q^{h}_{\epsilon,ij,ij-1}\right)^3} \partial^{h}_{x_2} u^{h}_{ij,ij-1}}{h_2} \right],
\end{aligned}
\tag{6.109}
$$

$$
w^{h}_{ij} = Q^{h}_{\epsilon,ij} \left(\frac{u^{h}_{i+1j} - u^{h}_{ij}}{h_1^2 Q^{h}_{\epsilon,ij,i+1j}} + \frac{u^{h}_{ij+1} - u^{h}_{ij}}{h_2^2 Q^{h}_{\epsilon,ij,ij+1}} - \frac{u^{h}_{ij} - u^{h}_{i-1j}}{h_1^2 Q^{h}_{\epsilon,ij,i-1j}} - \frac{u^{h}_{ij} - u^{h}_{ij-1}}{h_2^2 Q^{h}_{\epsilon,ij,ij-1}} \right) \text{ on } \omega_h,
$$

$$
u^{h}_{ij} |_{t=0} = \mathcal{P}\left(u_{ini}\right)_{ij} \text{ on } \overline{\omega}_h, \tag{6.110}
$$

$$
u^{h}_{ij} = g_{ij} \text{ and } w^{h}_{ij} = 0 \text{ on } \partial\omega_h, \tag{6.111}
$$

where $Q^{h}_{\epsilon,ij}$ is given by (6.103) and $Q^{h}_{\epsilon,ij,i+1j}$, $Q^{h}_{\epsilon,ij,ij+1}$, $Q^{h}_{\epsilon,ij,i-1j}$ and $Q^{h}_{\epsilon,ij,ij-1}$ are given by (6.97)–(6.100), $\mathbb{E}^{h}_{ij,\overline{ij}}$ is given by (6.85), $w^{h}_{ij,\overline{ij}}$ by (6.82)–(6.83) and as (6.69)–(6.72). $\partial^{h}_{x_1} u^{h}_{ij,\overline{ij}}$ and $\partial^{h}_{x_2} u^{h}_{ij,\overline{ij}}$ is approximated by (6.65)–(6.68).
The **complementary finite volume** semi-discrete numerical scheme for the **level-set formulation of the isotropic Willmore flow with the Neumann boundary conditions** is given by (6.109)–(6.110), (6.73)–(6.76) and (6.86)–(6.89).

Evaluation of anisotropic mean curvature of graphs For admissible anisotropy γ, the anisotropic mean curvature of graphs is given by equation (5.25). Integrating it over a finite volume Ω_{ij} and applying the Stokes formula

$$
\int_{\Omega_{ij}} H_\gamma \mathrm{dx} = \int_{\Omega_{ij}} \nabla \cdot \left(\nabla_{\mathbf{p}} \gamma\right) \mathrm{dx} = \int_{\Gamma_{ij}} \nabla_{\mathbf{p}} \gamma \cdot \nu \mathrm{d}\mathcal{H}^{n-1}. \tag{6.112}
$$

The approximation reads

$$
\int_{\Omega_{ij}} H_\gamma \mathrm{dx} \approx \mu\left(\Omega\right) H^{h}_{\gamma,ij} = \sum_{v_{\overline{ij}} \in \mathcal{N}_{ij}} l_{ij,\overline{ij}} \nabla_{\mathbf{p}} \gamma_{ij,\overline{ij}} \nu_{ij,\overline{ij}} \mathrm{d}\mathcal{H}^{n-1}, \tag{6.113}
$$

where

$$
\nabla_{\mathbf{p}} \gamma_{ij,\overline{ij}} = \left(\partial_{p_1} \gamma_{ij,\overline{ij}}, \partial_{p_2} \gamma_{ij,\overline{ij}}\right)^T = \left(\partial_{p_1} \gamma \left(\nabla \varphi^{h}_{ij,\overline{ij}}, -1\right), \partial_{p_2} \gamma \left(\nabla \varphi^{h}_{ij,\overline{ij}}, -1\right)\right)^T. \tag{6.114}
$$

For the regular dual mesh (6.54) we have

$$
\begin{aligned}
H^h_{\gamma,ij} &= \frac{1}{h_1 h_2}\Big(h_2 \nabla_{\mathbf{p}}\gamma_{ij,i+1j}\cdot(1,0)^T + h_1\nabla_{\mathbf{p}}\gamma_{ij,ij+1}\cdot(0,1)^T \\
&+ h_2 \nabla_{\mathbf{p}}\gamma_{ij,i-1j}\cdot(-1,0)^T + h_1\nabla_{\mathbf{p}}\gamma_{ij,ij-1}\cdot(0,-1)^T \Big) \\
&= \left(\frac{\partial_{p_1}\gamma_{ij,i+1j} - \partial_{p_1}\gamma_{ij,i-1,j}}{h_1} + \frac{\partial_{p_2}\gamma_{ij,ij+1} - \partial_{p_2}\gamma_{ij,ij-1}}{h_2} \right). \qquad (6.115)
\end{aligned}
$$

In the case of the Neumann boundary conditions from $\nabla_{\mathbf{p}}\gamma\cdot\nu = 0$ we set:

$$
\begin{aligned}
\text{if } i = 1 \text{ then } \nu = (-1,0) &\Rightarrow \partial_{p_1}\gamma_{1j,0j} = 0, & (6.116)\\
\text{if } i = N_1 - 1 \text{ then } \nu = (1,0) &\Rightarrow \partial_{p_1}\gamma_{N_1-1j,N_1j} = 0, & (6.117)\\
\text{if } j = 1 \text{ then } \nu = (0,-1) &\Rightarrow \partial_{p_2}\gamma_{i1,i0} = 0, & (6.118)\\
\text{if } j = N_2 - 1 \text{ then } \nu = (0,1) &\Rightarrow \partial_{p_2}\gamma_{iN_2-1,iN_2} = 0. & (6.119)
\end{aligned}
$$

The approximation of $\nabla_{\mathbf{p}}\gamma_{ij,\bar{i}\bar{j}}$ for general anisotropies is discussed later in the Sections 6.3.

Anisotropic Willmore flow of graphs From (6.115) we see the approximation of $w_\gamma = QH_\gamma$ on the finite volume Ω_{ij} as

$$
\begin{aligned}
w^h_{\gamma,ij} &= \frac{Q^h_{ij}}{\mu(\Omega_{ij})} \sum_{v_{\bar{i}\bar{j}}\in\mathcal{N}_{ij}} l_{ij,\bar{i}\bar{j}} \nabla_{\mathbf{p}}\gamma_{ij,\bar{i}\bar{j}}\nu_{ij,\bar{i}\bar{j}} \\
&= Q^h_{ij}\left(\frac{\partial_{p_1}\gamma_{ij,i+1j} - \partial_{p_1}\gamma_{ij,i-1,j}}{h_1} + \frac{\partial_{p_2}\gamma_{ij,ij+1} - \partial_{p_2}\gamma_{ij,ij-1}}{h_2} \right),
\end{aligned}
$$

and we also define

$$
w^h_{\gamma,ij,i+1j} = \frac{1}{2}\left(w^h_{\gamma,ij} + w^h_{\gamma,i+1j} \right) \quad , \quad w^h_{\gamma,ij,ij+1} = \frac{1}{2}\left(w^h_{\gamma,ij} + w^h_{\gamma,ij+1} \right), \qquad (6.120)
$$

$$
w^h_{\gamma,ij,i-1j} = \frac{1}{2}\left(w^h_{\gamma,ij} + w^h_{\gamma,i-1j} \right) \quad , \quad w^h_{\gamma,ij,ij-1} = \frac{1}{2}\left(w^h_{\gamma,ij} + w^h_{\gamma,ij-1} \right). \qquad (6.121)
$$

Integrating (5.81) over Ω_{ij} and applying the Stokes theorem we get

$$
\int_{\Omega_{ij}} \frac{1}{Q}\partial_t\varphi \mathrm{dx} = -\int_{\Gamma_{ij}} \mathbb{E}_\gamma \nabla w_\gamma \nu - \frac{1}{2}\frac{w_\gamma^2}{Q^3}\partial_\nu\varphi \mathrm{d}\mathcal{H}^{n-1} \qquad (6.122)
$$

where ν is the unit outer normal of the boundary Γ_{ij}. As before, the left hand side is approximated as follows:

$$
\int_{\Omega_{ij}} \frac{1}{Q}\partial_t\varphi \mathrm{dx} \approx \frac{\mu(\Omega_{ij})}{Q^h_{ij}}\frac{\mathrm{d}}{\mathrm{d}t}\varphi^h_{ij} = h_1 h_2 \frac{1}{Q^h_{ij}}\frac{\mathrm{d}}{\mathrm{d}t}\varphi^h_{ij}, \qquad (6.123)
$$

where we again assumed that φ^h_{ij} and Q^h_{ij} are constant on the element v_{ij}. For the integral on the right hand side of (6.122) we have

$$
-\int_{\Gamma_{ij}} \mathbb{E}_\gamma \nabla w_\gamma \nu - \frac{1}{2}\frac{w_\gamma^2}{Q^3}\partial_\nu\varphi \mathrm{d}\mathcal{H}^{n-1} \approx -\sum_{v_{\bar{i}\bar{j}}\in\mathcal{N}_{ij}} l_{ij,\bar{i}\bar{j}} \left(\mathbb{E}^h_{\gamma,ij,\bar{i}\bar{j}} \nabla w^h_{\gamma,ij,\bar{i}\bar{j}}\nu_{ij,\bar{i}\bar{j}} - \frac{1}{2}\frac{\left(w^h_{\gamma,ij,\bar{i}\bar{j}}\right)^2}{\left(Q^h_{ij,\bar{i}\bar{j}}\right)^3} \nabla_{ij,\bar{i}\bar{j}}\varphi^h_{ij}\nu_{ij,\bar{i}\bar{j}} \right). \qquad (6.124)
$$

with the usual notation. Putting (6.123) and (6.124) together gives

$$\frac{\mathrm{d}}{\mathrm{d}t}\varphi^h_{ij} = -\frac{Q^h_{ij}}{\mu\left(\Omega_{ij}\right)}\sum_{\overline{ij}\in\mathcal{N}_{ij}} l_{ij,\overline{ij}}\left(\mathbb{E}^h_{\gamma,ij,\overline{ij}}\nabla w^h_{\gamma,ij,\overline{ij}}\nu_{ij,\overline{ij}} - \frac{1}{2}\frac{\left(w^h_{\gamma,ij,\overline{ij}}\right)^2}{\left(Q^h_{ij,\overline{ij}}\right)^3}\nabla_{ij\overline{ij}}\varphi^h_{ij}\nu_{ij,\overline{ij}}\right).$$

In the terms of the regular dual mesh (6.54) we get

$$\begin{aligned}
\frac{\mathrm{d}}{\mathrm{d}t}\varphi^h_{ij} &= -\frac{Q^h_{ij}}{h_1h_2}\Bigg[h_2\left(\mathbb{E}^h_{\gamma,ij,i+1j}\nabla w^h_{\gamma,ij,i+1j}\left(1,0\right)^T - \frac{1}{2}\frac{\left(w^h_{\gamma,ij,i+1j}\right)^2}{\left(Q^h_{ij,i+1j}\right)^3}\nabla\varphi^h_{ij,i+1j}\left(1,0\right)^T\right)\\
&+ h_1\left(\mathbb{E}^h_{\gamma,ij,ij+1}\nabla w^h_{\gamma,ij,ij+1}\left(0,1\right)^T - \frac{1}{2}\frac{\left(w^h_{\gamma,ij,ij+1}\right)^2}{\left(Q^h_{ij,ij+1}\right)^3}\nabla\varphi^h_{ij,ij+1}\left(0,1\right)^T\right)\\
&+ h_2\left(\mathbb{E}^h_{\gamma,ij,i-1j}\nabla w^h_{\gamma,ij,i-1j}\left(-1,0\right)^T - \frac{1}{2}\frac{\left(w^h_{\gamma,ij,i-1j}\right)^2}{\left(Q^h_{ij,i-1j}\right)^3}\nabla\varphi^h_{ij,i-1j}\left(-1,0\right)^T\right)\\
&+ h_1\left(\mathbb{E}^h_{\gamma,ij,ij-1}\nabla w^h_{\gamma,ij,ij-1}\left(0,-1\right)^T - \frac{1}{2}\frac{\left(w^h_{\gamma,ij,ij-1}\right)^2}{\left(Q^h_{ij,ij-1}\right)^3}\nabla\varphi^h_{ij,ij-1}\left(0,-1\right)^T\right)\Bigg],
\end{aligned}$$

and so

$$\begin{aligned}
\frac{\mathrm{d}}{\mathrm{d}t}\varphi^h_{ij} &= -Q^h_{ij}\Bigg[\frac{1}{h_1}\left(\mathbb{E}^h_{\gamma,11,ij,i+1j}\partial^h_{x_1}w^h_{\gamma,ij,i+1j} + \mathbb{E}^h_{\gamma,12,ij,i+1j}\partial^h_{x_2}w^h_{\gamma,ij,i+1j} - \frac{1}{2}\frac{\left(w^h_{\gamma,ij,i+1j}\right)^2}{\left(Q^h_{ij,i+1j}\right)^3}\partial_{x_1}\varphi^h_{ij,i+1j}\right)\\
&+ \frac{1}{h_2}\left(\mathbb{E}^h_{\gamma,21,ij,ij+1}\partial^h_{x_1}w^h_{\gamma,ij,ij+1} + \mathbb{E}^h_{\gamma,22,ij,ij+1}\partial^h_{x_2}w^h_{\gamma,ij,ij+1} - \frac{1}{2}\frac{\left(w^h_{\gamma,ij,ij+1}\right)^2}{\left(Q^h_{ij,ij+1}\right)^3}\partial^h_{x_2}\varphi^h_{ij,ij+1}\right)\\
&- \frac{1}{h_1}\left(\mathbb{E}^h_{\gamma,11,ij,i-1j}\partial^h_{x_1}w^h_{\gamma,ij,i-1j} + \mathbb{E}^h_{\gamma,12,ij,i-1j}\partial^h_{x_2}w^h_{\gamma,ij,i-1j} - \frac{1}{2}\frac{\left(w^h_{\gamma,ij,i-1j}\right)^2}{\left(Q^h_{ij,i-1j}\right)^3}\partial^h_{x_1}\varphi^h_{ij,i-1j}\right)\\
&- \frac{1}{h_2}\left(\mathbb{E}^h_{\gamma,21,ij,ij-1}\partial^h_{x_1}w^h_{\gamma,ij,ij-1} + \mathbb{E}^h_{\gamma,22,ij,ij-1}\partial^h_{x_2}w^h_{\gamma,ij,ij-1} - \frac{1}{2}\frac{\left(w^h_{\gamma,ij,ij-1}\right)^2}{\left(Q^h_{ij,ij-1}\right)^3}\partial^h_{x_2}\varphi^h_{ij,ij-1}\right)\Bigg],
\end{aligned}$$

where for

$$\mathbb{E}^h_{\gamma,ij,\overline{ij}} = \begin{pmatrix} \mathbb{E}^h_{\gamma,11,ij,\overline{ij}} & \mathbb{E}^h_{\gamma,12,ij,\overline{ij}} \\ \mathbb{E}^h_{\gamma,21,ij,\overline{ij}} & \mathbb{E}^h_{\gamma,22,ij,\overline{ij}} \end{pmatrix}, \tag{6.125}$$

we have

$$\begin{aligned}
\mathbb{E}^h_{\gamma,ij,i+1j} &= \partial_{p_1}\partial_{p_1}\gamma\left(\nabla\varphi^h_{ij,i+1j},-1\right) \quad , \quad \mathbb{E}^h_{\gamma,ij,ij+1} = \partial_{p_1}\partial_{p_2}\gamma\left(\nabla\varphi^h_{ij,ij+1},-1\right),\\
\mathbb{E}^h_{\gamma,ij,i-1j} &= \partial_{p_1}\partial_{p_1}\gamma\left(\nabla\varphi^h_{ij,i-1j},-1\right) \quad , \quad \mathbb{E}^h_{\gamma,ij,ij-1} = \partial_{p_1}\partial_{p_2}\gamma\left(\nabla\varphi^h_{ij,ij-1},-1\right).
\end{aligned}$$

The Neumann boundary conditions $\partial_\nu \varphi = 0$ on $\partial\Omega$ take the following discrete form

$$\text{if } i = 1 \text{ then } \nu = (-1,0) \quad \Rightarrow \quad \frac{1}{h_1}\left(\varphi^h_{1,j} - \varphi^h_{0,j}\right) = 0, \tag{6.126}$$

$$\text{if } i = N_1 - 1 \text{ then } \nu = (1,0) \quad \Rightarrow \quad \frac{1}{h_1}\left(\varphi^h_{N_1,j} - \varphi^h_{N_1-1,j}\right) = 0, \tag{6.127}$$

$$\text{if } j = 1 \text{ then } \nu = (0,-1) \quad \Rightarrow \quad \frac{1}{h_2}\left(\varphi^h_{i,1} - \varphi^h_{i,0}\right) = 0, \tag{6.128}$$

$$\text{if } j = N_2 - 1 \text{ then } \nu = (0,1) \quad \Rightarrow \quad \frac{1}{h_2}\left(\varphi^h_{i,N_2} - \varphi^h_{i,N_2-1}\right) = 0 \tag{6.129}$$

and from (5.80) we get

$$\text{if } i = 1 \text{ then } \nu = (-1,0) \quad \Rightarrow \quad \mathbb{E}_{\gamma,11,1j,0j}\partial_{x_1} w^h_{\gamma,1j,0j} + \mathbb{E}_{\gamma,12,1j,0j}\partial_{x_2} w^h_{\gamma,1j,0j} = 0, \tag{6.130}$$

$$\begin{aligned}\text{if } i = N_1 - 1 \text{ then } \nu = (1,0) \quad \Rightarrow \quad & \mathbb{E}_{\gamma,11,N_1-1j,N_1j}\partial_{x_1} w^h_{\gamma,N_1-1j,N_1j} + \\ & \mathbb{E}_{\gamma,12,N_1-1j,N_1j}\partial_{x_2} w^h_{\gamma,N_1-1j,N_1j} = 0,\end{aligned} \tag{6.131}$$

$$\text{if } j = 1 \text{ then } \nu = (0,-1) \quad \Rightarrow \quad \mathbb{E}_{\gamma,21,i1,i0}\partial_{x_1} w^h_{\gamma,i1,i0} + \mathbb{E}_{\gamma,22,i1,i0}\partial_{x_2} w^h_{\gamma,i1,i0} = 0, \tag{6.132}$$

$$\begin{aligned}\text{if } j = N_2 - 1 \text{ then } \nu = (0,1) \quad \Rightarrow \quad & \mathbb{E}_{\gamma,21,iN_2-1,iN_2}\partial_{x_1} w^h_{\gamma,iN_2-1.iN_2} + \\ & \mathbb{E}_{\gamma,22,iN_2-1,iN_2}\partial_{x_2} w^h_{\gamma,iN_2-1,N_2} = 0.\end{aligned} \tag{6.133}$$

Numerical schemes for the anisotropic graph formulations We get the following schemes:

Scheme 6.2.18. The **complementary finite volume** semi-discrete numerical scheme for the **anisotropic Willmore flow of graphs with the Dirichlet boundary conditions** takes the following form

$$
\begin{aligned}
\frac{\mathrm{d}}{\mathrm{d}t}\varphi^h_{ij} &= Q_{ij}\left[\frac{\mathbb{E}^h_{\gamma,11,ij,i+1j}\partial^h_{x_1}w^h_{\gamma,ij,i+1j}+\mathbb{E}^h_{\gamma,12,ij,i+1j}\partial^h_{x_2}w^h_{\gamma,ij,i+1j}-\frac{1}{2}\frac{\left(w^h_{\gamma,ij,i+1j}\right)^2}{\left(Q^h_{ij,i+1j}\right)^3}\partial^h_{x_1}\varphi^h_{ij,i+1j}}{h_1}\right.\\
&+\frac{\mathbb{E}^h_{\gamma,21,ij,ij+1}\partial^h_{x_1}w^h_{\gamma,ij,ij+1}+\mathbb{E}^h_{\gamma,22,ij,ij+1}\partial^h_{x_2}w^h_{\gamma,ij,ij+1}-\frac{1}{2}\frac{\left(w^h_{\gamma,ij,ij+1}\right)^2}{\left(Q^h_{ij,ij+1}\right)^3}\partial^h_{x_2}\varphi^h_{ij,ij+1}}{h_2}\\
&-\frac{\mathbb{E}^h_{\gamma,11,ij,i-1j}\partial^h_{x_1}w^h_{\gamma,ij,i-1j}+\mathbb{E}^h_{\gamma,12,ij,i-1j}\partial^h_{x_2}w^h_{\gamma,ij,i-1j}-\frac{1}{2}\frac{\left(w^h_{\gamma,ij,i-1j}\right)^2}{\left(Q^h_{ij,i-1j}\right)^3}\partial^h_{x_1}\varphi^h_{ij,i-1j}}{h_1}\\
&-\left.\frac{\mathbb{E}^h_{\gamma,21,ij,ij-1}\partial^h_{x_1}w^h_{\gamma,ij,ij-1}+\mathbb{E}^h_{\gamma,22,ij,ij-1}\partial^h_{x_2}w^h_{\gamma,ij,ij-1}-\frac{1}{2}\frac{\left(w^h_{\gamma,ij,ij-1}\right)^2}{\left(Q^h_{ij,ij-1}\right)^3}\partial^h_{x_2}\varphi^h_{ij,ij-1}}{h_2}\right],
\end{aligned}
\tag{6.134}
$$

$$
\begin{aligned}
w^h_{\gamma,ij} &= Q^h_{ij}\left(\frac{\partial_{p_1}\gamma_{ij,i+1j}-\partial_{p_1}\gamma_{ij,i-1,j}}{h_1}+\frac{\partial_{p_2}\gamma_{ij,ij+1}-\partial_{p_2}\gamma_{ij,ij-1}}{h_2}\right) \text{ on } \omega_h,\\
\varphi^h_{ij}\,|_{t=0} &= \mathcal{P}\left(\varphi_{ini}\right)_{ij} \text{ on } \overline{\omega}_h, && (6.135)\\
\varphi^h_{ij} &= g_{ij} \text{ and } w^h_{ij}=0 \text{ on } \partial\omega_h, && (6.136)
\end{aligned}
$$

where Q^h_{ij} is given by (6.78) and $Q^h_{ij,i+1j}$, $Q^h_{ij,ij+1}$, $Q^h_{ij,i-1j}$ and $Q^h_{ij,ij-1}$ are given by (6.61)–(6.64), $\mathbb{E}^h_{\gamma,ij,\overline{ij}}$ is given by (6.125), $w^h_{\gamma,ij,\overline{ij}}$ by (6.120)–(6.121). $\partial^h_{x_1}\varphi^h_{ij,\overline{ij}}$ and $\partial^h_{x_2}\varphi^h_{ij,\overline{ij}}$ is approximated by (6.65)–(6.68).
The **complementary finite volume** semi-discrete numerical scheme for the **anisotropic Willmore flow of graphs with the Neumann boundary conditions** is given by (6.134)–(6.136), (6.126)–(6.129) and (6.130)–(6.133).

Scheme 6.2.19. The **complementary finite volume** semi-discrete numerical scheme for the **anisotropic mean-curvature flow of graphs with the Dirichlet boundary conditions** takes the form

$$\frac{\mathrm{d}}{\mathrm{dt}}\varphi_{ij}^h = Q_{ij}^h\left(\frac{\partial_{p_1}\gamma_{ij,i+1j}-\partial_{p_1}\gamma_{ij,i-1,j}}{h_1}+\frac{\partial_{p_2}\gamma_{ij,ij+1}-\partial_{p_2}\gamma_{ij,ij-1}}{h_2}\right) \text{ on } \omega_h, \quad (6.137)$$

$$\varphi_{ij}^h\,|_{t=0} = \mathcal{P}\left(\varphi_{ini}\right)_{ij} \text{ on } \overline{\omega}_h, \quad (6.138)$$

$$\varphi_{ij}^h = g_{ij} \text{ on } \partial\omega_h, \quad (6.139)$$

where Q_{ij}^h is given by (6.78) and $\nabla_{\mathbf{p}}\gamma_{ij,\overline{ij}} = \left(\partial_{p_1}\gamma_{ij,\overline{ij}}, \partial_{p_2}\gamma_{ij,\overline{ij}}\right)^T$ is given by (6.114).
The **complementary finite volume** semi-discrete numerical scheme for the **anisotropic mean-curvature flow of graphs with the Neumann boundary conditions** is given by (6.137)–(6.139) and (6.116)–(6.119).

Evaluation of anisotropic mean curvature for the level-set formulation Taking the right-hand side of the equation (5.30), integrating over a finite volume Ω_{ij} and applying the Stokes formula we get

$$\int_{\Omega_{ij}} H_\gamma \mathrm{dx} = \int_{\Omega_{ij}} \nabla\cdot\left(\nabla_{\mathbf{p}}\gamma\left(\nabla u\right)\right)\mathrm{dx} = \int_{\Gamma_{ij}} \nabla_{\mathbf{p}}\gamma\left(\nabla u\right)\cdot\nu \mathrm{d}\mathcal{H}^{n-1}, \quad (6.140)$$

which gives

$$\int_{\Omega_{ij}} H_\gamma \mathrm{dx} \approx \mu\left(\Omega\right) H_{\gamma,ij}^h = \sum_{v_{\overline{ij}}\in\mathcal{N}_{ij}} l_{ij,\overline{ij}} \nabla_{\mathbf{p}}\gamma_{ij,\overline{ij}}\nu_{ij,\overline{ij}}\mathrm{d}\mathcal{H}^{n-1}, \quad (6.141)$$

for

$$\nabla_{\mathbf{p}}\gamma_{ij,\overline{ij}} = \left(\partial_{p_1}\gamma_{ij,\overline{ij}}, \partial_{p_2}\gamma_{ij,\overline{ij}}\right)^T = \left(\partial_{p_1}\gamma\left(\nabla u_{ij,\overline{ij}}^h\right), \partial_{p_2}\gamma\left(\nabla u_{ij,\overline{ij}}^h\right)\right)^T. \quad (6.142)$$

On the regular dual mesh (6.54) we get

$$\begin{aligned} H_{\gamma,ij}^h &= \frac{1}{h_1h_2}\Big(h_2\nabla_{\mathbf{p}}\gamma_{ij,i+1j}\cdot(1,0)^T + h_1\nabla_{\mathbf{p}}\gamma_{ij,ij+1}\cdot(0,1)^T \\ &+ h_2\nabla_{\mathbf{p}}\gamma_{ij,i-1j}\cdot(-1,0)^T + h_1\nabla_{\mathbf{p}}\gamma_{ij,ij-1}\cdot(0,-1)^T\Big) \\ &= \left(\frac{\partial_{p_1}\gamma_{ij,i+1j}-\partial_{p_1}\gamma_{ij,i-1,j}}{h_1}+\frac{\partial_{p_2}\gamma_{ij,ij+1}-\partial_{p_2}\gamma_{ij,ij-1}}{h_2}\right). \end{aligned} \quad (6.143)$$

The Neumann boundary conditions from $\nabla_{\mathbf{p}}\gamma\cdot\nu=0$ are approximated as follows:

$$\text{if } i=1 \text{ then } \nu=(-1,0) \Rightarrow \partial_{p_1}\gamma_{1j,0j}=0, \quad (6.144)$$

$$\text{if } i=N_1-1 \text{ then } \nu=(1,0) \Rightarrow \partial_{p_1}\gamma_{N_1-1j,N_1j}=0, \quad (6.145)$$

$$\text{if } j=1 \text{ then } \nu=(0,-1) \Rightarrow \partial_{p_2}\gamma_{i1,i0}=0, \quad (6.146)$$

$$\text{if } j=N_2-1 \text{ then } \nu=(0,1) \Rightarrow \partial_{p_2}\gamma_{iN_2-1,iN_2}=0. \quad (6.147)$$

Anisotropic level-set formulation of the Willmore flow As for the isotropic level-set formulation, we start with the approximation of $w_\gamma = Q_\epsilon H_\gamma$. For the finite volume Ω_{ij} we get

$$\begin{aligned} w^h_{\gamma,ij} &= \frac{Q^h_{\epsilon,ij}}{\mu\left(\Omega_{ij}\right)} \sum_{v_{\overline{ij}} \in \mathcal{N}_{ij}} l_{ij,\overline{ij}} \nabla_{\mathbf{p}} \gamma_{ij,\overline{ij}} \nu_{ij,\overline{ij}} \\ &= Q^h_{\epsilon,ij} \left(\frac{\partial_{p_1}\gamma_{ij,i+1j} - \partial_{p_1}\gamma_{ij,i-1,j}}{h_1} + \frac{\partial_{p_2}\gamma_{ij,ij+1} - \partial_{p_2}\gamma_{ij,ij-1}}{h_2} \right), \end{aligned}$$

where $Q^h_{\epsilon,ij,\overline{ij}}$ is given by (6.103), $Q^h_{\epsilon,ij,i+1j}$, $Q^h_{\epsilon,ij,ij+1}$, $Q^h_{\epsilon,ij,i-1j}$ and $Q^h_{\epsilon,ij,ij-1}$ are given by (6.97)–(6.100) and we also define $w^h_{\gamma,ij,i+1j}$, $w^h_{\gamma,ij,ij+1}$, $w^h_{\gamma,ij,i-1j}$ and $w^h_{\gamma,ij,ij-1}$ by (6.120)–(6.121). We integrate the equation (5.89) over the finite volume Ω_{ij} and we apply the Stokes theorem to get

$$\int_{\Omega_{ij}} \frac{1}{Q_\epsilon} \partial_t u \mathrm{dx} = - \int_{\Gamma_{ij}} \mathbb{E}_\gamma \nabla w_\gamma \nu - \frac{1}{2} \frac{w^2_\gamma}{Q^3_\epsilon} \partial_\nu u \mathrm{d}\mathcal{H}^{n-1}, \tag{6.148}$$

which gives

$$\frac{\mu\left(\Omega_{ij}\right)}{Q^h_{\epsilon,ij}} \frac{\mathrm{d}}{\mathrm{d}t} u^h_{ij} = - \sum_{v_{\overline{ij}} \in \mathcal{N}_{ij}} l_{ij,\overline{ij}} \left(\mathbb{E}^h_{\gamma,ij,\overline{ij}} \nabla w^h_{\gamma,ij,\overline{ij}} \nu_{ij,\overline{ij}} - \frac{1}{2} \frac{\left(w^h_{\gamma,ij,\overline{ij}}\right)^2}{\left(Q^h_{\epsilon,ij,\overline{ij}}\right)^3} \nabla u^h_{ij,\overline{ij}} \nu_{ij,\overline{ij}} \right), \tag{6.149}$$

where for

$$\mathbb{E}^h_{\gamma,ij,\overline{ij}} = \begin{pmatrix} \mathbb{E}^h_{\gamma,11,ij,\overline{ij}} & \mathbb{E}^h_{\gamma,12,ij,\overline{ij}} \\ \mathbb{E}^h_{\gamma,21,ij,\overline{ij}} & \mathbb{E}^h_{\gamma,22,ij,\overline{ij}} \end{pmatrix}, \tag{6.150}$$

we have

$$\begin{aligned} \mathbb{E}^h_{\gamma,ij,i+1j} &= \partial_{p_1}\partial_{p_1}\gamma\left(\nabla u^h_{ij,i+1j}\right) \quad , \quad \mathbb{E}^h_{\gamma,ij,ij+1} = \partial_{p_1}\partial_{p_2}\gamma\left(\nabla u^h_{ij,ij+1}\right), \\ \mathbb{E}^h_{\gamma,ij,i-1j} &= \partial_{p_1}\partial_{p_1}\gamma\left(\nabla u^h_{ij,i-1j}\right) \quad , \quad \mathbb{E}^h_{\gamma,ij,ij-1} = \partial_{p_1}\partial_{p_2}\gamma\left(\nabla u^h_{ij,ij-1}\right). \end{aligned}$$

and we set

$$w^h_{\gamma,ij,i+1j} = \frac{1}{2}\left(w^h_{\gamma,ij} + w^h_{\gamma,i+1j}\right) \quad , \quad w^h_{\gamma,ij,ij+1} = \frac{1}{2}\left(w^h_{\gamma,ij} + w^h_{\gamma,ij+1}\right), \tag{6.151}$$

$$w^h_{\gamma,ij,i-1j} = \frac{1}{2}\left(w^h_{\gamma,ij} + w^h_{\gamma,i-1j}\right) \quad , \quad w^h_{\gamma,ij,ij-1} = \frac{1}{2}\left(w^h_{\gamma,ij} + w^h_{\gamma,ij-1}\right). \tag{6.152}$$

In terms of the regular dual mesh (6.54) it reads

$$\begin{aligned} \frac{\mathrm{d}}{\mathrm{d}t} u^h_{ij} &= Q^h_{\epsilon,ij} \left[\frac{1}{h_1} \left(\mathbb{E}^h_{\gamma,11,ij,i+1j} \partial^h_{x_1} w^h_{\gamma,ij,i+1j} + \mathbb{E}^h_{12,ij,i+1j} \partial^h_{x_2} w^h_{\gamma,ij,i+1j} - \frac{1}{2} \frac{\left(w^h_{\gamma,ij,i+1j}\right)^2}{\left(Q^h_{\epsilon,ij,i+1j}\right)^3} \partial^h_{x_1} u^h_{ij,i+1j} \right) \right. \\ &+ \frac{1}{h_2} \left(\mathbb{E}^h_{\gamma,21,ij,ij+1} \partial^h_{x_1} w^h_{\gamma,ij,ij+1} + \mathbb{E}^h_{\gamma,22,ij,ij+1} \partial^h_{x_2} w^h_{\gamma,ij,ij+1} - \frac{1}{2} \frac{\left(w^h_{\gamma,ij,ij+1}\right)^2}{\left(Q^h_{\epsilon,ij,ij+1}\right)^3} \partial^h_{x_2} u^h_{ij,ij+1} \right) \\ &- \frac{1}{h_1} \left(\mathbb{E}^h_{\gamma,11,ij,i-1j} \partial^h_{x_1} w^h_{\gamma,ij,i-1j} + \mathbb{E}^h_{\gamma,12,ij,i-1j} \partial^h_{x_2} w^h_{\gamma,ij,i-1j} - \frac{1}{2} \frac{\left(w^h_{\gamma,ij,i-1j}\right)^2}{\left(Q^h_{\epsilon,ij,i-1j}\right)^3} \partial^h_{x_1} u^h_{ij,i-1j} \right) \\ &- \left. \frac{1}{h_2} \left(\mathbb{E}^h_{\gamma,21,ij,ij-1} \partial^h_{x_1} w^h_{\gamma,ij,ij-1} + \mathbb{E}^h_{\gamma,22,ij,ij-1} \partial^h_{x_2} w^h_{\gamma,ij,ij-1} - \frac{1}{2} \frac{\left(w^h_{\gamma,ij,ij-1}\right)^2}{\left(Q^h_{\epsilon,ij,ij-1}\right)^3} \partial^h_{x_2} u^h_{ij,ij-1} \right) \right]. \end{aligned}$$

The Neumann boundary conditions $\partial_\nu \varphi = 0$ on $\partial\Omega$ take the following discrete form

$$
\begin{aligned}
\text{if } i = 1 \text{ then } \nu = (-1,0) \quad &\Rightarrow \quad \frac{1}{h_1}\left(\varphi^h_{1,j} - \varphi^h_{0,j}\right) = 0, &(6.153)\\
\text{if } i = N_1 - 1 \text{ then } \nu = (1,0) \quad &\Rightarrow \quad \frac{1}{h_1}\left(\varphi^h_{N_1,j} - \varphi^h_{N_1-1,j}\right) = 0, &(6.154)\\
\text{if } j = 1 \text{ then } \nu = (0,-1) \quad &\Rightarrow \quad \frac{1}{h_2}\left(\varphi^h_{i,1} - \varphi^h_{i,0}\right) = 0, &(6.155)\\
\text{if } j = N_2 - 1 \text{ then } \nu = (0,1) \quad &\Rightarrow \quad \frac{1}{h_2}\left(\varphi^h_{i,N_2} - \varphi^h_{i,N_2-1}\right) = 0 &(6.156)
\end{aligned}
$$

and from (5.80) we get

$$
\begin{aligned}
\text{if } i = 1 \text{ then } \nu = (-1,0) \quad &\Rightarrow \quad \mathbb{E}_{\gamma,11,1j,0j}\partial_{x_1} w^h_{\gamma,1j,0j} + \mathbb{E}_{\gamma,12,1j,0j}\partial_{x_2} w^h_{\gamma,1j,0j} = 0, &(6.157)\\
\text{if } i = N_1 - 1 \text{ then } \nu = (1,0) \quad &\Rightarrow \quad \mathbb{E}_{\gamma,11,N_1-1j,N_1j}\partial_{x_1} w^h_{\gamma,N_1-1j,N_1j} + \\
&\qquad \mathbb{E}_{\gamma,12,N_1-1j,N_1j}\partial_{x_2} w^h_{\gamma,N_1-1j,N_1j} = 0, &(6.158)\\
\text{if } j = 1 \text{ then } \nu = (0,-1) \quad &\Rightarrow \quad \mathbb{E}_{\gamma,21,i1,i0}\partial_{x_1} w^h_{\gamma,i1,i0} + \mathbb{E}_{\gamma,22,i1,i0}\partial_{x_2} w^h_{\gamma,i1,i0} = 0, &(6.159)\\
\text{if } j = N_2 - 1 \text{ then } \nu = (0,1) \quad &\Rightarrow \quad \mathbb{E}_{\gamma,21,iN_2-1,iN_2}\partial_{x_1} w^h_{\gamma,iN_2-1.iN_2} + \\
&\qquad \mathbb{E}_{\gamma,22,iN_2-1,iN_2}\partial_{x_2} w^h_{\gamma,iN_2-1,N_2} = 0. &(6.160)
\end{aligned}
$$

Numerical schemes for the anisotropic level-set formulations We conclude with the following schemes:

Scheme 6.2.20. The **complementary finite volume** semi-discrete numerical scheme for the **level-set formulation of the anisotropic mean-curvature flow with the Dirichlet boundary conditions** takes the form

$$
\frac{\mathrm{d}}{\mathrm{dt}} u^h_{ij} = Q^h_{\epsilon,ij}\left(\frac{\partial_{p_1}\gamma_{ij,i+1j} - \partial_{p_1}\gamma_{ij,i-1,j}}{h_1} + \frac{\partial_{p_2}\gamma_{ij,ij+1} - \partial_{p_2}\gamma_{ij,ij-1}}{h_2}\right) \text{ on } \omega_h, \tag{6.161}
$$

$$
u^h_{ij}\,|_{t=0} = \mathcal{P}\left(u_{ini}\right)_{ij} \text{ on } \overline{\omega}_h, \tag{6.162}
$$

$$
u^h_{ij} = g_{ij} \text{ on } \partial\omega_h, \tag{6.163}
$$

where $Q^h_{\epsilon,ij}$ is given by (6.103) and and $\nabla_{\mathbf{p}}\gamma_{ij,\overline{ij}} = \left(\partial_{p_1}\gamma_{ij,\overline{ij}}, \partial_{p_2}\gamma_{ij,\overline{ij}}\right)^T$ is given by (6.142). The **complementary finite volume** semi-discrete numerical scheme for the **level-set formulation of the anisotropic mean-curvature flow with the Neumann boundary conditions** is given by (6.161)–(6.162) and (6.144)–(6.147).

Scheme 6.2.21. The **complementary finite volume** semi-discrete numerical scheme for the **level-set formulation of the anisotropic Willmore flow with the Dirichlet boundary conditions** takes the form

$$
\begin{aligned}
\frac{\mathrm{d}}{\mathrm{d}t} u_{ij}^h &= Q_{\epsilon,ij}^h \Bigg[\frac{\mathbb{E}_{11,ij,i+1j}^h \partial_{x_1}^h w_{ij,i+1j}^h + \mathbb{E}_{12,ij,i+1j}^h \partial_{x_2}^h w_{ij,i+1j}^h - \frac{1}{2} \frac{\left(w_{ij,i+1j}^h\right)^2}{\left(Q_{\epsilon,ij,i+1j}^h\right)^3} \partial_{x_1}^h u_{ij,i+1j}^h}{h_1} \\
&+ \frac{\mathbb{E}_{21,ij,ij+1}^h \partial_{x_1}^h w_{ij,ij+1}^h + \mathbb{E}_{22,ij,ij+1}^h \partial_{x_2}^h w_{ij,ij+1}^h - \frac{1}{2} \frac{\left(w_{ij,ij+1}^h\right)^2}{\left(Q_{\epsilon,ij,ij+1}^h\right)^3} \partial_{x_2}^h u_{ij,ij+1}^h}{h_2} \\
&- \frac{\mathbb{E}_{11,ij,i-1j}^h \partial_{x_1}^h w_{ij,i-1j}^h + \mathbb{E}_{12,ij,i-1j}^h \partial_{x_2}^h w_{ij,i-1j}^h - \frac{1}{2} \frac{\left(w_{ij,i-1j}^h\right)^2}{\left(Q_{\epsilon,ij,i-1j}^h\right)^3} \partial_{x_1}^h u_{ij,i-1j}^h}{h_1} \\
&- \frac{\mathbb{E}_{21,ij,ij-1}^h \partial_{x_1}^h w_{ij,ij-1}^h + \mathbb{E}_{22,ij,ij-1}^h \partial_{x_2}^h w_{ij,ij-1}^h - \frac{1}{2} \frac{\left(w_{ij,ij-1}^h\right)^2}{\left(Q_{\epsilon,ij,ij-1}^h\right)^3} \partial_{x_2}^h u_{ij,ij-1}^h}{h_2} \Bigg],
\end{aligned} \tag{6.164}
$$

$$
w_{ij}^h = Q_{\epsilon,ij}^h \left(\frac{u_{i+1j}^h - u_{ij}^h}{h_1^2 Q_{\epsilon,ij,i+1j}^h} + \frac{u_{ij+1}^h - u_{ij}^h}{h_2^2 Q_{\epsilon,ij,ij+1}^h} - \frac{u_{ij}^h - u_{i-1j}^h}{h_1^2 Q_{\epsilon,ij,i-1j}^h} - \frac{u_{ij}^h - u_{ij-1}^h}{h_2^2 Q_{\epsilon,ij,ij-1}^h} \right) \text{ on } \omega_h, \tag{6.165}
$$

$$
u_{ij}^h \,|_{t=0} = \mathcal{P}\left(u_{ini}\right)_{ij} \text{ on } \overline{\omega}_h, \tag{6.166}
$$

$$
u_{ij}^h = g_{ij} \text{ and } w_{ij}^h = 0 \text{ on } \partial\omega_h, \tag{6.167}
$$

where $Q_{\epsilon,ij}^h$ is given by (6.103) and $Q_{\epsilon,ij,i+1j}^h$, $Q_{\epsilon,ij,ij+1}^h$, $Q_{\epsilon,ij,i-1j}^h$ and $Q_{\epsilon,ij,ij-1}^h$ are given by (6.97)–(6.100), $\mathbb{E}_{ij,\overline{ij}}$ is given by (6.85), $w_{ij,\overline{ij}}$ by (6.82)–(6.83) and as (6.69)–(6.72). $\partial_{x_1} u_{ij,\overline{ij}}^h$ and $\partial_{x_2} u_{ij,\overline{ij}}^h$ is approximated by (6.65)–(6.68).
The **complementary finite volume** semi-discrete numerical scheme for the **level-set formulation of the anisotropic Willmore flow with the Neumann boundary conditions** is given by (6.164)–(6.166), (6.144)–(6.147) and (6.157)–(6.160).

Remark 6.2.22. We can see that in general we get implicit boundary conditions of the form (6.116)-(6.119), (6.144)-(6.147), (6.130)-(6.133) and (6.157)-(6.160). These equations are non-linear in u_{ij}^h resp. w_{ij}^h on $\partial\omega_h$ and therefore it is not trivial to solve them. As a result we do not know these quantities on $\partial\omega_h$. In section 6.3.2, we will see that it is important for the semi-implicit scheme and we will show how to approximate the quantities we mentioned on the boundaries.

Remark 6.2.23. In the Figure 6.7 we show the stencil of the complementary finite volume schemes for the fourth order problem (6.2.18) and (6.2.21). It is a 21 point stencil (resp. a 25 point stencil in the case of the anisotropy 5.111). One can see that the stencil is symmetric and it is smaller then the stencil for the central schemes (see Figure 6.3).

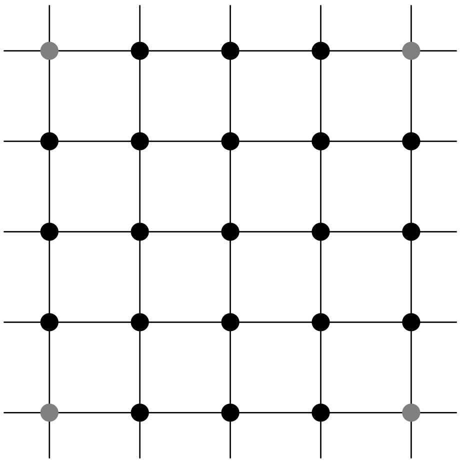

Figure 6.7.: Stencil of the numerical schemes (6.2.15), (6.2.17), (6.2.18) and (6.2.21) is symmetric and compact. Grey points represent the stencil of the schemes with the anisotropy (5.111)

Comparison with finite difference approach

Now we aim to derive the same schemes as in the previous section (i.e. schemes (6.2.14), (6.2.15), (6.2.16), (6.2.15), (6.2.19), (6.2.18), (6.2.20) and (6.2.21)) in terms of the finite difference method. The essence of this approach is in a definition of a finer numerical grid

$$\Omega_h = \left\{ (ih_1, jh_2) \mid i = \frac{1}{2}, 1, \cdots N_1 - \frac{1}{2}; j = \frac{1}{2}, 1 \cdots N_2 - \frac{1}{2} \right\}, \tag{6.168}$$

In comparison with the mesh ω_h we have added new nodes which are counterparts of the boundaries of the finite volumes of the dual mesh (6.54). The values of the grid function u^h_{ij} on Ω_h are obtained by the following interpolation mapping:

Definition 6.2.24. *The interpolation mapping $\mathcal{I}\left(u^h, i, j, r, s\right) : \omega_h \to \Omega_h$ is linear mapping defined for $r, s \in \{-1, 1\}$ as:*

$$\begin{aligned}
\mathcal{I}\left(u^h, i, j, r, 0\right) &= \frac{1}{2}\left(u^h_{i+r,j} + u^h_{ij}\right), \\
\mathcal{I}\left(u^h, i, j, 0, s\right) &= \frac{1}{2}\left(u^h_{i,j+s} + u^h_{ij}\right), \\
\mathcal{I}\left(u^h, i, j, r, s\right) &= \frac{1}{4}\left(u^h_{i+r,j+s} + u^h_{i+r,j} + u^h_{i,j+s} + u^h_{ij}\right).
\end{aligned}$$

For $r, s \in \{-1, 0, 1\}$ we set $u^h_{i+\frac{r}{2},j+\frac{s}{2}} = \mathcal{I}\left(u^h, i, j, r, s\right)$. By uppercase, we denote a grid function with doubled indices

$$U^h_{kl} = u^h_{\frac{k}{2}\frac{l}{2}}, \tag{6.169}$$

for $k = 0, \cdots, 2N_1$ and $l = 0, \cdots, 2N_2$. We extend the notation for finite differences on the finer grid as

$$\begin{aligned}
U^h_{f.,kl} &= 2\frac{U^h_{k+1,l} - U^h_{kl}}{h} &, \quad U^h_{b.,kl} &= 2\frac{U^h_{kl} - U^h_{k-1,l}}{h}, \\
U^h_{.f,kl} &= 2\frac{U^h_{k,l+1} - U^h_{kl}}{h} &, \quad U^h_{.b,kl} &= 2\frac{U^h_{kl} - U^h_{k,l-1}}{h}, \\
U^h_{c.,kl} &= \frac{1}{2}\left(U^h_{f.,kl} + U^h_{b.,kl}\right) &, \quad U^h_{.c,kl} &= \frac{1}{2}\left(U^h_{.f,kl} + U^h_{.b,kl}\right)
\end{aligned}$$

To approximate gradient of u we define

$$\nabla_h u_{ij}^h = \left(U_{c.,2i,2j}^h, U_{.c,2i,2j}^h\right) \quad \text{for} \quad i = 1, \cdots N_1 - 1,\ j = 1, \cdots, N_2 - 1$$

Note that since we define $\nabla_h u_{ij}^h$ in terms of U_{kl}^h we can also write $\nabla_h u_{i\pm\frac{1}{2},j\pm\frac{1}{2}}^h$ for $i = 1 \cdots N_1 - 1$ and $j = 1, \cdots N_2 - 1$. The discrete divergence operator is defined in the same manner.

For the graph formulation we denote

$$Q_{i\pm\frac{1}{2},j\pm\frac{1}{2}}^h = \sqrt{1 + \left|\nabla_h \varphi_{i\pm\frac{1}{2},j\pm\frac{1}{2}}^h\right|^2} \quad \text{resp.} \quad Q_{ij}^h = \frac{1}{4} \sum_{\substack{\zeta,\eta\in\{-1,1)\\ |\zeta|+|\eta|=1}} Q_{i+\frac{\zeta}{2},j+\frac{\eta}{2}}^h, \tag{6.170}$$

$$H_{\gamma,ij}^h = \nabla_h \cdot \nabla_{\mathbf{p}} \gamma_{ij} = \nabla_h \cdot \left(\partial_{p_1}\gamma_{ij}, \partial_{p_2}\gamma_{ij}\right)^T, \tag{6.171}$$

$$\mathbb{E}_{\gamma,i\pm\frac{1}{2},j\pm\frac{1}{2}}^h = \mathbb{E}_\gamma\left(\nabla_h \varphi_{i\pm\frac{1}{2},j\pm\frac{1}{2}}^h\right) = \nabla_{\mathbf{p}} \otimes \nabla_{\mathbf{p}} \gamma\left(\varphi_{i\pm\frac{1}{2},j\pm\frac{1}{2}}^h, -1\right). \tag{6.172}$$

for $i = 1, \cdots N_1 - 1$ and $j = 1, \cdots, N_2 - 1$ where

$$\left(\partial_{p_1}\gamma_{ij}, \partial_{p_2}\gamma_{ij}\right)^T = \left(\partial_{p_1}\gamma\left(\nabla_h \varphi_{ij}^h, -1\right), \partial_{p_2}\left(\nabla_h \varphi_{ij}^h, -1\right)\right)^T. \tag{6.173}$$

Remark 6.2.25. We demonstrate the meaning of the approximation on the isotropic mean curvature. It gives

$$H_{\gamma,ij}^h = \nabla_h \cdot \left(\frac{\nabla_h \varphi_{ij}^h}{Q_{ij}^h}\right).$$

Since we want to evaluate the discrete divergence ∇_h at the point x_{ij}, we will use the neighbours $x_{i\pm\frac{1}{2},j\pm\frac{1}{2}}$. We get

$$H_{\gamma,ij}^h = \frac{1}{h_1}\left(\frac{\partial_{x_1}^h u_{i+\frac{1}{2},j}^h}{Q_{i+\frac{1}{2},j}^h} - \frac{\partial_{x_1}^h u_{i-\frac{1}{2},j}^h}{Q_{i-\frac{1}{2},j}^h}\right) + \frac{1}{h_2}\left(\frac{\partial_{x_2}^h u_{i,j+\frac{1}{2}}^h}{Q_{i,j-\frac{1}{2}}^h} - \frac{\partial_{x_2}^h u_{i,j-\frac{1}{2}}^h}{Q_{i,j-\frac{1}{2}}^h}\right),$$

and simple substitution for $\partial_{x_l}^h u_{i\pm\frac{1}{2},j\pm\frac{1}{2}}^h$ for $l = 1, 2$ gives

$$H_{\gamma,ij}^h = \frac{1}{h_1^2}\left(\frac{u_{i+1,j}^h - u_{ij}^h}{Q_{i+\frac{1}{2},j}^h} - \frac{u_{ij}^h - u_{i-1,j}^h}{Q_{i-\frac{1}{2},j}^h}\right) + \frac{1}{h_2^2}\left(\frac{u_{i,j+1}^h - u_{ij}^h}{Q_{i,j-\frac{1}{2}}^h} - \frac{u_{ij}^h - u_{i,j-1}^h}{Q_{i,j-\frac{1}{2}}^h}\right),$$

Remark 6.2.26. In case when we compute $\nabla_h H_{\gamma,ij}^h$ or $\nabla_h w_{ij}^h$, having $H_{\gamma,i+\frac{r}{2},j+\frac{s}{2}}$ or $w_{i+\frac{r}{2},j+\frac{s}{2}}^h$ for $r, s \in \{-1, 0, 1\}$ is required. We have two possibilities how to achieve these quantities - either exact evaluation by substituting $\nabla_h u_{i+\frac{r}{2},j+\frac{s}{2}}^h$ as $H_{\gamma,i+\frac{r}{2},j+\frac{s}{2}}^h := H_\gamma\left(\nabla_h u_{i+\frac{r}{2},j+\frac{s}{2}}^h\right)$, or by means of the interpolation mapping (6.2.24) on $H_{\gamma,ij}^h$ as $H_{\gamma,i+\frac{r}{2},j+\frac{s}{2}}^h := \mathcal{I}\left(H_\gamma^h, i, j, r, s\right)$. Numerical experiments show that the latter approach gives the same accuracy of the scheme. Moreover, implementation of such schemes is significantly easier and more efficient. Therefore we choose the interpolation.

Now we introduce the following schemes (we consider only the anisotropic problems):

Scheme 6.2.27. The **finite difference** semi-discrete approximation of the **mean-curvature flow of graphs with the Dirichlet boundary conditions** with the anisotropy given by γ reads as

$$\frac{d\varphi_{ij}^h}{dt} = Q_{ij}^h \left(\frac{\partial_{p_1}\gamma_{ij,i+1j} - \partial_{p_1}\gamma_{ij,i-1,j}}{h_1} + \frac{\partial_{p_2}\gamma_{ij,ij+1} - \partial_{p_2}\gamma_{ij,ij-1}}{h_2} \right) \text{ on } \omega_h, \quad (6.174)$$

$$\varphi_{ij}^h \mid_{t=0} = \mathcal{P}\left(\varphi_{ini}\right)_{ij} \text{ on } \overline{\omega}_h, \quad (6.175)$$

$$\varphi_{ij}^h = g_{ij} \text{ on } \partial\omega_h,$$

where Q_{ij}^h is given by (6.170), $\partial_{p_1}\gamma_{ij}$, $\partial_{p_2}\gamma_{ij}$ by (6.173). The **finite difference** semi-discrete approximation of the **mean-curvature flow of graphs with the Neumann boundary conditions** with the anisotropy function γ is given by (6.174)–(6.175) and

$$\gamma_{p_1,i-\frac{1}{2},j} = 0 \text{ for } i = 1, \quad \gamma_{p_1,i+\frac{1}{2},j} = 0 \text{ for } i = N_1 - 1, \quad (6.176)$$

$$\gamma_{p_2,i,j-\frac{1}{2}} = 0 \text{ for } j = 1, \quad \gamma_{p_2,i,j+\frac{1}{2}} = 0 \text{ for } j = N_2 - 1. \quad (6.177)$$

Scheme 6.2.28. The **finite difference** semi-discrete approximation of the **anisotropic Willmore flow of graphs with the Dirichlet boundary conditions** with the anisotropy given by γ reads as

$$\frac{d\varphi_{ij}^h}{dt} = -Q_{ij}^h \nabla_h \cdot \left[\mathbb{E}_{\gamma,ij}^h \nabla_h w_{\gamma,ij}^h - \frac{1}{2} \frac{\left(w_{\gamma,ij}^h\right)^2}{\left(Q_{ij}^h\right)^3} \nabla_h \varphi_{ij}^h \right] \text{ on } \omega_h, \tag{6.178}$$

$$w_{\gamma,ij}^h = Q_{ij}^h \left(\frac{\partial_{p_1}\gamma_{ij,i+1j} - \partial_{p_1}\gamma_{ij,i-1,j}}{h_1} + \frac{\partial_{p_2}\gamma_{ij,ij+1} - \partial_{p_2}\gamma_{ij,ij-1}}{h_2} \right) \text{ on } \omega_h, \tag{6.179}$$

$$\varphi_{ij}^h\,|_{t=0} = \mathcal{P}\left(\varphi_{ini}\right)_{ij} \text{ on } \overline{\omega}_h, \tag{6.180}$$

$$\varphi_{ij}^h = g_{ij} \text{ and } w_{\gamma,ij}^h = 0 \text{ on } \partial\omega_h. \tag{6.181}$$

where Q_{ij}^h is given by (6.170), $\mathbb{E}_{\gamma,ij}^h$ by (6.172) and $\partial_{p_1}\gamma_{ij}$, $\partial_{p_2}\gamma_{ij}$ by (6.173). The **finite difference** semi-discrete approximation of the **anisotropic Willmore flow of graphs with the Neumann boundary conditions** with the anisotropy function γ is given by (6.178)–(6.180) and

$$\mathbb{E}_{11,i-\frac{1}{2},j}\partial_{x_1} w_{\gamma,i-\frac{1}{2},j}^h + \mathbb{E}_{12,i-\frac{1}{2},j}\partial_{x_2} w_{\gamma,1-\frac{1}{2},j}^h = 0 \text{ for } i = 1, \tag{6.182}$$

$$\mathbb{E}_{11,i+\frac{1}{2},j}\partial_{x_1} w_{\gamma,i+\frac{1}{2},j}^h + \mathbb{E}_{12,i+\frac{1}{2},j}\partial_{x_2} w_{\gamma,i+\frac{1}{2},j}^h = 0 \text{ for } i = N_1 - 1, \tag{6.183}$$

$$\mathbb{E}_{21,i,j-\frac{1}{2}}\partial_{x_1} w_{\gamma,i,j-\frac{1}{2}}^h + \mathbb{E}_{22,i,j-\frac{1}{2}}\partial_{x_2} w_{\gamma,i,j-\frac{1}{2}}^h = 0 \text{ for } j = 1, \tag{6.184}$$

$$\mathbb{E}_{21,i,j+\frac{1}{2}}\partial_{x_1} w_{\gamma,i,j+\frac{1}{2}}^h + \mathbb{E}_{22,i,j+\frac{1}{2}}\partial_{x_2} w_{\gamma,i,j+\frac{1}{2}}^h = 0 \text{ for } j = N_2 - 1, \tag{6.185}$$

together with $\partial_\nu^h \varphi_{ij}^h = 0$ on $\partial\omega_h$.

For the level-set formulation we denote

$$Q_{\epsilon,i\pm\frac{1}{2},j\pm\frac{1}{2}}^h = \sqrt{\epsilon^2 + \left|\nabla_h u_{i\pm\frac{1}{2},j\pm\frac{1}{2}}^h\right|^2} \quad \text{resp.} \quad Q_{ij}^h = \frac{1}{4} \sum_{\substack{\zeta,\eta\in\{-1,1)\\ |\zeta|+|\eta|=1}} Q_{i+\frac{\zeta}{2},j+\frac{\eta}{2}}^h, \tag{6.186}$$

$$H_{\gamma,ij}^h = \nabla_h \cdot \nabla_{\mathbf{p}}\gamma_{ij} = \nabla_h \cdot \left(\partial_{p_1}\gamma_{ij}, \partial_{p_2}\gamma_{ij}\right)^T, \tag{6.187}$$

$$\mathbb{E}_{\gamma,i\pm\frac{1}{2},j\pm\frac{1}{2}}^h = \mathbb{E}_\gamma\left(\nabla_h \varphi_{i\pm\frac{1}{2},j\pm\frac{1}{2}}^h\right) = \nabla_{\mathbf{p}} \otimes \nabla_{\mathbf{p}}\gamma\left(\varphi_{i\pm\frac{1}{2},j\pm\frac{1}{2}}^h\right). \tag{6.188}$$

for $i = 1, \cdots N_1 - 1$ and $j = 1, \cdots, N_2 - 1$ where

$$\left(\partial_{p_1}\gamma_{ij}, \partial_{p_2}\gamma_{ij}\right)^T = \left(\partial_{p_1}\gamma\left(\nabla_h \varphi_{ij}^h\right), \partial_{p_2}\left(\nabla_h \varphi_{ij}^h\right)\right)^T. \tag{6.189}$$

It allows us to introduce the following schemes:

Scheme 6.2.29. The **finite difference** semi-discrete approximation of the **level-set formulation of the mean-curvature flow with the Dirichlet boundary conditions** with the anisotropy given by γ reads as:

$$\begin{aligned} \frac{du^h_{ij}}{dt} &= Q^h_{ij} H^h_{\gamma,ij} \text{ on } \omega_h, && (6.190)\\ u^h_{ij} \mid_{t=0} &= \mathcal{P}\left(u_{ini}\right)_{ij} \text{ on } \overline{\omega}_h, && (6.191)\\ u^h_{ij} &= g_{ij} \text{ on } \partial\omega_h, \end{aligned}$$

where Q^h_{ij} is given by (6.186), $\mathbb{E}^h_{\gamma,ij}$ by (6.188) and $\partial_{p_1}\gamma_{ij}$, $\partial_{p_2}\gamma_{ij}$ by (6.189).
The **finite difference** semi-discrete approximation of the **level-set formulation of the mean-curvature flow with the Neumann boundary conditions** with the anisotropy function γ is given by (6.190)–(6.191) and

$$\begin{aligned} \gamma_{p_1,i-\frac{1}{2},j} &= 0 \text{ for } i=1, \quad \gamma_{p_1,i+\frac{1}{2},j} = 0 \text{ for } i = N_1-1, && (6.192)\\ \gamma_{p_2,i,j-\frac{1}{2}} &= 0 \text{ for } j=1, \quad \gamma_{p_2,i,j+\frac{1}{2}} = 0 \text{ for } j = N_2-1. && (6.193) \end{aligned}$$

Scheme 6.2.30. The **finite difference** semidiscrete approximation of the **anisotropic level-set formulation of the Willmore flow with the Dirichlet boundary conditions** with the anisotropy function γ reads as

$$\begin{aligned} \frac{du^h_{ij}}{dt} &= -Q^h_{ij}\nabla_h \cdot \left[\mathbb{E}^h_{\gamma,ij}\nabla_h w^h_{\gamma,ij} - \frac{1}{2}\frac{\left(w^h_{\gamma,ij}\right)^2}{\left(Q^h_{ij}\right)^3}\nabla_h u^h_{ij}\right] \text{ on } \omega_h, && (6.194)\\ w^h_{\gamma,ij} &= Q^h_{ij} H^h_{\gamma,ij}, \text{ on } \omega_h, && (6.195)\\ u^h_{ij} \mid_{t=0} &= \mathcal{P}\left(u_{ini}\right)_{ij} \text{ on } \overline{\omega}_h, && (6.196)\\ u^h_{ij} &= g_{ij} \text{ and } w^h_{\gamma,ij} = 0 \text{ on } \partial\omega_h, \end{aligned}$$

where Q^h_{ij} is given by (6.186), $\mathbb{E}^h_{\gamma,ij}$ by (6.188) and $\partial_{p_1}\gamma_{ij}$, $\partial_{p_2}\gamma_{ij}$ by (6.189).
The **finite difference** semidiscrete approximation of the **anisotropic level-set formulation of the Willmore flow with the Neumann boundary conditions** with the anisotropy function γ is given by (6.194)–(6.196) and

$$\begin{aligned} \mathbb{E}^h_{11,i-\frac{1}{2},j}\partial_{x_1} w^h_{\gamma,i-\frac{1}{2},j} + \mathbb{E}^h_{12,i-\frac{1}{2},j}\partial_{x_2} w^h_{\gamma,1-\frac{1}{2},j} &= 0 \text{ for } i = 1, && (6.197)\\ \mathbb{E}^h_{11,i+\frac{1}{2},j}\partial_{x_1} w^h_{\gamma,i+\frac{1}{2},j} + \mathbb{E}^h_{12,i+\frac{1}{2},j}\partial_{x_2} w^h_{\gamma,i+\frac{1}{2},j} &= 0 \text{ for } i = N_1-1, && (6.198)\\ \mathbb{E}^h_{21,i,j-\frac{1}{2}}\partial_{x_1} w^h_{\gamma,i,j-\frac{1}{2}} + \mathbb{E}^h_{22,i,j-\frac{1}{2}}\partial_{x_2} w^h_{\gamma,i,j-\frac{1}{2}} &= 0 \text{ for } j = 1, && (6.199)\\ \mathbb{E}^h_{21,i,j+\frac{1}{2}}\partial_{x_1} w^h_{\gamma,i,j+\frac{1}{2}} + \mathbb{E}^h_{22,i,j+\frac{1}{2}}\partial_{x_2} w^h_{\gamma,i,j+\frac{1}{2}} &= 0 \text{ for } j = N_2-1, && (6.200) \end{aligned}$$

together with $\partial^h_\nu u^h_{ij} = 0$ on $\partial\omega_h$.

Remark: In comparison with the complementary finite volume schemes (6.2.14), (6.2.15), (6.2.16), (6.2.15), (6.2.19), (6.2.18), (6.2.20) and (6.2.21) the finite difference schemes (6.2.27), (6.2.28), (6.2.29) and (6.2.30) are less general because they are restricted to regular orthogonal numerical grids. On the other hand, we can see that they are expressed in more compact form which is more similar to the original mathematical formulation. In the next part, it will allows us to treat these schemes as the one-sided or central finite difference numerical schemes and show some energy properties in the case of the Willmore flow of graphs. We remind that in this text we study all numerical schemes only on the regular orthogonal numerical grids and in this case the complementary finite volume schemes (6.2.14), (6.2.15), (6.2.16), (6.2.15), (6.2.19), (6.2.18), (6.2.20), (6.2.21) and they finite difference counterparts (6.2.27), (6.2.28), (6.2.29) and (6.2.30) give the same results - moreover they lead to the same implementation.

Energy equality of the Willmore flow of graphs

We prove analogy to (5.2.11). First, we need to extend the definitions of the scalar products for the grid functions on the finner grid. Assume having the grid functions $f, g : \overline{\Omega}_h \to \mathbb{R}$, $\boldsymbol{f} : \overline{\omega}_h \to \mathbb{R}^2$ and the related finner grid functions $F, G, \boldsymbol{F}$ defined by (6.169) we define

$$
\begin{aligned}
[F,G]_{pq}^{PQ} &= \frac{h_1 h_2}{4} \sum_{k=p,l=q}^{P,Q} F_{kl} G_{kl}, \quad (f,g)_h = (F,G)_h = [F,G]_{11}^{2N_1-1,2N_1-1}, && (6.201)\\
(f, g_{c.})_c &= (F, G_{c.})_c = \frac{1}{2}\left([F, G_{f.}]_{0,1}^{2N_1-1,2N_2-1} + [F, G_{b.}]_{1,1}^{2N_1,2N_2-1} \right), && (6.202)\\
(f, g_{.c})_c &= (F, G_{.c})_c = \frac{1}{2}\left([F, G_{.f}]_{1,0}^{2N_1-1,2N_2-1} + [F, G_{.b}]_{1,1}^{2N_1-1,2N_2} \right), && (6.203)\\
(\mathbf{f}, \nabla_h G)_c &= (\mathbf{F}, \nabla_h G)_c = \left(F^1, G_{c.}\right)_c + \left(F^2, G_{.c}\right)_c. && (6.204)
\end{aligned}
$$

In this section, all scalar products are summed over the finner grid. We need to transform the discrete Green formulas from central difference case to the finner grid functions.

Lemma 6.2.31. *Let $u : \overline{\omega}_h \to \mathbb{R}$, $\mathbf{v} : \overline{\omega}_h \to \mathbb{R}^2$. Then the Green formula is valid:*

$$
\begin{aligned}
(\nabla_h u, \mathbf{v})_h &= -(u, \nabla_h \cdot \mathbf{v})_c + \frac{h_2}{2} \sum_{l=1}^{2N-1} \left[(U_{2N-1,l} + U_{2N,l}) V^1_{2N,l} - (U_{0l} + U_{1l}) V^1_{0l} \right] \\
&\quad + \frac{h_1}{2} \sum_{k=1}^{2N-1} \left[(U_{k,2N-1} + U_{k,2N}) V^2_{k,2N} - (U_{k0} + U_{k1}) V^2_{k0} \right].
\end{aligned}
$$

Proof. Writing $(\nabla_h u, \mathbf{v})_h = (\nabla_c U, \mathbf{V})_h$ and applying (6.45) on the finner grid functions U and $\mathbf{V}$ we obtain (6.205). □

Corollary 6.2.32. *Let $p, u, v : \bar{\omega}_h \to \mathbb{R}$ and $v \mid_{\partial\omega} = 0$. Then*

$$
(\nabla_h \cdot (p \nabla_h u), v)_h = -(p \nabla_h u, \nabla_h v)_c. \tag{6.205}
$$

Proof. The proof is now really trivial. □

Theorem 6.2.33. *For the solution φ^h, w^h of (6.178)–(6.179) and $w^h = 0 \mid_{\partial\omega_h}$ we have*

$$
\left(\left(\varphi_t^h\right)^2, \frac{1}{Q^h} \right)_h + \frac{d}{dt} \left(\left(H_\gamma^h\right)^2, Q^h \right)_h = 0.
$$

Proof. The proof is the same as the proof of (6.48) but with the notation (6.201)-(6.204). □

6.3. Time discretisation

In the previous section we derived several semi-discrete schemes (6.2.2), (6.2.3), (6.2.8), (6.2.9), (6.2.27) and (6.2.28). They can be written in general as

$$\begin{aligned} \frac{\mathrm{d}u^h_{ij}}{\mathrm{dt}} &= f\left(t, u^h\right)_{ij} \text{ for } t > 0, && (6.206)\\ u^h_{ij}\left(t_0\right) &= u^h_{0,ij}, && (6.207) \end{aligned}$$

for $i = 1, \cdots N_1, j = 1, \cdots N_2$. Here F is a mapping $f : \Psi \to \mathbb{R}^N$ and Ψ is a domain $\Psi \subset \mathbb{R}^{N+1}$. If $f \in C\left(\Psi\right)$ and $\frac{\partial f^k}{\partial x_l} \in C\left(\Psi\right)$ for $k, l = 1, \cdots N$ then from Pontryagin [87] we have that for all $[t_0, \phi_{0,ij}] \in \Psi$ there exists $\delta > 0$ and $\phi^h_{ij} : (-\delta + t_0, t_0 + \delta) \to \mathbb{R}^N$ for $i = 1, \cdots N_1, j = 1, \cdots N_2$ for which

$$\begin{aligned} \frac{\mathrm{d}\phi^h_{ij}}{\mathrm{dt}} &= f\left(t, \phi^h\right)_{ij}, && (6.208)\\ \phi^h_{ij}\left(t_0\right) &= \phi_{0,ij}, && (6.209) \end{aligned}$$

for $i = 1, \cdots N_1, j = 1, \cdots N_2$. Moreover, if there is $\psi^h_{ij} : I \to \mathbb{R}^N$ for open non-empty interval I and $t_0 \in I$ such that (6.208)–(6.209) holds for ψ^h_{ij} on I then $\phi^h_{ij} = \psi^h_{ij}$ on $I \cap (-\delta + t_0, t_0 + \delta)$ for $i = 1, \cdots N_1, j = 1, \cdots N_2$.

To complete the discretisation we need to choose appropriate time discretisation. We have three possibilities: explicit, semi-implicit and fully-implicit discretisation in time. In this text we deal only with with the explicit and semi-implicit schemes.

6.3.1. Explicit schemes

Since we use highly nonlinear equations, the natural choice is the use of some explicit scheme. The great advantage of the explicit schemes is their high accuracy and the fact that they are easier to implement in comparison with the semi-implicit schemes requiring matrix solvers. In many articles, the fourth order Runge-Kutta kind solvers were successfully used [9, 10, 11, 7]. The Merson solver [97] belongs to this class of solvers. Moreover it offers automatic choice of the time step which makes it more robust. We will solve a system of ordinary differential equations having a form

$$\frac{\mathrm{d}u^h_{ij}}{\mathrm{dt}} = f\left(t, u^h\right)_{ij}, \tag{6.210}$$

where f is given by the right-hand side of some of the semidiscrete schemes (6.2.2), (6.2.3), (6.2.8), (6.2.9),(6.2.27) and (6.2.28). The following algorithm represents the solver for the explicit schemes which we present later in this text:

Algorithm 6.3.1. The explicit Runge-Kutta-Merson solver consist of the following steps:

1. Compute the grid functions k^1_{ij}, k^2_{ij}, k^3_{ij}, k^4_{ij}, k^5_{ij} as:

$$
\begin{aligned}
k^1_{ij} &:= \tau f\left(t, u^h\right)_{ij} \\
k^2_{ij} &:= \tau f\left(t + \frac{1}{3}\tau, u^h + \frac{1}{3}k^1\right)_{ij} \\
k^3_{ij} &:= \tau f\left(t + \frac{1}{3}\tau, u^h + \frac{1}{6}k^1 + \frac{1}{6}k^2\right)_{ij} \\
k^4_{ij} &:= \tau f\left(t + \frac{1}{2}\tau, u^h + \frac{1}{8}k^1 + \frac{3}{8}k^3\right)_{ij} \\
k^5_{ij} &:= \tau f\left(t + \tau, u^h + \frac{1}{2}k^1 - \frac{3}{2}k^3 + 2k^4\right)_{ij}.
\end{aligned}
$$

   for $i = 0, \cdots N_1$ and $j = 0, \cdots, N_2$.

2. Evaluate the error of the approximation with the current time step τ as

$$e := \max_{\substack{i=0,\cdots,N_1 \\ j=0,\cdots,N_2}} \frac{1}{3}\left|\frac{1}{5}k^1_{ij} - \frac{9}{10}k^3_{ij} + \frac{4}{5}k^4_{ij} - \frac{1}{10}k^5_{ij}\right|. \tag{6.211}$$

3. If this error is smaller then given tolerance ϵ update u^h as:

$$u^h_{ij} := u^h_{ij} + \frac{1}{6}\left(k^1_{ij} + 4k^4_{ij} + k^5_{ij}\right), \tag{6.212}$$

   for $i = 0, \cdots N_1$, $j = 0, \cdots, N_2$ and set

$$t := t + \tau.$$

4. Independently on the previous condition update τ as:

$$\tau := \min\left\{\tau \cdot \frac{4}{5}\left(\frac{\epsilon}{e}\right)^{\frac{1}{5}}, T - t\right\}. \tag{6.213}$$

5. Repeat whole process with the new τ i.e. go to the step 1.

Depending on the form of the right-hand side $f\left(t, u^h\right)_{ij}$ of (6.210) we obtain the following schemes:

Scheme 6.3.2. The **explicit one-sided finite difference** approximation of the **mean-curvature flow** with the anisotropy γ is given by the algorithm 6.3.1 where for the right-hand side of (6.210) we substitute the right-hand side of (6.10).

Scheme 6.3.3. The **explicit one-sided finite difference** approximation of the **Willmore flow** with the anisotropy γ is given by the algorithm 6.3.1 where for the right-hand side of (6.210) we substitute the right-hand side of (6.13).

Scheme 6.3.4. The **explicit central finite difference** approximation of the **mean-curvature flow** with the anisotropy γ is given by the algorithm 6.3.1 where for the right-hand side of (6.210) we substitute the right-hand side of (6.39).

Scheme 6.3.5. The **explicit central finite difference** approximation of the **Willmore flow** with the anisotropy γ is given by the algorithm 6.3.1 where for the right-hand side of (6.210) we substitute the right-hand side of (6.41).

Scheme 6.3.6. The **explicit finite difference** approximation of the **mean-curvature flow** with the anisotropy γ is given by the algorithm 6.3.1 where for the right-hand side of (6.210) we substitute the right-hand side of (6.174).

Scheme 6.3.7. The **explicit finite difference** approximation of the **Willmore flow** with the anisotropy γ is given by the algorithm 6.3.1 where for the right-hand side of (6.210) we substitute the right-hand side of (6.178).

Remark: The discretisation of the terms depending on given anisotropy, as they are expressed in the Section 5.3, is very straightforward. We just substitute appropriate finite differences approximating ∇u for $\mathbf{p}$.

6.3.2. Semi-implicit schemes

This section shows the semi-implicit schemes for the semi-discrete finite volume schemes (6.2.27) and (6.2.28). We omit the one-sided schemes (6.2.2) and (6.2.3) as well as the central schemes (6.2.8) and (6.2.9) because of their disadvantages in comparison with first ones ((6.2.27) and (6.2.28)). We discussed it in Sections 6.2.1 and 6.2.2. We study only the graph formulation. We would proceed in the same way for the level-set method. We also omit the isotropic problems since they are only special cases of more general anisotropic problems.

We assume having fixed time step τ such that $\tau = T/k$ for some $k \in \mathbb{N}^+$ and we denote

$$u_{ij}^n := u_{ij}\left(ih_1, jh_2, n\tau\right) \text{ for the grid function } u : \overline{\omega}_h \times [0, T) \to \mathbb{R}.$$

The semi-implicit schemes for the non-linear partial differential equations are always some kind of linearisation because we want to end up with a system of linear equations. The main difficulties come with the discretisation of the anisotropic mean-curvature H_γ. In general we have

$$H_\gamma = \nabla \cdot \left(\nabla_{\mathbf{p}} \gamma\right) = \partial_{x_1} \partial_{p_1} \gamma + \partial_{x_2} \partial_{p_2} \gamma.$$

We assume that we may write

$$\partial_{p_i} \gamma = \gamma_{i,1}^* p_1 + \gamma_{i,2}^* p_2 \text{ for } i = 1, 2.$$

Then we may write

$$\begin{aligned} H_\gamma\left(\varphi\right) &= \nabla \cdot \left(\nabla_{\mathbf{p}} \gamma \left(\nabla \varphi, -1\right)\right) \\ &= \partial_{x_1}\left[\gamma_{11}^*\left(\nabla\varphi, -1\right)\partial_{x_1}\varphi + \gamma_{12}^*\left(\nabla\varphi, -1\right)\partial_{x_2}\varphi\right] \\ &+ \partial_{x_2}\left[\gamma_{21}^*\left(\nabla\varphi, -1\right)\partial_{x_1}\varphi + \gamma_{22}^*\left(\nabla\varphi, -1\right)\partial_{x_2}\varphi\right]. \end{aligned}$$

The idea is to discretise $H_{\gamma,ij}^n$ as

$$\begin{aligned} H_{\gamma,ij}^n &= \partial_{x_1}^h\left(\gamma_{11,ij}^{*,n-1}\partial_{x_1}^h u_{ij}^n + \gamma_{12,ij}^{*,n-1}\partial_{x_2}^h u_{ij}^n\right) + \partial_{x_2}^h\left(\gamma_{21,ij}^{*,n-1}\partial_{x_1}^h u_{ij}^n + \gamma_{22,ij}^{*,n-1}\partial_{x_2}^h u_{ij}^n\right), \\ &= \frac{1}{h_1}\left(\gamma_{11,i+\frac{1}{2},j}^{*,n-1}\partial_{x_1}^h u_{i+\frac{1}{2},j}^n + \gamma_{12,i+\frac{1}{2},j}^{*,n-1}\partial_{x_2}^h u_{i+\frac{1}{2},j}^n\right. \\ &\quad \left. -\gamma_{11,i-\frac{1}{2},j}^{*,n-1}\partial_{x_1}^h u_{i-\frac{1}{2},j}^n - \gamma_{12,i-\frac{1}{2},j}^{*,n-1}\partial_{x_2}^h u_{i-\frac{1}{2},j}^n\right) \\ &+ \frac{1}{h_2}\left(\gamma_{21,i,j+\frac{1}{2}}^{*,n-1}\partial_{x_1}^h u_{i,j+\frac{1}{2}}^n + \gamma_{22,i,j+\frac{1}{2}}^{*,n-1}\partial_{x_2}^h u_{i,j+\frac{1}{2}}^n\right. \\ &\quad \left. - \gamma_{21,i,j-\frac{1}{2}}^{*,n-1}\partial_{x_1}^h u_{i,j-\frac{1}{2}}^n - \gamma_{22,i,j-\frac{1}{2}}^{*,n-1}\partial_{x_2}^h u_{i,j-\frac{1}{2}}^n\right), \end{aligned} \tag{6.214}$$

where we denote $\left(\partial^h_{x_1} u^n_{ij}, \partial^h_{x_2} u^n_{ij}\right)^T = \nabla_h u^n_{ij}$. In the same manner we discretise the boundary conditions (6.144)-(6.147).

With this notation in hand, we may introduce the following schemes – the choice of the time step (n or $n-1$) for each term is important:

Scheme 6.3.8. The **semi-implicit** numerical scheme for the finite difference **anisotropic mean-curvature flow graphs with the Dirichlet boundary conditions** has a form

$$\begin{aligned} \frac{u^n_{ij} - u^{n-1}_{ij}}{\tau} &= Q^{n-1}_{ij} \left(\partial^h_{x_1} \left(\gamma^{*,n-1}_{11,ij} \partial^h_{x_1} u^n_{ij} + \gamma^{*,n-1}_{12,ij} \partial^h_{x_2} u^n_{ij} \right) \right. \\ &+ \left. \partial^h_{x_2} \left(\gamma^{*,n-1}_{21,ij} \partial^h_{x_1} u^n_{ij} + \gamma^{*,n-1}_{22,ij} \partial^h_{x_2} u^n_{ij} \right) \right) \text{ on } \omega_h, && (6.215) \\ u^0_{ij} &= \mathcal{P}\left(u_{ini}\right)_{ij} \text{ on } \overline{\omega}_h, && (6.216) \\ u^n_{ij} &= g_{ij} \text{ on } \partial\omega_h, \end{aligned}$$

where Q^h_{ij} is given by (6.170), $\partial_{p_1}\gamma_{ij}$, $\partial_{p_2}\gamma_{ij}$ by (6.173).
The **semi-implicit** numerical scheme for the finite difference **anisotropic mean-curvature flow graphs with the Neumann boundary conditions** is given by (6.215)–(6.216) and

$$\begin{aligned} \gamma^{*,n-1}_{11,i-\frac{1}{2},j} \partial^h_{x_1} u^n_{i-\frac{1}{2},j} + \gamma^{*,n-1}_{12,i-\frac{1}{2},j} \partial^h_{x_2} u^n_{i-\frac{1}{2},j} &= 0 \text{ for } i = 1, && (6.217) \\ \gamma^{*,n-1}_{11,i+\frac{1}{2},j} \partial^h_{x_1} u^n_{i+\frac{1}{2},j} + \gamma^{*,n-1}_{12,i+\frac{1}{2},j} \partial^h_{x_2} u^n_{i+\frac{1}{2},j} &= 0 \text{ for } i = N_1 - 1, && (6.218) \\ \gamma^{*,n-1}_{21,i,j-\frac{1}{2}} \partial^h_{x_1} u^n_{i,j-\frac{1}{2}} + \gamma^{*,n-1}_{22,i,j-\frac{1}{2}} \partial^h_{x_2} u^n_{i,j-\frac{1}{2}} &= 0 \text{ for } j = 1, && (6.219) \\ \gamma^{*,n-1}_{21,i,j+\frac{1}{2}} \partial^h_{x_1} u^n_{i,j+\frac{1}{2}} + \gamma^{*,n-1}_{22,i,j+\frac{1}{2}} \partial^h_{x_2} u^n_{i,j+\frac{1}{2}} &= 0 \text{ for } j = N_2 - 1. && (6.220) \end{aligned}$$

For the **level-set formulation** we replace Q^h_{ij} in (6.215) by $Q^h_{\epsilon,ij}$ given by (6.186) and $\partial_{p_1}\gamma_{ij}$, $\partial_{p_2}\gamma_{ij}$ is defined by (6.173).

Scheme 6.3.9. The **semi-implicit** numerical scheme for the finite difference **anisotropic Willmore flow of graphs with the Dirichlet boundary conditions** has a form

$$\frac{u_{ij}^n - u_{ij}^{n-1}}{\tau} = -Q_{ij}^{n-1}\nabla_h \cdot \left(\mathbb{E}_{\gamma,ij}^{n-1} \nabla_h w_{ij}^n - \frac{1}{2}\frac{\left(w_{ij}^{n-1}\right)^2}{\left(Q_{ij}^{n-1}\right)^3} \nabla_h u_{ij}^n \right) \text{ on } \omega_h, \tag{6.221}$$

$$\begin{aligned} w_{ij}^{n-1} &= Q_{ij}^{n-1} H_{\gamma,ij}^{n-1} \text{ on } \omega_h, \\ w_{ij}^n &= Q_{ij}^{n-1}\left(\partial_{x_1}^h \left(\gamma_{11,ij}^{*,n-1} \partial_{x_1}^h u_{ij}^n + \gamma_{12,ij}^{*,n-1} \partial_{x_2}^h u_{ij}^n \right) \right. \\ &+ \left. \partial_{x_2}^h \left(\gamma_{21,ij}^{*,n-1} \partial_{x_1}^h u_{ij}^n + \gamma_{22,ij}^{*,n-1} \partial_{x_2}^h u_{ij}^n \right)\right) \text{ on } \omega_h, \\ u_{ij}^h\,|_{t=0} &= \mathcal{P}\left(u_{ini}\right)_{ij} \text{ on } \overline{\omega}_h, \\ u_{ij}^n &= g_{ij} \text{ and } w_{ij}^n = 0 \text{ on } \partial\omega_h, \end{aligned} \tag{6.222}$$

where Q_{ij}^h is given by (6.170), $\mathbb{E}_{\gamma,ij}^h$ by (6.172) and $\partial_{p_1}\gamma_{ij}$, $\partial_{p_2}\gamma_{ij}$ by (6.173).
The **semi-implicit** numerical scheme for the finite difference **anisotropic Willmore flow of graphs with the Neumann boundary conditions** is given by (6.221)–(6.222) and

$$\text{if } i = 1 \text{ then } \nu = (-1,0) \;\Rightarrow\; \frac{1}{h_1}\left(u_{1,j}^n - u_{0,j}^n\right) = 0, \tag{6.223}$$

$$\text{if } i = N_1 - 1 \text{ then } \nu = (1,0) \;\Rightarrow\; \frac{1}{h_1}\left(u_{N_1,j}^n - u_{\gamma,N_1-1,j}^n\right) = 0, \tag{6.224}$$

$$\text{if } j = 1 \text{ then } \nu = (0,-1) \;\Rightarrow\; \frac{1}{h_2}\left(u_{i,1}^n - u_{i,0}^n\right) = 0, \tag{6.225}$$

$$\text{if } j = N_2 - 1 \text{ then } \nu = (0,1) \;\Rightarrow\; \frac{1}{h_2}\left(u_{i,N_2}^n - u_{i,N_2-1}^n\right) = 0 \tag{6.226}$$

and

$$\frac{\mathbb{E}_{11,i-\frac{1}{2},j}^{n-1}}{h_1}\left(w_{i,j}^n - w_{i-1,j}^{n-1}\right) + \frac{\mathbb{E}_{12,i-\frac{1}{2},j}^{n-1}}{4h_1h_2}\left(w_{i,j+1}^n + w_{i-1,j+1}^{n-1} - w_{i,j-1}^n - w_{i-1,j-1}^{n-1}\right) = 0 \quad \text{for } i = 1, \tag{6.227}$$

$$\frac{\mathbb{E}_{11,i+\frac{1}{2},j}^{n-1}}{h_1}\left(w_{i+1,j}^{n-1} - w_{ij}^n\right) + \frac{\mathbb{E}_{12,i+\frac{1}{2},j}^{n-1}}{4h_1h_2}\left(w_{i,j+1}^n + w_{i+1,j+1}^{n-1} - w_{i,j-1}^n - w_{i+1,j-1}^{n-1}\right) = 0 \quad \text{for } i = N_1 - 1, \tag{6.228}$$

$$\frac{\mathbb{E}_{21,i,j-\frac{1}{2}}^{n-1}}{4h_1h_2}\left(w_{i+1,j}^n + w_{i+1,j-1}^{n-1} - w_{i-1,j}^n - w_{i-1,j-1}^{n-1}\right) + \frac{\mathbb{E}_{22,i,j-\frac{1}{2}}^{n-1}}{h_2}\left(w_{ij}^n - w_{i,j-1}^{n-1}\right) = 0 \quad \text{for } j = 1, \tag{6.229}$$

$$\frac{\mathbb{E}_{21,i,j+\frac{1}{2}}^{n-1}}{4h_1h_2}\left(w_{i+1,j}^n + w_{i+1,j+1}^{n-1} - w_{i-1,j}^n - w_{i-1,j+1}^{n-1}\right) + \frac{\mathbb{E}_{22,i,j+\frac{1}{2}}^{n-1}}{h_2}\left(w_{i,j+1}^{n-1} - w_{ij}^n\right) = 0 \quad \text{for } j = N_2 - 1. \tag{6.230}$$

For the **level-set formulation** we replace Q_{ij}^h in (6.215) by $Q_{\epsilon,ij}^h$ given by (6.186), $\mathbb{E}_{\gamma,ij}^h$ is defined by (6.188) and $\partial_{p_1}\gamma_{ij}$ with $\partial_{p_2}\gamma_{ij}$ by (6.173).

The linear system of the semi-implicit scheme for the mean-curvature flow

To implement the scheme (6.3.8) we need to find the coefficients of the linear system related to it. From (6.215) we see that for $i = 1, \cdots N_1 - 1, j = 1, \cdots, N_2 - 1$

$$
\begin{aligned}
H^n_{\gamma,ij} &= \nabla_h \cdot \left(\gamma^{*,n-1}_{11,ij} \partial^h_{x_1} u^n_{ij} + \gamma^{*,n-1}_{12,ij} \partial^h_{x_2} u^n_{ij}, \gamma^{*,n-1}_{21} \partial^h_{x_1} u^n_{ij} + \gamma^{*,n-1}_{22} \partial^h_{x_2} u^n_{ij} \right)^T \\
&= \frac{1}{h_1} \left(\gamma^{*,n-1}_{11,i+\frac{1}{2},j} \partial^h_{x_1} u^n_{i+\frac{1}{2},j} + \gamma^{*,n-1}_{12,i+\frac{1}{2},j} \partial^h_{x_2} u^n_{i+\frac{1}{2},j} \right. \\
&- \left. \gamma^{*,n-1}_{11,i-\frac{1}{2},j} \partial^h_{x_1} u^n_{i-\frac{1}{2},j} + \gamma^{*,n-1}_{12,i-\frac{1}{2},j} \partial^h_{x_2} u^n_{i-\frac{1}{2},j} \right) \\
&+ \frac{1}{h_2} \left(\gamma^{*,n-1}_{21,i,j+\frac{1}{2}} \partial^h_{x_1} u^n_{i,j+\frac{1}{2}} + \gamma^{*,n-1}_{22,i,j+\frac{1}{2}} \partial^h_{x_2} u^n_{i,j+\frac{1}{2}} \right. \\
&- \left. \gamma^{*,n-1}_{21,i,j-\frac{1}{2}} \partial^h_{x_1} u^n_{i,j-\frac{1}{2}} + \gamma^{*,n-1}_{22,i,j-\frac{1}{2}} \partial^h_{x_2} u^n_{i,j-\frac{1}{2}} \right)
\end{aligned}
$$

Substituting appropriate approximations of $\partial^h_{x_m} u_{i \pm k\frac{1}{2}, j \pm l\frac{1}{2}}$ for $m = 1, 2,\ k, l \in \{0, 1\}$ and $|k| + |l| = 1$ we get

$$
\begin{aligned}
H^n_{\gamma,ij} &= \frac{\gamma^*_{11,i+\frac{1}{2},j}}{h_1^2} \left(u^n_{i+1,j} - u^n_{ij} \right) - \frac{\gamma^*_{11,i-\frac{1}{2},j}}{h_1^2} \left(u^n_{ij} - u^n_{i-1,j} \right) \\
&+ \frac{\gamma^*_{12,i+\frac{1}{2},j}}{4h_1h_2} \left(u^n_{i+1,j+1} + u^n_{i,j+1} - u^n_{i+1,j-1} - u^n_{i,j-1} \right) \\
&- \frac{\gamma^*_{12,i-\frac{1}{2},j}}{4h_1h_2} \left(u^n_{i,j+1} + u^n_{i-1,j+1} - u^n_{i,j-1} - u^n_{i-1,j-1} \right) \\
&+ \frac{\gamma^*_{21,i,j+\frac{1}{2}}}{4h_1h_2} \left(u^n_{i+1,j+1} + u^n_{i+1,j} - u^n_{i-1,j+1} - u^n_{i-1,j} \right) \\
&- \frac{\gamma^*_{21,i,j-\frac{1}{2}}}{4h_1h_2} \left(u^n_{i+1,j-1} + u^n_{i+1,j} - u^n_{i-1,j-1} - u^n_{i-1,j} \right) \\
&+ \frac{\gamma^*_{22,i,j+\frac{1}{2}}}{h_2^2} \left(u^n_{i,j+1} - u^n_{ij} \right) - \frac{\gamma^*_{22,i,j-\frac{1}{2}}}{h_2^2} \left(u^n_{ij} - u^n_{i,j-1} \right)
\end{aligned}
\tag{6.231}
$$

or denoting

$$
C^{0,0}_{H,ij} := \left(-\frac{\gamma^*_{11,i+\frac{1}{2},j}}{h_1^2} - \frac{\gamma^*_{11,i-\frac{1}{2},j}}{h_1^2} - \frac{\gamma^*_{22,i,j+\frac{1}{2}}}{h_2^2} - \frac{\gamma^*_{22,i,j-\frac{1}{2}}}{h_2^2} \right),
$$

$$
\begin{aligned}
C^{1,0}_{H,ij} &:= \left(\frac{\gamma^*_{11,i+\frac{1}{2},j}}{h_1^2} + \frac{\gamma^*_{21,i,j+\frac{1}{2}}}{4h_1h_2} - \frac{\gamma^*_{21,i,j-\frac{1}{2}}}{4h_1h_2} \right),\ C^{1,1}_{H,ij} := \left(\frac{\gamma^*_{12,i+\frac{1}{2},j}}{4h_1h_2} + \frac{\gamma^*_{21,i,j+\frac{1}{2}}}{4h_1h_2} \right), \\
C^{0,1}_{H,ij} &:= \left(\frac{\gamma^*_{12,i+\frac{1}{2},j}}{4h_1h_2} - \frac{\gamma^*_{12,i-\frac{1}{2},j}}{4h_1h_2} + \frac{\gamma^*_{22,i,j+\frac{1}{2}}}{h_2^2} \right),\ C^{1,-1}_{H,ij} := \left(-\frac{\gamma^*_{12,i+\frac{1}{2},j}}{4h_1h_2} - \frac{\gamma^*_{21,i,j-\frac{1}{2}}}{4h_1h_2} \right), \\
C^{-1,0}_{H,ij} &:= \left(\frac{\gamma^*_{11,i-\frac{1}{2},j}}{h_1^2} - \frac{\gamma^*_{21,i,j+\frac{1}{2}}}{4h_1h_2} + \frac{\gamma^*_{21,i,j-\frac{1}{2}}}{4h_1h_2} \right),\ C^{-1,1}_{H,ij} := \left(-\frac{\gamma^*_{12,i-\frac{1}{2},j}}{4h_1h_2} - \frac{\gamma^*_{21,i,j+\frac{1}{2}}}{4h_1h_2} \right), \\
C^{0,-1}_{H,ij} &:= \left(-\frac{\gamma^*_{12,i+\frac{1}{2},j}}{4h_1h_2} + \frac{\gamma^*_{12,i-\frac{1}{2},j}}{4h_1h_2} + \frac{\gamma^*_{22,i,j-\frac{1}{2}}}{h_2^2} \right),\ C^{-1,-1}_{H,ij} := \left(\frac{\gamma^*_{12,i-\frac{1}{2},j}}{4h_1h_2} + \frac{\gamma^*_{21,i,j-\frac{1}{2}}}{4h_1h_2} \right),
\end{aligned}
$$

and

$$C^{r,s}_{w,ij} := Q^{n-1}_{ij} C^{r,s}_{H,ij} \text{ for } r,s \in \{-1,0,1\} \tag{6.232}$$

we may write

$$H^n_{\gamma,ij} = \sum_{r,s\in\{-1,0,1\}} C^{r,s}_{H,ij} u^n_{i+r,j+s}, \tag{6.233}$$

resp.

$$w^n_{ij} = \sum_{r,s\in\{-1,0,1\}} C^{r,s}_{w,ij} u^n_{i+r,j+s}, \tag{6.234}$$

and (6.215) now reads as

$$\boxed{u^n_{ij} - \tau \sum_{r,s\in\{-1,0,1\}} C^{r,s}_{w,ij} u^n_{i+r,j+s} = u^{n-1}_{ij}.} \tag{6.235}$$

Discretisation of the Neumann boundary conditions (6.217)-(6.220) gives

$$\begin{aligned}
\frac{\gamma^{*,n-1}_{11,i-\frac{1}{2},j}}{h_1}\left(u^n_{ij} - u^n_{i-1,j}\right) + \frac{\gamma^{*,n-1}_{12,i-\frac{1}{2},j}}{4h_1h_2}\left(u^n_{i,j+1} + u^n_{i-1,j+1} - u^n_{i,j-1} - u^n_{i-1,j-1}\right) &= 0 \qquad (6.236)\\
&\ \text{for } i = 1,\\
\frac{\gamma^{*,n-1}_{11,i+\frac{1}{2},j}}{h_1}\left(u^n_{i+1,j} - u^n_{i,j}\right) + \frac{\gamma^{*,n-1}_{12,i+\frac{1}{2},j}}{4h_1h_2}\left(u^n_{i+1,j+1} + u^n_{i,j+1} - u^n_{i+1,j-1} - u^n_{i,j-1}\right) &= 0 \qquad (6.237)\\
&\ \text{for } i = N_1 - 1,\\
\frac{\gamma^{*,n-1}_{21,i,j-\frac{1}{2}}}{4h_1h_2}\left(u^n_{i+1,j-1} + u^n_{i+1,j} - u^n_{i-1,j-1} - u^n_{i-1,j}\right) + \frac{\gamma^{*,n-1}_{22,i,j-\frac{1}{2}}}{h_2}\left(u^n_{ij} - u^n_{i,j-1}\right) &= 0 \qquad (6.238)\\
&\ \text{for } j = 1,\\
\frac{\gamma^{*,n-1}_{21,i,j+\frac{1}{2}}}{4h_1h_2}\left(u^n_{i+1,j+1} + u^n_{i+1,j} - u^n_{i-1,j+1} - u^n_{i-1,j}\right) + \frac{\gamma^{*,n-1}_{22,i,j+\frac{1}{2}}}{h_2}\left(u^n_{i,j+1} - u^n_{ij}\right) &= 0 \qquad (6.239)\\
&\ \text{for } j = N_2 - 1,
\end{aligned}$$

which we will use to define the values of u^n_{ij} on $\partial\omega_h$. There is, however, ambiguity for the values at the corners of $\bar{\omega}_h$. Take for example the value u^n_{00}. It appears in two equations (6.236) and (6.238). This is because in the corner of $\partial\omega_h$ the outer normal is not defined and so the boundary condition $\nabla_{\mathbf{p}}\gamma \cdot \nu = 0$ does not make sense. For example for this corner node we have (for $i = j = 1$ from (6.236) and (6.238)):

$$\frac{\gamma^{*,n-1}_{11,\frac{1}{2},1}}{h_1}\left(u^n_{1,1} - u^n_{0,1}\right) + \frac{\gamma^{*,n-1}_{12,\frac{1}{2},1}}{4h_1h_2}\left(u^n_{1,2} + u^n_{0,2} - u^n_{1,0} - u^n_{0,0}\right) = 0, \tag{6.240}$$

$$\frac{\gamma^{*,n-1}_{21,1,\frac{1}{2}}}{4h_1h_2}\left(u^n_{2,0} + u^n_{2,1} - u^n_{0,0} - u^n_{0,1}\right) + \frac{\gamma^{*,n-1}_{22,1,\frac{1}{2}}}{h_2}\left(u^n_{1,1} - u^n_{1,0}\right) = 0 \tag{6.241}$$

Summing these two equations we get:

$$\begin{aligned}
&C^{0,0}_{w,0,0}u^n_{0,0} + C^{1,0}_{w,0,0}u^n_{1,0} + C^{0,1}_{w,0,0}u^n_{0,1} + C^{1,1}_{w,0,0}u^n_{1,1}\\
&+C^{1,2}_{w,0,0}u^n_{1,2} + C^{0,2}_{w,0,0}u^n_{0,2} + C^{2,1}_{w,0,0}u^n_{2,0} + C^{2,0}_{w,0,0}u^n_{2,1} = 0, \qquad (6.242)
\end{aligned}$$

for

$$
\begin{aligned}
C_{w,0,0}^{0,0} &:= -\frac{\gamma_{12,\frac{1}{2},1}^{*,n-1}}{4h_1h_2} - \frac{\gamma_{21,1,\frac{1}{2}}^{*,n-1}}{4h_1h_2}, \quad C_{w,0,0}^{1,0} := -\frac{\gamma_{12,\frac{1}{2},1}^{*,n-1}}{4h_1h_2} - \frac{\gamma_{22,1,\frac{1}{2}}^{*,n-1}}{h_2},\\
C_{w,0,0}^{0,1} &:= -\frac{\gamma_{11,\frac{1}{2},1}^{*,n-1}}{h_1} - \frac{\gamma_{21,1,\frac{1}{2}}^{*,n-1}}{4h_1h_2}, \quad C_{w,0,0}^{1,1} := \frac{\gamma_{11,\frac{1}{2},1}^{*,n-1}}{h_1} + \frac{\gamma_{22,1,\frac{1}{2}}^{*,n-1}}{h_2},\\
C_{w,0,0}^{1,2} &:= C_{w,0,0}^{0,2} = \frac{\gamma_{12,\frac{1}{2},1}^{*,n-1}}{4h_1h_2}, \qquad C_{w,0,0}^{2,1} := C_{w,0,0}^{2,0} = \frac{\gamma_{21,1,\frac{1}{2}}^{*,n-1}}{4h_1h_2}.
\end{aligned}
$$

In the same way from (6.236) and (6.239) with $i=1$ and $j=N_2-1$ we get equation for u_{0,N_2}^n

$$
\begin{aligned}
&C_{w,0,N_2}^{0,0}u_{0,N_2}^n + C_{w,0,N_2}^{1,0}u_{1,N_2}^n + C_{w,0,N_2}^{0,-1}u_{0,N_2-1}^n + C_{w,0,N_2}^{1,-1}u_{1,N_2-1}^n\\
&+C_{w,0,N_2}^{1,-2}u_{1,N_2-2}^n + C_{w,0,N_2}^{0,-2}u_{0,N_2-2}^n + C_{w,0,N_2}^{2,-1}u_{2,N_2}^n + C_{w,0,N_2}^{2,0}u_{2,N_2-1}^n = 0,
\end{aligned} \tag{6.243}
$$

for

$$
\begin{aligned}
C_{w,0,N_2}^{0,0} &:= \frac{\gamma_{12,\frac{1}{2},N_2-1}^{*,n-1}}{4h_1h_2} - \frac{\gamma_{21,1,N_2-\frac{1}{2}}^{*,n-1}}{4h_1h_2}, C_{w,0,N_2}^{1,0} := \frac{\gamma_{12,\frac{1}{2},N_2-1}^{*,n-1}}{4h_1h_2} + \frac{\gamma_{22,1,N_2-\frac{1}{2}}^{*,n-1}}{h_2},\\
C_{w,0,N_2}^{0,-1} &:= -\frac{\gamma_{11,\frac{1}{2},N_2-1}^{*,n-1}}{h_1} - \frac{\gamma_{21,1,N_2-\frac{1}{2}}^{*,n-1}}{4h_1h_2}, C_{w,0,N_2}^{1,-1} := \frac{\gamma_{11,\frac{1}{2},N_2-1}^{*,n-1}}{h_1} + \frac{\gamma_{22,1,N_2-\frac{1}{2}}^{*,n-1}}{h_2},\\
C_{w,0,N_2}^{1,-2} &:= C_{w,0,N_2}^{0,-2} := -\frac{\gamma_{12,\frac{1}{2},N_2-1}^{*,n-1}}{4h_1h_2}, C_{w,0,N_2}^{2,-1} := C_{w,0,N_2}^{2,0} := \frac{\gamma_{21,1,N_2-\frac{1}{2}}^{*,n-1}}{4h_1h_2}
\end{aligned}
$$

from (6.237) and (6.238) with $i=N_1-1$ and $j=1$ we get equation for $u_{N_1,0}$

$$
\begin{aligned}
&C_{w,N_1,0}^{0,0}u_{N_1,0}^n + C_{w,N_1,0}^{-1,0}u_{N_1-1,0}^n + C_{w,N_1,0}^{0,1}u_{N_1,1}^n + C_{w,N_1,0}^{-1,1}u_{N_1-1,1}^n\\
&+C_{w,N_1,0}^{-1,2}u_{N_1-1,2}^n + C_{w,N_1,0}^{0,2}u_{N_1,2}^n + C_{w,N_1,0}^{-2,1}u_{N_1-2,1}^n + C_{w,N_1,0}^{-2,0}u_{N_1-2,0}^n = 0,
\end{aligned} \tag{6.244}
$$

for

$$
\begin{aligned}
C_{w,N_1,0}^{0,0} &:= -\frac{\gamma_{12,N_1+\frac{1}{2},1}^{*,n-1}}{4h_1h_2} + \frac{\gamma_{21,N_1-1,\frac{1}{2}}^{*,n-1}}{4h_1h_2}, C_{w,N_1,0}^{-1,0} := -\frac{\gamma_{12,N_1+\frac{1}{2},1}^{*,n-1}}{4h_1h_2} - \frac{\gamma_{22,N_1-1,\frac{1}{2}}^{*,n-1}}{h_2},\\
C_{w,N_1,0}^{0,1} &:= \frac{\gamma_{11,N_1+\frac{1}{2},1}^{*,n-1}}{h_1} + \frac{\gamma_{21,N_1-1,\frac{1}{2}}^{*,n-1}}{4h_1h_2}, C_{w,N_1,0}^{-1,1} := -\frac{\gamma_{11,N_1+\frac{1}{2},1}^{*,n-1}}{h_1} + \frac{\gamma_{22,N_1-1,\frac{1}{2}}^{*,n-1}}{h_2},\\
C_{w,N_1,0}^{-1,2} &:= C_{w,N_1,0}^{0,2} := \frac{\gamma_{12,N_1+\frac{1}{2},1}^{*,n-1}}{4h_1h_2}, C_{w,N_1,0}^{-2,1} := C_{w,N_1,0}^{-2,0} := -\frac{\gamma_{21,N_1-1,\frac{1}{2}}^{*,n-1}}{4h_1h_2},
\end{aligned}
$$

and from (6.237) and (6.239) with $i=N_1-1$ and $j=N_2-1$ we get equation for u_{N_1,N_2}

$$
\begin{aligned}
&C_{w,N_1,N_2}^{0,0}u_{N_1,N_2}^n + C_{w,N_1,N_2}^{-1,0}u_{N_1-1,N_2}^n + C_{w,N_1,N_2}^{0,-1}u_{N_1,N_2-1}^n\\
&+C_{w,N_1,N_2}^{-1,-1}u_{N_1-1,N_2-1}^n + C_{w,N_1,N_2}^{-1,-2}u_{N_1-1,N_2-2}^n + C_{w,N_1,N_2}^{0,-2}u_{N_1,N_2-2}^n\\
&+C_{w,N_1,N_2}^{-2,-1}u_{N_1-2,N_2-1}^n + C_{w,N_1,N_2}^{-2,0}u_{N_1-2,N_2}^n = 0,
\end{aligned} \tag{6.245}
$$

$$C^{0,0}_{w,N_1,N_2} := \frac{\gamma^{*,n-1}_{12,N_1-\frac{1}{2},N_2-1}}{4h_1h_2} + \frac{\gamma^{*,n-1}_{21,N_1-1,N_2-\frac{1}{2}}}{4h_1h_2}, \qquad C^{-1,0}_{w,N_1,N_2} := \frac{\gamma^{*,n-1}_{12,N_1-\frac{1}{2},N_2-1}}{4h_1h_2} + \frac{\gamma^{*,n-1}_{22,N_1-1,N_2-\frac{1}{2}}}{h_2},$$
$$C^{0,-1}_{w,N_1,N_2} := \frac{\gamma^{*,n-1}_{11,N_1-\frac{1}{2},N_2-1}}{h_1} + \frac{\gamma^{*,n-1}_{21,N_1-1,N_2-\frac{1}{2}}}{4h_1h_2}, \qquad C^{-1,-1}_{w,N_1,N_2} := -\frac{\gamma^{*,n-1}_{11,N_1-\frac{1}{2},N_2-1}}{h_1} - \frac{\gamma^{*,n-1}_{22,N_1-1,N_2-\frac{1}{2}}}{h_2},$$
$$C^{-1,-2}_{w,N_1,N_2} := C^{0,-2}_{w,N_1,N_2} := -\frac{\gamma^{*,n-1}_{12,N_1-\frac{1}{2},N_2-1}}{4h_1h_2}, \qquad C^{-2,-1}_{w,N_1,N_2} := C^{-2,0}_{w,N_1,N_2} := -\frac{\gamma^{*,n-1}_{21,N_1-1,N_2-\frac{1}{2}}}{4h_1h_2}.$$

Now from the equation (6.236) we get system of equations for u^n_{ij} for $i=0$ and $j=1,\cdots,N_2-1$

$$C^{0,0}_{w,0,j}u^n_{0,j} + C^{1,0}_{w,0,j}u^n_{1,j} + C^{0,1}_{w,0,j}u^n_{0,j+1} + C^{0,-1}_{w,0,j}u^n_{0,j-1} + C^{1,-1}_{w,0,j}u^n_{1,j-1} + C^{1,1}_{w,0,j}u^n_{1,j+1} = 0, \quad (6.246)$$

for

$$\begin{aligned} C^{0,0}_{w,0,j} &:= -C^{1,0}_{w,0,j} = -\frac{\gamma^{*,n-1}_{11,\frac{1}{2},j}}{h_1}, \\ C^{0,1}_{w,0,j} &:= -C^{0,-1}_{w,0,j} := -C^{1,-1}_{w,0,j} := C^{1,1}_{w,0,j} := \frac{\gamma^{*,n-1}_{12,\frac{1}{2},j}}{4h_1h_2}, \end{aligned}$$

from (6.237) we get system of equations for u^n_{ij} for $i=N_1$ and $j=1,\cdots,N_2-1$

$$\begin{aligned} C^{0,0}_{w,N_1,j}u^n_{N_1,j} + C^{-1,0}_{w,N_1,j}u^n_{N_1-1,j} + C^{0,1}_{w,N_1,j}u^n_{N_1,j+1} & \\ + C^{0,-1}_{w,N_1,j}u^n_{N_1,j-1} + C^{-1,-1}_{w,N_1,j}u^n_{N_1-1,j-1} + C^{-1,1}_{w,N_1,j}u^n_{N_1-1,j+1} &= 0, \end{aligned} \quad (6.247)$$

for

$$\begin{aligned} C^{0,0}_{w,N_1,j} := -C^{-1,0}_{w,N_1,j} &:= \frac{\gamma^{*,n-1}_{11,N_1+\frac{1}{2},j}}{h_1}, \\ C^{0,1}_{w,N_1,j} := -C^{0,-1}_{w,N_1,j} := -C^{-1,-1}_{w,N_1,j} := C^{-1,1}_{w,N_1,j} &:= \frac{\gamma^{*,n-1}_{12,N_1+\frac{1}{2},j}}{4h_1h_2}, \end{aligned}$$

from (6.238) we get system of equations for u^n_{ij} for $i=1\cdots,N_1-1$ and $j=0$

$$C^{0,0}_{w,i,0}u^n_{i,0} + C^{0,1}_{w,i,0}u^n_{i,1} + C^{1,0}_{w,i,0}u^n_{i+1,0} + C^{-1,0}_{w,i,0}u^n_{i-1,0} + C^{1,1}_{w,i,0}u^n_{i+1,1} + C^{-1,1}_{w,i,0}u^n_{i-1,1} = 0, \quad (6.248)$$

for

$$\begin{aligned} C^{0,0}_{w,i,0} &:= -C^{0,1}_{w,i,0} := -\frac{\gamma^{*,n-1}_{22,i,j-\frac{1}{2}}}{h_2}, \\ C^{1,0}_{w,i,0} &:= -C^{-1,0}_{w,i,0} := C^{1,1}_{w,i,0} := -C^{-1,1}_{w,i,0} := \frac{\gamma^{*,n-1}_{21,i,\frac{1}{2}}}{4h_1h_2}, \end{aligned}$$

and from (6.239) we get system of equations for u^n_{ij} for $i=1\cdots,N_1-1$ and $j=N_2$

$$\begin{aligned} C^{0,0}_{w,i,N_2}u^n_{i,N_2} + C^{0,-1}_{w,i,N_2}u^n_{i,N_2-1} + C^{1,0}_{w,i,N_2}u^n_{i+1,N_2} & \\ + C^{-1,0}_{w,i,N_2}u^n_{i-1,N_2} + C^{1,-1}_{w,i,N_2}u^n_{i+1,N_2-1} + C^{-1,-1}_{w,i,N_2}u^n_{i-1,N_2-1} &= 0, \end{aligned} \quad (6.249)$$

for

$$C^{0,0}_{w,i,N_2} \quad := \quad -C^{0,-1}_{w,i,N_2} := \frac{\gamma^{*,n-1}_{22,i,N_2-\frac{1}{2}}}{h_2}, \tag{6.250}$$

$$C^{1,0}_{w,i,N_2} \quad := \quad -C^{-1,0}_{w,i,N_2} := C^{1,-1}_{w,i,N_2} := -C^{-1,-1}_{w,i,N_2} := \frac{\gamma^{*,n-1}_{21,i,N_2-\frac{1}{2}}}{4h_1h_2}. \tag{6.251}$$

So, in general we have nine-point stencil for w^n_{ij} given by the coefficients $C^{r,s}_{w,ij}$ for $r,s \in \{-2,-1,0,1,2\}$ (r and s can be ± 2 only at the corner nodes) using which we can assembly the final linear system. In the matrix form it reads

$$\mathbb{A}^{MC}\left(\mathbf{u}^{n-1}\right)\mathbf{u}^n = \mathbf{b}\left(\mathbf{u}^{n-1}\right). \tag{6.252}$$

Let us index the rows and columns corresponding to some u^n_{ij} by

$$I(i,j) = J(i,j) = iN_2 + j \tag{6.253}$$

where we will use I for the rows of $\mathbb{A}\left(\mathbf{u}^{n-1}\right)$ and J for its columns. We also define the inverse mapping

$$i = i(I) \quad = \quad I \text{ div } N_2 \text{ resp. } i = i(J) = J \text{ div } N_2, \tag{6.254}$$

$$j = j(I) \quad = \quad I \bmod N_2 \text{ resp. } j = j(J) = J \bmod N_2. \tag{6.255}$$

If we set $C^{r,s}_{w,ij} = 0$ for all such i,j,r,s that $C^{r,s}_{w,ij}$ was not defined so far, the matrix $\mathbb{A}_{MC}$ is given by the following algorithm.

Algorithm 6.3.10. Setup of the linear system matrix for the semi-implicit mean-curvature flow consist of the following steps:

1. set $A^{MC}_{IJ} := 0$ for all $I,J = 0,\cdots N_1N_2$ and $b_I := 0$ for all $I = 0,\cdots N_1N_2$
2. for the row $I = 0,\cdots N_1N_2$ do
3. if $(i(I),j(I)) \in \partial\omega_h$ set the boundary conditions
4. set $A^{MC}_{II} := 1$, $b_I := g^n_{ij}$ for the Dirichlet boundary conditions
5. for $r,s \in \{-2,-1,0,1,2\}$, $J = J(i+r,j+s)$ $A^{MC}_{IJ} := C^{r,s}_{w,ij}$, $b_I := 0$ for the Neumann boundary conditions
6. else set $A_{II} := 1$, $b_I := u^{n-1}_{ij}$
7. for $r,s \in \{-1,0,1\}$, $J = J(i+r,j+s)$ $A^{MC}_{IJ} := A^{MC}_{IJ} - \tau C^{r,s}_{w,ij}$.

The linear system of the semi-implicit scheme for the Willmore flow

The equation (6.221) gives

$$u^n_{ij} + \tau Q^{n-1}_{ij}\nabla_h \cdot \left(\mathbb{E}^{n-1}_{\gamma,ij}\nabla_h w^n_{ij} - \frac{1}{2}\frac{\left(w^{n-1}_{ij}\right)^2}{\left(Q^{n-1}_{ij}\right)^3}\nabla_h u^n_{ij} \right) \quad = \quad u^{n-1}_{ij} \tag{6.256}$$

which gives

$$
\begin{aligned}
& u_{ij}^{n} + \tau Q_{ij}^{n-1} \cdot \\
& \left[\frac{1}{h_1} \left(\mathbb{E}_{\gamma,11,i+\frac{1}{2},j}^{n-1} \partial_{x_1}^{h} w_{i+\frac{1}{2},j}^{n} + \mathbb{E}_{\gamma,12,i+\frac{1}{2},j}^{n-1} \partial_{x_2}^{h} w_{i+\frac{1}{2},j}^{n} - \frac{1}{2} \frac{\left(w_{i+\frac{1}{2},j}^{n-1}\right)^2}{\left(Q_{i+\frac{1}{2},j}^{n-1}\right)^3} \partial_{x_1} u_{i+\frac{1}{2},j}^{n} \right. \right. \\
& \qquad \left. - \mathbb{E}_{\gamma,11,i-\frac{1}{2},j}^{n-1} \partial_{x_1}^{h} w_{i-\frac{1}{2},j}^{n} - \mathbb{E}_{\gamma,12,i-\frac{1}{2},j}^{n-1} \partial_{x_2}^{h} w_{i-\frac{1}{2},j}^{n} + \frac{1}{2} \frac{\left(w_{i-\frac{1}{2},j}^{n-1}\right)^2}{\left(Q_{i-\frac{1}{2},j}^{n-1}\right)^3} \partial_{x_1} u_{i-\frac{1}{2},j}^{n} \right) \\
& \quad + \frac{1}{h_2} \left(\mathbb{E}_{\gamma,21,i,j+\frac{1}{2}}^{n-1} \partial_{x_1}^{h} w_{i,j+\frac{1}{2}}^{n} + \mathbb{E}_{\gamma,22,i,j+\frac{1}{2}}^{n-1} \partial_{x_2}^{h} w_{i,j+\frac{1}{2}}^{n} - \frac{1}{2} \frac{\left(w_{i,j+\frac{1}{2}}^{n-1}\right)^2}{\left(Q_{i,j+\frac{1}{2}}^{n-1}\right)^3} \partial_{x_2} u_{i,j+\frac{1}{2}}^{n} \right. \\
& \qquad \left. \left. - \mathbb{E}_{\gamma,21,i,j-\frac{1}{2}}^{n-1} \partial_{x_1}^{h} w_{i,j-\frac{1}{2}}^{n} - \mathbb{E}_{\gamma,22,i,j-\frac{1}{2}}^{n-1} \partial_{x_2}^{h} w_{i,j-\frac{1}{2}}^{n} + \frac{1}{2} \frac{\left(w_{i,j-\frac{1}{2}}^{n-1}\right)^2}{\left(Q_{i,j-\frac{1}{2}}^{n-1}\right)^3} \partial_{x_2} u_{i,j-\frac{1}{2}}^{n} \right) \right] = u_{ij}^{n-1},
\end{aligned}
$$

and the approximations of the partial derivatives of u_{ij} and w_{ij} gives

$$
\begin{aligned}
& u_{ij}^{n} + \tau Q_{ij}^{n-1} \cdot \\
& \left[\frac{\mathbb{E}_{\gamma,11,i+\frac{1}{2},j}^{n-1}}{h_1^2} \left(w_{i+1,j}^{n} - w_{ij}^{n}\right) + \frac{\mathbb{E}_{\gamma,12,i+\frac{1}{2},j}^{n-1}}{4h_1h_2} \left(w_{i,j+1}^{n} + w_{i+1,j+1}^{n} - w_{i,j-1}^{n} - w_{i+1,j-1}^{n}\right) \right. \\
& - \frac{\mathbb{E}_{\gamma,11,i-\frac{1}{2},j}^{n-1}}{h_1^2} \left(w_{ij}^{n} - w_{i-1,j}^{n}\right) - \frac{\mathbb{E}_{\gamma,12,i-\frac{1}{2},j}^{n-1}}{4h_1h_2} \left(w_{i,j+1}^{n} + w_{i-1,j+1}^{n} - w_{i,j-1}^{n} - w_{i-1,j-1}^{n}\right) \\
& \qquad - \frac{1}{2h_1^2} \frac{\left(w_{i+\frac{1}{2},j}^{n-1}\right)^2}{\left(Q_{i+\frac{1}{2},j}^{n-1}\right)^3} \left(u_{i+1,j}^{n} - u_{ij}^{n}\right) + \frac{1}{2h_1^2} \frac{\left(w_{i-\frac{1}{2},j}^{n-1}\right)^2}{\left(Q_{i-\frac{1}{2},j}^{n-1}\right)^3} \left(u_{ij}^{n} - u_{i-1,j}\right) \\
& + \frac{\mathbb{E}_{\gamma,21,i,j+\frac{1}{2}}^{n-1}}{4h_1h_2} \left(w_{i+1,j}^{n} + w_{i+1,j+1}^{n} - w_{i-1,j}^{n} - w_{i-1,j+1}^{n}\right) + \frac{\mathbb{E}_{\gamma,22,i,j+\frac{1}{2}}^{n-1}}{h_2^2} \left(w_{i,j+1}^{n} - w_{ij}^{n}\right) \\
& - \frac{\mathbb{E}_{\gamma,21,i,j-\frac{1}{2}}^{n-1}}{4h_1h_2} \left(w_{i+1,j}^{n} + w_{i+1,j-1}^{n} - w_{i-1,j}^{n} - w_{i-1,j-1}^{n}\right) - \frac{\mathbb{E}_{\gamma,22,i,j-\frac{1}{2}}^{n-1}}{h_2^2} \left(w_{ij}^{n} - w_{i-1,j}^{n}\right) \\
& \qquad \left. - \frac{1}{2h_2^2} \frac{\left(w_{i,j+\frac{1}{2}}^{n-1}\right)^2}{\left(Q_{i,j+\frac{1}{2}}^{n-1}\right)^3} \left(u_{i,j+1}^{n} - u_{ij}^{n}\right) + \frac{1}{2h_2^2} \frac{\left(w_{i,j-\frac{1}{2}}^{n-1}\right)^2}{\left(Q_{i,j-\frac{1}{2}}^{n-1}\right)^3} \left(u_{ij}^{n} - u_{i,j-1}^{n}\right) \right] = u_{ij}^{n-1}.
\end{aligned}
$$

Let us now again introduce supporting coefficients $C_{\mathbb{E},ij}^{r,s}$ for $r, s \in \{-1, 0, 1\}$

$$
\begin{aligned}
C^{0,0}_{\mathbb{E},ij} &:= \tau Q^{n-1}_{ij}\left(-\frac{\mathbb{E}^{n-1}_{\gamma,11,i+\frac{1}{2},j}}{h_1^2}-\frac{\mathbb{E}^{n-1}_{\gamma,11,i-\frac{1}{2},j}}{h_1^2}-\frac{\mathbb{E}^{n-1}_{\gamma,22,i,j+\frac{1}{2}}}{h_2^2}-\frac{\mathbb{E}^{n-1}_{\gamma,22,i,j-\frac{1}{2}}}{h_2^2}\right),\\
C^{1,0}_{\mathbb{E},ij} &:= \tau Q^{n-1}_{ij}\left(\frac{\mathbb{E}^{n-1}_{\gamma,11,i+\frac{1}{2},j}}{h_1^2}+\frac{\mathbb{E}^{n-1}_{\gamma,21,i,j+\frac{1}{2}}}{4h_1h_2}-\frac{\mathbb{E}^{n-1}_{\gamma,21,i,j-\frac{1}{2}}}{4h_1h_2}\right),\\
C^{1,1}_{\mathbb{E},ij} &:= \tau Q^{n-1}_{ij}\left(\frac{\mathbb{E}^{n-1}_{\gamma,12,i+\frac{1}{2},j}}{4h_1h_2}+\frac{\mathbb{E}^{n-1}_{\gamma,21,i,j+\frac{1}{2}}}{4h_1h_2}\right),\\
C^{0,1}_{\mathbb{E},ij} &:= \tau Q^{n-1}_{ij}\left(\frac{\mathbb{E}^{n-1}_{\gamma,12,i+\frac{1}{2},j}}{4h_1h_2}-\frac{\mathbb{E}^{n-1}_{\gamma,12,i-\frac{1}{2},j}}{4h_1h_2}+\frac{\mathbb{E}^{n-1}_{\gamma,22,i,j+\frac{1}{2}}}{h_2^2}\right),\\
C^{-1,1}_{\mathbb{E},ij} &:= \tau Q^{n-1}_{ij}\left(\frac{-\mathbb{E}^{n-1}_{\gamma,12,i-\frac{1}{2},j}}{4h_1h_2}-\frac{\mathbb{E}^{n-1}_{\gamma,21,i,j+\frac{1}{2}}}{4h_1h_2}\right),
\end{aligned}
$$

$$
\begin{aligned}
C^{-1,0}_{\mathbb{E},ij} &:= \tau Q^{n-1}_{ij}\left(\frac{\mathbb{E}^{n-1}_{\gamma,11,i-\frac{1}{2},j}}{h_1^2}-\frac{\mathbb{E}^{n-1}_{\gamma,21,i,j+\frac{1}{2}}}{4h_1h_2}+\frac{\mathbb{E}^{n-1}_{\gamma,21,i,j-\frac{1}{2}}}{4h_1h_2}+\frac{\mathbb{E}^{n-1}_{\gamma,22,i,j-\frac{1}{2}}}{h_2^2}\right),\\
C^{-1,-1}_{\mathbb{E},ij} &:= \tau Q^{n-1}_{ij}\left(\frac{\mathbb{E}^{n-1}_{\gamma,12,i-\frac{1}{2},j}}{4h_1h_2}+\frac{\mathbb{E}^{n-1}_{\gamma,21,i,j-\frac{1}{2}}}{4h_1h_2}\right),\\
C^{0,-1}_{\mathbb{E},ij} &:= \tau Q^{n-1}_{ij}\left(-\frac{\mathbb{E}^{n-1}_{\gamma,12,i+\frac{1}{2},j}}{4h_1h_2}+\frac{\mathbb{E}^{n-1}_{\gamma,12,i-\frac{1}{2},j}}{4h_1h_2}\right),\\
C^{1,-1}_{\mathbb{E},ij} &:= \tau Q^{n-1}_{ij}\left(\frac{-\mathbb{E}^{n-1}_{\gamma,12,i+\frac{1}{2},j}}{4h_1h_2}-\frac{\mathbb{E}^{n-1}_{\gamma,21,i,j-\frac{1}{2}}}{4h_1h_2}\right),
\end{aligned}
$$

and $C^{r,s}_{wQ,ij}$ for $r,s\in\{-1,0,1\}$ and $|r|=|s|=1$

$$
\begin{aligned}
C^{1,0}_{wQ,ij} &:= \tau Q^{n-1}_{ij}\left(-\frac{1}{2h_1^2}\frac{\left(w^{n-1}_{i+\frac{1}{2},j}\right)^2}{\left(Q^{n-1}_{i+\frac{1}{2},j}\right)^3}\right), \quad C^{0,1}_{wQ,ij} := \tau Q^{n-1}_{ij}\left(-\frac{1}{2h_2^2}\frac{\left(w^{n-1}_{i,j+\frac{1}{2}}\right)^2}{\left(Q^{n-1}_{i,j+\frac{1}{2}}\right)^3}\right)\\
C^{-1,0}_{wQ,ij} &:= \tau Q^{n-1}_{ij}\left(-\frac{1}{2h_1^2}\frac{\left(w^{n-1}_{i-\frac{1}{2},j}\right)^2}{\left(Q^{n-1}_{i-\frac{1}{2},j}\right)^3}\right), \quad C^{0,-1}_{wQ,ij} := \tau Q^{n-1}_{ij}\left(-\frac{1}{2h_2^2}\frac{\left(w^{n-1}_{i,j-\frac{1}{2}}\right)^2}{\left(Q^{n-1}_{i,j-\frac{1}{2}}\right)^3}\right)
\end{aligned}
$$

and also

$$
C^{0,0}_{wQ,ij} := -\sum_{r,s\in\{-1,0,1\};|r|=|s|=1} C^{r,s}_{wQ,ij}.
$$

Then we may write

$$
u^n_{ij} + \sum_{r,s\in\{-1,0,1\}} C^{r,s}_{\mathbb{E},ij} w^n_{i+r,j+s} + \sum_{r',s'\in\{-1,0,1\};|r'|+|s'|=1} C^{r',s'}_{wQ,ij} u^n_{i+r',j+s'} = u^{n-1}_{ij}, \tag{6.257}
$$

for $i = 1, \cdots N_1 - 1$, $j = 1, \cdots, N_2 - 1$. We expand $w^n_{i+r,j+s}$ using the coefficients $C^{r',s'}_{w,i+r,j+s}$ for $0 < i + r < N_1$ and $0 < j + r < N_2$, otherwise we replace w^n_{ij} by w^{n-1}_{ij}. At the end we have

$$\boxed{\begin{aligned} u^n_{ij} + \sum_{\substack{r,s\in\{-1,0,1\}\\(i+r,j+s)\in\omega_h}} C^{r,s}_{\mathbb{E},ij} \sum_{r',s'\in\{-1,0,1\}} C^{r,s}_{w,i+r,j+s} u^n_{i+r+r',j+s+s'} & \qquad (6.258)\\ + \sum_{\substack{r',s'\in\{-1,0,1\}\\|r'|+|s'|=1}} C^{r',s'}_{wQ,ij} u^n_{i+r',j+s'} \quad &= \quad u^{n-1}_{ij},\\ u^n_{ij} + \sum_{\substack{r',s'\in\{-1,0,1\}\\|r'|+|s'|=1}} C^{r',s'}_{wQ,ij} u^n_{i+r',j+s'} \quad &= \quad u^{n-1}_{ij}\\ - \sum_{\substack{r,s\in\{-1,0,1\}\\(i+r,j+s)\in\partial\omega_h}} C^{r,s}_{\mathbb{E},ij} w^{n-1}_{i+r,j+s}, & \qquad (6.259)\end{aligned}}$$

which is again a system of linear equations in u^n_{ij} for $i = 1, \cdots N_1 - 1$, $j = 1, \cdots, N_2 - 1$ and it can be written in a matrix form,

$$\mathbb{A}\left(\mathbf{u}^{n-1}\right)\mathbf{u}^n = \mathbf{b}\left(\mathbf{u}^{n-1}, \mathbf{w}_{n-1}\right). \tag{6.260}$$

What remains now, is to solve the boundary conditions. The Dirichlet problem is trivial to solve. In case of the Neumann problem we must deal with the equations (6.227)-(6.230) - solving the Neumann boundary conditions on u^h_{ij} i.e. $\partial^h_{\mathbf{n}} u^h_{ij} = 0$ on $\partial\omega_h$ is also trivial. To solve (6.227)-(6.230) proceed as follows. For the node $w^{n-1}_{0,0}$ we get from (6.227) and (6.229) for $i = 1$ and $j = 1$

$$\begin{aligned} C^{0,0}_{\mathbb{E},0,0} w^{n-1}_{0,0} + C^{0,1}_{\mathbb{E},0,0} w^{n-1}_{0,1} + C^{1,0}_{\mathbb{E},0,0} w^{n-1}_{1,0} + C^{1,1}_{\mathbb{E},0,0} w^{n-1}_{1,1} + &\\ C^{0,2}_{\mathbb{E},0,0} w^{n-1}_{0,2} + C^{2,0}_{\mathbb{E},0,0} w^{n-1}_{2,0} + C^{1,2}_{\mathbb{E},0,0} w^{n-1}_{1,2} + C^{2,1}_{\mathbb{E},0,0} w^{n-1}_{2,1} \quad &= \quad 0 \end{aligned} \tag{6.261}$$

where

$$\begin{aligned} C^{0,0}_{\mathbb{E},0,0} &:= -\frac{\mathbb{E}^{n-1}_{12,\frac{1}{2},1}}{4h_1h_2} - \frac{\mathbb{E}^{n-1}_{21,1,\frac{1}{2}}}{4h_1h_2}, \quad C^{0,1}_{\mathbb{E},0,0} := -\frac{\mathbb{E}^{n-1}_{11,\frac{1}{2},1}}{h_1} - \frac{\mathbb{E}^{n-1}_{21,1,\frac{1}{2}}}{4h_1h_2},\\ C^{1,0}_{\mathbb{E},0,0} &:= -\frac{\mathbb{E}^{n-1}_{12,\frac{1}{2},1}}{4h_1h_2} - \frac{\mathbb{E}^{n-1}_{22,1,\frac{1}{2}}}{h_2}, \quad C^{1,1}_{\mathbb{E},0,0} := \frac{\mathbb{E}^{n-1}_{11,\frac{1}{2},1}}{h_1} + \frac{\mathbb{E}^{n-1}_{22,1,\frac{1}{2}}}{h_2},\\ C^{0,2}_{\mathbb{E},0,0} &:= C^{1,2}_{\mathbb{E},0,0} := \frac{\mathbb{E}^{n-1}_{12,\frac{1}{2},1}}{4h_1h_2}, \quad C^{2,0}_{\mathbb{E},0,0} := C^{2,1}_{\mathbb{E},0,0} := \frac{\mathbb{E}^{n-1}_{21,1,\frac{1}{2}}}{4h_1h_2}, \end{aligned}$$

for the node $w^{n-1}_{N_1,0}$ we have from (6.228) and (6.229) with $i = N_1 - 1$ and $j = 1$

$$\begin{aligned} C^{0,0}_{\mathbb{E},N_1,0} w^{n-1}_{N_1,0} + C^{0,1}_{\mathbb{E},N_1,0} w^{n-1}_{N_1,1} + C^{-1,0}_{\mathbb{E},N_1,0} w^{n-1}_{N_1-1,0} + C^{-1,1}_{\mathbb{E},N_1,0} w^{n-1}_{N_1-1,1} &\\ + C^{0,2}_{\mathbb{E},N_1,0} w^{n-1}_{N_1,2} + C^{-2,0}_{\mathbb{E},N_1,0} w^{n-1}_{N_1-2,0} + C^{-1,2}_{\mathbb{E},N_1,0} w^{n-1}_{N_1-1,2} + C^{-2,1}_{\mathbb{E},N_1,0} w^{n-1}_{N_1-2,1} \quad &= \quad 0 \end{aligned} \tag{6.262}$$

where

$$
\begin{aligned}
C^{0,0}_{\mathbb{E},N_1,0} &:= -\frac{\mathbb{E}^{n-1}_{12,N_1-\frac{1}{2},1}}{4h_1h_2} + \frac{\mathbb{E}^{n-1}_{21,N_1-1,\frac{1}{2}}}{4h_1h_2}, \quad C^{0,1}_{\mathbb{E},N_1,0} := \frac{\mathbb{E}^{n-1}_{11,N_1-\frac{1}{2},1}}{h_1} + \frac{\mathbb{E}^{n-1}_{21,N_1-1,\frac{1}{2}}}{4h_1h_2},\\
C^{-1,0}_{\mathbb{E},N_1,0} &:= -\frac{\mathbb{E}^{n-1}_{12,N_1-\frac{1}{2},1}}{4h_1h_2} - \frac{\mathbb{E}^{n-1}_{22,N_1-1,\frac{1}{2}}}{h_2}, \quad C^{-1,1}_{\mathbb{E},N_1,0} := -\frac{\mathbb{E}^{n-1}_{11,N_1-\frac{1}{2},1}}{h_1} + \frac{\mathbb{E}^{n-1}_{22,N_1-1,\frac{1}{2}}}{h_2},\\
C^{0,2}_{\mathbb{E},N_1,0} &:= C^{-1,2}_{\mathbb{E},N_1,0} := \frac{\mathbb{E}^{n-1}_{12,N_1-\frac{1}{2},1}}{4h_1h_2}, \quad C^{-2,0}_{\mathbb{E},N_1,0} := C^{-2,1}_{\mathbb{E},N_1,0} := -\frac{\mathbb{E}^{n-1}_{21,N_1-1,\frac{1}{2}}}{4h_1h_2}.
\end{aligned}
$$

For the node w^{n-1}_{0,N_2} we take (6.227) and (6.230) with $i = 1$ and $j = N_2 - 1$. It gives

$$
\begin{aligned}
&C^{0,0}_{\mathbb{E},0,N_2} w^{n-1}_{0,N_2} + C^{0,-1}_{\mathbb{E},0,N_2} w^{n-1}_{0,N_2-1} + C^{1,0}_{\mathbb{E},0,N_2} w^{n-1}_{1,N_2} + C^{1,-1}_{\mathbb{E},0,N_2} w^{n-1}_{1,N_2-1}\\
&+C^{0,-2}_{\mathbb{E},0,N_2} w^{n-1}_{0,N_2-2} + C^{2,0}_{\mathbb{E},0,N_2} w^{n-1}_{2,N_2} + C^{1,-2}_{\mathbb{E},0,N_2} w^{n-1}_{1,N_2-2} + C^{2,-1}_{\mathbb{E},0,N_2} w^{n-1}_{2,N_2-1} = 0 \qquad (6.263)
\end{aligned}
$$

for

$$
\begin{aligned}
C^{0,0}_{\mathbb{E},0,N_2} &:= \frac{\mathbb{E}^{n-1}_{12,\frac{1}{2},N_2-1}}{4h_1h_2} - \frac{\mathbb{E}^{n-1}_{21,1,N_2-\frac{1}{2}}}{4h_1h_2}, \quad C^{0,-1}_{\mathbb{E},0,N_2} := -\frac{\mathbb{E}^{n-1}_{11,\frac{1}{2},N_2-1}}{h_1} - \frac{\mathbb{E}^{n-1}_{21,1,N_2-\frac{1}{2}}}{4h_1h_2},\\
C^{1,0}_{\mathbb{E},0,N_2} &:= \frac{\mathbb{E}^{n-1}_{12,\frac{1}{2},N_2-1}}{4h_1h_2} + \frac{\mathbb{E}^{n-1}_{22,1,N_2-\frac{1}{2}}}{h_2}, \quad C^{1,-1}_{\mathbb{E},0,N_2} := \frac{\mathbb{E}^{n-1}_{11,\frac{1}{2},N_2-1}}{h_1} - \frac{\mathbb{E}^{n-1}_{22,1,N_2-\frac{1}{2}}}{h_2},\\
C^{0,-2}_{\mathbb{E},0,N_2} &:= C^{1,-2}_{\mathbb{E},0,N_2} := -\frac{\mathbb{E}^{n-1}_{12,\frac{1}{2},N_2-1}}{4h_1h_2}, \quad C^{2,0}_{\mathbb{E},0,N_2} := C^{2,-1}_{\mathbb{E},0,N_2} := \frac{\mathbb{E}^{n-1}_{21,1,N_2-\frac{1}{2}}}{4h_1h_2},
\end{aligned}
$$

and from (6.228) and (6.230) with $i = N_1 - 1$ and $j = N_2 - 1$ we get

$$
\begin{aligned}
&C^{0,0}_{\mathbb{E},N_1,N_2} w^{n-1}_{N_1,N_2} + C^{0,-1}_{\mathbb{E},N_1,N_2} w^{n-1}_{N_1,N_2-1} + C^{-1,0}_{\mathbb{E},N_1,N_2} w^{n-1}_{N_1-1,N_2}\\
&+C^{-1,-1}_{\mathbb{E},N_1,N_2} w^{n-1}_{N_1-1,N_2-1} + C^{0,-2}_{\mathbb{E},N_1,N_2} w^{n-1}_{N_1,N_2-2} + C^{-2,0}_{\mathbb{E},N_1,N_2} w^{n-1}_{N_1-2,N_2}\\
&+C^{-1,-2}_{\mathbb{E},N_1,N_2} w^{n-1}_{N_1-1,N_2-2} + C^{-2,-1}_{\mathbb{E},N_1,N_2} w^{n-1}_{N_1-2,N_2-1} = 0 \qquad (6.264)
\end{aligned}
$$

where

$$
\begin{aligned}
C^{0,0}_{\mathbb{E},N_1,N_2} &:= \frac{\mathbb{E}^{n-1}_{12,N_1-\frac{1}{2},N_2-1}}{4h_1h_2} + \frac{\mathbb{E}^{n-1}_{21,N_1-1,N_2-\frac{1}{2}}}{4h_1h_2}, \quad C^{0,-1}_{\mathbb{E},N_1,N_2} := \frac{\mathbb{E}^{n-1}_{11,N_1-\frac{1}{2},N_2-1}}{h_1} + \frac{\mathbb{E}^{n-1}_{21,N_1-1,N_2-\frac{1}{2}}}{4h_1h_2},\\
C^{-1,0}_{\mathbb{E},N_1,N_2} &:= \frac{\mathbb{E}^{n-1}_{12,N_1-\frac{1}{2},N_2-1}}{4h_1h_2} + \frac{\mathbb{E}^{n-1}_{22,N_1-1,N_2-\frac{1}{2}}}{h_2}, \quad C^{-1,-1}_{\mathbb{E},N_1,N_2} := -\frac{\mathbb{E}^{n-1}_{11,N_1-\frac{1}{2},N_2-1}}{h_1} - \frac{\mathbb{E}^{n-1}_{22,N_1-1,N_2-\frac{1}{2}}}{h_2},\\
C^{0,-2}_{\mathbb{E},N_1,N_2} &:= C^{-1,-2}_{\mathbb{E},N_1,N_2} := -\frac{\mathbb{E}^{n-1}_{12,N_1-\frac{1}{2},N_2-1}}{4h_1h_2}, \quad C^{-2,0}_{\mathbb{E},N_1,N_2} := C^{-2,-1}_{\mathbb{E},N_1,N_2} := -\frac{\mathbb{E}^{n-1}_{21,N_1-1,N_2-\frac{1}{2}}}{4h_1h_2}.
\end{aligned}
$$

Proceeding to the equation (6.227) with $i = 1$ and $j = 1, \cdots, N_2-1$ we get a system of equations

$$
\begin{aligned}
&C^{0,0}_{\mathbb{E},0,j} w^{n-1}_{0,j} + C^{1,0}_{\mathbb{E},0,j} w^{n-1}_{1,j} + C^{0,1}_{\mathbb{E},0,j} w^{n-1}_{0,j+1}\\
&+C^{0,-1}_{\mathbb{E},0,j} w^{n-1}_{0,j-1} + C^{1,1}_{\mathbb{E},0,j} w^{n-1}_{1,j+1} + C^{1,-1}_{\mathbb{E},0,j} w^{n-1}_{1,j-1} = 0 \qquad (6.265)
\end{aligned}
$$

for

$$
\begin{aligned}
C^{0,0}_{\mathbb{E},0,j} &:= -C^{1,0}_{\mathbb{E},0,j} := -\frac{\mathbb{E}^{n-1}_{11,\frac{1}{2},j}}{h_1},\\
C^{0,1}_{\mathbb{E},0,j} &:= -C^{0,-1}_{\mathbb{E},0,j} := -C^{1,-1}_{\mathbb{E},0,j} := C^{1,1}_{\mathbb{E},0,j} := \frac{\mathbb{E}^{n-1}_{12,\frac{1}{2},j}}{4h_1h_2},
\end{aligned}
$$

from (6.228) with $i = N_1 - 1$ and $j = 1, \cdots, N_2 - 1$ we get

$$\begin{aligned} C^{0,0}_{\mathbb{E},N_1,j} w^{n-1}_{N_1,j} + C^{-1,0}_{\mathbb{E},N_1,j} w^{n-1}_{N_1-1,j} + C^{0,1}_{\mathbb{E},N_1,j} w^{n-1}_{N_1,j+1} & \\ + C^{0,-1}_{\mathbb{E},N_1,j} w^{n-1}_{N_1,j-1} + C^{-1,1}_{\mathbb{E},N_1,j} w^{n-1}_{N_1-1,j+1} + C^{-1,-1}_{\mathbb{E},N_1,j} w^{n-1}_{N_1-1,j-1} &= 0 \end{aligned} \tag{6.266}$$

for

$$\begin{aligned} C^{0,0}_{\mathbb{E},N_1,j} &:= -C^{-1,0}_{\mathbb{E},N_1,j} := \frac{\mathbb{E}^{n-1}_{11,N_1-\frac{1}{2},j}}{h_1}, \\ C^{0,1}_{\mathbb{E},N_1,j} &:= -C^{0,-1}_{\mathbb{E},N_1,j} := -C^{-1,-1}_{\mathbb{E},N_1,j} := C^{-1,1}_{\mathbb{E},N_1,j} := \frac{\mathbb{E}^{n-1}_{12,N_1-\frac{1}{2},j}}{4h_1h_2} \end{aligned}$$

from (6.229) with $i = 1, \cdots, N_1 - 1$ and $j = 1$ we get

$$\begin{aligned} C^{0,0}_{\mathbb{E},i,0} w^{n-1}_{i,0} + C^{-1,0}_{\mathbb{E},i,0} w^{n-1}_{i-1,0} + C^{1,0}_{\mathbb{E},i,0} w^{n-1}_{i+1,0} & \\ + C^{0,1}_{\mathbb{E},i,0} w^{n-1}_{i,1} + C^{1,1}_{\mathbb{E},i,0} w^{n-1}_{i+1,1} + C^{-1,1}_{\mathbb{E},i,0} w^{n-1}_{i-1,1} &= 0 \end{aligned} \tag{6.267}$$

where

$$\begin{aligned} C^{0,0}_{\mathbb{E},i,0} &:= -C^{0,1}_{\mathbb{E},i,0} := -\frac{\mathbb{E}^{n-1}_{22,i,\frac{1}{2}}}{h_2}, \\ C^{1,0}_{\mathbb{E},i,0} &:= -C^{-1,0}_{\mathbb{E},i,0} := -C^{-1,1}_{\mathbb{E},i,0} := C^{1,1}_{\mathbb{E},i,0} := \frac{\mathbb{E}^{n-1}_{21,i,\frac{1}{2}}}{4h_1h_2}, \end{aligned}$$

and finally from (6.230) with $i = 1, \cdots, N_1 - 1$ and $j = N_2 - 1$ we get

$$\begin{aligned} C^{0,0}_{\mathbb{E},i,N_2} w^{n-1}_{i,N_2} + C^{-1,0}_{\mathbb{E},i,N_2} w^{n-1}_{i-1,N_2} + C^{1,0}_{\mathbb{E},i,N_2} w^{n-1}_{i+1,N_2} & \\ + C^{0,-1}_{\mathbb{E},i,N_2} w^{n-1}_{i,N_2-1} + C^{1,-1}_{\mathbb{E},i,N_2} w^{n-1}_{i+1,N_2-1} + C^{-1,-1}_{\mathbb{E},i,N_2} w^{n-1}_{i-1,N_2-1} &= 0 \end{aligned} \tag{6.268}$$

where

$$\begin{aligned} C^{0,0}_{\mathbb{E},i,N_2} &:= -C^{0,-1}_{\mathbb{E},i,N_2} := \frac{\mathbb{E}^{n-1}_{22,i,N_2-\frac{1}{2}}}{h_2}, \\ C^{1,0}_{\mathbb{E},i,N_2} &:= -C^{-1,0}_{\mathbb{E},i,N_2} := -C^{-1,-1}_{\mathbb{E},i,N_2} := C^{1,-1}_{\mathbb{E},i,N_2} := \frac{\mathbb{E}^{n-1}_{21,i,N_2-\frac{1}{2}}}{4h_1h_2}. \end{aligned}$$

As before, we end up with a system of linear equations using which we are able to extend w^{n-1}_{ij} from ω_h to $\bar{\omega}_h$. The resulting algorithm reads:

Algorithm 6.3.11. Algorithm for the extension of w^h_{ij} to $\bar{\omega}_h$:

1. set $A^{w_{ext}}_{IJ} := 0$ for all $I, J = 0, \cdots N_1N_2$ and $b_I := 0$ for all $I = 0, \cdots N_1N_2$
2. for the row $I = 0, \cdots N_1N_2$ do
3. if $(i(I), j(I)) \in \omega_h$ set

$$A^{w_{ext}}_{II} := 1 \text{ and } b_I := w^h_{i(I),j(I)}$$

4. if $(i(I), j(I)) \in \partial\omega_h$ set

$$A^{w_{ext}}_{IJ(i+r,j+s)} := C^{r,s}_{\mathbb{E},i,j} \text{ and } b_I := 0,$$

for $i = u(I)$, $j = j(I)$ and $r, s \in \{-2, -1, 0, 1, 2\}$

5. solve the linear system
$$\mathbb{A}^{w_{ext}}\mathbf{w}^h = \mathbf{b}.$$

The algorithm for assembling the linear system matrix for the semi-implicit scheme for the Willmore flow is as follows:

Algorithm 6.3.12. Setup of the linear system matrix for the semi-implicit Willmore flow consists of the following steps:

1. set $A^W_{IJ} := 0$ for all $I, J = 0, \cdots N_1 N_2$ and $b_I := 0$ for all $I = 0, \cdots N_1 N_2$
2. evaluate $w^{n-1}_{\gamma,ij} := Q^{n-1}_{ij} \nabla \cdot \nabla_{\mathbf{p}} \gamma \left(\nabla u^{n-1}_{ij} \right)$ on ω_h
3. in case of the Neumann boundary conditions extend w^h_{ij} on $\bar{\omega}^h$ using the algorithm (6.3.11)
4. for the row $I = 0, \cdots N_1 N_2$ do
5. if $(i(I), j(I)) \in \partial\omega_h$ set the boundary conditions:
6. for the Dirichlet boundary conditions set
$$A^W_{II} := 1, b_I := g^{n-1}_{ij}, \text{ and } w^{n-1}_{ij} := 0,$$
7. for the Neumann boundary conditions set $b_I := 0$ and
$$\begin{array}{rll} \text{if } i = i\,(I,J) = 0 & \text{set} & A^W_{II} := -1 \text{ and } A^W_{I,J(i+1,j)} := 1, \\ \text{if } i = i\,(I,J) = N_1 & \text{set} & A^W_{II} := 1 \text{ and } A^W_{I,J(i-1,j)} := -1, \\ \text{if } j = j\,(I,J) = 0 & \text{set} & A^W_{II} := -1 \text{ and } A^W_{I,J(i,j+1)} := 1, \\ \text{if } j = j\,(I,J) = N_2 & \text{set} & A^W_{II} := 1 \text{ and } A^W_{I,J(i,j-1)} := -1, \end{array}$$
8. else set $A_{II} := 1$, $b_I := u^{n-1}_{ij}$
9. for all $r, s = -1, 0, 1$ do
10. for all $r', s' = -1, 0, 1$ and $|r'| + |s'| = 1$ set
$$A_{IJ} := A_{IJ} + C^{r',s'}_{wQ,i+r',j+s'} \text{ for } J = J\left(i + r', j + s'\right)$$
11. if $(i + r, j + s) \in \omega_h$ do
12. for all $r', s' = -1, 0, 1$ set
$$A_{IJ} := A_{IJ} + C^{r,s}_{\mathbb{E},ij} C^{r,s}_{w,i+r,j+s} \text{ for } J = J\left(i + r + r', j + s + s'\right)$$
13. if $(i + r, j + s) \in \partial\omega_h$ do set
$$b_I := b_I - C^{r,s}_{\mathbb{E},ij} w^{n-1}_{i+r,j+s}$$

6.4. Numerical scheme for the parametric approach

We will now describe numerical schemes for the parametric approach . It is a simplified version of the scheme introduced in [77]. Since we use the parametric approach only for a comparison with the level-set method, we consider only schemes of the semi-implicit nature. We discretise the evolved plane curve by points x_i^n for $i = 1, \cdots, N$ and $n = 1, \cdots, M$. The index i denotes the space discretisation and index n stands for the time stepping. We remind that since we constrain ourselves only to closed planar curves, we set the periodic boundary conditions $x_{-1}^n = x_{N-1}^n$, $x_0^n = x_N^n$, $x_{N+1}^n = x_1^n$ and $x_{N+2}^n = x_1^n$ for all $n = 1, \cdots, M$. For a uniform division of the time interval $[0, T]$ we get $\tau = T/M$ and with the uniform division of the parametrisation interval $[0, 1]$, we get $h = 1/N$ and we may write $x_i^n = x(ih, n\tau)$. To solve the system (5.123)-(5.125) we also discretise the quantities g, κ, α, β with their discrete counterparts r_i^n, κ_i^n, α_i^n and β_i^n. For the approximation of the local lengths r_i^n we set

$$r_i^n = \left| x_i^n - x_{i-1}^n \right| . \tag{6.269}$$

α_i^n and β_i^n represent normal and tangential velocity of the node x_i^n. Discrete curvature κ_i^n is piecewise constant approximation of κ in the so-called flowing finite volume $\left[\tilde{x}_{i-1}^n, \tilde{x}_i^n\right]$ for $\tilde{x}_i^n = \frac{x_{i-1}^n + x_i^n}{2}$. We also define local length of the flowing volume

$$q_i^n \approx \left| \tilde{x}_{i+1}^n - \tilde{x}_i^n \right| \approx \frac{1}{2}\left(r_{i+1}^n + r_i^n \right) \tag{6.270}$$

For the approximation of the curvature κ (see the Figure 6.8), we introduce the tangential vector $R_i^n = x_i^n - x_{i-1}^n$. From (4.3) we see that κ is in fact a change of angle between the tangential vectors adjacent to the vector R_i. Since κ_i^n is constant approximation of κ in the flowing volume $\left[\tilde{x}_i^n, \tilde{x}_{i+1}^n\right]$, we will evaluate it in the node x_i^n. We measure the change of the angle between R_{i-1}^n and R_{i+1}^n related to the local length r_i^n. It is given by

$$\Delta\theta = \arccos\left(\frac{R_{i+1}^n \cdot R_{i-1}^n}{\left|R_{i+1}^n\right| \left|R_{i-1}^n\right|} \right).$$

To keep the correct sign of κ (positive for convex and negative for concave parts) we multiply it by the orientation of R_{i+1}^n and R_{i-1}^n which is

$$\operatorname{sign}\left(R_{i+1}^n \wedge R_{i-1} \right) = \operatorname{sign}\det\left(R_{i+1}^n, R_{i-1}^n \right).$$

Putting it all together, we have

$$\begin{aligned} \kappa_i^n = \partial_s\theta \approx \frac{\Delta\theta}{\Delta s} &= \frac{1}{q_{i-1}^n + q_i^n} \operatorname{sign}\left(R_{i+1}^n \wedge R_{i-1}^n \right) \arccos\left(\frac{R_{i+1}^n \cdot R_{i-1}^n}{r_{i+1}^n r_{i-1}^n} \right) \\ &\approx \frac{1}{2r_i^n} \operatorname{sign}\left(R_{i+1}^n \wedge R_{i-1}^n \right) \arccos\left(\frac{R_{i+1}^n \cdot R_{i-1}^n}{r_{i+1}^n r_{i-1}^n} \right). \end{aligned}$$

where we used the fact that

$$q_{i-1}^n + q_i^n = \frac{1}{2}\left(r_{i-1}^n + r_i^n \right) + \frac{1}{2}\left(r_i^n + r_{i+1}^n \right) = r_i^n + \frac{1}{2} r_{i-1}^n + \frac{1}{2} r_{i+1}^n \approx 2r_i^n.$$

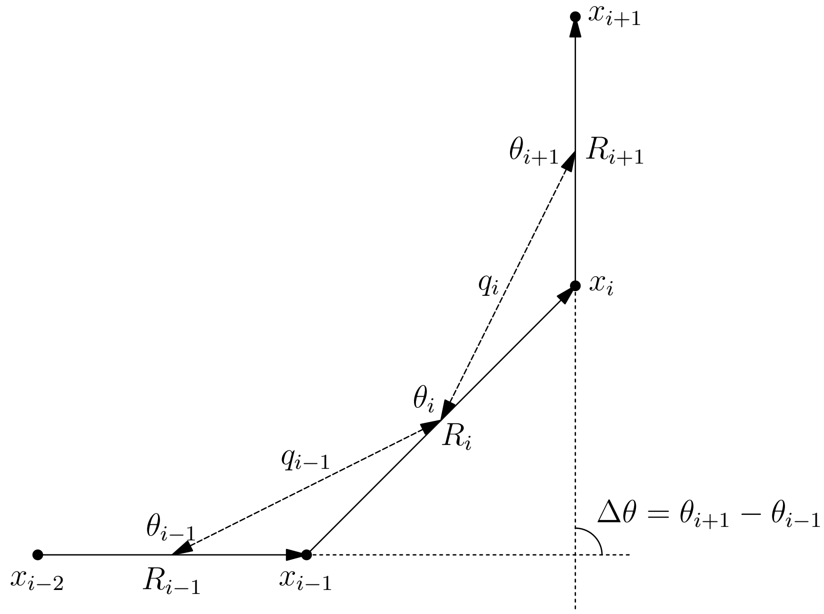

Figure 6.8.: Curvature approximation for the Lagrangian method is given as a change of the angles θ_{i+1} and θ_{i-1} corresponding to the tangential vectors R_{i+1} and R_{i-1} divided by the distance $q_{i-1} + q_i$.

Having κ_i^n in hand, we may proceed to the discretisation of β from (5.4.1) and (5.4.2). The first one is trivial. In the case of (5.4.2) we need to evaluate the second derivative of κ at $\tilde{x}_i^n$, it is

$$\begin{aligned}\partial_s^2 \kappa\left(\tilde{x}_i^n\right) &= \frac{\partial_s \kappa\left(x_i^n\right) - \partial_s \kappa\left(x_{i-1}^n\right)}{r_i^n} \\ &= \frac{1}{r_i^n}\left(\frac{\kappa\left(\tilde{x}_{i+1}^n\right) - \kappa\left(\tilde{x}_i^n\right)}{q_i^n} - \frac{\kappa\left(\tilde{x}_i^n\right) - \kappa\left(\tilde{x}_{i-1}^n\right)}{q_{i-1}^n}\right) \\ &= \frac{1}{r_i^n}\left(\frac{\kappa_{i+1}^n - \kappa_i^n}{q_i^n} - \frac{\kappa_i^n - \kappa_{i-1}^n}{q_{i-1}^n}\right).\end{aligned}$$

To approximate α we integrate the equation (5.124) over the volume $[x_{i-1}, x_i]$ and obtain

$$\int_{x_{i-1}}^{x_i} \partial_s \alpha \mathrm{d}s = \int_{x_{i-1}}^{x_i} \kappa\beta - \langle\kappa\beta\rangle_{\Gamma(t)} + \omega\left(\frac{L}{g} - 1\right)\mathrm{d}s,$$

which gives

$$\alpha_i - \alpha_{i-1} = r_i\left(\kappa_i\beta_i - \langle\kappa\beta\rangle_{\Gamma(t)}\right) + \omega\left(\frac{L}{N} - r_i\right).$$

Denoting

$$L^n = \sum_{l=1}^N r_l^n \text{ and } B^n = \frac{1}{L^n}\sum_{l=1}^N r_l^n \kappa_l^n \beta_l^n,$$

and setting $\alpha_0^n = 0$ we have

$$\alpha_i^n = \alpha_{i-1}^n + r_i^{n-1}\left(\kappa_i^{n-1}\beta_i^{n-1} - B^{n-1}\right) + \omega\left(\frac{L^{n-1}}{n} - r_i^{n-1}\right),$$

for $i = 1, \cdots N$. Finally we may proceed to the discretisation of the equation

$$\partial_t \mathbf{x} = \beta \mathbf{n} + \alpha \mathbf{t}. \tag{6.271}$$

Since we aim to derive a semi-implicit scheme, we would like to express $\beta\mathbf{n}$ in terms of partial derivatives of $\mathbf{x}$ w.r. to s. For the mean-curvature flow from (4.4) we have $\beta\mathbf{n} = \kappa\mathbf{n} = -\partial_s^2\mathbf{x}$. It is approximated as follows:

$$\partial_s^2 \mathbf{x}(x_i) \approx \frac{\partial_s \mathbf{x}(\tilde{x}_{i+1}) - \partial_s \mathbf{x}(\tilde{x}_i)}{q_i} \approx \frac{1}{q_i}\left(\frac{x_{i+1} - x_i}{r_{i+1}} - \frac{x_i - x_{i-1}}{r_i}\right).$$

To discretise $\beta\mathbf{n}$ with β given by (5.4.2) i.e. $\beta = -\partial_s^2\kappa - \frac{1}{2}\kappa^3$ we start with the fourth derivative of the positional vector $\mathbf{x}$:

$$\begin{aligned}
\partial_s^4 \mathbf{x} &= \partial_s^3 \mathbf{t} = -\partial_s^2(\kappa\mathbf{n}) = -\partial_s(\partial_s k\mathbf{n} + \kappa\partial_s\mathbf{n}) = -\partial_s^2\kappa\mathbf{n} - 2\partial_s\kappa\partial_s\mathbf{n} - \kappa\partial_s^2\mathbf{n} \\
&= -\partial_s^2\kappa\mathbf{n} - 2\partial_s\kappa(\kappa\mathbf{t}) - \kappa\partial_s(\kappa\mathbf{t}) = -\partial_s^2\kappa\mathbf{n} - 2\partial_s\kappa(\kappa\mathbf{t}) - \kappa\partial_s\kappa\mathbf{t} - \kappa^2\partial_s\mathbf{t} \\
&= -\partial_s^2\kappa\mathbf{n} - 3\partial_s\kappa(\kappa\mathbf{t}) - \kappa^2\partial_s\mathbf{t} = -\partial_s^2\kappa\mathbf{n} - \frac{3}{2}\partial_s(\kappa^2)\partial_s\mathbf{x} - \kappa^2\partial_s^2\mathbf{x}.
\end{aligned}$$

It means:

$$\partial_s^2\kappa\mathbf{n} = -\partial_s^4\mathbf{x} - \kappa^2\partial_s^2\mathbf{x} - \frac{3}{2}\partial_s(\kappa^2)\partial_s\mathbf{x},$$

and together with $\kappa\mathbf{n} = -\partial_s\mathbf{t} = -\partial_s^2\mathbf{x}$ we have:

$$\begin{aligned}
\left(\partial_s^2\kappa + \frac{1}{2}\kappa^3\right)\mathbf{n} &= -\partial_s^4\mathbf{x} - \frac{3}{2}\partial_s(\kappa^2)\partial_s\mathbf{x} - \kappa^2\partial_s^2\mathbf{x} - \frac{1}{2}\kappa^2\partial_s^2\mathbf{x} \\
&= -\partial_s^4\mathbf{x} - \frac{3}{2}\partial_s(\kappa^2)\partial_s\mathbf{x} - \frac{3}{2}\kappa^2\partial_s^2\mathbf{x} \\
&= -\partial_s^4\mathbf{x} - \frac{3}{2}\partial_s(\kappa^2\partial_s\mathbf{x}).
\end{aligned}$$

The approximation of $\partial_s^4\mathbf{x}$ is as follows:

$$\begin{aligned}
\partial_s^4\mathbf{x}(x_i) &\approx \frac{\partial_s^3\mathbf{x}(\tilde{x}_{i+1}) - \partial_s^3\mathbf{x}(\tilde{x})}{q_i} \\
&\approx \frac{1}{q_i}\left(\frac{\partial_s^2\mathbf{x}(x_{i+1}) - \partial_s^2\mathbf{x}(x_i)}{r_{i+1}} - \frac{\partial_s^2\mathbf{x}(x_i) - \partial_s^2\mathbf{x}(x_{i-1})}{r_i}\right) \\
&\approx \frac{1}{q_i r_{i+1}}\left(\frac{\partial_s\mathbf{x}(\tilde{x}_{i+2}) - \partial_s\mathbf{x}(\tilde{x}_{i+1})}{q_{i+1}} - \frac{\partial_s\mathbf{x}(\tilde{x}_{i+1}) - \partial_s\mathbf{x}(\tilde{x}_i)}{q_i}\right) \\
&- \frac{1}{q_i r_i}\left(\frac{\partial_s\mathbf{x}(\tilde{x}_{i+1}) - \partial_s\mathbf{x}(\tilde{x}_i)}{q_i} - \frac{\partial_s\mathbf{x}(\tilde{x}_i) - \partial_s\mathbf{x}(\tilde{x}_{i-1})}{q_{i-1}}\right) \\
&\approx \frac{1}{q_i q_{i+1} r_{i+1}}\left(\frac{x_{i+2} - x_{i+1}}{r_{i+2}} - \frac{x_{i+1} - x_i}{r_{i+1}}\right) \\
&- \frac{1}{q_i^2 r_{i+1}}\left(\frac{x_{i+1} - x_i}{r_{i+1}} - \frac{x_i - x_{i-1}}{r_i}\right) \\
&- \frac{1}{q_i^2 r_i}\left(\frac{x_{i+1} - x_i}{r_{i+1}} - \frac{x_i - x_{i-1}}{r_i}\right) \\
&+ \frac{1}{q_i q_{i-1} r_i}\left(\frac{x_i - x_{i-1}}{r_i} - \frac{x_{i-1} - x_{i-2}}{r_{i-1}}\right).
\end{aligned}$$

The second term is discretised as:

$$\begin{aligned} \frac{3}{2}\partial_s\left(\kappa^2\partial_s\mathbf{x}\right) &\approx \frac{3}{2}\frac{\left(\kappa^2\partial_s x\right)(\tilde{x}_{i+1}) - \left(\kappa^2\partial_s x\right)(\tilde{x}_i)}{q_i} \\ &\approx \frac{3}{2}\frac{1}{q_i}\left(\kappa_{i+1}^2\frac{x_{i+1}-x_i}{r_{i+1}} - \kappa_i^2\frac{x_i-x_{i-1}}{r_i}\right). \end{aligned}$$

To complete the space discretisation of (6.271) we need only to solve the tangential term:

$$\alpha\mathbf{t} \approx \alpha_i\frac{\tilde{x}_{i+1}-\tilde{x}_i}{q_i} = \frac{\alpha_i}{2}\frac{x_{i+1}-x_{i-1}}{q_i}.$$

We replace the time derivative in (6.271) by backward difference. We conclude with the following algorithm:

Algorithm 6.4.1. The semi-implicit parametric approach with asymptotically uniform redistribution:

1. Evaluate the local length r_i^n for $i = 1, \cdots N$ by

$$r_i^n = \left|x_i^n - x_{i-1}^n\right|, \tag{6.272}$$

   and apply the periodic boundary conditions $r_{-1}^n = r_{N-1}^n$, $r_0^n = r_N^n$, $r_{N+1}^n = r_1^n$ and $r_{N+2}^n = r_1^n$.

2. Evaluate the curvature κ_i^n for $i = 1, \cdots N$ by

$$\kappa_i^n = \frac{1}{2r_i^n}\operatorname{sign}\left(R_{i+1}^n \wedge R_{i-1}^n\right)\arccos\left(\frac{R_{i+1}^n \cdot R_{i-1}^n}{r_{i+1}^n r_{i-1}^n}\right), \tag{6.273}$$

   for $R_i^n = x_i^n - x_{i-1}^n$ and with the periodic boundary conditions $\kappa_{-1}^n = \kappa_{N-1}^n$, $\kappa_0^n = \kappa_N^n$, $\kappa_{N+1}^n = \kappa_1^n$ and $\kappa_{N+2}^n = \kappa_1^n$.

3. Evaluate the normal velocity β_i^n:
   a) In the case of the mean-curvature flow set

$$\beta_i^n = \kappa_i^n, \text{ for } i = -1, \cdots N+2 \tag{6.274}$$

   b) In the case of the Willmore flow set

$$\beta_i^n = -\frac{1}{r_i^n}\left(\frac{\kappa_{i+1}^n - \kappa_i^n}{q_i^n} - \frac{\kappa_i^n - \kappa_{i-1}^n}{q_{i-1}^n}\right) - \frac{1}{2}\left(\kappa_i^n\right)^3 \text{ for } i = 1, \cdots, N \tag{6.275}$$

   where $q_i = \frac{1}{2}\left(r_i^n + r_{i+1}^n\right)$ and apply the periodic boundary conditions $\beta_{-1}^n = \beta_{N-1}^n$, $\beta_0^n = \beta_N^n$, $\beta_{N+1}^n = \beta_1^n$ and $\beta_{N+2}^n = \beta_1^n$.

4. Evaluate the tangential velocity α_i^n by

$$\begin{aligned} L^n &= \sum_{l=1}^N r_l^n,\ B^n = \frac{1}{L^n}\sum_{l=1}^N r_l^n\kappa_l^n\beta_l^n,\ \omega = \delta_1 + \delta_2 B^n \\ \alpha_0^n &= 0, \\ \alpha_i^n &= \alpha_{i-1}^n + r_i^{n-1}\left(\kappa_i^{n-1}\beta_i^{n-1} - B^{n-1}\right) + \omega\left(\frac{L^{n-1}}{n} - r_i^{n-1}\right), \end{aligned} \tag{6.276}$$

   for $i = 1, \cdots, N$.

5. Solve:
   a) Tridiagonal system for the mean-curvature flow:
   $$B_i^n x_{i-1}^n + C_i^n x_i^n + D_i^n x_{i+1}^n = F_i^n, \tag{6.277}$$
   where
   $$\begin{aligned} C_i^n &= \frac{q_i^n}{\tau} - \left(B_i^n + D_i^n\right), \quad F_i^n = \frac{q_i^n}{\tau} x_i^{n-1}, \\ B_i^n &= \frac{1}{r_i^n}, \quad D_i^n = \frac{1}{r_{i+1}^n}. \end{aligned}$$
   b) Pentadiagonal system for the surface diffusion flow: where
   c) Pentadiagonal system for the Willmore flow:
   $$A_i^n x_{i-2}^n + B_i^n x_{i-1}^n + C_i^n x_i^n + D_i^n x_{i+1}^n + E_{i+2}^n = F_i^n, \tag{6.278}$$
   where
   $$\begin{aligned} A_i^n &= \frac{1}{r_i^n q_{i-1}^n r_{i-1}^n}, \quad C_i^n = \frac{q_i^n}{\tau} - \left(A_i^n + B_i^n + D_i^n + E_i^n\right), \\ E_i^n &= \frac{1}{r_{i+1}^n q_{i+1}^n r_{i+2}^n}, \quad F_i^n = \frac{q_i^n}{\tau} x_i^{n-1}, \\ B_i^n &= -\left(\frac{1}{r_i^n q_{i-1}^n r_{i-1}^n} + \frac{1}{(r_i^n)^2 q_{i-1}^n} + \frac{1}{(r_i^n)^2 q_i^n} + \frac{1}{r_i^n q_i^n r_{i+1}^n}\right) \\ &\quad + \frac{3}{2}\frac{(\kappa_i^n)^2}{r_i^n} + \frac{\alpha_i^n}{2} \\ D_i^n &= -\left(\frac{1}{r_i^n q_i^n r_{i+1}^n} + \frac{1}{(r_{i+1}^n)^2 q_i^n} + \frac{1}{(r_{i+1}^n)^2 q_{i+1}^n} + \frac{1}{r_{i+1}^n q_{i+1}^n r_{i+2}^n}\right) \\ &\quad + \frac{3}{2}\frac{(\kappa_{i+1}^n)^2}{r_{i+1}^n} - \frac{\alpha_i^n}{2}. \end{aligned}$$

6.5. Numerical solution of eikonal equations

In this section we discuss possible numerical schemes to the eikonal equations (5.136) and (5.137). We will see that the main difficulties come from the necessity to get a scheme which will ensure convergence towards the viscosity solution of (5.136) resp. (5.137). We also require that in case of the level-set function redistancing , the zero level-set curve (hypersurface) Γ will be preserved.

We start with the time dependent equation (5.137). In the case of general Hamilton-Jacobi equation of the from
$$u_t + H\left(\mathbf{x}, \nabla u\left(\mathbf{x}\right)\right) = 0, \tag{6.279}$$
for H uniformly continuous, Ostrov [86], Bardi and Osher [4] show convergence of monotone numerical schemes to the viscosity solution of (6.279). For the definition of the monotone schemes see for example a book by Feistauer, Felcman and Straškraba [50].

Definition 6.5.1. *Assume numerical scheme for the solution of (6.279) (for the simplicity only in $\mathbb{R}^1$) which can be written in a form*
$$u_i^{n+1} = \Phi\left(u_{i-l}^n, \cdots, u_i^n, \cdots, u_{i+l}^n\right).$$
The scheme is called **monotone** *iff Φ is nondecreasing in all its arguments:*
$$a_j \le b_j, \text{ for } j = 1, \cdots, 2l+1 \Rightarrow \Phi\left(a_1, \cdots a_{2l+1}\right) \le \Phi\left(b_1, \cdots, b_{2l+1}\right).$$

In [80] we compared the following monotone iterative schemes for (5.137): a **regularised scheme** , an **upwind scheme** and **the Godunov scheme** .

6.5.1. Regularised scheme

The idea of the regularised scheme comes directly from the method of the vanishing viscosity. The scheme has a form

Scheme 6.5.2. The regularised finite difference numerical scheme for the equation (5.137) reads as:

$$\begin{aligned} \frac{u_{ij}^{n+1} - u_{ij}^{n}}{\tau} &= \operatorname{sign}\left(u_{ij}^{0}\right)\left(1 - \left|\nabla_c u_{ij}\right|\right) + \epsilon \Delta_h u_{ij}^{n} \text{ on } \omega_h, \\ u_{ij}^{h}\ |_{t=0} &= \mathcal{P}\left(u_{ini}\right)_{ij} \text{ on } \overline{\omega}_h, \\ \partial_{\mathbf{n}}^{h} u_{ij}^{h} &= 1 \text{ on } \partial\omega_h \text{ (the Neumann b.c.)}, \end{aligned}$$

for

$$\Delta_h u_{ij}^{h} = \frac{u_{i-1,j}^{h} - 2u_{ij} + u_{i+1,j}^{h}}{h_1^2} + \frac{u_{i,j-1}^{h} - 2u_{ij} + u_{i,j+1}^{h}}{h_2^2}.$$

6.5.2. Upwind scheme

The methods based on the upwind schemes are well known from the numerical methods for the equation containing advection. For the first order Hamilton-Jacobi equation of the form

$$u_t + F\left(\mathbf{x}, u\right)\left|\nabla u\right| = 0, \tag{6.280}$$

the upwind scheme reads as

$$\frac{u_{ij}^{n+1} - u_{ij}^{n}}{\tau} = \left[F_{ij}\right]_{+} \nabla_U^{+}\left(u_{ij}^{n}\right) + \left[F_{ij}\right]_{-} \nabla_U^{-}\left(u_{ij}^{n}\right) \tag{6.281}$$

where

$$\nabla_U^{+} u_{ij}^{h} = \left(\left[u_{b.,ij}\right]_{+}^{2} + \left[u_{f.,ij}\right]_{-}^{2} + \left[u_{.b,ij}\right]_{+}^{2} + \left[u_{.f,ij}\right]_{-}^{2}\right)^{\frac{1}{2}}, \tag{6.282}$$

$$\nabla_U^{-} u_{ij}^{h} = \left(\left[u_{f.,ij}\right]_{+}^{2} + \left[u_{b.,ij}\right]_{-}^{2} + \left[u_{.f,ij}\right]_{+}^{2} + \left[u_{.b,ij}\right]_{-}^{2}\right)^{\frac{1}{2}}. \tag{6.283}$$

and we use the notation $[a]_{+} = \max\{a, 0\}$ and $[a]_{-} = \min\{a, 0\}$. At the boundaries we replace:

$$u_{b.,ij} \text{ by } u_{f.,ij} \text{ for } i = 0 \quad \text{and} \quad u_{f.,ij} \text{ by } u_{b.,ij} \text{ for } i = N_1, \tag{6.284}$$

$$u_{.b,ij} \text{ by } u_{.f,ij} \text{ for } j = 0 \quad \text{and} \quad u_{.f,ij} \text{ by } u_{.b,ij} \text{ for } j = N_2. \tag{6.285}$$

For (5.137) we have:

Scheme 6.5.3. The upwind finite difference numerical scheme for the equation (5.137) reads as:

$$\begin{aligned} \frac{u_{ij}^{n+1} - n_{ij}^{k}}{\tau} &= \left[\operatorname{sign}\left(u_{ij}^{0}\right)\right]_{+} \nabla_U^{+}\left(u_{ij}^{n}\right) + \left[\operatorname{sign}\left(u_{ij}^{0}\right)\right]_{-} \nabla_U^{-}\left(u_{ij}^{n}\right) - \operatorname{sign}\left(u_{ij}^{0}\right) \text{ on } \omega_h, \\ u_{ij}^{h}\ |_{t=0} &= \mathcal{P}\left(u_{ini}\right)_{ij} \text{ on } \overline{\omega}_h, \end{aligned}$$

where ∇_U^{+} and ∇_U^{-} are given by (6.283) and (6.283).

6.5.3. Godunov scheme

The Godunov scheme – see Bardi and Osher [4] – is similar to the upwind scheme. For equation (6.280) it has a form

$$\frac{u_{ij}^{k+1}-u_{ij}^{k}}{\tau}=[F_{ij}]_{+}\nabla_{M}^{+}\left(u_{ij}^{k}\right)+[F_{ij}]_{-}\nabla_{M}^{-}\left(u_{ij}^{k}\right)$$

where

$$\nabla_{M}^{+} = \left(\max\left([u_{b.,ij}]_{+},-[u_{f.,ij}]_{-}\right)^{2}+\max\left([u_{.b,ij}]_{+},-[u_{.f,ij}]_{-}\right)^{2}\right)^{\frac{1}{2}}, \tag{6.286}$$

$$\nabla_{M}^{-} = \left(\max\left([u_{f.,ij}]_{+},-[u_{b.,ij}]_{-}\right)^{2}+\max\left([u_{.f,ij}]_{+},-[u_{.b,ij}]_{-}\right)^{2}\right)^{\frac{1}{2}}, \tag{6.287}$$

and the finite differences at the boundaries are handled in the same way as for the upwind scheme using (6.284) and (6.285). In $\mathbb{R}^2$ the scheme for the equation (5.137) has a form:

Scheme 6.5.4. The Godunov finite difference numerical scheme for the equation (5.137) reads as:

$$\begin{aligned}\frac{u_{ij}^{k+1}-u_{ij}^{k}}{\tau} &= \left[sign\ u_{ij}^{0}\right]_{+}\nabla_{M}^{+}\left(u_{ij}^{k}\right)+\left[sign\ u_{ij}^{0}\right]_{-}\nabla_{M}^{-}\left(u_{ij}^{k}\right)-sign\ u_{ij}^{0},\\ u_{ij}^{h}\,|_{t=0} &= \mathcal{P}\left(u_{ini}\right)_{ij}\ \text{ on } \overline{\omega}_{h},\end{aligned}$$

where ∇_M^+ and ∇_M^- are given by (6.286) and (6.287).

6.5.4. Interface preserving re-distancing

In [80], we show that the above mentioned schemes do not preserve the zero level-set sufficiently. Moreover, in some cases when the evolution of (5.137) is computed for a time long enough, the zero level-set may totally disappear. We have achieved these results independently on the works of Sussman and others [70, 69, 93, 94] where we can read: "The evolution equation for the interface (5.137) conserves the volume of the domain bounded by the curve defined implicitly by the equation $u_0(\mathbf{x})=0$. This is due to the fact that it does not change the position of the boundary (zero level-set). In numerical computation this is not true anymore."

The authors of [94] propose a method for better preserving of the zero level-set based on the conserving of the volume of IntΓ. If H is the Heaviside function defined as

$$H(u)=\begin{cases}1 & \text{if} \quad u>0\\ 0 & \text{if} \quad u\le 0\end{cases}, \tag{6.288}$$

then we want

$$\partial_t\int_\Omega H(u)\,\mathrm{dx}=0. \tag{6.289}$$

It is a condition for the preserving of the volume of IntΓ. Let us denote

$$L(u_0,u)=\mathrm{sign}(u_0)(1-|\nabla u|).$$

Instead of (5.137) we consider a modified evolution equation

$$\partial_t u = L(u_0, u) + \lambda f(u), \tag{6.290}$$

where λ is a function only of t determined by

$$\partial_t \int_\Omega H(u)\,\mathrm{dx} = \int_\Omega H'(u)\,\partial_t u = \int_\Omega H'(u)\left(L(u_0,u) + \lambda f(u)\right) = 0,$$

which gives

$$\lambda = \frac{-\int_\Omega H'(u)\, L(u_0,u)}{\int_\Omega H'(u)\, f(u)}.$$

To correct u only near the zero level-set we set

$$f(u) = H'(u)\,|\nabla u|.$$

For the numerical implementation, we consider the dual mesh (6.54), take a finite volume v_{ij} for $0 < i < N_1$, $0 < j < N_2$, i and j fixed, and denote Ω_{ij} its interior. We want to preserve the volume of Γ interior on each Ω_{ij}. It means that $\partial_t \int_{\Omega_{ij}} H(u)\,\mathrm{dx} = 0$ should hold. It gives us

$$\begin{aligned}
\frac{\mathrm{d}}{\mathrm{dt}} u^h_{ij} &= L\left(u^h_0, u^h\right) + \lambda_{ij} f\left(u^h\right), \\
\lambda_{ij} &= \frac{-\int_{\Omega_{ij}} H'\left(u^h\right) L\left(u^h_0, u^h\right)}{\int_{\Omega_{ij}} H'\left(u^h\right) f\left(u^h\right)}.
\end{aligned}$$

The Heaviside and the sign function are discretise as

$$\begin{aligned}
H_h\left(u^h\right) &= \begin{cases} 1 & \text{if} \quad u^h > h \\ 0 & \text{if} \quad u^h < -h \\ \frac{1}{2}\left(1 + \frac{u}{h} + \frac{1}{\pi}\sin\left(\pi\frac{u}{h}\right)\right) & \text{otherwise} \end{cases}, \\
\mathrm{sign}_h\left(u^h\right) &= 2\left(H_h\left(u^h\right) - \frac{1}{2}\right).
\end{aligned}$$

The partial derivatives of u are approximated as

$$\begin{aligned}
\partial^h_{x_1} u_{ij} &\approx \begin{cases} u_{f\cdot,ij} & \text{if } u_{f\cdot,ij} u^h \mathrm{sign}\left(u_{0,ij}\right) < 0 \text{ and } \left(u_{b\cdot,ij} + u_{f\cdot,ij}\right)\mathrm{sign}\left(u_{0,ij}\right) < 0 \\ u_{b\cdot,ij} & \text{if } u_{b\cdot,ij} u^h \mathrm{sign}\left(u_{0,ij}\right) > 0 \text{ and } \left(u_{b\cdot,ij} + u_{f\cdot,ij}\right)\mathrm{sign}\left(u_{0,ij}\right) > 0 \\ 0 & \text{if } u_{b\cdot,ij}\mathrm{sign}\left(u_{0,ij}\right) < 0 \text{and } u_{f\cdot,ij}\mathrm{sign}\left(u_{0,ij}\right) > 0 \end{cases} \\
\partial^h_{x_2} u_{ij} &\approx \begin{cases} u_{\cdot f,ij} & \text{if } u_{\cdot f,ij} u^h \mathrm{sign}\left(u_{0,ij}\right) < 0 \text{ and } \left(u_{\cdot b,ij} + u_{\cdot f,ij}\right)\mathrm{sign}\left(u_{0,ij}\right) < 0 \\ u_{\cdot b,ij} & \text{if } u_{\cdot b,ij} u^h \mathrm{sign}\left(u_{0,ij}\right) > 0 \text{ and } \left(u_{\cdot b,ij} + u_{\cdot f,ij}\right)\mathrm{sign}\left(u_{0,ij}\right) > 0 \\ 0 & \text{if } u_{\cdot b,ij}\mathrm{sign}\left(u_{0,ij}\right) < 0 \text{and } u_{\cdot f,ij}\mathrm{sign}\left(u_{0,ij}\right) > 0 \end{cases}
\end{aligned}$$

and the numerical scheme reads as:

Scheme 6.5.5. The zero level-set preserving explicit finite difference numerical scheme for the level-set function redistancing with the first order discretisation reads as

$$\begin{aligned}
\tilde{u}^{n+1}_{ij} &= u^n_{ij} + \tau L\left(u^h_0, u^n\right), \\
u^{n+1}_{ij} &= \tilde{u}^{n+1}_{ij} + \tau \lambda_{ij} H'_h\left(u^h_0\right)\left|\nabla u^h_{0,ij}\right|, \\
\lambda_{ij} &= \frac{-\int_{\Omega_{ij}} H'_h\left(u^h_0\right) \frac{\tilde{u}^{n+1}_{ij} - u^h_{0,ij}}{\tau}\,\mathrm{dx}}{\int_{\Omega_{ij}} \left[H'_h\left(u^h_{0,ij}\right)\right]^2 \left|\nabla u^h_{0,ij}\right|\mathrm{dx}},
\end{aligned} \tag{6.291}$$

where τ is fixed time step.

The integrals over the finite volume Ω_{ij} are approximated as

$$\int_{\Omega_{ij}} g\mathrm{dx} \approx \frac{h^2}{24}\left(16g_{ij} + \sum_{m,n=-1;(m,n)\neq(0,0)}^{1} g_{i+m,j+n}\right).$$

The discretisation of the constraint removes the leading order term of the error in

$$\int_{\Omega_{ij}} \left(H_h\left(u^{n+1}\right) - H_h\left(u_0\right)\right).$$

The Taylor expansion gives

$$\begin{aligned}&\int_{\Omega_{ij}} \left(H_h\left(u^{n+1}\right) - H_h\left(u_0\right)\right)\\ &= \int_{\Omega_{ij}} H_h'\left(u_0\right)\left(u^{n+1} - u_0\right) + \int_{\Omega_{ij}} H_h''\left(u_0\right)\frac{\left(u^{n+1} - u_0\right)^2}{2} + \cdots\end{aligned}$$

If we assume that λ_{ij} is constant on Ω_{ij} then we may write

$$\begin{aligned}&\int_{\Omega_{ij}} H_h'\left(u_0\right)\left(u^{n+1} - u_0\right)\\ &= \int_{\Omega_{ij}} H_h'\left(u_0\right)\left(\tilde{u}^{n+1} + \tau\lambda_{ij}H'\left(u_0\right)\left|\nabla u_0\right| - u_0\right)\\ &= \tau\left[\int_{\Omega_{ij}} H_h'\left(u_0\right)\frac{\tilde{u}^{n+1} - u_0}{\tau}\mathrm{dx} + \lambda_{ij}\int_{\Omega_{ij}}\left(H_h'\left(u_0\right)\right)^2\left|\nabla u_0\right|\mathrm{dx}\right] = 0,\end{aligned}$$

where the we substituted from (6.291).

6.5.5. Direct methods

At the end of this section we only refer to some direct methods which might be used for finding a viscosity solution of an equation

$$\left|\nabla u\left(\mathbf{x}\right)\right| = F\left(\mathbf{x}\right) \text{ on } \mathbb{R}^n \text{ and } u = g \text{ on } \Gamma \subset \mathbb{R}^n, \tag{6.292}$$

where the boundary conditions are given on some subset Γ where u is fixed. Γ might be for example some hypersurface to which we want to construct the (signed) distance function – in this case $g = 0$. We should also imposed some compatibility condition on g to ensure that (6.292) has a solution. Let us assume that such solution exists. Discretisation of the left hand side of (6.292) using some of the monotones scheme gives linear system which might by solved by some appropriate solver of linear systems. However, better understanding of this equation allows us to develop much more efficient methods. Very simply said, we should construct the solution first at the regions closer to Γ. It corresponds well with the fact that (6.292) simulates a monotonically advancing front, for example water front. Assume that $n = 2$, $g \equiv 0$ and Γ is a planar curve representing the front moving in $\mathbb{R}^2$ with speed $v\left(\mathbf{x}\right) = 1/F\left(\mathbf{x}\right)$ depending on the space variable $\mathbf{x}$ (v is only scalar now and it says, in what speed the particles of the front can move at given point $\mathbf{x}$). $\Gamma\left(t\right)$ given as $\Gamma\left(t\right) \equiv \left\{\mathbf{x} \in \mathbb{R}^2 \mid u\left(\mathbf{x}\right)\right\} = t$ is just the shape of the advancing front at time t. Realizing this fact, it is really natural that we construct the approximate solution first at the nodes of the numerical mesh which are closest to $\Gamma\mid_{t=0}$ and the we proceed to further regions following the front.

This idea led to the first method optimised just for (6.292). It was **the fast marching method** by Sethian [61]. This method splits all nodes of the numerical mesh to fixed points (those where we already know the approximate solution), tentative points (they are usually neighbours of the fixed points and therefore we can approximate the solution there using the values from the fixed points) and unknown points (they are too far from the regions where we know the approximate solution so that we do not even try to guess their values). At each iteration of the algorithm we seek for the tentative point with the smallest value. This point is the closest one to the region where we know the solution. We fix this point, update values of its neighbours and mark them as tentative. It is an efficient method which allows us to construct the solution only in some small neighbourhood of Γ. It is useful especially for **the narrow band methods** . The main disadvantage of this method is the necessity of searching the tentative point with the smallest value. This can significantly slowdown whole method. Heap sort is usually preferred for this task.

Tsai, Cheng and Zhao [102, 58] introduced **the fast sweeping method** . This method eliminates any seeking. It consists of the Gauss-Seidel type iterations called sweepings. At each sweeping we immediately use new values at nodes we went already through as it is usual for the Gauss-Seidel iterations. If the direction of the sweeping agree with the direction at which the front is propagating we construct the correct approximate solution very efficiently. To cover all the directions the front can propagate, we change the direction of the sweepings every time we finish one sweeping and start another. It is not difficult to prove that if $f \equiv 1$ we can get the approximate solution after 4 iterations – see Qian, Zhang and Zhao [88]. The fast sweeping method is simple to implement and at the same time it is very efficient.

In [80] we introduced so called **the front tracing method**. It combines advantages of both methods. It also avoids the necessity of seeking for the smallest tentative node and at the same time it allows to construct the approximate solution only in some small neighbourhood of Γ which is not possible with the fast sweeping method. In cases when f is not constant and generates more complex characteristics (lines along which the front is moving) the fast sweeping method may require more then 4 iterations. At this situation the front tracking method might perform even better then the fast sweeping method. The disadvantage of the front tracking method is in its higher complexity (it is also why we do not explain this method in this text) and the fact that it is not trivial to extend it to higher dimensions which is trivial for both fast marching and fast sweeping method.

For our numerical simulations we preferred mainly the fast sweeping method.

7. Computational studies

7.1. Experimental order of convergence

In this chapter, we describe methods which we use for the measuring of the experimental order of convergence and we also present many qualitative results obtained using the numerical schemes we described in this thesis.

7.1.1. Experimental order of convergence for the graph formulation

To our best knowledge, there is no analytical solution for the graph formulation of the mean-curvature flow or Willmore flow. To study the experimental convergence, we solve a modified problems of the form

$$\begin{aligned} \partial_t \varphi &= Q(\varphi) \nabla \cdot \left(\frac{\nabla \varphi}{Q(\varphi)} \right) + F_{MC}(\varphi) \quad \text{on } (0, \mathrm{T}\rangle \times \Omega, \qquad (7.1) \\ \varphi \mid_{t=0} &= \varphi_{ini} \quad \text{on } \Omega, \end{aligned}$$

with the Dirichlet boundary condition

$$\varphi = g \quad \text{on } \partial\Omega,$$

for the isotropic graph formulation of the mean-curvature flow and

$$\partial_t \varphi = -Q(\varphi) \nabla \cdot \left(\frac{1}{Q(\varphi)} \mathbb{P}(\varphi) \nabla w(\varphi) - \frac{1}{2} \frac{w^2(\varphi)}{Q^3(\varphi)} \nabla \varphi \right) + F_W(\varphi) \text{ on } \Omega \times (0, T], \qquad (7.2)$$

$$w = QH \text{ on } \Omega \times [0, T], \qquad (7.3)$$

$$\varphi \mid_{t=0} = \varphi_{ini} \text{ on } \Omega,$$

with the Dirichlet boundary conditions

$$\varphi = g, w = 0 \text{ on } \partial\Omega,$$

for the isotropic graph formulation of the Willmore flow. We choose F_{MC} and F_W such that (7.1) and (7.2)–(7.3) have analytical solution. Having a function $\zeta(\mathbf{x}, t)$ and setting

$$F_{MC}(\zeta) = -Q(\zeta) \nabla \cdot \left(\frac{\nabla \zeta}{Q(\zeta)} \right) + \partial_t \zeta, \qquad (7.4)$$

and

$$\boxed{\begin{aligned} F_W(\zeta) &= Q(\zeta)\nabla\cdot\left(\frac{1}{Q(\zeta)}\mathbb{P}(\zeta)\nabla w(\zeta)-\frac{1}{2}\frac{w^2(\zeta)}{Q^3(\zeta)}\nabla\zeta\right)+\partial_t\zeta, &(7.5)\\ w(\zeta) &= Q(\zeta)\nabla\cdot\left(\frac{\nabla\zeta}{Q(\zeta)}\right)\text{ on }\Omega\times[0,T]. &(7.6)\end{aligned}}$$

We express all necessary quantities in terms of the function ζ:

$$\begin{aligned}
Q &:= \sqrt{\epsilon^2+\zeta_x^2+\zeta_y^2},\\
Q_x &:= (\zeta_x\zeta_{xx}+\zeta_y\zeta_{xy})/Q,\\
Q_y &:= (\zeta_y\zeta_{yy}+\zeta_x\zeta_{xy})/Q,\\
Q_{xx} &:= \left(\zeta_{xx}^2+\zeta_x\zeta_{xxx}+\zeta_{xy}^2+\zeta_y\zeta_{xxy}-Q_x^2\right)/Q,\\
Q_{xy} &:= (\zeta_{xy}\zeta_{xx}+\zeta_x\zeta_{xxy}+\zeta_{yy}\zeta_{xy}+\zeta_y\zeta_{xyy}-Q_xQ_y)/Q,\\
Q_{yy} &:= \left(\zeta_{yy}^2+\zeta_y\zeta_{yyy}+\zeta_{xy}^2+\zeta_x\zeta_{xyy}-Q_y^2\right)/Q,\\
Q_{xxx} &:= (3\zeta_{xx}\zeta_{xxx}+\zeta_x\zeta_{xxxx}+2\zeta_{xy}\zeta_{xxy}+\zeta_{xy}\zeta_{xxy}+\zeta_y\zeta_{xxxy}-3Q_xQ_xx)/Q,\\
Q_{xxy} &:= (2\zeta_{xx}\zeta_{xxy}+\zeta_{xy}\zeta_{xxx}+\zeta_x\zeta_{xxxy}+2\zeta_{xy}\zeta_{xyy}+\zeta_{yy}\zeta_{xxy}+\zeta_y\zeta_{xxyy}\\
&\quad -2Q_xQ_{xy}-Q_{xx}Q_y)/Q,\\
Q_{xyy} &:= (2\zeta_{yy}\zeta_{xyy}+\zeta_{xy}\zeta_{yyy}+\zeta_y\zeta_{xyyy}+2\zeta_{xy}\zeta_{xxy}+\zeta_{xx}\zeta_{xyy}+\zeta_x\zeta_{xxyy}\\
&\quad -2Q_yQ_{xy}-Q_{yy}Q_x)/Q,\\
Q_{yyy} &:= (3\zeta_{yy}\zeta_{yyy}+\zeta_y\zeta_{yyyy}+2\zeta_{xy}\zeta_{xyy}+\zeta_{xy}\zeta_{xyy}+\zeta_x\zeta_{xyyy}-3Q_yQ_{yy})/Q,
\end{aligned}$$

$$\begin{aligned}
H &:= (\zeta_{xx}+\zeta_{yy})/Q-(\zeta_xQ_x+\zeta_yQ_y)/Q^2,\\
H_x &:= (\zeta_{xxx}+\zeta_{xyy})/Q+2Q_x(\zeta_xQ_x+\zeta_yQ_y)/Q^3-\\
&\quad (2\zeta_{xx}Q_x+\zeta_{yy}Q_x+\zeta_xQ_{xx}+\zeta_{xy}Q_y+\zeta_yQ_{xy})/Q^2,\\
H_y &:= (\zeta_{yyy}+\zeta_{xxy})/Q+2Q_y(\zeta_xQ_x+\zeta_yQ_y)/Q^3-\\
&\quad (2\zeta_{yy}Q_y+\zeta_{xx}Q_y+\zeta_yQ_{yy}+\zeta_{xy}Q_x+\zeta_xQ_{xy})/Q^2,\\
H_{xy} &:= (\zeta_{xxxy}+\zeta_{xyyy})/Q-[Q_x(\zeta_{xxy}+\zeta_{yyy})+Q_y(\zeta_{xxx}+\zeta_{xyy})+\\
&\quad Q_{xy}(\zeta_{xx}+\zeta_{yy})+\zeta_{xxy}Q_x+\zeta_{xy}Q_{xx}+\zeta_{xx}Q_{xy}+\zeta_xQ_{xxy}+\\
&\quad \zeta_{xyy}Q_y+\zeta_{yy}Q_{xy}+\zeta_{xy}Q_{yy}+\zeta_yQ_{xyy}]/Q^2+\\
&\quad 2(Q_xQ_y(\zeta_{xx}+\zeta_{yy})+Q_x(\zeta_{xy}Q_x+\zeta_xQ_{xy}+\zeta_{yy}Q_y+\zeta_yQ_{yy})+\\
&\quad Q_y(\zeta_{xx}Q_x+\zeta_xQ_{xx}+\zeta_{xy}Q_y+\zeta_yQ_{xy})+Q_{xy}(\zeta_xQ_x+\zeta_yQ_y)]/Q^3-\\
&\quad 6[Q_xQ_y(\zeta_xQ_x+\zeta_yQ_y)]/Q^4,\\
H_{xx} &:= (\zeta_{xxxx}+\zeta_{xxyy})/Q-(Q_x\zeta_{xyy}+3\zeta_{xxx}Q_x+3\zeta_{xx}Q_{xx}+\zeta_xQ_{xxx}+\\
&\quad \zeta_{xyy}Q_x+\zeta_{yy}Q_{xx}+\zeta_{xxy}Q_y+2\zeta_{xy}Q_{xy}+\zeta_yQ_{xxy})/Q^2+\\
&\quad 2[Q_{xx}(\zeta_xQ_x+\zeta_yQ_y)+Q_x(3\zeta_{xx}Q_x+2\zeta_xQ_{xx}+2\zeta_{xy}Q_y+\zeta_yQ_{xy}+\\
&\quad \zeta_{yy}Q_x+\zeta_yQ_{xy})]/Q^3-6\left[Q_x^2(\zeta_xQ_x+\zeta_yQ_y)\right]/Q^4,\\
H_{yy} &:= (\zeta_{yyyy}+\zeta_{xxyy})/Q-[Q_y\zeta_{xxy}+3\zeta_{yyy}Q_y+3\zeta_{yy}Q_{yy}+\zeta_yQ_{yyy}+\\
&\quad \zeta_{xxy}Q_y+\zeta_{xx}Q_{yy}+\zeta_{xyy}Q_x+2\zeta_{xy}Q_{xy}+\zeta_xQ_{xyy})/Q^2+\\
&\quad 2[Q_{yy}(\zeta_yQ_y+\zeta_xQ_x)+Q_y(3\zeta_{yy}Q_y+2\zeta_yQ_{yy}+2\zeta_{xy}Q_x+\zeta_xQ_{xy}+\\
&\quad \zeta_{xx}Q_y+\zeta_xQ_{xy})]/Q^3-6\left[Q_y^2(\zeta_yQ_y+\zeta_xQ_x)\right]/Q^4,
\end{aligned}$$

$$\begin{aligned}
w &:= QH, \\
w_x &:= Q_x H + Q H_x, \\
w_y &:= Q_y H + Q H_y, \\
w_{xy} &:= Q_{xy} H + Q_y H_x + Q_x H_y + Q H_{xy}, \\
w_{xx} &:= Q_{xx} H + 2 Q_x H_x + Q H_{xx}, \\
w_{yy} &:= Q_{yy} H + 2 Q_x H_x + Q H_{yy}.
\end{aligned}$$

$$\begin{aligned}
E_{11}^W &:= 1/Q - \zeta_x^2/Q^3, \\
E_{12}^W &:= -\zeta_x \zeta_y / Q^3, \\
E_{22}^W &:= 1/Q - \zeta_y^2/Q^3, \\
E_{11,x}^W &:= -Q_x/Q^2 - 2\zeta_x \zeta_x x/Q^3 + 3 Q_x \zeta_x^2 / Q^4, \\
E_{12,x}^W &:= -\left(\zeta_{xx}\zeta_y + \zeta_x \zeta_{xy}\right)/Q^3 + 3 Q_x \zeta_x \zeta_y / Q^4, \\
E_{12,y}^W &:= -\left(\zeta_{xy}\zeta_y + \zeta_x \zeta_{yy}\right)/Q^3 + 3 Q_y \zeta_x \zeta_y / Q^4, \\
E_{22,y}^W &:= -Q_y/Q^2 - 2\zeta_y \zeta_{yy}/Q^3 + 3 Q_y \zeta_y^2 / Q^4,
\end{aligned}$$

We get that (7.4) reads

$$\boxed{F_{MC} := -w + \partial_t \zeta} \tag{7.7}$$

and for (7.5) we get

$$\boxed{\begin{aligned}
F_W := & -Q\left[E_{11,x}^W w_x + E_{11}^W w_{xx} + E_{22,y}^W w_y + E_{22}^W w_{yy}\right. \\
& + \quad E_{12,x}^W w_y + E_{12}^W w_{xy} + E_{12,y}^W w_x + E_{12}^W w_{xy} \\
& -\frac{1}{2}\left(\left(2 w w_x \zeta_x + w^2 \zeta_{xx} + 2 w w_y \zeta_y + w^2 \zeta_{yy}\right)/Q^3\right. \\
& - \quad \left.\left. 3 w^2 \left(\zeta_x Q_x + \zeta_y Q_y\right)/Q^4\right)\right] + \partial_t \zeta.
\end{aligned}} \tag{7.8}$$

As an analytical solution $\zeta(\mathbf{x}, t)$ of (7.1) and (7.2)–(7.3) we chose the following function

$$\boxed{\zeta(x,y) := \cos(\pi t) \frac{1}{r^{2n}} \left(x^n - r^n\right)\left(y^n - r^n\right) \exp\left(-\sigma\left(x^2 + y^2\right)\right) \text{ on } \Omega \times [0,T],} \tag{7.9}$$

for $\Omega \equiv [-r, r]^2$. Then we get

$$\begin{aligned}
\zeta_x &:= \cos(\pi t)/r^{2n}\left(y^n - r^n\right) n x^{n-1} \exp\left(-\sigma\left(x^2+y^2\right)\right) - 2\sigma x \zeta, \\
\zeta_y &:= \cos(\pi t)/r^{2n}\left(x^n - r^n\right) n y^{n-1} \exp\left(-\sigma\left(x^2+y^2\right)\right) - 2\sigma x \zeta, \\
\zeta_{xx} &:= \cos(\pi t)/r^{2n}\left(y^n - r^n\right)\left(n(n-1)x^{n-2} - 2\sigma n x^n\right) \exp\left(-\sigma\left(x^2+y^2\right)\right) - 2\sigma\left(\zeta + x\zeta_x\right), \\
\zeta_{xy} &:= \cos(\pi t)/r^{2n}\left(n^2 y^{n-1} x^{n-1} \exp\left(-\sigma\left(x^2+y^2\right)\right)\right) - 2\sigma\left(y\zeta_x - x\zeta_y\right) - 4\sigma^2 x y \zeta, \\
\zeta_{yy} &:= \cos(\pi t)/r^{2n}\left(x^n - r^n\right)\left(n(n-1)y^{n-2} - 2\sigma n y^n\right) \exp\left(-\sigma\left(x^2+y^2\right)\right) - 2\sigma\left(\zeta + y\zeta_y\right),
\end{aligned}$$

$$
\begin{aligned}
\zeta_{xxx} &:= \cos(\pi t)/r^{2n}(y^n - r^n)\left(n(n-1)(n-2)x^{n-3} - 2\sigma n(2n-1)x^{n-1} + 4\sigma^2 n x^{n+1}\right) \\
&\quad \exp\left(-\sigma\left(x^2+y^2\right)\right) - 2\sigma\left(2\zeta_x + x\zeta_{xx}\right), \\
\zeta_{xxy} &:= \cos(\pi t)/r^{2n}\left(n^2(n-1)x^{n-2}y^{n-1} - 2\sigma n^2 x^n y^{n-1}\right)\exp\left(-\sigma\left(x^2+y^2\right)\right) \\
&\quad -2\sigma y\zeta_{xx} - 4\sigma^2 y\left(\zeta + x\zeta_x\right) - 2\sigma\zeta_y - 2\sigma x\zeta_{xy}, \\
\zeta_{xyy} &:= \cos(\pi t)/r^{2n}\left(n^2(n-1)x^{n-1}y^{n-2} - 2\sigma n^2 x^{n-1}y^n\right)\exp\left(-\sigma\left(x^2+y^2\right)\right) \\
&\quad -2\sigma x\zeta_{yy} - 4\sigma^2 x\left(\zeta + y\zeta_y\right) - 2\sigma\zeta_x - 2\sigma y\zeta_{xy}, \\
\zeta_{yyy} &:= \cos(\pi t)/r^{2n}(x^n - r^n)\left(n(n-1)(n-2)y^{n-3} - 2\sigma n(2n-1)y^{n-1} + 4\sigma^2 n y^{n+1}\right) \\
&\quad \exp\left(-\sigma\left(x^2+y^2\right)\right) - 2\sigma\left(2\zeta_y + y\zeta_{yy}\right),
\end{aligned}
$$

$$
\begin{aligned}
\zeta_{xxxx} &:= \cos(\pi t)/r^{2n}(y^n - r^n)\exp\left(-\sigma\left(x^2+y^2\right)\right) \\
&\quad \left(n(n-1)(n-2)(n-3)x^{n-4} - 6\sigma n(n-1)(n-1)x^{n-2} + 12\sigma^2 n^2 x^n - 8\sigma^3 n x^{n+2}\right) \\
&\quad -2\sigma\left(3\zeta_{xx} + x\zeta_{xxx}\right), \\
\zeta_{xxxy} &:= \cos(\pi t)/r^{2n}\left(n(n-1)(n-2)x^{n-3} - 2\sigma n(2n-1)x^{n-1} + 4c^2 n x^{n+1}\right) \\
&\quad \left(ny^{n-1} - 2\sigma y(y^n - 1)\right)\exp\left(-\sigma\left(x^2+y^2\right)\right) - 2\sigma\left(2\zeta_{xy} + x\zeta_{xxy}\right), \\
\zeta_{xxyy} &:= \cos(\pi t)/r^{2n}\exp\left(-\sigma\left(x^2+y^2\right)\right) \\
&\quad \left(n^2(n-1)^2 x^{n-2}y^{n-2} - 2\sigma n^2(n-1)x^n y^{n-2} - 2\sigma n^2(n-1)x^{n-2}y^n + 4\sigma^2 n^2 x^n y^n\right) \\
&\quad -2\sigma\left(\zeta_{xx} + \zeta_{yy} + y\zeta_{xxy} + x\zeta_{xyy}\right) - 4\sigma^2\left(\zeta + x\zeta_x + y\zeta_y + xy\zeta_{xy}\right), \\
\zeta_{xyyy} &:= \cos(\pi t)/r^{2n}\left(n(n-1)(n-2)y^{n-3} - 2\sigma n(2n-1)y^{n-1} + 4\sigma^2 n y^{n+1}\right) \\
&\quad \left(nx^{n-1} - 2\sigma x(x^n - 1)\right)\exp\left(-\sigma\left(x^2+y^2\right)\right) - 2\sigma\left(2\zeta_{xy} + y\zeta_{xyy}\right), \\
\zeta_{yyyy} &:= \cos(\pi t)/r^{2n}(x^n - r^n)\exp\left(-\sigma\left(x^2+y^2\right)\right) \\
&\quad \left(n(n-1)(n-2)(n-3)y^{n-4} - 6\sigma n(n-1)(n-1)y^{n-2} + 12\sigma^2 n^2 y^n - 8\sigma^3 n y^{n+2}\right) \\
&\quad -2\sigma\left(3\zeta_{yy} + y\zeta_{yyy}\right).
\end{aligned}
$$

For given T, we evaluate the errors in the norms of the spaces $L_1(\Omega;[0,T])$, $L_2(\Omega;[0,T])$ and $L_\infty(\Omega;[0,T])$ resp. their approximations

$$\left\|\varphi^h - \mathcal{P}_h(\zeta)\right\|_{L_1(\omega_h;[0,T])}^{h,\tau} := \sum_{k=0}^{M}\tau\sum_{i=0,j=0}^{N_1,N_2}\left|\varphi_{ij}^h(k\tau) - \zeta(-r+ih,-r+jh,k\tau)\right|h^2, \tag{7.10}$$

$$\left\|\varphi^h - \mathcal{P}_h(\zeta)\right\|_{L_2(\omega_h;[0,T])}^{h,\tau} := \left(\sum_{k=0}^{M}\tau\sum_{i=0,j=0}^{N_1,N_2}\left(\varphi_{ij}^h(k\tau) - \zeta(-r+ih,-r+jh,k\tau)\right)^2 h^2\right)^{\frac{1}{2}}, \tag{7.11}$$

$$\left\|\varphi^h - \mathcal{P}_h(\zeta)\right\|_{L_\infty(\omega_h;[0,T])}^{h,\tau} := \max_{k=0,\cdots,M}\max_{\substack{i=0,\cdots,N_1\\ j=0,\cdots,N_2}}\left|\varphi_{ij}^h(k\tau) - \zeta(-r+ih,-r+jh,k\tau)\right|, \tag{7.12}$$

for $\tau = T/M$. We would like to emphasise that τ does not correspond with the time step of a solver. In case of the explicit schemes, the time step is adaptively set by the solver. For the semi-implicit scheme the time step is proportional to h^2.

The experimental order of convergence is evaluated as follows - for two approximations φ^{h_1} and φ^{h_2} obtained by the discretisation with the space steps h_1 and h_2 we compute the approximation errors Err_{h_1} and Err_{h_2} in one norm of (7.10)–(7.12) as

$$\boxed{EOC\left(Err_{h_1}, Err_{h_2}\right) := \frac{\log\left(Err_{h_1}/Err_{h_2}\right)}{\log\left(h_1/h_2\right)}.} \tag{7.13}$$

The results for the numerical schemes for the mean-curvature flow of graphs (6.3.2), (6.3.4), (6.3.6), (6.3.8) and the Willmore flow of graphs (6.3.3), (6.3.5), (6.3.7), (6.3.9) are presented in the Numerical experiments (7.1.1)-(7.1.8) resp. Figures (7.1)-(7.16). One can see that the one-sided schemes approximate both φ and w with the EOC equal to 1 - see Tables (7.1), (7.2), (7.7) and (7.8). For this class of schemes we tested only the explicit versions. On the other hand, the central schemes approximate the quantities φ and H resp. w with the second order of accuracy except of the approximation of w in the case of the Willmore flow. Here, only the error in L_∞ norm decreases with the second order. It follows from Tables (7.3), (7.4), (7.9) and (7.10). Note also, that the central schemes require significantly less CPU time in comparison with the one-sided schemes, the only exception here is the finest mesh for the Willmore flow. Even for this class of schemes we tested only the ones with the explicit discretisation in time. Finally the complementary finite volume schemes with the explicit time discretisation also give EOC equal to 2 - see Tables (7.5), (7.6), (7.11) and (7.12). Concerning the CPU time requirement, it is comparable with the one-sided schemes. For this class of scheme we also implemented the semi-implicit counterparts. The results can be found in Tables (7.13), (7.14), (7.15) and (7.16). We achieved again the approximation of the second order and we see that, except of the mean-curvature flow, the semi-implicit schemes are computationally much more efficient.

h	$\|\cdot\|^{h,\tau}_{L_1(\omega_h;[0,T])}$		$\|\cdot\|^{h,\tau}_{L_2(\omega_h;[0,T])}$		$\|\cdot\|^{h,\tau}_{L_\infty(\omega_h;[0,T])}$		CPU/sec.
	Error	**EOC**	Error	**EOC**	Error.	**EOC**	
1/2	0.003227		0.00394		0.02163		1
1/4	0.001216	**1.408**	0.001544	**1.351**	0.01125	**0.9428**	1
1/8	0.000541	**1.168**	0.0007301	**1.081**	0.00477	**1.238**	3
1/16	0.0002576	**1.07**	0.0003602	**1.02**	0.002178	**1.131**	8
1/32	0.0001262	**1.03**	0.0001795	**1.005**	0.001046	**1.058**	31
1/64	6.26e-05	**1.011**	8.967e-05	**1.001**	0.0005103	**1.036**	292

Figure 7.1.: EOC of the approximation of φ for the **explicit one-sided** numerical scheme for the **mean-curvature flow of graphs** (6.3.2). See the Numerical experiment 7.1.1.

h	$\|\cdot\|^{h,\tau}_{L_1(\omega_h;[0,T])}$		$\|\cdot\|^{h,\tau}_{L_2(\omega_h;[0,T])}$		$\|\cdot\|^{h,\tau}_{L_\infty(\omega_h;[0,T])}$	
	Error	**EOC**	Error	**EOC**	Error.	**EOC**
1/2	0.02809		0.04154		0.292	
1/4	0.01383	**1.023**	0.02267	**0.8739**	0.2004	**0.543**
1/8	0.006039	**1.195**	0.01211	**0.9041**	0.105	**0.9328**
1/16	0.002888	**1.064**	0.006139	**0.9804**	0.05569	**0.9148**
1/32	0.00142	**1.024**	0.00308	**0.9952**	0.02727	**1.03**
1/64	0.000706	**1.009**	0.001541	**0.9988**	0.01346	**1.019**

Figure 7.2.: EOC of the approximation of w for the **explicit one-sided** numerical scheme for the **mean-curvature flow of graphs** (6.3.2). See the Numerical experiment 7.1.1.

Numerical experiment 7.1.1. EOC for the explicit one-sided finite difference numerical scheme for the mean-curvature flow of graphs. **Computational domain:** $\Omega \equiv [-4, 4]^2$. **Initial condition:**

$$\varphi_{ini}(x, y) := \frac{1}{r^{2n}} (x^n - r^n)(y^n - r^n) \exp\left(-\sigma \left(x^2 + y^2\right)\right)$$

for $r = 4, n = 4, \sigma = 1$. **Final time:** $T = 0.1$. **Space steps:** 0.5×0.5, 0.25×0.25, 0.125×0.125, 0.0625×0.0625, 0.03125×0.03125 and 0.015625×0.015625. **Time step:** Adaptive. **Numerical scheme:** 6.3.2. **Figure:** 7.1 and 7.2. **Remark:** The approximation of φ and w is of the first order.

h	$\|\cdot\|^{h,\tau}_{L_1(\omega_h;[0,T])}$		$\|\cdot\|^{h,\tau}_{L_2(\omega_h;[0,T])}$		$\|\cdot\|^{h,\tau}_{L_\infty(\omega_h;[0,T])}$		CPU/sec.
	Error	**EOC**	Error	**EOC**	Error.	**EOC**	
1/2	0.01267		0.01914		0.167		1
1/4	0.003319	**1.932**	0.00459	**2.06**	0.04993	**1.742**	1
1/8	0.0008469	**1.971**	0.001111	**2.047**	0.00921	**2.439**	3
1/16	0.0002127	**1.993**	0.0002771	**2.003**	0.002137	**2.107**	6
1/32	5.324e-05	**1.998**	6.925e-05	**2**	0.000528	**2.017**	14
1/64	1.331e-05	**2**	1.731e-05	**2**	0.0001316	**2.004**	98

Figure 7.3.: EOC of the approximation of φ for the **explicit central** numerical scheme for the **mean-curvature flow of graphs** (6.3.4). See the Numerical experiment 7.1.2.

h	$\|\cdot\|^{h,\tau}_{L_1(\omega_h;[0,T])}$		$\|\cdot\|^{h,\tau}_{L_2(\omega_h;[0,T])}$		$\|\cdot\|^{h,\tau}_{L_\infty(\omega_h;[0,T])}$	
	Error	**EOC**	Error	**EOC**	Error.	**EOC**
1/2	0.05449		0.06402		0.3501	
1/4	0.02439	**1.16**	0.03808	**0.7494**	0.4347	**-0.312**
1/8	0.007615	**1.679**	0.01356	**1.489**	0.1864	**1.221**
1/16	0.002055	**1.89**	0.003667	**1.887**	0.05047	**1.885**
1/32	0.000523	**1.974**	0.0009342	**1.973**	0.01286	**1.972**
1/64	0.0001313	**1.994**	0.0002347	**1.993**	0.003231	**1.993**

Figure 7.4.: EOC of the approximation of w for the **explicit central** numerical scheme for the **mean-curvature flow of graphs** (6.3.4). See the Numerical experiment 7.1.2.

Numerical experiment 7.1.2. EOC for the explicit central finite difference numerical scheme for the mean-curvature flow of graphs. **Computational domain:** $\Omega \equiv [-4, 4]^2$. **Initial condition:**

$$\varphi_{ini}(x, y) := \frac{1}{r^{2n}} (x^n - r^n)(y^n - r^n) \exp\left(-\sigma \left(x^2 + y^2\right)\right)$$

for $r = 4, n = 4, \sigma = 1$. **Final time:** $T = 0.1$. **Time step:** Adaptive. **Numerical scheme:** 6.3.4. **Figure:** 7.3 and 7.4. **Remark:** The approximation of φ and w is of the second order.

h	$\|\cdot\|^{h,\tau}_{L_1(\omega_h;[0,T])}$		$\|\cdot\|^{h,\tau}_{L_2(\omega_h;[0,T])}$		$\|\cdot\|^{h,\tau}_{L_\infty(\omega_h;[0,T])}$		CPU/sec.
	Error	**EOC**	Error	**EOC**	Error.	**EOC**	
1/2	0.003339		0.004452		0.02897		1
1/4	0.0008226	**2.021**	0.0009809	**2.182**	0.005666	**2.354**	1
1/8	0.0002085	**1.98**	0.0002458	**1.997**	0.001335	**2.086**	3
1/16	5.226e-05	**1.996**	6.152e-05	**1.998**	0.0003299	**2.016**	6
1/32	1.307e-05	**2**	1.539e-05	**1.999**	8.226e-05	**2.004**	29
1/64	3.268e-06	**2**	3.847e-06	**2**	2.055e-05	**2.001**	368

Figure 7.5.: EOC of the approximation of φ for the **explicit complementary finite volume** numerical scheme for the **mean-curvature flow of graphs** (6.3.6). See the Numerical experiment 7.1.3.

h	$\|\cdot\|^{h,\tau}_{L_1(\omega_h;[0,T])}$		$\|\cdot\|^{h,\tau}_{L_2(\omega_h;[0,T])}$		$\|\cdot\|^{h,\tau}_{L_\infty(\omega_h;[0,T])}$	
	Error	**EOC**	Error	**EOC**	Error.	**EOC**
1/2	0.02175		0.03425		0.2702	
1/4	0.006553	**1.731**	0.008048	**2.09**	0.08475	**1.673**
1/8	0.001721	**1.929**	0.001988	**2.017**	0.02168	**1.967**
1/16	0.000438	**1.974**	0.0005028	**1.983**	0.005449	**1.993**
1/32	0.0001099	**1.995**	0.0001261	**1.996**	0.001364	**1.998**
1/64	2.762e-05	**1.993**	3.155e-05	**1.998**	0.0003411	**2**

Figure 7.6.: EOC of the approximation of w for the **explicit finite difference** numerical scheme for the **mean-curvature flow of graphs** (6.3.6). See the Numerical experiment 7.1.3.

Numerical experiment 7.1.3. EOC for the explicit finite difference numerical scheme for the mean-curvature flow of graphs. **Computational domain:** $\Omega \equiv [-4,4]^2$. **Initial condition:**

$$\varphi_{ini}(x,y) := \frac{1}{r^{2n}}(x^n - r^n)(y^n - r^n)\exp\left(-\sigma\left(x^2+y^2\right)\right)$$

for $r=4, n=4, \sigma=1$. **Final time:** $T=0.1$. **Time step:** Adaptive. **Numerical scheme:** 6.3.6. **Figure:** 7.5 and 7.6. **Remark:** The approximation of φ and w is of the second order.

h	$\|\cdot\|^{h,\tau}_{L_1(\omega_h;[0,T])}$		$\|\cdot\|^{h,\tau}_{L_2(\omega_h;[0,T])}$		$\|\cdot\|^{h,\tau}_{L_\infty(\omega_h;[0,T])}$		CPU/sec.
	Error	**EOC**	Error	**EOC**	Error.	**EOC**	
1/2	0.05847		0.1215		0.6986		3
1/4	0.004741	**3.624**	0.00441	**4.785**	0.01577	**5.47**	5
1/8	0.001783	**1.411**	0.002152	**1.035**	0.009123	**0.7894**	65
1/16	0.000602	**1.566**	0.00073	**1.56**	0.003162	**1.529**	3672
1/32	0.0002489	**1.274**	0.0003037	**1.265**	0.001246	**1.344**	273181

Figure 7.7.: EOC of the approximation of φ for the **explicit one-sided** numerical scheme for the **Willmore flow of graphs** (6.3.3). See the Numerical experiment 7.1.4.

h	$\|\cdot\|^{h,\tau}_{L_1(\omega_h;[0,T])}$		$\|\cdot\|^{h,\tau}_{L_2(\omega_h;[0,T])}$		$\|\cdot\|^{h,\tau}_{L_\infty(\omega_h;[0,T])}$	
	Error	**EOC**	Error	**EOC**	Error.	**EOC**
1/2	0.3495		0.8077		4.281	
1/4	0.04469	**2.968**	0.06361	**3.667**	0.5434	**2.978**
1/8	0.01728	**1.37**	0.02333	**1.447**	0.1226	**2.148**
1/16	0.007537	**1.197**	0.01089	**1.099**	0.05642	**1.119**
1/32	0.003566	**1.08**	0.005345	**1.027**	0.02793	**1.014**

Figure 7.8.: EOC of the approximation of w for the **explicit one-sided** numerical scheme for the **Willmore flow of graphs** (6.3.3). See the Numerical experiment 7.1.4.

Numerical experiment 7.1.4. EOC for the explicit one-sided finite difference numerical scheme for the Willmore flow of graphs. **Computational domain:** $\Omega \equiv [-4,4]^2$. **Initial condition:**

$$\varphi_{ini}(x,y) := \frac{1}{r^{2n}}\left(x^n - r^n\right)\left(y^n - r^n\right)\exp\left(-\sigma\left(x^2+y^2\right)\right)$$

for $r=4, n=4, \sigma=1$. **Final time:** $T=0.1$. **Space steps:** 0.5×0.5, 0.25×0.25, 0.125×0.125, 0.0625×0.0625 and 0.03125×0.03125. **Time step:** Adaptive. **Numerical scheme:** 6.3.3. **Figure:** 7.7 and 7.8. **Remark:** The approximation of φ and w is of the first order.

h	$\|\cdot\|^{h,\tau}_{L_1(\omega_h;[0,T])}$		$\|\cdot\|^{h,\tau}_{L_2(\omega_h;[0,T])}$		$\|\cdot\|^{h,\tau}_{L_\infty(\omega_h;[0,T])}$		CPU/sec.
	Error	**EOC**	Error	**EOC**	Error.	**EOC**	
1/2	0.2631		0.8637		9.058		4
1/4	0.04963	**2.406**	0.07862	**3.458**	0.3746	**4.596**	6
1/8	0.005386	**3.204**	0.004646	**4.081**	0.02642	**3.826**	14
1/16	0.001284	**2.068**	0.001061	**2.13**	0.004619	**2.516**	291
1/32	0.0002489	**2.367**	0.0003037	**1.805**	0.001246	**1.89**	268116

Figure 7.9.: EOC of the approximation of φ for the **explicit central** numerical scheme for the **Willmore flow of graphs** (6.3.5). See the Numerical experiment 7.1.5.

h	$\|\cdot\|^{h,\tau}_{L_1(\omega_h;[0,T])}$		$\|\cdot\|^{h,\tau}_{L_2(\omega_h;[0,T])}$		$\|\cdot\|^{h,\tau}_{L_\infty(\omega_h;[0,T])}$	
	Error	**EOC**	Error	**EOC**	Error.	**EOC**
1/2	0.5269		0.5517		1.838	
1/4	0.2113	**1.318**	0.2962	**0.8974**	2.192	**-0.2537**
1/8	0.03547	**2.575**	0.04777	**2.632**	0.5783	**1.922**
1/16	0.009032	**1.974**	0.01212	**1.979**	0.1307	**2.145**
1/32	0.003566	**1.341**	0.005345	**1.181**	0.02793	**2.227**

Figure 7.10.: EOC of the approximation of w for the **explicit central** numerical scheme for the **Willmore flow of graphs** (6.3.5). See the Numerical experiment 7.1.5.

Numerical experiment 7.1.5. EOC for the explicit central finite difference numerical scheme for the Willmore flow of graphs. **Computational domain:** $\Omega \equiv [-4,4]^2$. **Initial condition:**

$$\varphi_{ini}(x,y) := \frac{1}{r^{2n}}\left(x^n - r^n\right)\left(y^n - r^n\right)\exp\left(-\sigma\left(x^2+y^2\right)\right)$$

for $r=4, n=4, \sigma=1$. **Final time:** $T=0.1$. **Space steps:** 0.5×0.5, 0.25×0.25, 0.125×0.125, 0.0625×0.0625 and 0.03125×0.03125. **Time step:** Adaptive. **Numerical scheme:** 6.3.5. **Figure:** 7.9 and 7.10. **Remark:** The approximation of u is of the first order and the approximation of w is of the first order except of the error in the norm $\|\cdot\|^{h,\tau}_{L_\infty(\omega_h;[0,T])}$ where the approximation is of the second order.

h	$\|\cdot\|^{h,\tau}_{L_1(\omega_h;[0,T])}$		$\|\cdot\|^{h,\tau}_{L_2(\omega_h;[0,T])}$		$\|\cdot\|^{h,\tau}_{L_\infty(\omega_h;[0,T])}$		CPU/sec.
	Error	**EOC**	Error	**EOC**	Error.	**EOC**	
1/2	0.0992		0.202		1.049		3
1/4	0.00437	**4.505**	0.004395	**5.523**	0.02826	**5.214**	5
1/8	0.0009964	**2.133**	0.000755	**2.541**	0.001687	**4.066**	77
1/16	0.0002499	**1.995**	0.0001894	**1.995**	0.0004223	**1.999**	4494
1/32	6.256e-05	**1.998**	4.74e-05	**1.999**	0.0001057	**1.998**	328300

Figure 7.11.: EOC of the approximation of φ for the **explicit finite difference** numerical scheme for the **Willmore flow of graphs** (6.3.7). See the Numerical experiment 7.1.6.

h	$\|\cdot\|^{h,\tau}_{L_1(\omega_h;[0,T])}$		$\|\cdot\|^{h,\tau}_{L_2(\omega_h;[0,T])}$		$\|\cdot\|^{h,\tau}_{L_\infty(\omega_h;[0,T])}$	
	Error	**EOC**	Error	**EOC**	Error.	**EOC**
1/2	0.4846		0.8378		3.652	
1/4	0.03197	**3.922**	0.04893	**4.098**	0.5334	**2.776**
1/8	0.007023	**2.187**	0.00779	**2.651**	0.08812	**2.598**
1/16	0.001763	**1.994**	0.001911	**2.028**	0.02102	**2.068**
1/32	0.0004408	**2**	0.0004755	**2.007**	0.0052	**2.015**

Figure 7.12.: EOC of the approximation of w for the **explicit finite difference** numerical scheme for the **Willmore flow of graphs** (6.3.7). See the Numerical experiment 7.1.6.

Numerical experiment 7.1.6. EOC for the explicit finite difference numerical scheme for the Willmore flow of graphs. **Computational domain:** $\Omega \equiv [-4,4]^2$. **Initial condition:**

$$\varphi_{ini}(x,y) := \frac{1}{r^{2n}}\left(x^n - r^n\right)\left(y^n - r^n\right)\exp\left(-\sigma\left(x^2+y^2\right)\right)$$

for $r=4, n=4, \sigma=1$. **Final time:** $T=0.1$. **Space steps:** 0.5×0.5, 0.25×0.25, 0.125×0.125, 0.0625×0.0625 and 0.03125×0.03125. **Time step:** Adaptive. **Numerical scheme:** 6.3.7. **Figure:** 7.11 and 7.12. **Remark:** The approximation of φ and w is of the second order.

h	$\lVert\cdot\rVert^{h,\tau}_{L_1(\omega_h;[0,T])}$		$\lVert\cdot\rVert^{h,\tau}_{L_2(\omega_h;[0,T])}$		$\lVert\cdot\rVert^{h,\tau}_{L_\infty(\omega_h;[0,T])}$		CPU/sec.
	Error	**EOC**	Error	**EOC**	Error.	**EOC**	
1/2	0.0033		0.004406		0.02867		0
		2.014		**2.176**		**2.345**	
1/4	0.0008171		0.0009751		0.005642		0
		1.976		**1.993**		**2.083**	
1/8	0.0002078		0.000245		0.001332		2
		1.994		**1.996**		**2.015**	
1/16	5.216e-05		6.143e-05		0.0003296		15
		1.998		**1.998**		**2.003**	
1/32	1.306e-05		1.537e-05		8.221e-05		101
		1.999		**1.999**		**2.001**	
1/64	3.266e-06		3.845e-06		2.054e-05		823

Figure 7.13.: EOC of the approximation of φ for the **semi-implicit finite difference** numerical scheme for the **mean-curvature flow of graphs** (6.3.8). See the Numerical experiment 7.1.7.

h	$\lVert\cdot\rVert^{h,\tau}_{L_1(\omega_h;[0,T])}$		$\lVert\cdot\rVert^{h,\tau}_{L_2(\omega_h;[0,T])}$		$\lVert\cdot\rVert^{h,\tau}_{L_\infty(\omega_h;[0,T])}$	
	Error	**EOC**	Error	**EOC**	Error.	**EOC**
1/2	0.01955		0.03179		0.2601	
		1.643		**2.026**		**1.628**
1/4	0.006261		0.007808		0.08415	
		1.899		**1.998**		**1.96**
1/8	0.001679		0.001955		0.02162	
		1.957		**1.972**		**1.99**
1/16	0.0004324		0.0004985		0.005442	
		1.984		**1.988**		**1.996**
1/32	0.0001093		0.0001257		0.001364	
		1.994		**1.996**		**1.999**
1/64	2.745e-05		3.15e-05		0.0003411	

Figure 7.14.: EOC of the approximation of w for the **semi-implicit finite difference** numerical scheme for the **mean-curvature flow of graphs** (6.3.8). See the Numerical experiment 7.1.7.

Numerical experiment 7.1.7. EOC for the semi-implicit finite difference numerical scheme for the mean-curvature flow of graphs. **Computational domain:** $\Omega \equiv [-4,4]^2$. **Initial condition:**

$$\varphi_{ini}(x,y) := \frac{1}{r^{2n}}\left(x^n - r^n\right)\left(y^n - r^n\right)\exp\left(-\sigma\left(x^2+y^2\right)\right)$$

for $r=4, n=4, \sigma=1$. **Final time:** $T=0.1$. **Space steps:** 0.5×0.5, 0.25×0.25, 0.125×0.125, 0.0625×0.0625, 0.03125×0.03125 and 0.015625×0.015625. **Time step:** Depends on the space steps - $5\cdot10^{-3}$, $2.5\cdot10^{-3}$, $1.25\cdot10^{-3}$, $6.25\cdot10^{-4}$, $3.125\cdot10^{-4}$ and $1.5625\cdot10^{-4}$. **Numerical scheme:** 6.3.8. **Figure:** 7.13 and 7.14. **Remark:** The approximation of φ and w is of the second order.

h	$\|\cdot\|^{h,\tau}_{L_1(\omega_h;[0,T])}$		$\|\cdot\|^{h,\tau}_{L_2(\omega_h;[0,T])}$		$\|\cdot\|^{h,\tau}_{L_\infty(\omega_h;[0,T])}$		CPU/sec.
	Error	**EOC**	Error	**EOC**	Error.	**EOC**	
1/2	0.0925		0.1856		0.9748		0
1/4	0.0043	**4.427**	0.004341	**5.418**	0.02809	**5.117**	5
1/8	0.0009945	**2.112**	0.0007539	**2.526**	0.001685	**4.06**	34
1/16	0.0002498	**1.993**	0.0001893	**1.994**	0.0004221	**1.997**	1106
1/32	6.247e-05	**2**	4.736e-05	**1.999**	0.0001057	**1.997**	29804

Figure 7.15.: EOC of the approximation of φ for the **semi-implicit finite difference** numerical scheme for the **Willmore flow of graphs** (6.3.9). See the Numerical experiment 7.1.8.

h	$\|\cdot\|^{h,\tau}_{L_1(\omega_h;[0,T])}$		$\|\cdot\|^{h,\tau}_{L_2(\omega_h;[0,T])}$		$\|\cdot\|^{h,\tau}_{L_\infty(\omega_h;[0,T])}$	
	Error	**EOC**	Error	**EOC**	Error.	**EOC**
1/2	0.3897		0.7456		3.812	
1/4	0.03144	**3.632**	0.0486	**3.94**	0.5327	**2.839**
1/8	0.007006	**2.166**	0.007785	**2.642**	0.08811	**2.596**
1/16	0.001762	**1.991**	0.00191	**2.027**	0.02102	**2.068**
1/32	0.0004407	**2**	0.0004755	**2.006**	0.0052	**2.015**

Figure 7.16.: EOC of the approximation of w for the **semi-implicit finite difference** numerical scheme for the **Willmore flow of graphs** (6.3.9). See the Numerical experiment 7.1.8.

Numerical experiment 7.1.8. EOC for the semi-implicit finite difference numerical scheme for the Willmore flow of graphs. **Computational domain:** $\Omega \equiv [-4,4]^2$. **Initial condition:**

$$\varphi_{ini}(x,y) := \frac{1}{r^{2n}}\left(x^n - r^n\right)\left(y^n - r^n\right)\exp\left(-\sigma\left(x^2+y^2\right)\right)$$

for $r=4, n=4, \sigma=1$. **Final time:** $T=0.1$. **Space steps:** 0.5×0.5, 0.25×0.25, 0.125×0.125, 0.0625×0.0625 and 0.03125×0.03125. **Time step:** Depends on the space steps - $2.5\cdot 10^{-3}$, $6.25\cdot 10^{-4}$, $1.5625\cdot 10^{-4}$, $3.90625\cdot 10^{-5}$ and $9.765625\cdot 10^{-6}$. **Numerical scheme:** 6.3.9. **Figure:** 7.15 and 7.16. **Remark:** The approximation of φ and w is of the second order.

7.1.2. Experimental order of convergence for the level-set formulation

For the isotropic level-set formulations of the mean-curvature flow and the Willmore flow, there exist analytical solutions. As an initial condition we always choose a circle with radius r_0. For all the evolutionary laws, the initial curve remains the circle, however the radius may change. We want to find formulas describing the rate of change. It is easy to see that the curvature of circle with radius $r(t)$ equals

$$\kappa(t) = -\frac{1}{r(t)}.$$

For the mean-curvature flow from (5.19) resp. (5.4.1) we have that

$$\partial_t r(t) = -\frac{1}{r(t)},$$

which is an ordinary differential equation. Solving it we get:

A circle with initial radius r_0 driven by **mean-curvature flow**

$$V = H$$

evolves with respect to the following relation for the radius

$$r(t) = \sqrt{r_0^2 - 2t}. \tag{7.14}$$

In case of the Willmore flow we look at the Definition 5.2.5 resp. (5.4.2) and obtain

$$\partial_t r(t) = \frac{1}{2}\frac{1}{r^3}, \tag{7.15}$$

solution of which gives:

A circle with initial radius r_0 driven by the **Willmore flow**

$$V = -\Delta_\Gamma H - \frac{1}{2}H^3 + 2KH$$

evolves with respect to the following relation for the radius r

$$r(t) = \left(2t + r_0^4\right)^{\frac{1}{4}}. \tag{7.16}$$

The errors of the approximation are evaluated in similar manner as for the graph formulation. Having an exact solution $\Gamma(t)$ and an approximated solution $\Gamma_h(t)$, the error of the approximation at point $\mathbf{x} \in \Gamma_h(t)$ is given by

$$\mathrm{Err}(\Gamma_h(t), \mathbf{x}) = \min_{\mathbf{y}\in\Gamma(t)} |\mathbf{x} - \mathbf{y}|.$$

Employing the norms of spaces $L_1(\Gamma(t); [0,T])$, resp. $L_2(\Gamma(t); [0,T])$ resp. $L_\infty(\Gamma(t); [0,T])$, we get the global error of the approximation $\Gamma_h(t)$ of $\Gamma(t)$ during the evolution up to time T. If $\Gamma(t)$ is a circle with its centre in the origin we may approximate the local error $\mathrm{Err}(\Gamma_h(t), \mathbf{x})$ by

$$\mathrm{Err}(\Gamma_h(t), \mathbf{x}) \approx ||\mathbf{x}| - r(t)|,$$

For function $\alpha^h(t)$ defined on $\Gamma_h(t)$ as $\alpha_i^h(t) = \alpha(x_i(t), t)$ where $\Gamma_h(t)$ is approximated by points x_i for $i = 1, \cdots, N$, we define the discrete norms as

$$\begin{aligned}
\left\|\alpha^h\right\|_{L_1(\Gamma_h;[0,T])}^{h,\tau} &:= \sum_{k=0}^{M} \tau \sum_{i=0}^{N} \left|\alpha_i^h(k\tau)\right| q_i,\\
\left\|\alpha^h\right\|_{L_2(\Gamma_h;[0,T])}^{h,\tau} &:= \left(\sum_{k=0}^{M} \tau \sum_{i=0}^{N} \left(\alpha_i^h(k\tau)\right)^2 q_i\right)^{\frac{1}{2}},\\
\left\|\alpha^h\right\|_{L_\infty(\Gamma_h;[0,T])}^{h,\tau} &:= \max_{k=0,\cdots,M}\max_{i=0,\cdots,N} \left|\alpha_i^h(k\tau)\right|,
\end{aligned}$$

where q_i is given by (6.270). We leave the superscript h in the norm notation $\|\cdot\|^{h,\tau}_{L_\cdot(\Gamma_h;[0,T])}$ to express the dependence on the numerical grid ω_h which was used for the level-set method. Experimental order of convergence with errors on two different numerical grids with space steps h_1 and h_2 is given by (7.13).

The reader can find obtained experimental order of convergence in Tables 7.17–7.19.

h	$\|\cdot\|^{h,\tau}_{L_1(\Gamma_h(t);[0,T])}$		$\|\cdot\|^{h,\tau}_{L_2(\Gamma_h(t);[0,T])}$		$\|\cdot\|^{h,\tau}_{L_\infty(\Gamma_h(t);[0,T])}$		CPU/sec.
	Error	**EOC**	Error	**EOC**	Error.	**EOC**	
1/16	1.601e-05		0.0001282		0.00223		1
1/32	3.11e-06	**2.364**	2.517e-05	**2.349**	0.0004446	**2.326**	2
1/64	7.864e-07	**1.919**	6.394e-06	**1.913**	0.0001175	**1.858**	5
1/128	1.954e-07	**2.078**	1.562e-06	**2.104**	2.94e-05	**2.068**	13
1/256	4.631e-08	**2.077**	3.748e-07	**2.059**	7.329e-06	**2.004**	148
1/512	1.145e-08	**2.016**	9.386e-08	**1.998**	1.84e-06	**1.994**	2688
1/1024	2.876e-09	**1.992**	2.35e-08	**1.998**	4.592e-07	**2.002**	41270

Figure 7.17.: EOC of the approximation of $\Gamma(t)$ for the **explicit finite difference** numerical scheme for the **level-set formulation of the mean-curvature flow**. See the Numerical experiment 7.1.9.

Numerical experiment 7.1.9. EOC for the explicit finite difference numerical scheme for the level-set formulation of the mean-curvature flow. **Computational domain:** $\Omega \equiv [-0.5, 0.5]^2$. **Initial condition:** Circle given by $x^2 + y^2 = 0.25^2$. **Boundary conditions:** $\partial_\nu u = 1$ on $\partial\Omega$. **Final time:** $T = 0.02$. **Space steps:** $1/16 \times 1/16$, $1/32 \times 1/32$, $1/64 \times 1/64$, $1/128 \times 1/128$, $1/256 \times 1/256$, $1/512 \times 1/512$ and $1/1024 \times 1/1024$. **Time step:** Adaptive. **Level-set:** regularisation $\epsilon = 10^{-15}$, no re-distancing. **Numerical scheme:** 6.3.6 **Figure:** 7.17. **Remark:** –

h	$\|\cdot\|^{h,\tau}_{L_1(\Gamma_h(t);[0,T])}$		$\|\cdot\|^{h,\tau}_{L_2(\Gamma_h(t);[0,T])}$		$\|\cdot\|^{h,\tau}_{L_\infty(\Gamma_h(t);[0,T])}$		CPU/sec.
	Error	**EOC**	Error	**EOC**	Error.	**EOC**	
1/16	1.648e-05		0.0001318		0.002276		0
1/32	3.218e-06	**2.884**	2.57e-05	**2.886**	0.0004519	**2.855**	3
1/64	8.13e-07	**1.877**	6.55e-06	**1.865**	0.0001184	**1.828**	56
1/128	2.027e-07	**1.95**	1.602e-06	**1.977**	2.948e-05	**1.951**	1068
1/256	4.793e-08	**2.13**	3.844e-07	**2.107**	7.433e-06	**2.035**	16446
1/512	1.192e-08	**2.032**	9.658e-08	**2.017**	1.854e-06	**2.027**	267354

Figure 7.18.: EOC of the approximation of $\Gamma(t)$ for the **semi-implicit finite difference numerical** scheme for the **level-set formulation of the mean-curvature flow**. See the Numerical experiment 7.1.10.

Numerical experiment 7.1.10. EOC for the semi-implicit finite difference numerical scheme for the level-set formulation of the mean-curvature flow. **Computational domain:** $\Omega \equiv [-0.5, 0.5]^2$. **Initial condition:** Circle given by $x^2 + y^2 = 0.25^2$. **Boundary conditions:** $\partial_\nu u = 1$ on $\partial\Omega$. **Final time:** $T = 0.02$. **Space steps:** $1/16 \times 1/16$, $1/32 \times 1/32$, $1/64 \times 1/64$, $1/128 \times 1/128$, $1/256 \times 1/256$ and $1/512 \times 1/512$. **Time step:** Depends on the space step – $2 \cdot 10^{-4}$,$5 \cdot 10^{-5}$,$1.25 \cdot 10^{-5}$,$3.125 \cdot 10^{-6}$,$7.8125 \cdot 10^{-7}$ and $1.953125 \cdot 10^{-7}$. **Level-set:** regularisation $\epsilon = 10^{-15}$, no re-distancing. **Numerical scheme:** 6.3.8 **Figure:** 7.18. **Remark:** –

h	$\|\cdot\|^{h,\tau}_{L_1(\Gamma_h(t);[0,T])}$		$\|\cdot\|^{h,\tau}_{L_2(\Gamma_h(t);[0,T])}$		$\|\cdot\|^{h,\tau}_{L_\infty(\Gamma_h(t);[0,T])}$		CPU/sec.
	Error	**EOC**	Error	**EOC**	Error.	**EOC**	
1/16	0.2715		0.1499		0.1092		0
		4.974		**4.719**		**3.711**	
1/32	0.01877		0.01188		0.01488		11
		-0.6891		**-0.5915**		**0.003516**	
1/64	0.02958		0.01756		0.01484		683
		0.3735		**0.3481**		**0.2768**	
1/128	0.02275		0.01375		0.01222		59127

Figure 7.19.: EOC of the approximation of $\Gamma(t)$ for the **semi-implicit finite difference numerical** scheme for the **level-set formulation of the Willmore flow**. See the Numerical experiment 7.1.11.

Numerical experiment 7.1.11. EOC for the semi-implicit finite difference numerical scheme for the level-set formulation of the Willmore flow. **Computational domain:** $\Omega \equiv [-0.5, 0.5]^2$. **Initial condition:** Circle given by $x^2 + y^2 = 0.25^2$. **Boundary conditions:** $\partial_\nu u = 1$ on $\partial\Omega$. **Final time:** $T = 0.02$. **Space steps:** $1/16 \times 1/16$, $1/32 \times 1/32$, $1/64 \times 1/64$, $1/128 \times 1/128$, $1/256 \times 1/256$ and $1/512 \times 1/512$. **Time step:** Depends on the space step – $0.01, 2.5 \cdot 10^{-3}, 6.25 \cdot 10^{-4}$ and $1.5625 \cdot 10^{-4}$. **Level-set:** regularisation depends on the space step $\epsilon = 0.4472$, 0.3162,0.2236 and 0.1581, re-distancing depends on the space step $\tau_{redist} = 0.025$, 0.0125, $6.25 \cdot 10^{-3}$ and $3.125 \cdot 10^{-3}$. **Numerical scheme:** 6.3.9 **Figure:** 7.19. **Remark:** –

7.2. Numerical experiments

In this part we bring almost 100 numerical experiments. They demonstrate differences between all the classes of the schemes we derived in this text i.e. one-sided finite differences, central finite differences and the complementary finite volumes schemes. We show both the graph and the level-set formulation. For all initial conditions the reader can see comparison of the evolutions given by the mean-curvature flow and the Willmore flow. We will be also interested in a comparison of the explicit and semi-implicit schemes. First of all, we test the schemes on the graph formulation then we proceed to the level-set method. In both cases we start with the isotropic problems and then we show examples of few anisotropies.

7.2.1. Graph formulation

Let us begin with the one-sided finite difference schemes. Numerical experiments 7.2.1–7.2.4 and Figures 7.20 – 7.23 show that the scheme 6.3.2 for the mean-curvature flow performs well. However, we can see significant loss of symmetry when we approximate the Willmore flow - see Figure 7.21 related to the experiment 7.2.2. It is even more evident on the Figure 7.23 and the experiment 7.2.4 where we can see that the scheme 6.3.3 in fact failed to converge to the correct solution. We have already mentioned that this class of schemes suffers from non-symmetric stencils. Therefore in [82] we proposed to use the central differences.

The results obtained by the finite difference method with use of the central differences (i.e. schemes 6.3.4 – 6.3.5) are on Figures 7.20 – 7.27 resp. experiments 7.20 – 7.2.8. One can see that these schemes preserve the symmetry sufficiently even for the Willmore flow. The disadvantage is that they do not perform well for discontinuous initial conditions in the experiments 7.2.7 – 7.2.8. For the fourth order problem (experiment 7.2.8) we had to add some artificial viscosity C_{visc} from 100 to 1000. This, however, decreases the accuracy of the scheme. It makes this class of schemes not very good choice. Moreover, large stencil in the case of the fourth order problems is not convenient for the semi-implicit schemes.

The rest of the results was obtained just by the complementary finite volumes method either in explicit or semi-implicit form. Figures 7.2.9 – 7.39 and numerical experiments 7.28 – 7.2.20 demonstrate the isotropic problems. The level lines always show good preserving of the symmetry when the initial condition is symmetric.

For Figures 7.36 – 7.39 and the numerical experiments 7.2.17 – 7.2.20 the Neumann boundary conditions were imposed.

The effect of the anisotropy (5.111) can be seen on Figures 7.40 – 7.51 and numerical experiments 7.2.21 – 7.2.24. First of all, the quadratic form $\mathbb{G}$ is set such that the level-lines turn into ellipses oriented along the axis y. By setting up even the non-diagonal elements to non-zero values (Figures 7.42 – 7.43 and experiments 7.2.23 – 7.2.24), we get a deformation along the line $x = y$. The Neumann boundary conditions were imposed in the case of the numerical experiments7.2.25 – 7.2.32, results of which can be seen on the Figures 7.44 – 7.51. We have tested both, the deformation along the axis y (experiments 7.2.25 – 7.2.26, 7.2.29 – 7.2.30 and Figures 7.44 – 7.45 and 7.48 – 7.49) and along the line $x = y$ (experiments 7.2.27 – 7.2.28, 7.2.31 – 7.2.32 and Figures 7.46 – 7.47 and 7.50 – 7.51).

The anisotropy (5.113) has been studied at the experiments 7.2.33 – 7.2.44 and Figures 7.52 – 7.44. This anisotropy turns the level-lines into squares or rectangles which have the same orientation as the coordinate system. When this anisotropy is inserted into the fourth order problems, we get really highly non-linear problems. If we employ the explicit schemes, we get very small time steps even on quite coarse meshes. For example the numerical experiment 7.2.34 (Figure 7.53) was performed with space step $h = 0.01$ and the adaptive algorithm at the Merson method set the time step to 10^{-12}. The computation was running for more then 8 months on 2

CPU AMD Opteron 270 (4 cores) and it did not reach a steady state. The semi-implicit scheme here gave comparable results with much higher efficiency. It is the reason why we were not able to show the steady states for all simulations. We can, however, see that even with such high non-linearity, the complementary finite volume schemes are able to handle discontinuities like the ones we can see at the experiments 7.2.35 – 7.2.36 and Figures 7.54 – 7.55. We, of course, show experiments with the Neumann boundary conditions 7.2.41 – 7.2.44, see Figures 7.60 – 7.63.

The last anisotropy we consider is the l_m-norm (5.114) for $m = 16$. The results are presented on Figures 7.64 – 7.75 and numerical experiments 7.2.45 – 7.2.56. This anisotropy leads to even stronger non-linearity. The semi-implicit schemes often require very small time steps too. The explicit schemes then may be better choice.

Numerical experiment 7.2.1. Test of the **explicit one-sided finite difference** numerical scheme for the **isotropic mean-curvature flow of graphs**

$$\begin{aligned} \partial_t \varphi &= Q \nabla \cdot \left(\frac{\nabla \varphi}{Q} \right) \quad \text{on } \left(0, \mathrm{T}\right\rangle \times \Omega, \\ \varphi \mid_{t=0} &= \sin(2\pi x) \sin(2\pi y) \quad \text{on } \Omega, \end{aligned}$$

with the Dirichlet boundary condition

$$\varphi = 0 \quad \text{on } \partial\Omega.$$

Computational domain: $\Omega \equiv [0,1]^2$.
Final time: $T = 0.05$.
Space steps: $h = 0.01$.
Time step: Adaptive.
Numerical scheme: 6.3.2
Figure: 7.20.
Remark: In the case of the mean-curvature flow of graphs the scheme (6.3.2) performs sufficiently.

Numerical experiment 7.2.2. Test of the **explicit one-sided finite difference** numerical scheme for the **isotropic Willmore flow of graphs**

$$\begin{aligned} \partial_t \varphi &= -Q \nabla \cdot \left(\frac{1}{Q} \mathbb{P} \nabla w - \frac{1}{2} \frac{w^2}{Q^3} \nabla \varphi \right) \text{ on } \Omega \times (0, T], \\ w &= Q \nabla \cdot \left(\frac{\nabla \varphi}{Q} \right) \text{ on } \Omega \times [0, T], \\ \varphi \mid_{t=0} &= \sin(2\pi x) \sin(2\pi y) \text{ on } \Omega, \end{aligned}$$

with the Dirichlet boundary conditions

$$\varphi = 0, w = 0 \text{ on } \partial\Omega.$$

Computational domain: $\Omega \equiv [0,1]^2$.
Final time: $T = 0.002$.
Space steps: $h = 0.01$.
Time step: Adaptive.
Numerical scheme: 6.3.3
Figure: 7.21.
Remark: In the case of the Willmore flow of graphs we see that the scheme (6.3.3) does not preserve the symmetry of the initial condition.

Isotropic graph formulation of the mean-curvature flow

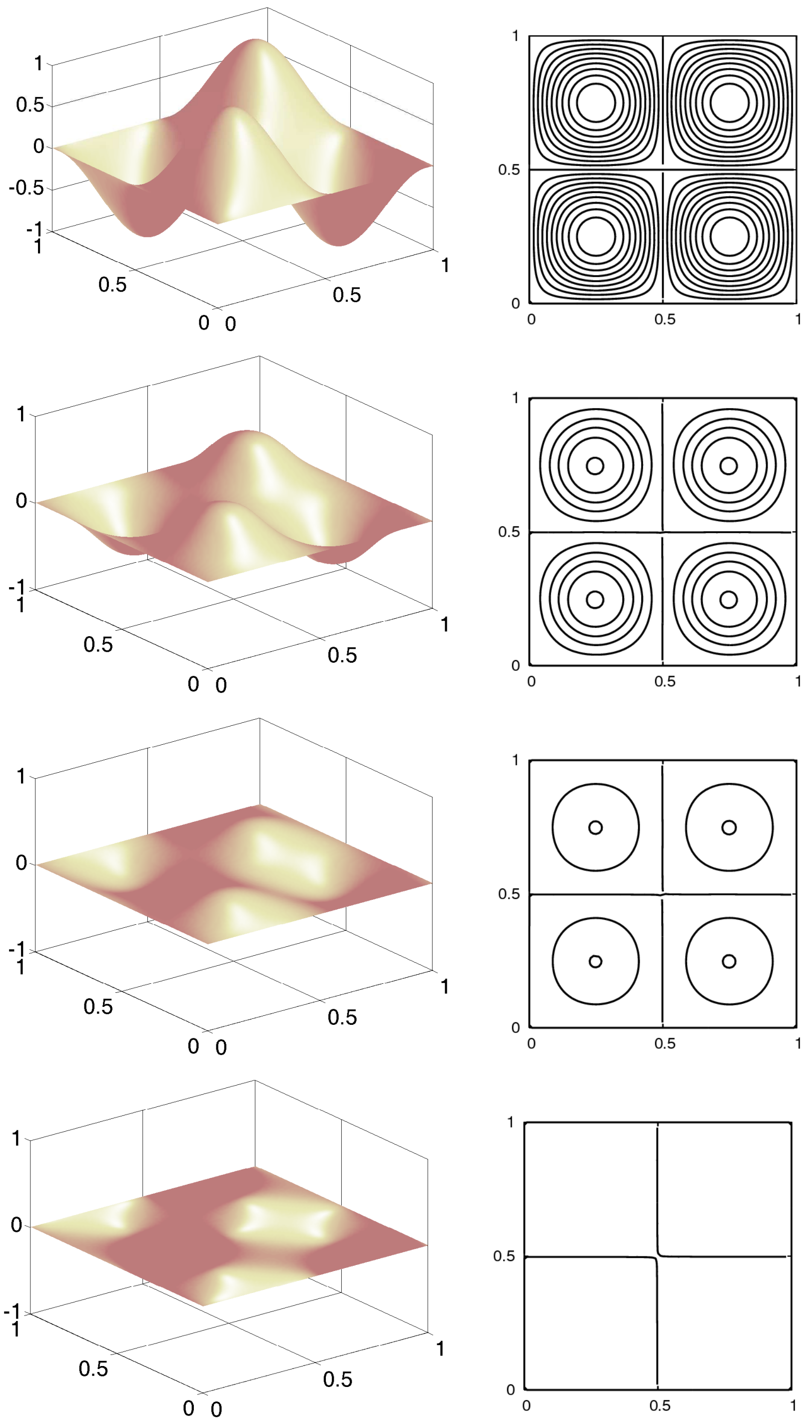

Figure 7.20.: **The explicit one-sided finite difference** numerical scheme for **the isotropic mean-curvature flow of graphs** at times $t = 0$, $t = 0.0125$, $t = 0.025$ and $t = 0.05$ (graph of φ on the left, level-lines of φ on the right). See the Numerical experiment 7.2.1.

Isotropic graph formulation of the Willmore flow

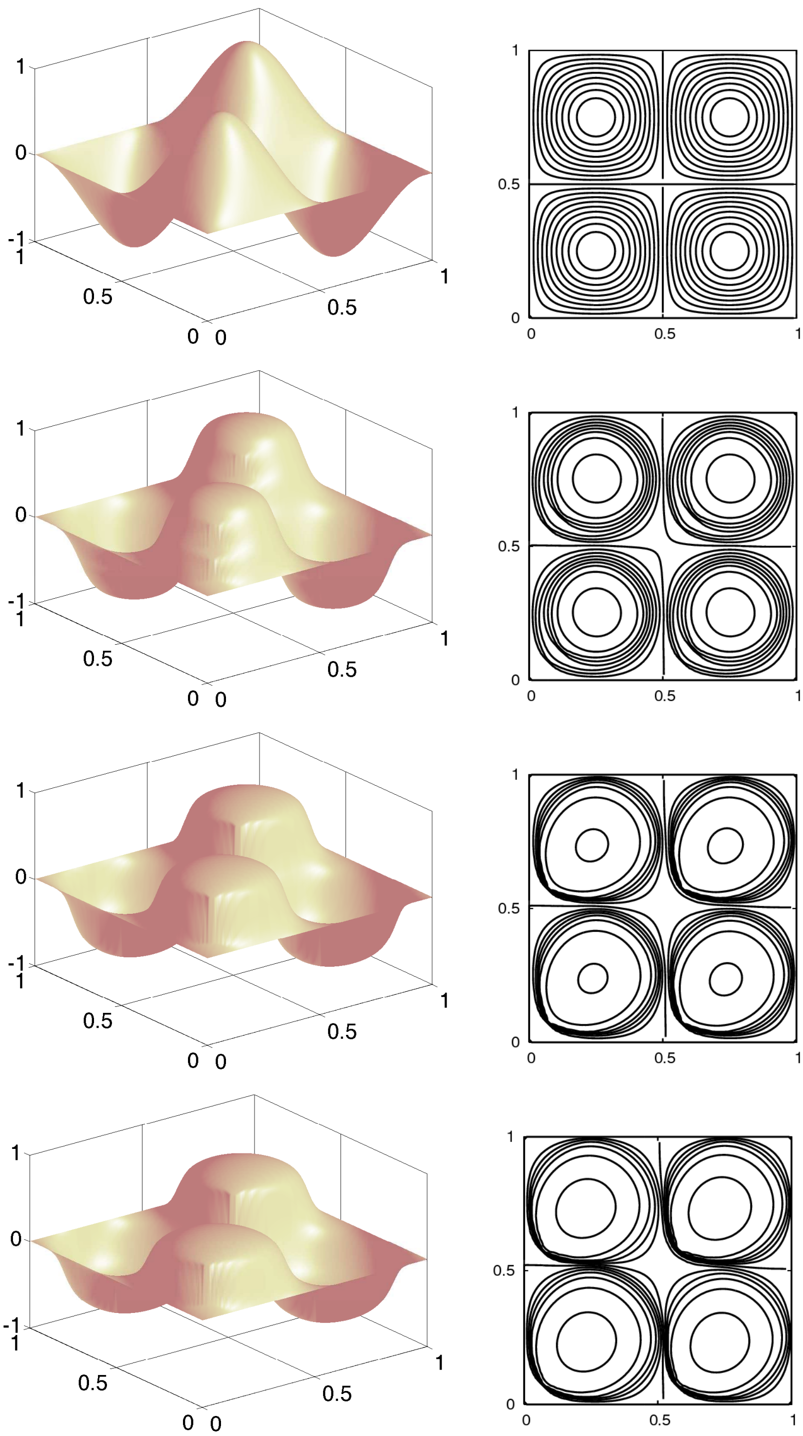

Figure 7.21.: **The explicit one-sided finite difference** numerical scheme for **the isotropic Willmore flow of graphs** at times $t = 0$, $t = 0.0001$, $t = 0.0005$ and $t = 0.001$ (graph of φ on the left, level-lines of φ on the right). See the Numerical experiment 7.2.2.

Numerical experiment 7.2.3. Test of the **explicit one-sided finite difference** numerical scheme for the **isotropic mean-curvature flow of graphs**

$$\begin{aligned}\partial_t \varphi &= Q\nabla \cdot \left(\frac{\nabla \varphi}{Q}\right) \quad \text{on } (0, \mathrm{T}\rangle \times \Omega, \\ \varphi\,|_{t=0} &= \operatorname{sign}\left(x^2+y^2-0.1\right)+1 \quad \text{on } \Omega,\end{aligned}$$

with the Dirichlet boundary condition

$$\varphi = 0 \quad \text{on } \partial\Omega.$$

Computational domain: $\Omega \equiv [-0.5, 0.5]^2$.
Final time: $T = 0.25$.
Space steps: $h = 0.01$.
Time step: Adaptive.
Numerical scheme: 6.3.2
Figure: 7.22.
Remark: The scheme (6.3.2) performs well even for discontinuous initial condition.

Numerical experiment 7.2.4. Test of the **explicit one-sided finite difference** numerical scheme for the **isotropic Willmore flow of graphs**

$$\begin{aligned}\partial_t \varphi &= -Q\nabla \cdot \left(\frac{1}{Q}\mathbb{P}\nabla w - \frac{1}{2}\frac{w^2}{Q^3}\nabla\varphi\right) \text{ on } \Omega \times (0, T]\,, \\ w &= Q\nabla \cdot \left(\frac{\nabla \varphi}{Q}\right) \text{ on } \Omega \times [0, T]\,, \\ \varphi\,|_{t=0} &= \operatorname{sign}\left(x^2+y^2-0.1\right)+1 \text{ on } \Omega,\end{aligned}$$

with the Dirichlet boundary conditions

$$\varphi = 0, w = 0 \text{ on } \partial\Omega.$$

Computational domain: $\Omega \equiv [-0.5, 0.5]^2$.
Final time: $T = 0.03$.
Space steps: $h = 0.01$.
Time step: Adaptive.
Numerical scheme: 6.3.3
Figure: 7.23.
Remark: With discontinuous initial condition the Numerical scheme (6.3.3) completely fails to find approximate solution.

Isotropic graph formulation of the mean-curvature flow

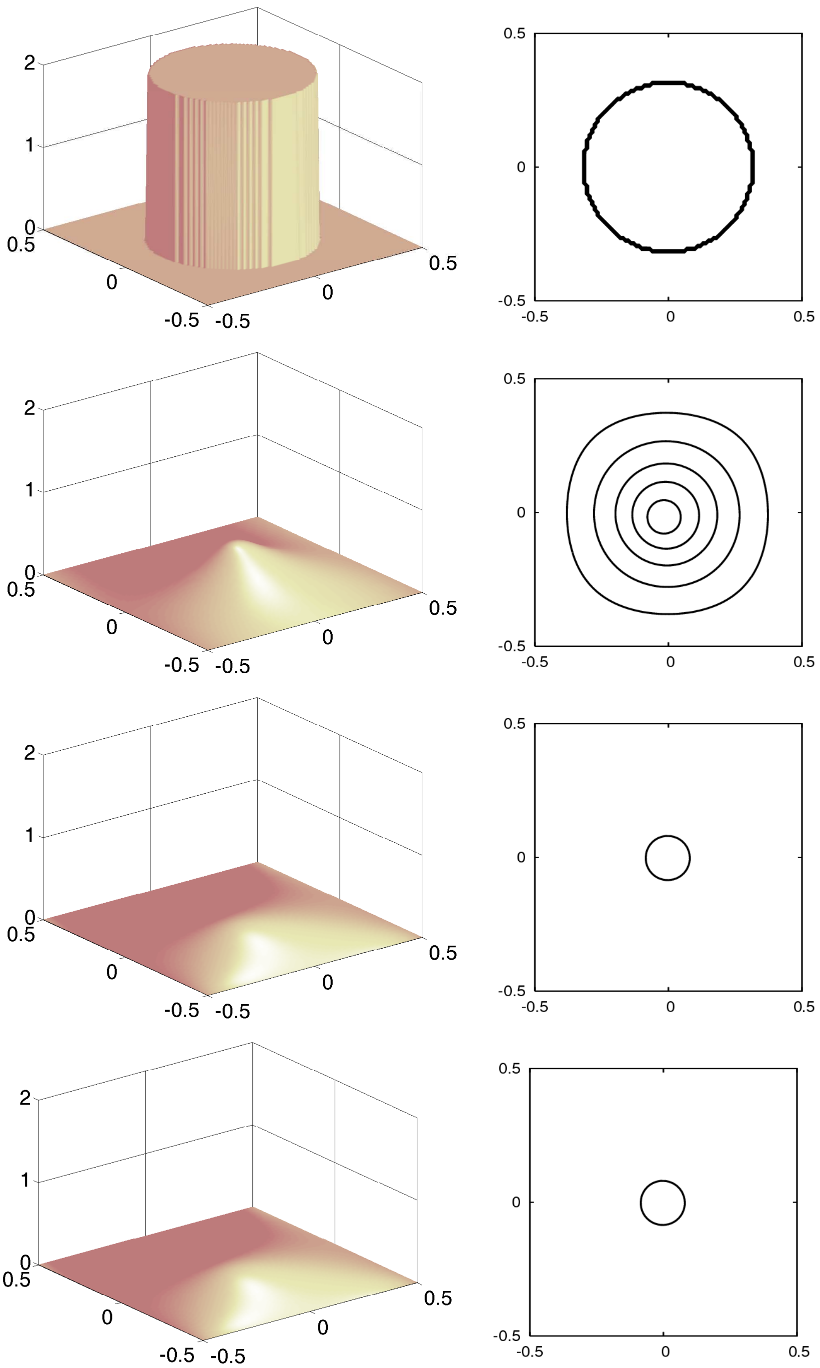

Figure 7.22.: **The explicit one-sided finite difference** numerical scheme for **the mean-curvature flow of graphs** at times $t = 0$, $t = 0.0125$, $t = 0.0625$ and $t = 0.125$ (graph of φ on the left, level-lines of φ on the right). See the Numerical experiment 7.2.3.

Isotropic graph formulation of the Willmore flow

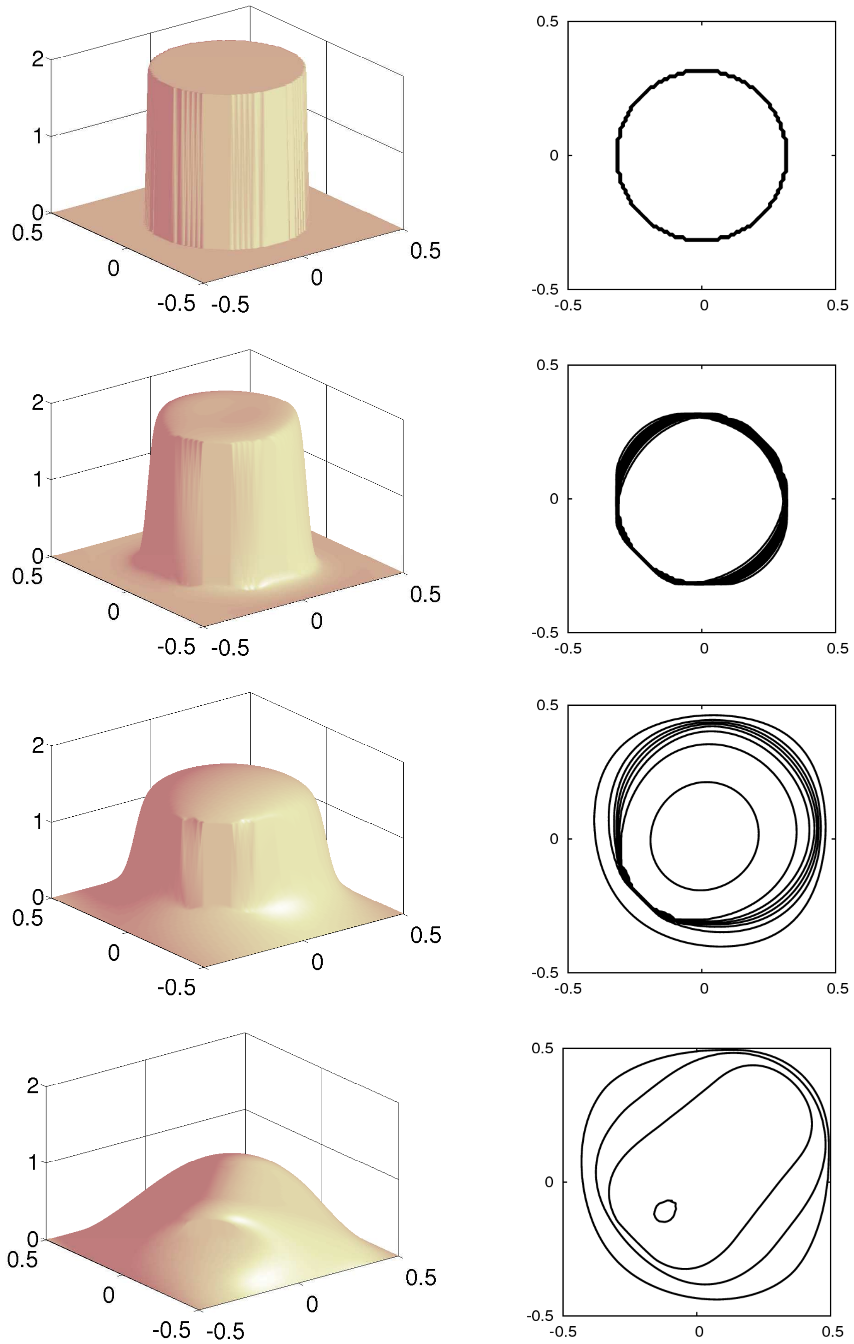

Figure 7.23.: **The explicit one-sided finite difference** numerical scheme for **the Willmore flow of graphs** at times $t = 0$, $t = 1 \cdot 10^{-5}$, $t = 0.01$ and $t = 0.03$ (graph of φ on the left, level-lines of φ on the right). See the Numerical experiment 7.2.4.

Numerical experiment 7.2.5. Test of the **explicit central finite difference** numerical scheme for the **isotropic mean-curvature flow of graphs**

$$\begin{aligned}\partial_t \varphi &= Q\nabla \cdot \left(\frac{\nabla \varphi}{Q}\right) \quad \text{on } (0,\mathrm{T}\rangle \times \Omega,\\ \varphi\,|_{t=0} &= \sin(2\pi x)\sin(2\pi y) \quad \text{on } \Omega,\end{aligned}$$

with the Dirichlet boundary condition

$$\varphi = 0 \quad \text{on } \partial\Omega.$$

Computational domain: $\Omega \equiv [0,1]^2$.
Final time: $T = 0.05$.
Space steps: $h = 0.01$.
Time step: Adaptive.
Numerical scheme: 6.3.4
Figure: 7.20.
Remark: In the case of the mean-curvature flow of graphs the scheme (6.3.4) performs well.

Numerical experiment 7.2.6. Test of the **explicit central finite difference** numerical scheme for the **isotropic Willmore flow of graphs**

$$\begin{aligned}\partial_t \varphi &= -Q\nabla \cdot \left(\frac{1}{Q}\mathbb{P}\nabla w - \frac{1}{2}\frac{w^2}{Q^3}\nabla\varphi\right) \text{ on } \Omega \times (0,T]\,,\\ w &= Q\nabla \cdot \left(\frac{\nabla \varphi}{Q}\right) \text{ on } \Omega \times [0,T]\,,\\ \varphi\,|_{t=0} &= \sin(2\pi x)\sin(2\pi y) \text{ on } \Omega,\end{aligned}$$

with the Dirichlet boundary conditions

$$\varphi = 0, w = 0 \text{ on } \partial\Omega.$$

Computational domain: $\Omega \equiv [0,1]^2$.
Final time: $T = 0.002$.
Space steps: $h = 0.01$.
Time step: Adaptive.
Numerical scheme: 6.3.5
Figure: 7.25.
Remark: In the case of the Willmore flow of graphs we see that the scheme (6.3.5) preserves the symmetry of the solution well.

Isotropic graph formulation of the mean-curvature flow

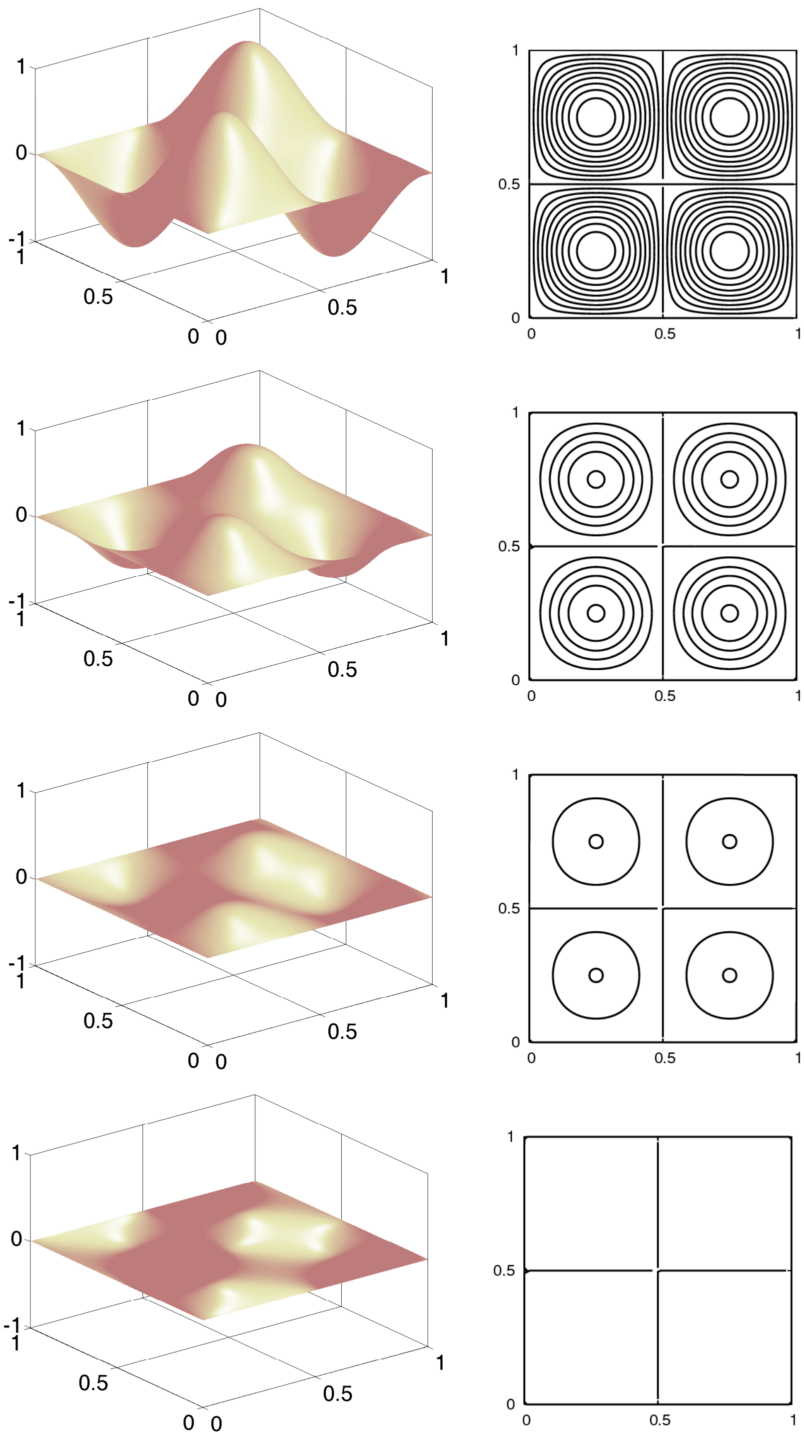

Figure 7.24.: The **explicit central finite difference** numerical scheme for the **isotropic mean-curvature flow of graphs** at times $t = 0$, $t = 0.0125$, $t = 0.025$ and $t = 0.05$ (graph of u on the left, level-lines of u on the right). See the Numerical experiment 7.2.5.

Isotropic graph formulation of the Willmore flow

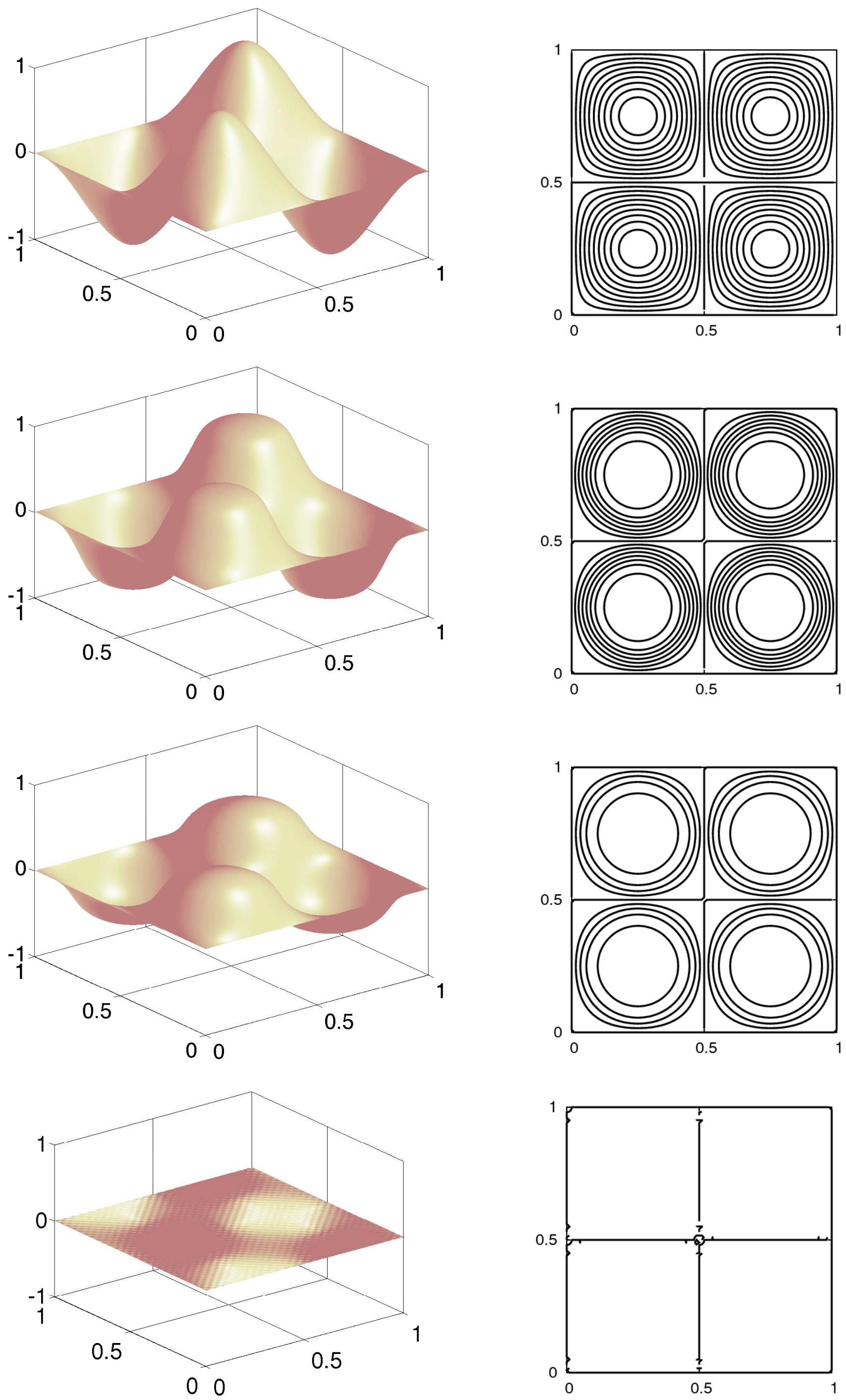

Figure 7.25.: The **explicit central finite difference** numerical scheme for the **isotropic Willmore flow of graphs** at times $t = 0$, $t = 0.0001$, $t = 0.0005$ and $t = 0.002$ (graph of u on the left, level-lines of u on the right). See the Numerical experiment 7.2.6.

Numerical experiment 7.2.7. Test of the **explicit central finite difference** numerical scheme for the **isotropic mean-curvature flow of graphs**

$$\begin{aligned} \partial_t \varphi &= Q\nabla \cdot \left(\frac{\nabla \varphi}{Q}\right) \quad \text{on } (0, \mathrm{T}\rangle \times \Omega, \\ \varphi\mid_{t=0} &= \operatorname{sign}\left(x^2+y^2-0.1\right)+1 \quad \text{on } \Omega, \end{aligned}$$

with the Dirichlet boundary condition

$$\varphi = 0 \quad \text{on } \partial\Omega.$$

Computational domain: $\Omega \equiv [-0.5, 0.5]^2$.
Initial condition: $u_{ini}(x,y) := \operatorname{sign}\left(x^2+y^2-0.1\right)+1$.
Boundary conditions: $u = w = 0$ on $\partial\Omega$.
Final time: $T = 0.25$.
Space steps: $h = 0.01$.
Time step: Adaptive.
Numerical scheme: 6.3.4
Figure: 7.26.
Remark: In the case of the mean-curvature flow of graphs with discontinuous initial condition the scheme (6.3.4) performs sufficiently.

Numerical experiment 7.2.8. Test of the **explicit central finite difference** numerical scheme for the **isotropic Willmore flow of graphs**

$$\begin{aligned} \partial_t \varphi &= -Q\nabla \cdot \left(\frac{1}{Q}\mathbb{P}\nabla w - \frac{1}{2}\frac{w^2}{Q^3}\nabla\varphi\right) \text{ on } \Omega \times (0, T], \\ w &= Q\nabla \cdot \left(\frac{\nabla \varphi}{Q}\right) \text{ on } \Omega \times [0, T], \\ \varphi\mid_{t=0} &= \operatorname{sign}\left(x^2+y^2-0.1\right)+1 \text{ on } \Omega, \end{aligned}$$

with the Dirichlet boundary conditions

$$\varphi = 0, w = 0 \text{ on } \partial\Omega.$$

Computational domain: $\Omega \equiv [-0.5, 0.5]^2$.
Final time: $T = 0.125$.
Space steps: $h = 0.01$.
Time step: Adaptive.
Numerical scheme: 6.3.5
Figure: 7.27.
Remark: In the case of the Willmore flow of graphs we see that the scheme (6.3.5) preserves the symmetry of the solution. However, strong artificial viscosity $C_{visc} = 1000$ have to be added to avoid oscillations.

Isotropic graph formulation of the mean-curvature flow

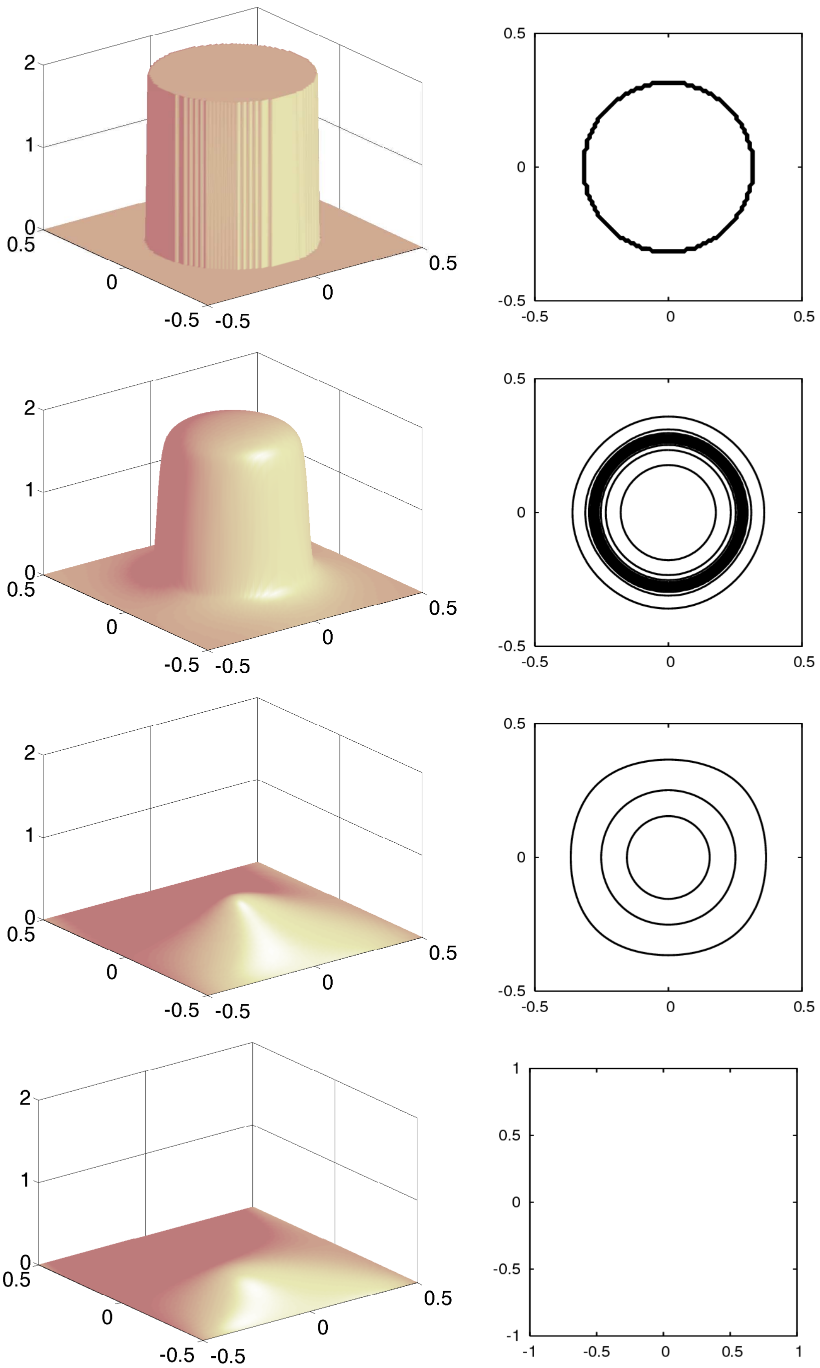

Figure 7.26.: The **explicit central finite difference** numerical scheme for the **isotropic mean-curvature flow of graphs** at times $t = 0$, $t = 0.0125$, $t = 0.0625$ and $t = 0.125$ (graph of u on the left, level-lines of u on the right). See the Numerical experiment 7.2.7.

Isotropic graph formulation of the Willmore flow

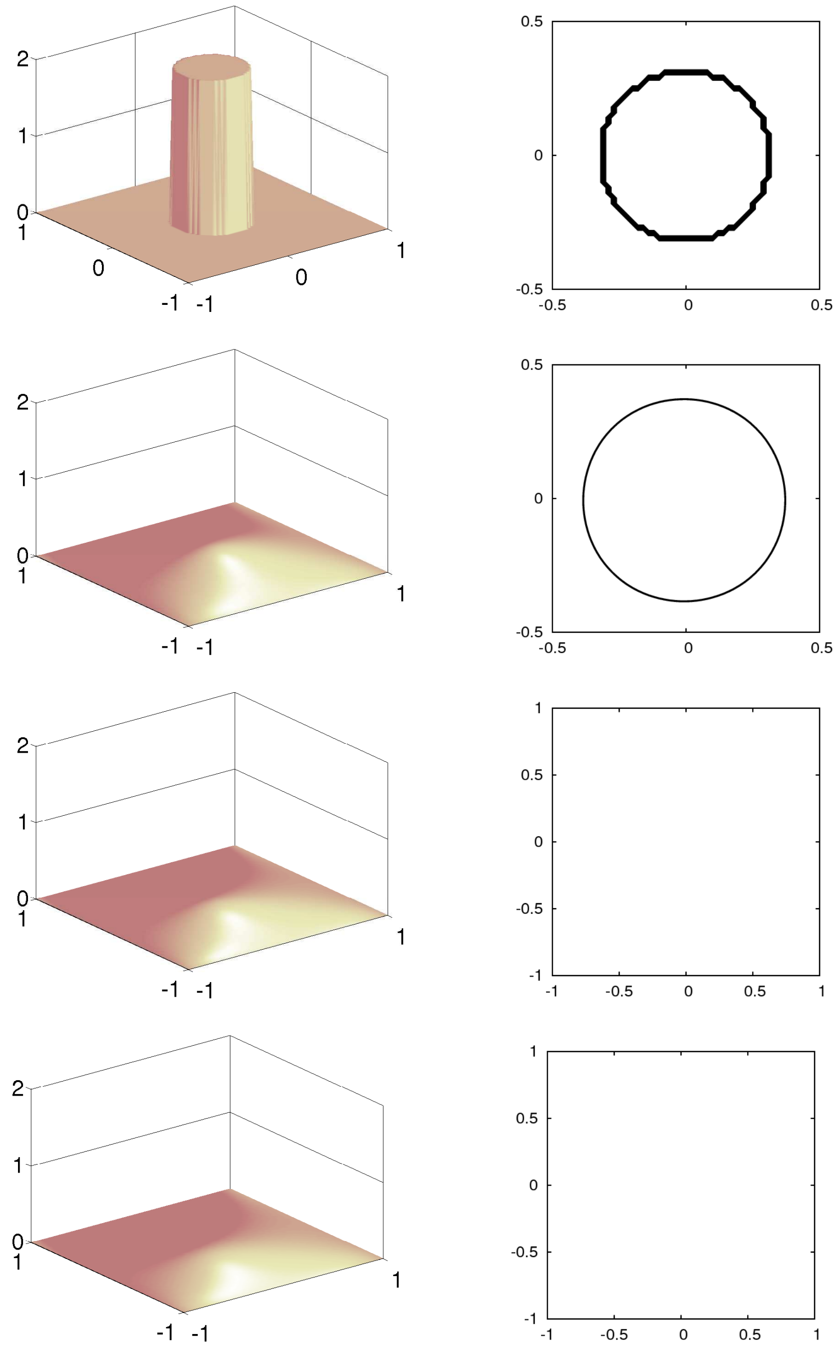

Figure 7.27.: The **explicit central finite difference** numerical scheme for the **isotropic Willmore flow of graphs** at times $t = 0$, $t = 0.00625$, $t = 0.03125$ and $t = 0.125$ (graph of u on the left, level-lines of u on the right). See the Numerical experiment 7.2.8.

Numerical experiment 7.2.9. Test of the **explicit finite difference** numerical scheme for the **isotropic mean-curvature flow of graphs**

$$\begin{aligned} \partial_t \varphi &= Q \nabla \cdot \left(\frac{\nabla \varphi}{Q} \right) \quad \text{on } (0, \mathrm{T}\rangle \times \Omega, \\ \varphi \,|_{t=0} &= \sin(2\pi x) \sin(2\pi y) \quad \text{on } \Omega, \end{aligned}$$

with the Dirichlet boundary condition

$$\varphi = 0 \quad \text{on } \partial\Omega.$$

Computational domain: $\Omega \equiv [0,1]^2$.
Final time: $T = 0.05$.
Space steps: $h = 0.01$.
Time step: Adaptive.
Numerical scheme: 6.3.6
Figure: 7.28.
Remark: In the case of the mean-curvature flow of graphs the scheme (6.3.6) preserves the symmetry of the solution well.

Numerical experiment 7.2.10. Test of the **explicit finite difference** numerical scheme for the **isotropic Willmore flow of graphs**

$$\begin{aligned} \partial_t \varphi &= -Q \nabla \cdot \left(\frac{1}{Q} \mathbb{P} \nabla w - \frac{1}{2} \frac{w^2}{Q^3} \nabla \varphi \right) \text{ on } \Omega \times (0, T], \\ w &= Q \nabla \cdot \left(\frac{\nabla \varphi}{Q} \right) \text{ on } \Omega \times [0, T], \\ \varphi \,|_{t=0} &= \sin(2\pi x) \sin(2\pi y) \text{ on } \Omega, \end{aligned}$$

with the Dirichlet boundary conditions

$$\varphi = 0, w = 0 \text{ on } \partial\Omega.$$

Computational domain: $\Omega \equiv [0,1]^2$.
Final time: $T = 0.004$.
Space steps: $h = 0.01$.
Time step: Adaptive.
Numerical scheme: 6.3.7
Figure: 7.29.
Remark: In the case of the Willmore flow of graphs we see that the scheme (6.3.7) preserves the symmetry of the solution well.

Isotropic graph formulation of the mean-curvature flow

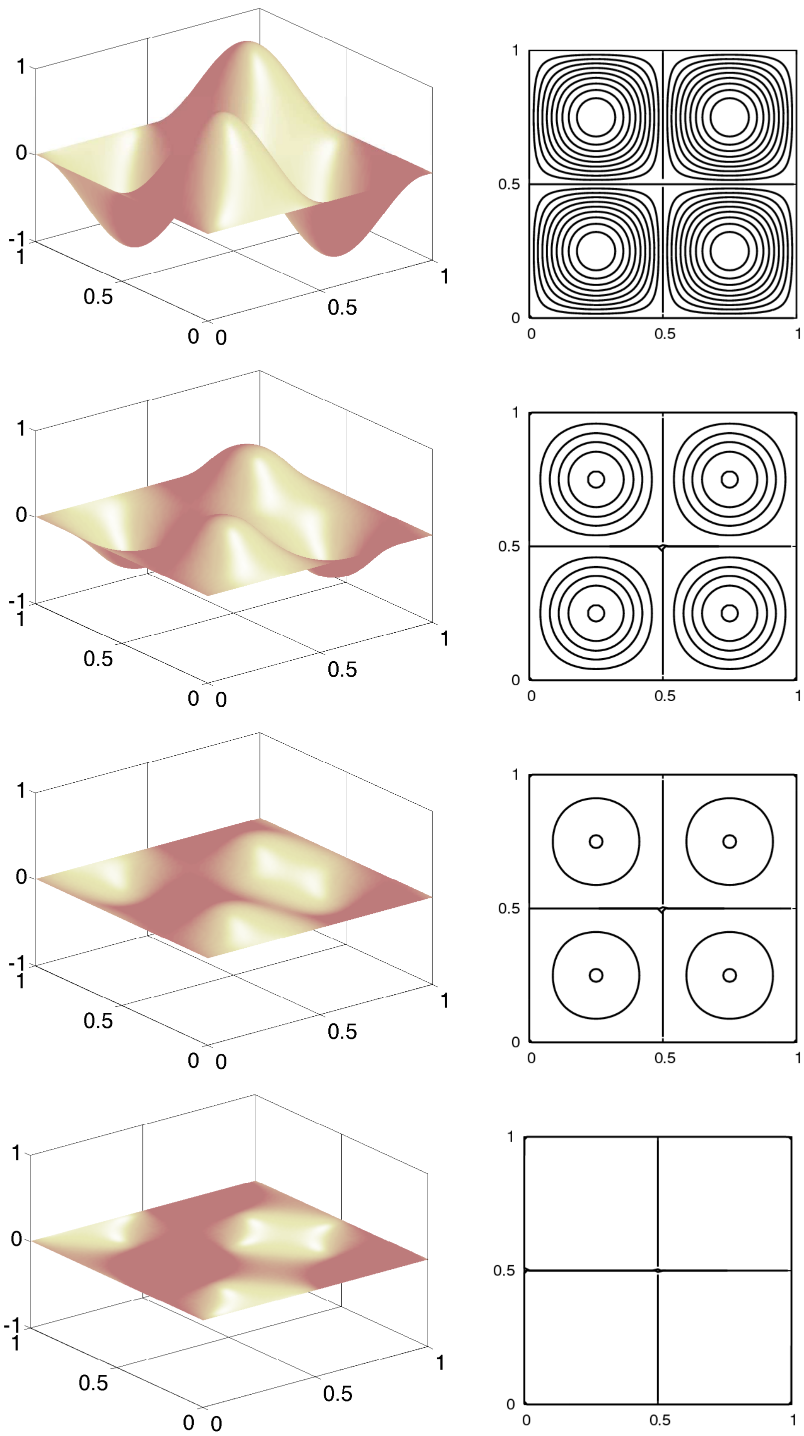

Figure 7.28.: **The explicit finite difference** numerical scheme for the **mean-curvature flow of graphs** at times $t = 0$, $t = 0.0125$, $t = 0.025$ and $t = 0.05$ (graph of u on the left, level-lines of u on the right). See the Numerical experiment 7.2.9.

Isotropic graph formulation of the Willmore flow

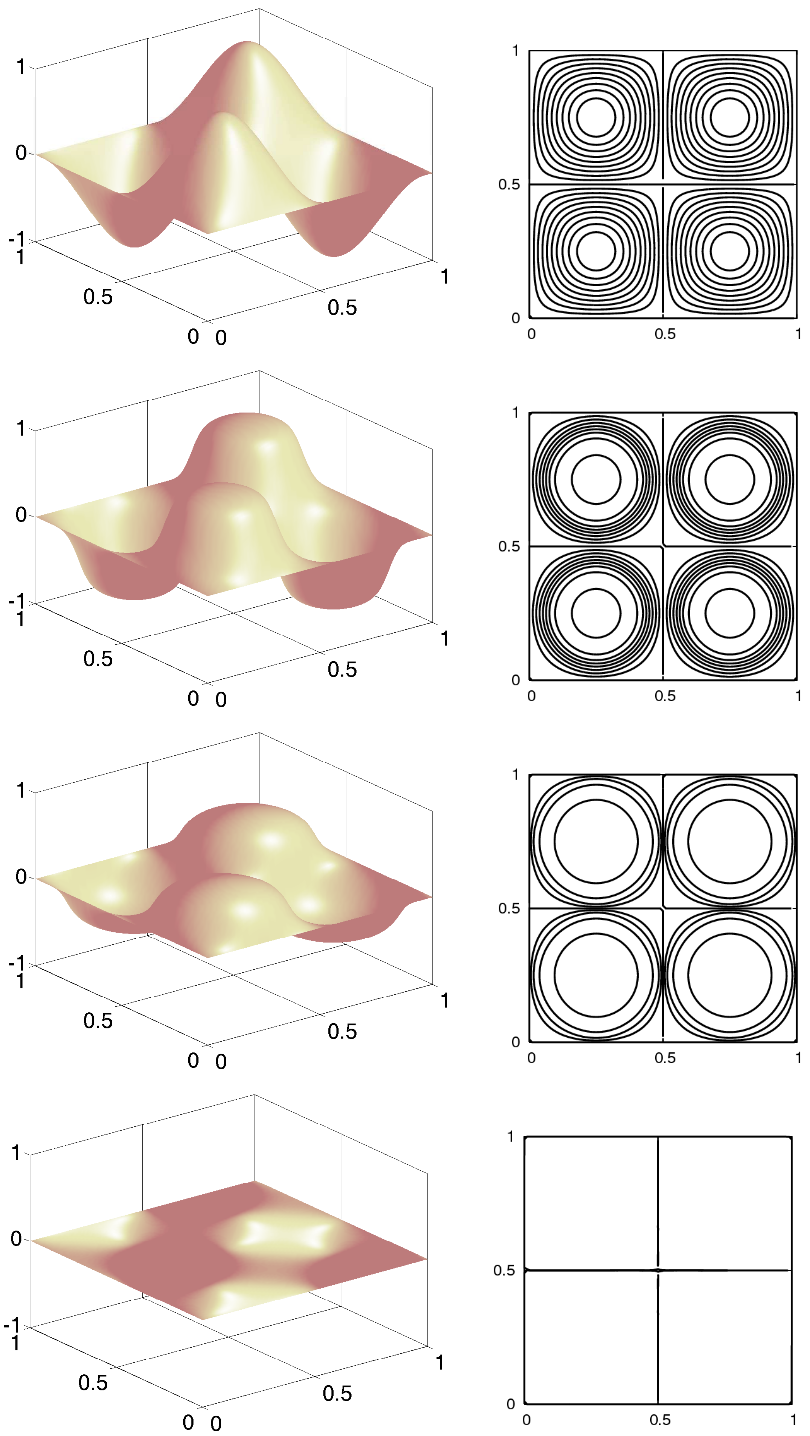

Figure 7.29.: **The explicit finite difference** numerical scheme for the **Willmore flow of graphs** at times $t = 0$, $t = 0.0001$, $t = 0.002$ and $t = 0.004$ (graph of u on the left, level-lines of u on the right). See the Numerical experiment 7.2.10.

Numerical experiment 7.2.11. Test of the **explicit finite difference** numerical scheme for the **isotropic mean-curvature flow of graphs**

$$
\begin{aligned}
\partial_t \varphi &= Q \nabla \cdot \left(\frac{\nabla \varphi}{Q} \right) \quad \text{on } (0, \mathrm{T}\rangle \times \Omega, \\
\varphi \mid_{t=0} &= \operatorname{sign}\left(x^2 + y^2 - 0.1\right) + 1 \quad \text{on } \Omega,
\end{aligned}
$$

with the Dirichlet boundary condition

$$
\varphi = 0 \quad \text{on } \partial\Omega.
$$

Computational domain: $\Omega \equiv [-0.5, 0.5]^2$.
Final time: $T = 0.25$.
Space steps: $h = 0.01$.
Time step: Adaptive.
Numerical scheme: 6.3.6
Figure: 7.30.
Remark: In the case of the mean-curvature flow of graphs with discontinuous initial condition the scheme (6.3.6) performs sufficiently.

Numerical experiment 7.2.12. Test of the **explicit central finite difference** numerical scheme for the **isotropic Willmore flow of graphs**

$$
\begin{aligned}
\partial_t \varphi &= -Q \nabla \cdot \left(\frac{1}{Q} \mathbb{P} \nabla w - \frac{1}{2} \frac{w^2}{Q^3} \nabla \varphi \right) \text{ on } \Omega \times (0, T] \,, \\
w &= Q \nabla \cdot \left(\frac{\nabla \varphi}{Q} \right) \text{ on } \Omega \times [0, T] \,, \\
\varphi \mid_{t=0} &= \operatorname{sign}\left(x^2 + y^2 - 0.1\right) + 1 \text{ on } \Omega,
\end{aligned}
$$

with the Dirichlet boundary conditions

$$
\varphi = 0, w = 0 \text{ on } \partial\Omega.
$$

Computational domain: $\Omega \equiv [-0.5, 0.5]^2$.
Final time: $T = 0.125$.
Space steps: $h = 0.01$.
Time step: Adaptive.
Numerical scheme: 6.3.7
Figure: 7.31.
Remark: In the case of the Willmore flow of graphs with discontinuous initial condition the scheme (6.3.7) performs well.

Isotropic graph formulation of the mean-curvature flow

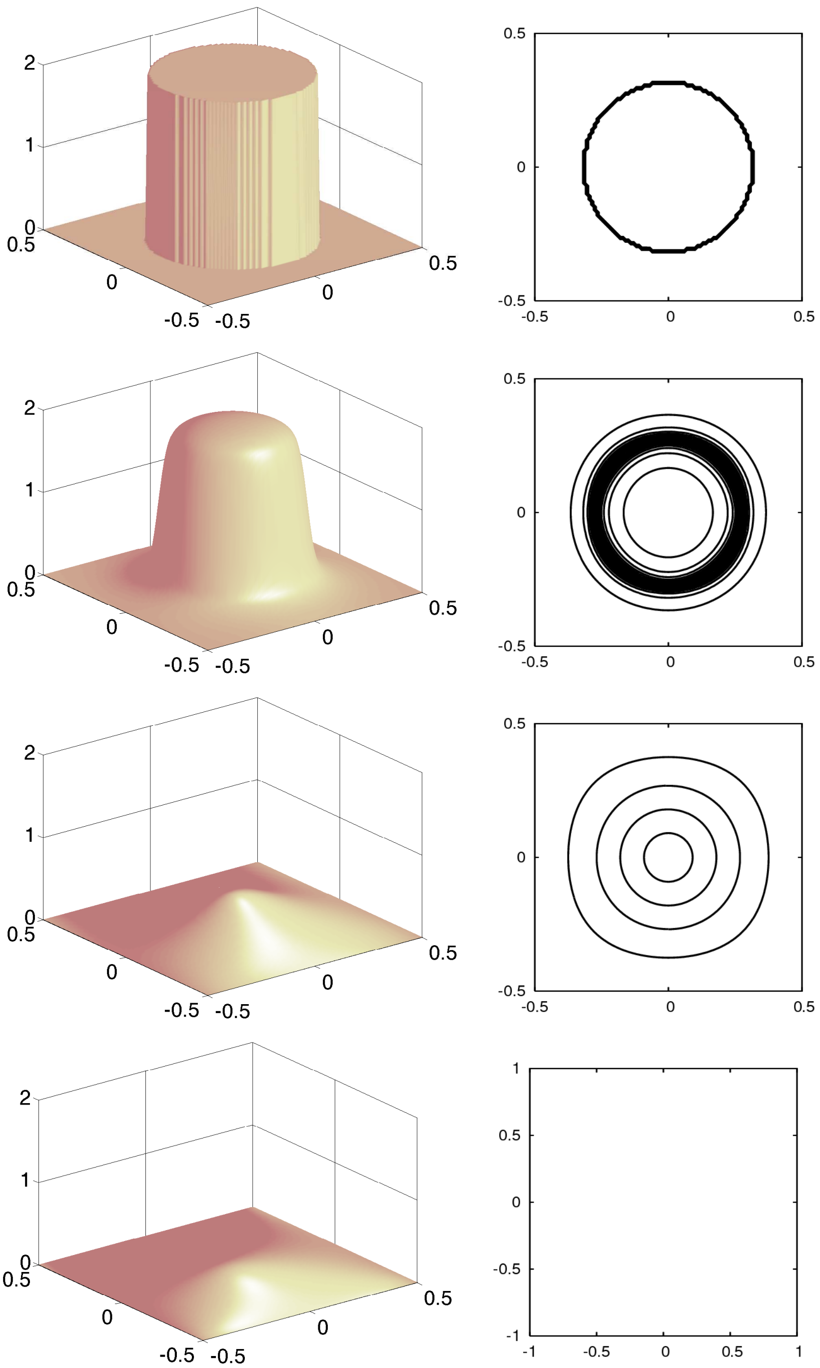

Figure 7.30.: **The explicit finite difference** numerical scheme for the **mean-curvature flow of graphs** at times $t = 0$, $t = 0.0125$, $t = 0.0625$ and $t = 0.125$ (graph of u on the left, level-lines of u on the right). See the Numerical experiment 7.2.11.

Isotropic graph formulation of the Willmore flow

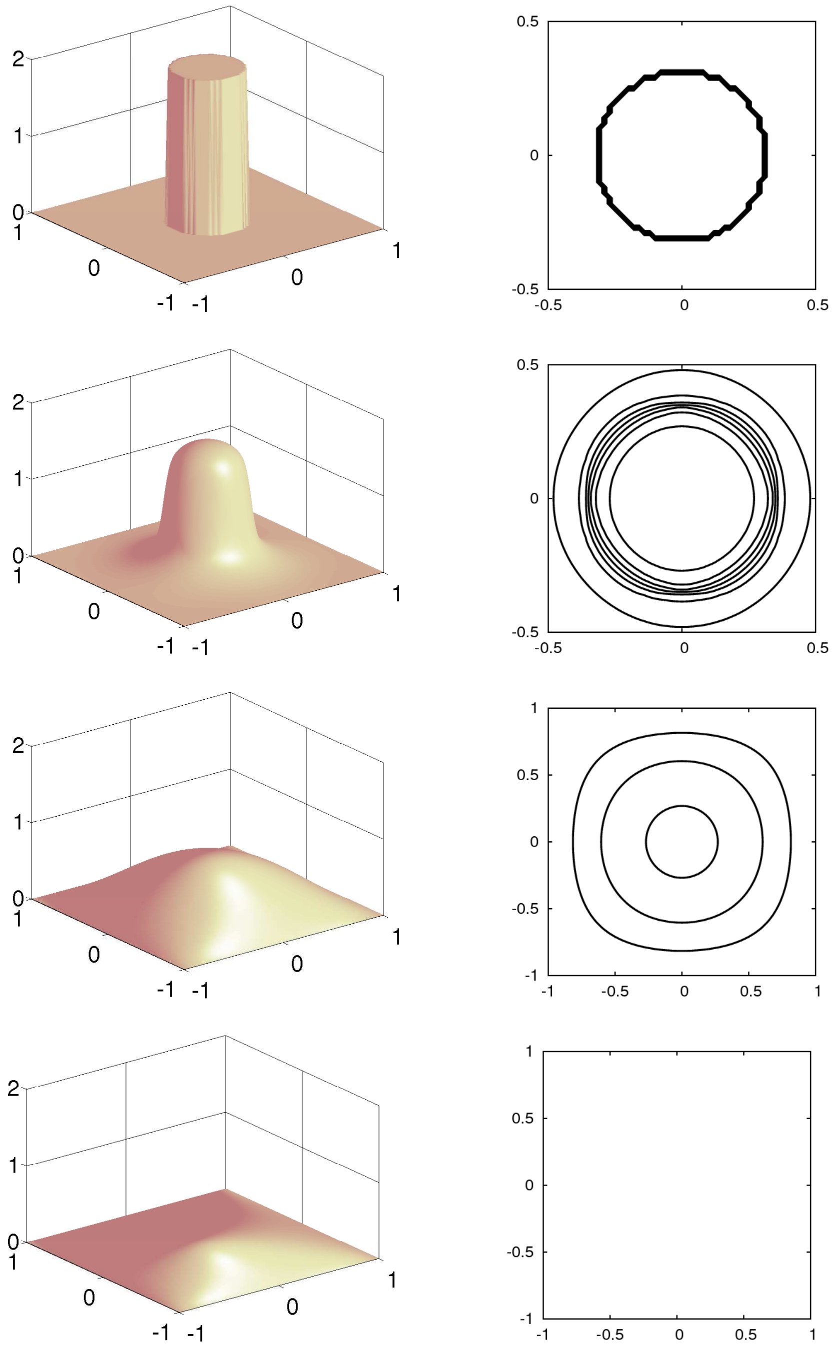

Figure 7.31.: **The explicit finite difference** numerical scheme for the **Willmore flow of graphs** at times $t = 0$, $t = 0.00625$, $t = 0.03125$ and $t = 0.125$ (graph of u on the left, level-lines of u on the right). See the Numerical experiment 7.2.12.

Numerical experiment 7.2.13. Test of the **explicit finite difference** numerical scheme for the **isotropic mean-curvature flow of graphs**

$$
\begin{aligned}
\partial_t \varphi &= Q \nabla \cdot \left(\frac{\nabla \varphi}{Q} \right) \quad \text{on } (0, \mathrm{T}\rangle \times \Omega, \\
\varphi \mid_{t=0} &= \sin \left(\pi \tanh \left(5 \left(\left(x^2 + y^2 \right) - 0.25 \right) \right) \right) \quad \text{on } \Omega,
\end{aligned}
$$

with the Dirichlet boundary condition

$$
\varphi = 0 \quad \text{on } \partial\Omega.
$$

Computational domain: $\Omega \equiv [-1, 1]^2$.
Final time: $T = 0.125$.
Space steps: $h = 0.02$.
Time step: Adaptive.
Numerical scheme: 6.3.6.
Figure: 7.32.
Remark: –

Numerical experiment 7.2.14. Test of the **explicit finite difference** numerical scheme for the **isotropic Willmore flow of graphs**

$$
\begin{aligned}
\partial_t \varphi &= Q \nabla \cdot \left(\frac{\nabla \varphi}{Q} \right) \quad \text{on } (0, \mathrm{T}\rangle \times \Omega, \\
\varphi \mid_{t=0} &= \sin \left(\pi \tanh \left(5 \left(\left(x^2 + y^2 \right) - 0.25 \right) \right) \right) \quad \text{on } \Omega,
\end{aligned}
$$

with the Dirichlet boundary condition

$$
\varphi = 0 \quad \text{on } \partial\Omega.
$$

Computational domain: $\Omega \equiv [-1, 1]^2$.
Final time: $T = 0.1$.
Space steps: $h = 0.02$.
Time step: Adaptive.
Numerical scheme: 6.3.7
Figure: 7.33.
Remark: –

Isotropic graph formulation of the mean-curvature flow

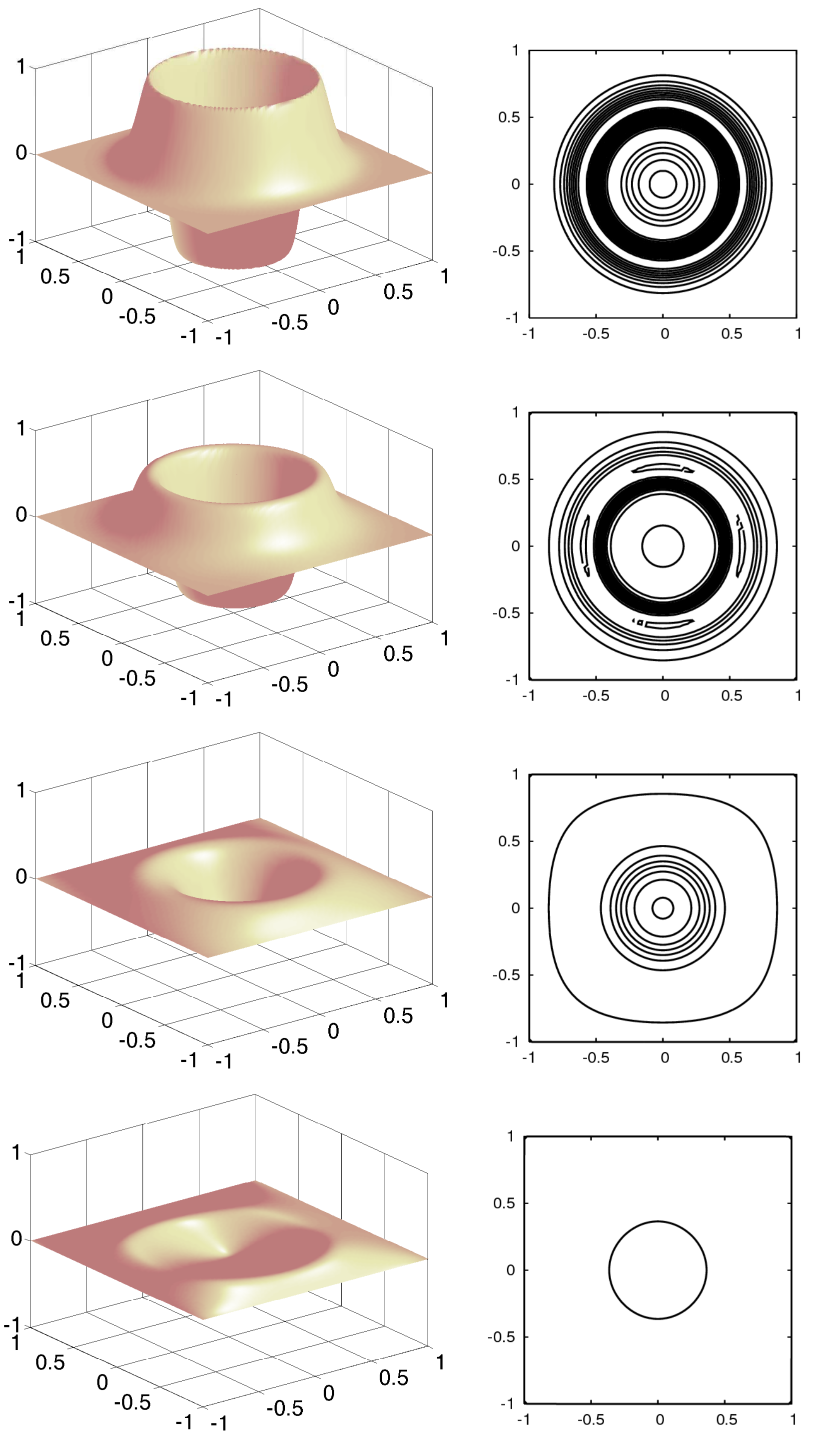

Figure 7.32.: **The explicit finite difference** numerical scheme for the **mean-curvature flow of graphs** at times $t = 0$, $t = 0.0125$, $t = 0.0625$ and $t = 0.125$ (graph of u on the left, level-lines of u on the right). See the Numerical experiment 7.2.13.

Isotropic graph formulation of the Willmore flow

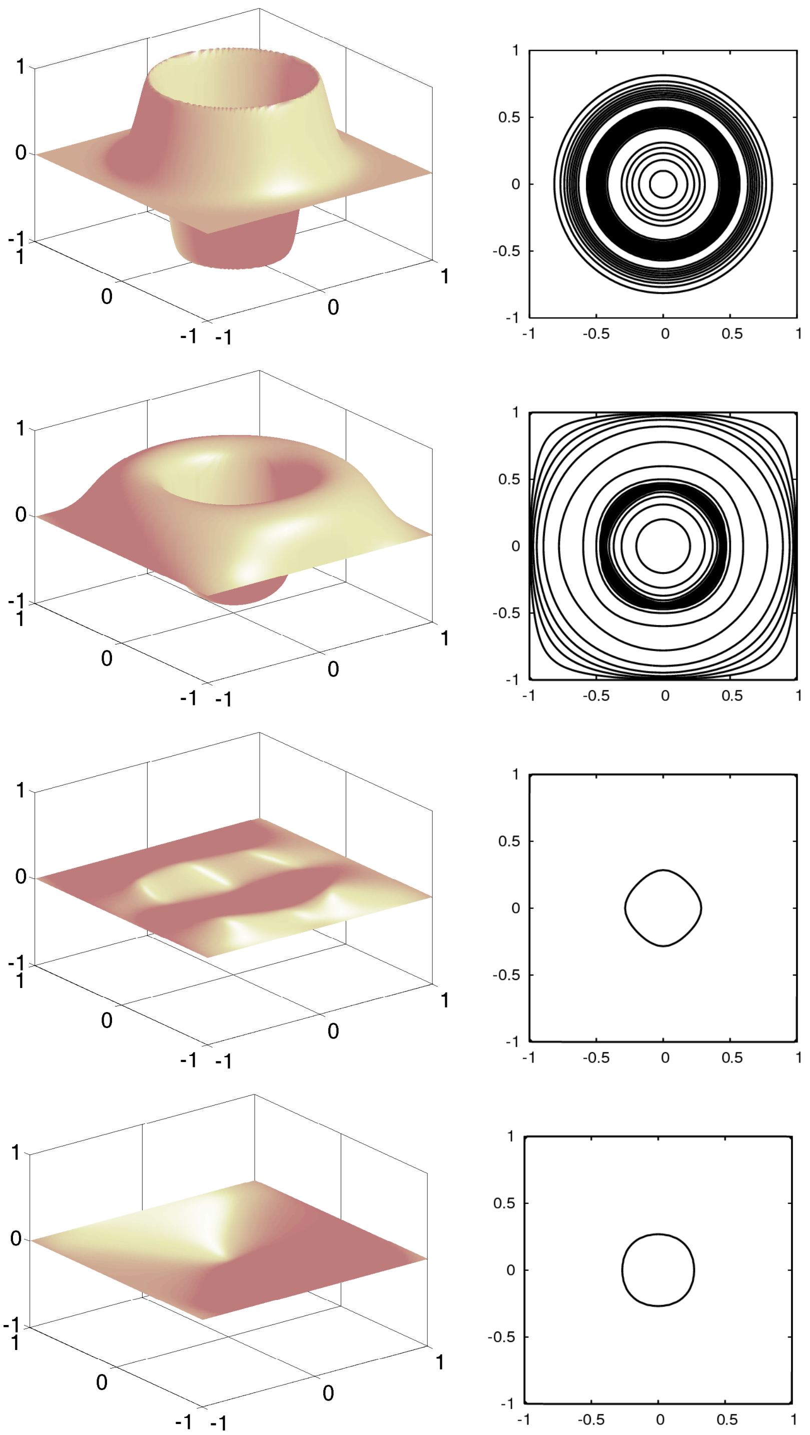

Figure 7.33.: **The explicit finite difference** numerical scheme for the **Willmore flow of graphs** at times $t = 0$, $t = 0.00625$, $t = 0.025$ and steady state at $t = 0.1$ (graph of u on the left, level-lines of u on the right). See the Numerical experiment 7.2.14.

Numerical experiment 7.2.15. Test of the **explicit finite difference** numerical scheme for the **isotropic mean-curvature flow of graphs**

$$\begin{aligned}\partial_t \varphi &= Q\nabla\cdot\left(\frac{\nabla\varphi}{Q}\right) \quad \text{on } (0,\mathrm{T}\rangle\times\Omega,\\ \varphi\mid_{t=0} &= -0.5\sin^2(\pi x)\cdot\left(1-(y-2)^2\right)\left(1-\tanh\left(10\left(\sqrt{x^2+y^2}-0.6\right)\right)\right) \quad \text{on } \Omega,\end{aligned}$$

with the Dirichlet boundary condition

$$\varphi = 0 \quad \text{on } \partial\Omega.$$

Computational domain: $\Omega\equiv[-1,1]^2$.
Initial condition:
$u_{ini}(x,y) := -0.5\sin^2(\pi x)\cdot\left(1-(y-2)^2\right)\left(1-\tanh\left(10\left(\sqrt{x^2+y^2}-0.6\right)\right)\right)$.
Boundary conditions: $u = w = 0$ on $\partial\Omega$.
Final time: $T = 0.5$.
Space steps: $h = 0.02$.
Time step: Adaptive.
Numerical scheme: 6.3.6
Figure: 7.34.
Remark: –

Numerical experiment 7.2.16. Test of the **explicit finite difference** numerical scheme for the **isotropic Willmore flow of graphs**

$$\begin{aligned}\partial_t \varphi &= Q\nabla\cdot\left(\frac{\nabla\varphi}{Q}\right) \quad \text{on } (0,\mathrm{T}\rangle\times\Omega,\\ \varphi\mid_{t=0} &= -0.5\sin^2(\pi x)\cdot\left(1-(y-2)^2\right)\left(1-\tanh\left(10\left(\sqrt{x^2+y^2}-0.6\right)\right)\right) \quad \text{on } \Omega,\end{aligned}$$

with the Dirichlet boundary condition

$$\varphi = 0 \quad \text{on } \partial\Omega.$$

Computational domain: $\Omega\equiv[-1,1]^2$.
Final time: $T = 0.5$.
Space steps: $h = 0.02$.
Time step: Adaptive.
Numerical scheme: 6.3.7
Figure: 7.35.
Remark: –

Isotropic graph formulation of the mean-curvature flow

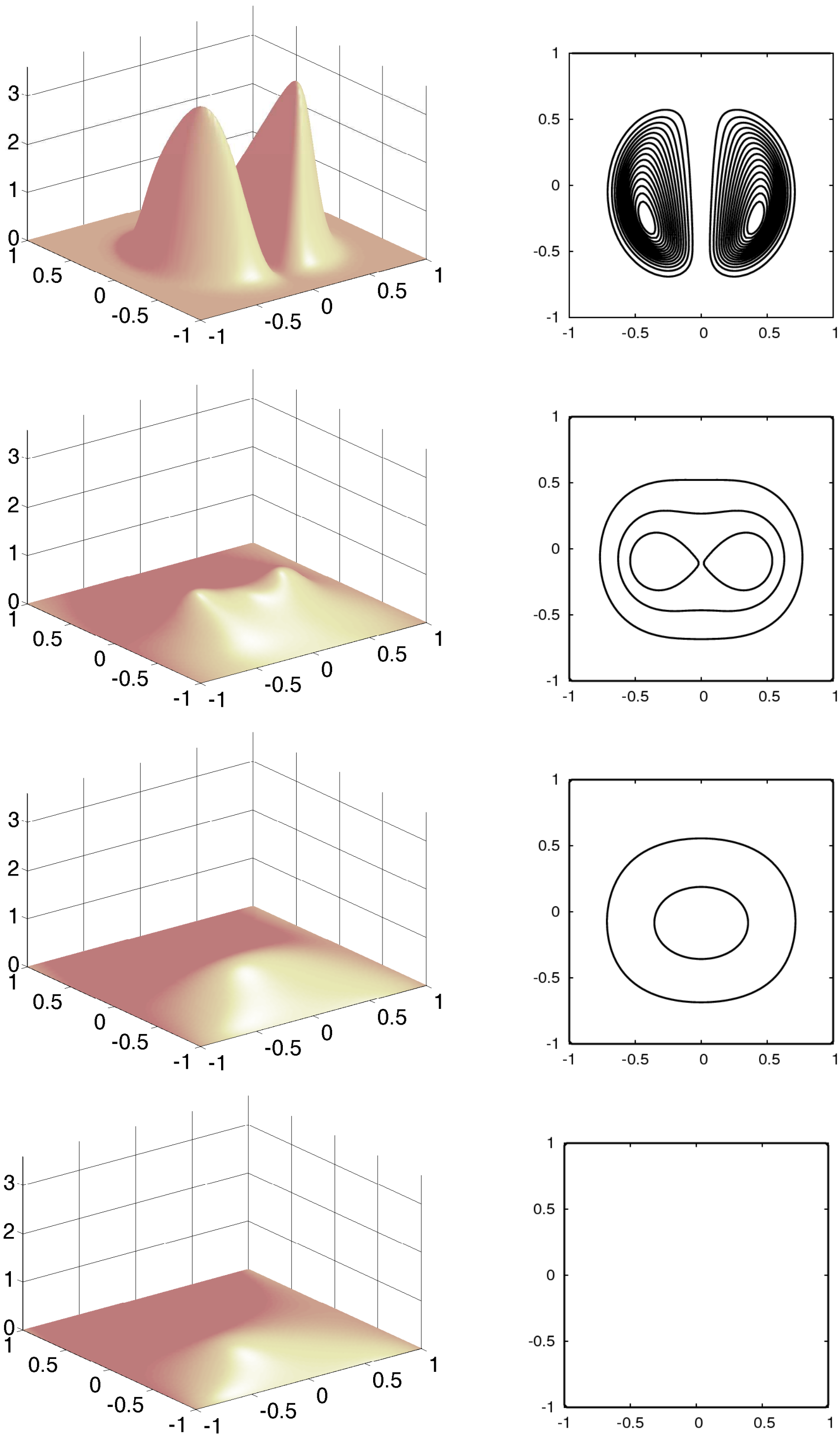

Figure 7.34.: **The explicit finite difference** numerical scheme for the **mean-curvature flow of graphs** at times $t = 0$, $t = 0.0625$, $t = 0.125$ and $t = 0.5$ (graph of u on the left, level-lines of u on the right). See the Numerical experiment 7.2.15.

Isotropic graph formulation of the Willmore flow

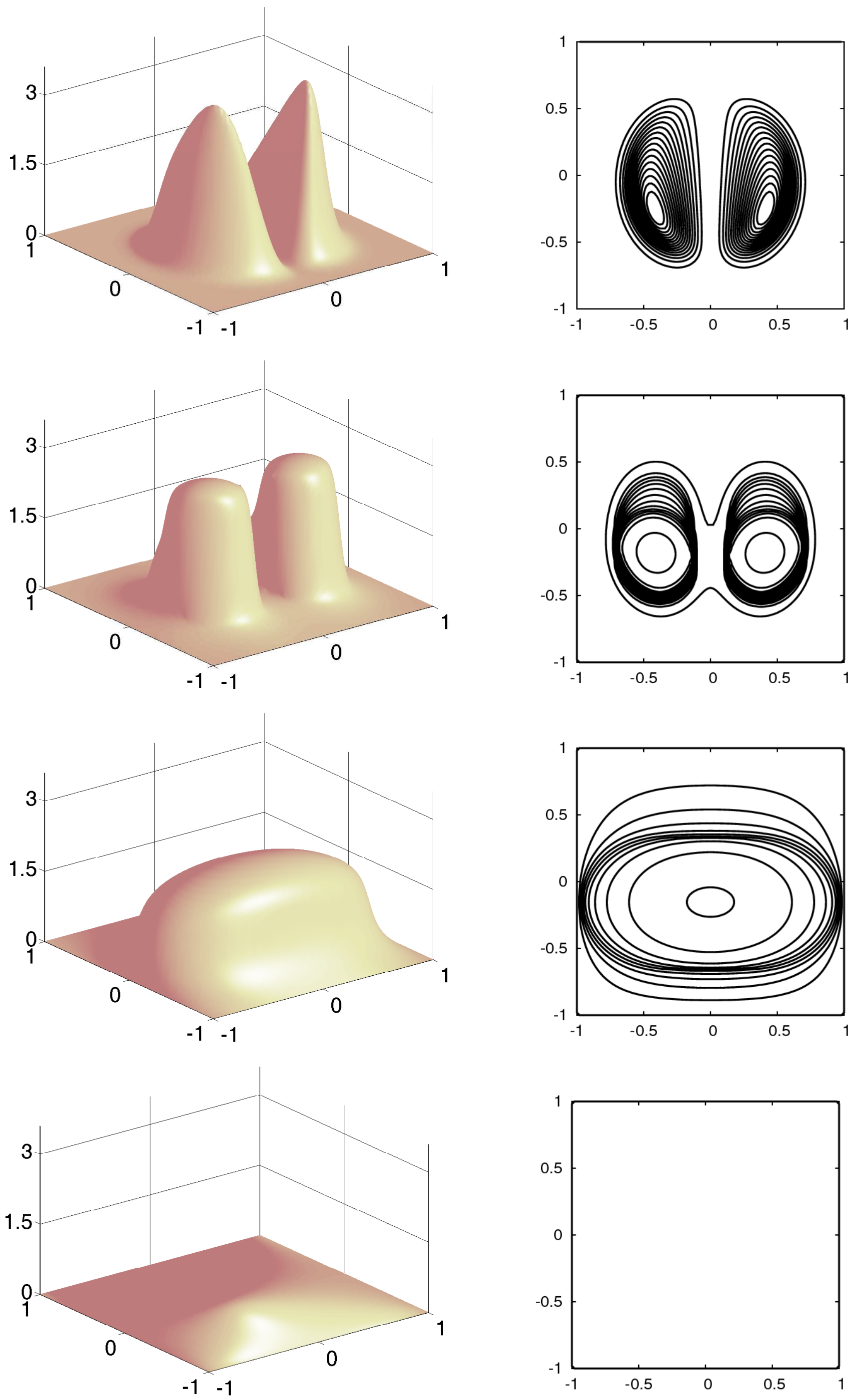

Figure 7.35.: **The explicit finite difference** numerical scheme for the **Willmore flow of graphs** at times $t = 0$, $t = 0.00125$, $t = 0.025$ and $t = 0.5$ (graph of u on the left, level-lines of u on the right). See the Numerical experiment 7.2.16.

Numerical experiment 7.2.17. Test of the **explicit finite difference** numerical scheme for the **isotropic mean-curvature flow of graphs**

$$\begin{aligned}\partial_t \varphi &= Q\nabla\cdot\left(\frac{\nabla\varphi}{Q}\right) \quad \text{on } (0,\mathrm{T}\rangle\times\Omega,\\ \varphi\mid_{t=0} &= \sin(2\pi x)\sin(2\pi y) \quad \text{on } \Omega,\end{aligned}$$

with the Neumann boundary condition

$$\partial_\nu\varphi = 0 \quad \text{on } \partial\Omega.$$

Computational domain: $\Omega\equiv[0,1]^2$.
Initial condition: $u_{ini}(x,y) := \sin(2\pi x)\sin(2\pi y)$.
Boundary conditions: $\partial_{\mathbf{n}}u = \partial_{\mathbf{n}}w = 0$ on $\partial\Omega$.
Final time: $T = 0.125$.
Space steps: $h = 0.01$.
Time step: Adaptive.
Numerical scheme: 6.3.6
Figure: 7.36.
Remark: See the Numerical experiment 7.2.9 with the same initial condition but the Dirichlet boundary conditions.

Numerical experiment 7.2.18. Test of the **explicit finite difference** numerical scheme for the **isotropic Willmore flow of graphs**

$$\begin{aligned}\partial_t \varphi &= Q\nabla\cdot\left(\frac{\nabla\varphi}{Q}\right) \quad \text{on } (0,\mathrm{T}\rangle\times\Omega,\\ \varphi\mid_{t=0} &= \sin(2\pi x)\sin(2\pi y) \quad \text{on } \Omega,\end{aligned}$$

with the Neumann boundary condition

$$\partial_\nu\varphi = \partial_\nu w = 0 \quad \text{on } \partial\Omega.$$

Computational domain: $\Omega\equiv[0,1]^2$.
Final time: $T = 0.025$.
Space steps: $h = 0.01$.
Time step: Adaptive.
Numerical scheme: 6.3.7
Figure: 7.37.
Remark: See the Numerical experiment 7.2.10 with the same initial condition but the Dirichlet boundary conditions.

Isotropic graph formulation of the mean-curvature flow

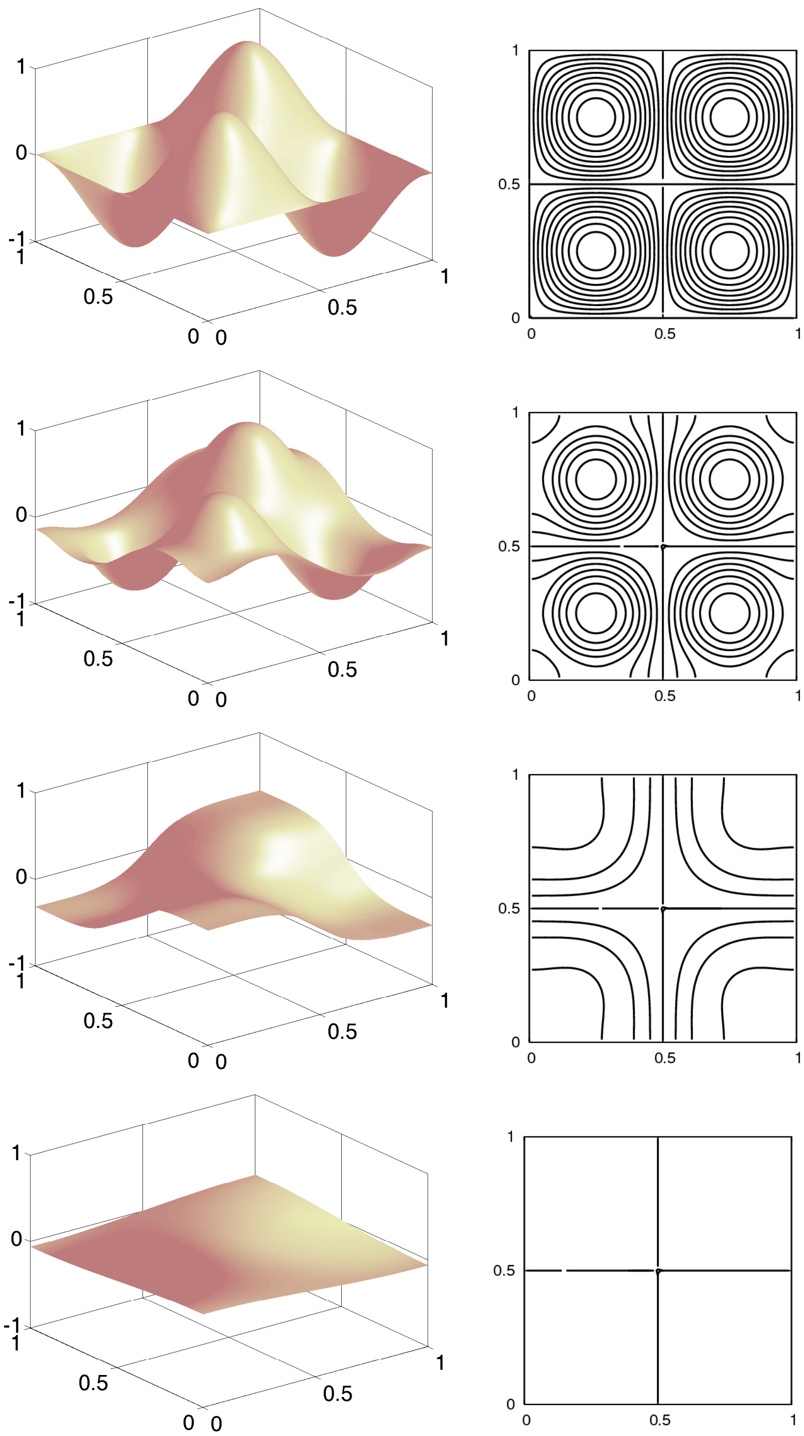

Figure 7.36.: **The explicit finite difference** numerical scheme for the **mean-curvature flow of graphs** at times $t = 0$, $t = 0.005$, $t = 0.025$ and $t = 0.125$ (graph of u on the left, level-lines of u on the right). See the Numerical experiment 7.2.17.

Isotropic graph formulation of the Willmore flow

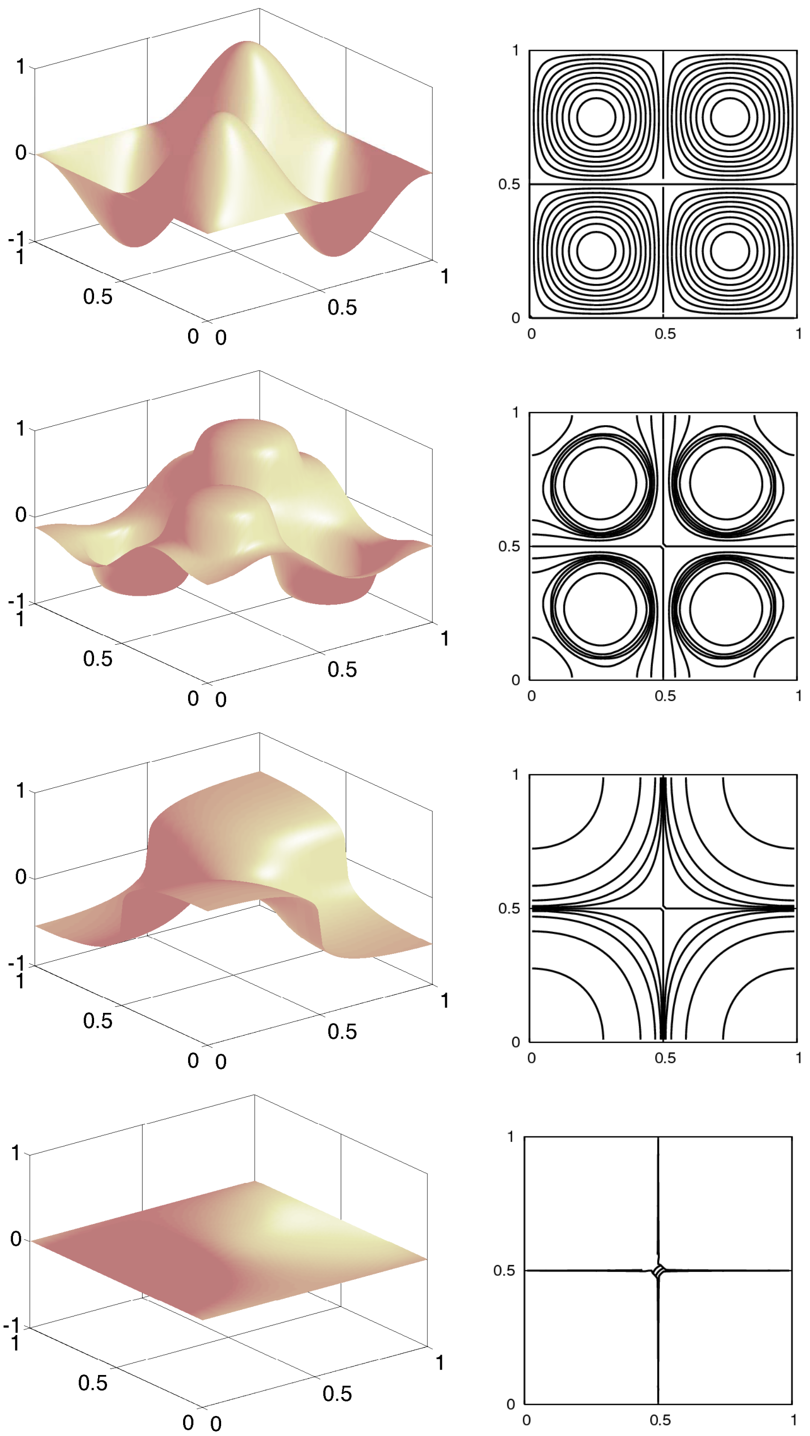

Figure 7.37.: **The explicit finite difference** numerical scheme for the **Willmore flow of graphs** at times $t = 0$, $t = 0.00025$, $t = 0.00125$ and $t = 0.025$ (graph of u on the left, level-lines of u on the right). See the Numerical experiment 7.2.18.

Numerical experiment 7.2.19. Test of the **explicit finite difference** numerical scheme for the **isotropic mean-curvature flow of graphs**

$$\begin{aligned} \partial_t\varphi &= Q\nabla\cdot\left(\frac{\nabla\varphi}{Q}\right) \quad \text{on } (0,\mathrm{T}\rangle\times\Omega, \\ \varphi\,|_{t=0} &= \sin\left(3\pi\sqrt{x^2+y^2}\right) \quad \text{on } \Omega, \end{aligned}$$

with the Neumann boundary condition

$$\partial_\nu\varphi = 0 \quad \text{on } \partial\Omega.$$

Computational domain: $\Omega\equiv[-2,2]^2$.
Final time: $T = 0.5$.
Space steps: $h = 0.04$.
Time step: Adaptive.
Numerical scheme: 6.3.6
Figure: 7.38.
Remark: –

Numerical experiment 7.2.20. Test of the **explicit finite difference** numerical scheme for the **isotropic Willmore flow of graphs**

$$\begin{aligned} \partial_t\varphi &= Q\nabla\cdot\left(\frac{\nabla\varphi}{Q}\right) \quad \text{on } (0,\mathrm{T}\rangle\times\Omega, \\ \varphi\,|_{t=0} &= \sin\left(3\pi\sqrt{x^2+y^2}\right) \quad \text{on } \Omega, \end{aligned}$$

with the Neumann boundary condition

$$\partial_\nu\varphi = \partial_\nu w0 \quad \text{on } \partial\Omega.$$

Computational domain: $\Omega\equiv[-2,2]^2$.
Initial condition: $u_{ini}(x,y) := \sin\left(3\pi\sqrt{x^2+y^2}\right)$.
Boundary conditions: $\partial_{\mathbf{n}}u = \partial_{\mathbf{n}}w = 0$ on $\partial\Omega$.
Final time: $T = 0.1$.
Space steps: $h = 0.04$.
Time step: Adaptive.
Numerical scheme: 6.3.7
Figure: 7.39.
Remark: –

Isotropic graph formulation of the mean-curvature flow

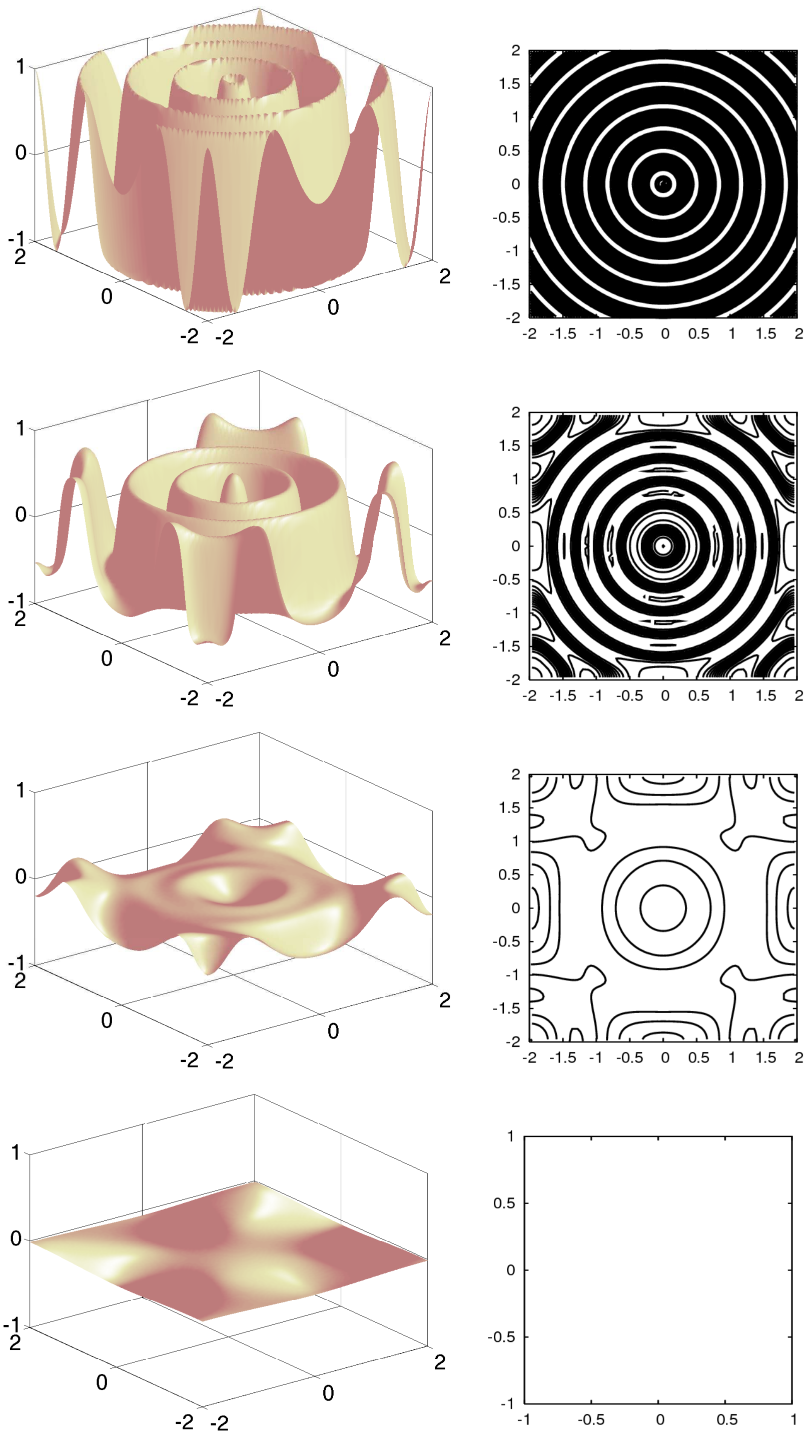

Figure 7.38.: **The explicit finite difference** numerical scheme for the **mean-curvature flow of graphs** at times $t = 0$, $t = 0.025$, $t = 0.1$ and $t = 0.5$ (graph of u on the left, level-lines of u on the right). See the Numerical experiment 7.2.19.

Isotropic graph formulation of the Willmore flow

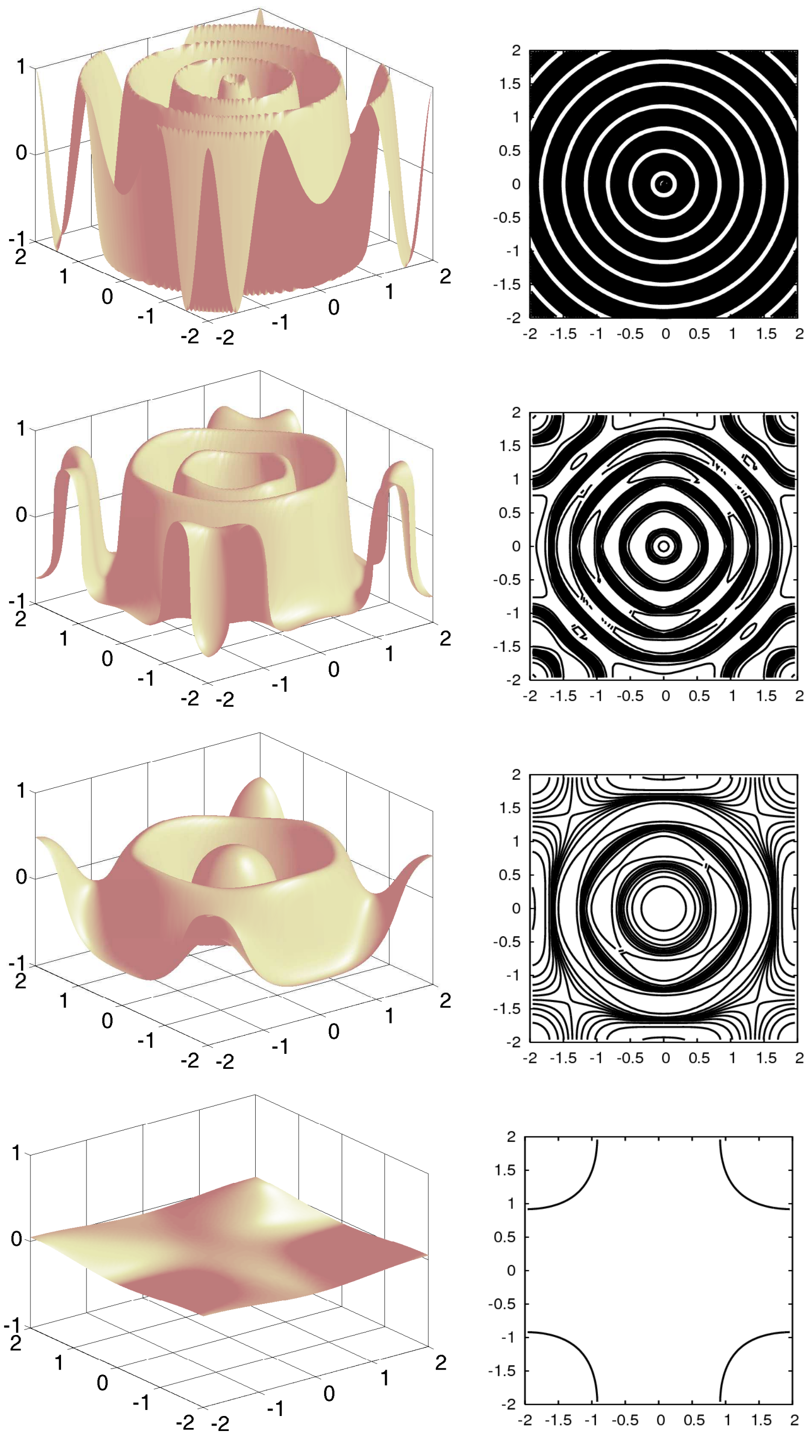

Figure 7.39.: **The explicit finite difference** numerical scheme for the **Willmore flow of graphs** at times $t = 0$, $t = 0.01$, $t = 0.025$ and $t = 0.1$ (graph of u on the left, level-lines of u on the right). See the Numerical experiment 7.2.20.

Numerical experiment 7.2.21. Test of the **explicit finite difference** numerical scheme for the **anisotropic mean-curvature flow of graphs**

$$
\begin{aligned}
\partial_t \varphi &= Q \nabla_{\mathbf{p}} \gamma_{\mathbb{G}} \left(\nabla \varphi, -1 \right) \quad \text{on } (0, \mathrm{T}\rangle \times \Omega \\
\varphi \mid_{t=0} &= \operatorname{sign}\left(x^2 + y^2 - 0.1 \right) + 1 \quad \text{on } \Omega
\end{aligned}
$$

where the anisotropy function $\gamma_{\mathbb{G}}$ is given by

$$
\gamma_{\mathbb{G}} \left(\nabla \varphi, -1 \right) := \sqrt{1 + \nabla \varphi^T \mathbb{G} \nabla \varphi}, \text{ for } \mathbb{G} := \begin{pmatrix} 2 & 0 \\ 0 & 1 \end{pmatrix}
$$

and we apply the Dirichlet boundary conditions

$$
\varphi = 0 \quad \text{on } \partial\Omega.
$$

Computational domain: $\Omega \equiv [-0.5, 0.5]^2$.
Final time: $T = 0.1$.
Space steps: $h = 0.01$.
Time step: Adaptive.
Numerical scheme: 6.3.6
Figure: 7.40.
Remark: Compare with the Numerical experiment 7.2.11.

Numerical experiment 7.2.22. Test of the **explicit finite difference** numerical scheme for the **anisotropic Willmore flow of graphs**

$$
\begin{aligned}
\partial_t \varphi &= -Q \nabla \cdot \left(\mathbb{E}_\gamma \nabla w_\gamma - \frac{1}{2} \frac{w_\gamma^2}{Q^3} \nabla \varphi \right) \quad \text{on } (0, T) \times \Omega, \\
w_\gamma &= Q H_\gamma \quad \text{on } (0, T) \times \Omega, \\
\varphi \mid_{t=0} &= \operatorname{sign}\left(x^2 + y^2 - 0.1 \right) + 1 \quad \text{on } \Omega,
\end{aligned}
$$

where the anisotropy function $\gamma_{\mathbb{G}}$ is given by

$$
\gamma_{\mathbb{G}} \left(\nabla \varphi, -1 \right) := \sqrt{1 + \nabla \varphi^T \mathbb{G} \nabla \varphi}, \text{ for } \mathbb{G} := \begin{pmatrix} 2 & 0 \\ 0 & 1 \end{pmatrix}
$$

and we apply the Dirichlet boundary conditions

$$
\varphi = w_\gamma = 0 \quad \text{on } \partial\Omega.
$$

Computational domain: $\Omega \equiv [-1, 1]^2$.
Final time: $T = 0.001$.
Space steps: $h = 0.02$.
Time step: Adaptive.
Numerical scheme: 6.3.7
Figure: 7.41.
Remark: Compare with the Numerical experiment 7.2.12.

Anisotropic graph formulation of the mean-curvature flow

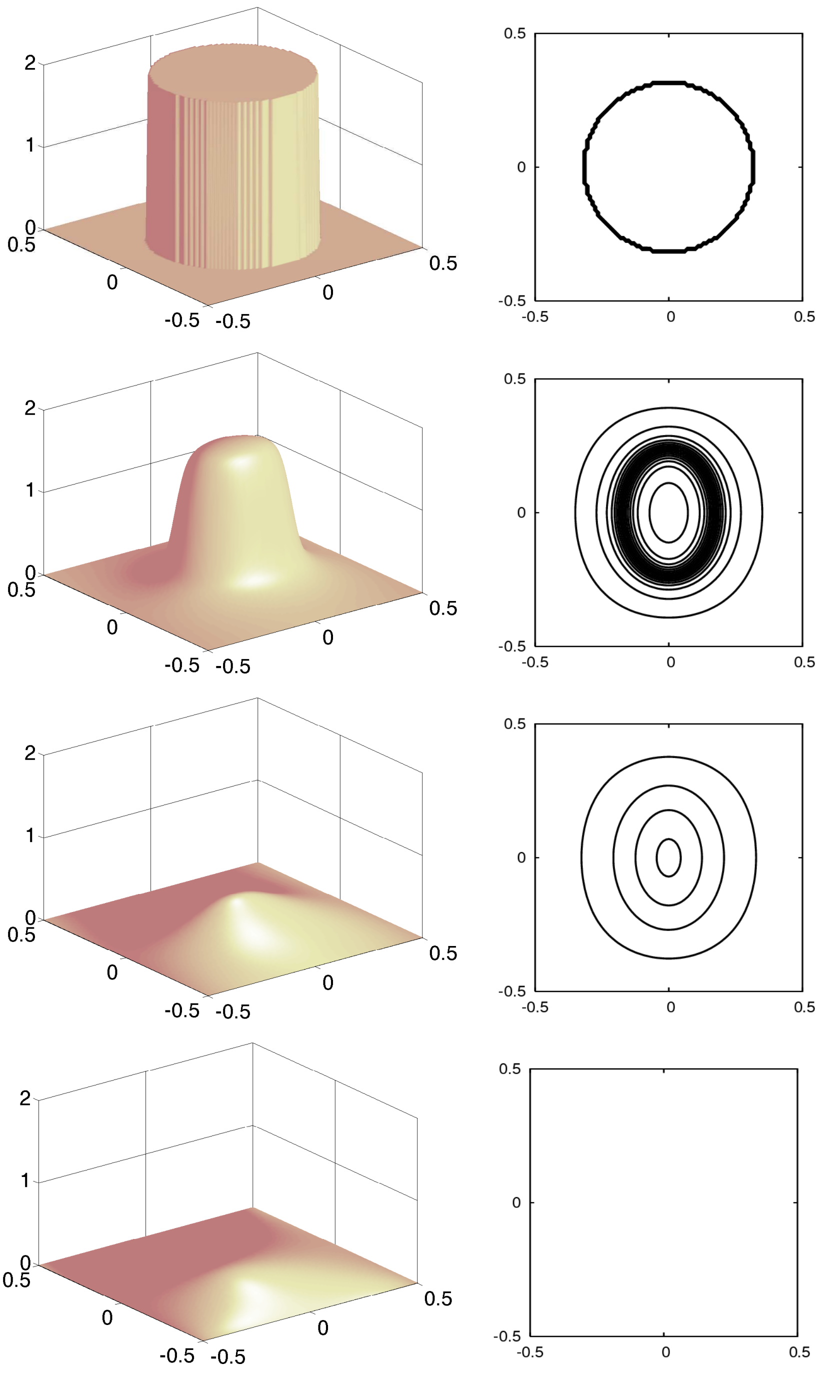

Figure 7.40.: **The explicit finite difference** numerical scheme for the **anisotropic mean-curvature flow of graphs** at times $t = 0$, $t = 0.025$, $t = 0.05$ and $t = 0.1$ (graph of φ on the left, level-lines of φ on the right). See the Numerical experiment 7.2.21.

Anisotropic graph formulation of the Willmore flow

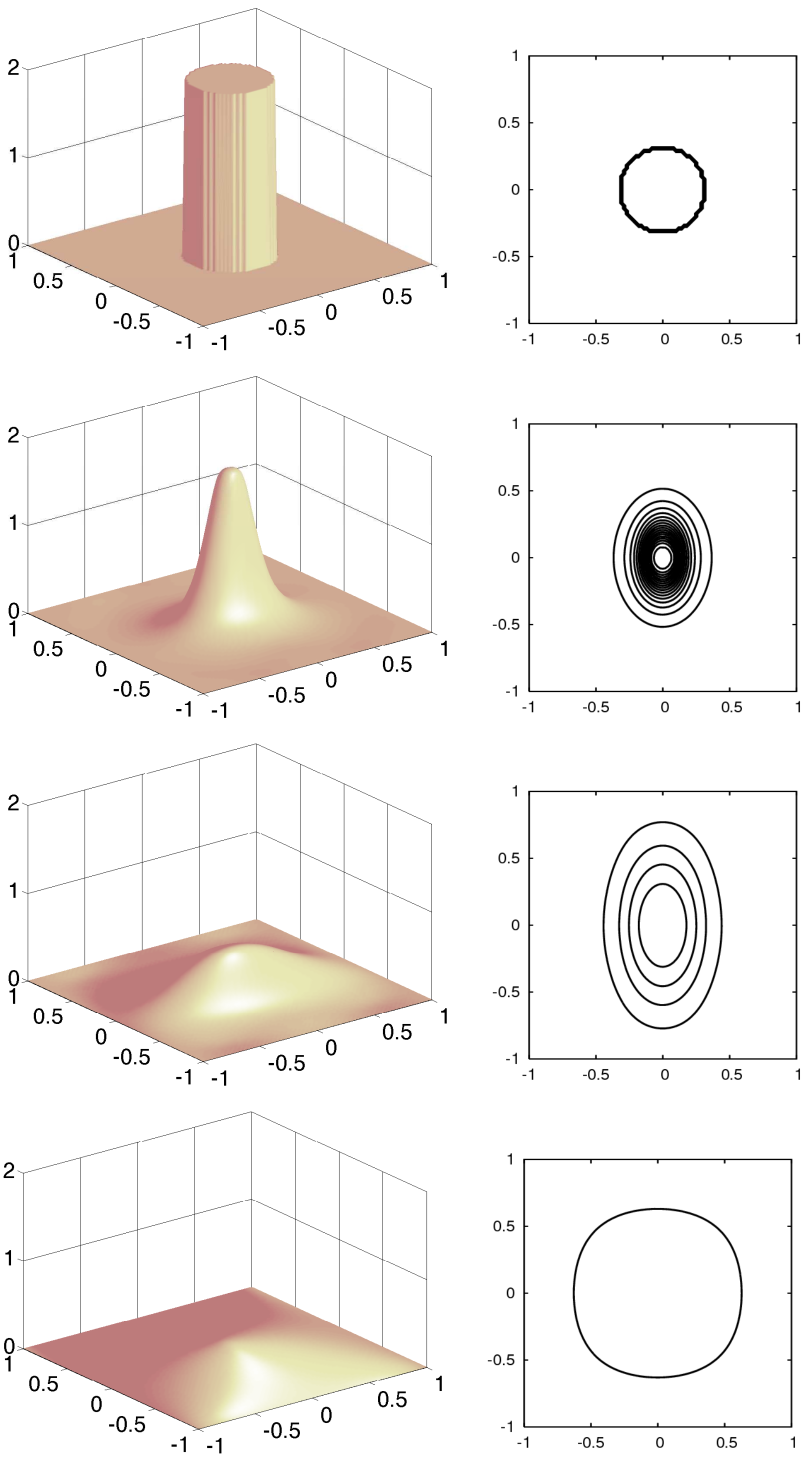

Figure 7.41.: **The explicit finite difference** numerical scheme for the **anisotropic Willmore flow of graphs** at times $t = 0$, $t = 5 \cdot 10^{-5}$, $t = 2.5 \cdot 10^{-4}$ and $t = 0.001$ (graph of φ on the left, level-lines of φ on the right). See the Numerical experiment 7.2.22.

Numerical experiment 7.2.23. Test of the **explicit finite difference** numerical scheme for the **anisotropic mean-curvature flow of graphs**

$$\begin{aligned}\partial_t \varphi &= Q \nabla_{\mathbf{p}} \gamma_{\mathbb{G}} \left(\nabla \varphi, -1 \right) \quad \text{on } (0, \mathrm{T}\rangle \times \Omega \\ \varphi \mid_{t=0} &= \operatorname{sign}\left(x^2 + y^2 - 0.1 \right) + 1 \quad \text{on } \Omega\end{aligned}$$

where the anisotropy function $\gamma_{\mathbb{G}}$ is given by

$$\gamma_{\mathbb{G}} \left(\nabla \varphi, -1 \right) := \sqrt{1 + \nabla \varphi^T \mathbb{G} \nabla \varphi}, \text{ for } \mathbb{G} := \begin{pmatrix} 2 & 1 \\ 1 & 2 \end{pmatrix}$$

and we apply the Dirichlet boundary conditions

$$\varphi = 0 \quad \text{on } \partial \Omega.$$

Computational domain: $\Omega \equiv [-0.5, 0.5]^2$.
Final time: $T = 0.0625$.
Space steps: $h = 0.01$.
Time step: Adaptive.
Numerical scheme: 6.3.6
Figure: 7.42.
Remark: Compare with the Numerical experiment 7.2.11.

Numerical experiment 7.2.24. Test of the **explicit finite difference** numerical scheme for the **anisotropic Willmore flow of graphs**

$$\begin{aligned}\partial_t \varphi &= -Q \nabla \cdot \left(\mathbb{E}_\gamma \nabla w_\gamma - \frac{1}{2} \frac{w_\gamma^2}{Q^3} \nabla \varphi \right) \quad \text{on } (0, T) \times \Omega, \\ w_\gamma &= Q H_\gamma \quad \text{on } (0, T) \times \Omega, \\ \varphi \mid_{t=0} &= \operatorname{sign}\left(x^2 + y^2 - 0.1 \right) + 1 \quad \text{on } \Omega,\end{aligned}$$

where the anisotropy function $\gamma_{\mathbb{G}}$ is given by

$$\gamma_{\mathbb{G}} \left(\nabla \varphi, -1 \right) := \sqrt{1 + \nabla \varphi^T \mathbb{G} \nabla \varphi}, \text{ for } \mathbb{G} := \begin{pmatrix} 2 & 1 \\ 1 & 2 \end{pmatrix}$$

and we apply the Dirichlet boundary conditions

$$\varphi = w_\gamma = 0 \quad \text{on } \partial \Omega.$$

Computational domain: $\Omega \equiv [-1, 1]^2$.
Final time: $T = 0.01$.
Space steps: $h = 0.02$.
Time step: Adaptive.
Numerical scheme: 6.3.7
Figure: 7.43.
Remark: Compare with the Numerical experiment 7.2.12.

Anisotropic graph formulation of the mean-curvature flow

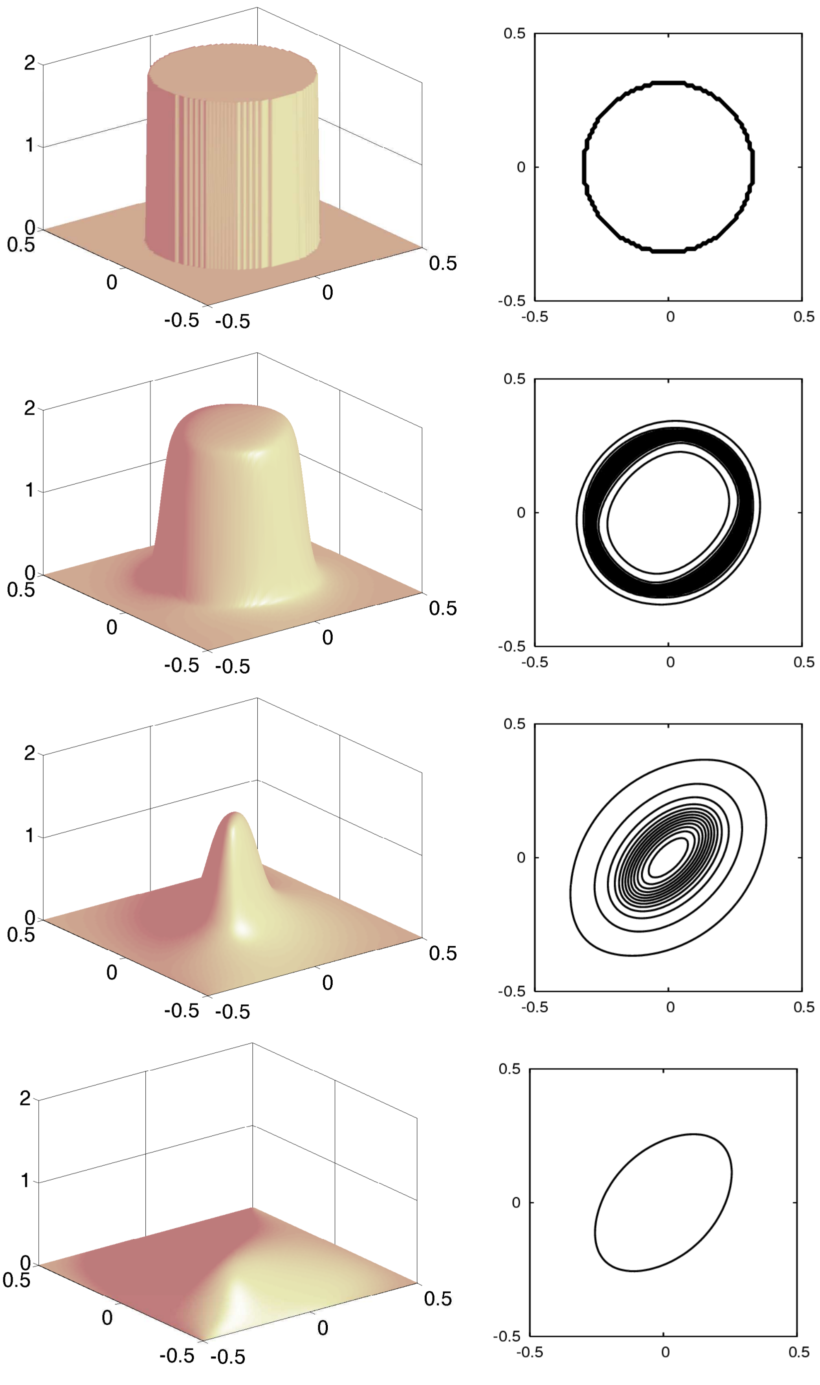

Figure 7.42.: **The explicit finite difference** numerical scheme for the **anisotropic mean-curvature flow of graphs** at times $t = 0$, $t = 0.00625$, $t = 0.03125$ and $t = 0.0625$ (graph of φ on the left, level-lines of φ on the right). See the Numerical experiment 7.2.23.

Anisotropic graph formulation of the Willmore flow

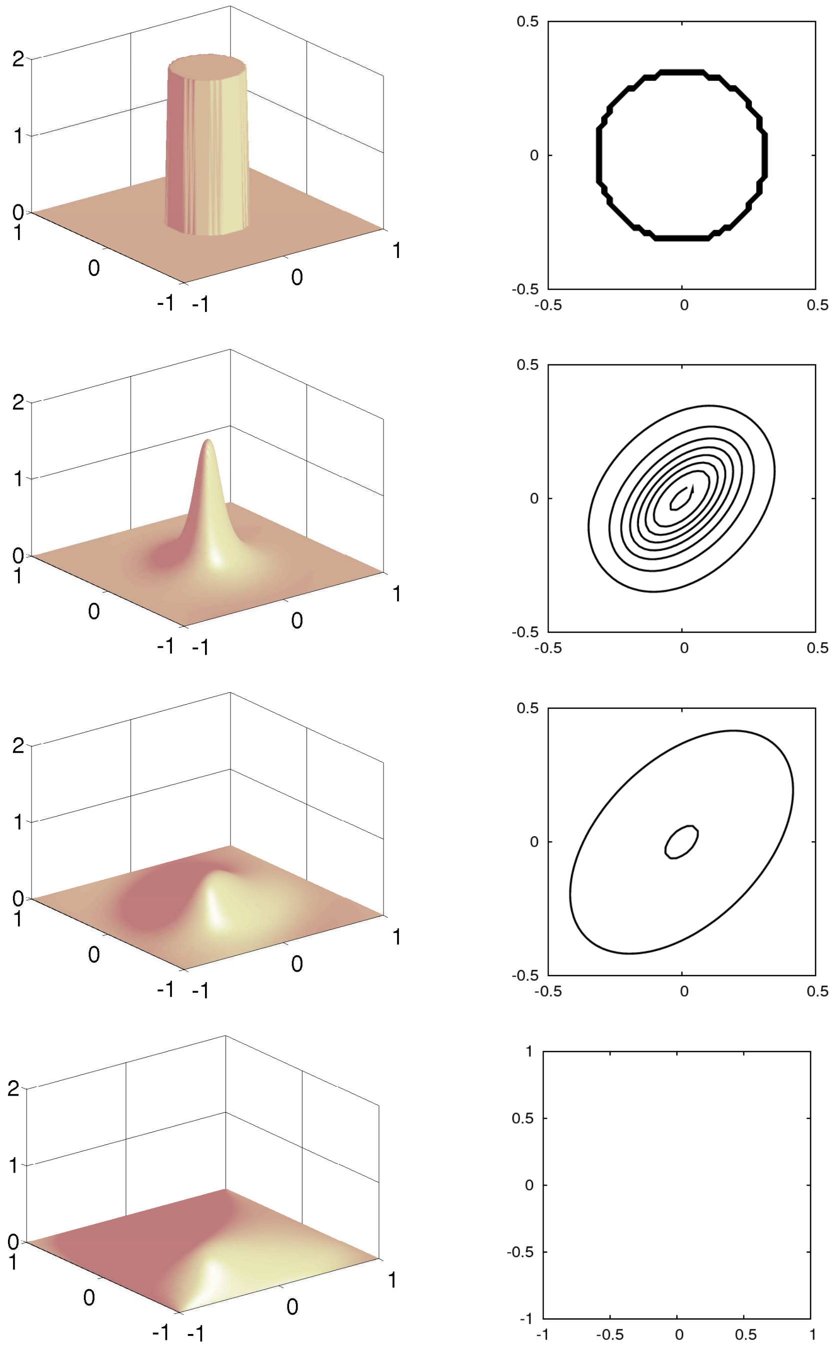

Figure 7.43.: **The explicit finite difference** numerical scheme for the **anisotropic Willmore flow of graphs** at times $t = 0$, $t = 0.0001$, $t = 0.0005$ and $t = 0.01$ (graph of φ on the left, level-lines of φ on the right). See the Numerical experiment 7.2.24.

Numerical experiment 7.2.25. Test of the **explicit finite difference** numerical scheme for the **anisotropic mean-curvature flow of graphs**

$$\begin{aligned} \partial_t \varphi &= Q \nabla_{\mathbf{p}} \gamma_{\mathbb{G}} (\nabla \varphi, -1) \quad \text{on } (0, \mathrm{T}\rangle \times \Omega \\ \varphi \,|_{t=0} &= \sin(2\pi x) \sin(2\pi y) \quad \text{on } \Omega \end{aligned}$$

where the anisotropy function $\gamma_{\mathbb{G}}$ is given by

$$\gamma_{\mathbb{G}} (\nabla \varphi, -1) := \sqrt{1 + \nabla \varphi^T \mathbb{G} \nabla \varphi}, \text{ for } \mathbb{G} := \begin{pmatrix} 10 & 0 \\ 0 & 1 \end{pmatrix}$$

and we apply the Neumann boundary conditions

$$\nabla_{\mathbf{p}} \gamma \cdot \nu = 0 \quad \text{on } \partial\Omega.$$

Computational domain: $\Omega \equiv [0,1]^2$.
Final time: $T = 0.125$.
Space steps: $h = 0.01$.
Time step: $\tau = 2 \cdot 10^{-5}$.
Numerical scheme: 6.3.8
Figure: 7.44.
Remark: Compare with the Numerical experiment 7.2.17.

Numerical experiment 7.2.26. Test of the **explicit finite difference** numerical scheme for the **anisotropic Willmore flow of graphs**

$$\begin{aligned} \partial_t \varphi &= -Q \nabla \cdot \left(\mathbb{E}_\gamma \nabla w_\gamma - \frac{1}{2} \frac{w_\gamma^2}{Q^3} \nabla \varphi \right) \quad \text{on } (0, T) \times \Omega, \\ w_\gamma &= Q H_\gamma \quad \text{on } (0, T) \times \Omega, \\ \varphi \,|_{t=0} &= \sin(2\pi x) \sin(2\pi y) \quad \text{on } \Omega, \end{aligned}$$

where the anisotropy function $\gamma_{\mathbb{G}}$ is given by

$$\gamma_{\mathbb{G}} (\nabla \varphi, -1) := \sqrt{1 + \nabla \varphi^T \mathbb{G} \nabla \varphi}, \text{ for } \mathbb{G} := \begin{pmatrix} 10 & 0 \\ 0 & 1 \end{pmatrix}$$

and we apply the Neumann boundary conditions

$$\partial_\nu \varphi = \mathbb{E}_\gamma \nabla w_\gamma \cdot \nu = 0 \quad \text{on } \partial\Omega.$$

Computational domain: $\Omega \equiv [0,1]^2$.
Final time: $T = 10^{-4}$.
Space steps: $h = 0.01$.
Time step: Adaptive.
Numerical scheme: 6.3.7
Figure: 7.45.
Remark: Compare with the Numerical experiment 7.2.18.

Anisotropic graph formulation of the mean-curvature flow

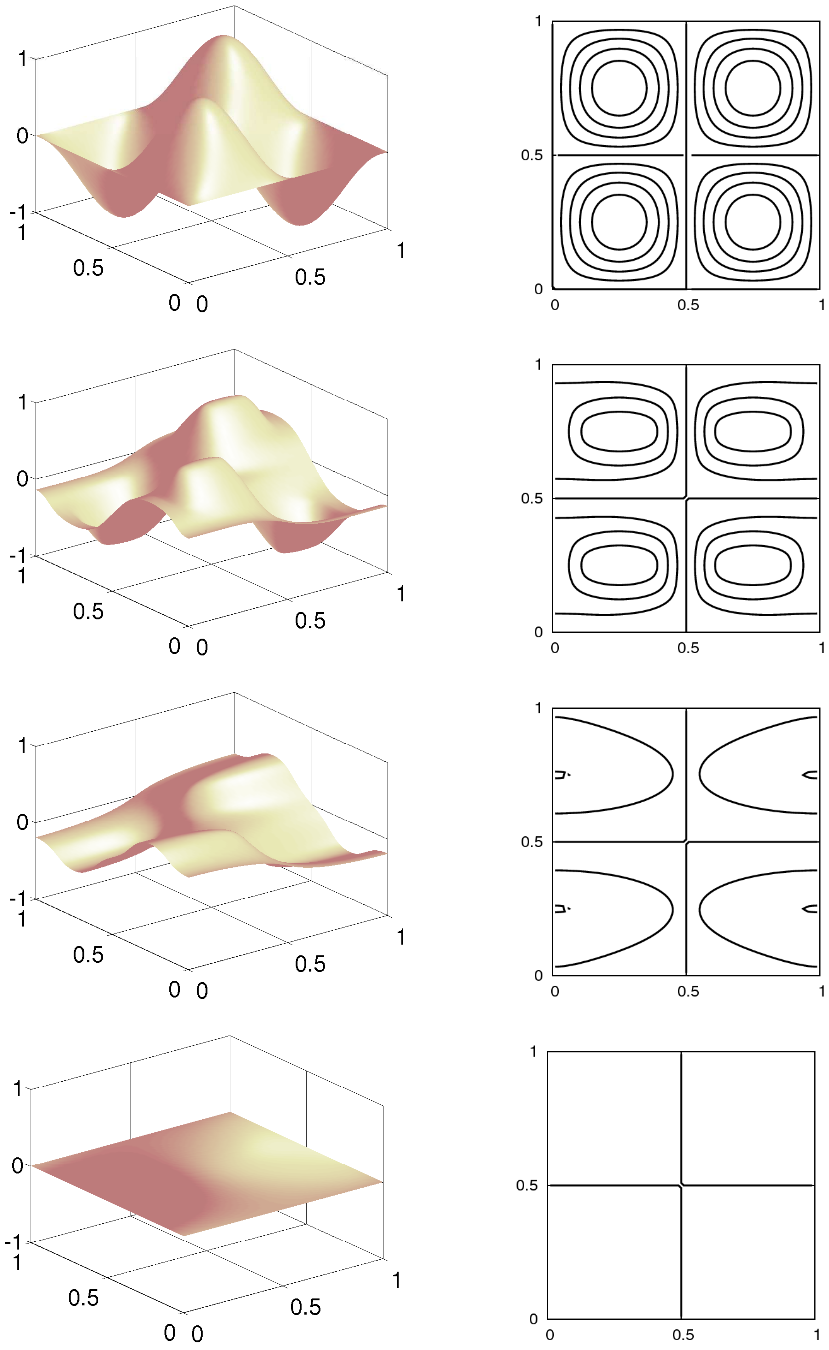

Figure 7.44.: The semi-implicit finite difference numerical scheme for the **anisotropic mean-curvature flow of graphs** at times $t = 0$, $t = 0.0025$, $t = 0.01$ and $t = 0.125$ (graph of φ on the left, level-lines of φ on the right). See the Numerical experiment 7.2.25.

Anisotropic graph formulation of the Willmore flow

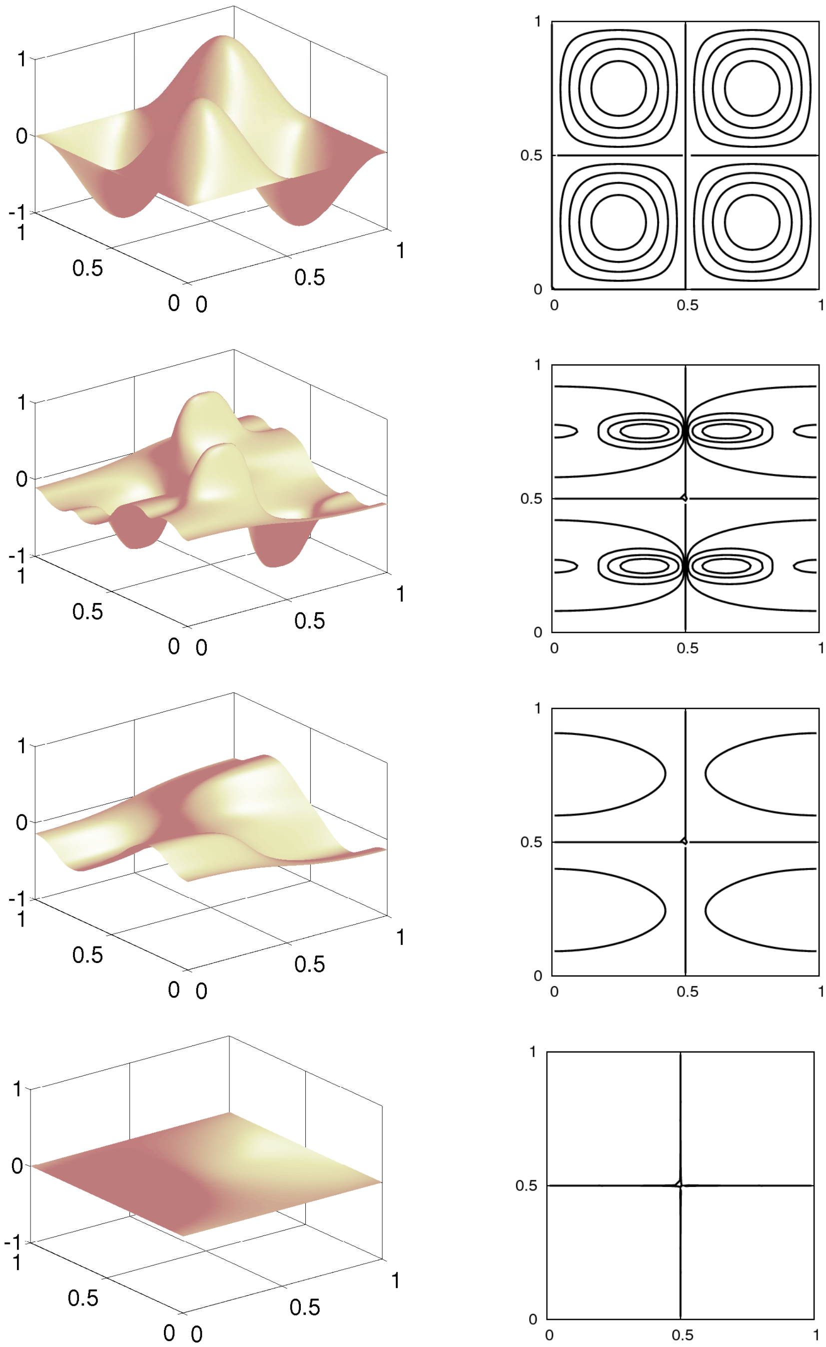

Figure 7.45.: **The explicit finite difference** numerical scheme for the **anisotropic Willmore flow of graphs** at times $t = 0$, $t = 10^{-6}$, $t = 4 \cdot 10^{-6}$ and $t = 0.0001$ (graph of φ on the left, level-lines of φ on the right). See the Numerical experiment 7.2.26.

Numerical experiment 7.2.27. Test of the **explicit finite difference** numerical scheme for the **anisotropic mean-curvature flow of graphs**

$$
\begin{aligned}
\partial_t \varphi &= Q \nabla_{\mathbf{p}} \gamma_{\mathbb{G}} \left(\nabla \varphi, -1 \right) \quad \text{on } (0, \mathrm{T}\rangle \times \Omega \\
\varphi \mid_{t=0} &= \sin\left(2\pi x\right) \sin\left(2\pi y\right) \quad \text{on } \Omega
\end{aligned}
$$

where the anisotropy function $\gamma_{\mathbb{G}}$ is given by

$$
\gamma_{\mathbb{G}} \left(\nabla \varphi, -1 \right) := \sqrt{1 + \nabla \varphi^T \mathbb{G} \nabla \varphi}, \text{ for } \mathbb{G} := \begin{pmatrix} 11 & 10 \\ 10 & 11 \end{pmatrix}
$$

and we apply the Neumann boundary conditions

$$
\nabla_{\mathbf{p}} \gamma \nu = 0 \quad \text{on } \partial \Omega.
$$

Computational domain: $\Omega \equiv [0,1]^2$.
Final time: $T = 0.025$.
Space steps: $h = 0.01$.
Time step: Adaptive.
Numerical scheme: 6.3.6
Figure: 7.46.
Remark: Compare with the Numerical experiment 7.2.17.

Numerical experiment 7.2.28. Test of the **explicit finite difference** numerical scheme for the **anisotropic Willmore flow of graphs**

$$
\begin{aligned}
\partial_t \varphi &= -Q \nabla \cdot \left(\mathbb{E}_\gamma \nabla w_\gamma - \frac{1}{2} \frac{w_\gamma^2}{Q^3} \nabla \varphi \right) \quad \text{on } (0, T) \times \Omega, \\
w_\gamma &= Q H_\gamma \quad \text{on } (0, T) \times \Omega, \\
\varphi \mid_{t=0} &= \sin\left(2\pi x\right) \sin\left(2\pi y\right) \quad \text{on } \Omega,
\end{aligned}
$$

where the anisotropy function $\gamma_{\mathbb{G}}$ is given by

$$
\gamma_{\mathbb{G}} \left(\nabla \varphi, -1 \right) := \sqrt{1 + \nabla \varphi^T \mathbb{G} \nabla \varphi}, \text{ for } \mathbb{G} := \begin{pmatrix} 11 & 10 \\ 10 & 11 \end{pmatrix}
$$

and we apply the Neumann boundary conditions

$$
\partial_\nu \varphi = \mathbb{E}_\gamma \nabla w_\gamma \cdot \nu = 0 \quad \text{on } \partial \Omega.
$$

Computational domain: $\Omega \equiv [0,1]^2$.
Final time: $T = 10^{-5}$.
Space steps: $h = 0.01$.
Time step: Adaptive.
Numerical scheme: 6.3.7
Figure: 7.47.
Remark: Compare with the Numerical experiment 7.2.18.

Anisotropic graph formulation of the mean-curvature flow

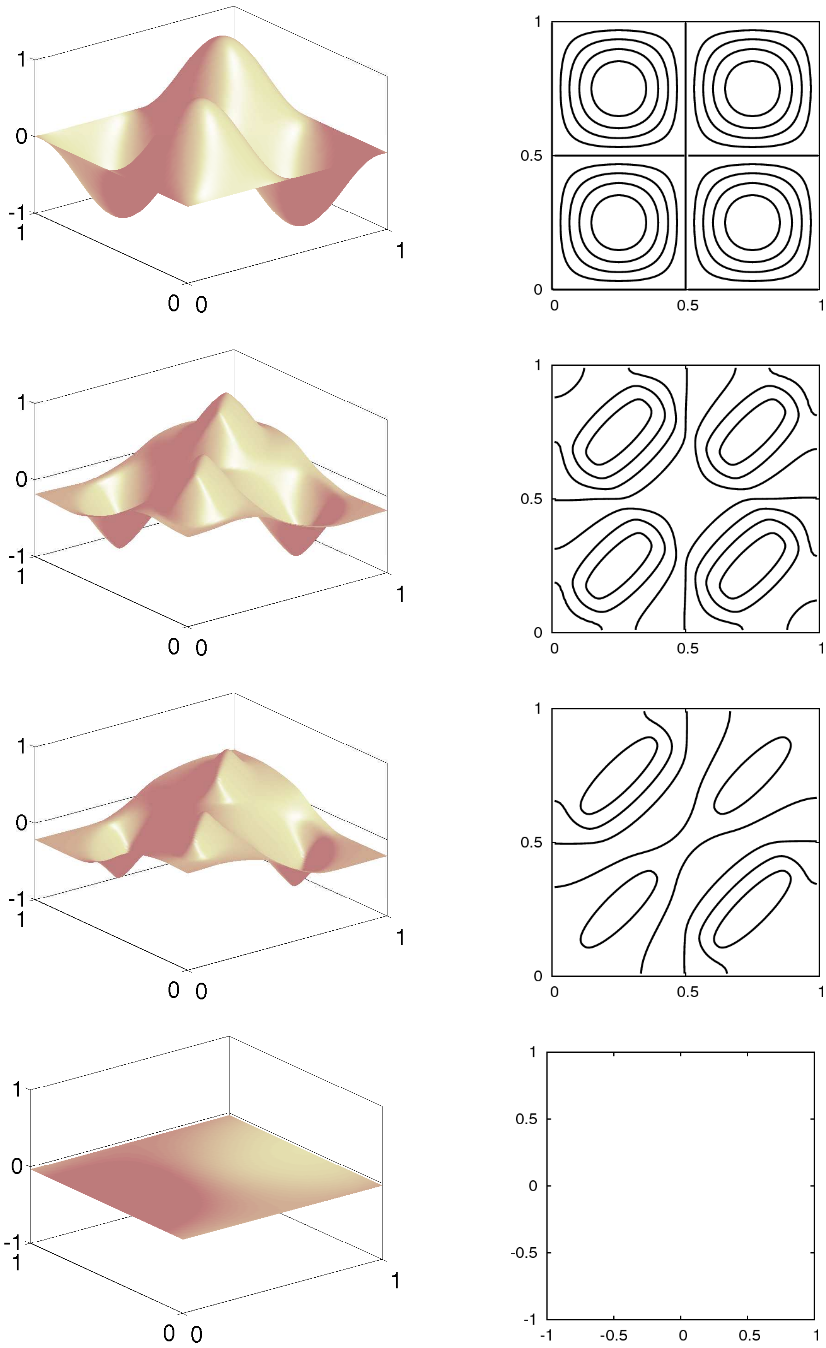

Figure 7.46.: **The explicit finite difference** numerical scheme for the **anisotropic mean-curvature flow of graphs** at times $t = 0$, $t = 0.001$, $t = 0.002$ and $t = 0.025$ (graph of φ on the left, level-lines of φ on the right). See the Numerical experiment 7.2.27.

Anisotropic graph formulation of the Willmore flow

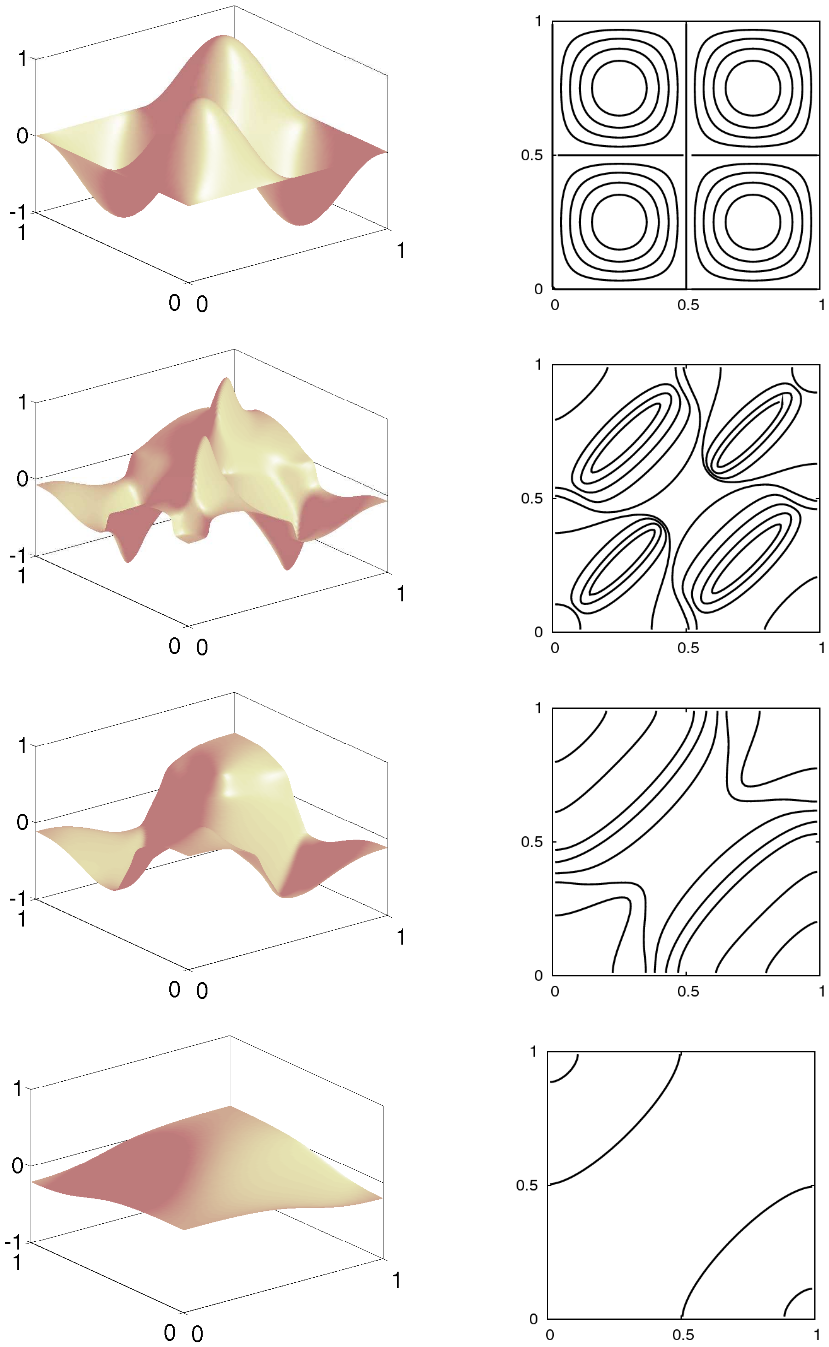

Figure 7.47.: **The explicit finite difference** numerical scheme for the **anisotropic Willmore flow of graphs** at times $t = 0$, $t = 3 \cdot 10^{-7}$, $t = 10^{-6}$ and $t = 5 \cdot 10^{-5}$ (graph of φ on the left, level-lines of φ on the right). See the Numerical experiment 7.2.28.

Numerical experiment 7.2.29. Test of the **explicit finite difference** numerical scheme for the **anisotropic mean-curvature flow of graphs**

$$\begin{aligned} \partial_t \varphi &= Q \nabla_{\mathbf{p}} \gamma_{\mathbb{G}} (\nabla \varphi, -1) \quad \text{on } (0, \mathrm{T}\rangle \times \Omega \\ \varphi \mid_{t=0} &= \sin\left(3\pi \sqrt{x^2 + y^2}\right) \quad \text{on } \Omega \end{aligned}$$

where the anisotropy function $\gamma_{\mathbb{G}}$ is given by

$$\gamma_{\mathbb{G}} (\nabla \varphi, -1) := \sqrt{1 + \nabla \varphi^T \mathbb{G} \nabla \varphi}, \text{ for } \mathbb{G} := \begin{pmatrix} 8 & 0 \\ 0 & 1 \end{pmatrix}$$

and we apply the Neumann boundary conditions

$$\nabla_{\mathbf{p}} \gamma \cdot \nu = 0 \quad \text{on } \partial\Omega.$$

Computational domain: $\Omega \equiv [-2, 2]^2$.
Final time: $T = 0.25$.
Space steps: $h = 0.04$.
Time step: $\tau = 5 \cdot 10^{-4}$.
Numerical scheme: 6.3.8
Figure: 7.48.
Remark: Compare with the Numerical experiment 7.2.19.

Numerical experiment 7.2.30. Test of the **explicit finite difference** numerical scheme for the **anisotropic Willmore flow of graphs**

$$\begin{aligned} \partial_t \varphi &= -Q \nabla \cdot \left(\mathbb{E}_\gamma \nabla w_\gamma - \frac{1}{2} \frac{w_\gamma^2}{Q^3} \nabla \varphi \right) \quad \text{on } (0, T) \times \Omega, \\ w_\gamma &= Q H_\gamma \quad \text{on } (0, T) \times \Omega, \\ \varphi \mid_{t=0} &= \sin\left(3\pi \sqrt{x^2 + y^2}\right) \quad \text{on } \Omega, \end{aligned}$$

where the anisotropy function $\gamma_{\mathbb{G}}$ is given by

$$\gamma_{\mathbb{G}} (\nabla \varphi, -1) := \sqrt{1 + \nabla \varphi^T \mathbb{G} \nabla \varphi}, \text{ for } \mathbb{G} := \begin{pmatrix} 8 & 0 \\ 0 & 1 \end{pmatrix}$$

and we apply the Neumann boundary conditions

$$\partial_\nu \varphi = \mathbb{E}_\gamma \nabla w_\gamma \cdot \nu = 0 \quad \text{on } \partial\Omega.$$

Computational domain: $\Omega \equiv [-2, 2]^2$.
Final time: $T = 0.001$.
Space steps: $h = 0.04$.
Time step: Adaptive.
Numerical scheme: 6.3.7
Figure: 7.49.
Remark: Compare with the Numerical experiment 7.2.20.

Anisotropic graph formulation of the mean-curvature flow

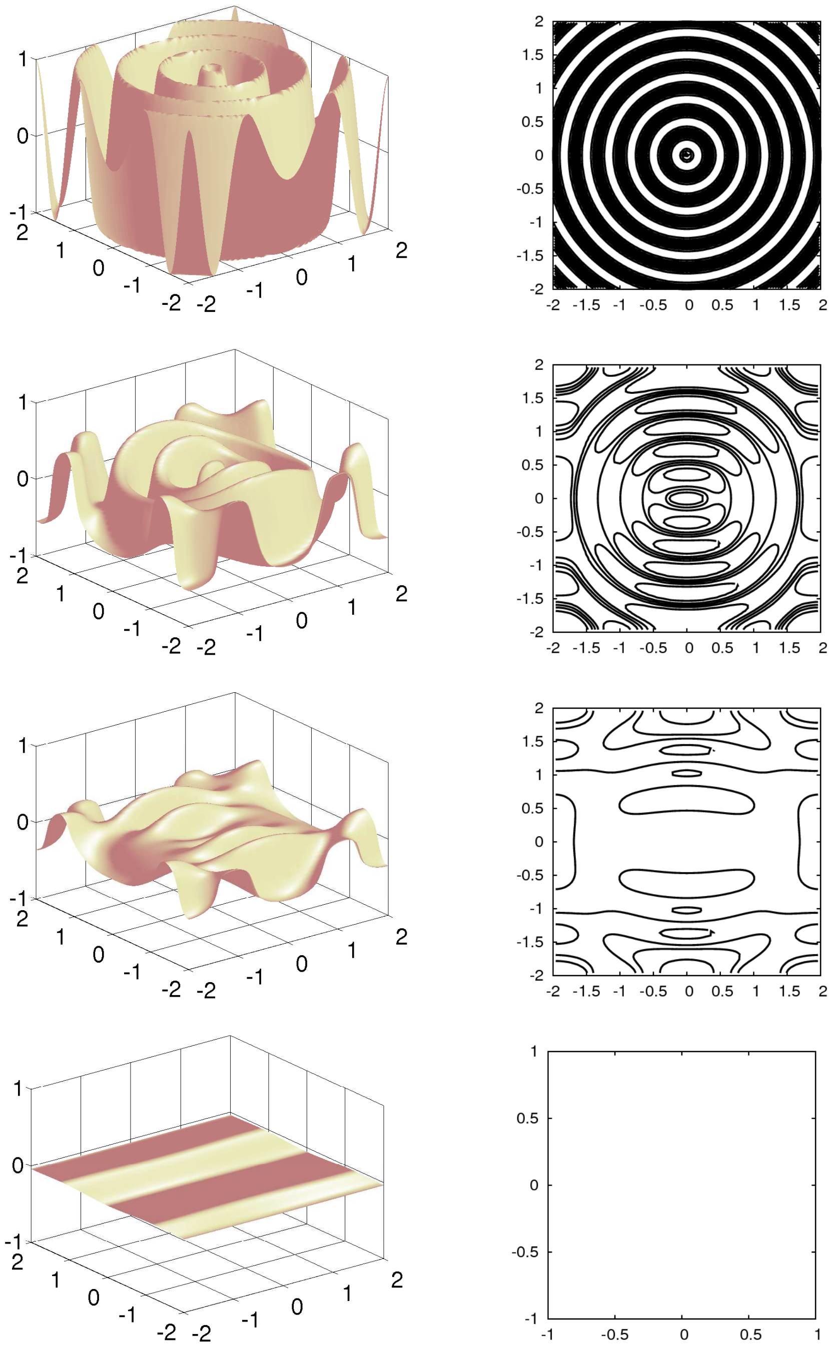

Figure 7.48.: **The semi-implicit finite difference** numerical scheme for the **anisotropic mean-curvature flow of graphs** at times $t = 0$, $t = 0.02$, $t = 0.08$ and $t = 0.25$ (graph of φ on the left, level-lines of φ on the right). See the Numerical experiment 7.2.29.

Anisotropic graph formulation of the Willmore flow

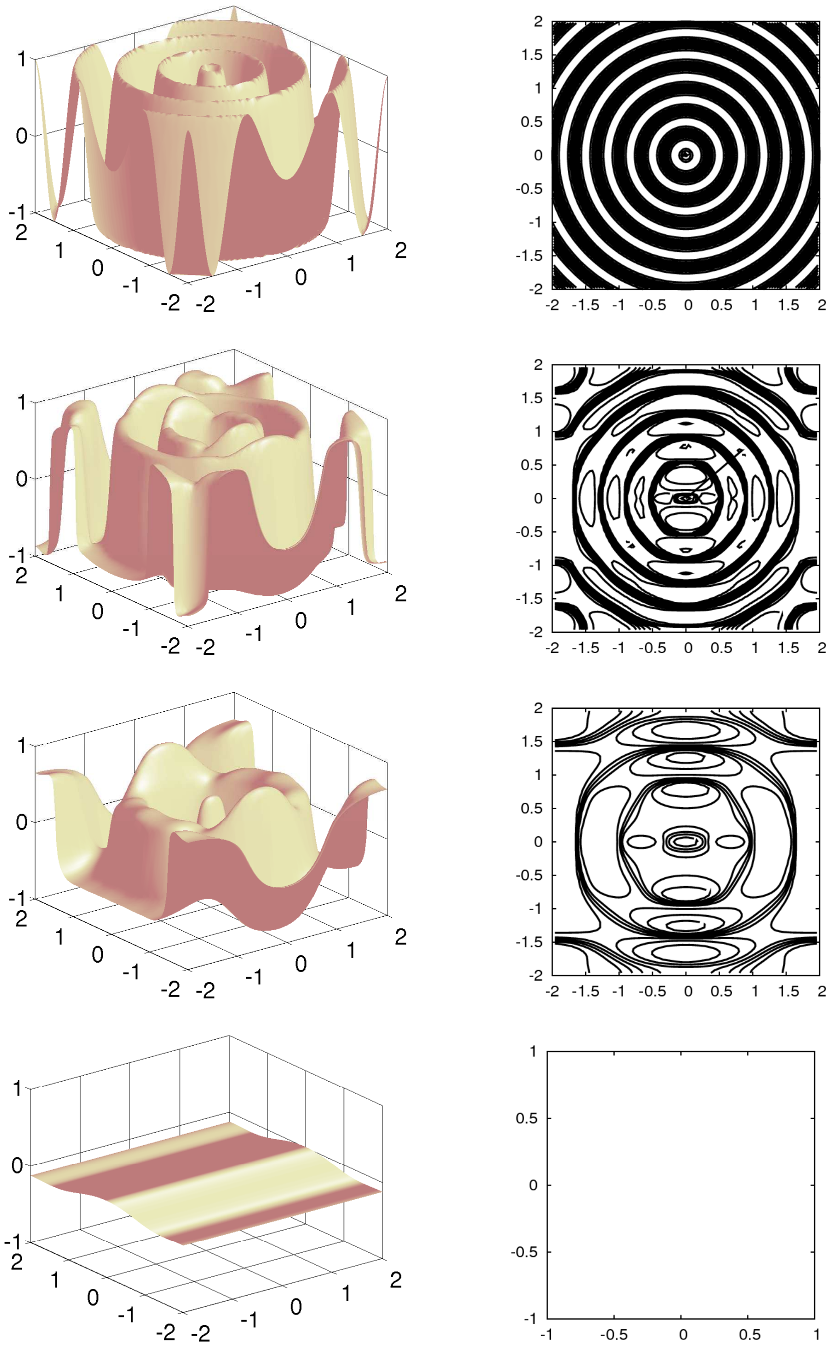

Figure 7.49.: **The explicit finite difference** numerical scheme for the **anisotropic Willmore flow of graphs** at times $t = 0$, $t = 1.6 \cdot 10^{-5}$, $t = 1.28 \cdot 10^{-4}$ and $t = 0.001$ (graph of φ on the left, level-lines of φ on the right). See the Numerical experiment 7.2.30.

Numerical experiment 7.2.31. Test of the **explicit finite difference** numerical scheme for the **anisotropic mean-curvature flow of graphs**

$$\begin{aligned} \partial_t \varphi &= Q \nabla_{\mathbf{p}} \gamma_{\mathbb{G}} (\nabla \varphi, -1) \quad \text{on } (0, \mathrm{T}\rangle \times \Omega \\ \varphi\mid_{t=0} &= \sin\left(3\pi\sqrt{x^2+y^2}\right) \quad \text{on } \Omega \end{aligned}$$

where the anisotropy function $\gamma_{\mathbb{G}}$ is given by

$$\gamma_{\mathbb{G}} (\nabla \varphi, -1) := \sqrt{1 + \nabla \varphi^T \mathbb{G} \nabla \varphi}, \text{ for } \mathbb{G} := \begin{pmatrix} 10 & 8 \\ 8 & 10 \end{pmatrix}$$

and we apply the Neumann boundary conditions

$$\nabla_{\mathbf{p}} \gamma \nu = 0 \quad \text{on } \partial\Omega.$$

Computational domain: $\Omega \equiv [-2,2]^2$.
Final time: $T = 0.25$.
Space steps: $h = 0.04$.
Time step: Adaptive.
Numerical scheme: 6.3.6
Figure: 7.50.
Remark: Compare with the Numerical experiment 7.2.19.

Numerical experiment 7.2.32. Test of the **explicit finite difference** numerical scheme for the **anisotropic Willmore flow of graphs**

$$\begin{aligned} \partial_t \varphi &= -Q \nabla \cdot \left(\mathbb{E}_\gamma \nabla w_\gamma - \frac{1}{2} \frac{w_\gamma^2}{Q^3} \nabla \varphi \right) \quad \text{on } (0,T) \times \Omega, \\ w_\gamma &= Q H_\gamma \quad \text{on } (0,T) \times \Omega, \\ \varphi\mid_{t=0} &= \sin\left(3\pi\sqrt{x^2+y^2}\right) \quad \text{on } \Omega, \end{aligned}$$

where the anisotropy function $\gamma_{\mathbb{G}}$ is given by

$$\gamma_{\mathbb{G}} (\nabla \varphi, -1) := \sqrt{1 + \nabla \varphi^T \mathbb{G} \nabla \varphi}, \text{ for } \mathbb{G} := \begin{pmatrix} 10 & 8 \\ 8 & 10 \end{pmatrix}$$

and we apply the Neumann boundary conditions

$$\partial_\nu \varphi = \mathbb{E}_\gamma \nabla w_\gamma \cdot \nu = 0 \quad \text{on } \partial\Omega.$$

Computational domain: $\Omega \equiv [-2,2]^2$.
Final time: $T = 1.024 \cdot 10^{-3}$.
Space steps: $h = 0.04$.
Time step: Adaptive.
Numerical scheme: 6.3.7
Figure: 7.51.
Remark: Compare with the Numerical experiment 7.2.20.

Anisotropic graph formulation of the mean-curvature flow

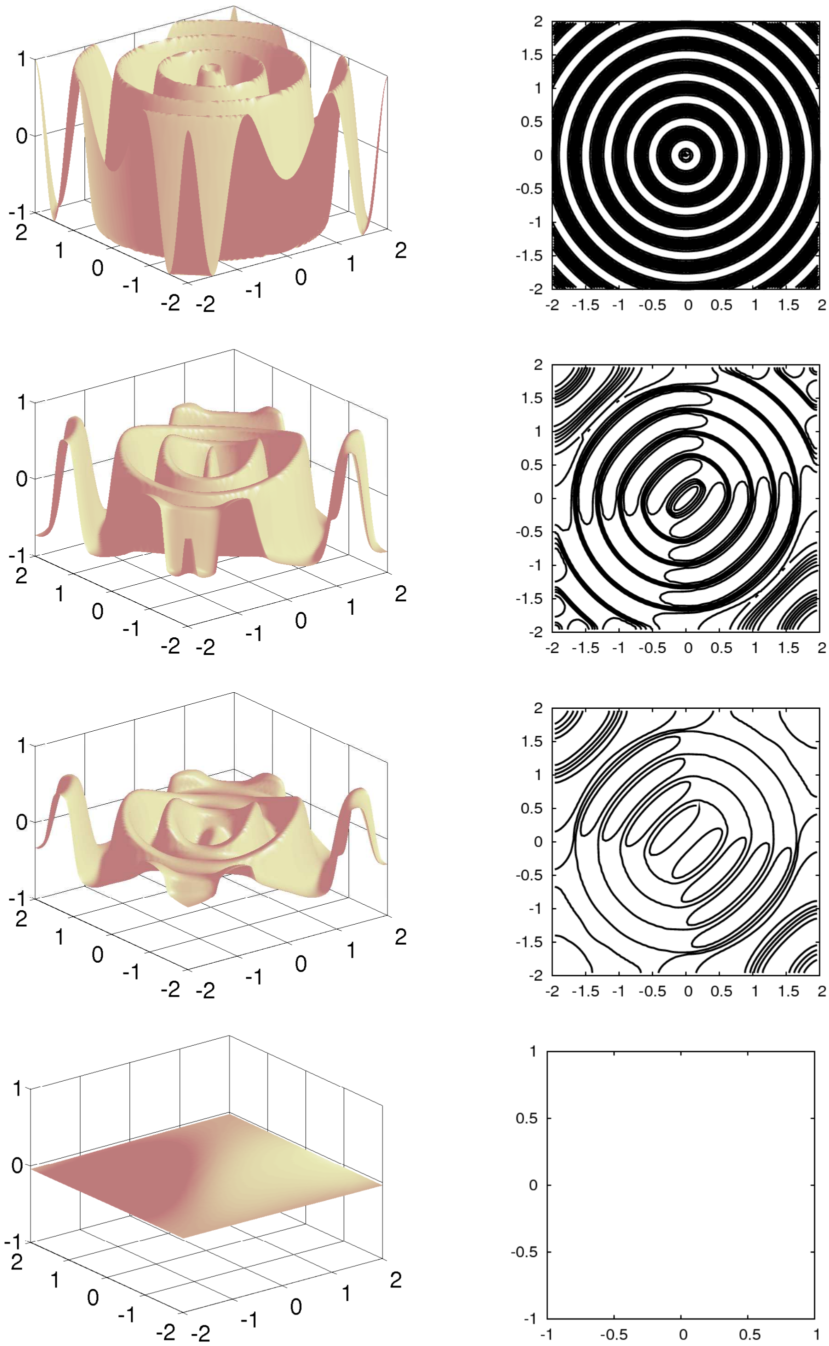

Figure 7.50.: **The explicit finite difference** numerical scheme for the **anisotropic mean-curvature flow of graphs** at times $t = 0$, $t = 0.01$, $t = 0.04$ and $t = 0.25$ (graph of φ on the left, level-lines of φ on the right). See the Numerical experiment 7.2.31.

Anisotropic graph formulation of the Willmore flow

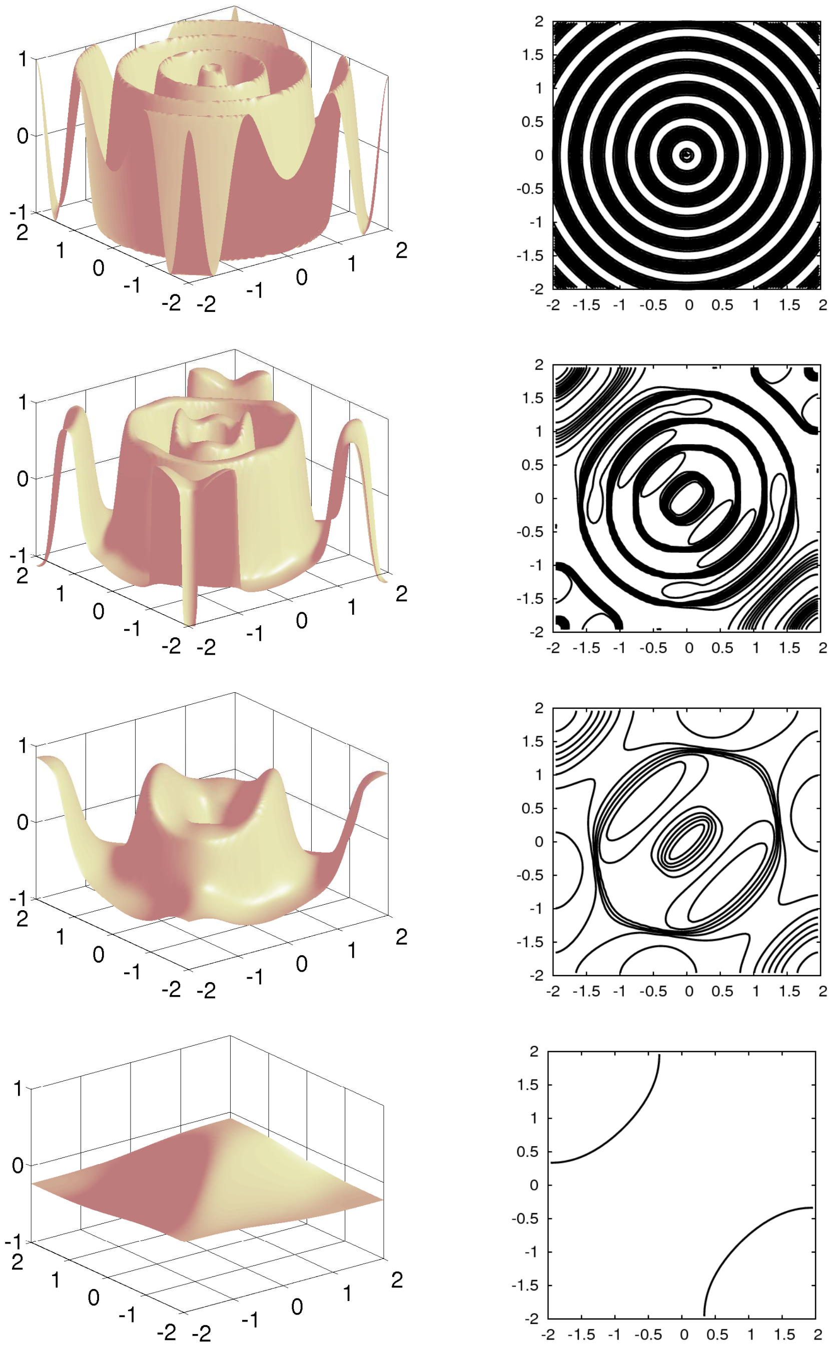

Figure 7.51.: **The explicit finite difference** numerical scheme for the **anisotropic Willmore flow of graphs** at times $t = 0$, $t = 8 \cdot 10^{-6}$, $t = 6.4 \cdot 10^{-5}$ and $t = 1.024 \cdot 10^{-3}$ (graph of φ on the left, level-lines of φ on the right). See the Numerical experiment 7.2.32.

Numerical experiment 7.2.33. Test of the **explicit finite difference** numerical scheme for the **anisotropic mean-curvature flow of graphs**

$$\begin{aligned} \partial_t \varphi &= Q \nabla_{\mathbf{p}} \gamma_{abs} \left(\nabla \varphi, -1 \right) \quad \text{on } (0, \mathrm{T}\rangle \times \Omega \\ \varphi \mid_{t=0} &= \sin\left(2\pi x\right) \sin\left(2\pi y\right) \quad \text{on } \Omega \end{aligned}$$

where the anisotropy function γ_{abs} is given by

$$\gamma_{abs}\left(\mathbf{P}\right) = \sum_{i=1}^{3} \sqrt{P_i^2 + \epsilon_{abs} \sum_{j=1}^{3} P_j^2} \text{ for } \epsilon_{abs} = 0.001,$$

and we apply the Dirichlet boundary conditions

$$\varphi = 0 \quad \text{on } \partial\Omega.$$

Computational domain: $\Omega \equiv [0,1]^2$.
Final time: $T = 0.025$.
Space steps: $h = 0.01$.
Time step: Adaptive.
Numerical scheme: 6.3.6
Figure: 7.52.
Remark: Compare with the Numerical experiment 7.2.9.

Numerical experiment 7.2.34. Test of the **explicit finite difference** numerical scheme for the **anisotropic Willmore flow of graphs**

$$\begin{aligned} \partial_t \varphi &= -Q \nabla \cdot \left(\mathbb{E}_\gamma \nabla w_\gamma - \frac{1}{2} \frac{w_\gamma^2}{Q^3} \nabla \varphi \right) \quad \text{on } (0, T) \times \Omega, \\ w_\gamma &= Q H_\gamma \quad \text{on } (0, T) \times \Omega, \\ \varphi \mid_{t=0} &= \sin\left(3\pi \sqrt{x^2 + y^2} \right) \quad \text{on } \Omega, \end{aligned}$$

where the anisotropy function γ_{abs} is given by

$$\gamma_{abs}\left(\mathbf{P}\right) = \sum_{i=1}^{3} \sqrt{P_i^2 + \epsilon_{abs} \sum_{j=1}^{3} P_j^2} \text{ for } \epsilon_{abs} = 0.001,$$

and we apply the Dirichlet boundary conditions

$$\varphi = w_\gamma = 0 \quad \text{on } \partial\Omega.$$

Computational domain: $\Omega \equiv [0,1]^2$.
Final time: $T = 1.5 \cdot 10^{-3}$.
Space steps: $h = 0.01$.
Time step: Adaptive.
Numerical scheme: 6.3.7
Figure: 7.53.
Remark: Compare with the Numerical experiment 7.2.10.

Anisotropic graph formulation of the mean-curvature flow

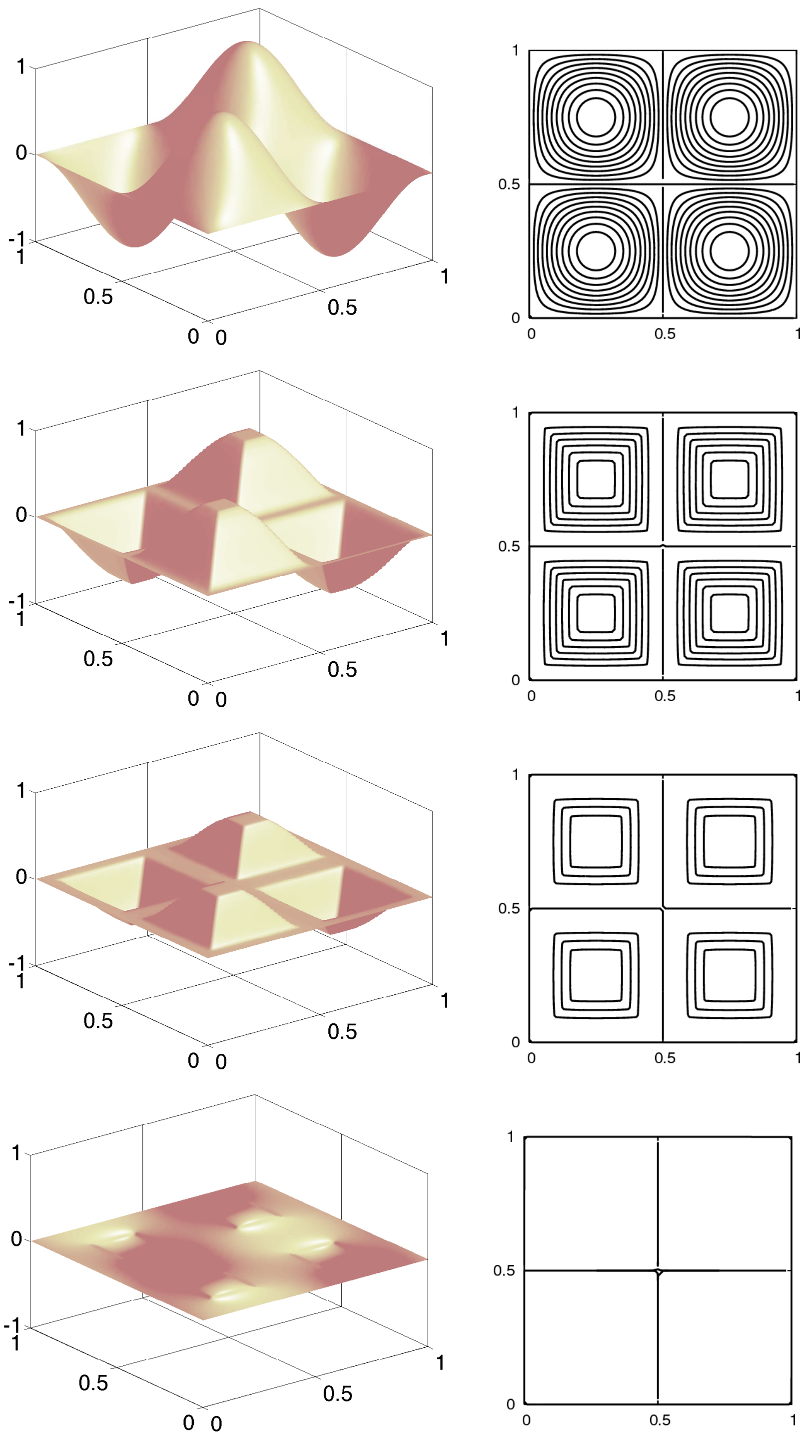

Figure 7.52.: **The explicit finite difference** numerical scheme for the **anisotropic mean-curvature flow of graphs** at times $t = 0$, $t = 0.00625$, $t = 0.0125$ and $t = 0.025$ (graph of φ on the left, level-lines of φ on the right). See the Numerical experiment 7.2.33.

Anisotropic graph formulation of the Willmore flow

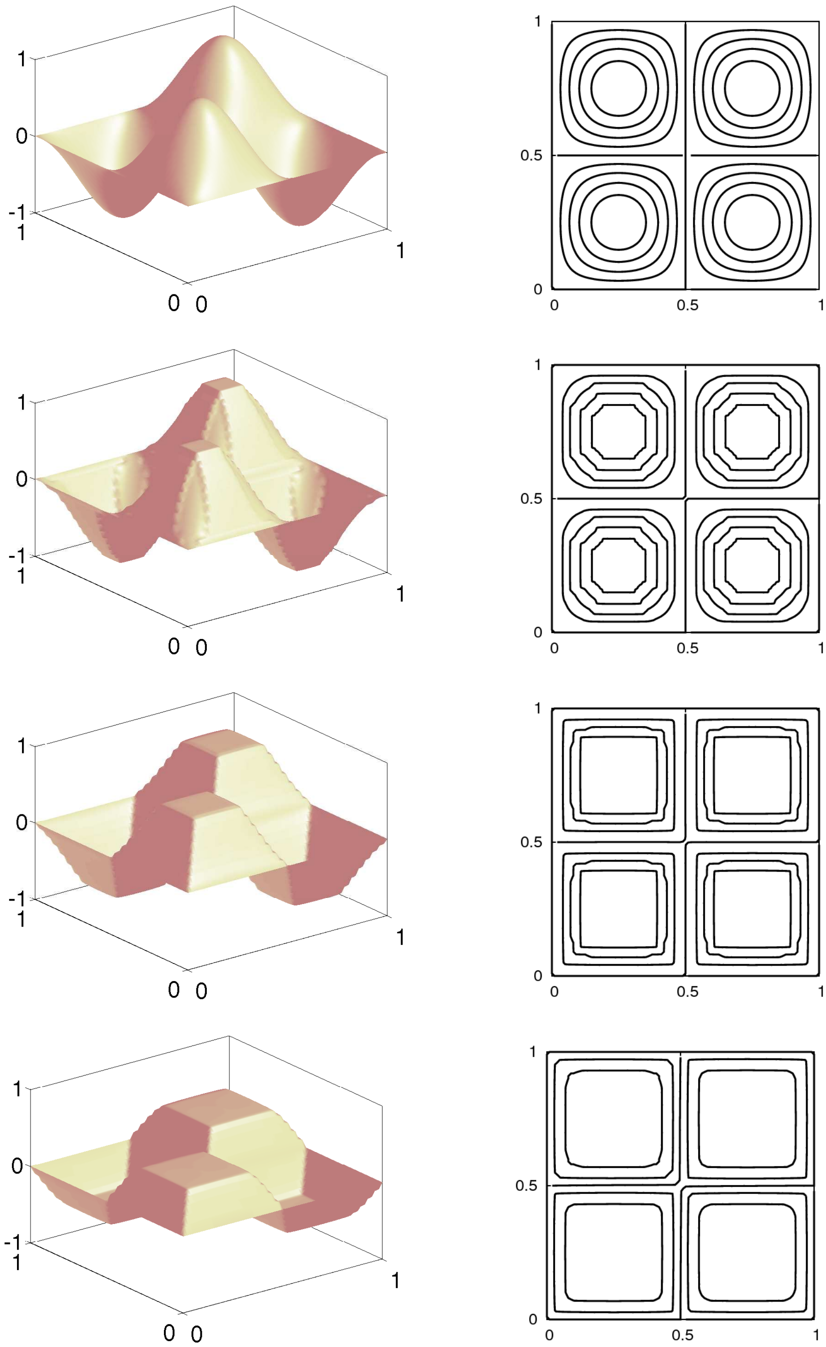

Figure 7.53.: **The explicit finite difference** numerical scheme for the **anisotropic Willmore flow of graphs** at times $t = 0$, $t = 4 \cdot 10^{-6}$, $t = 2.56 \cdot 10^{-4}$ and $t = 1.5 \cdot 10^{-3}$ (graph of φ on the left, level-lines of φ on the right). See the Numerical experiment 7.2.34.

Numerical experiment 7.2.35. Test of the **explicit finite difference** numerical scheme for the **anisotropic mean-curvature flow of graphs**

$$\begin{aligned} \partial_t \varphi &= Q \nabla_{\mathbf{p}} \gamma_{abs} \left(\nabla \varphi, -1 \right) \quad \text{on } (0, \mathrm{T}\rangle \times \Omega \\ \varphi \mid_{t=0} &= \operatorname{sign}\left(x^2 + y^2 - 0.1 \right) + 1 \quad \text{on } \Omega \end{aligned}$$

where the anisotropy function γ_{abs} is given by

$$\gamma_{abs}\left(\mathbf{P}\right) = \sum_{i=1}^{3} \sqrt{P_i^2 + \epsilon_{abs} \sum_{j=1}^{3} P_j^2} \text{ for } \epsilon_{abs} = 0.001,$$

and we apply the Dirichlet boundary conditions

$$\varphi = 0 \quad \text{on } \partial\Omega.$$

Computational domain: $\Omega \equiv [-0.5, 0.5]^2$.
Final time: $T = 0.0625$.
Space steps: $h = 0.01$.
Time step: Adaptive.
Numerical scheme: 6.3.6
Figure: 7.54.
Remark: Compare with the Numerical experiment 7.2.11.

Numerical experiment 7.2.36. Test of the **explicit finite difference** numerical scheme for the **anisotropic Willmore flow of graphs**

$$\begin{aligned} \partial_t \varphi &= -Q \nabla \cdot \left(\mathbb{E}_\gamma \nabla w_\gamma - \frac{1}{2} \frac{w_\gamma^2}{Q^3} \nabla \varphi \right) \quad \text{on } (0, T) \times \Omega, \\ w_\gamma &= Q H_\gamma \quad \text{on } (0, T) \times \Omega, \\ \varphi \mid_{t=0} &= \operatorname{sign}\left(x^2 + y^2 - 0.1 \right) + 1 \quad \text{on } \Omega, \end{aligned}$$

where the anisotropy function γ_{abs} is given by

$$\gamma_{abs}\left(\mathbf{P}\right) = \sum_{i=1}^{3} \sqrt{P_i^2 + \epsilon_{abs} \sum_{j=1}^{3} P_j^2},$$

and we apply the Dirichlet boundary conditions

$$\varphi = w_\gamma = 0 \quad \text{on } \partial\Omega.$$

Computational domain: $\Omega \equiv [-0.5, 0.5]^2$.
Final time: $T = 2.048 \cdot 10^{-3}$.
Space steps: $h = 0.01$.
Time step: $\tau = 10^{-5}$.
Numerical scheme: 6.3.9
Figure: 7.55.
Remark: Compare with the Numerical experiment 7.2.12. Note small asymmetry on the third image cause probably by use of the semi-implicit scheme.

Anisotropic graph formulation of the mean-curvature flow

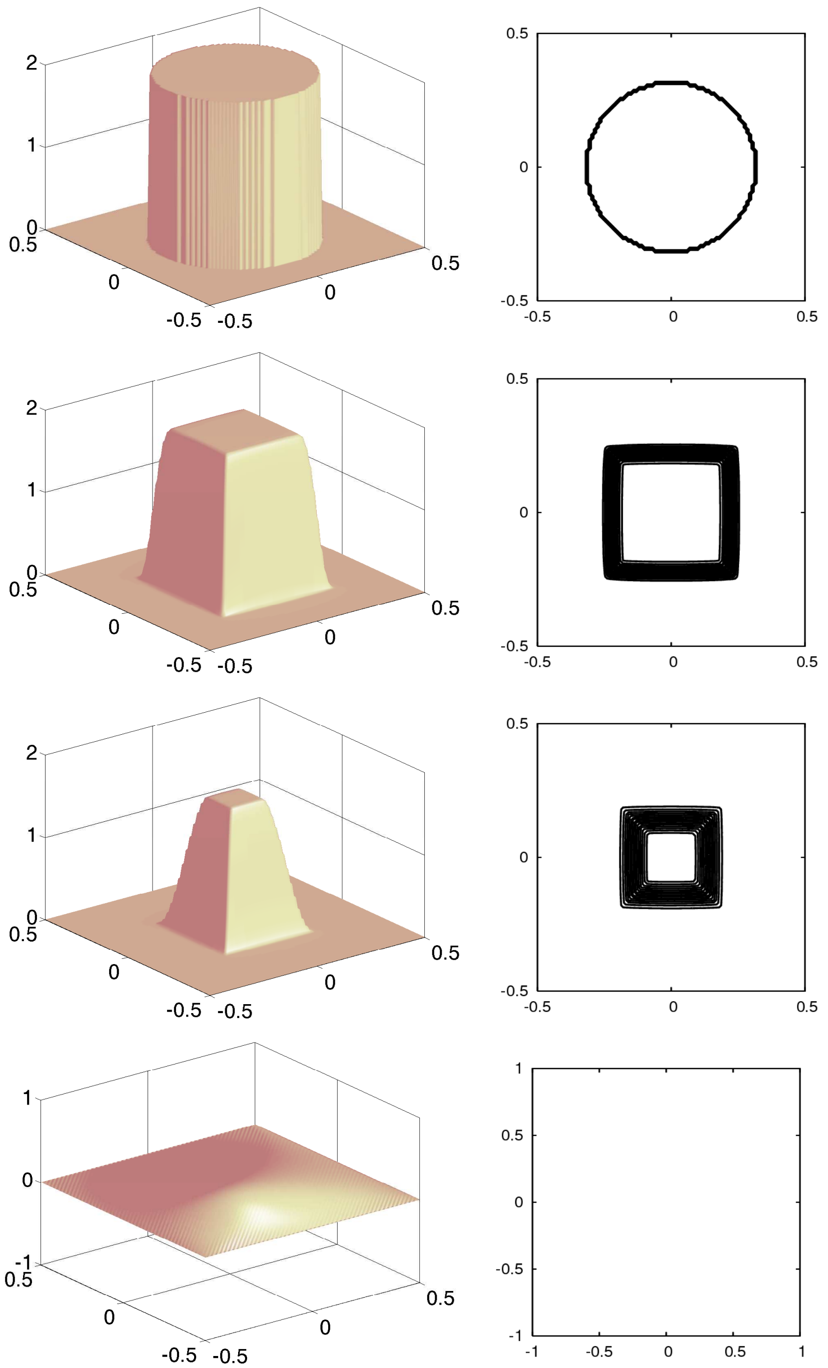

Figure 7.54.: **The explicit finite difference** numerical scheme for the **anisotropic mean-curvature flow of graphs** at times $t = 0$, $t = 0.015625$, $t = 0.03125$ and $t = 0.0625$ (graph of φ on the left, level-lines of φ on the right). See the Numerical experiment 7.2.35.

Anisotropic graph formulation of the Willmore flow

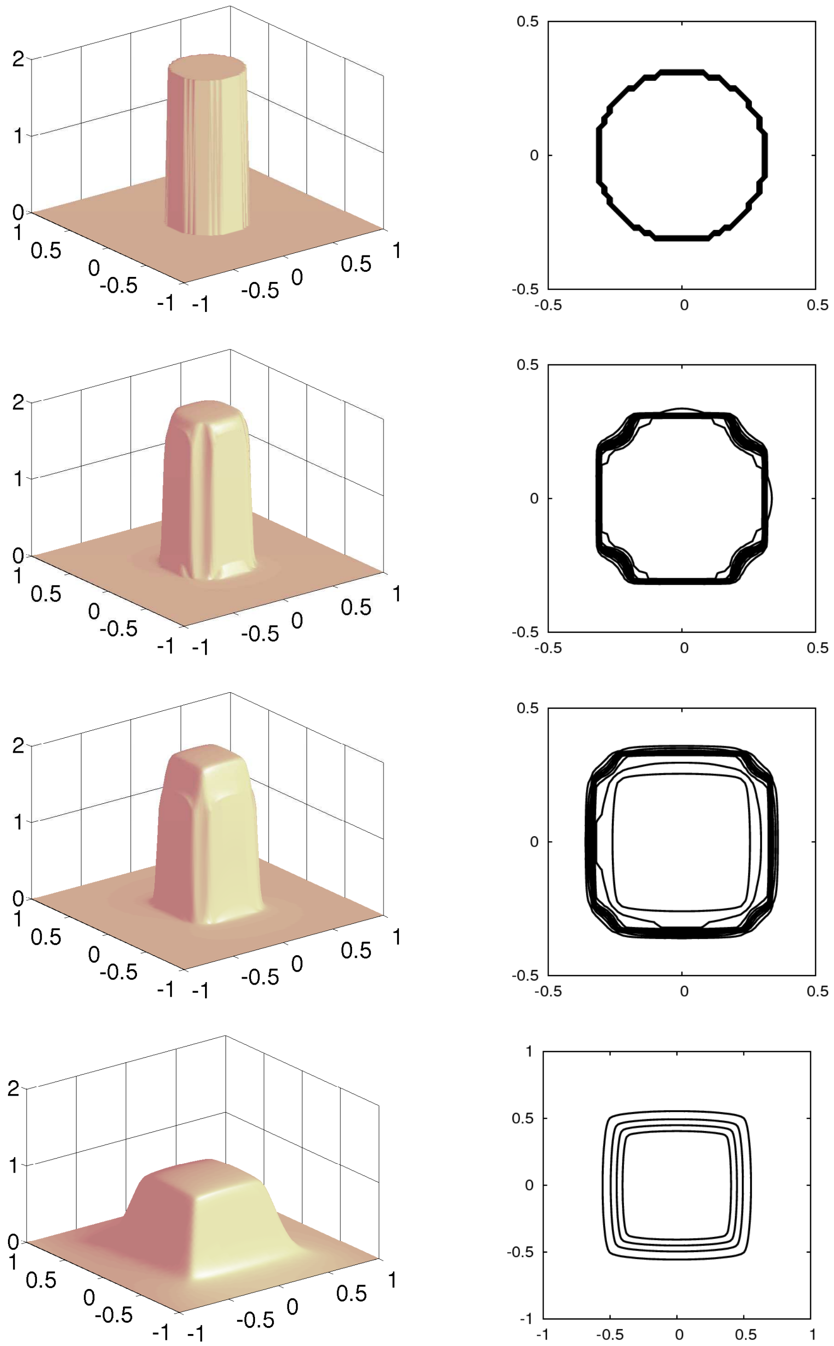

Figure 7.55.: **The semi-implicit finite difference** numerical scheme for the **anisotropic Willmore flow of graphs** at times $t = 0$, $t = 4 \cdot 10^{-6}$, $t = 1.6 \cdot 10^{-5}$ and $t = 2.048 \cdot 10^{-3}$ (graph of φ on the left, level-lines of φ on the right). See the Numerical experiment 7.2.36.

Numerical experiment 7.2.37. Test of the **explicit finite difference** numerical scheme for the **anisotropic mean-curvature flow of graphs**

$$\begin{aligned}\partial_t\varphi &= Q\nabla_{\mathbf{p}}\gamma_{abs}\left(\nabla\varphi,-1\right) \quad \text{on } (0,\mathrm{T}\rangle\times\Omega \\ \varphi\mid_{t=0} &= \sin\left(\pi\tanh\left(5\left(\left(x^2+y^2\right)-0.25\right)\right)\right), \quad \text{on } \Omega\end{aligned}$$

where the anisotropy function γ_{abs} is given by

$$\gamma_{abs}\left(\mathbf{P}\right)=\sum_{i=1}^{3}\sqrt{P_i^2+\epsilon_{abs}\sum_{j=1}^{3}P_j^2} \text{ for } \epsilon_{abs}=0.001,$$

and we apply the Dirichlet boundary conditions

$$\varphi=0 \quad \text{on } \partial\Omega.$$

Computational domain: $\Omega\equiv[-1,1]^2$.
Final time: $T=0.125$.
Space steps: $h=0.02$.
Time step: Adaptive.
Numerical scheme: 6.3.6
Figure: 7.56.
Remark: Compare with the Numerical experiment 7.2.13.

Numerical experiment 7.2.38. Test of the **explicit finite difference** numerical scheme for the **anisotropic Willmore flow of graphs**

$$\begin{aligned}\partial_t\varphi &= -Q\nabla\cdot\left(\mathbb{E}_\gamma\nabla w_\gamma-\frac{1}{2}\frac{w_\gamma^2}{Q^3}\nabla\varphi\right) \quad \text{on } (0,T)\times\Omega, \\ w_\gamma &= QH_\gamma \quad \text{on } (0,T)\times\Omega, \\ \varphi\mid_{t=0} &= \sin\left(\pi\tanh\left(5\left(\left(x^2+y^2\right)-0.25\right)\right)\right) \quad \text{on } \Omega,\end{aligned}$$

where the anisotropy function γ_{abs} is given by

$$\gamma_{abs}\left(\mathbf{P}\right)=\sum_{i=1}^{3}\sqrt{P_i^2+\epsilon_{abs}\sum_{j=1}^{3}P_j^2} \text{ for } \epsilon_{abs}=0.001,$$

and we apply the Dirichlet boundary conditions

$$\varphi=w_\gamma=0 \quad \text{on } \partial\Omega.$$

Computational domain: $\Omega\equiv[-1,1]^2$.
Final time: $T=2\cdot10^{-4}$.
Space steps: $h=0.02$.
Time step: $\tau=10^{-8}$.
Numerical scheme: 6.3.9
Figure: 7.57.
Remark: Compare with the Numerical experiment 7.2.14.

Anisotropic graph formulation of the mean-curvature flow

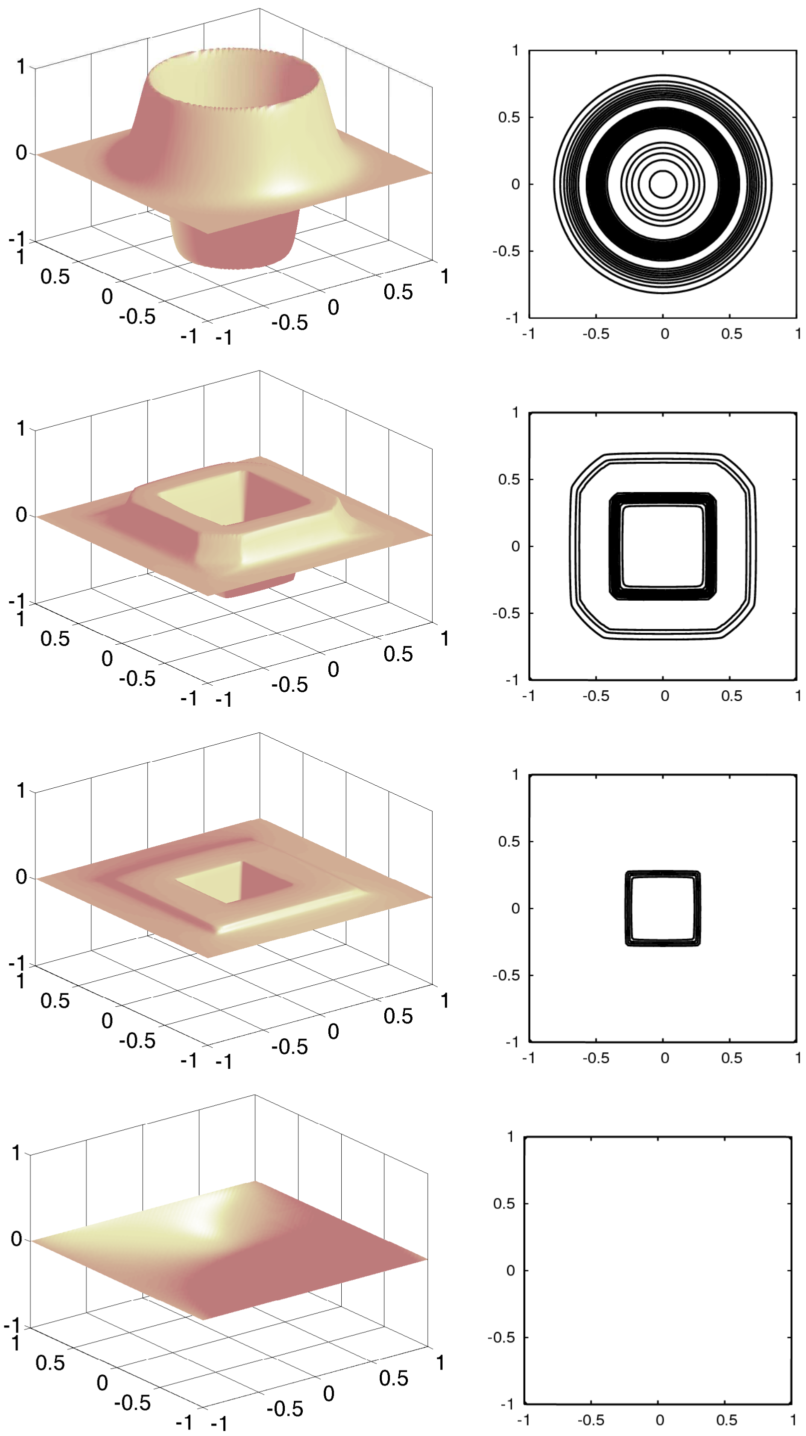

Figure 7.56.: **The explicit finite difference** numerical scheme for the **anisotropic mean-curvature flow of graphs** at times $t = 0$, $t = 0.03125$, $t = 0.0625$ and $t = 0.125$ (graph of φ on the left, level-lines of φ on the right). See the Numerical experiment 7.2.37.

Anisotropic graph formulation of the Willmore flow

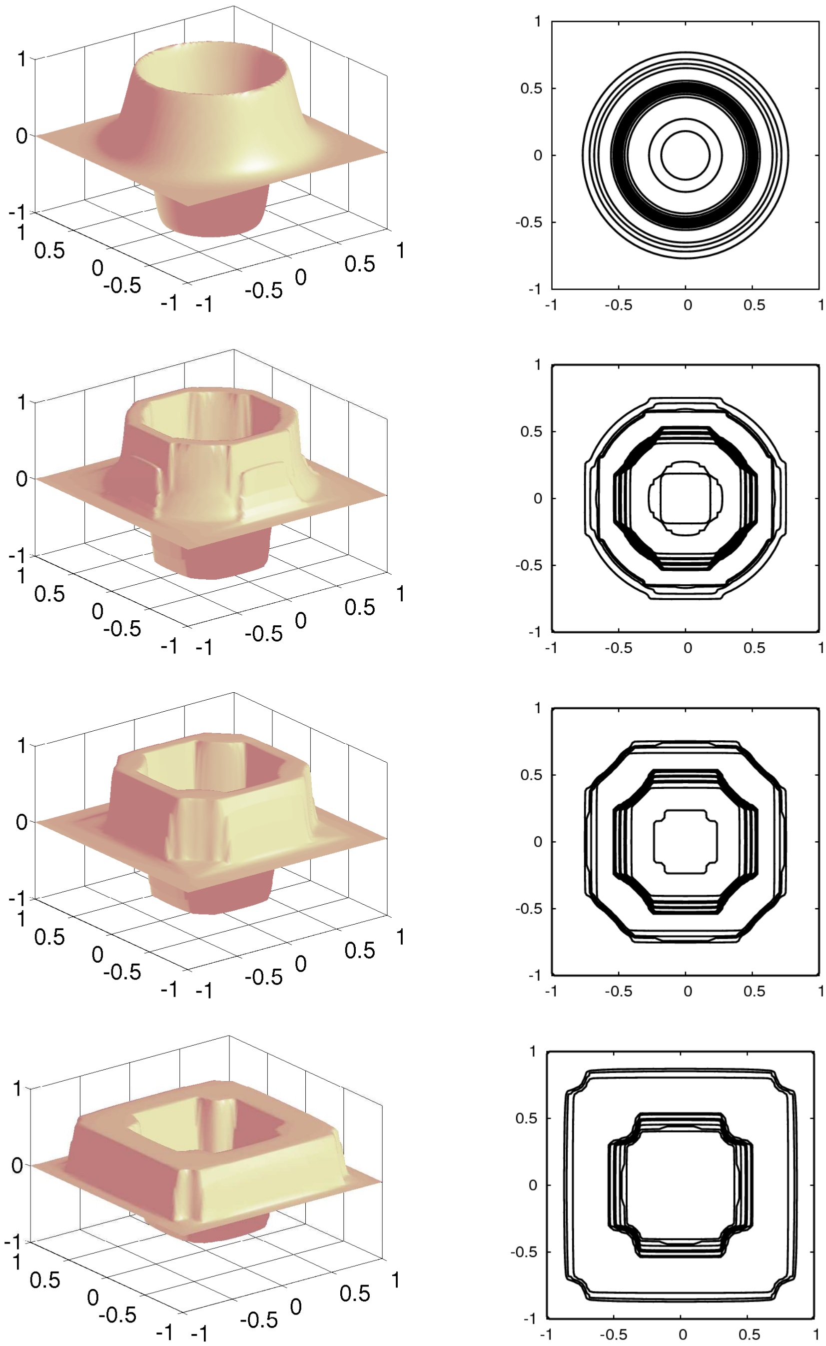

Figure 7.57.: **The semi-implicit finite difference** numerical scheme for the **anisotropic Willmore flow of graphs** at times $t = 0$, $t = 4 \cdot 10^{-6}$, $t = 3.2 \cdot 10^{-5}$ and $t = 2 \cdot 10^{-4}$ - it is not a steady state solution - (graph of φ on the left, level-lines of φ on the right). See the Numerical experiment 7.2.38.

Numerical experiment 7.2.39. Test of the **explicit finite difference** numerical scheme for the **anisotropic mean-curvature flow of graphs**

$$\begin{aligned}\partial_t \varphi &= Q \nabla_{\mathbf{p}} \gamma_{abs} \left(\nabla \varphi, -1\right) \quad \text{on } \left(0, \mathrm{T}\right\rangle \times \Omega \\ \varphi \mid_{t=0} &= -0.5 \sin^2 \left(\pi x\right) \cdot \left(1 - \left(y-2\right)^2\right) \left(1 - \tanh\left(10\left(\sqrt{x^2+y^2} - 0.6\right)\right)\right) \quad \text{on } \Omega\end{aligned}$$

where the anisotropy function γ_{abs} is given by

$$\gamma_{abs}\left(\mathbf{P}\right) = \sum_{i=1}^{3} \sqrt{P_i^2 + \epsilon_{abs} \sum_{j=1}^{3} P_j^2} \text{ for } \epsilon_{abs} = 0.001,$$

and we apply the Dirichlet boundary conditions

$$\varphi = 0 \quad \text{on } \partial\Omega.$$

Computational domain: $\Omega \equiv \left[-1, 1\right]^2$.
Final time: $T = 0.125$.
Space steps: $h = 0.02$.
Time step: Adaptive.
Numerical scheme: 6.3.6
Figure: 7.58.
Remark: Compare with the Numerical experiment 7.2.15.

Numerical experiment 7.2.40. Test of the **explicit finite difference** numerical scheme for the **anisotropic Willmore flow of graphs**

$$\begin{aligned}\partial_t \varphi &= -Q \nabla \cdot \left(\mathbb{E}_\gamma \nabla w_\gamma - \frac{1}{2} \frac{w_\gamma^2}{Q^3} \nabla \varphi\right) \quad \text{on } \left(0, T\right) \times \Omega, \\ w_\gamma &= Q H_\gamma \quad \text{on } \left(0, T\right) \times \Omega, \\ \varphi \mid_{t=0} &= -0.5 \sin^2 \left(\pi x\right) \cdot \left(1 - \left(y-2\right)^2\right) \left(1 - \tanh\left(10\left(\sqrt{x^2+y^2} - 0.6\right)\right)\right) \quad \text{on } \Omega,\end{aligned}$$

where the anisotropy function γ_{abs} is given by

$$\gamma_{abs}\left(\mathbf{P}\right) = \sum_{i=1}^{3} \sqrt{P_i^2 + \epsilon_{abs} \sum_{j=1}^{3} P_j^2} \text{ for } \epsilon_{abs} = 0.001,$$

and we apply the Dirichlet boundary conditions

$$\varphi = w_\gamma = 0 \quad \text{on } \partial\Omega.$$

Computational domain: $\Omega \equiv \left[-1, 1\right]^2$.
Final time: $T = 0.012$.
Space steps: $h = 0.02$.
Time step: Adaptive.
Numerical scheme: 6.3.7
Figure: 7.59.
Remark: Compare with the Numerical experiment 7.2.16.

Anisotropic graph formulation of the mean-curvature flow

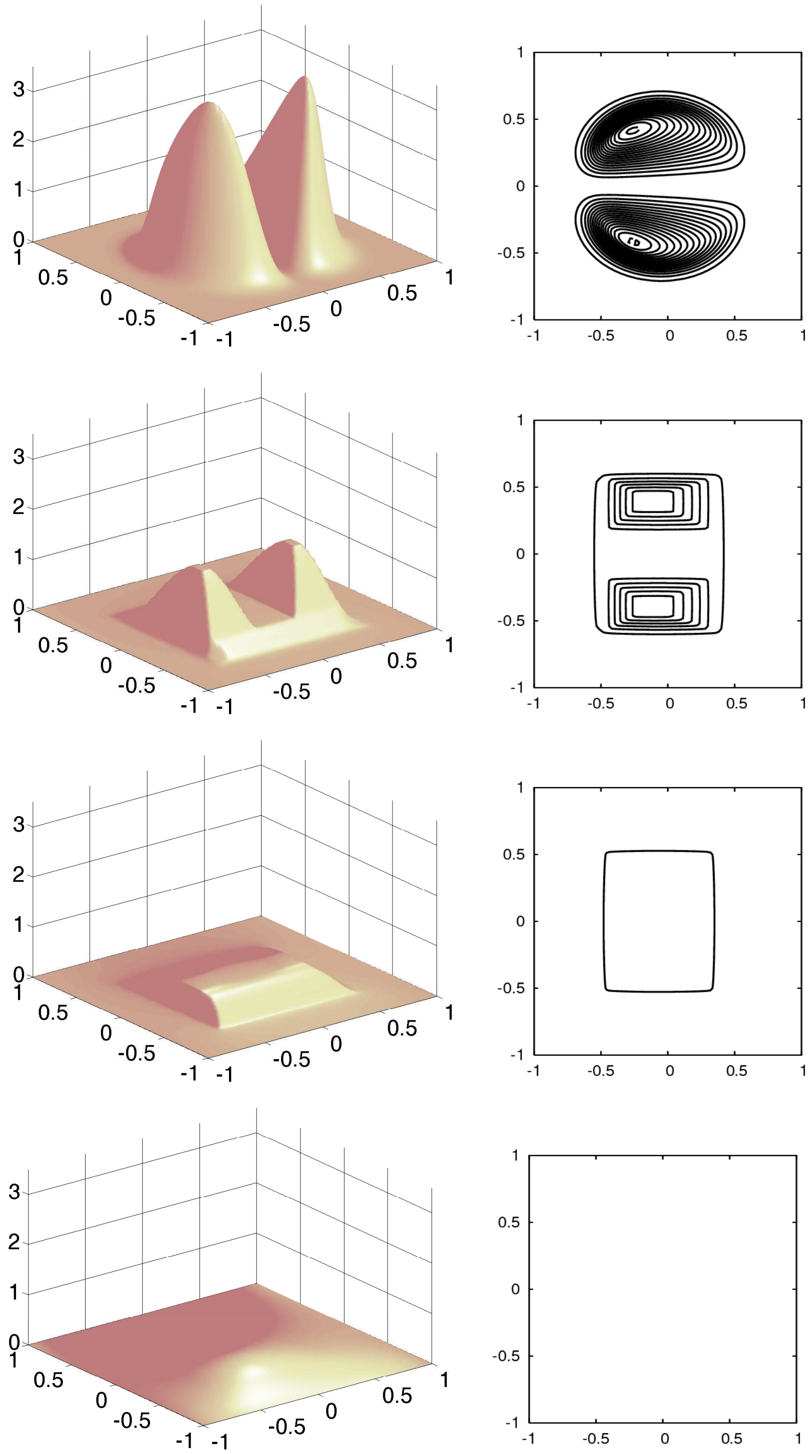

Figure 7.58.: **The explicit finite difference** numerical scheme for the **anisotropic mean-curvature flow of graphs** at times $t = 0$, $t = 0.03125$, $t = 0.0625$ and $t = 0.125$ (graph of φ on the left, level-lines of φ on the right). See the Numerical experiment 7.2.39.

Anisotropic graph formulation of the Willmore flow

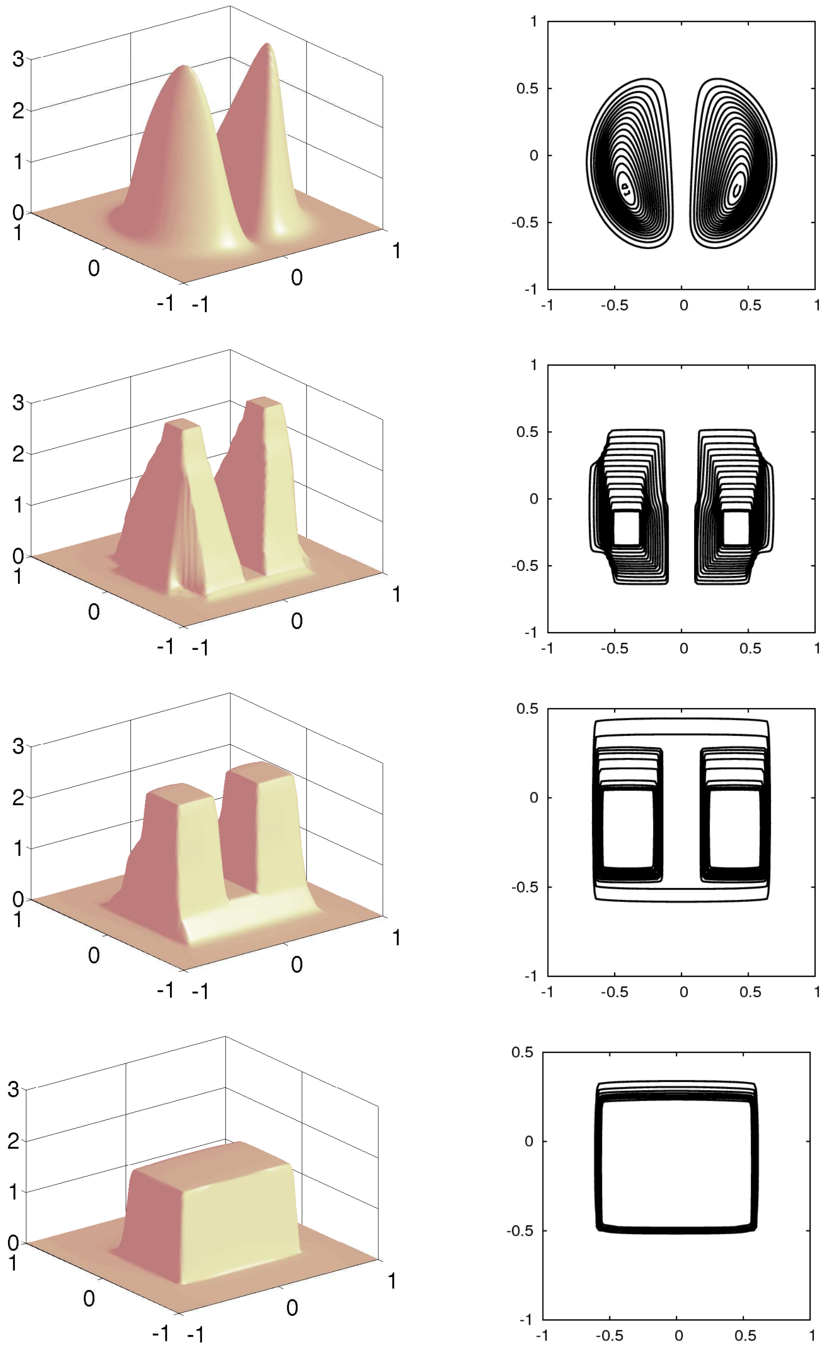

Figure 7.59.: **The explicit finite difference** numerical scheme for the **anisotropic Willmore flow of graphs** at times $t = 0$, $t = 9.6 \cdot 10^{-4}$, $t = 1.536 \cdot 10^{-3}$ and $t = 0.012$ (graph of φ on the left, level-lines of φ on the right). See the Numerical experiment 7.2.40.

Numerical experiment 7.2.41. Test of the **explicit finite difference** numerical scheme for the **anisotropic mean-curvature flow of graphs**

$$\begin{aligned}\partial_t \varphi &= Q\nabla_{\mathbf{p}}\gamma_{abs}\left(\nabla\varphi,-1\right) \quad \text{on } (0,\mathrm{T}\rangle\times\Omega\\ \varphi\mid_{t=0} &= \sin\left(2\pi x\right)\sin\left(2\pi y\right) \quad \text{on } \Omega\end{aligned}$$

where the anisotropy function γ_{abs} is given by

$$\gamma_{abs}\left(\mathbf{P}\right)=\sum_{i=1}^{3}\sqrt{P_i^2+\epsilon_{abs}\sum_{j=1}^{3}P_j^2} \text{ for } \epsilon_{abs}=0.001,$$

and we apply the Neumann boundary conditions

$$\nabla_{\mathbf{p}}\gamma\nu=0 \quad \text{on } \partial\Omega.$$

Computational domain: $\Omega\equiv[0,1]^2$.
Final time: $T=0.7$.
Space steps: $h=0.01$.
Time step: Adaptive.
Numerical scheme: 6.3.6
Figure: 7.60.
Remark: Compare with the Numerical experiment 7.2.17.

Numerical experiment 7.2.42. Test of the **explicit finite difference** numerical scheme for the **anisotropic Willmore flow of graphs**

$$\begin{aligned}\partial_t \varphi &= -Q\nabla\cdot\left(\mathbb{E}_\gamma\nabla w_\gamma-\frac{1}{2}\frac{w_\gamma^2}{Q^3}\nabla\varphi\right) \quad \text{on } (0,T)\times\Omega,\\ w_\gamma &= QH_\gamma \quad \text{on } (0,T)\times\Omega,\\ \varphi\mid_{t=0} &= \sin\left(2\pi x\right)\sin\left(2\pi y\right) \quad \text{on } \Omega,\end{aligned}$$

where the anisotropy function γ_{abs} is given by

$$\gamma_{abs}\left(\mathbf{P}\right)=\sum_{i=1}^{3}\sqrt{P_i^2+\epsilon_{abs}\sum_{j=1}^{3}P_j^2} \text{ for } \epsilon_{abs}=0.001,$$

and we apply the Neumann boundary conditions

$$\partial_\nu\varphi=\mathbb{E}_\gamma\nabla w_\gamma\cdot\nu=0 \quad \text{on } \partial\Omega.$$

Computational domain: $\Omega\equiv[0,1]^2$.
Final time: $T=0.004$.
Space steps: $h=0.01$.
Time step: $\tau=5\cdot10^{-10}$.
Numerical scheme: 6.3.9
Figure: 7.61.
Remark: Compare with the Numerical experiment 7.2.18.

Anisotropic graph formulation of the mean-curvature flow

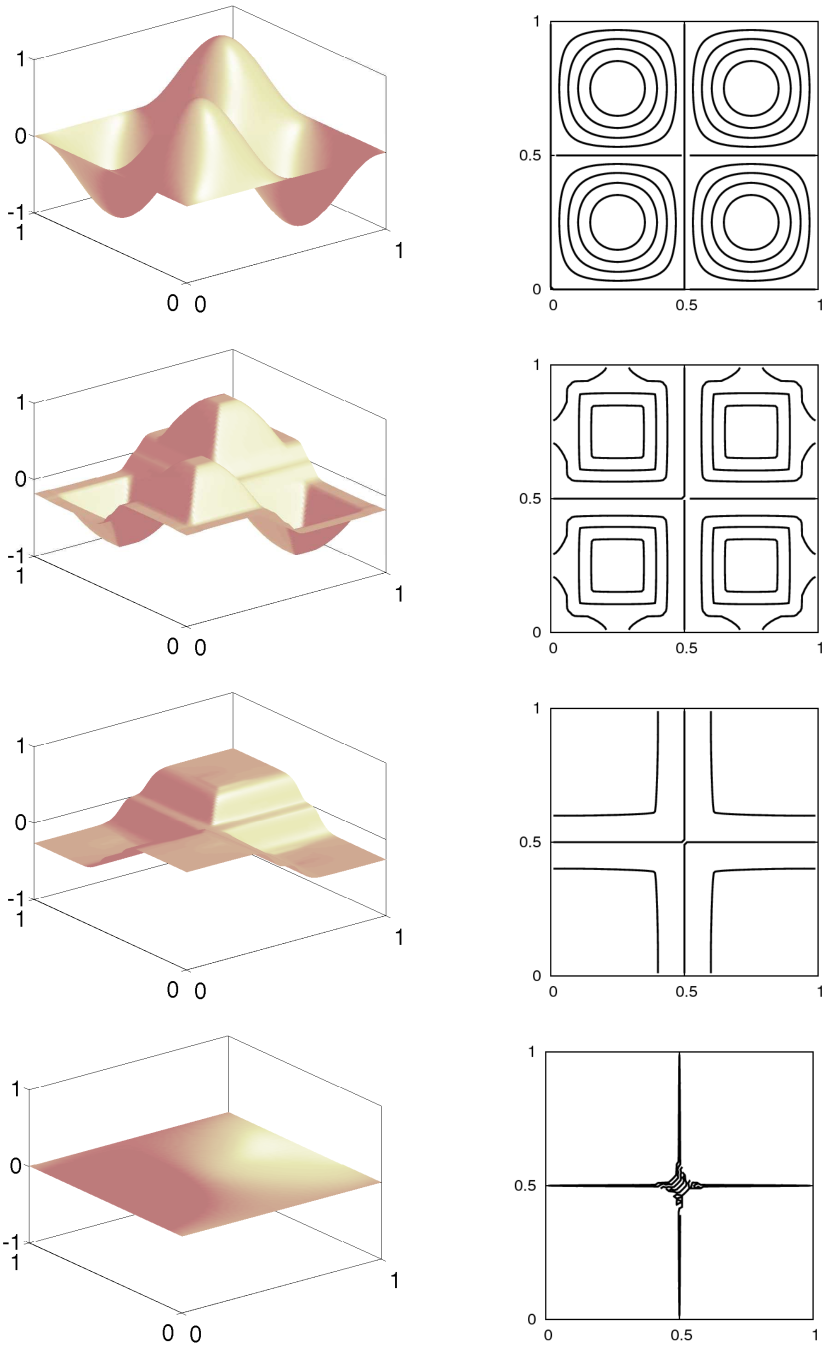

Figure 7.60.: **The explicit finite difference** numerical scheme for the **anisotropic mean-curvature flow of graphs** at times $t = 0$, $t = 0.04$, $t = 0.16$ and $t = 0.7$ (graph of φ on the left, level-lines of φ on the right). See the Numerical experiment 7.2.41.

Anisotropic graph formulation of the Willmore flow

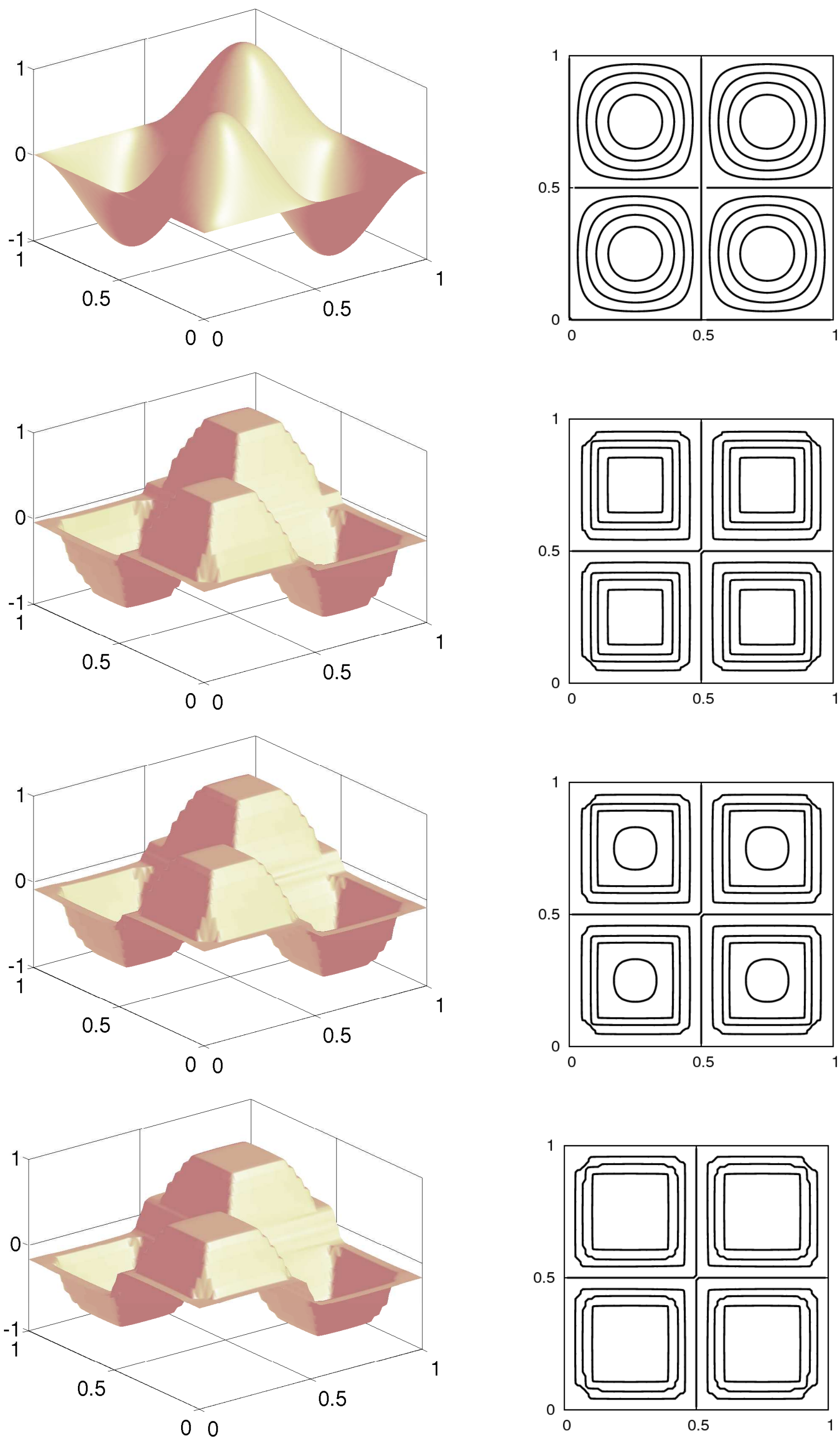

Figure 7.61.: **The semi-implicit finite difference** numerical scheme for the **anisotropic Willmore flow of graphs** at times $t = 0$, $t = 0.0001$, $t = 0.0002$ and $t = 0.0004$ (graph of φ on the left, level-lines of φ on the right) – not a steady state. See the Numerical experiment 7.2.42.

Numerical experiment 7.2.43. Test of the **explicit finite difference** numerical scheme for the **anisotropic mean-curvature flow of graphs**

$$\begin{aligned}\partial_t \varphi &= Q \nabla_{\mathbf{p}} \gamma_{abs} (\nabla \varphi, -1) \quad \text{on } (0, \mathrm{T}\rangle \times \Omega \\ \varphi\,|_{t=0} &= \sin\left(3\pi \sqrt{x^2+y^2}\right) \quad \text{on } \Omega\end{aligned}$$

where the anisotropy function γ_{abs} is given by

$$\gamma_{abs}(\mathbf{P}) = \sum_{i=1}^{3} \sqrt{P_i^2 + \epsilon_{abs} \sum_{j=1}^{3} P_j^2} \text{ for } \epsilon_{abs} = 0.001,$$

and we apply the Neumann boundary conditions

$$\nabla_{\mathbf{p}} \gamma \nu = 0 \quad \text{on } \partial\Omega.$$

Computational domain: $\Omega \equiv [-2, 2]^2$.
Final time: $T = 0.5$.
Space steps: $h = 0.04$.
Time step: Adaptive.
Numerical scheme: 6.3.6
Figure: 7.62.
Remark: Compare with the Numerical experiment 7.2.19.

Numerical experiment 7.2.44. Test of the **explicit finite difference** numerical scheme for the **anisotropic Willmore flow of graphs**

$$\begin{aligned}\partial_t \varphi &= -Q \nabla \cdot \left(\mathbb{E}_\gamma \nabla w_\gamma - \frac{1}{2} \frac{w_\gamma^2}{Q^3} \nabla \varphi \right) \quad \text{on } (0, T) \times \Omega, \\ w_\gamma &= Q H_\gamma \quad \text{on } (0, T) \times \Omega, \\ \varphi\,|_{t=0} &= \sin(2\pi x) \sin(2\pi y) \quad \text{on } \Omega,\end{aligned}$$

where the anisotropy function γ_{abs} is given by

$$\gamma_{abs}(\mathbf{P}) = \sum_{i=1}^{3} \sqrt{P_i^2 + \epsilon_{abs} \sum_{j=1}^{3} P_j^2} \text{ for } \epsilon_{abs} = 0.001,$$

and we apply the Neumann boundary conditions

$$\partial_\nu \varphi = \mathbb{E}_\gamma \nabla w_\gamma \cdot \nu = 0 \quad \text{on } \partial\Omega.$$

Computational domain: $\Omega \equiv [-2, 2]^2$.
Final time: $T = 0.006$.
Space steps: $h = 0.04$.
Time step: Adaptive.
Numerical scheme: 6.3.7
Figure: 7.63.
Remark: Compare with the Numerical experiment 7.2.20. The computation has been stopped after 70 days of running on 4 CPUs Opteron 2261.

Anisotropic graph formulation of the mean-curvature flow

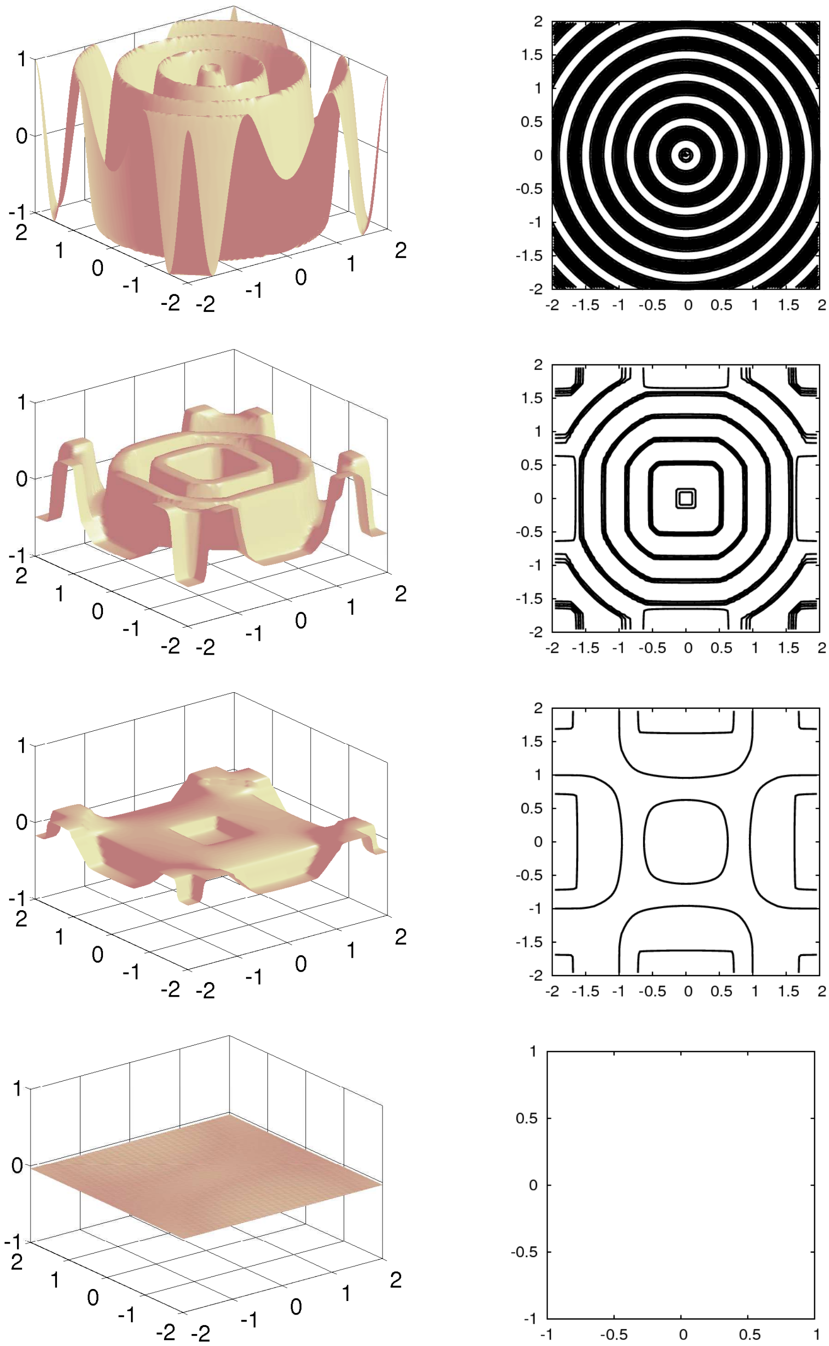

Figure 7.62.: **The explicit finite difference** numerical scheme for the **anisotropic mean-curvature flow of graphs** at times $t = 0$, $t = 0.04$, $t = 0.08$ and $t = 0.5$ (graph of φ on the left, level-lines of φ on the right). See the Numerical experiment 7.2.43.

Anisotropic graph formulation of the Willmore flow

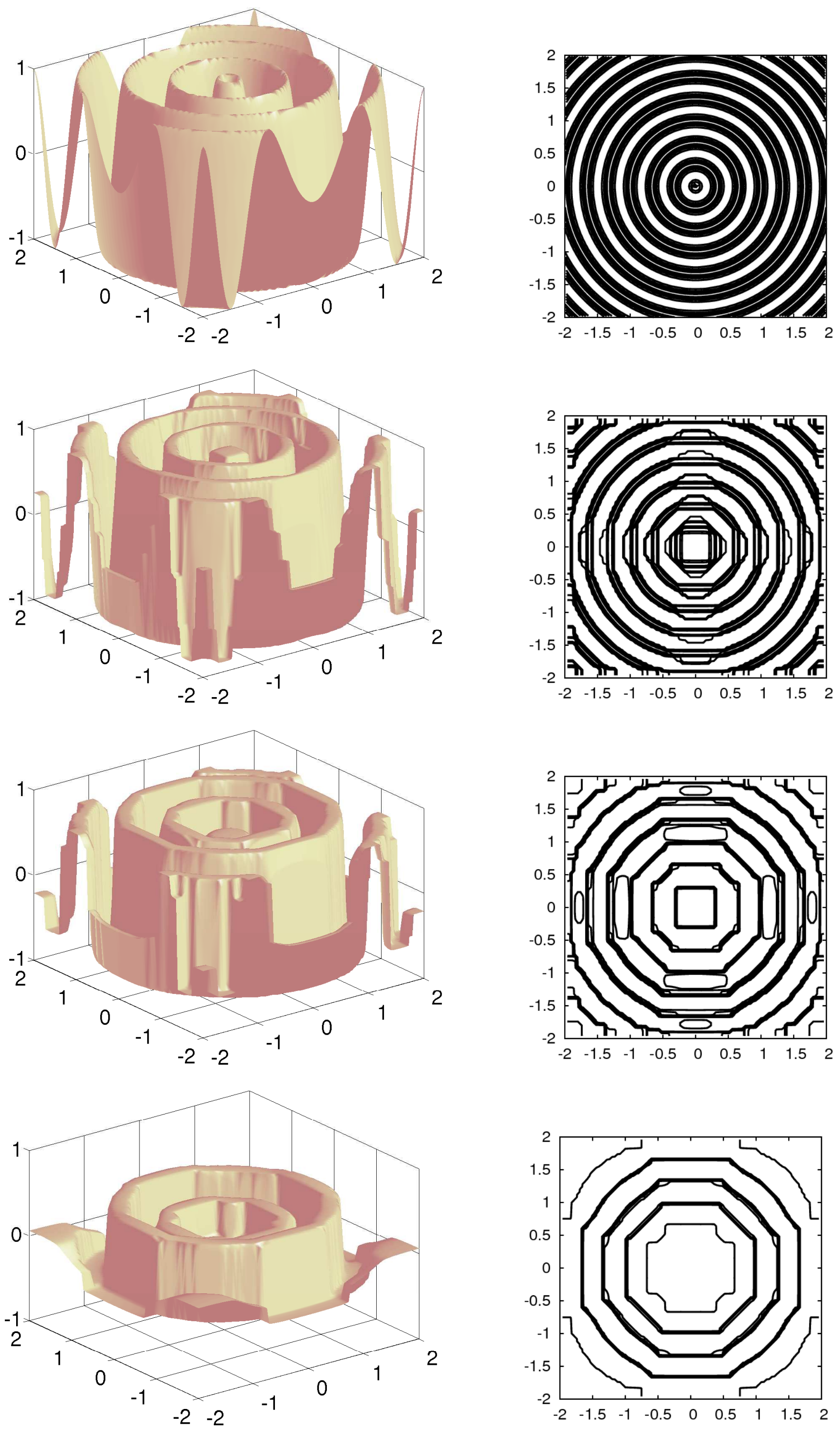

Figure 7.63.: **The explicit finite difference** numerical scheme for the **anisotropic Willmore flow of graphs** at times $t = 0$, $t = 5 \cdot 10^{-5}$, $t = 0.001$ and $t = 0.006$ – not a steady state (graph of φ on the left, level-lines of φ on the right). See the Numerical experiment 7.2.44.

Numerical experiment 7.2.45. Test of the **explicit finite difference** numerical scheme for the **anisotropic mean-curvature flow of graphs**

$$\begin{aligned} \partial_t \varphi &= Q \nabla_{\mathbf{p}} \gamma_{l^{16}} (\nabla \varphi, -1) \quad \text{on } (0, \mathrm{T}\rangle \times \Omega \\ \varphi \mid_{t=0} &= \sin(2\pi x) \sin(2\pi y)) \quad \text{on } \Omega \end{aligned}$$

where the anisotropy function $\gamma_{l^{16}}$ is given by

$$\gamma_{l^{16}} (\mathbf{P}) = \left(\sum_{i=1}^{3} |P_i|^{16} \right)^{\frac{1}{16}}$$

and we apply the Dirichlet boundary conditions

$$\varphi = 0 \quad \text{on } \partial\Omega.$$

Computational domain: $\Omega \equiv [0,1]^2$.
Final time: $T = 0.1$.
Space steps: $h = 0.01$.
Time step: $\tau = 0.005$.
Numerical scheme: 6.3.8
Figure: 7.64.
Remark: In case of l^m anisotropy the solution of the mean-curvature flow of graphs seems to converge to non-trivial steady state. Compare with the Numerical experiment 7.2.9.

Numerical experiment 7.2.46. Test of the **explicit finite difference** numerical scheme for the **anisotropic Willmore flow of graphs**

$$\begin{aligned} \partial_t \varphi &= -Q \nabla \cdot \left(\mathbb{E}_\gamma \nabla w_\gamma - \frac{1}{2} \frac{w_\gamma^2}{Q^3} \nabla \varphi \right) \quad \text{on } (0, T\rangle \times \Omega, \\ w_\gamma &= Q H_\gamma \quad \text{on } (0, T\rangle \times \Omega, \\ \varphi \mid_{t=0} &= \sin(2\pi x) \sin(2\pi y) \quad \text{on } \Omega, \end{aligned}$$

where the anisotropy function $\gamma_{l^{16}}$ is given by

$$\gamma_{l^{16}} (\mathbf{P}) = \left(\sum_{i=1}^{3} |P_i|^{16} \right)^{\frac{1}{16}}$$

and we apply the Dirichlet boundary conditions

$$\varphi = w_\gamma = 0 \quad \text{on } \partial\Omega.$$

Computational domain: $\Omega \equiv [0,1]^2$.
Final time: $T = 0.0004$.
Space steps: $h = 0.01$.
Time step: Adaptive.
Numerical scheme: 6.3.7
Figure: 7.65
Remark: –

Anisotropic graph formulation of the mean-curvature flow

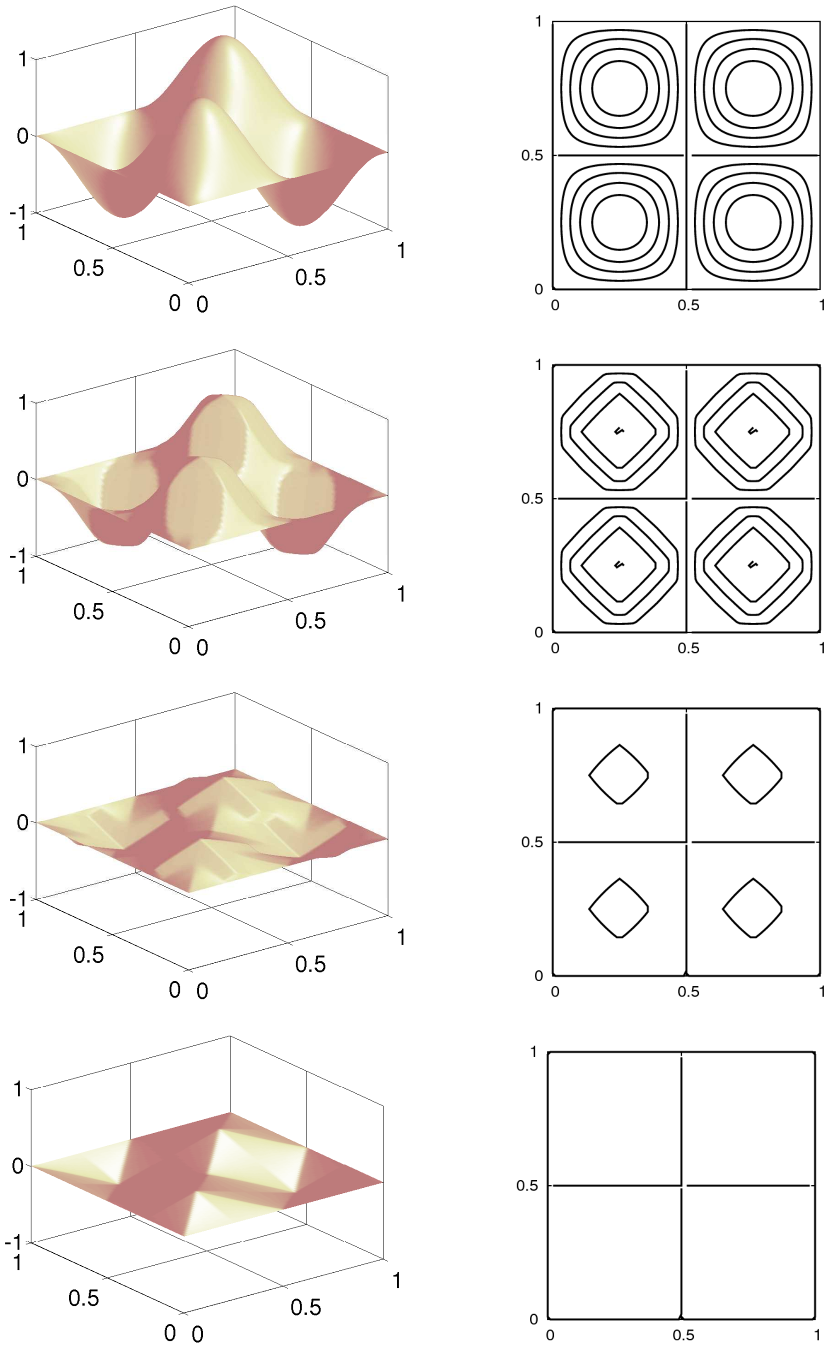

Figure 7.64.: The semi-implicit finite difference numerical scheme for the **anisotropic mean-curvature flow of graphs** at times $t = 0$, $t = 0.005$, $t = 0.025$ and $t = 0.1$ (graph of φ on the left, level-lines of φ on the right). See the Numerical experiment 7.2.45.

Anisotropic graph formulation of the Willmore flow

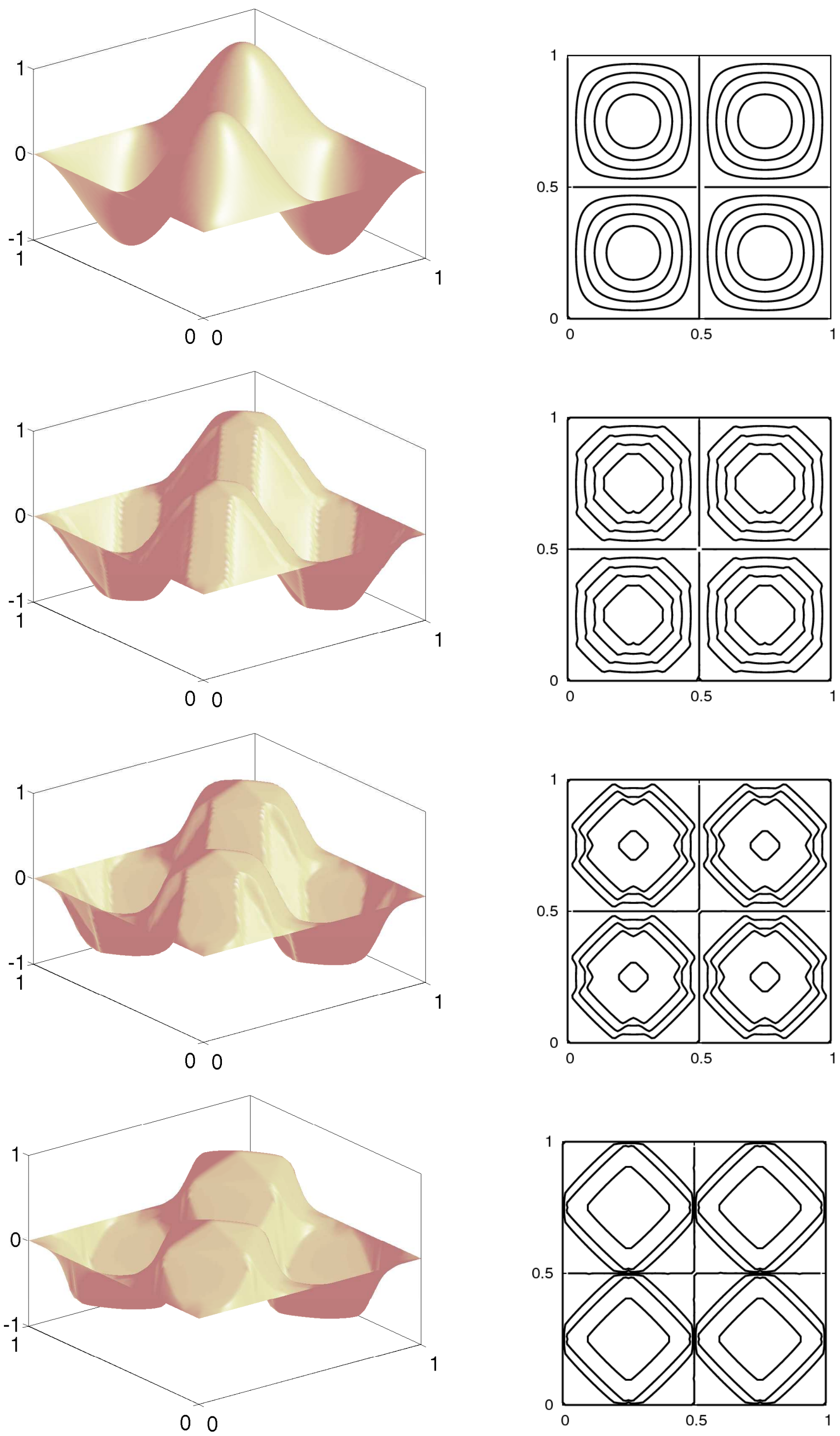

Figure 7.65.: The explicit finite difference numerical scheme for the **anisotropic Willmore flow of graphs** at times $t = 0$, $t = 2 \cdot 10^{-5}$, $t = 0.0001$ and $t = 0.0004$ (graph of φ on the left, level-lines of φ on the right) – not a steady state. See the Numerical experiment 7.2.46.

Numerical experiment 7.2.47. Test of the **explicit finite difference** numerical scheme for the **anisotropic mean-curvature flow of graphs**

$$\begin{aligned}\partial_t \varphi &= Q \nabla_{\mathbf{p}} \gamma_{l^{16}} (\nabla \varphi, -1) \quad \text{on } (0, \mathrm{T}\rangle \times \Omega \\ \varphi \mid_{t=0} &= \operatorname{sign}\left(x^2 + y^2 - 0.1\right) + 1 \quad \text{on } \Omega\end{aligned}$$

where the anisotropy function $\gamma_{l^{16}}$ is given by

$$\gamma_{l^{16}} (\mathbf{P}) = \left(\sum_{i=1}^{3} |P_i|^{16} \right)^{\frac{1}{16}}$$

and we apply the Dirichlet boundary conditions

$$\varphi = 0 \quad \text{on } \partial\Omega.$$

Computational domain: $\Omega \equiv [-0.5, 0.5]^2$.
Final time: $T = 0.0625$.
Space steps: $h = 0.01$.
Time step: $\tau = 10^{-5}$.
Numerical scheme: 6.3.8
Figure: 7.66
Remark: Compare with the Numerical experiment 7.2.11.

Numerical experiment 7.2.48. Test of the **explicit finite difference** numerical scheme for the **anisotropic Willmore flow of graphs**

$$\begin{aligned}\partial_t \varphi &= -Q \nabla \cdot \left(\mathbb{E}_\gamma \nabla w_\gamma - \frac{1}{2} \frac{w_\gamma^2}{Q^3} \nabla \varphi \right) \quad \text{on } (0, T) \times \Omega, \\ w_\gamma &= Q H_\gamma \quad \text{on } (0, T) \times \Omega, \\ \varphi \mid_{t=0} &= \operatorname{sign}\left(x^2 + y^2 - 0.1\right) + 1 \quad \text{on } \Omega,\end{aligned}$$

where the anisotropy function $\gamma_{l^{16}}$ is given by

$$\gamma_{l^{16}} (\mathbf{P}) = \left(\sum_{i=1}^{3} |P_i|^{16} \right)^{\frac{1}{16}}$$

and we apply the Dirichlet boundary conditions

$$\varphi = w_\gamma = 0 \quad \text{on } \partial\Omega.$$

Computational domain: $\Omega \equiv [-0.5, 0.5]^2$.
Final time: $T = 0.025$.
Space steps: $h = 0.01$.
Time step: $\tau = 5 \cdot 10^{-9}$.
Numerical scheme: 6.3.9
Figure: 7.67.
Remark: In case of l^m anisotropy the solution of the Willmore flow of graphs seems to converge to non-trivial steady state. Compare with the Numerical experiment 7.2.12.

Anisotropic graph formulation of the mean-curvature flow

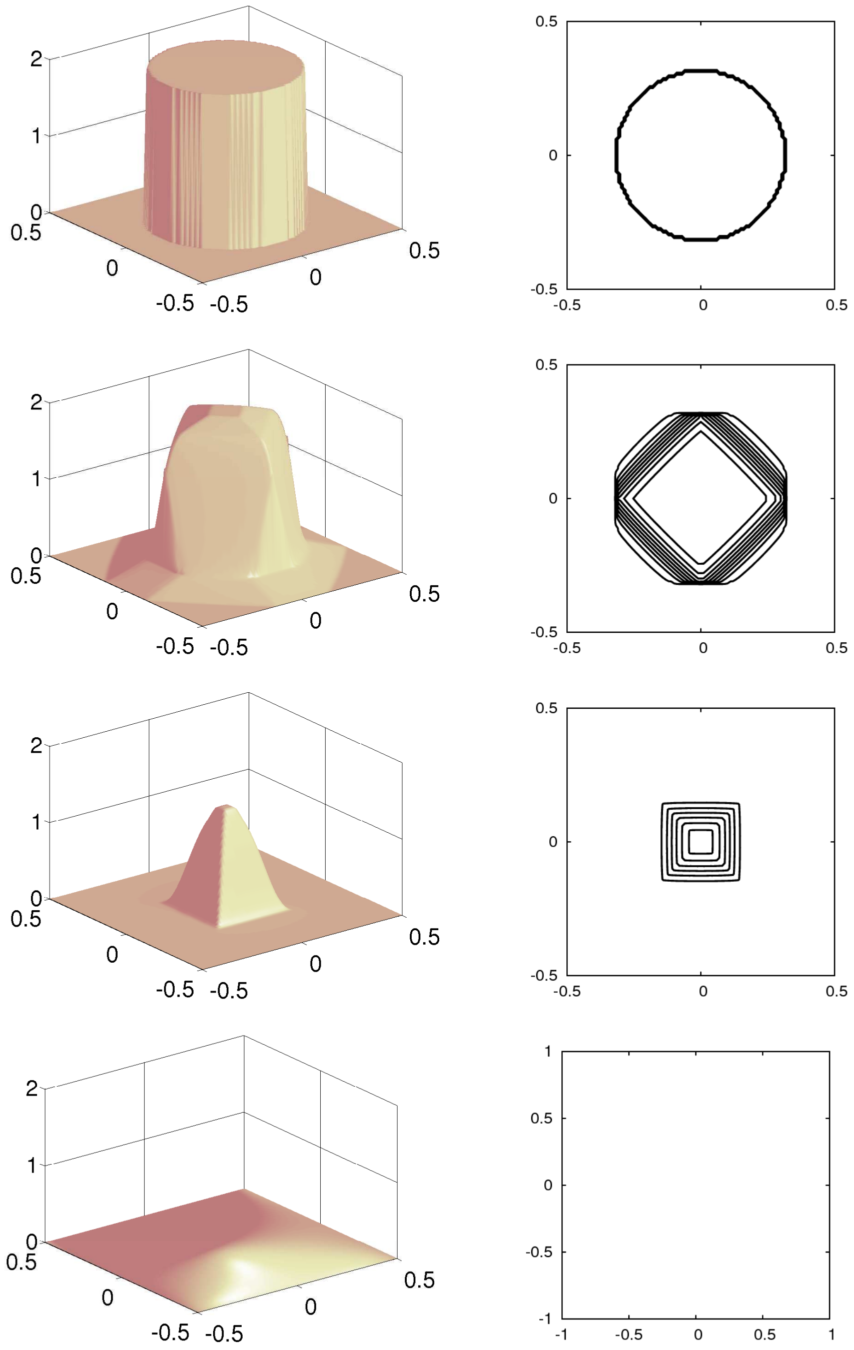

Figure 7.66.: The semi-implicit finite difference numerical scheme for the **anisotropic mean-curvature flow of graphs** at times $t = 0$, $t = 0.0125$, $t = 0.0375$ and $t = 0.0625$ (graph of φ on the left, level-lines of φ on the right). See the Numerical experiment 7.2.47.

Anisotropic graph formulation of the Willmore flow

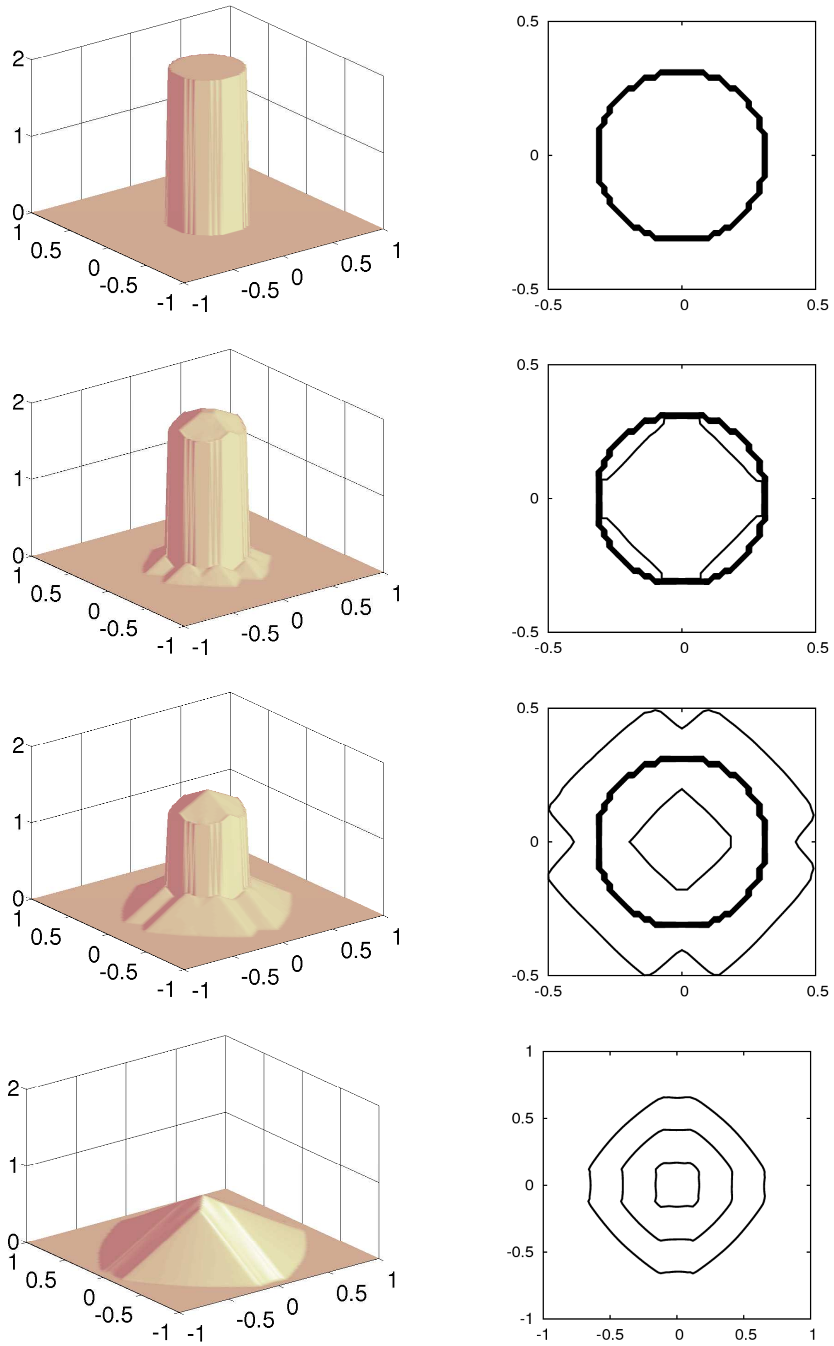

Figure 7.67.: The semi-implicit finite difference numerical scheme for the **anisotropic Willmore flow of graphs** at times $t = 0$, $t = 0.0001$, $t = 0.005$ and $t = 0.025$ (graph of φ on the left, level-lines of φ on the right). See the Numerical experiment 7.2.48.

Numerical experiment 7.2.49. Test of the **explicit finite difference** numerical scheme for the **anisotropic mean-curvature flow of graphs**

$$\begin{aligned}\partial_t \varphi &= Q \nabla_{\mathbf{p}} \gamma_{l^{16}} \left(\nabla \varphi, -1 \right) \quad \text{on } (0, \mathrm{T}\rangle \times \Omega \\ \varphi\,|_{t=0} &= \sin\left(\pi \tanh\left(5\left(\left(x^2+y^2\right)-0.25\right)\right)\right) \quad \text{on } \Omega\end{aligned}$$

where the anisotropy function $\gamma_{l^{16}}$ is given by

$$\gamma_{l^{16}}\left(\mathbf{P}\right) = \left(\sum_{i=1}^{3} |P_i|^{16} \right)^{\frac{1}{16}}$$

and we apply the Dirichlet boundary conditions

$$\varphi = 0 \quad \text{on } \partial\Omega.$$

Computational domain: $\Omega \equiv [-1, 1]^2$.
Final time: $T = 1.0$.
Space steps: $h = 0.02$.
Time step: $\tau = 1.25 \cdot 10^{-4}$.
Numerical scheme: 6.3.8
Figure: 7.68.
Remark: In case of l^m anisotropy the solution of the mean-curvature flow of graphs seems to converge to non-trivial steady state. Compare with the Numerical experiment 7.2.13.

Numerical experiment 7.2.50. Test of the **explicit finite difference** numerical scheme for the **anisotropic Willmore flow of graphs**

$$\begin{aligned}\partial_t \varphi &= -Q \nabla \cdot \left(\mathbb{E}_\gamma \nabla w_\gamma - \frac{1}{2} \frac{w_\gamma^2}{Q^3} \nabla \varphi \right) \quad \text{on } (0, T\rangle \times \Omega, \\ w_\gamma &= Q H_\gamma \quad \text{on } (0, T\rangle \times \Omega, \\ \varphi\,|_{t=0} &= \sin\left(\pi \tanh\left(5\left(\left(x^2+y^2\right)-0.25\right)\right)\right) \quad \text{on } \Omega,\end{aligned}$$

where the anisotropy function $\gamma_{l^{16}}$ is given by

$$\gamma_{l^{16}}\left(\mathbf{P}\right) = \left(\sum_{i=1}^{3} |P_i|^{16} \right)^{\frac{1}{16}}$$

and we apply the Dirichlet boundary conditions

$$\varphi = w_\gamma = 0 \quad \text{on } \partial\Omega.$$

Computational domain: $\Omega \equiv [-1, 1]^2$.
Final time: $T = 0.1$.
Space steps: $h = 0.04$.
Time step: Adaptive.
Numerical scheme: 6.3.7
Figure: 7.69
Remark: The solution at the time $t = 0.1$ seems to be a steady state solution.

Anisotropic graph formulation of the mean-curvature flow

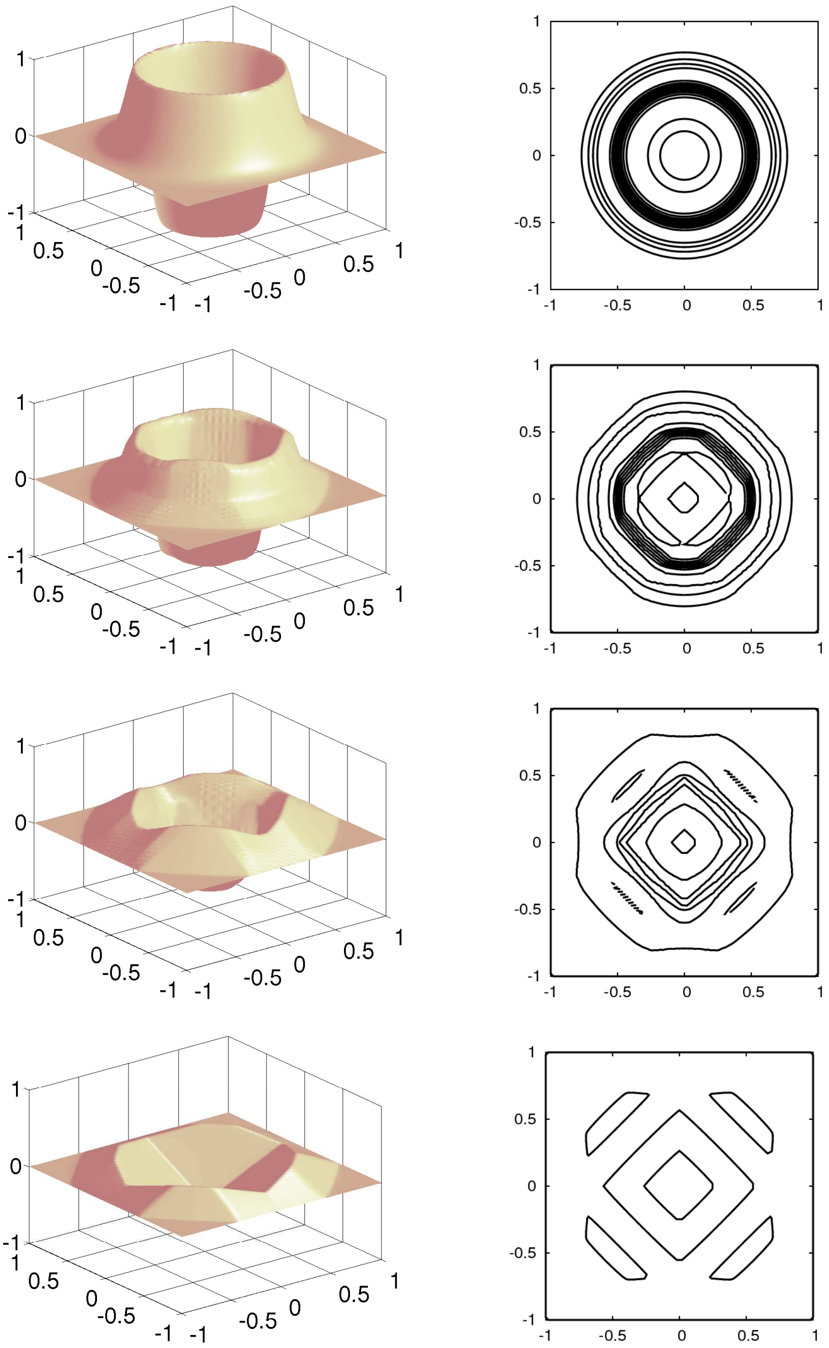

Figure 7.68.: The semi-implicit finite difference numerical scheme for the **anisotropic mean-curvature flow of graphs** at times $t = 0$, $t = 0.01$, $t = 0.04$ and $t = 1.0$ (graph of φ on the left, level-lines of φ on the right). See the Numerical experiment 7.2.49.

Anisotropic graph formulation of the Willmore flow

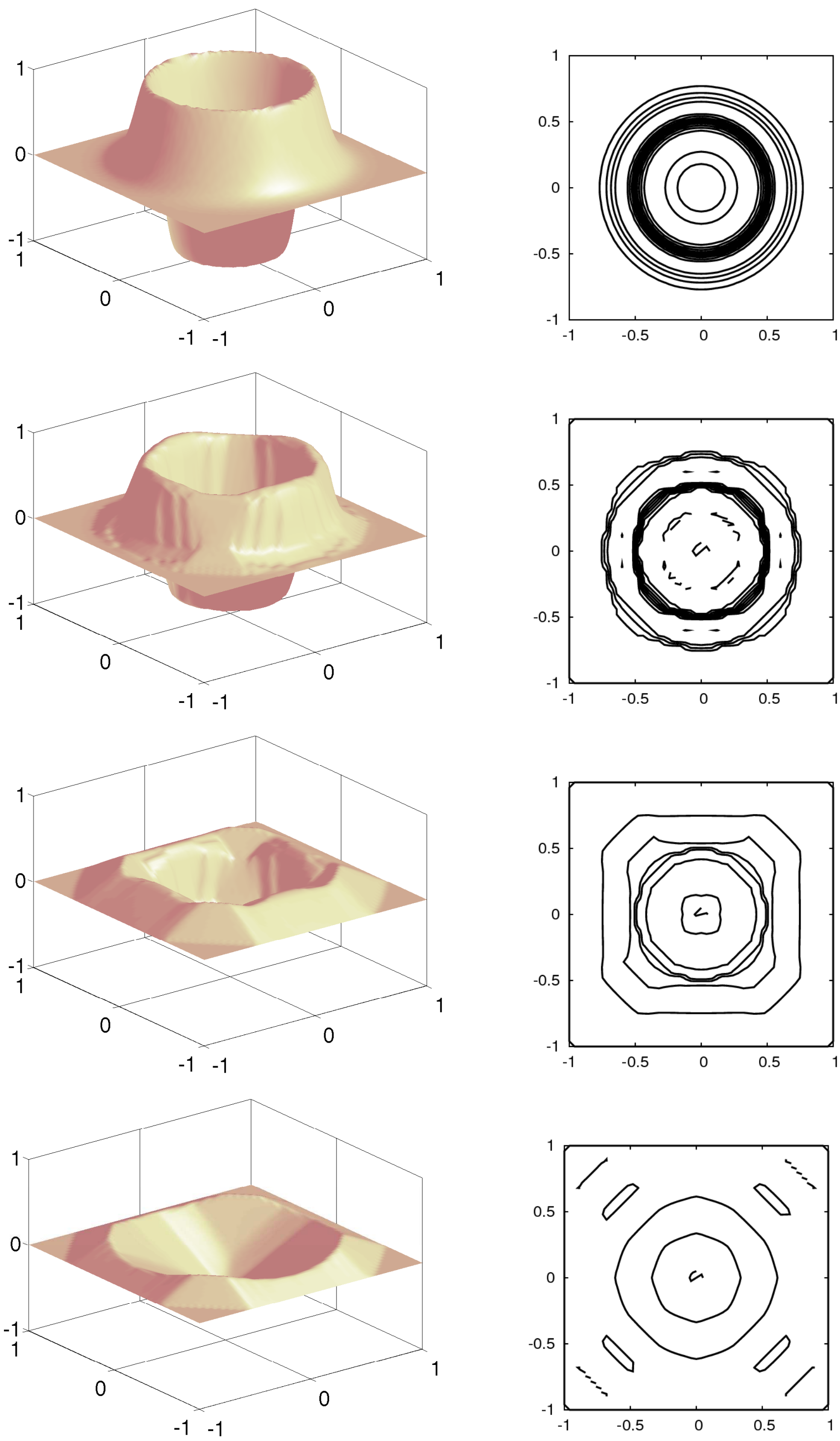

Figure 7.69.: The semi-implicit finite difference numerical scheme for the **anisotropic Willmore flow of graphs** at times $t = 0$, $t = 0.001$, $t = 0.01$ and $t = 0.1$ (graph of φ on the left, level-lines of φ on the right). See the Numerical experiment 7.2.50.

Numerical experiment 7.2.51. Test of the **explicit finite difference** numerical scheme for the **anisotropic mean-curvature flow of graphs**

$$
\begin{aligned}
\partial_t \varphi &= Q \nabla_{\mathbf{p}} \gamma_{l^{16}} \left(\nabla \varphi, -1 \right) \quad \text{on } (0, \mathrm{T}\rangle \times \Omega \\
\varphi \mid_{t=0} &= -0.5 \sin^2 \left(\pi x \right) \cdot \left(1 - \left(y - 2 \right)^2 \right) \left(1 - \tanh \left(10 \left(\sqrt{x^2 + y^2} - 0.6 \right) \right) \right) \quad \text{on } \Omega
\end{aligned}
$$

where the anisotropy function $\gamma_{l^{16}}$ is given by

$$
\gamma_{l^{16}} \left(\mathbf{P} \right) = \left(\sum_{i=1}^{3} \left| P_i \right|^{16} \right)^{\frac{1}{16}}
$$

and we apply the Dirichlet boundary conditions

$$
\varphi = 0 \quad \text{on } \partial \Omega.
$$

Computational domain: $\Omega \equiv [-1, 1]^2$.
Final time: $T = 0.125$.
Space steps: $h = 0.02$.
Time step: $\tau = 2.5 \cdot 10^{-4}$.
Numerical scheme: 6.3.8
Figure: 7.70.
Remark: In case of l^m anisotropy the solution of the mean-curvature flow of graphs seems to converge to non-trivial steady state. Compare with the Numerical experiment 7.2.15.

Numerical experiment 7.2.52. Test of the **explicit finite difference** numerical scheme for the **anisotropic Willmore flow of graphs**

$$
\begin{aligned}
\partial_t \varphi &= -Q \nabla \cdot \left(\mathbb{E}_\gamma \nabla w_\gamma - \frac{1}{2} \frac{w_\gamma^2}{Q^3} \nabla \varphi \right) \quad \text{on } (0, T) \times \Omega, \\
w_\gamma &= Q H_\gamma \quad \text{on } (0, T) \times \Omega, \\
\varphi \mid_{t=0} &= -0.5 \sin^2 \left(\pi x \right) \cdot \left(1 - \left(y - 2 \right)^2 \right) \left(1 - \tanh \left(10 \left(\sqrt{x^2 + y^2} - 0.6 \right) \right) \right) \quad \text{on } \Omega,
\end{aligned}
$$

where the anisotropy function $\gamma_{l^{16}}$ is given by

$$
\gamma_{l^{16}} \left(\mathbf{P} \right) = \left(\sum_{i=1}^{3} \left| P_i \right|^{16} \right)^{\frac{1}{16}}
$$

and we apply the Neumann boundary conditions

$$
\varphi = w_\gamma = 0 \quad \text{on } \partial \Omega.
$$

Computational domain: $\Omega \equiv [-1, 1]^2$.
Final time: $T = 0.009$.
Space steps: $h = 0.02$.
Time step: Adaptive.
Numerical scheme: 6.3.7
Figure: 7.2.52.
Remark: The computation has been stopped after 50 days of running on 4 CPUs Opteron 270 2 GHz.

Anisotropic graph formulation of the mean-curvature flow

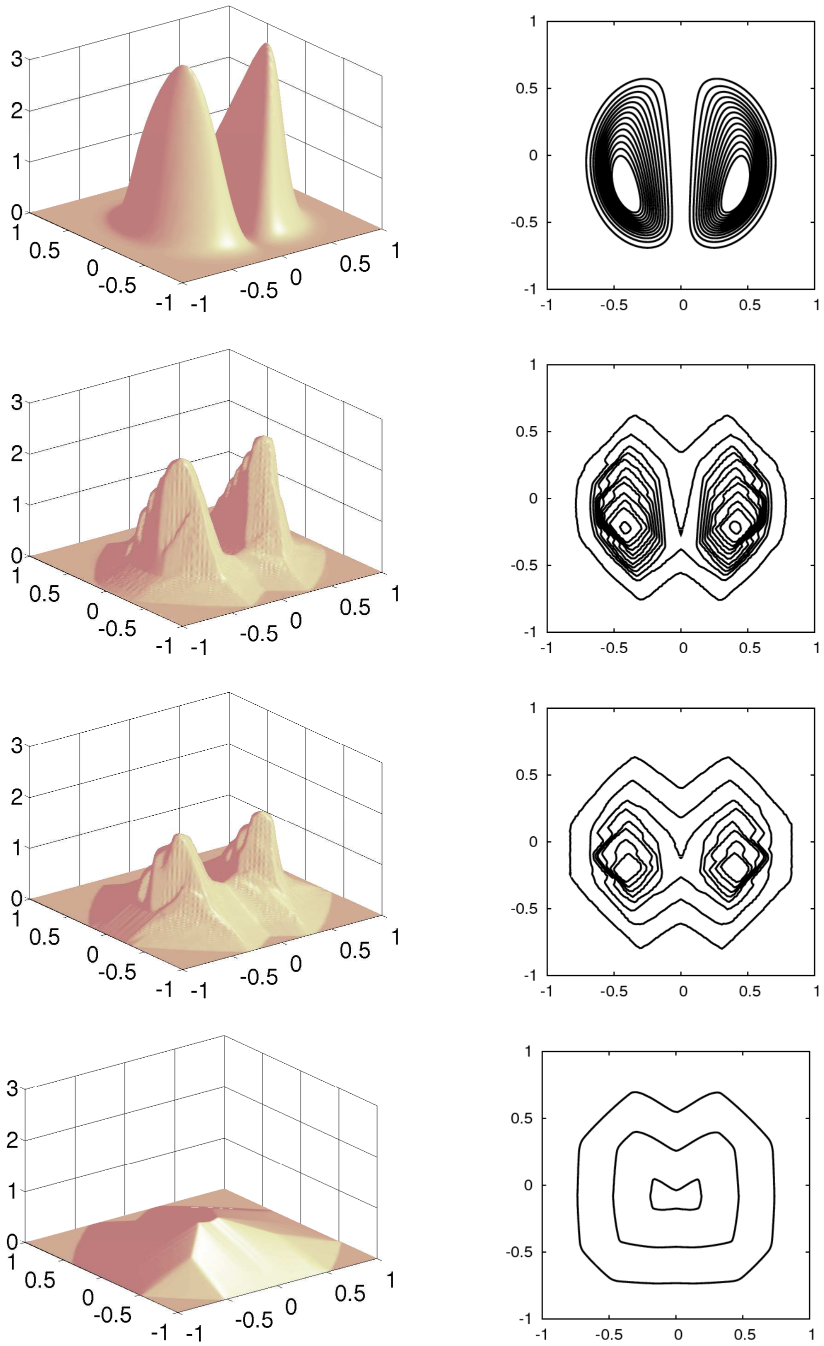

Figure 7.70.: The semi-implicit finite difference numerical scheme for the **anisotropic mean-curvature flow of graphs** at times $t = 0$, $t = 0.02$, $t = 0.04$ and $t = 1.0$ (graph of φ on the left, level-lines of φ on the right). See the Numerical experiment 7.2.51.

Anisotropic graph formulation of the Willmore flow

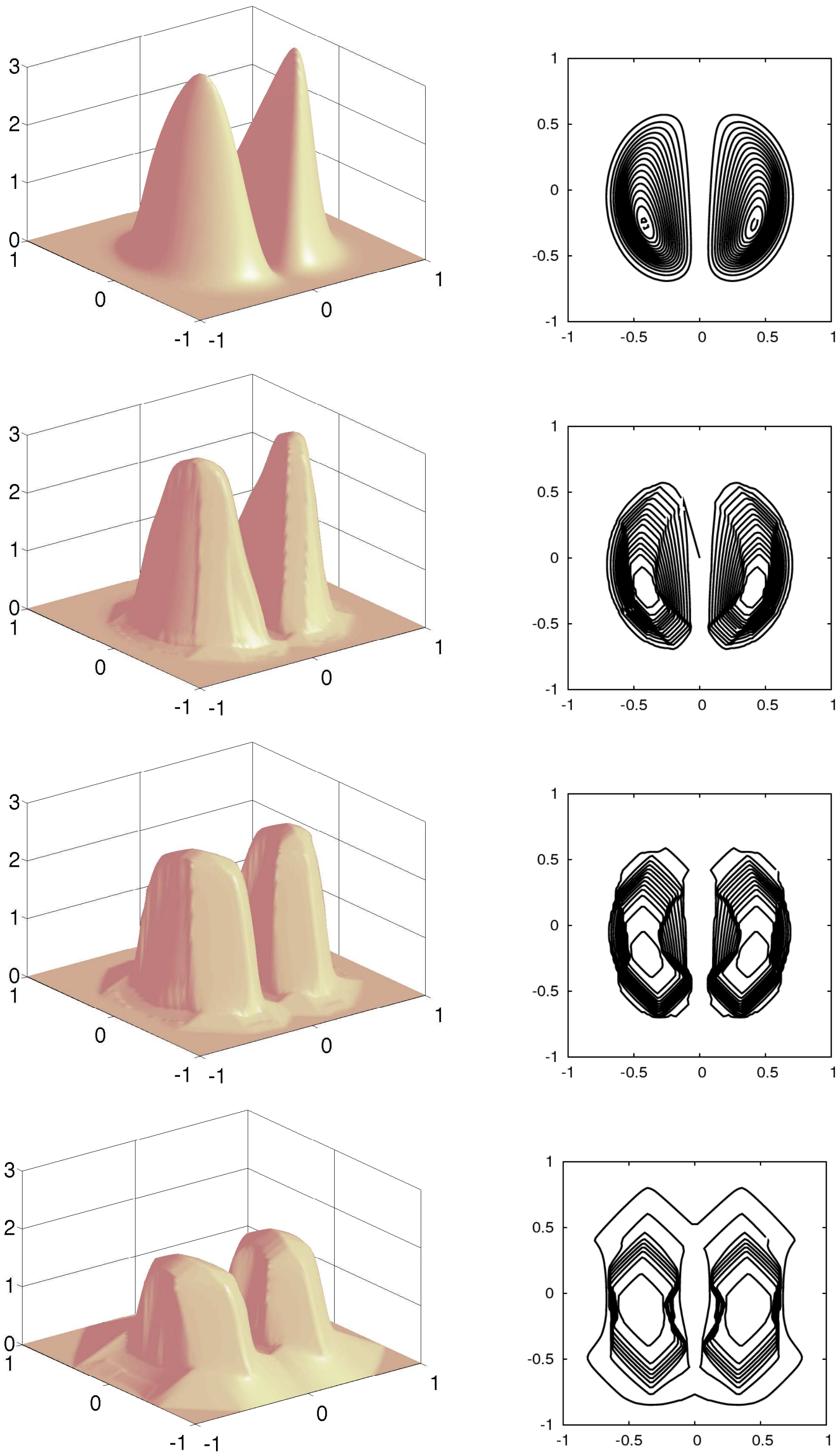

Figure 7.71.: The semi-implicit finite difference numerical scheme for the **anisotropic Willmore flow of graphs** at times $t = 0$, $t = 0.0001$, $t = 0.001$ and $t = 0.009$ – not a steady state (graph of φ on the left, level-lines of φ on the right). See the Numerical experiment 7.2.52.

Numerical experiment 7.2.53. Test of the **explicit finite difference** numerical scheme for the **anisotropic mean-curvature flow of graphs**

$$\begin{aligned}\partial_t \varphi &= Q \nabla_{\mathbf{p}} \gamma_{l^{16}} \left(\nabla \varphi, -1 \right) \quad \text{on } \left(0, \mathrm{T} \right\rangle \times \Omega \\ \varphi \left|_{t=0} \right. &= \sin \left(2\pi x \right) \sin \left(2\pi y \right) \quad \text{on } \Omega\end{aligned}$$

where the anisotropy function $\gamma_{l^{16}}$ is given by

$$\gamma_{l^{16}} \left(\mathbf{P} \right) = \left(\sum_{i=1}^{3} \left| P_i \right|^{16} \right)^{\frac{1}{16}}$$

and we apply the Neumann boundary conditions

$$\nabla_{\mathbf{p}} \gamma \nu = 0 \quad \text{on } \partial \Omega.$$

Computational domain: $\Omega \equiv [0, 1]^2$.
Boundary conditions: $\nabla_{\mathbf{p}} \gamma \nu = 0$ on $\partial \Omega$.
Final time: $T = 10^4$.
Space steps: $h = 0.01$.
Time step: Adaptive.
Numerical scheme: 6.3.6
Figure: 7.72
Remark: In case of l^m anisotropy the solution of the mean-curvature flow of graphs seems to converge to non-trivial steady state. Compare with the Numerical experiment 7.2.17.

Numerical experiment 7.2.54. Test of the **explicit finite difference** numerical scheme for the **anisotropic Willmore flow of graphs**

$$\begin{aligned}\partial_t \varphi &= -Q \nabla \cdot \left(\mathbb{E}_\gamma \nabla w_\gamma - \frac{1}{2} \frac{w_\gamma^2}{Q^3} \nabla \varphi \right) \quad \text{on } \left(0, T \right) \times \Omega, \\ w_\gamma &= Q H_\gamma \quad \text{on } \left(0, T \right) \times \Omega, \\ \varphi \left|_{t=0} \right. &= \sin \left(2\pi x \right) \sin \left(2\pi y \right) \quad \text{on } \Omega,\end{aligned}$$

where the anisotropy function $\gamma_{l^{16}}$ is given by

$$\gamma_{l^{16}} \left(\mathbf{P} \right) = \left(\sum_{i=1}^{3} \left| P_i \right|^{16} \right)^{\frac{1}{16}}$$

and we apply the Neumann boundary conditions

$$\partial_\nu \varphi = \mathbb{E}_\gamma \nabla w_\gamma \cdot \nu = 0 \quad \text{on } \partial \Omega.$$

Computational domain: $\Omega \equiv [0, 1]^2$.
Final time: $T = 0.005$.
Space steps: $h = 0.02$.
Time step: Adaptive.
Numerical scheme: 6.3.7
Figure: 7.73.
Remark: –

Anisotropic graph formulation of the mean-curvature flow

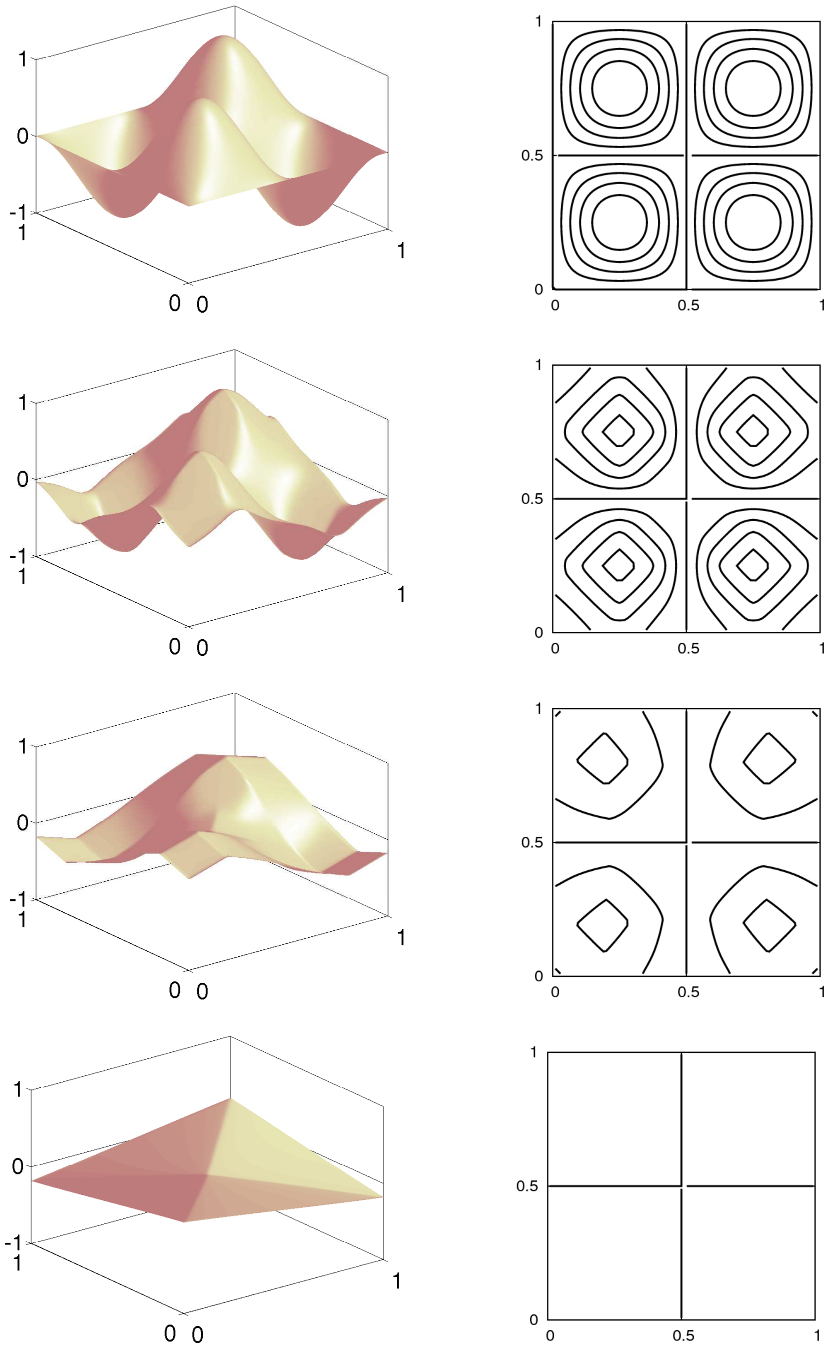

Figure 7.72.: **The explicit finite difference** numerical scheme for the **anisotropic mean-curvature flow of graphs** at times $t = 0$, $t = 0.001$, $t = 0.008$ and $t = 10^4$ (graph of φ on the left, level-lines of φ on the right). See the Numerical experiment 7.2.53.

Anisotropic graph formulation of the Willmore flow

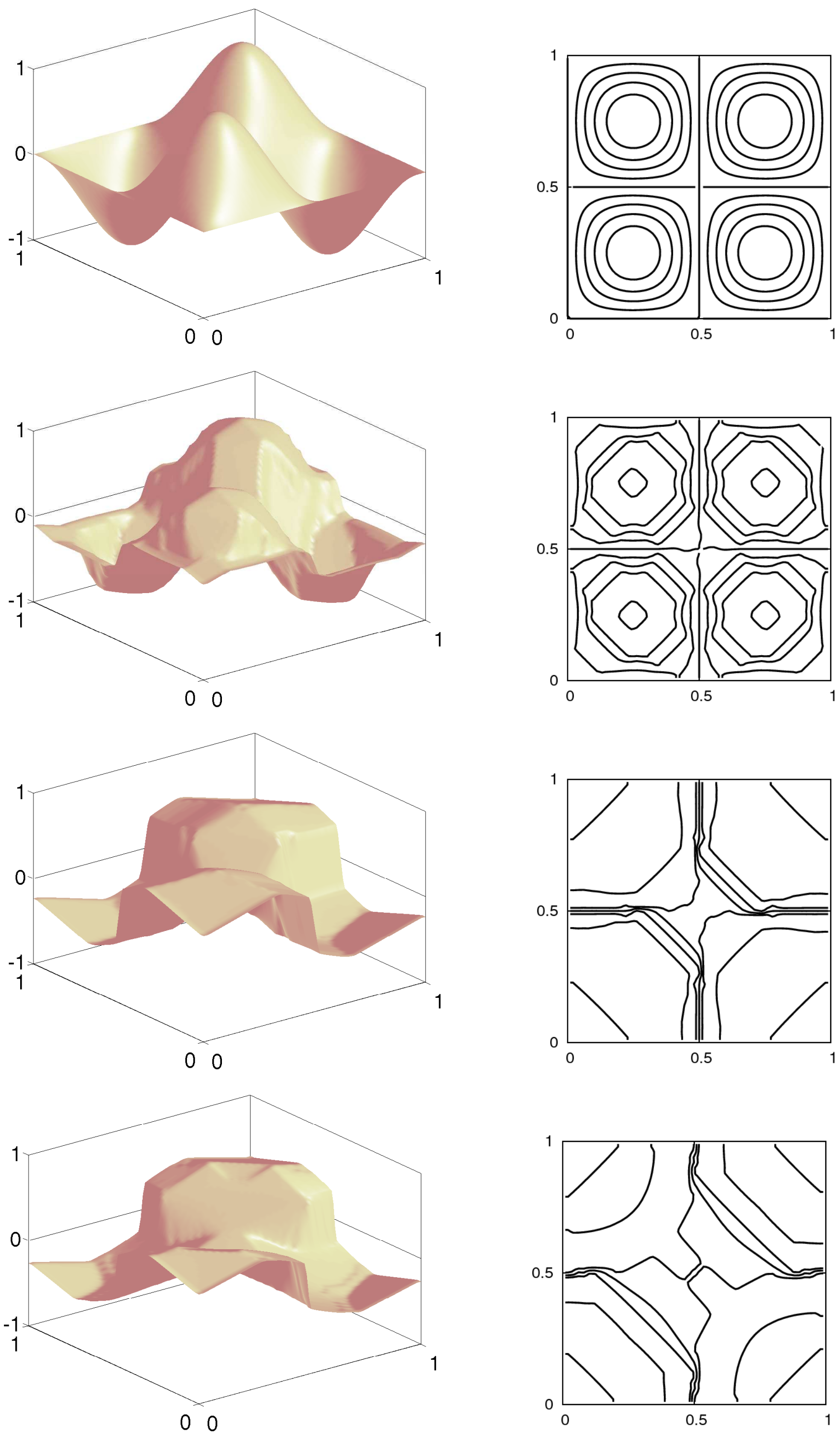

Figure 7.73.: **The explicit finite difference** numerical scheme for the **anisotropic Willmore flow of graphs** at times $t = 0$, $t = 0.0001$, $t = 0.001$ and $t = 0.005$ (graph of φ on the left, level-lines of φ on the right). See the Numerical experiment 7.2.54.

Numerical experiment 7.2.55. Test of the **explicit finite difference** numerical scheme for the **anisotropic mean-curvature flow of graphs**

$$
\begin{aligned}
\partial_t \varphi &= Q \nabla_{\mathbf{p}} \gamma_{l^{16}} \left(\nabla \varphi, -1 \right) \quad \text{on } (0, \mathrm{T}\rangle \times \Omega \\
\varphi \mid_{t=0} &= \sin \left(3\pi \sqrt{x^2 + y^2} \right) \quad \text{on } \Omega
\end{aligned}
$$

where the anisotropy function $\gamma_{l^{16}}$ is given by

$$
\gamma_{l^{16}} \left(\mathbf{P} \right) = \left(\sum_{i=1}^{3} \left| P_i \right|^{16} \right)^{\frac{1}{16}}
$$

and we apply the Dirichlet boundary conditions

$$
\varphi = 0 \quad \text{on } \partial\Omega.
$$

Computational domain: $\Omega \equiv [-2, 2]^2$.
Final time: $T = 5 \cdot 10^5$.
Space steps: $h = 0.04$.
Time step: Adaptive.
Numerical scheme: 6.3.6
Figure: 7.74.
Remark: In case of l^m anisotropy the solution of the mean-curvature flow of graphs seems to converge to non-trivial steady state. Compare with the Numerical experiment 7.2.19.

Numerical experiment 7.2.56. Test of the **explicit finite difference** numerical scheme for the **anisotropic Willmore flow of graphs**

$$
\begin{aligned}
\partial_t \varphi &= -Q \nabla \cdot \left(\mathbb{E}_\gamma \nabla w_\gamma - \frac{1}{2} \frac{w_\gamma^2}{Q^3} \nabla \varphi \right) \quad \text{on } (0, T) \times \Omega, \\
w_\gamma &= Q H_\gamma \quad \text{on } (0, T) \times \Omega, \\
\varphi \mid_{t=0} &= \sin \left(3\pi \sqrt{x^2 + y^2} \right) \quad \text{on } \Omega,
\end{aligned}
$$

where the anisotropy function $\gamma_{l^{16}}$ is given by

$$
\gamma_{l^{16}} \left(\mathbf{P} \right) = \left(\sum_{i=1}^{3} \left| P_i \right|^{16} \right)^{\frac{1}{16}}
$$

and we apply the Neumann boundary conditions

$$
\varphi = w_\gamma = 0 \quad \text{on } \partial\Omega.
$$

Computational domain: $\Omega \equiv [-2, 2]^2$.
Final time: $T = 0.1$.
Space steps: $h = 0.04$.
Time step: Adaptive.
Numerical scheme: 6.3.7
Figure: 7.75
Remark:

Anisotropic graph formulation of the mean-curvature flow

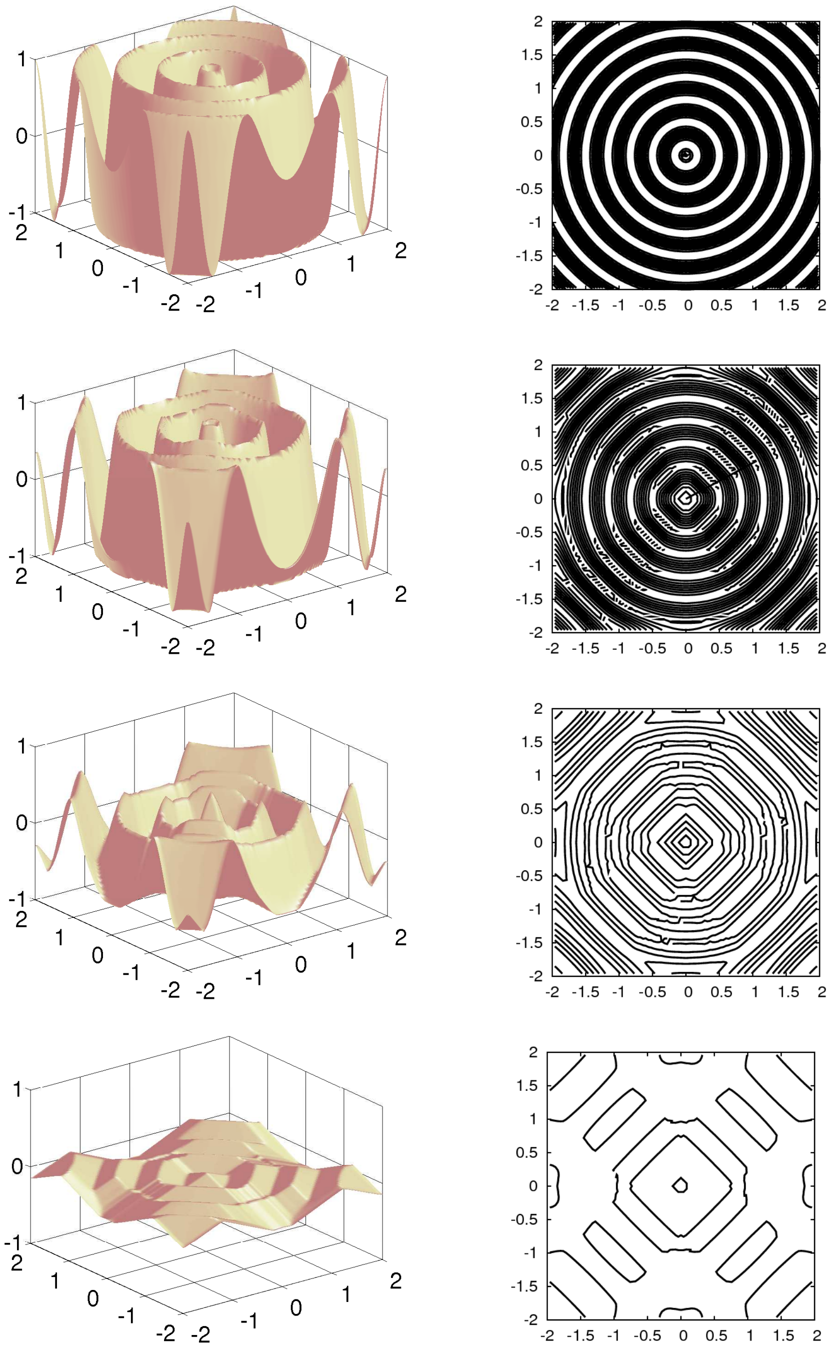

Figure 7.74.: **The explicit finite difference** numerical scheme for the **anisotropic mean-curvature flow of graphs** at times $t = 0$, $t = 0.001$, $t = 0.008$ and $t = 5 \cdot 10^5$ (graph of φ on the left, level-lines of φ on the right). See the Numerical experiment 7.2.55.

Anisotropic graph formulation of the Willmore flow

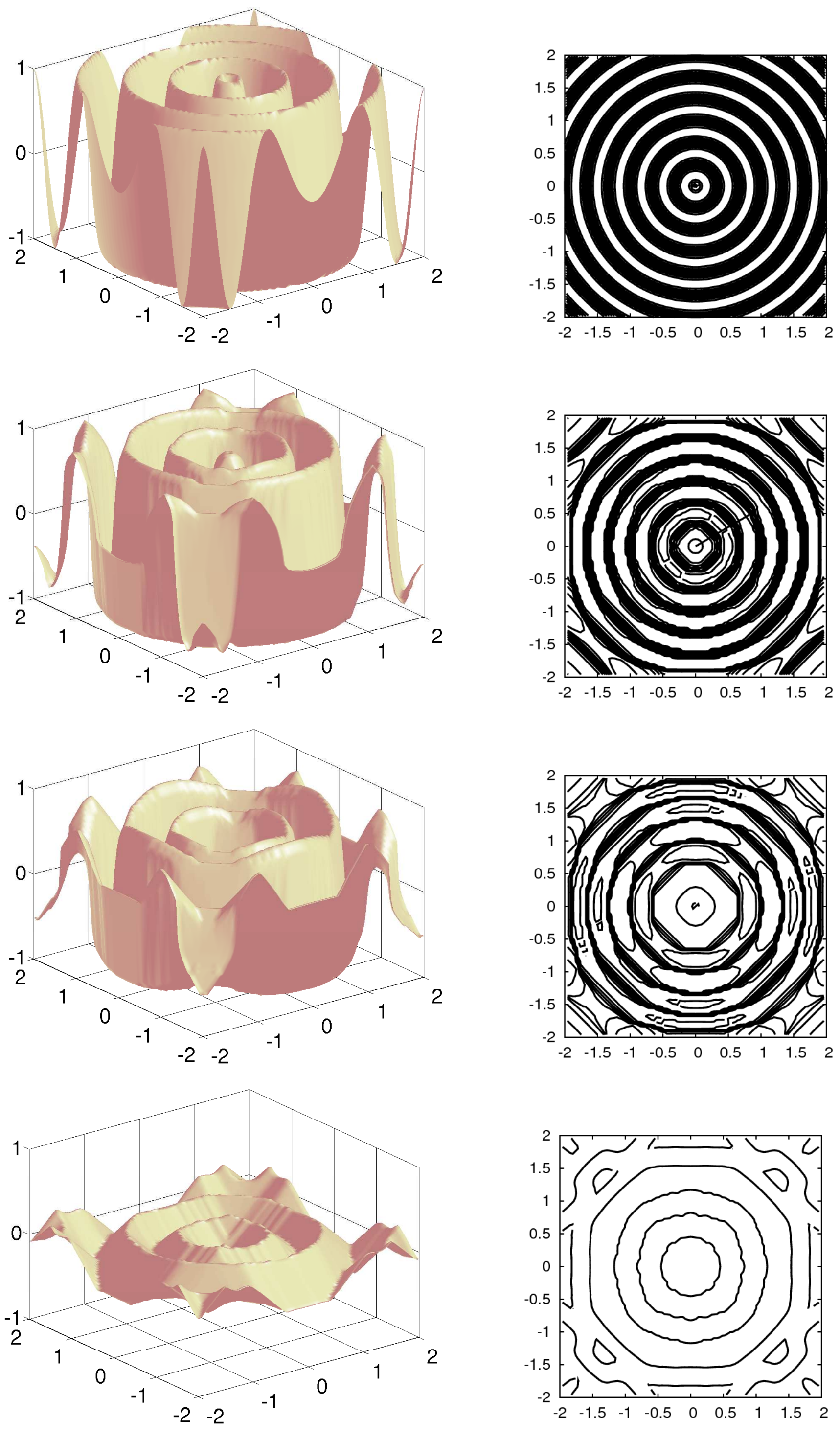

Figure 7.75.: **The explicit finite difference** numerical scheme for the **anisotropic Willmore flow of graphs** at times $t = 0$, $t = 0.001$, $t = 0.01$ and $t = 0.1$ (graph of φ on the left, level-lines of φ on the right). See the Numerical experiment 7.2.56.

7.2.2. Level-set formulation

The numerical experiments for the level-set formulation consist of two parts. In the first one we compare the level-set method with the parametric approach on the isotropic problems. The results are shown on the Figures 7.76 – 7.83 and set-ups of the experiments are described in the Numerical experiments 7.2.57 – 7.2.64. Except of the last experiment 7.2.64 we have always employed the semi-implicit versions of the complementary finite volume schemes. We have considered initial curves with sharp corners and also curves which are not convex. In all cases we show comparison of the evolutions driven by the mean-curvature and the Willmore flow. All the experiments show very good agreement of the results obtained by both methods. We also show evolution of the level-set function which is important too. One can see that its deformation is most significant in the case of the Willmore flow.

The second part demonstrates anisotropic level-set method, but now it is not compared to the parametric approach. One can find the results on the Numerical experiments 7.2.65 – 7.2.96 the Figures 7.84 – 7.115. As well as in case of the isotropic evolutions, we also show the level-set function evolution. One can see, that the numerical schemes we propose, are able to drive the curves towards appearance of sharp corners even in cases of the fourth order problems.

Numerical experiment 7.2.57. Comparison of the **explicit finite difference** numerical scheme for the **isotropic level-set formulation of the mean-curvature flow**

$$
\begin{aligned}
\frac{\partial_t u}{Q_\epsilon} &= \nabla \cdot \left(\frac{\nabla u}{Q_\epsilon} \right) \quad \text{on } \langle 0, \mathrm{T} \rangle \times \Omega, \\
u \mid_{t=0} &= u_{ini} \quad \text{on } \Omega,
\end{aligned}
$$

with the Neumann boundary conditions

$$
\partial_\nu u = 1 \quad \text{on } \partial\Omega,
$$

and the parametric approach.

$$
\partial_t \mathbf{x} = k\mathbf{n}.
$$

The initial condition is an ellipse given by $\left(\frac{x}{1.5}\right)^2 + \left(\frac{y}{0.75}\right)^2 = 1$.
Computational domain: $\Omega \equiv [-2, 2]^2$.
Final time: $T = 0.5$.
Level-set: 200×200 nodes, regularisation $\epsilon = 10^{-5}$, no re-distancing.
Parametric approach: 100 nodes, redistribution $\epsilon_1 = 1$, $\delta_1 = 1$ and $\delta_2 = 1$.
Time step: 0.0005 - level-set method, 0.001 - parametric approach.
Numerical scheme: 6.3.8, 6.4.1 for the mean-curvature flow
Figure: 7.76.
Remark: One can see that both methods, level-set and parametric, give equivalent results.

Numerical experiment 7.2.58. Comparison of the **semi-implicit finite difference** numerical scheme for the **isotropic level-set formulation of the Willmore flow**

$$
\begin{aligned}
\partial_t \varphi &= -Q\nabla \cdot \left(\frac{1}{Q} \mathbb{P} \nabla w - \frac{1}{2} \frac{w^2}{Q^3} \nabla \varphi \right) \text{ on } \Omega \times (0, T], \\
w &= QH \text{ on } \Omega \times [0, T], \\
\varphi \mid_{t=0} &= \varphi_{ini} \text{ on } \Omega,
\end{aligned}
$$

with the Neumann boundary conditions

$$
\partial_\nu u = 1, \quad \partial_\nu w = 0 \quad \text{on } \partial\Omega,
$$

and the parametric approach.

$$
\partial_t \mathbf{x} = \left(-\partial_s^2 k - \frac{1}{2} k^3 \right) \mathbf{n}.
$$

The initial condition is an ellipse given by $\left(\frac{x}{1.5}\right)^2 + \left(\frac{y}{0.75}\right)^2 = 1$.
Computational domain: $\Omega \equiv [-2, 2]^2$.
Final time: $T = 0.5$.
Level-set: 100×100 nodes, regularisation $\epsilon = 0.04$, no re-distancing.
Parametric approach: 100 nodes, redistribution $\epsilon_1 = 1$, $\delta_1 = 1$ and $\delta_2 = 1$.
Time step: 10^{-6} - level-set method, 0.001 - parametric approach.
Numerical scheme: 6.3.9, 6.4.1 for the Willmore flow
Figure: 7.77.
Remark: One can see that both methods, level-set and parametric, give equivalent results.

Isotropic level-set formulation of the mean-curvature flow

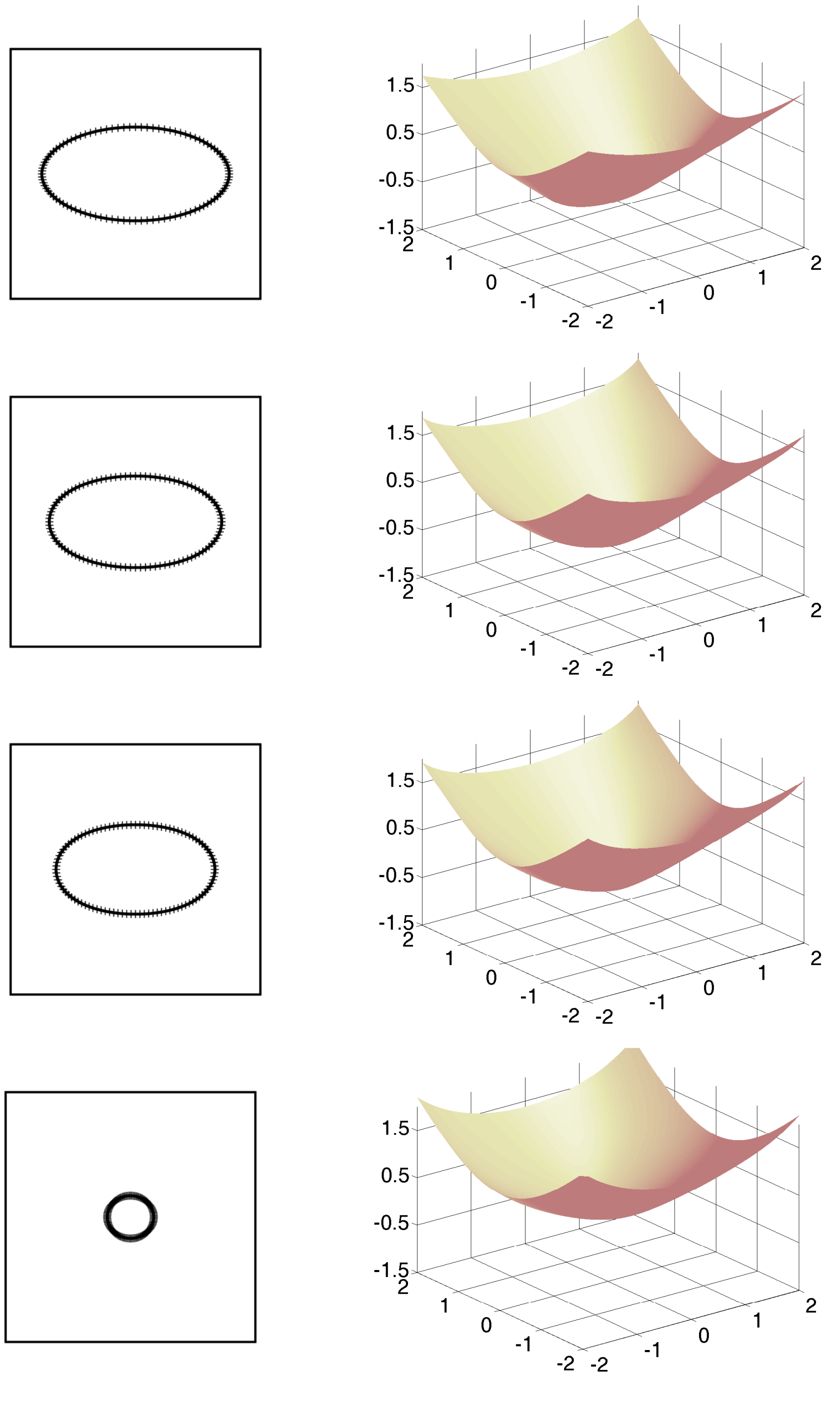

Figure 7.76.: Comparison of the parametric (crosses) and level-set method (lines) for the **mean-curvature flow** at times $t = 0$, $t = 0.05$, $t = 0.1$ and $t = 0.5$. See the numerical experiment 7.2.57.

Isotropic level-set formulation of the Willmore flow

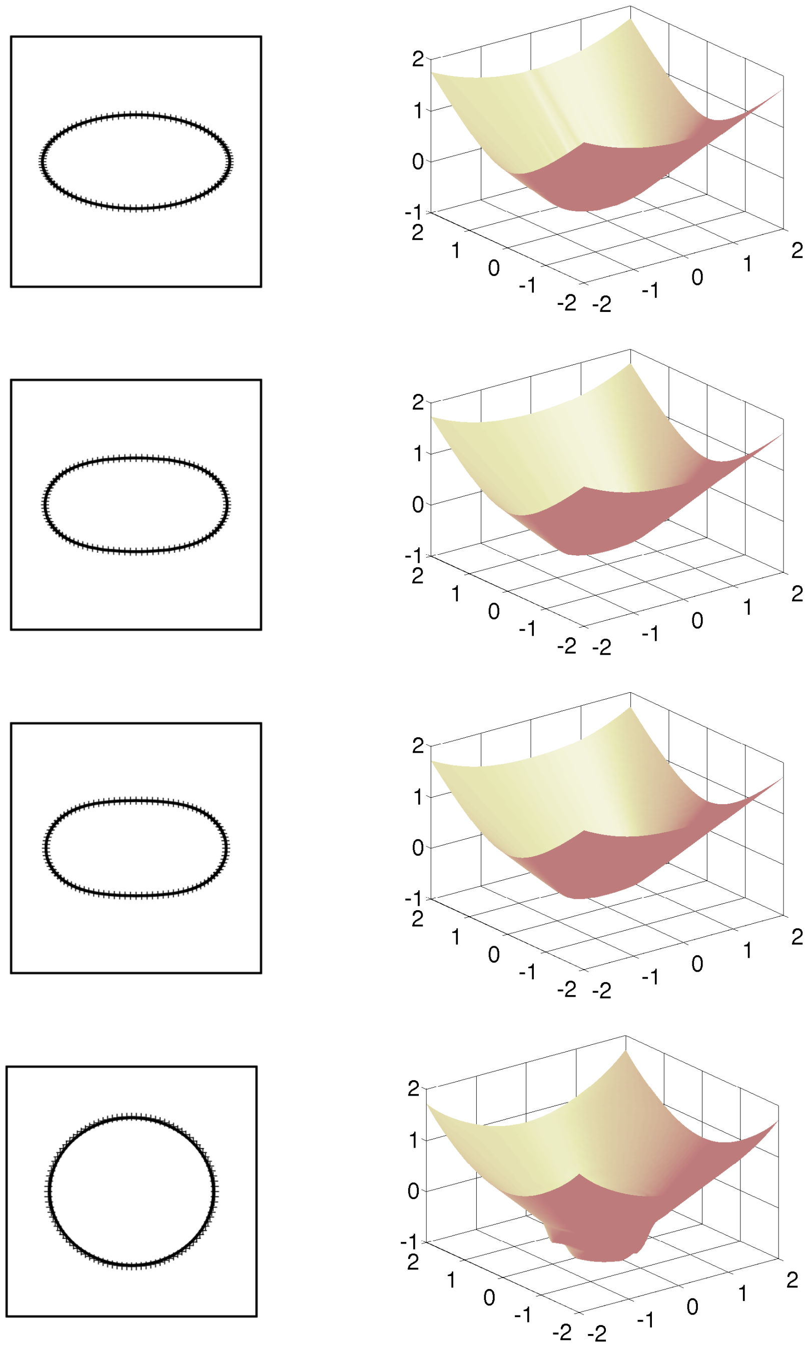

Figure 7.77.: Comparison of the parametric (crosses) and level-set method (lines) for the **Willmore flow** at times $t = 0$, $t = 0.01$, $t = 0.02$ and $t = 0.5$. See the numerical experiment 7.2.58.

Numerical experiment 7.2.59. Comparison of the **explicit finite difference** numerical scheme for the **isotropic level-set formulation of the mean-curvature flow**

$$
\begin{aligned}
\frac{\partial_t u}{Q_\epsilon} &= \nabla \cdot \left(\frac{\nabla u}{Q_\epsilon} \right) \quad \text{on } \left(0, \mathrm{T}\right\rangle \times \Omega, \\
u\,|_{t=0} &= u_{ini} \quad \text{on } \Omega,
\end{aligned}
$$

with the Neumann boundary conditions

$$\partial_\nu u = 1 \quad \text{on } \partial\Omega,$$

and the parametric approach.

$$\partial_t \mathbf{x} = k\mathbf{n}.$$

The initial condition is a square given by $(|x| - 0.75)(|y| - 0.75) = 0$.
Computational domain: $\Omega \equiv [-1, 1]^2$.
Initial condition: Square given by $(|x| - 0.75)(|y| - 0.75) = 0$.
Boundary conditions: $\partial u \nu = 1$ on $\partial\Omega$.
Final time: $T = 0.2$.
Level-set: 200×200 nodes, regularisation $\epsilon = 10^{-5}$, no re-distancing.
parametric approach: 150 nodes, redistribution $\epsilon_1 = 1$, $\delta_1 = 1000$ and $\delta_2 = 1$.
Time step: 10^{-6} - level-set method, 0.001 - parametric approach.
Numerical scheme: 6.3.8, 6.4.1 for the mean-curvature flow
Figure: 7.78.
Remark: One can see that both methods, level-set and parametric, give equivalent results.

Numerical experiment 7.2.60. Comparison of the **semi-implicit finite difference** numerical scheme for the **isotropic level-set formulation of the Willmore flow**

$$
\begin{aligned}
\partial_t \varphi &= -Q\nabla \cdot \left(\frac{1}{Q} \mathbb{P} \nabla w - \frac{1}{2} \frac{w^2}{Q^3} \nabla \varphi \right) \text{ on } \Omega \times (0, T]\,, \\
w &= QH \text{ on } \Omega \times [0, T]\,, \\
\varphi\,|_{t=0} &= \varphi_{ini} \text{ on } \Omega,
\end{aligned}
$$

with the Neumann boundary conditions

$$\partial_\nu u = 1, \quad \partial_\nu w = 0 \quad \text{on } \partial\Omega,$$

and the parametric approach.

$$\partial_t \mathbf{x} = \left(-\partial_s^2 k - \frac{1}{2} k^3 \right) \mathbf{n}.$$

The initial condition is an ellipse given by $\left(\frac{x}{1.5}\right)^2 + \left(\frac{y}{0.75}\right)^2 = 1$.
Computational domain: $\Omega \equiv [-1, 1]^2$.
Final time: $T = 0.2$.
Level-set: 100×100 nodes, regularisation $\epsilon = 0.002$, no re-distancing.
parametric approach: 200 nodes, redistribution $\epsilon_1 = 2$, $\delta_1 = 1$ and $\delta_2 = 0$.
Time step: $2 \cdot 10^{-7}$ - level-set method, 10^{-6} - parametric approach.
Numerical scheme: 6.3.9, 6.4.1 for the Willmore flow
Figure: 7.79.
Remark: One can see that both methods, level-set and parametric, give equivalent results.

Isotropic level-set formulation of the mean-curvature flow

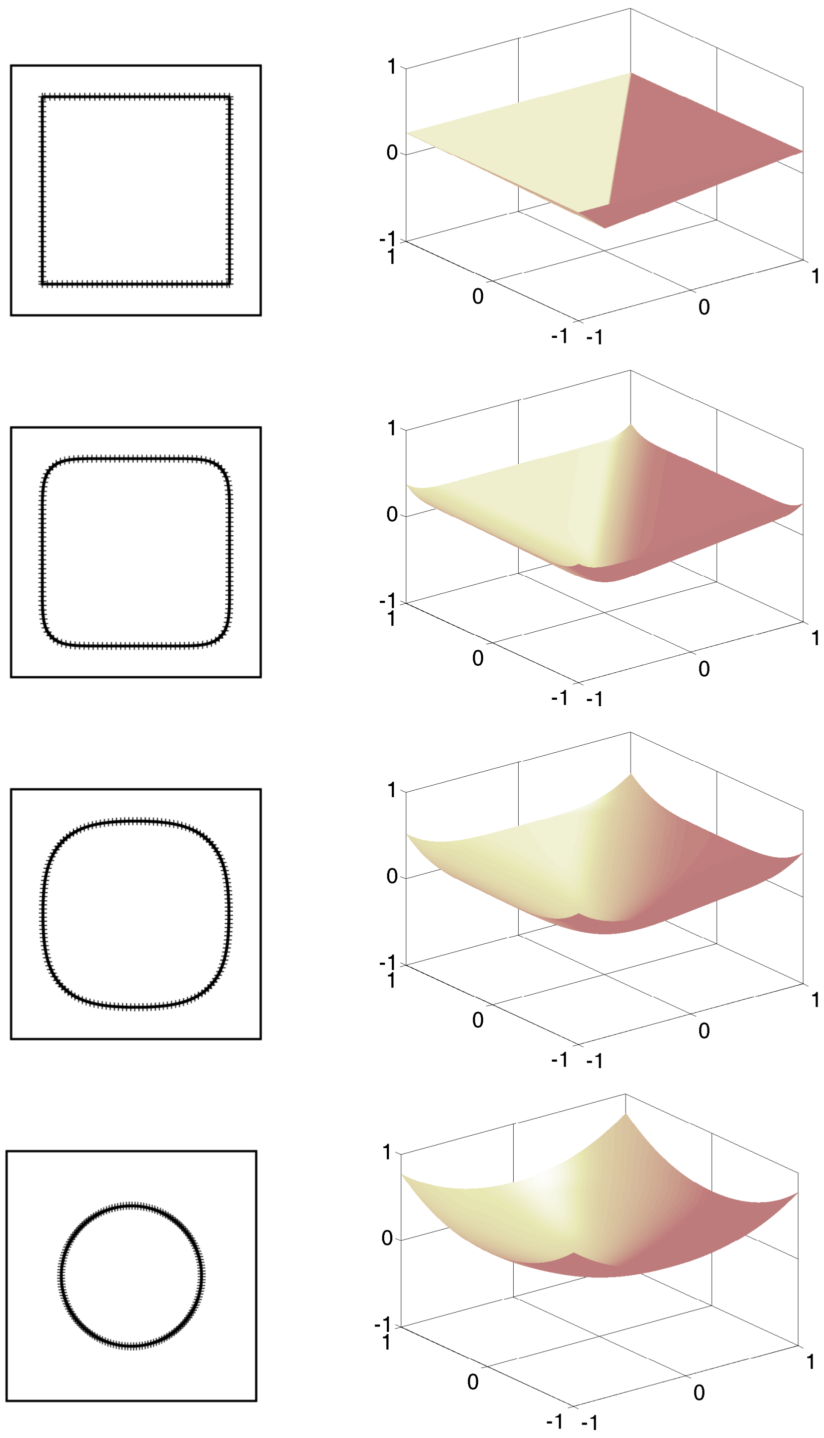

Figure 7.78.: Comparison of the parametric (crosses) and level-set method (lines) for the **mean-curvature flow** at times $t = 0$, $t = 0.01$, $t = 0.05$ and $t = 0.2$. See the numerical experiment 7.2.59.

Isotropic level-set formulation of the Willmore flow

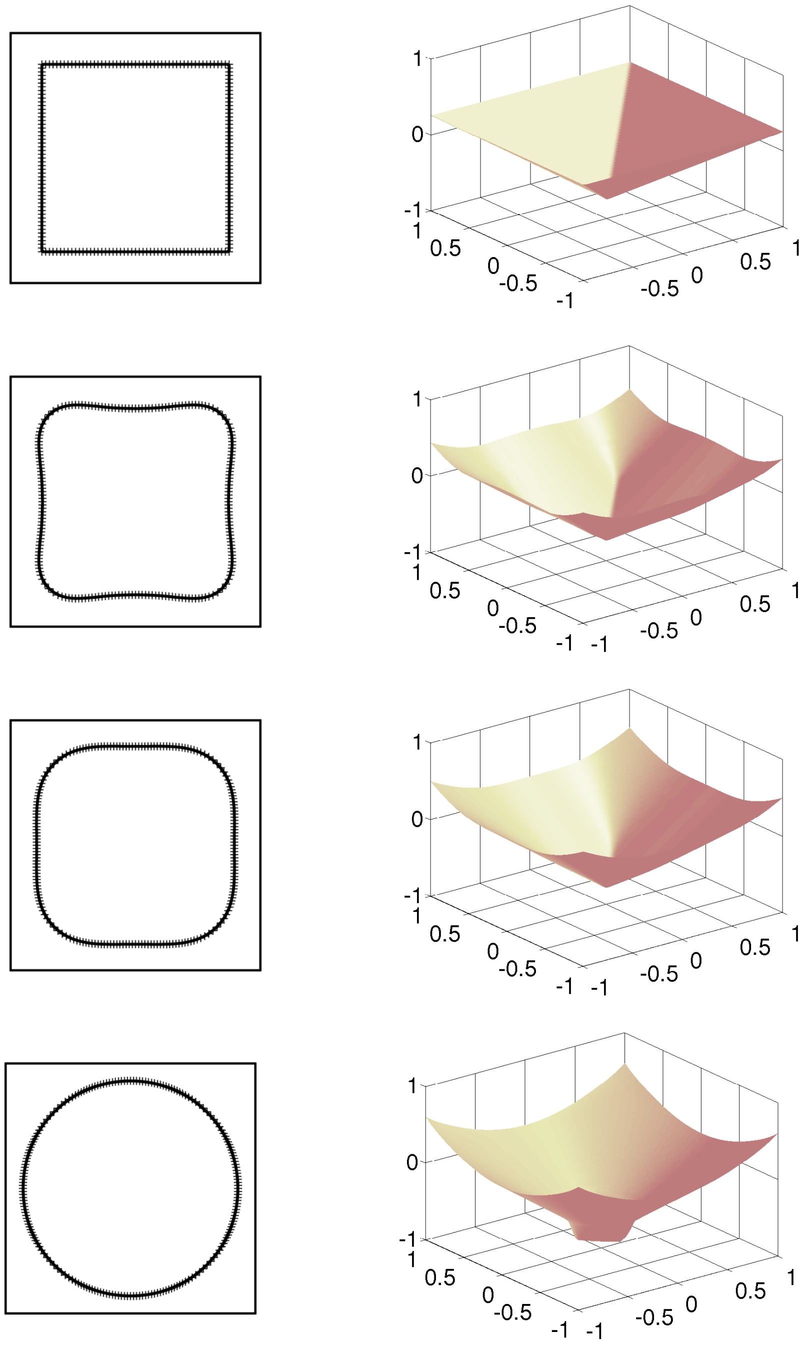

Figure 7.79.: Comparison of the parametric (crosses) and level-set method (lines) for the **Willmore flow** at times $t = 0$, $t = 0.01$, $t = 0.05$ and $t = 0.2$. See the numerical experiment 7.2.59.

Numerical experiment 7.2.61. Comparison of the **explicit finite difference** numerical scheme for the **isotropic level-set formulation of the mean-curvature flow**

$$\begin{aligned}\frac{\partial_t u}{Q_\epsilon} &= \nabla \cdot \left(\frac{\nabla u}{Q_\epsilon}\right) \quad \text{on } \langle 0, \mathrm{T}\rangle \times \Omega, \\ u\mid_{t=0} &= u_{ini} \quad \text{on } \Omega,\end{aligned}$$

with the Neumann boundary conditions

$$\partial_\nu u = 1 \quad \text{on } \partial\Omega,$$

and the parametric approach.

$$\partial_t \mathbf{x} = k\mathbf{n}.$$

The initial condition is an astroid given by $x^{2/3} + y^{2/3} = 0.75^{2/3}$. **Computational domain:** $\Omega \equiv [-1, 1]^2$.
Final time: $T = 0.05$.
Level-set: 130×130 nodes, regularisation $\epsilon = 10^{-5}$, no re-distancing.
Parametric approach: 150 nodes, redistribution $\epsilon_1 = 1$, $\delta_1 = 1$ and $\delta_2 = 1$.
Time step: 10^{-6} - level-set method, 10^{-5} - parametric approach.
Numerical scheme: 6.3.8, 6.4.1 for the mean-curvature flow
Figure: 7.80.
Remark: One can see that both methods, level-set and parametric, give equivalent results.

Numerical experiment 7.2.62. Comparison of the **semi-implicit finite difference** numerical scheme for the **isotropic level-set formulation of the Willmore flow**

$$\begin{aligned}\partial_t \varphi &= -Q\nabla \cdot \left(\frac{1}{Q}\mathbb{P}\nabla w - \frac{1}{2}\frac{w^2}{Q^3}\nabla\varphi\right) \text{ on } \Omega \times (0, T], \\ w &= QH \text{ on } \Omega \times [0, T], \\ \varphi\mid_{t=0} &= \varphi_{ini} \text{ on } \Omega,\end{aligned}$$

with the Neumann boundary conditions

$$\partial_\nu u = 1, \quad \partial_\nu w = 0 \quad \text{on } \partial\Omega,$$

and the parametric approach.

$$\partial_t \mathbf{x} = \left(-\partial_s^2 k - \frac{1}{2}k^3\right)\mathbf{n}.$$

The initial condition is an astroid given by $x^{2/3} + y^{2/3} = 0.75^{2/3}$.
Computational domain: $\Omega \equiv [-1, 1]^2$.
Final time: $T = 0.05$.
Level-set: 150×150 nodes, regularisation $\epsilon = 0.025$, re-distancing $\tau_{redist} = 10^{-4}$.
Parametric approach: 200 nodes, redistribution $\epsilon_1 = 0$, $\delta_1 = 1$ and $\delta_2 = 1$.
Time step: $2 \cdot 10^{-9}$ - level-set method, 10^{-9} - parametric approach.
Numerical scheme: 6.3.9, 6.4.1 for the Willmore flow
Figure: 7.81.
Remark: One can see that both methods, level-set and parametric, give equivalent results.

Isotropic level-set formulation of the mean-curvature flow

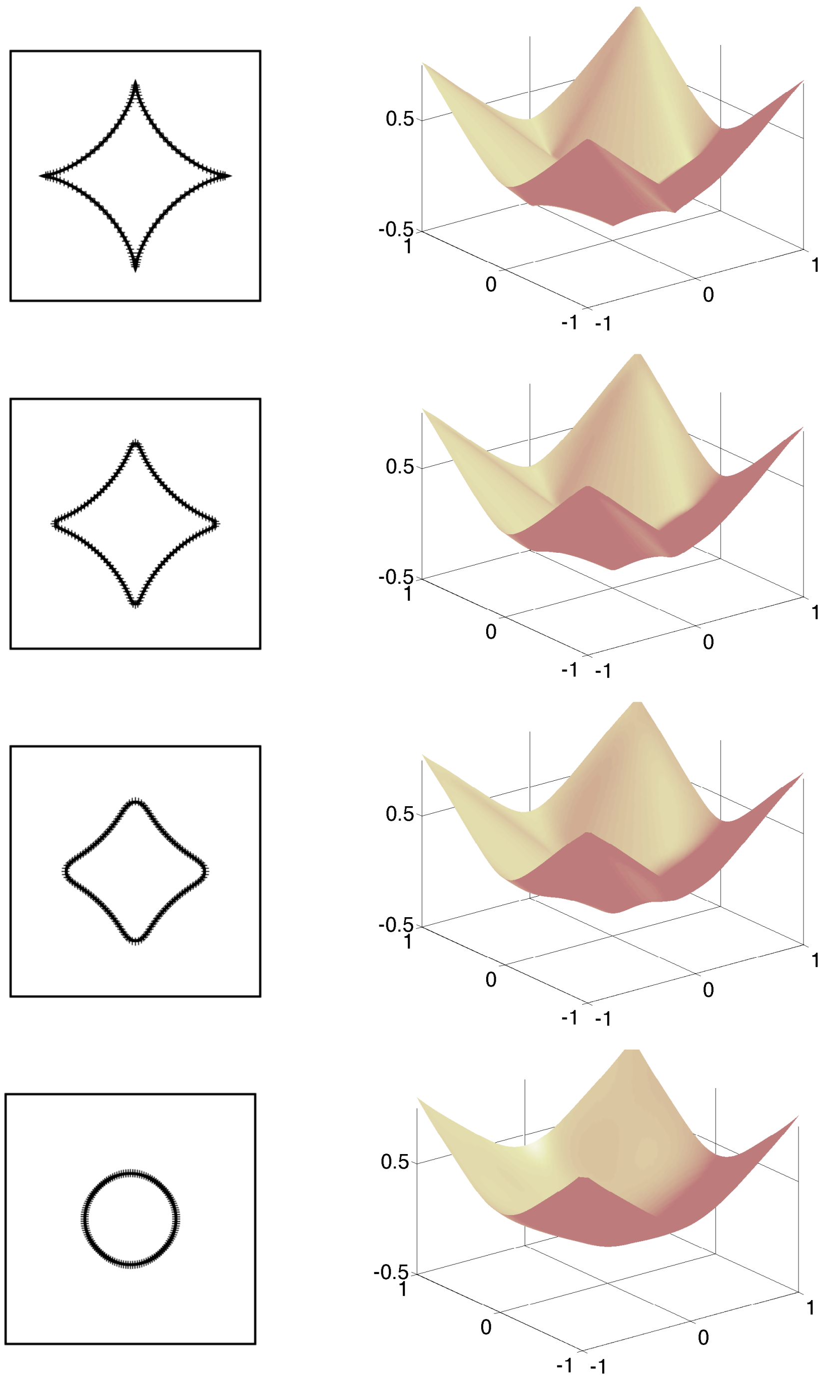

Figure 7.80.: Comparison of the parametric (crosses) and level-set method (lines) for the **mean-curvature flow** at times $t = 0$, $t = 0.001$, $t = 0.005$ and $t = 0.04$. See the numerical experiment 7.2.61.

Isotropic level-set formulation of the Willmore flow

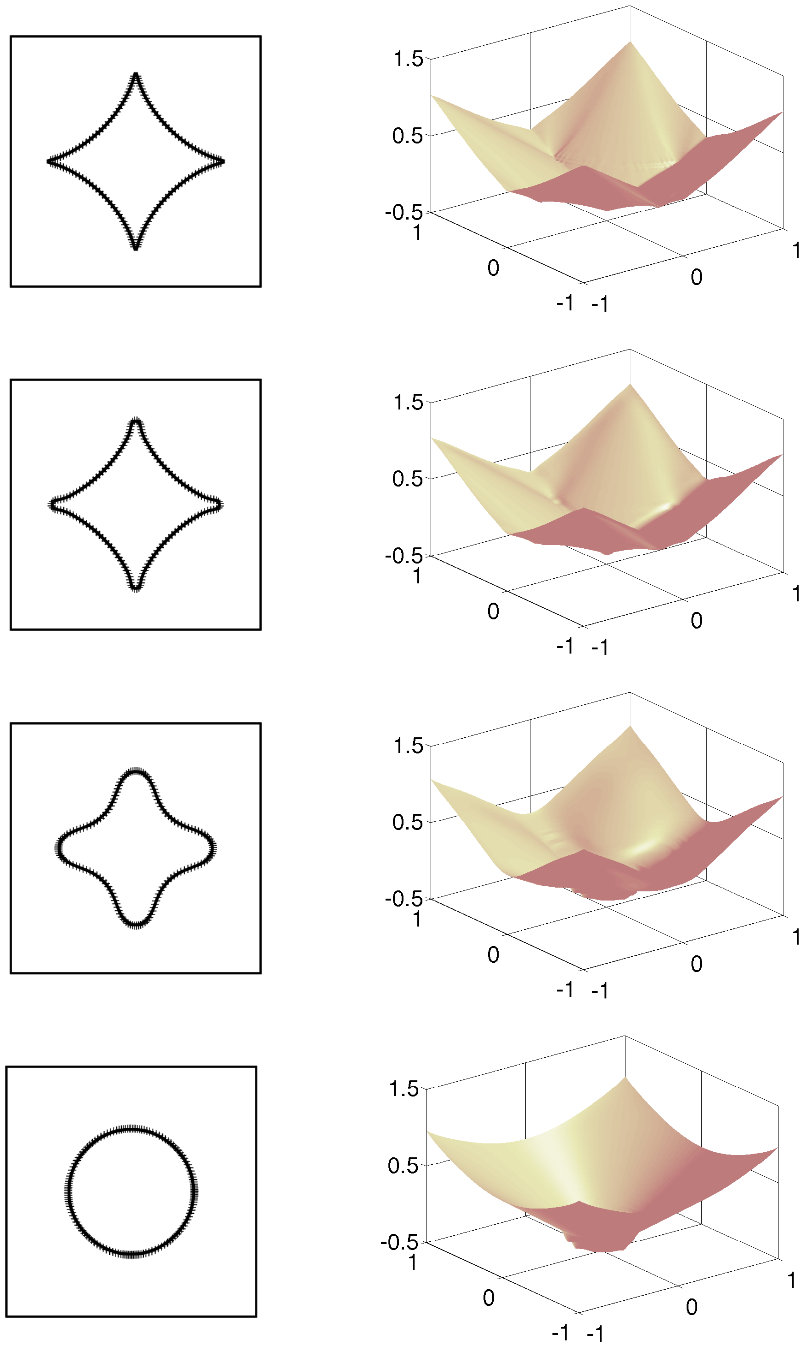

Figure 7.81.: Comparison of the parametric (crosses) and level-set method (lines) for the **Willmore flow** at times $t = 0$, $t = 10^{-6}$, $t = 10^{-4}$ and $t = 0.0015$. See the numerical experiment 7.2.62.

Numerical experiment 7.2.63. Comparison of the **explicit finite difference** numerical scheme for the **isotropic level-set formulation of the mean-curvature flow**

$$\begin{aligned} \frac{\partial_t u}{Q_\epsilon} &= \nabla \cdot \left(\frac{\nabla u}{Q_\epsilon} \right) \quad \text{on } (0, \mathrm{T}\rangle \times \Omega, \\ u\,|_{t=0} &= u_{ini} \quad \text{on } \Omega, \end{aligned}$$

with the Neumann boundary conditions

$$\partial_\nu u = 1 \quad \text{on } \partial\Omega,$$

and the parametric approach.

$$\partial_t \mathbf{x} = k\mathbf{n}.$$

The initial condition is a non-convex curve given by $x = 1 - 0.75\cos^2(6t)\cos t$, $y = 1 - 0.75\cos^2(6t)\sin t$ for $t \in [0, 2\pi)$.
Computational domain: $\Omega \equiv [-1.5, 1.5]^2$.
Final time: $T = 0.03$.
Level-set: 400×400 nodes, regularisation $\epsilon = 10^{-5}$, re-distancing $\tau_{redist} = 0$.
parametric approach: 400 nodes, redistribution $\epsilon_1 = 0$, $\delta_1 = 10$ and $\delta_2 = 1$.
Time step: Adaptive - level-set method, 10^{-5} - parametric approach.
Numerical scheme: 6.3.6, 6.4.1 for the mean-curvature flow
Figure: 7.82.
Remark: One can see that both methods, level-set and parametric, give equivalent results even with highly non-convex initial curve.

Numerical experiment 7.2.64. Comparison of the **explicit finite difference** numerical scheme for the **isotropic level-set formulation of the Willmore flow**

$$\begin{aligned}
\partial_t \varphi &= -Q \nabla \cdot \left(\frac{1}{Q} \mathbb{P} \nabla w - \frac{1}{2} \frac{w^2}{Q^3} \nabla \varphi \right) \text{ on } \Omega \times (0, T] \,, \\
w &= QH \text{ on } \Omega \times [0, T] \,, \\
\varphi \mid_{t=0} &= \varphi_{ini} \text{ on } \Omega,
\end{aligned}$$

with the Neumann boundary conditions

$$\partial_\nu u = 1, \quad \partial_\nu w = 0 \quad \text{on } \partial\Omega,$$

and the parametric approach.

$$\partial_t \mathbf{x} = \left(-\partial_s^2 k - \frac{1}{2} k^3 \right) \mathbf{n}.$$

The initial condition is a non-convex curve given by $x = 1 - 0.3 \cos^2(6t) \cos t,\ y = 1 - 0.3 \cos^2(6t) \sin t$ for $t \in [0, 2\pi)$.
Computational domain: $\Omega \equiv [-1.5, 1.5]^2$.
Final time: $T = 0.00032$.
Level-set: 200×200 nodes, regularisation $\epsilon = 0.05$, re-distancing $\tau_{redist} = 5 \cdot 10^{-5}$.
Parametric approach: 1000 nodes, redistribution $\epsilon_1 = 0$, $\delta_1 = 1$ and $\delta_2 = 1$.
Time step: Adaptive - level-set method, $2 \cdot 10^{-9}$ - parametric approach.
Numerical scheme: 6.2.30, 6.4.1 for the Willmore flow
Figure: 7.83.
Remark: One can see that both methods, level-set and parametric, give equivalent results. We would like to note, that the semi-implicit scheme for the level-set method failed to compute approximate solution at this experiment. We chose a bit different initial curve then in the experiment 7.2.63 because it would lead to splitting into more the one curve which is not possible to be handled by the parametric method.

Isotropic level-set formulation of the mean-curvature flow

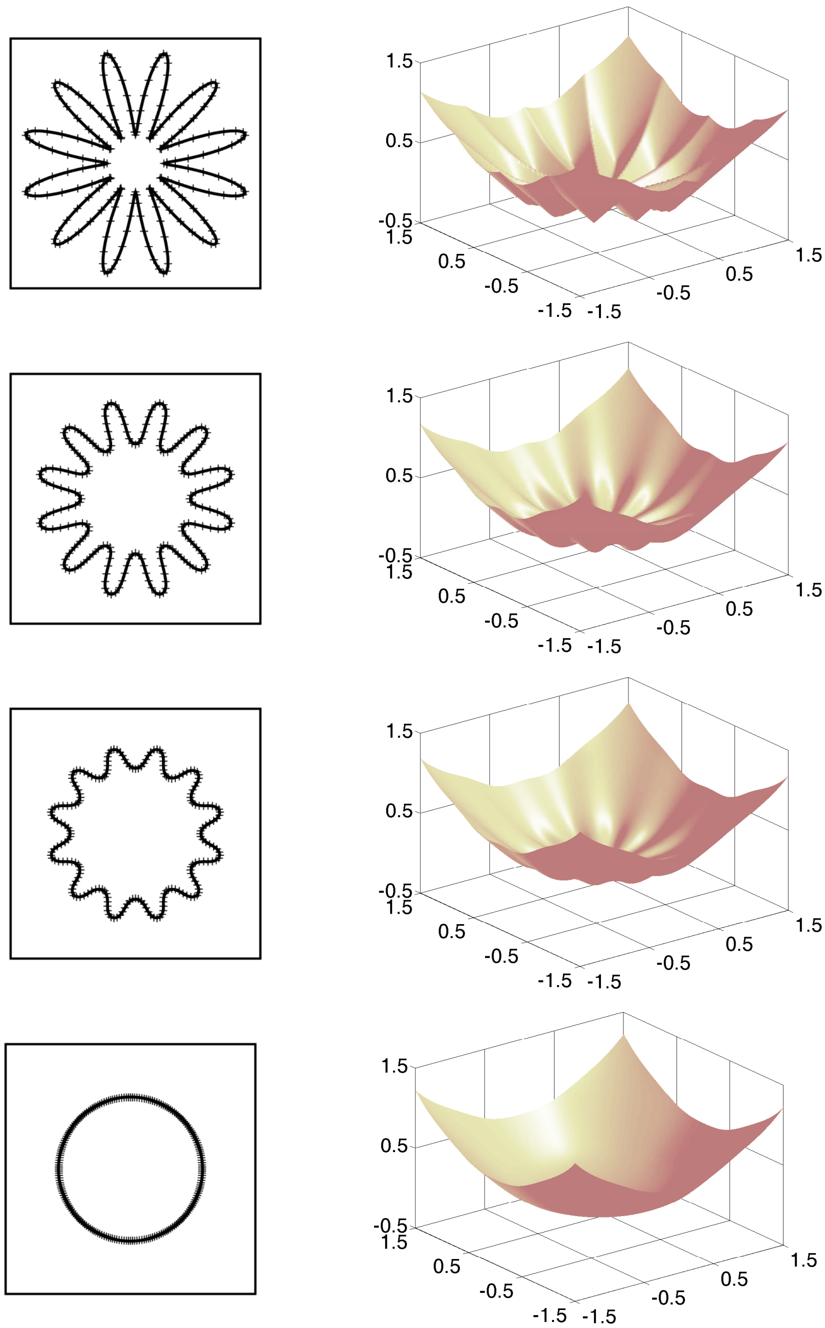

Figure 7.82.: Comparison of the parametric (crosses) and level-set method (lines) for the **mean-curvature flow** at times $t = 0$, $t = 0.005$, $t = 0.01$ and $t = 0.03$. See the numerical experiment 7.2.63.

Isotropic level-set formulation of the Willmore flow

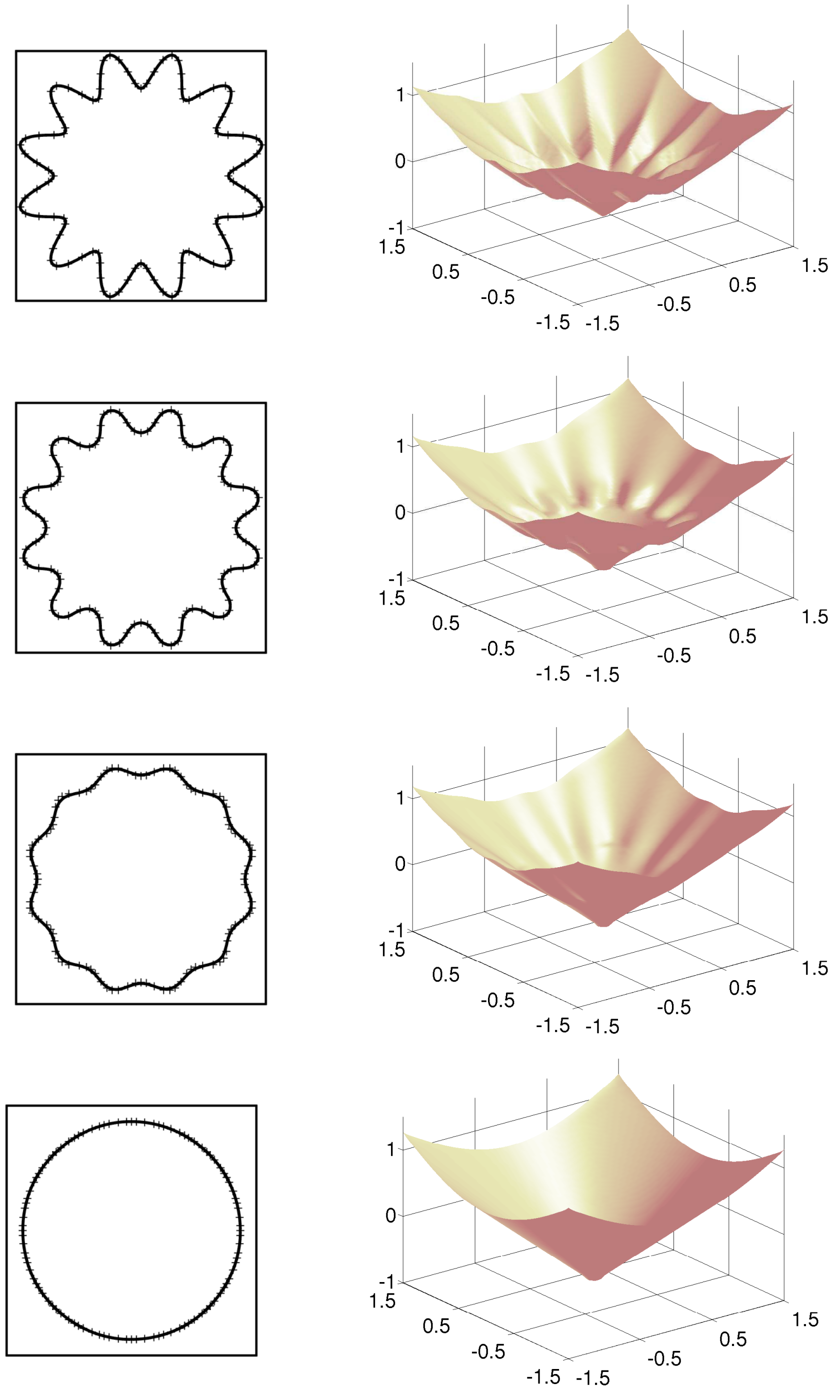

Figure 7.83.: Comparison of the parametric (crosses) and level-set method (lines) for the **Willmore flow** at times $t = 0$, $t = 8 \cdot 10^{-5}$, $t = 0.00016$ and $t = 0.00032$. See the numerical experiment 7.2.64.

Numerical experiment 7.2.65. Test of the **level-set formulation for the anisotropic mean-curvature flow**

$$\begin{aligned} \frac{\partial_t u}{Q_\epsilon} &= \nabla \cdot \left(\nabla_{\mathbf{p}} \gamma_{\mathbb{G}} \left(\nabla u\right)\right) \quad \text{on } (0, \mathrm{T}\rangle \times \Omega, \\ u\,|_{t=0} &= u_{ini} \quad \text{on } \Omega, \end{aligned}$$

with the Neumann boundary conditions

$$\nabla_{\mathbf{p}} \gamma_{\mathbb{G}} \nu = 1 \quad \text{on } \partial\Omega.$$

The anisotropy function $\gamma_{\mathbb{G}}$ is given by

$$\gamma_{\mathbb{G}}\left(\mathbf{p}, -1\right) := \sqrt{1 + \mathbf{p}^T \mathbb{G} \mathbf{p}}, \text{ for } \mathbb{G} := \begin{pmatrix} 10 & 0 \\ 0 & 1 \end{pmatrix},$$

and the initial condition is a circle given by $x^2 + y^2 = 1$.
Computational domain: $\Omega \equiv [-2, 2]^2$.
Final time: $T = 0.2$.
Level-set: 100×100 nodes, regularisation $\epsilon = 10^{-5}$, no re-distancing.
Time step: $\tau = 0.0005$.
Numerical scheme: 6.3.8
Figure: 7.84.
Remark: –

Numerical experiment 7.2.66. Test of the **level-set formulation for the anisotropic Willmore flow**

$$\begin{aligned} \frac{\partial_t u}{Q_\epsilon} &= -\nabla \cdot \left(\mathbb{E}_\gamma \nabla w_\gamma - \frac{1}{2} \frac{w_\gamma^2}{Q^3} \nabla u \right) \quad \text{on } (0, T) \times \Omega, \\ w_\gamma &= Q_\epsilon H_\gamma \quad \text{on } (0, T) \times \Omega, \\ u\,|_{t=0} &= u_{ini} \quad \text{on } \Omega, \end{aligned}$$

with the Neumann boundary conditions

$$\partial_\nu u = 1, \; \mathbb{E}_\gamma \nabla w_\gamma \cdot \nu = 0 \quad \text{on } \partial\Omega.$$

The anisotropy function $\gamma_{\mathbb{G}}$ is given by

$$\gamma_{\mathbb{G}}\left(\mathbf{p}, -1\right) := \sqrt{1 + \mathbf{p}^T \mathbb{G} \mathbf{p}}, \text{ for } \mathbb{G} := \begin{pmatrix} 10 & 0 \\ 0 & 1 \end{pmatrix},$$

and the initial condition is a circle given by $x^2 + y^2 = 1$.
Computational domain: $\Omega \equiv [-2, 2]^2$.
Final time: $T = 0.07$.
Level-set: 100×100 nodes, regularisation $\epsilon = 0.01$, no re-distancing.
Time step: $\tau = 2 \cdot 10^{-7}$.
Numerical scheme: 6.3.9
Figure: 7.85.
Remark: –

Anisotropic level-set formulation of the mean-curvature flow

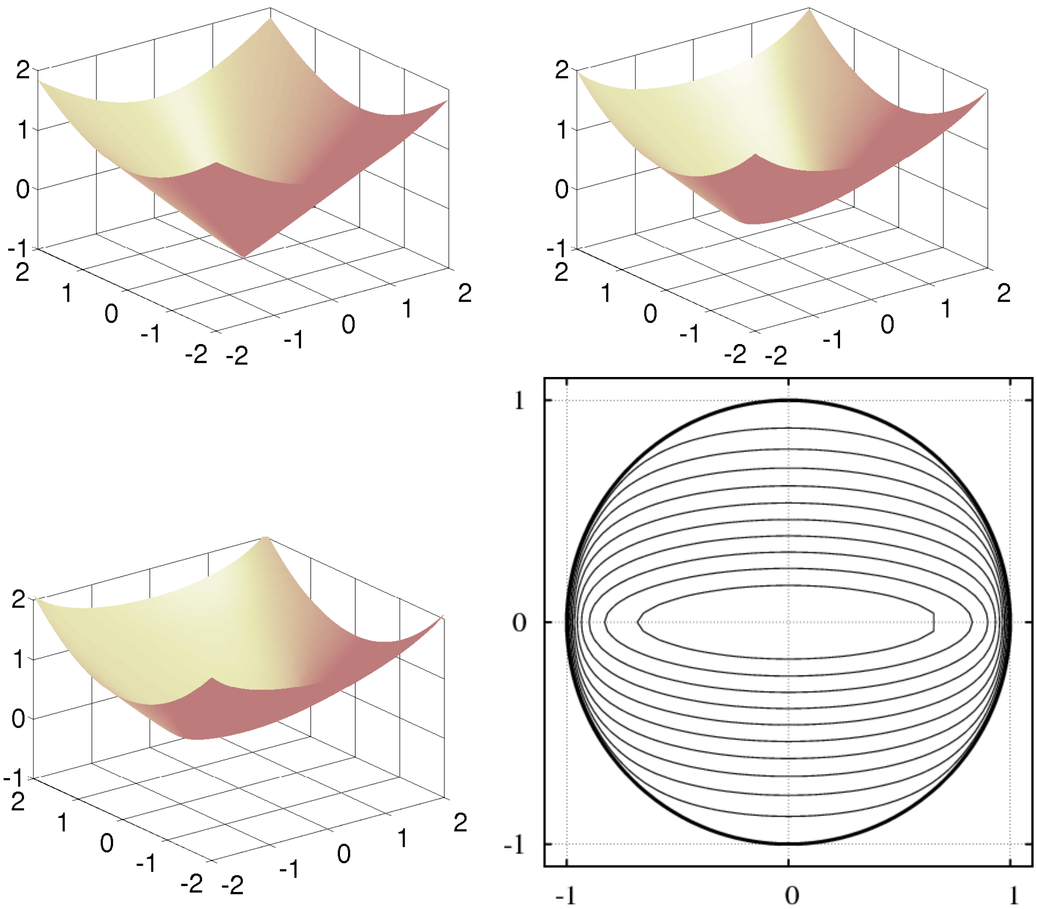

Figure 7.84.: Anisotropic level-set method for the **mean-curvature flow** – graphs of the level-set function at times $t = 0, t = 0.1$ and $t = 0.2$ and evolution of the initial curve until the time $t = 0.2$ with the time period 0.02. See the Numerical experiment 7.2.65

Anisotropic level-set formulation of the Willmore flow

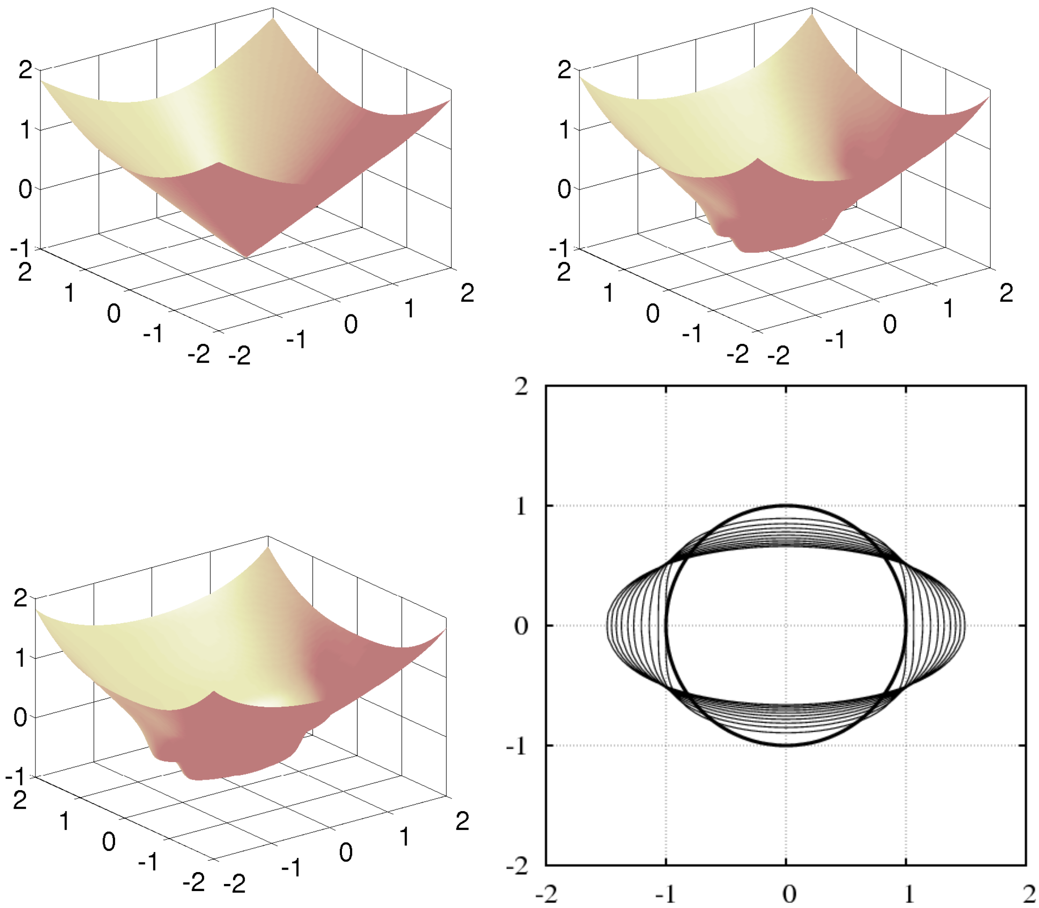

Figure 7.85.: Anisotropic level-set method for the **Willmore flow** – graphs of the level-set function at times $t = 0$, $t = 0.03$ and $t = 0.07$ and evolution of the initial curve until the time $t = 0.07$ with the time period 0.007. See the Numerical experiment 7.2.66

Numerical experiment 7.2.67. Test of the **level-set formulation for the anisotropic mean-curvature flow**

$$\begin{aligned}\frac{\partial_t u}{Q_\epsilon} &= \nabla\cdot\left(\nabla_{\mathbf{p}}\gamma_{\mathbb{G}}\left(\nabla u\right)\right) \quad \text{on } \left(0,\mathrm{T}\right\rangle\times\Omega,\\ u\left.\right|_{t=0} &= u_{ini} \quad \text{on } \Omega,\end{aligned}$$

with the Neumann boundary conditions

$$\nabla_{\mathbf{p}}\gamma_{\mathbb{G}}\nu = 1 \quad \text{on } \partial\Omega.$$

The anisotropy function $\gamma_{\mathbb{G}}$ is given by

$$\gamma_{\mathbb{G}}\left(\mathbf{p},-1\right) := \sqrt{1+\mathbf{p}^T\mathbb{G}\mathbf{p}}, \text{ for } \mathbb{G} := \begin{pmatrix} 11 & 10\\ 10 & 11\end{pmatrix},$$

and the initial condition is a circle given by $x^2+y^2=1$.
Computational domain: $\Omega\equiv[-2,2]^2$.
Final time: $T=0.16$.
Level-set: 100×100 nodes, regularisation $\epsilon=10^{-5}$, no re-distancing.
Time step: Adaptive.
Numerical scheme: 6.3.6
Figure: 7.86.
Remark: –

Numerical experiment 7.2.68. Test of the **level-set formulation for the anisotropic Willmore flow**

$$\begin{aligned}\frac{\partial_t u}{Q_\epsilon} &= -\nabla\cdot\left(\mathbb{E}_\gamma\nabla w_\gamma - \frac{1}{2}\frac{w_\gamma^2}{Q^3}\nabla u\right) \quad \text{on } \left(0,T\right)\times\Omega,\\ w_\gamma &= Q_\epsilon H_\gamma \quad \text{on } \left(0,T\right)\times\Omega,\\ u\left.\right|_{t=0} &= u_{ini} \quad \text{on } \Omega,\end{aligned}$$

with the Neumann boundary conditions

$$\partial_\nu u = 1,\ \mathbb{E}_\gamma\nabla w_\gamma\cdot\nu = 0 \quad \text{on } \partial\Omega.$$

The anisotropy function $\gamma_{\mathbb{G}}$ is given by

$$\gamma_{\mathbb{G}}\left(\mathbf{p},-1\right) := \sqrt{1+\mathbf{p}^T\mathbb{G}\mathbf{p}}, \text{ for } \mathbb{G} := \begin{pmatrix} 11 & 10\\ 10 & 11\end{pmatrix},$$

and the initial condition is a circle given by $x^2+y^2=1$.
Computational domain: $\Omega\equiv[-2,2]^2$.
Final time: $T=0.0008$.
Level-set: 100×100 nodes, regularisation $\epsilon=0.01$, no re-distancing.
Time step: Adaptive.
Numerical scheme: 6.3.7
Figure: 7.87.
Remark: –

Anisotropic level-set formulation of the mean-curvature flow

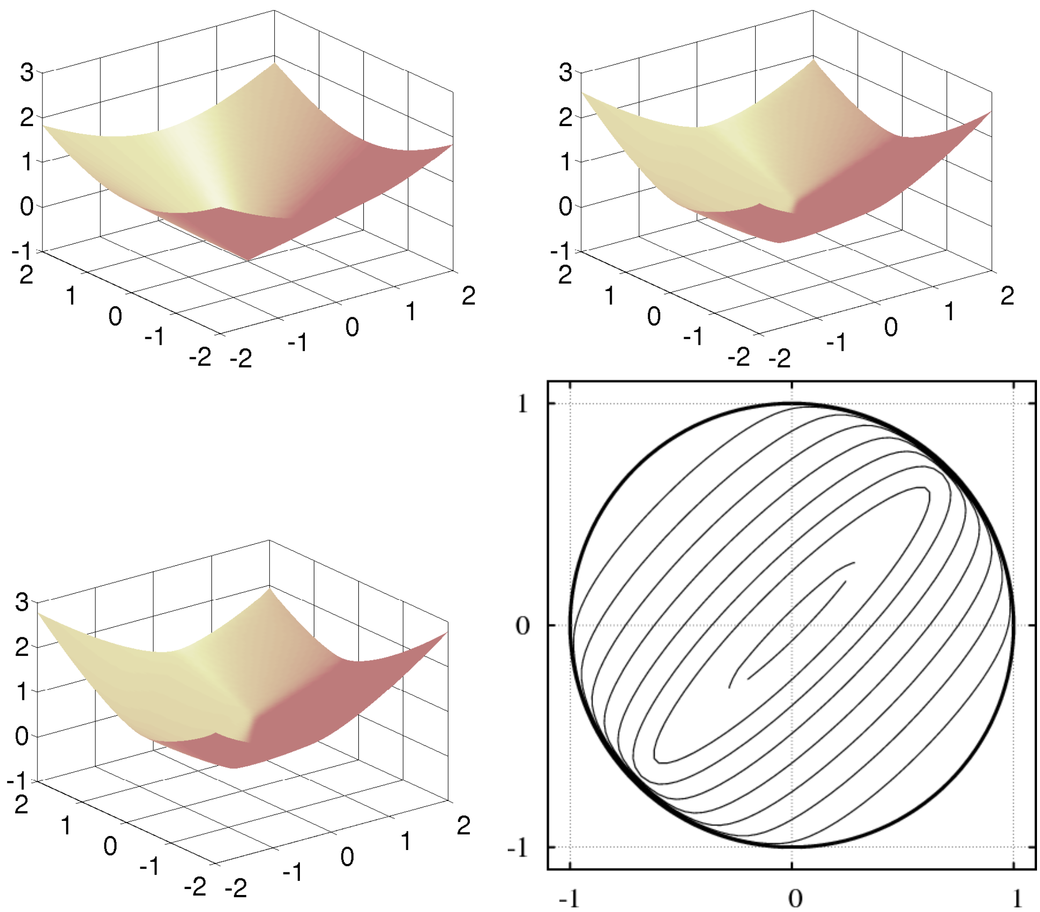

Figure 7.86.: Anisotropic level-set method for the **mean-curvature flow** – graphs of the level-set function at times $t = 0$, $t = 0.1$, $t = 0.16$ and evolution of the initial curve until the time $t = 0.16$ with the time period 0.02. See the Numerical experiment 7.2.67

Anisotropic level-set formulation of the Willmore flow

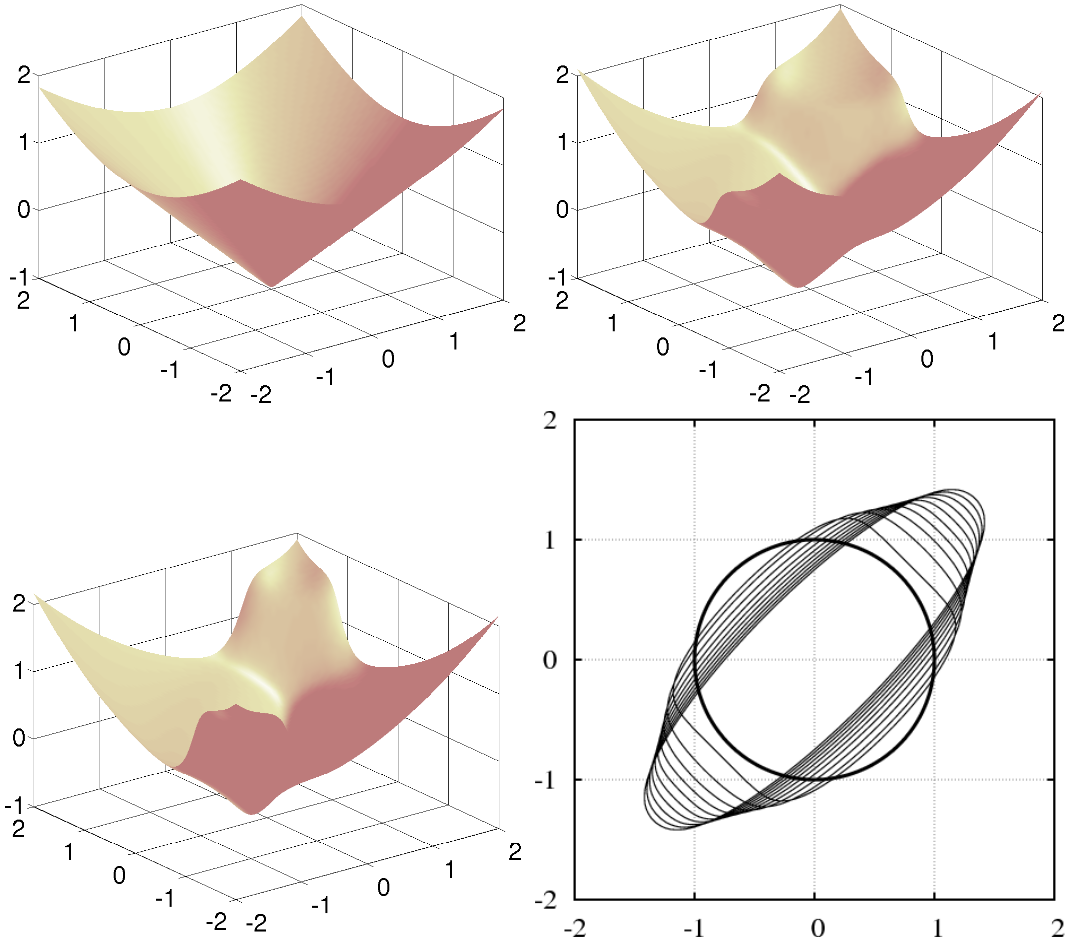

Figure 7.87.: Anisotropic level-set method for the **Willmore flow** – graphs of the level-set function at times $t = 0$, $t = 0.0004$, $t = 0.008$ and evolution of the circle until the time $t = 0.0008$ with the time period $8 \cdot 10^{-5}$. See the Numerical experiment 7.2.68

Numerical experiment 7.2.69. Test of the **level-set formulation for the anisotropic mean-curvature flow**

$$\begin{aligned}\frac{\partial_t u}{Q_\epsilon} &= \nabla \cdot \left(\nabla_{\mathbf{p}} \gamma_{\mathbb{G}} \left(\nabla u\right)\right) \quad \text{on } (0,\mathrm{T}\rangle \times \Omega,\\ u\left.\right|_{t=0} &= u_{ini} \quad \text{on } \Omega,\end{aligned}$$

with the Neumann boundary conditions

$$\nabla_{\mathbf{p}} \gamma_{\mathbb{G}} \nu = 1 \quad \text{on } \partial\Omega.$$

The anisotropy function $\gamma_{\mathbb{G}}$ is given by

$$\gamma_{\mathbb{G}}\left(\mathbf{p}, -1\right) := \sqrt{1 + \mathbf{p}^T \mathbb{G} \mathbf{p}}, \text{ for } \mathbb{G} := \begin{pmatrix} 10 & 0 \\ 0 & 1 \end{pmatrix},$$

and the initial condition is a square given by $\left(|x| - 0.75\right)\left(|y| - 0.75\right) = 0$.
Computational domain: $\Omega \equiv [-2, 2]^2$.
Final time: $T = 0.25$.
Level-set: 100×100 nodes, regularisation $\epsilon = 10^{-5}$, no re-distancing.
Time step: $\tau = 10^{-6}$.
Numerical scheme: 6.3.8
Figure: 7.88.
Remark: –

Numerical experiment 7.2.70. Test of the **level-set formulation for the anisotropic Willmore flow**

$$\begin{aligned}\frac{\partial_t u}{Q_\epsilon} &= -\nabla \cdot \left(\mathbb{E}_\gamma \nabla w_\gamma - \frac{1}{2}\frac{w_\gamma^2}{Q^3} \nabla u\right) \quad \text{on } (0,T) \times \Omega,\\ w_\gamma &= Q_\epsilon H_\gamma \quad \text{on } (0,T) \times \Omega,\\ u\left.\right|_{t=0} &= u_{ini} \quad \text{on } \Omega,\end{aligned}$$

with the Neumann boundary conditions

$$\partial_\nu u = 1, \; \mathbb{E}_\gamma \nabla w_\gamma \cdot \nu = 0 \quad \text{on } \partial\Omega.$$

The anisotropy function $\gamma_{\mathbb{G}}$ is given by

$$\gamma_{\mathbb{G}}\left(\mathbf{p}, -1\right) := \sqrt{1 + \mathbf{p}^T \mathbb{G} \mathbf{p}}, \text{ for } \mathbb{G} := \begin{pmatrix} 10 & 0 \\ 0 & 1 \end{pmatrix},$$

and the initial condition is a square given by $\left(|x| - 0.75\right)\left(|y| - 0.75\right) = 0$.
Computational domain: $\Omega \equiv [-3, 3]^2$.
Final time: $T = 0.0025$.
Level-set: 150×150 nodes, regularisation $\epsilon = 0.01$, no re-distancing.
Time step: $\tau = 10^{-8}$.
Numerical scheme: 6.3.9
Figure: 7.89.
Remark: –

Anisotropic level-set formulation of the mean-curvature flow

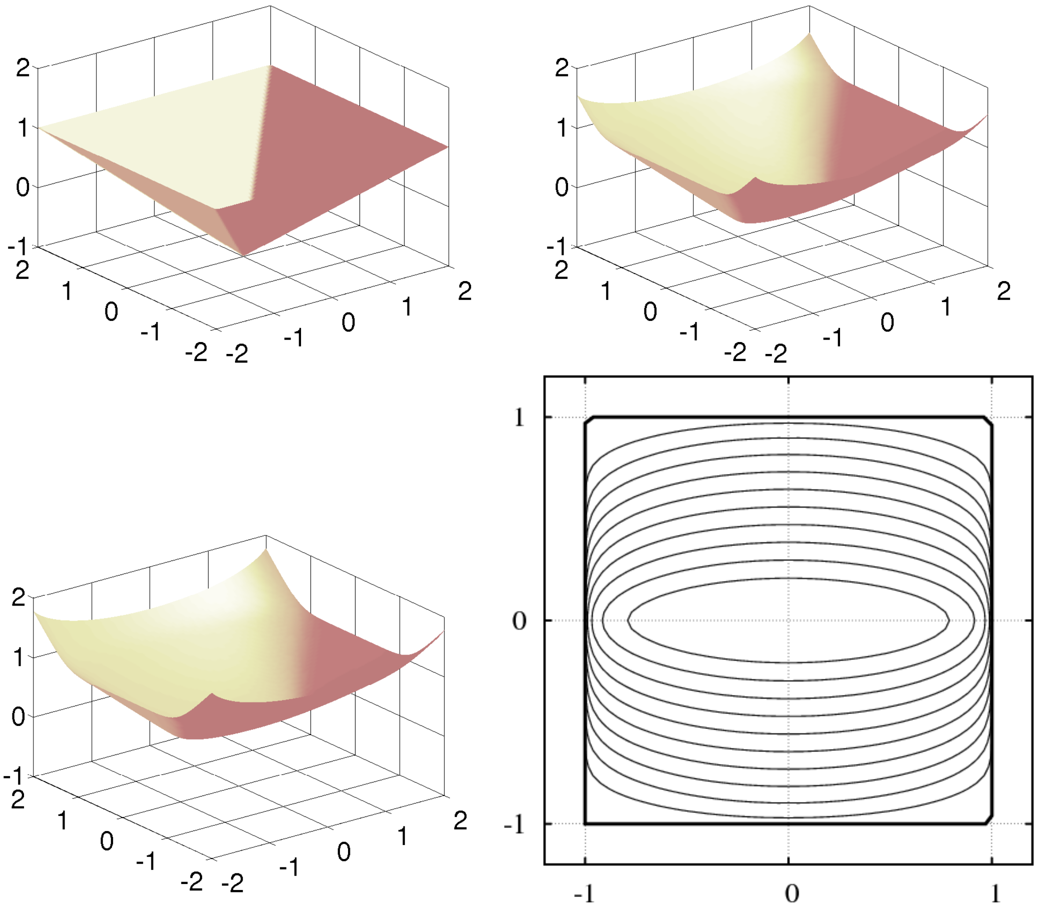

Figure 7.88.: Anisotropic level-set method for the **mean-curvature flow** – graphs of the level-set function at times $t = 0$, $t = 0.128$ and $t = 0.25$ and evolution of the circle until the time $t = 0.25$ with the time period 0.025. See the Numerical experiment 7.2.69

Anisotropic level-set formulation of the Willmore flow

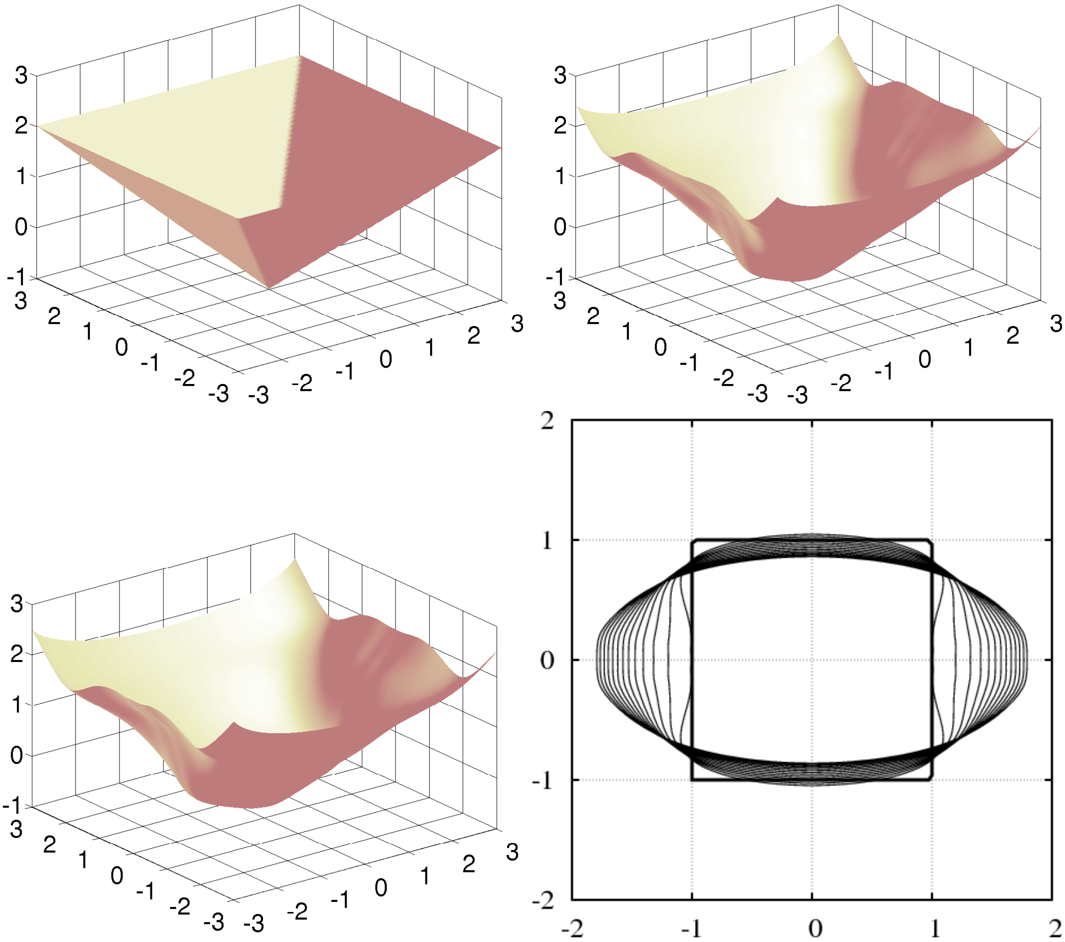

Figure 7.89.: Anisotropic level-set method for the **Willmore flow** – graphs of the level-set function at times $t = 0$, $t = 0.00125$, $t = 0.0025$ and evolution of the initial curve at the time $t = 0.0025$ with the time period 0.0001. See the Numerical experiment 7.2.70

Numerical experiment 7.2.71. Test of the **level-set formulation for the anisotropic mean-curvature flow**

$$\begin{aligned}\frac{\partial_t u}{Q_\epsilon} &= \nabla\cdot\left(\nabla_{\mathbf{p}}\gamma_{\mathbb{G}}\left(\nabla u\right)\right) \quad \text{on } \left(0,\mathrm{T}\right\rangle\times\Omega,\\ u\,|_{t=0} &= u_{ini} \quad \text{on } \Omega,\end{aligned}$$

with the Neumann boundary conditions

$$\nabla_{\mathbf{p}}\gamma_{\mathbb{G}}\nu = 1 \quad \text{on } \partial\Omega.$$

The anisotropy function $\gamma_{\mathbb{G}}$ is given by

$$\gamma_{\mathbb{G}}\left(\mathbf{p},-1\right) := \sqrt{1+\mathbf{p}^T\mathbb{G}\mathbf{p}}, \text{ for } \mathbb{G} := \begin{pmatrix} 11 & 10\\ 10 & 11\end{pmatrix},$$

and the initial condition is a square given by $\left(|x|-0.75\right)\left(|y|-0.75\right)=0$.
Computational domain: $\Omega\equiv\left[-2,2\right]^2$.
Final time: $T=0.2$.
Level-set: 100×100 nodes, regularisation $\epsilon=0.001$, no re-distancing.
Time step: Adaptive.
Numerical scheme: 6.3.6
Figure: 7.90.
Remark: –

Numerical experiment 7.2.72. Test of the **level-set formulation for the anisotropic Willmore flow**

$$\begin{aligned}\frac{\partial_t u}{Q_\epsilon} &= -\nabla\cdot\left(\mathbb{E}_\gamma\nabla w_\gamma - \frac{1}{2}\frac{w_\gamma^2}{Q^3}\nabla u\right) \quad \text{on } \left(0,T\right)\times\Omega,\\ w_\gamma &= Q_\epsilon H_\gamma \quad \text{on } \left(0,T\right)\times\Omega,\\ u\,|_{t=0} &= u_{ini} \quad \text{on } \Omega,\end{aligned}$$

with the Neumann boundary conditions

$$\partial_\nu u = 1,\ \mathbb{E}_\gamma\nabla w_\gamma\cdot\nu = 0 \quad \text{on } \partial\Omega.$$

The anisotropy function $\gamma_{\mathbb{G}}$ is given by

$$\gamma_{\mathbb{G}}\left(\mathbf{p},-1\right) := \sqrt{1+\mathbf{p}^T\mathbb{G}\mathbf{p}}, \text{ for } \mathbb{G} := \begin{pmatrix} 11 & 10\\ 10 & 11\end{pmatrix},$$

and the initial condition is a square given by $\left(|x|-0.75\right)\left(|y|-0.75\right)=0$.
Computational domain: $\Omega\equiv\left[-3,3\right]^2$.
Final time: $T=0.0008$.
Level-set: 150×150 nodes, regularisation $\epsilon=0.01$, no re-distancing.
Time step: Adaptive.
Numerical scheme: 6.3.7
Figure: 7.91.
Remark: –

Anisotropic level-set formulation of the mean-curvature flow

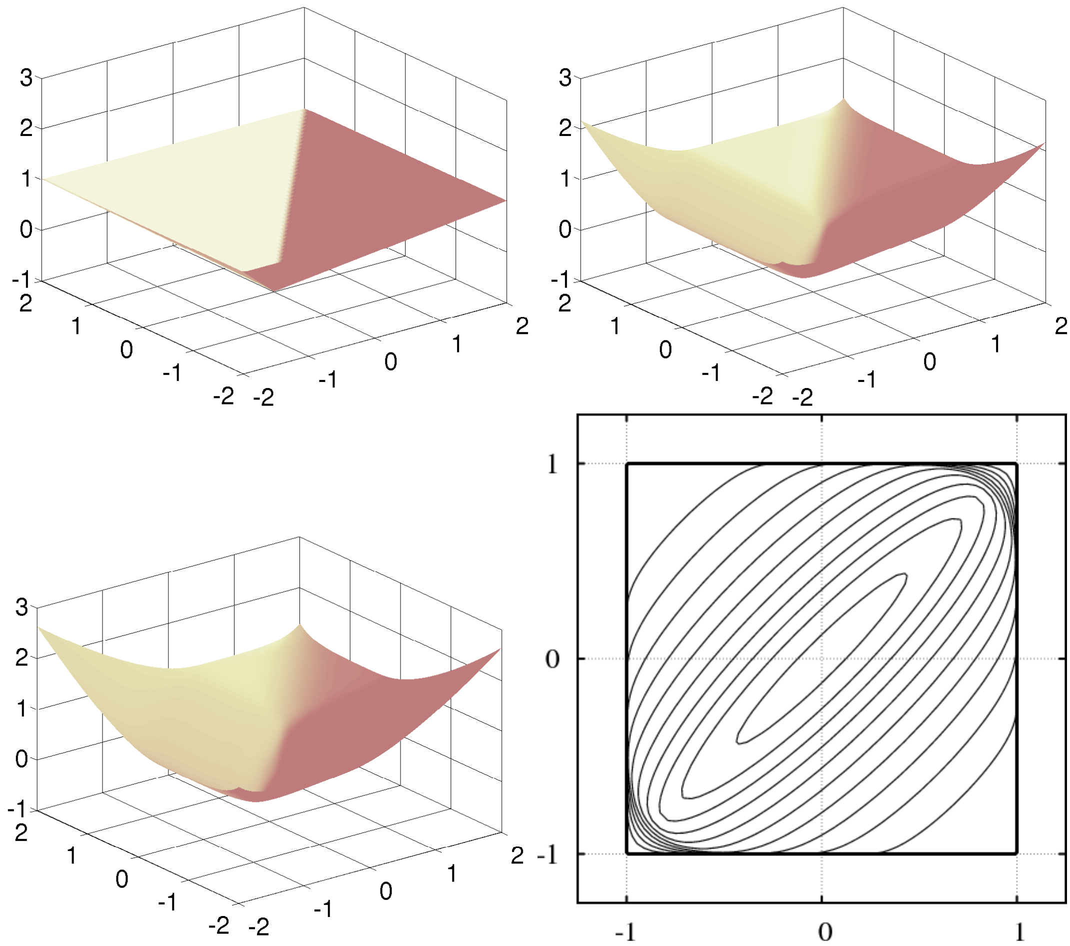

Figure 7.90.: Anisotropic level-set method for the **mean-curvature flow** – graphs of the level-set function at times $t = 0$, $t = 0.1$, $t = 0.2$ and evolution of the initial curve until the time $t = 0.2$ with the time period 0.02. See the Numerical experiment 7.2.71

Anisotropic level-set formulation of the Willmore flow

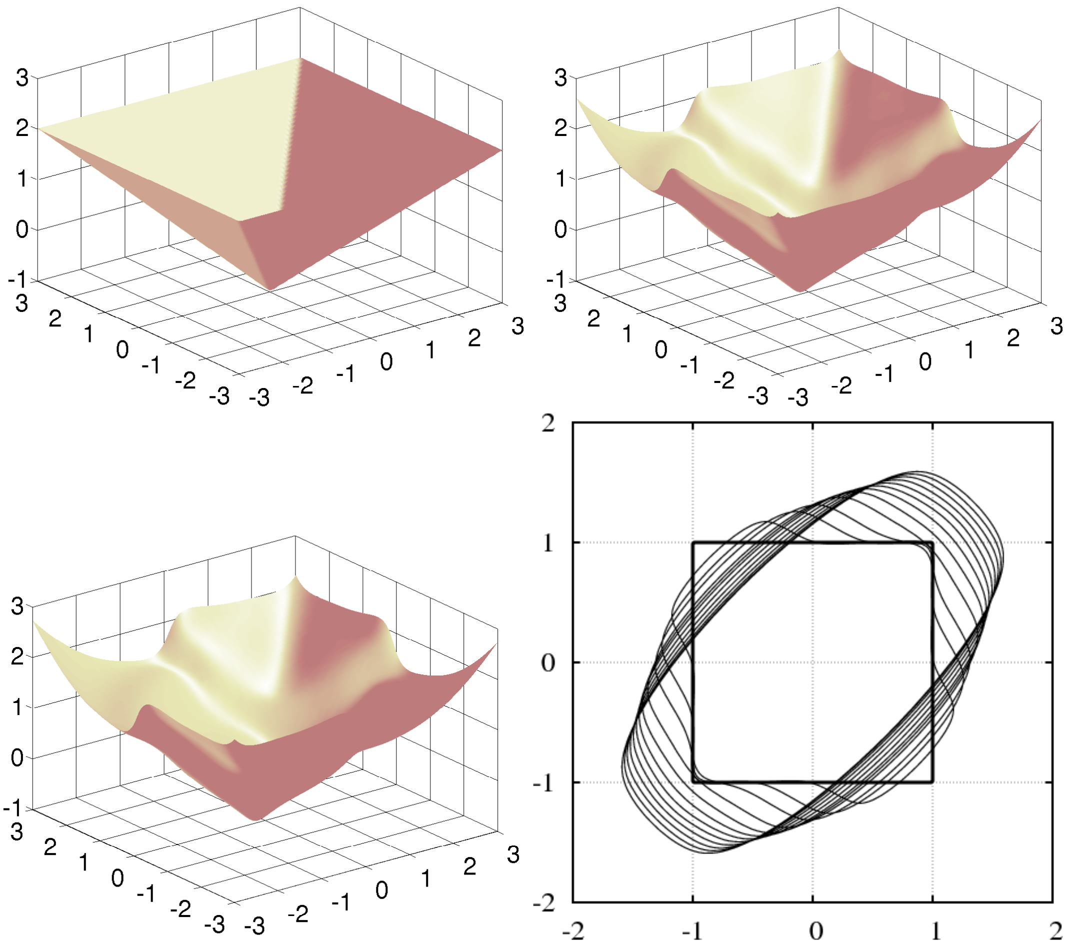

Figure 7.91.: Anisotropic level-set method for the **Willmore flow** – graphs of the level-set function at times $t = 0$, $t = 0.0004$, $t = 0.0008$ and evolution of the initial curve at times $t = 10^{-5}, 4 \cdot 10^{-5}, 8 \cdot 10^{-5}, 0.00016, 0.00024, \cdots, 0.0008$. See the Numerical experiment 7.2.72

Numerical experiment 7.2.73. Test of the **level-set formulation for the anisotropic mean-curvature flow**

$$\begin{aligned} \frac{\partial_t u}{Q_\epsilon} &= \nabla \cdot \left(\nabla_{\mathbf{p}} \gamma_{\mathbb{G}} \left(\nabla u\right)\right) \quad \text{on } (0, \mathrm{T}\rangle \times \Omega, \\ u\,|_{t=0} &= u_{ini} \quad \text{on } \Omega, \end{aligned}$$

with the Neumann boundary conditions

$$\nabla_{\mathbf{p}} \gamma_{\mathbb{G}} \nu = 1 \quad \text{on } \partial\Omega.$$

The anisotropy function $\gamma_{\mathbb{G}}$ is given by

$$\gamma_{\mathbb{G}}\left(\mathbf{p}, -1\right) := \sqrt{1 + \mathbf{p}^T \mathbb{G} \mathbf{p}}, \text{ for } \mathbb{G} := \begin{pmatrix} 10 & 0 \\ 0 & 1 \end{pmatrix},$$

and the initial condition is an astroid given by $x^{2/3} + y^{2/3} = 0.75^{2/3}$.
Computational domain: $\Omega \equiv [-1, 1]^2$.
Final time: $T = 0.0045$.
Level-set: 100×100 nodes, regularisation $\epsilon = 10^{-5}$, no re-distancing.
Time step: $\tau = 2 \cdot 10^{-5}$.
Numerical scheme: 6.3.8
Figure: 7.92.
Remark: –

Numerical experiment 7.2.74. Test of the **level-set formulation for the anisotropic Willmore flow**

$$\begin{aligned} \frac{\partial_t u}{Q_\epsilon} &= -\nabla \cdot \left(\mathbb{E}_\gamma \nabla w_\gamma - \frac{1}{2} \frac{w_\gamma^2}{Q^3} \nabla u\right) \quad \text{on } (0, T) \times \Omega, \\ w_\gamma &= Q_\epsilon H_\gamma \quad \text{on } (0, T) \times \Omega, \\ u\,|_{t=0} &= u_{ini} \quad \text{on } \Omega, \end{aligned}$$

with the Neumann boundary conditions

$$\partial_\nu u = 1, \ \mathbb{E}_\gamma \nabla w_\gamma \cdot \nu = 0 \quad \text{on } \partial\Omega.$$

The anisotropy function $\gamma_{\mathbb{G}}$ is given by

$$\gamma_{\mathbb{G}}\left(\mathbf{p}, -1\right) := \sqrt{1 + \mathbf{p}^T \mathbb{G} \mathbf{p}}, \text{ for } \mathbb{G} := \begin{pmatrix} 10 & 0 \\ 0 & 1 \end{pmatrix},$$

and the initial condition is an astroid given by $x^{2/3} + y^{2/3} = 0.75^{2/3}$.
Computational domain: $\Omega \equiv [-1, 1]^2$.
Final time: $T = 5 \cdot 10^{-4}$.
Level-set: 125×125 nodes, regularisation $\epsilon = 0.01$, no re-distancing.
Time step: $\tau = 10^{-9}$.
Numerical scheme: 6.3.9
Figure: 7.93.
Remark: –

Anisotropic level-set formulation of the mean-curvature flow

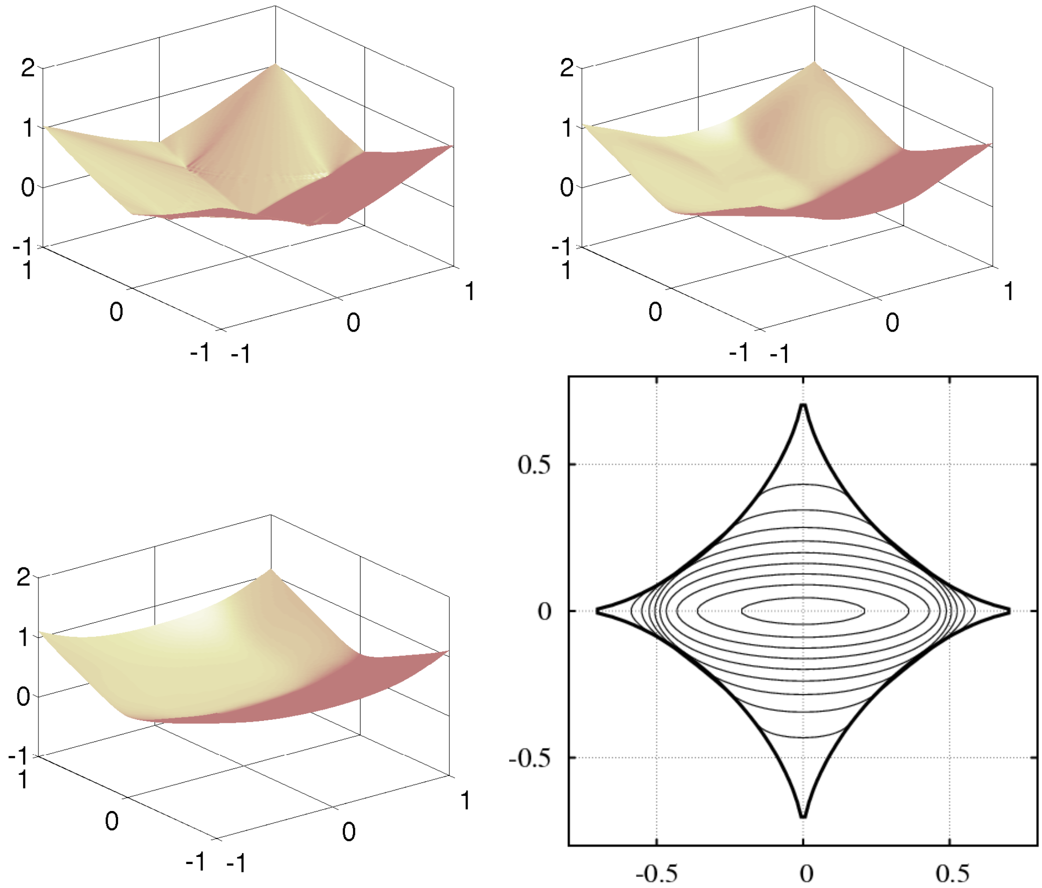

Figure 7.92.: Anisotropic level-set method for the **mean-curvature flow** – graphs if the level-set function at times $t = 0$, $t = 0.001$, $t = 0.0045$ and evolution of the initial curve until the time $t = 0.0045$ with the time period 0.005. See the Numerical experiment 7.2.73

Anisotropic level-set formulation of the Willmore flow

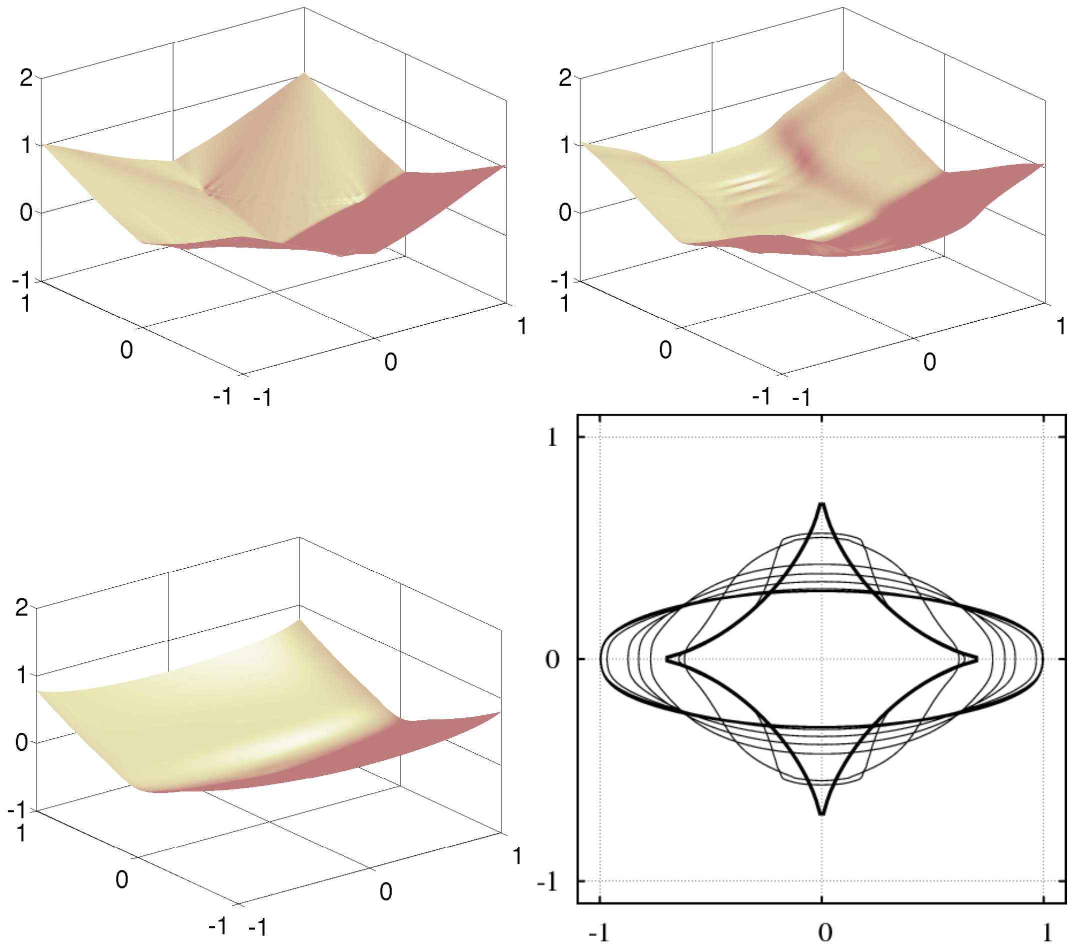

Figure 7.93.: Anisotropic level-set method for the **Willmore flow** – graphs of the level-set function at times $t = 0$, $t = 10^{-5}$, $t = 0.0005$ and evolution of the initial curve at times $t = 10^{-6}, 10^{-5}, 5 \cdot 10^{-5}, 0.00015, \cdots, 0.0005$. See the Numerical experiment 7.2.74

Numerical experiment 7.2.75. Test of the **level-set formulation for the anisotropic mean-curvature flow**

$$\begin{aligned} \frac{\partial_t u}{Q_\epsilon} &= \nabla \cdot \left(\nabla_{\mathbf{p}} \gamma_{\mathbb{G}} \left(\nabla u \right) \right) \quad \text{on } (0, \mathrm{T}\rangle \times \Omega, \\ u \,|_{t=0} &= u_{ini} \quad \text{on } \Omega, \end{aligned}$$

with the Neumann boundary conditions

$$\nabla_{\mathbf{p}} \gamma_{\mathbb{G}} \nu = 1 \quad \text{on } \partial\Omega.$$

The anisotropy function $\gamma_{\mathbb{G}}$ is given by

$$\gamma_{\mathbb{G}} \left(\mathbf{p}, -1 \right) := \sqrt{1 + \mathbf{p}^T \mathbb{G} \mathbf{p}}, \text{ for } \mathbb{G} := \begin{pmatrix} 11 & 10 \\ 10 & 11 \end{pmatrix},$$

and the initial condition is an astroid given by $x^{2/3} + y^{2/3} = 0.75^{2/3}$.
Computational domain: $\Omega \equiv [-1, 1]^2$.
Final time: $T = 0.033$.
Level-set: 100×100 nodes, regularisation $\epsilon = 0.001$, no re-distancing.
Time step: Adaptive.
Numerical scheme: 6.3.6
Figure: 7.94.
Remark: –

Numerical experiment 7.2.76. Test of the **level-set formulation for the anisotropic Willmore flow**

$$\begin{aligned} \frac{\partial_t u}{Q_\epsilon} &= -\nabla \cdot \left(\mathbb{E}_\gamma \nabla w_\gamma - \frac{1}{2} \frac{w_\gamma^2}{Q^3} \nabla u \right) \quad \text{on } (0, T) \times \Omega, \\ w_\gamma &= Q_\epsilon H_\gamma \quad \text{on } (0, T) \times \Omega, \\ u \,|_{t=0} &= u_{ini} \quad \text{on } \Omega, \end{aligned}$$

with the Neumann boundary conditions

$$\partial_\nu u = 1, \ \mathbb{E}_\gamma \nabla w_\gamma \cdot \nu = 0 \quad \text{on } \partial\Omega.$$

The anisotropy function $\gamma_{\mathbb{G}}$ is given by

$$\gamma_{\mathbb{G}} \left(\mathbf{p}, -1 \right) := \sqrt{1 + \mathbf{p}^T \mathbb{G} \mathbf{p}}, \text{ for } \mathbb{G} := \begin{pmatrix} 11 & 10 \\ 10 & 11 \end{pmatrix},$$

and the initial condition is an astroid given by $x^{2/3} + y^{2/3} = 0.75^{2/3}$.
Computational domain: $\Omega \equiv [-1, 1]^2$.
Final time: $T = 0.0001$.
Level-set: 125×125 nodes, regularisation $\epsilon = 0.01$, no re-distancing.
Time step: $\tau = 10^{-9}$.
Numerical scheme: 6.3.9
Figure: 7.95.
Remark: –

Anisotropic level-set formulation of the mean-curvature flow

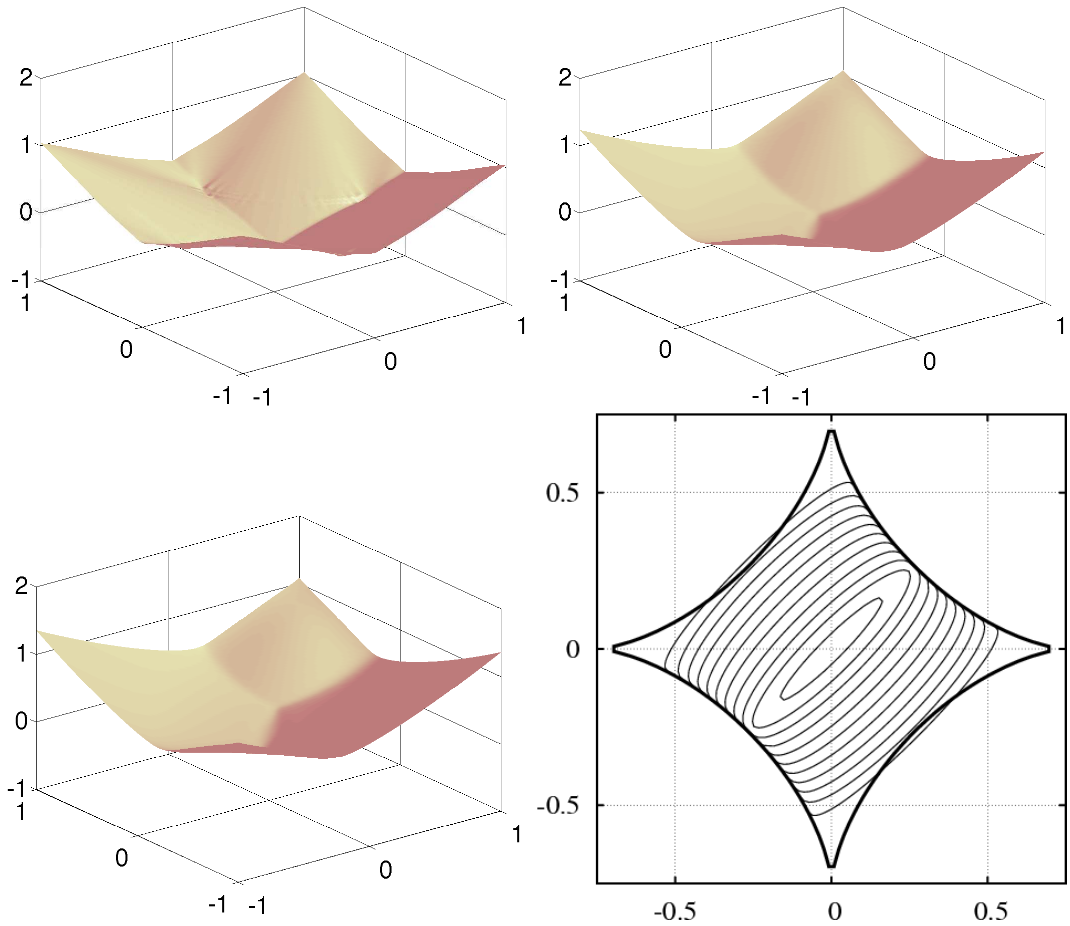

Figure 7.94.: Anisotropic level-set method for the **mean-curvature flow** – graphs of the level-set function at times $t = 0$, $t = 0.015$, $t = 0.033$ and evolution of the initial curve until the time $t = 0.033$ with the time period 0.003. See the Numerical experiment 7.2.75

Anisotropic level-set formulation of the Willmore flow

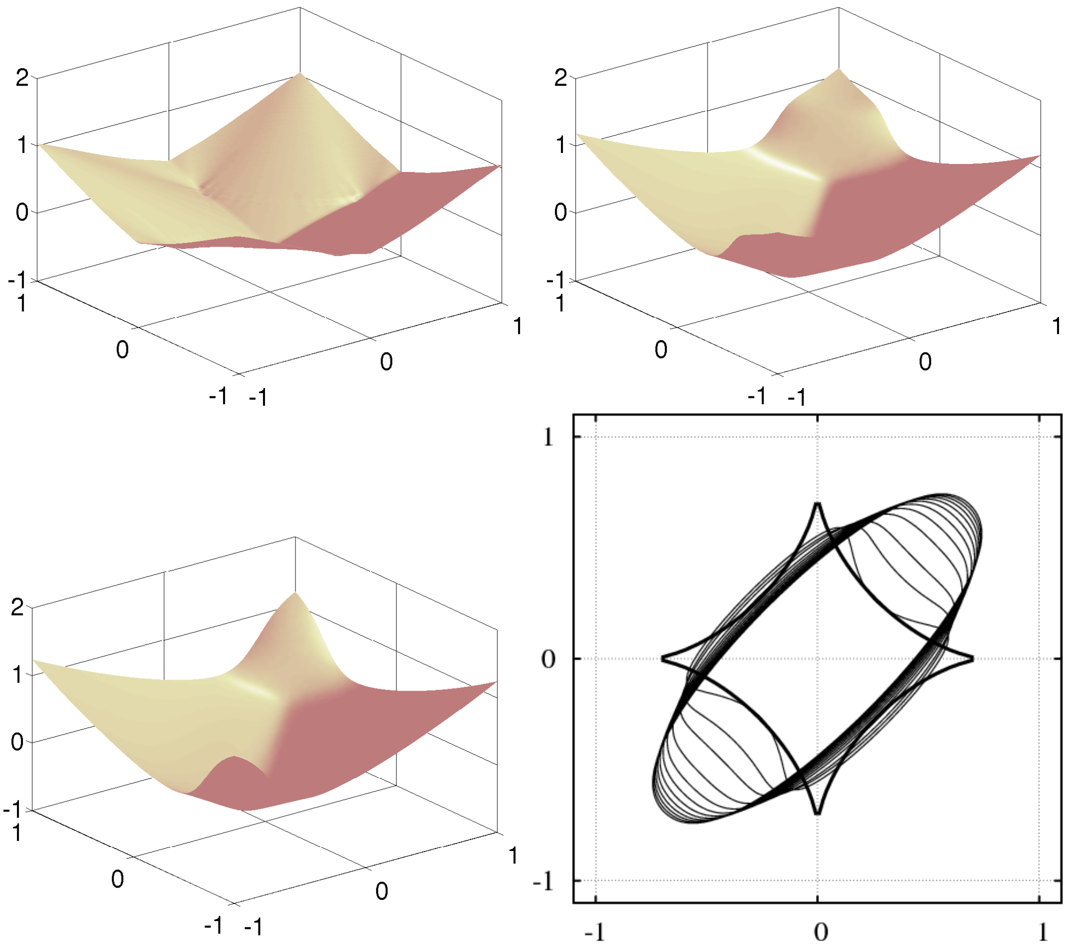

Figure 7.95.: Anisotropic level-set method for the **Willmore flow** – graphs of the level-set function at times $t = 0$, $t = 5 \cdot 10^{-5}$, $t = 0.0001$ and evolution of the initial curve at times $t = 10^{-6}, 5 \cdot 10^{-6}, 10^{-5}, 2 \cdot 10^{-5}, 3 \cdot 10^{-5}, \cdots, 0.0001$. See the Numerical experiment 7.2.76

Numerical experiment 7.2.77. Test of the **level-set formulation for the anisotropic mean-curvature flow**

$$
\begin{aligned}
\frac{\partial_t u}{Q_\epsilon} &= \nabla \cdot \left(\nabla_{\mathbf{p}} \gamma_{\mathbb{G}} \left(\nabla u\right)\right) \quad \text{on } \left(0, \mathrm{T}\right\rangle \times \Omega, \\
u\,|_{t=0} &= u_{ini} \quad \text{on } \Omega,
\end{aligned}
$$

with the Neumann boundary conditions

$$\nabla_{\mathbf{p}} \gamma_{\mathbb{G}} \nu = 1 \quad \text{on } \partial\Omega.$$

The anisotropy function $\gamma_{\mathbb{G}}$ is given by

$$\gamma_{\mathbb{G}} \left(\mathbf{p}, -1\right) := \sqrt{1 + \mathbf{p}^T \mathbb{G} \mathbf{p}}, \text{ for } \mathbb{G} := \begin{pmatrix} 10 & 0 \\ 0 & 1 \end{pmatrix},$$

and the initial condition is a curve given by

$$u\left(x, y\right) = \sqrt{x^2 + y^2} - 1 - 0.75 \sin \left(6 \arccos \frac{x}{\sqrt{x^2 + y^2}}\right) = 0$$

.
Computational domain: $\Omega \equiv \left[-1.5, 1.5\right]^2$.
Final time: $T = 0.1$.
Level-set: 250×250 nodes, regularisation $\epsilon = 10^{-5}$, no re-distancing.
Time step: Adaptive.
Numerical scheme: 6.3.6
Figure: 7.96.
Remark: –

Numerical experiment 7.2.78. Test of the **level-set formulation for the anisotropic Willmore flow**

$$\begin{aligned} \frac{\partial_t u}{Q_\epsilon} &= -\nabla \cdot \left(\mathbb{E}_\gamma \nabla w_\gamma - \frac{1}{2} \frac{w_\gamma^2}{Q^3} \nabla u \right) \quad \text{on } (0,T) \times \Omega, \\ w_\gamma &= Q_\epsilon H_\gamma \quad \text{on } (0,T) \times \Omega, \\ u \left.\right|_{t=0} &= u_{ini} \quad \text{on } \Omega, \end{aligned}$$

with the Neumann boundary conditions

$$\partial_\nu u = 1, \ \mathbb{E}_\gamma \nabla w_\gamma \cdot \nu = 0 \quad \text{on } \partial\Omega.$$

The anisotropy function $\gamma_{\mathbb{G}}$ is given by

$$\gamma_{\mathbb{G}} (\mathbf{p}, -1) := \sqrt{1 + \mathbf{p}^T \mathbb{G} \mathbf{p}}, \ \text{for } \mathbb{G} := \begin{pmatrix} 11 & 10 \\ 10 & 11 \end{pmatrix},$$

and the initial condition is a curve given by

$$u(x,y) = \sqrt{x^2+y^2} - 1 - 0.3 \sin \left(6 \arccos \frac{x}{\sqrt{x^2+y^2}} \right) = 0$$

.

Computational domain: $\Omega \equiv [-1.5, 1.5]^2$.
Final time: $T = 0.0012$.
Level-set: 100×100 nodes, regularisation $\epsilon = 0.01$, no re-distancing.
Time step: Adaptive.
Numerical scheme: 6.3.7
Figure: 7.93.
Remark: –

Anisotropic level-set formulation of the mean-curvature flow

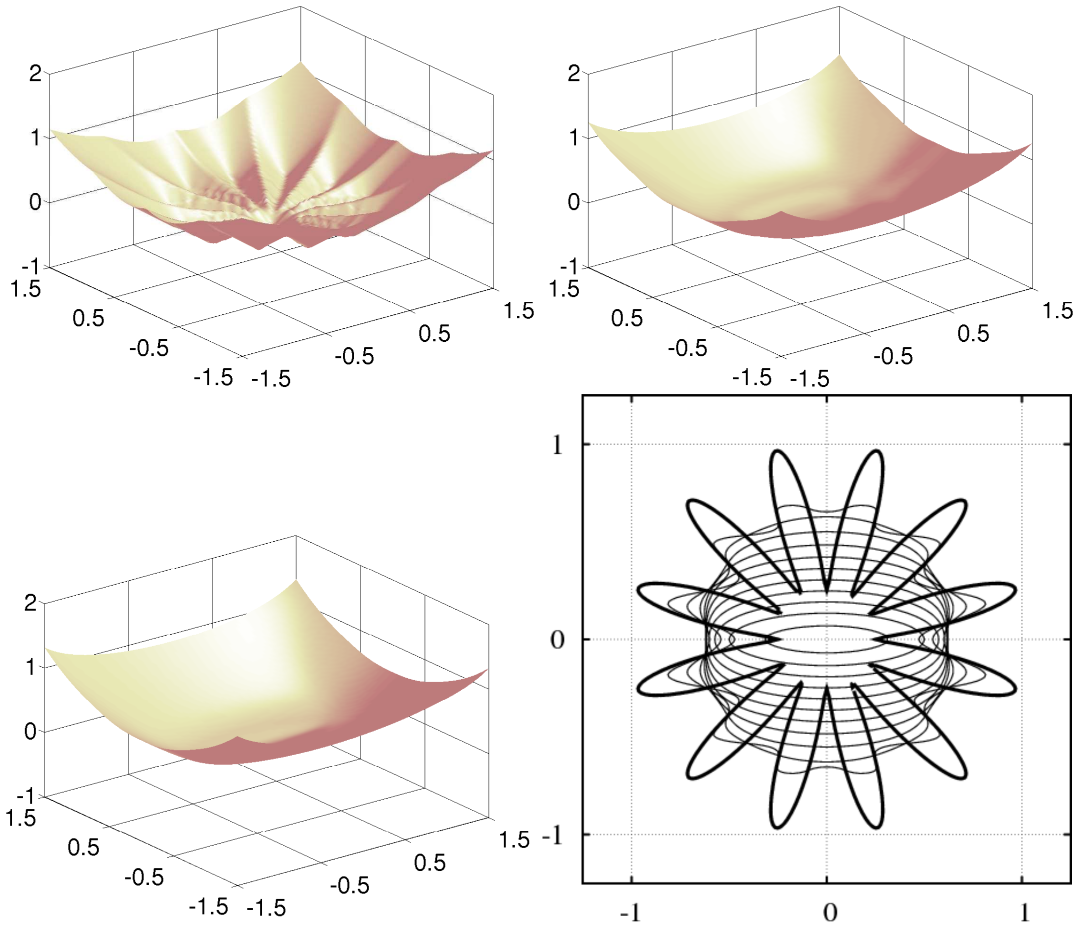

Figure 7.96.: Anisotropic level-set method for the **mean-curvature flow** – graphs of the level-set function at times $t = 0$, $t = 0.05$, $t = 0.1$ and evolution of the initial curve at times $t = 0.005, 0.01, 0.02, 0.03, \cdots, 0.1$. See the Numerical experiment 7.2.77

Anisotropic level-set formulation of the Willmore flow

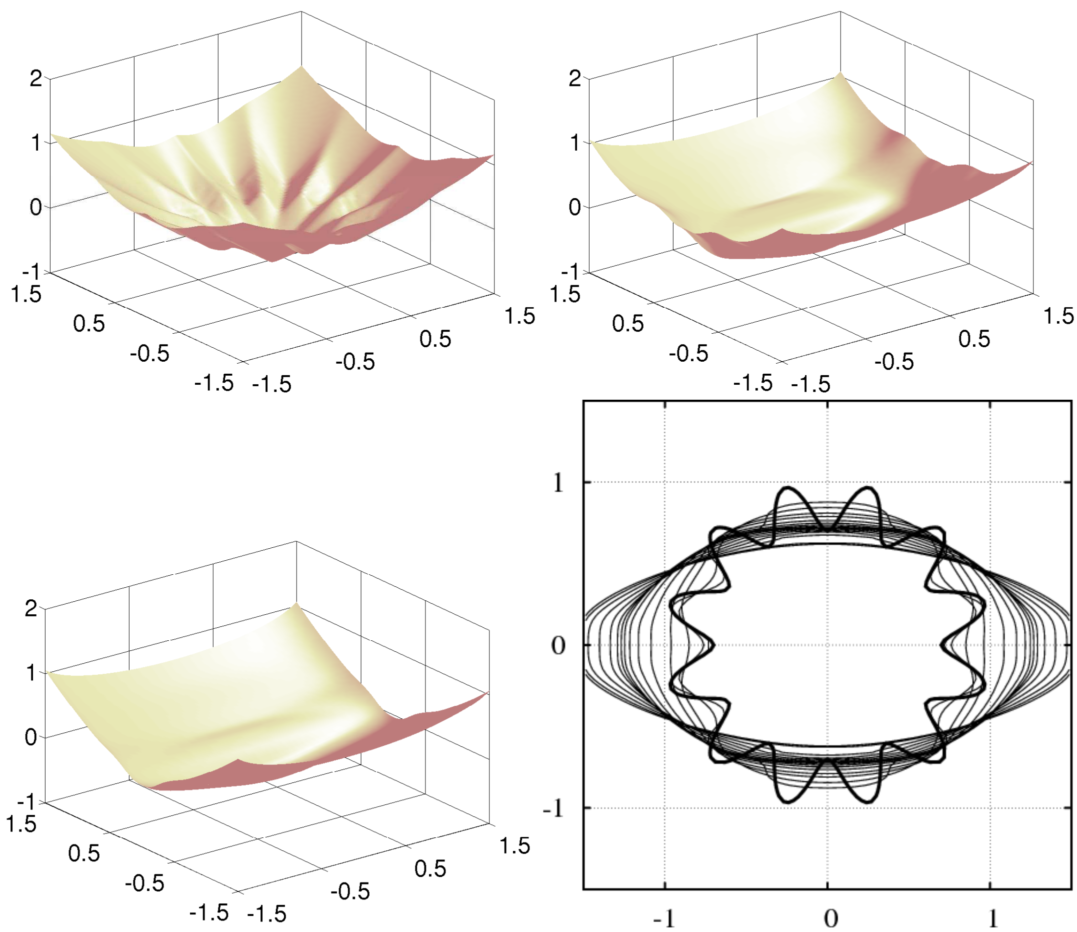

Figure 7.97.: Anisotropic level-set method for the **Willmore flow** – graphs of the level-set function at times $t = 0$, $t = 0.0006$, $t = 0.0012$ and evolution of the initial curve at times $t = 10^{-6}, 10^{-5}, 5 \cdot 10^{-5}, 0.0001, 0.0002, 0.0003, \cdots, 0.0012$. See the Numerical experiment 7.2.78

Numerical experiment 7.2.79. Test of the **level-set formulation for the anisotropic mean-curvature flow**

$$\begin{aligned} \frac{\partial_t u}{Q_\epsilon} &= \nabla \cdot \left(\nabla_{\mathbf{p}} \gamma_{\mathbb{G}} \left(\nabla u \right) \right) \quad \text{on } \langle 0, \mathrm{T} \rangle \times \Omega, \\ u \left|_{t=0} \right. &= u_{ini} \quad \text{on } \Omega, \end{aligned}$$

with the Neumann boundary conditions

$$\nabla_{\mathbf{p}} \gamma_{\mathbb{G}} \nu = 1 \quad \text{on } \partial \Omega.$$

The anisotropy function $\gamma_{\mathbb{G}}$ is given by

$$\gamma_{\mathbb{G}} \left(\mathbf{p}, -1 \right) := \sqrt{1 + \mathbf{p}^T \mathbb{G} \mathbf{p}}, \text{ for } \mathbb{G} := \begin{pmatrix} 11 & 10 \\ 10 & 11 \end{pmatrix},$$

and the initial condition is a curve given by

$$u \left(x, y \right) = \sqrt{x^2 + y^2} - 1 - 0.75 \sin \left(6 \arccos \frac{x}{\sqrt{x^2 + y^2}} \right) = 0$$

.
Computational domain: $\Omega \equiv \left[-1.5, 1.5 \right]^2$.
Final time: $T = 0.075$.
Level-set: 250×250 nodes, regularisation $\epsilon = 0.001$, no re-distancing.
Time step: Adaptive.
Numerical scheme: 6.3.6
Figure: 7.98.
Remark: –

Numerical experiment 7.2.80. Test of the **level-set formulation for the anisotropic Willmore flow**

$$\begin{aligned}\frac{\partial_t u}{Q_\epsilon} &= -\nabla \cdot \left(\mathbb{E}_\gamma \nabla w_\gamma - \frac{1}{2}\frac{w_\gamma^2}{Q^3} \nabla u \right) \quad \text{on } (0,T) \times \Omega, \\ w_\gamma &= Q_\epsilon H_\gamma \quad \text{on } (0,T) \times \Omega, \\ u\,|_{t=0} &= u_{ini} \quad \text{on } \Omega,\end{aligned}$$

with the Neumann boundary conditions

$$\partial_\nu u = 1, \; \mathbb{E}_\gamma \nabla w_\gamma \cdot \nu = 0 \quad \text{on } \partial\Omega.$$

The anisotropy function $\gamma_{\mathbb{G}}$ is given by

$$\gamma_{\mathbb{G}}(\mathbf{p}, -1) := \sqrt{1 + \mathbf{p}^T \mathbb{G} \mathbf{p}}, \text{ for } \mathbb{G} := \begin{pmatrix} 11 & 10 \\ 10 & 11 \end{pmatrix},$$

and the initial condition is a curve given by

$$u(x,y) = \sqrt{x^2+y^2} - 1 - 0.3 \sin\left(6 \arccos \frac{x}{\sqrt{x^2+y^2}} \right) = 0$$

.
Computational domain: $\Omega \equiv [-1.5, 1.5]^2$.
Final time: $T = 3 \cdot 10^{-4}$.
Level-set: 100×100 nodes, regularisation $\epsilon = 0.01$, no re-distancing.
Time step: Adaptive.
Numerical scheme: 6.3.7
Figure: 7.99.
Remark: –

Anisotropic level-set formulation of the mean-curvature flow

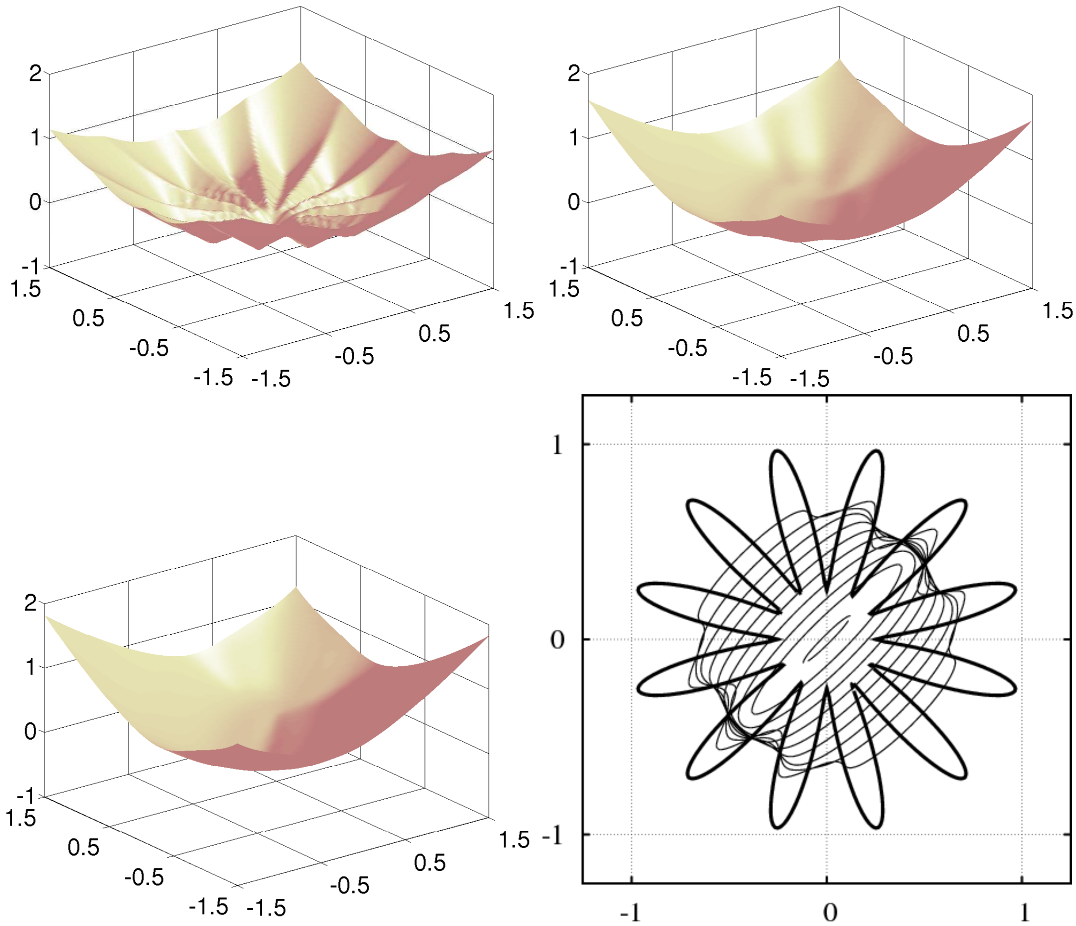

Figure 7.98.: Anisotropic level-set method for the **mean-curvature flow** – graphs of the level-set function at times $t = 0$, $t = 0.0375$, $t = 0.075$ and evolution of the initial curve until the time $t = 0.075$ with the time period 0.0075. See the Numerical experiment 7.2.79

Anisotropic level-set formulation of the Willmore flow

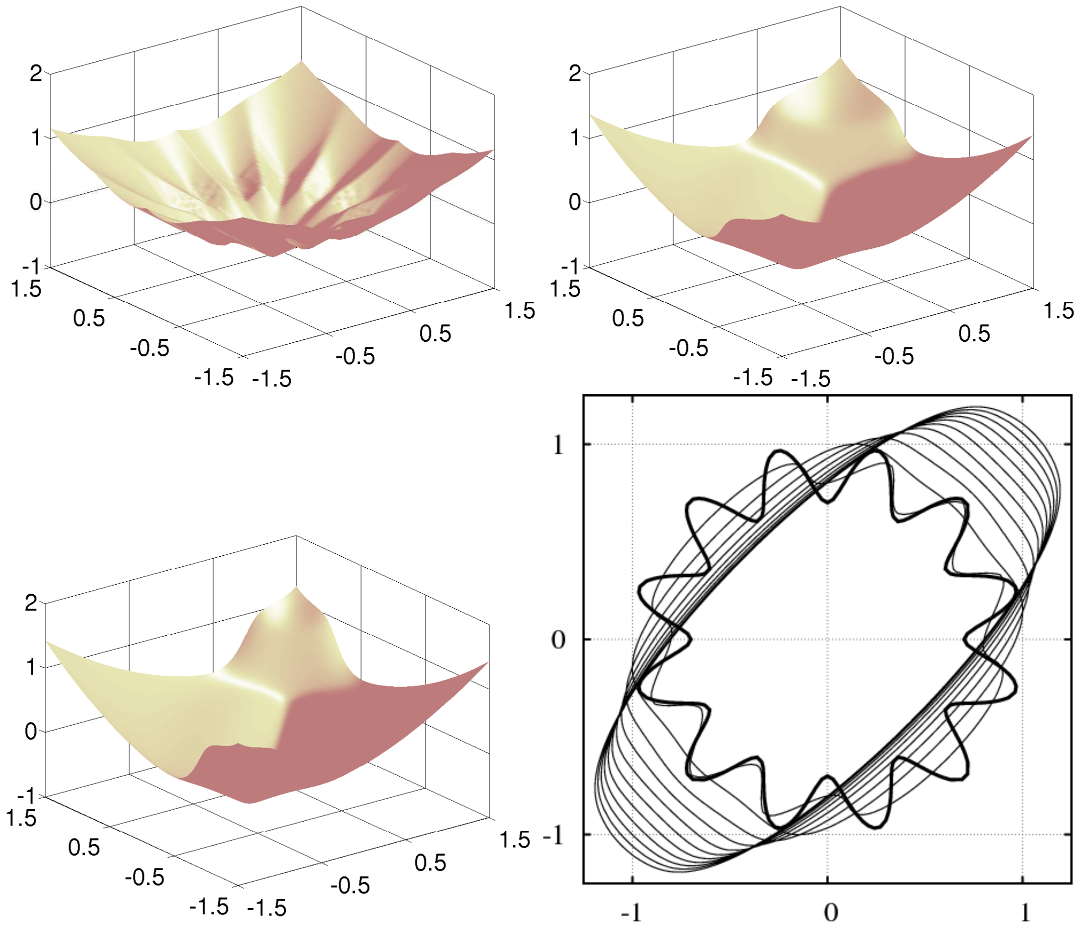

Figure 7.99.: Anisotropic level-set method for the **Willmore flow** – graphs of the level-set function at times $t = 0$, $t = 1.5 \cdot 10^{-4}$, $t = 3 \cdot 10^{-4}$ and evolution of the initial curve at times $t = 10^{-6}, 3 \cdot 10^{-5}, 6 \cdot 10^{-5}, 9 \cdot 10^{-5}, 0.00012, 0.00015, 0.00018, \cdots, 0.0003$. See the Numerical experiment 7.2.80

Numerical experiment 7.2.81. Test of the **level-set formulation for the anisotropic mean-curvature flow**

$$\begin{aligned} \frac{\partial_t u}{Q_\epsilon} &= \nabla \cdot \left(\nabla_{\mathbf{p}} \gamma_{abs} \left(\nabla u \right) \right) \quad \text{on } (0, \mathrm{T}\rangle \times \Omega, \\ u\,|_{t=0} &= u_{ini} \quad \text{on } \Omega, \end{aligned}$$

with the Neumann boundary conditions

$$\nabla_{\mathbf{p}} \gamma_{abs} \cdot \nu = 1 \quad \text{on } \partial\Omega.$$

The anisotropy function γ_{abs} is given by

$$\gamma_{abs}\left(\mathbf{P}\right) = \sum_{i=1}^{3} \sqrt{P_i^2 + \epsilon_{abs} \sum_{j=1}^{3} P_j^2}, \text{ for } \epsilon_{abs} = 0.001,$$

and the initial condition is a circle given by $x^2 + y^2 = 1$.
Computational domain: $\Omega \equiv [-2, 2]^2$.
Final time: $T = 0.36$.
Level-set: 100×100 nodes, regularisation $\epsilon = 10^{-5}$, no re-distancing.
Time step: Adaptive.
Numerical scheme: 6.3.6
Figure: 7.100.
Remark: –

Numerical experiment 7.2.82. Test of the **level-set formulation for the anisotropic Willmore flow**

$$\begin{aligned}\frac{\partial_t u}{Q_\epsilon} &= -\nabla\cdot\left(\mathbb{E}_\gamma\nabla w_\gamma - \frac{1}{2}\frac{w_\gamma^2}{Q^3}\nabla u\right) \quad \text{on } (0,T)\times\Omega,\\ w_\gamma &= Q_\epsilon H_\gamma \quad \text{on } (0,T)\times\Omega,\\ u\,|_{t=0} &= u_{ini} \quad \text{on } \Omega,\end{aligned}$$

with the Neumann boundary conditions

$$\partial_\nu u = 1,\ \mathbb{E}_\gamma\nabla w_\gamma\cdot\nu = 0 \quad \text{on } \partial\Omega.$$

The anisotropy function γ_{abs} is given by

$$\gamma_{abs}(\mathbf{P}) = \sum_{i=1}^{3}\sqrt{P_i^2 + \epsilon_{abs}\sum_{j=1}^{3}P_j^2},\ \text{for } \epsilon_{abs} = 0.001,$$

and the initial condition is a circle given by $x^2+y^2=1$.
Computational domain: $\Omega \equiv [-2,2]^2$.
Initial condition: Circle given by $x^2+y^2=1$.
Boundary conditions: $\partial_\nu u = 1$, $\mathbb{E}_\gamma\nabla w_\gamma\cdot\nu = 0$ on $\partial\Omega$.
Final time: $T = 0.1$.
Level-set: 100×100 nodes, regularisation $\epsilon = 0.01$, no re-distancing.
Time step: $\tau = 10^{-8}$.
Numerical scheme: 6.3.9
Figure: 7.101.
Remark: –

Anisotropic level-set formulation of the mean-curvature flow

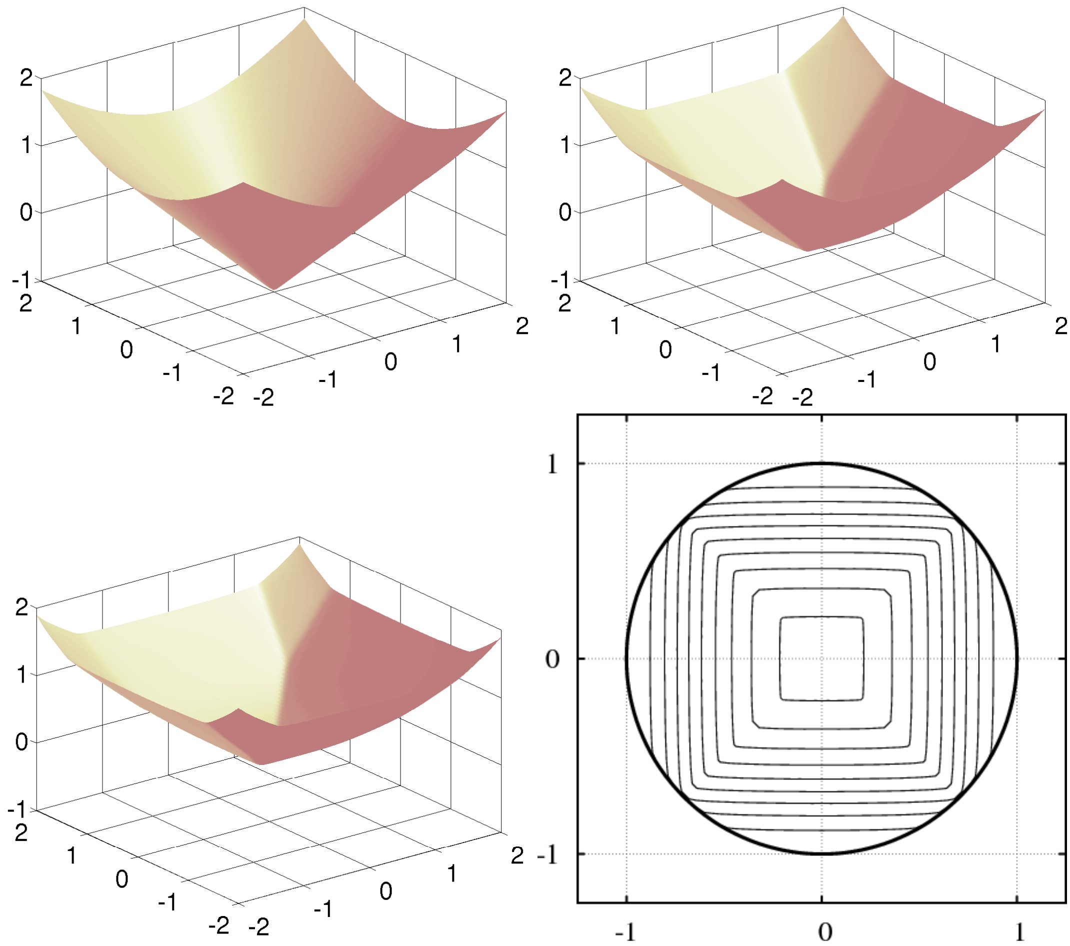

Figure 7.100.: Anisotropic level-set method for the **mean-curvature flow** – graphs of the level-set function at times $t = 0$,$t = 0.18$ and $t = 0.36$ and evolution of the initial curve until the time $t = 0.36$ with the time period 0.04. See the Numerical experiment 7.2.81

Anisotropic level-set formulation of the Willmore flow

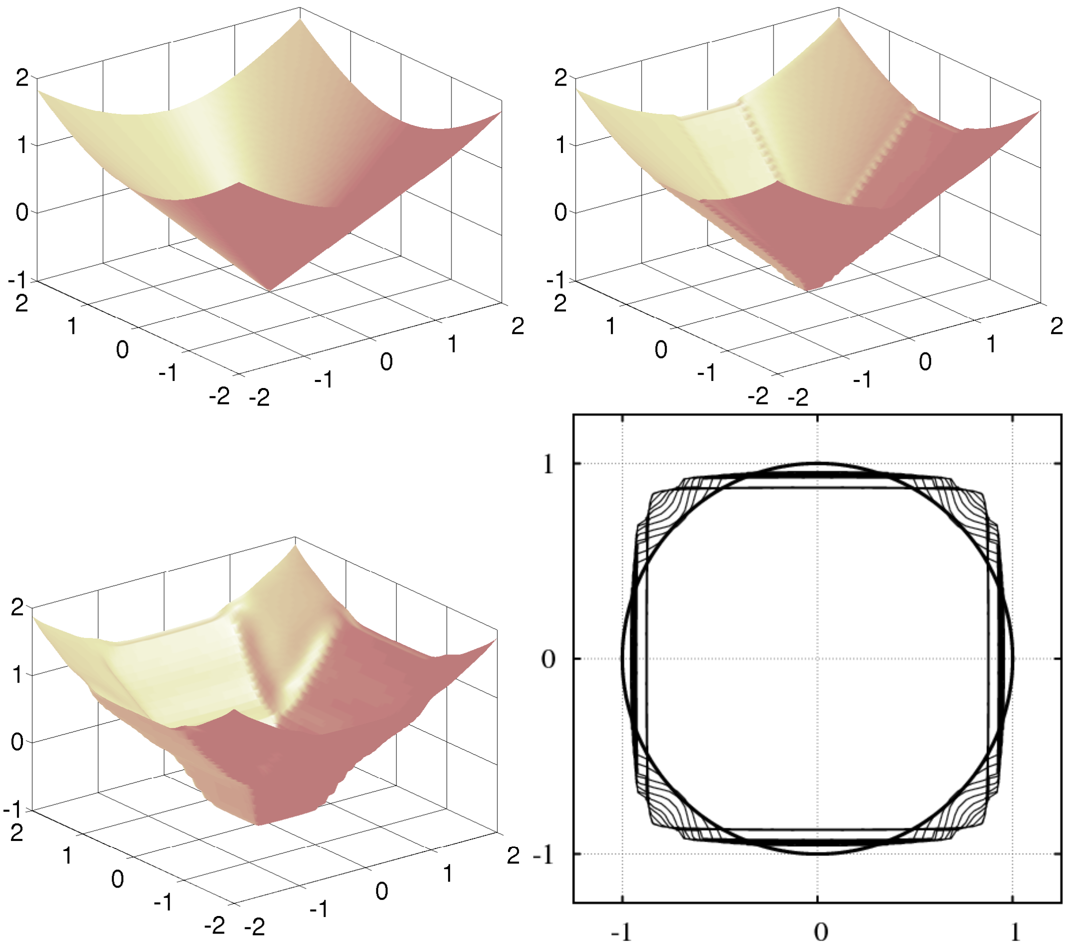

Figure 7.101.: Anisotropic level-set method for the **Willmore flow** – graphs of the level-set function at times $t = 0$, $t = 0.001$ and $t = 0.1$ and evolution of the curve at times $t = 0.001, 0.005, 0.01, 0.02, 0.03, \cdots, 0.1$. See the Numerical experiment 7.2.82

Numerical experiment 7.2.83. Test of the **level-set formulation for the anisotropic mean-curvature flow**

$$\begin{aligned}\frac{\partial_t u}{Q_\epsilon} &= \nabla\cdot\left(\nabla_{\mathbf{p}}\gamma_{abs}\left(\nabla u\right)\right) \quad \text{on } (0,\mathrm{T}\rangle\times\Omega,\\ u\mid_{t=0} &= u_{ini} \quad \text{on } \Omega,\end{aligned}$$

with the Neumann boundary conditions

$$\nabla_{\mathbf{p}}\gamma_{abs}\cdot\nu = 1 \quad \text{on } \partial\Omega.$$

The anisotropy function γ_{abs} is given by

$$\gamma_{abs}\left(\mathbf{P}\right) = \sum_{i=1}^{3}\sqrt{P_i^2+\epsilon_{abs}\sum_{j=1}^{3}P_j^2}, \text{ for } \epsilon_{abs}=0.001,$$

and the initial condition is a square given by $\left(|x|-0.75\right)\left(|y|-0.75\right)=0$.
Computational domain: $\Omega\equiv[-2,2]^2$.
Final time: $T=0.48$.
Level-set: 100×100 nodes, regularisation $\epsilon=0.001$, no re-distancing.
Time step: Adaptive.
Numerical scheme: 6.3.6.
Figure: 7.102.
Remark: –.

Numerical experiment 7.2.84. Test of the **level-set formulation for the anisotropic Willmore flow**

$$\begin{aligned}\frac{\partial_t u}{Q_\epsilon} &= -\nabla\cdot\left(\mathbb{E}_\gamma\nabla w_\gamma-\frac{1}{2}\frac{w_\gamma^2}{Q^3}\nabla u\right) \quad \text{on } (0,T)\times\Omega,\\ w_\gamma &= Q_\epsilon H_\gamma \quad \text{on } (0,T)\times\Omega,\\ u\mid_{t=0} &= u_{ini} \quad \text{on } \Omega,\end{aligned}$$

with the Neumann boundary conditions

$$\partial_\nu u = 1,\ \mathbb{E}_\gamma\nabla w_\gamma\cdot\nu = 0 \quad \text{on } \partial\Omega.$$

The anisotropy function γ_{abs} is given by

$$\gamma_{abs}\left(\mathbf{P}\right) = \sum_{i=1}^{3}\sqrt{P_i^2+\epsilon_{abs}\sum_{j=1}^{3}P_j^2}, \text{ for } \epsilon_{abs}=0.001,$$

and the initial condition is a square given by $\left(|x|-0.75\right)\left(|y|-0.75\right)=0$.
Computational domain: $\Omega\equiv[-2,2]^2$.
Final time: $T=0.003$.
Level-set: 100×100 nodes, regularisation $\epsilon=0.01$, no re-distancing.
Time step: $\tau=10^{-8}$.
Numerical scheme: 6.3.9.
Figure: 7.103.
Remark: –.

Anisotropic level-set formulation of the mean-curvature flow

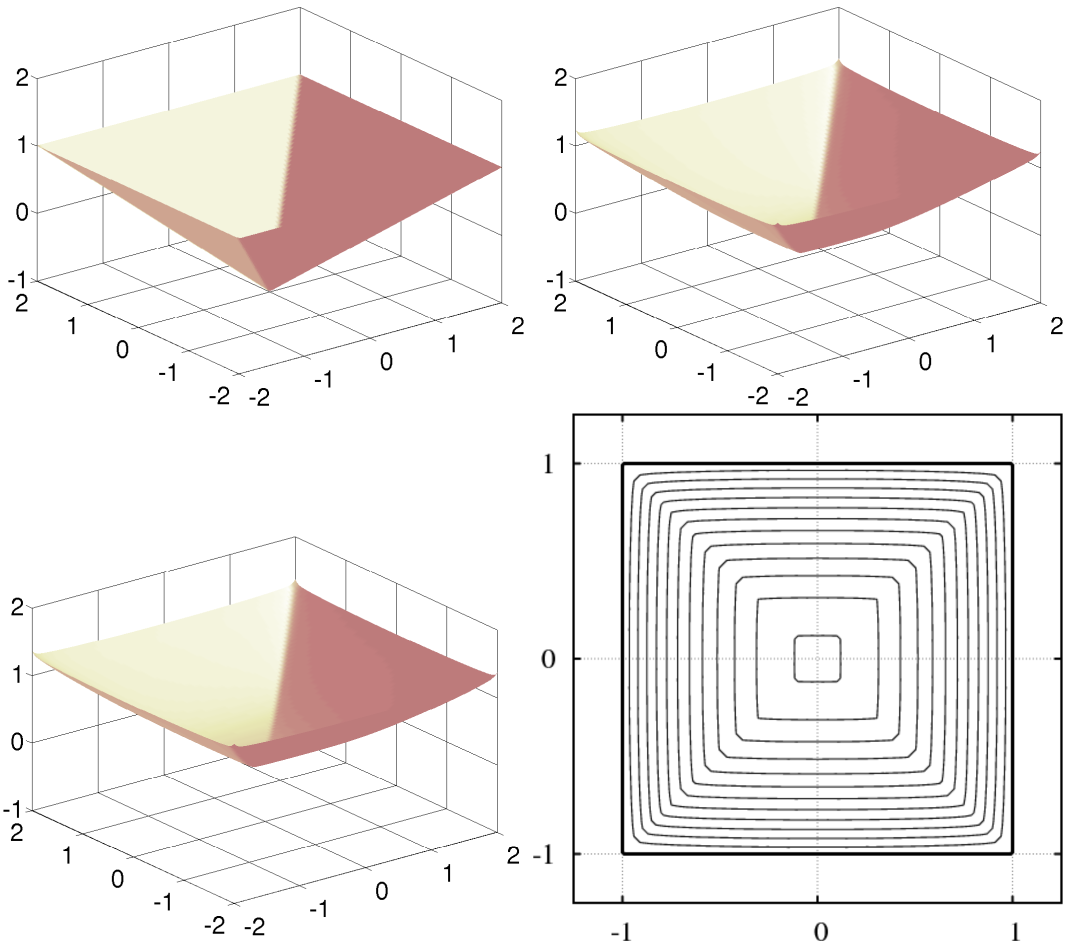

Figure 7.102.: Anisotropic level-set method for the **mean-curvature flow** – graphs of the level-set function at times $t = 0$, $t = 0.24$, $t = 0.48$ and evolution of the curve until the time $t = 0.48$ with the time period 0.04. See the Numerical experiment 7.2.83

Anisotropic level-set formulation of the Willmore flow

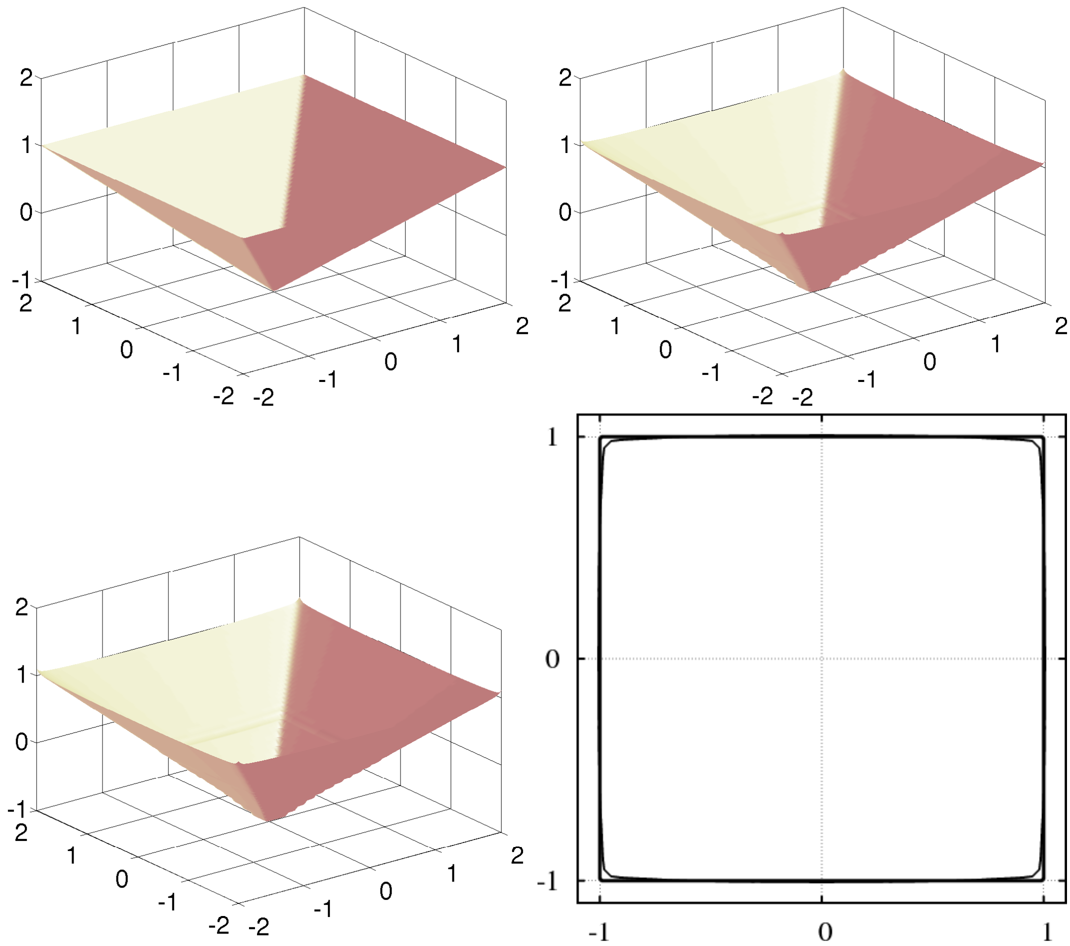

Figure 7.103.: Anisotropic level-set method for the **Willmore flow** – graphs of the level-set function at times $t = 0$, $t = 0.0015$, $t = 0.003$ and evolution of the initial curve until the time $t = 0.003$ with the time period 0.0003. See the Numerical experiment 7.2.84.

Numerical experiment 7.2.85. Test of the **level-set formulation for the anisotropic mean-curvature flow**

$$\begin{aligned} \frac{\partial_t u}{Q_\epsilon} &= \nabla \cdot \left(\nabla_{\mathbf{p}} \gamma_{abs} \left(\nabla u \right) \right) \quad \text{on } (0, \mathrm{T}\rangle \times \Omega, \\ u\,|_{t=0} &= u_{ini} \quad \text{on } \Omega, \end{aligned}$$

with the Neumann boundary conditions

$$\nabla_{\mathbf{p}} \gamma_{abs} \cdot \nu = 1 \quad \text{on } \partial\Omega.$$

The anisotropy function γ_{abs} is given by

$$\gamma_{abs}\left(\mathbf{P}\right) = \sum_{i=1}^{3} \sqrt{P_i^2 + \epsilon_{abs} \sum_{j=1}^{3} P_j^2}, \text{ for } \epsilon_{abs} = 0.001,$$

and the initial condition is an astroid given by $x^{2/3} + y^{2/3} = 0.75^{2/3}$.
Computational domain: $\Omega \equiv [-1, 1]^2$.
Final time: $T = 0.075$.
Level-set: 150×150 nodes, regularisation $\epsilon = 10^{-5}$, no re-distancing.
Time step: Adaptive.
Numerical scheme: 6.3.6.
Figure: 7.104.
Remark: –.

Numerical experiment 7.2.86. Test of the **level-set formulation for the anisotropic Willmore flow**

$$\begin{aligned} \frac{\partial_t u}{Q_\epsilon} &= -\nabla \cdot \left(\mathbb{E}_\gamma \nabla w_\gamma - \frac{1}{2} \frac{w_\gamma^2}{Q^3} \nabla u \right) \quad \text{on } (0, T) \times \Omega, \\ w_\gamma &= Q_\epsilon H_\gamma \quad \text{on } (0, T) \times \Omega, \\ u\,|_{t=0} &= u_{ini} \quad \text{on } \Omega, \end{aligned}$$

with the Neumann boundary conditions

$$\partial_\nu u = 1, \; \mathbb{E}_\gamma \nabla w_\gamma \cdot \nu = 0 \quad \text{on } \partial\Omega.$$

The anisotropy function γ_{abs} is given by

$$\gamma_{abs}\left(\mathbf{P}\right) = \sum_{i=1}^{3} \sqrt{P_i^2 + \epsilon_{abs} \sum_{j=1}^{3} P_j^2}, \text{ for } \epsilon_{abs} = 0.001,$$

and the initial condition is an astroid given by $x^{2/3} + y^{2/3} = 0.75^{2/3}$.
Computational domain: $\Omega \equiv [-1, 1]^2$.
Final time: 0.0012.
Level-set: 100×100 nodes, regularisation $\epsilon = 0.01$, no re-distancing.
Time step: Adaptive.
Numerical scheme: 6.3.9
Figure: 7.105.
Remark: The computation was stopped after 38 days of running on 2 CPU Core2 Duo 2.66 GHz.

Anisotropic level-set formulation of the mean-curvature flow

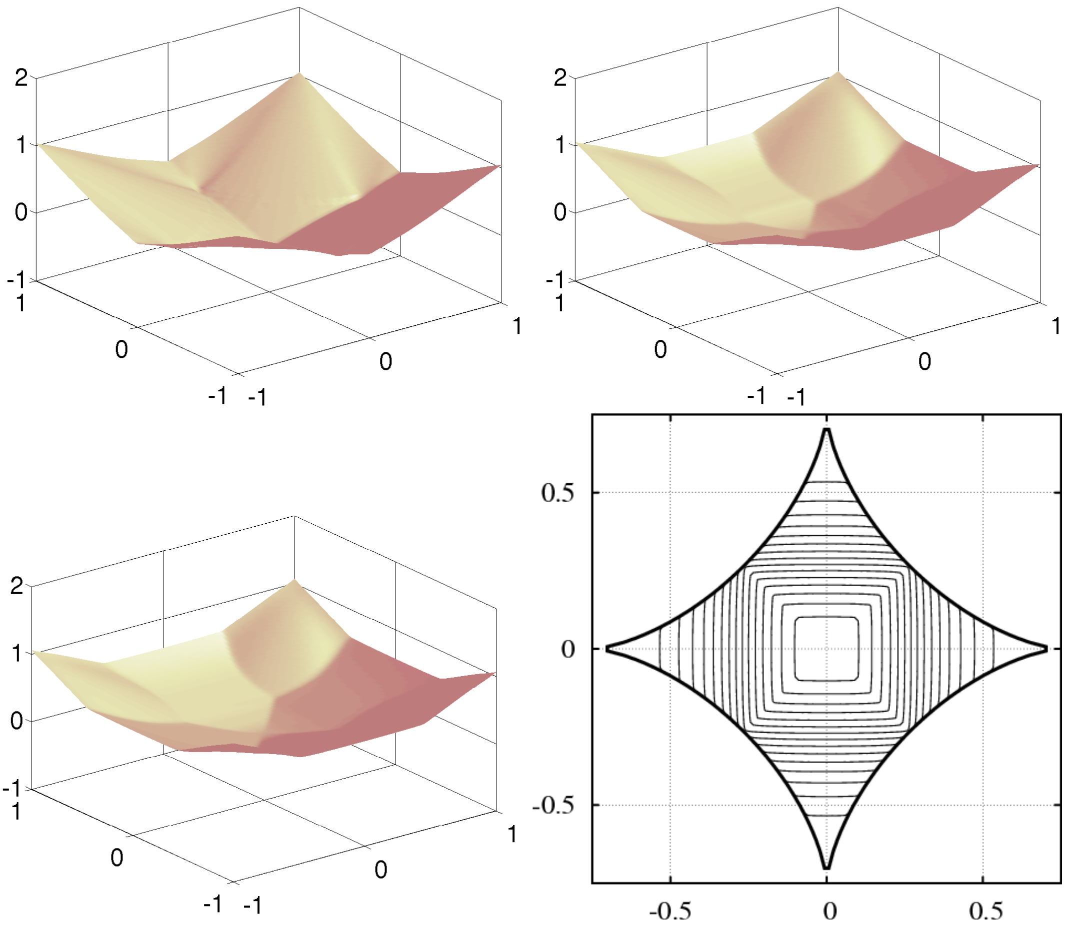

Figure 7.104.: Anisotropic level-set method for the **mean-curvature flow** – graphs if the level-set function at times $t = 0$, $t = 0.04$, $t = 0.075$ and evolution of the curve until the time $t = 0.075$ with the time period 0.05. See the Numerical experiment 7.2.85

Anisotropic level-set formulation of the Willmore flow

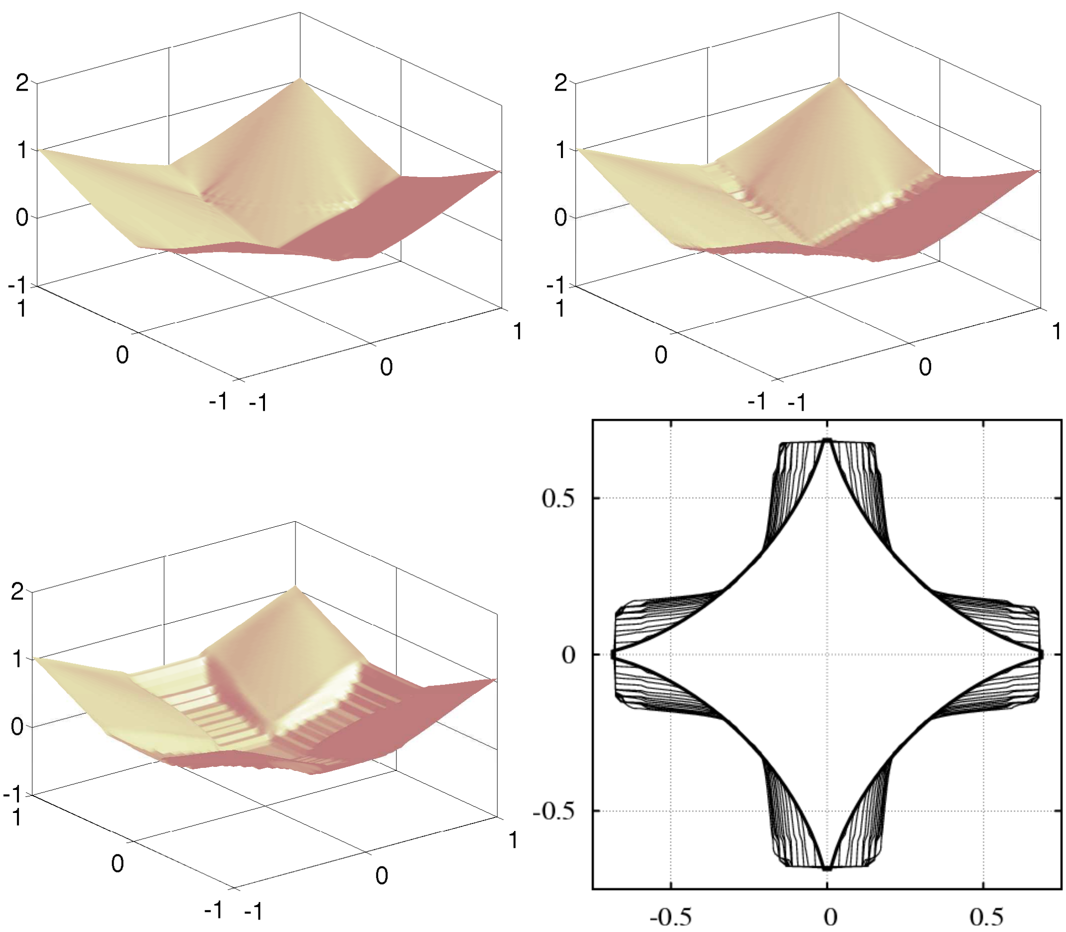

Figure 7.105.: Anisotropic level-set method for the **Willmore flow** – graphs of the level-set function at times $t = 0$, $t = 10^{-5}$, $t = 0.0012$ and evolution of the curve at times $t = 10^{-5}, 5 \cdot 10^{-5}, 0.0001, 0.0002 \cdots 0.0012$ – it is not a steady state. See the Numerical experiment 7.2.86

Numerical experiment 7.2.87. Test of the **level-set formulation for the anisotropic mean-curvature flow**

$$\begin{aligned}\frac{\partial_t u}{Q_\epsilon} &= \nabla \cdot \left(\nabla_{\mathbf{p}} \gamma_{abs} \left(\nabla u\right)\right) \quad \text{on } (0, \mathrm{T}\rangle \times \Omega, \\ u\,|_{t=0} &= u_{ini} \quad \text{on } \Omega,\end{aligned}$$

with the Neumann boundary conditions

$$\nabla_{\mathbf{p}} \gamma_{abs} \cdot \nu = 1 \quad \text{on } \partial\Omega.$$

The anisotropy function γ_{abs} is given by

$$\gamma_{abs}\left(\mathbf{P}\right) = \sum_{i=1}^{3} \sqrt{P_i^2 + \epsilon_{abs} \sum_{j=1}^{3} P_j^2}, \text{ for } \epsilon_{abs} = 0.001,$$

and the initial condition is a curve given by

$$u\left(x, y\right) = \sqrt{x^2 + y^2} - 1 - 0.75 \sin\left(6 \arccos \frac{x}{\sqrt{x^2 + y^2}}\right) = 0$$

.
Computational domain: $\Omega \equiv [-1.5, 1.5]^2$.
Final time: $T = 1.7$.
Level-set: 250×250 nodes, regularisation $\epsilon = 0.001$, no re-distancing.
Time step: Adaptive.
Numerical scheme: 6.3.6.
Figure: 7.106.
Remark: –.

Numerical experiment 7.2.88. Test of the **level-set formulation for the anisotropic Willmore flow**

$$\begin{aligned} \frac{\partial_t u}{Q_\epsilon} &= -\nabla \cdot \left(\mathbb{E}_\gamma \nabla w_\gamma - \frac{1}{2} \frac{w_\gamma^2}{Q^3} \nabla u \right) \quad \text{on } (0,T) \times \Omega, \\ w_\gamma &= Q_\epsilon H_\gamma \quad \text{on } (0,T) \times \Omega, \\ u \mid_{t=0} &= u_{ini} \quad \text{on } \Omega, \end{aligned}$$

with the Neumann boundary conditions

$$\partial_\nu u = 1, \; \mathbb{E}_\gamma \nabla w_\gamma \cdot \nu = 0 \quad \text{on } \partial\Omega.$$

The anisotropy function γ_{abs} is given by

$$\gamma_{abs}(\mathbf{P}) = \sum_{i=1}^{3} \sqrt{P_i^2 + \epsilon_{abs} \sum_{j=1}^{3} P_j^2}, \text{ for } \epsilon_{abs} = 0.001,$$

and the initial condition is a curve given by

$$u(x,y) = \sqrt{x^2+y^2} - 1 - 0.3 \sin\left(6 \arccos \frac{x}{\sqrt{x^2+y^2}} \right) = 0$$

.
Computational domain: $\Omega \equiv [-1.5, 1.5]^2$.
Final time: $T = 0.025$.
Level-set: 100×100 nodes, regularisation $\epsilon = 0.01$, no re-distancing.
Time step: Adaptive.
Numerical scheme: 6.3.7
Figure: 7.107.
Remark: –

Anisotropic level-set formulation of the mean-curvature flow

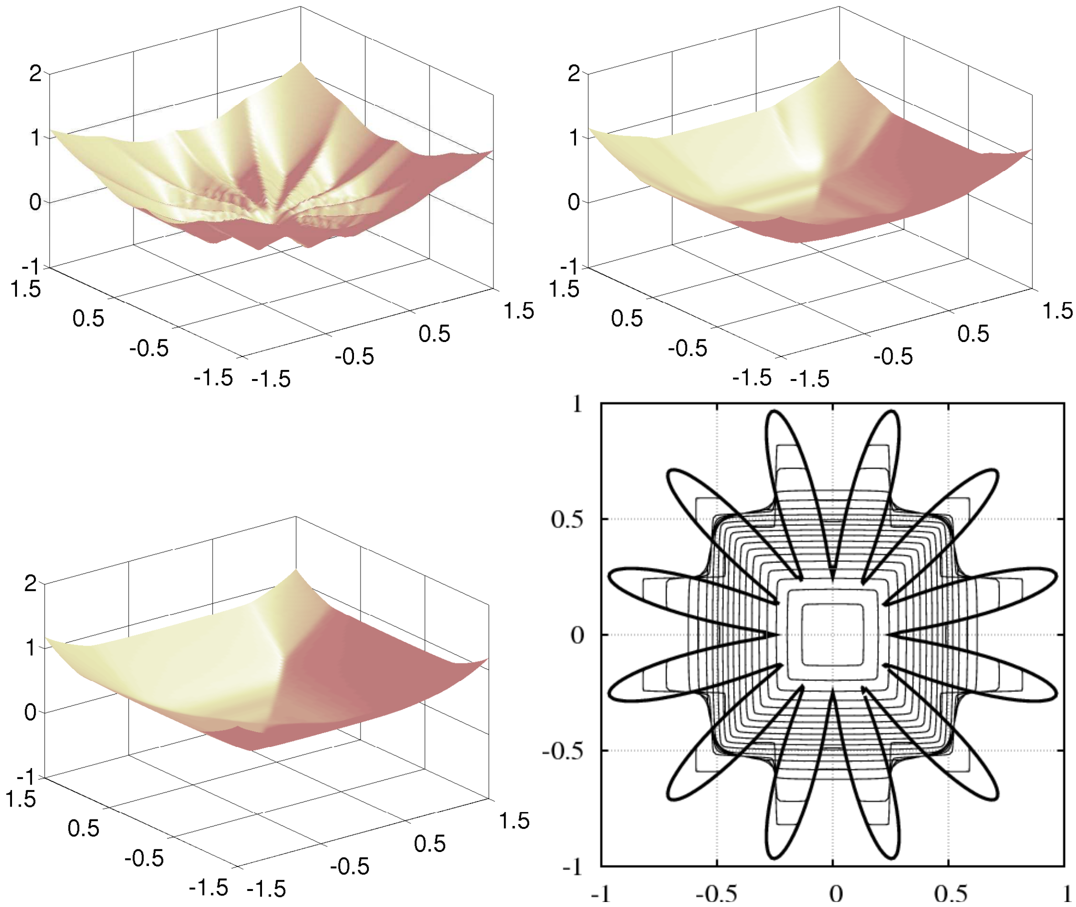

Figure 7.106.: Anisotropic level-set method for the **mean-curvature flow** – graphs of the level-set function at times $t = 0$, $t = 0.8$, $t = 1.7$ and evolution of the curve at times $t = 0.005, 0.01, 0.2, 0.3, 0.4, \cdots, 1.7$. See the Numerical experiment 7.2.87

Anisotropic level-set formulation of the Willmore flow

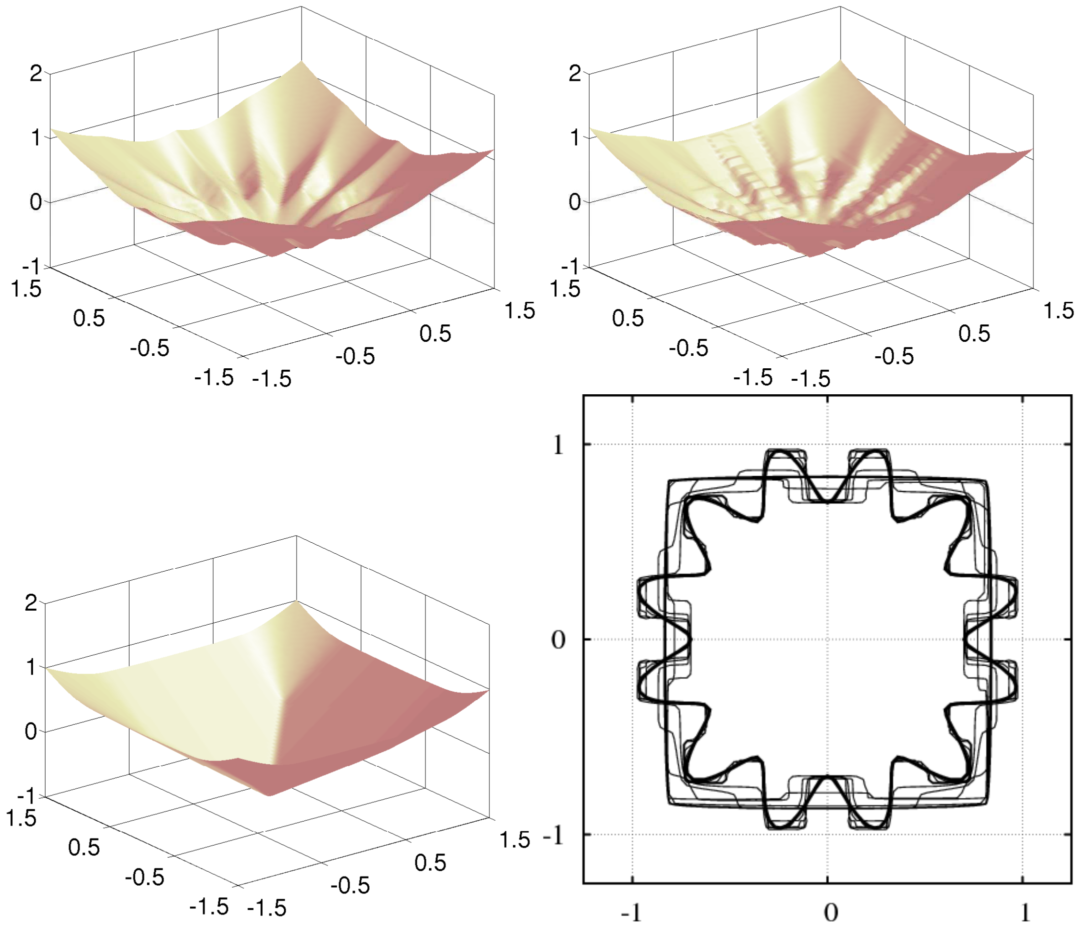

Figure 7.107.: Anisotropic level-set method for the **Willmore flow** – graphs of the level-set function at times $t = 0$, $t = 0.0001$, $t = 0.025$ and evolution of the initial curve at times $t = 10^{-5}, 0.0001, 0.00025, 0.0005, 0.001, 0.002, 0.0025, 0.003, 0.004, 0.005, \cdots, 0.025$. See the Numerical experiment 7.2.88

Numerical experiment 7.2.89. Test of the **level-set formulation for the anisotropic mean-curvature flow**

$$\begin{aligned} \frac{\partial_t u}{Q_\epsilon} &= \nabla \cdot \left(\nabla_{\mathbf{p}} \gamma_{l^{16}} \left(\nabla u \right) \right) \quad \text{on } (0, \mathrm{T}\rangle \times \Omega, \\ u\,|_{t=0} &= u_{ini} \quad \text{on } \Omega, \end{aligned}$$

with the Neumann boundary conditions

$$\nabla_{\mathbf{p}} \gamma_{abs} \cdot \nu = 1 \quad \text{on } \partial\Omega.$$

The anisotropy function $\gamma_{l^{16}}$ is given by

$$\gamma_{l^{16}} \left(\mathbf{P} \right) = \left(\sum_{i=1}^{3} |P_i|^{16} \right)^{\frac{1}{16}}$$

and the initial condition is a circle given by $x^2 + y^2 = 1$.
Computational domain: $\Omega \equiv [-2, 2]^2$.
Final time: $T = 0.55$.
Level-set: 100×100 nodes, regularisation $\epsilon = 10^{-5}$, no re-distancing.
Time step: Adaptive.
Numerical scheme: 6.3.6
Figure: 7.108.
Remark: –

Numerical experiment 7.2.90. Test of the **level-set formulation for the anisotropic Willmore flow**

$$\begin{aligned} \frac{\partial_t u}{Q_\epsilon} &= -\nabla \cdot \left(\mathbb{E}_\gamma \nabla w_\gamma - \frac{1}{2} \frac{w_\gamma^2}{Q^3} \nabla u \right) \quad \text{on } (0, T) \times \Omega, \\ w_\gamma &= Q_\epsilon H_\gamma \quad \text{on } (0, T) \times \Omega, \\ u\,|_{t=0} &= u_{ini} \quad \text{on } \Omega, \end{aligned}$$

with the Neumann boundary conditions

$$\partial_\nu u = 1, \ \mathbb{E}_\gamma \nabla w_\gamma \cdot \nu = 0 \quad \text{on } \partial\Omega.$$

The anisotropy function $\gamma_{l^{16}}$ is given by

$$\gamma_{l^{16}} \left(\mathbf{P} \right) = \left(\sum_{i=1}^{3} |P_i|^{16} \right)^{\frac{1}{16}}$$

and the initial condition is a circle given by $x^2 + y^2 = 1$.
Computational domain: $\Omega \equiv [-2, 2]^2$.
Final time: $T = 0.0375$.
Level-set: 100×100 nodes, regularisation $\epsilon = 0.01$, no re-distancing.
Time step: Adaptive.
Numerical scheme: 6.3.7
Figure: 7.109.
Remark: –

Anisotropic level-set formulation of the mean-curvature flow

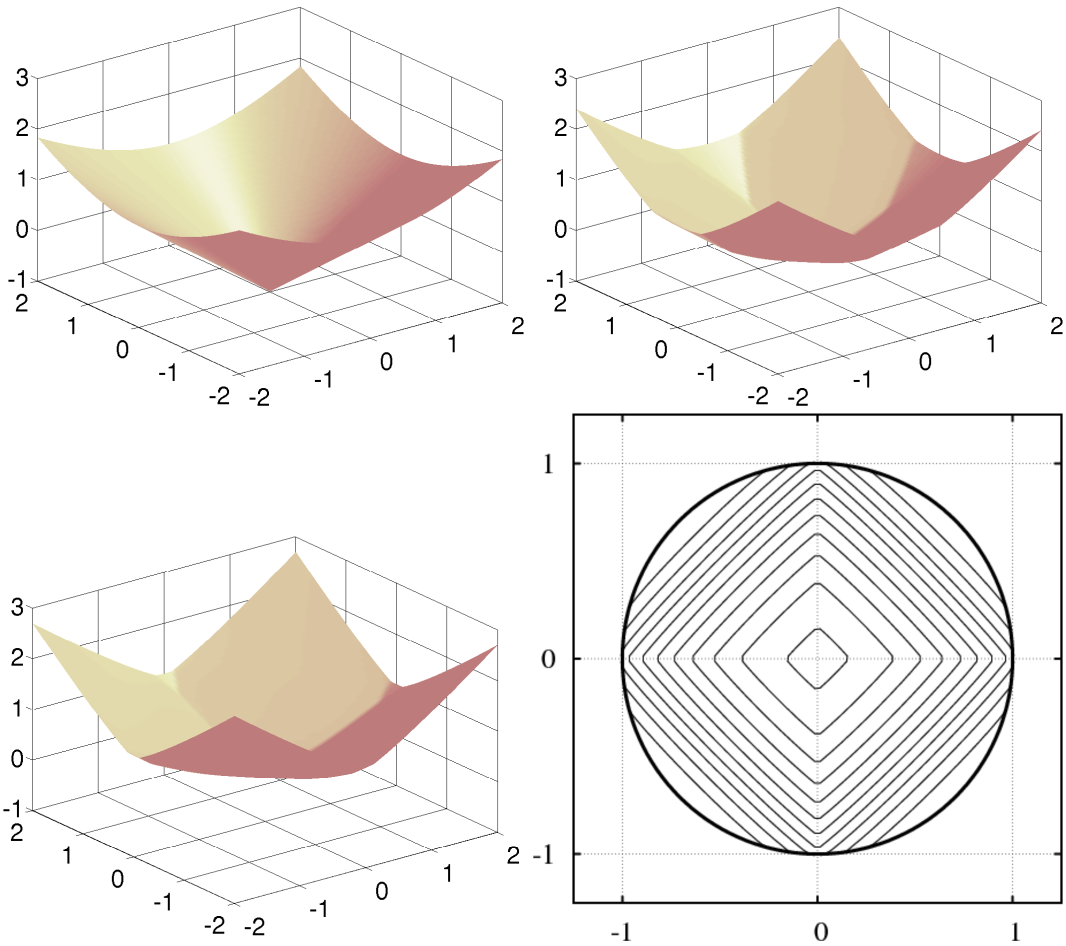

Figure 7.108.: Anisotropic level-set method for the **mean-curvature flow** – graphs of the level-set function at times $t = 0$,$t = 0.25$, $t = 0.55$ and evolution of the initial curve until the time $t = 0.55$ with the time period 0.05. See the Numerical experiment 7.2.89

Anisotropic level-set formulation of the Willmore flow

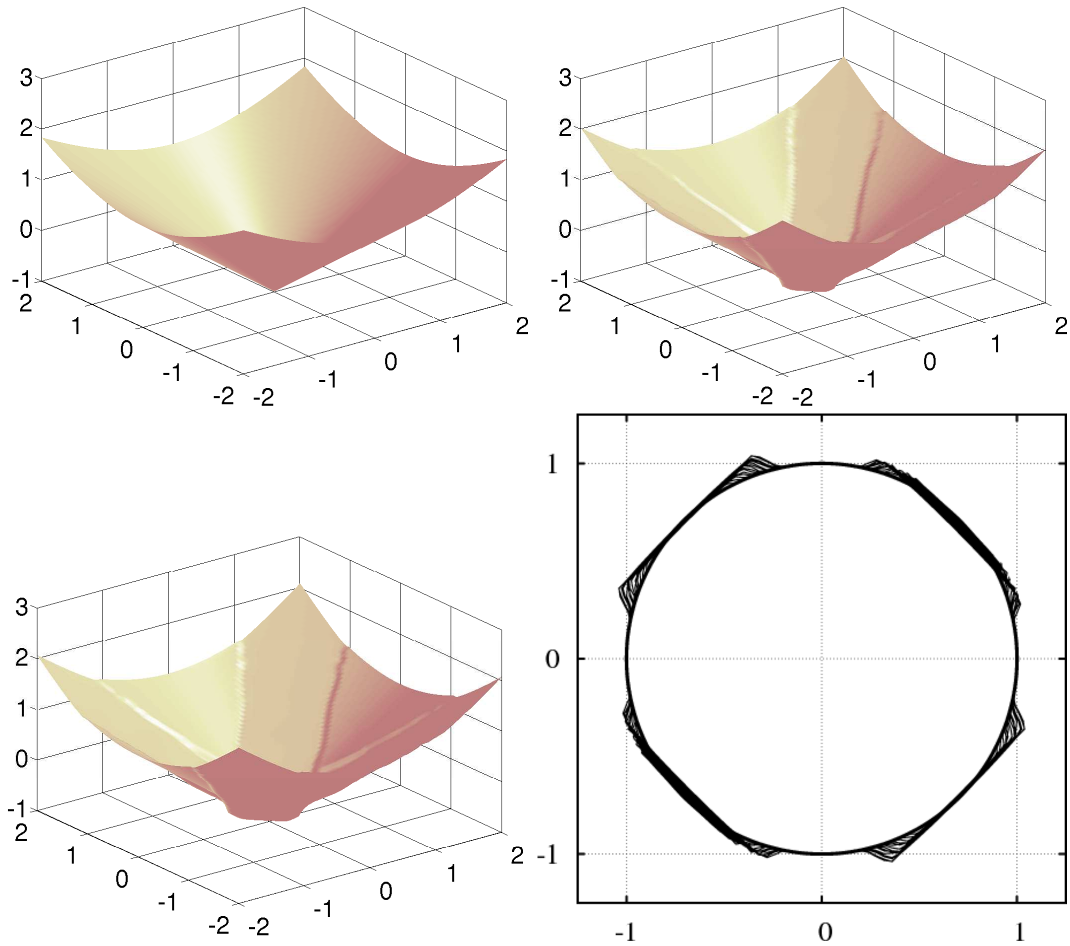

Figure 7.109.: Anisotropic level-set method for the **Willmore flow** – graphs of the level-set function at times $t = 0$, $t = 0.015$ and $t = 0.0375$ and evolution of the curve at times $t = 0.0, 0.0025, 0.005 \cdots 0.0375$ – not a steady state. See the Numerical experiment 7.2.90

Numerical experiment 7.2.91. Test of the **level-set formulation for the anisotropic mean-curvature flow**

$$\begin{aligned} \frac{\partial_t u}{Q_\epsilon} &= \nabla \cdot \left(\nabla_{\mathbf{p}} \gamma_{l^{16}} \left(\nabla u \right) \right) \quad \text{on } (0, \mathrm{T}\rangle \times \Omega, \\ u \mid_{t=0} &= u_{ini} \quad \text{on } \Omega, \end{aligned}$$

with the Neumann boundary conditions

$$\nabla_{\mathbf{p}} \gamma_{abs} \cdot \nu = 1 \quad \text{on } \partial\Omega.$$

The anisotropy function $\gamma_{l^{16}}$ is given by

$$\gamma_{l^{16}} \left(\mathbf{P} \right) = \left(\sum_{i=1}^{3} |P_i|^{16} \right)^{\frac{1}{16}}$$

and the initial condition is a square given by $\left(|x| - 0.75\right)\left(|y| - 0.75\right) = 0$.
Computational domain: $\Omega \equiv [-2, 2]^2$.
Final time: $T = 0.7$.
Level-set: 150×150 nodes, regularisation $\epsilon = 10^{-5}$, no re-distancing.
Time step: Adaptive.
Numerical scheme: 6.3.6.
Figure: 7.110.
Remark: –.

Numerical experiment 7.2.92. Test of the **level-set formulation for the anisotropic Willmore flow**

$$\begin{aligned} \frac{\partial_t u}{Q_\epsilon} &= -\nabla \cdot \left(\mathbb{E}_\gamma \nabla w_\gamma - \frac{1}{2} \frac{w_\gamma^2}{Q^3} \nabla u \right) \quad \text{on } (0, T) \times \Omega, \\ w_\gamma &= Q_\epsilon H_\gamma \quad \text{on } (0, T) \times \Omega, \\ u \mid_{t=0} &= u_{ini} \quad \text{on } \Omega, \end{aligned}$$

with the Neumann boundary conditions

$$\partial_\nu u = 1, \; \mathbb{E}_\gamma \nabla w_\gamma \cdot \nu = 0 \quad \text{on } \partial\Omega.$$

The anisotropy function $\gamma_{l^{16}}$ is given by

$$\gamma_{l^{16}} \left(\mathbf{P} \right) = \left(\sum_{i=1}^{3} |P_i|^{16} \right)^{\frac{1}{16}}$$

and the initial condition is a square given by $\left(|x| - 0.75\right)\left(|y| - 0.75\right) = 0$.
Computational domain: $\Omega \equiv [-2, 2]^2$.
Final time: $T = 0.025$.
Level-set: 100×100 nodes, regularisation $\epsilon = 0.05$, no re-distancing.
Time step: Adaptive.
Numerical scheme: 6.3.7.
Figure: 7.111.
Remark: –.

Anisotropic level-set formulation of the mean-curvature flow

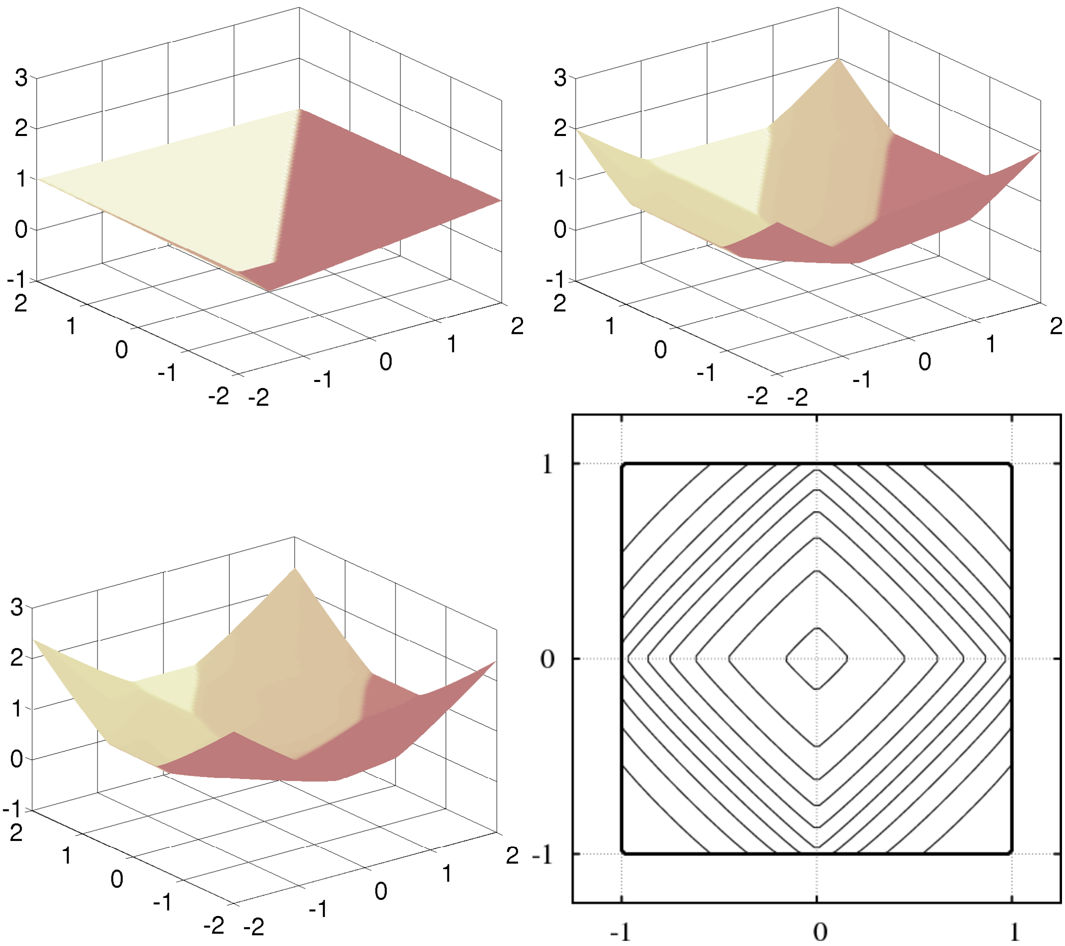

Figure 7.110.: Anisotropic level-set method for the **mean-curvature flow** – graphs of the level-set function at times $t = 0$, $t = 0.35$, $t = 0.7$ and evolution of the curve until the time $t = 0.7$ with the time period 0.07. See the Numerical experiment 7.2.91

Anisotropic level-set formulation of the Willmore flow

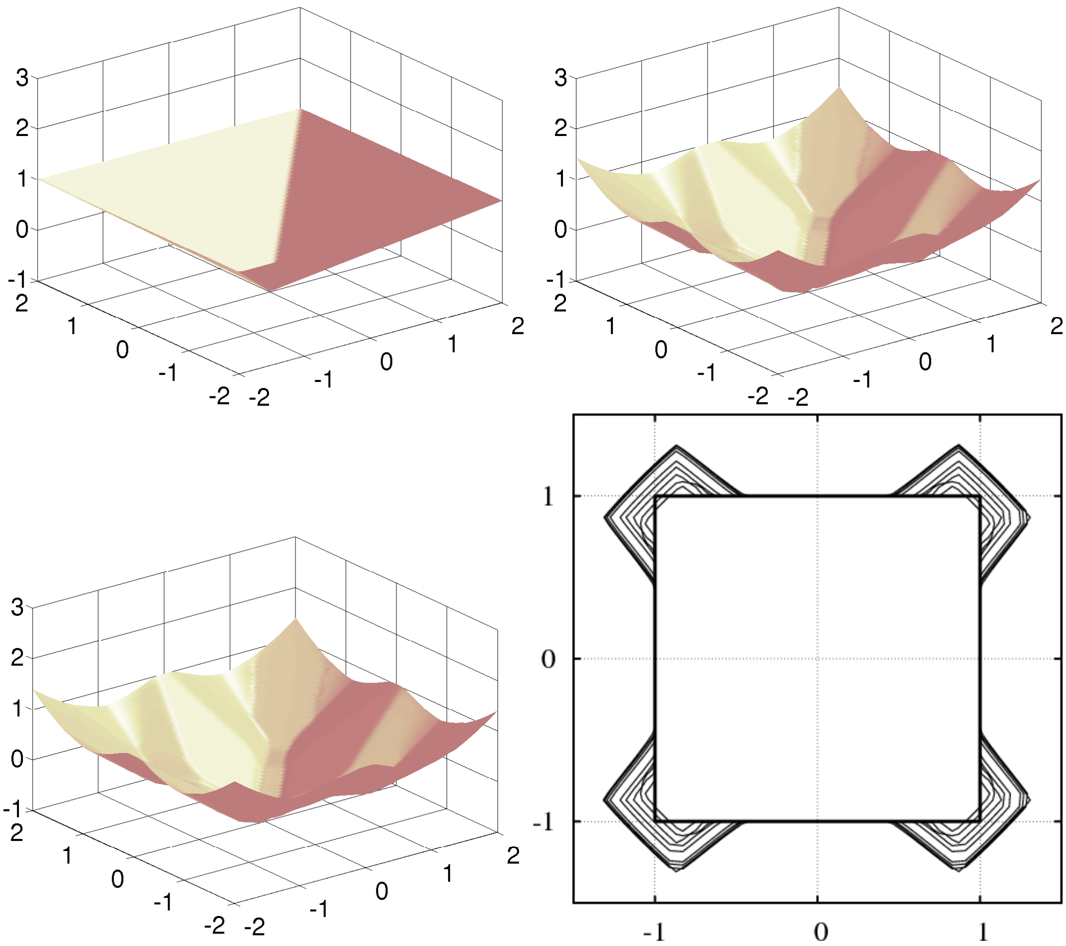

Figure 7.111.: Anisotropic level-set method for the **Willmore flow** – graphs of the level-set function at times $t = 0$, $t = 0.01$, $t = 0.025$ and evolution of the initial curve at times $t = 0.001, 0.002, 0.003, 0.004, 0.005, 0.01, 0.15 \cdots 0.025$ – not a steady state. See the Numerical experiment 7.2.92

Numerical experiment 7.2.93. Test of the **level-set formulation for the anisotropic mean-curvature flow**

$$
\begin{aligned}
\frac{\partial_t u}{Q_\epsilon} &= \nabla \cdot \left(\nabla_{\mathbf{p}} \gamma_{l^{16}} \left(\nabla u\right)\right) \quad \text{on } (0, \mathrm{T}\rangle \times \Omega, \\
u\left.\right|_{t=0} &= u_{ini} \quad \text{on } \Omega,
\end{aligned}
$$

with the Neumann boundary conditions

$$\nabla_{\mathbf{p}} \gamma_{abs} \cdot \nu = 1 \quad \text{on } \partial\Omega.$$

The anisotropy function $\gamma_{l^{16}}$ is given by

$$\gamma_{l^{16}}\left(\mathbf{P}\right) = \left(\sum_{i=1}^{3} \left|P_i\right|^{16}\right)^{\frac{1}{16}}$$

and the initial condition is an astroid given by $x^{2/3} + y^{2/3} = 0.75^{2/3}$.
Computational domain: $\Omega \equiv [-1, 1]^2$.
Anisotropy: $\gamma_{l^{16}}\left(\mathbf{P}\right) = \left(\sum_{i=1}^{3} \left|P_i\right|^{16}\right)^{\frac{1}{16}}$
Initial condition: Astroid given by $x^{2/3} + y^{2/3} = 0.75^{2/3}$.
Boundary conditions: $\nabla_{\mathbf{p}} \gamma \cdot \nu = 1$ on $\partial\Omega$.
Final time: $T = 0.115$.
Level-set: 150×150 nodes, regularisation $\epsilon = 10^{-5}$, no re-distancing.
Time step: Adaptive.
Numerical scheme: 6.3.6.
Figure: 7.112.
Remark: –.

Numerical experiment 7.2.94. Test of the **level-set formulation for the anisotropic Willmore flow**

$$\begin{aligned}\frac{\partial_t u}{Q_\epsilon} &= -\nabla\cdot\left(\mathbb{E}_\gamma\nabla w_\gamma - \frac{1}{2}\frac{w_\gamma^2}{Q^3}\nabla u\right) \quad \text{on } (0,T)\times\Omega,\\ w_\gamma &= Q_\epsilon H_\gamma \quad \text{on } (0,T)\times\Omega,\\ u\,|_{t=0} &= u_{ini} \quad \text{on } \Omega,\end{aligned}$$

with the Neumann boundary conditions

$$\partial_\nu u = 1,\ \mathbb{E}_\gamma\nabla w_\gamma\cdot\nu = 0 \quad \text{on } \partial\Omega.$$

The anisotropy function $\gamma_{l^{16}}$ is given by

$$\gamma_{l^{16}}(\mathbf{P}) = \left(\sum_{i=1}^{3}|P_i|^{16}\right)^{\frac{1}{16}}$$

and the initial condition is an astroid given by $x^{2/3}+y^{2/3}=0.75^{2/3}$.
Computational domain: $\Omega\equiv[-1,1]^2$.
Final time: 0.0009.
Level-set: 100×100 nodes, regularisation $\epsilon=0.05$, no re-distancing.
Time step: Adaptive.
Numerical scheme: 6.3.7
Figure: 7.113.
Remark: –

Anisotropic level-set formulation of the mean-curvature flow

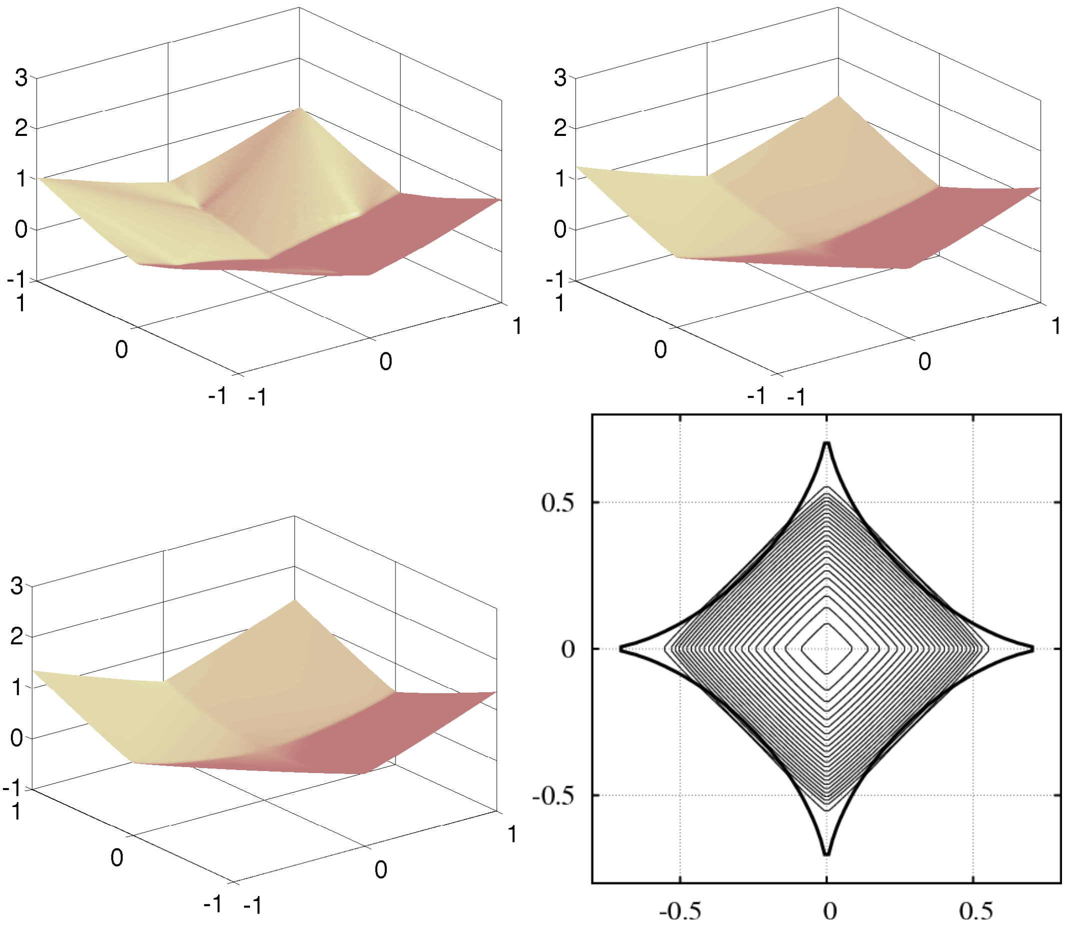

Figure 7.112.: Anisotropic level-set method for the **mean-curvature flow** – graphs if the level-set function at times $t = 0$, $t = 0.06$, $t = 0.115$ and evolution of the curve until the time $t = 0.115$ with the time period 0.005. See the Numerical experiment 7.2.93

Anisotropic level-set formulation of the Willmore flow

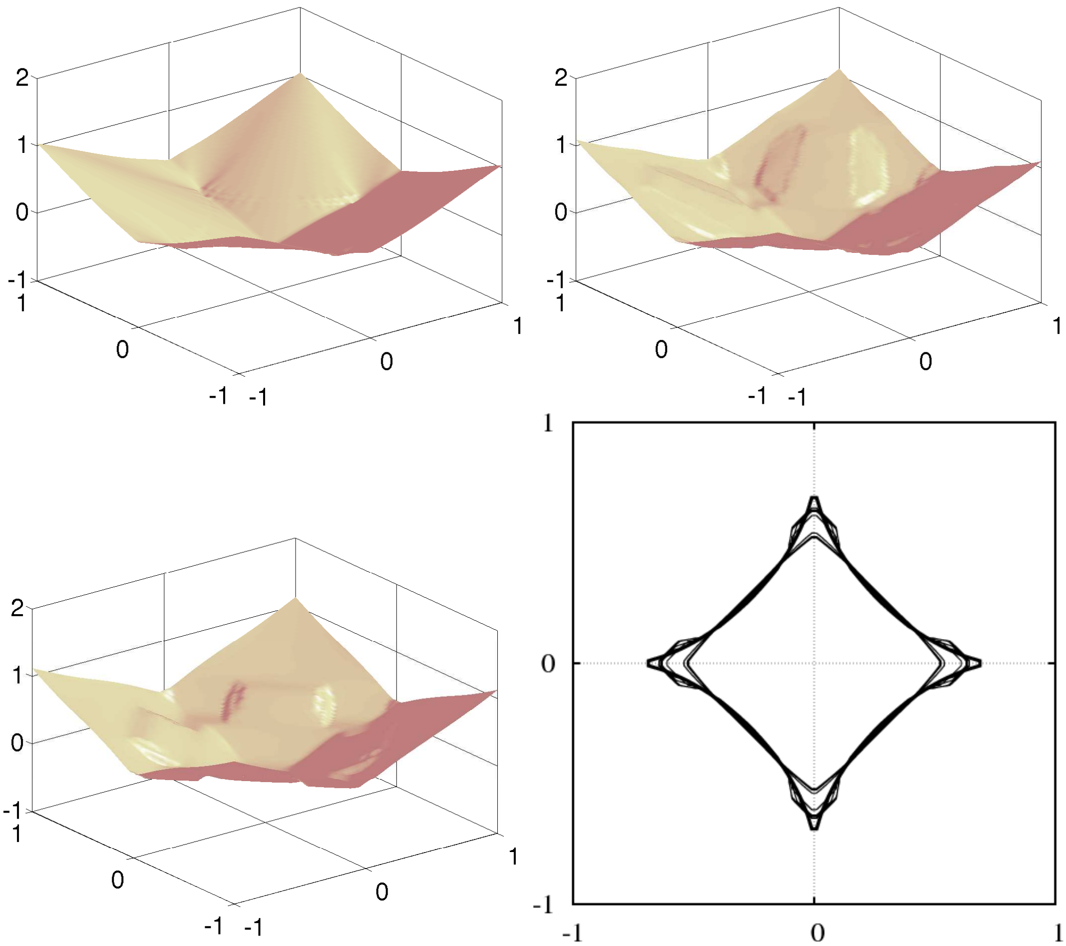

Figure 7.113.: Anisotropic level-set method for the **Willmore flow** – graphs of the level-set function at times $t = 0$, $t = 0.0001$, $t = 0.0009$ and evolution of the initial curve at times $t = 10^{-5}, 5 \cdot 10^{-5}, 0.0001, 0.0002, 0.0003, \cdots, 0.0009$. See the Numerical experiment 7.2.94

Numerical experiment 7.2.95. Test of the **level-set formulation for the anisotropic mean-curvature flow**

$$\begin{aligned} \frac{\partial_t u}{Q_\epsilon} &= \nabla \cdot \left(\nabla_{\mathbf{p}} \gamma_{l^{16}} \left(\nabla u \right) \right) \quad \text{on } (0, \mathrm{T}\rangle \times \Omega, \\ u \left|_{t=0}\right. &= u_{ini} \quad \text{on } \Omega, \end{aligned}$$

with the Neumann boundary conditions

$$\nabla_{\mathbf{p}} \gamma_{abs} \cdot \nu = 1 \quad \text{on } \partial\Omega.$$

The anisotropy function $\gamma_{l^{16}}$ is given by

$$\gamma_{l^{16}} \left(\mathbf{P} \right) = \left(\sum_{i=1}^{3} \left| P_i \right|^{16} \right)^{\frac{1}{16}}$$

and the initial condition is a curve given by

$$u \left(x, y \right) = \sqrt{x^2 + y^2} - 1 - 0.75 \sin \left(6 \arccos \frac{x}{\sqrt{x^2 + y^2}} \right) = 0$$

.
Computational domain: $\Omega \equiv \left[-1.5, 1.5 \right]^2$.
Final time: $T = 0.26$.
Level-set: 250×250 nodes, regularisation $\epsilon = 0.001$, no re-distancing.
Time step: Adaptive.
Numerical scheme: 6.3.6.
Figure: 7.114.
Remark: –.

Numerical experiment 7.2.96. Computational domain: $\Omega \equiv [-1.5, 1.5]^2$. Test of the **level-set formulation for the anisotropic Willmore flow**

$$\begin{aligned} \frac{\partial_t u}{Q_\epsilon} &= -\nabla \cdot \left(\mathbb{E}_\gamma \nabla w_\gamma - \frac{1}{2} \frac{w_\gamma^2}{Q^3} \nabla u \right) \quad \text{on } (0,T) \times \Omega, \\ w_\gamma &= Q_\epsilon H_\gamma \quad \text{on } (0,T) \times \Omega, \\ u \mid_{t=0} &= u_{ini} \quad \text{on } \Omega, \end{aligned}$$

with the Neumann boundary conditions

$$\partial_\nu u = 1, \; \mathbb{E}_\gamma \nabla w_\gamma \cdot \nu = 0 \quad \text{on } \partial\Omega.$$

The anisotropy function $\gamma_{l^{16}}$ is given by

$$\gamma_{l^{16}} (\mathbf{P}) = \left(\sum_{i=1}^{3} |P_i|^{16} \right)^{\frac{1}{16}}$$

and the initial condition is a curve given by

$$u(x,y) = \sqrt{x^2 + y^2} - 1 - 0.3 \sin \left(6 \arccos \frac{x}{\sqrt{x^2 + y^2}} \right) = 0$$

.

Final time: $T = 0.01$.
Level-set: 100×100 nodes, regularisation $\epsilon = 0.05$, no re-distancing.
Time step: Adaptive.
Numerical scheme: 6.3.7
Figure: 7.115.
Remark: –

Anisotropic level-set formulation of the mean-curvature flow

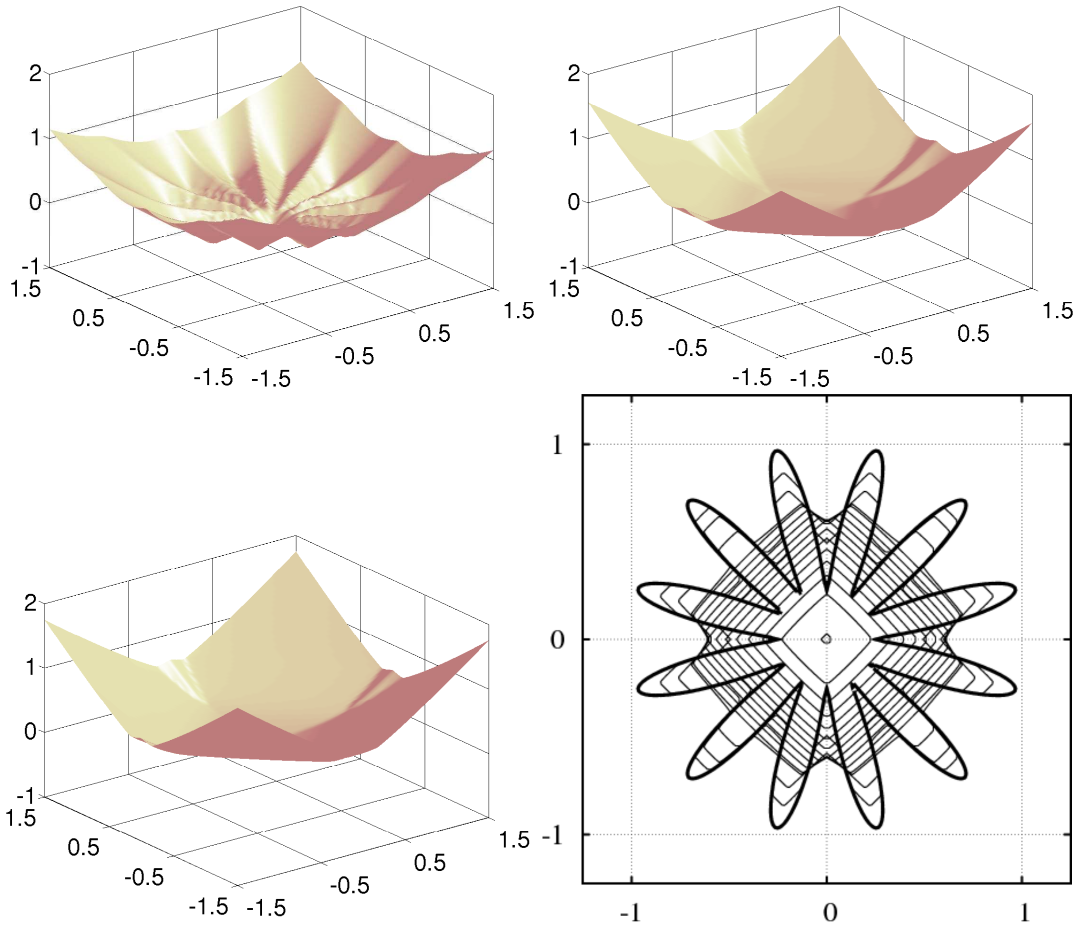

Figure 7.114.: Anisotropic level-set method for the **mean-curvature flow** – graphs if the level-set function at times $t = 0$, $t = 0.13$, $t = 0.26$ and evolution of the curve at times $t = 0.005, 0.01, 0.2, 0.3, \cdots, 0.26$. See the Numerical experiment 7.2.95

Anisotropic level-set formulation of the Willmore flow

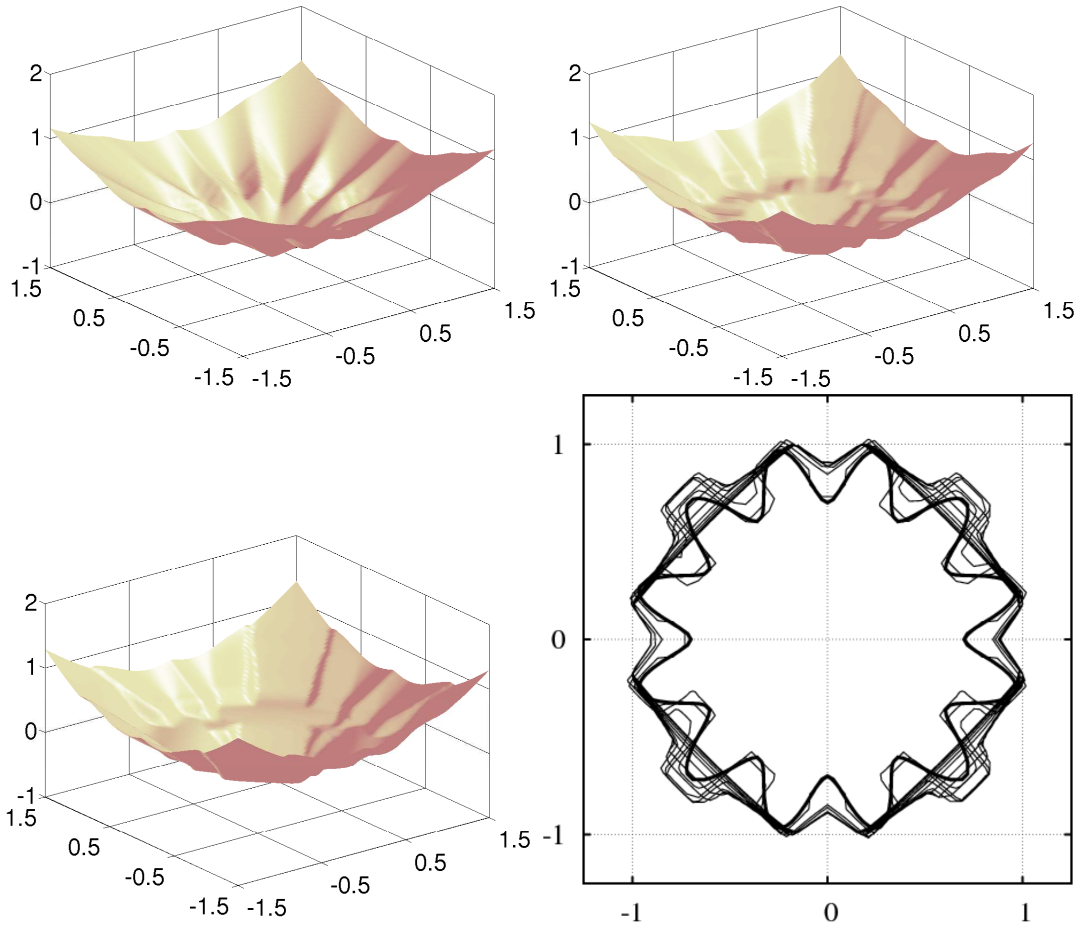

Figure 7.115.: Anisotropic level-set method for the **Willmore flow** – graphs of the level-set function at times $t = 0$, $t = 0.001$, $t = 0.01$ and evolution of the initial curve at times $t = 0.0001, 0.0005, 0.001, 0.002, \cdots, 0.01$. See the Numerical experiment 7.2.96

7.3. Summary

We summarise results of performed numerical experiments.

7.3.1. Discretisation in space

We proposed three different classes of schemes based on the discretisation in space:

- schemes based on the one-sided finite differences – 6.2.2 and 6.2.3
- schemes based in the central differences – 6.2.8 and 6.2.9
- complementary finite volume schemes resp. finite difference counterparts – 6.2.14–6.2.21 resp. 6.2.27 and 6.2.30

The Numerical experiments 7.2.2 and 7.2.4 show that the first class of schemes fails especially in the approximation of the Willmore flow. The main problem is in lack of symmetry of those schemes. Therefore we proposed replacing the one-sided finite differences by the central ones. They offer better approximation. However, Figure 6.2 shows, that in case of discontinuous functions, oscillations may appear. We tried to overcome this difficulty by introducing artificial viscosity term which was supposed to keep the approximate solution smooth enough. This approach, however, involve setting of a new parameter which is something we usually want to avoid from the numerical schemes. We found a better solution in complementary finite-volume schemes. They are symmetric (in the meaning of having symmetric stencil), they do not need any artificial parameter and they also have smaller stencil then the central schemes. This is important for the semi-implicit discretisation in time. Numerous tests, we performed in this thesis, show that the complementary finite-volume schemes appear appropriate for the space discretisation of the geometric partial differential equations.

7.3.2. Discretisation in time

We also have extensively tested two discretisations in time – the explicit and the semi-implicit ones. None of them outperforms the other. We solve really highly non-linear problems. From the nature of the semi-implicit schemes, we always have to undergo certain linearisation. It is necessary for turning non-linear algebraic problem into linear one. This always brings in some error of the approximation. The more non-nonlinear problem we solve the bigger this error is. Therefore the semi-implicit schemes do not seem to be good choice in case of strongly non-linear equations.

The disadvantage of the explicit schemes is in very small time step which is necessary for their stability. It decreases efficiency of the algorithm.

We expected that such situation may occur in case of the fourth order level-set methods. Here, the signed distance function of the initial curve is taken as an initial condition. It usually contains singular points at which the partial derivatives are not defined.

The results of our tests are surprising. In most cases we are able to get correct approximation using both kinds of time discretisation. Sometimes, however, the semi-implicit schemes fail completely – see the Numerical experiment 7.2.64 or the Willmore flow with anisotropy given by (5.114) in general. We were also surprised by the fact that the explicit schemes can be employed even for the fourth order level-set methods. We must, however, confess, that the explicit schemes require often a lot of CPU time. For example Numerical experiment 7.2.34 was running for more then 8 months on 4 CPUs Opteron 270 and still did not reach the steady state. The same but semi-implicit scheme performed almost ten times faster. On the other hand, in most of the experiments dealing with the mean-curvature flow,, both kinds of schemes required the same

CPU time and sometimes the explicit schemes were even faster – see the Numerical experiment 7.1.9 and 7.1.10. We would like to note that even for the semi-implicit schemes we had to set quite small time steps such that the iterative matrix solver (GMRES in most cases) converged in tens of iterations. Therefore a preconditioning, like ILU for example, do not speed up the computation at all. It also requires some CPU for initiation which is not advantageous in the situation when the iterative solver converges in few iterations.

The result of this comparison is that the explicit and the semi-implicit schemes are sufficient for the second-order problems and both offer approximately the same efficiency. For the fourth-order flows, fully implicit schemes based on the Newton solver might be more promising for development of efficient algorithm.

7.3.3. Second order vs. fourth order flows

We would like to emphasise one important fact concerning the level-set formulation for the mean-curvature flow. For both explicit and semi-implicit schemes, we were able to obtain experimental order of convergence equal almost exactly 2 with the regularising parameter $\epsilon = 10^{-15}$ – see the Numerical experiment 7.1.9 and 7.1.10. We did not have to change this parameter with respect to the space step h (moreover, in the case of the explicit scheme we did not have to set even the time step). It turns, especially the explicit scheme, into a black box which needs only the input data and does not require setting of any parameter.

We would like to achieve similar results even for the Willmore flow. Unfortunately, we did not succeed. The Numerical experiment 7.1.11 shows insufficient result obtained as an experimental order of convergence for the level-set formulation of the Willmore flow. Our computations performed for the surface-diffusion flow for [83] showed better EOC. Moreover, Numerical experiment 7.83 shows that the semi-implicit version of the Numerical scheme 6.2.30 may fail in case of highly non-convex initial curves. We also experienced serious difficulties in case of changes of topology with the level-set formulation of the Willmore flow – see [13].

As a result we see that the Willmore flow is the most difficult to approximate. Comparing the equation for the normal velocity for the surface-diffusion flow

$$V = \Delta_\Gamma H_\gamma \text{ on } \Gamma(t),$$

and for the Willmore flow

$$V = \Delta_\Gamma H + H \|W\|_F^2 - \frac{1}{2} H^3 \text{ on } \Gamma(t),$$

we see that the difficulties with the Willmore flow come from the terms $H \|W\|_F^2 - \frac{1}{2} H^3$ and not $\Delta_\Gamma H$, which is easier for numerical approximation when standing alone. We understand this as one of the most important results in this thesis.

In the future work we would like to study the Willmore flow in context of image processing and image inpainting. For this purpose we propose to study functional of bending energy (3.6)

$$\int_\Gamma \kappa_1^2 + \kappa_2^2 \mathrm{d}\mathcal{H}^{n-1} = \int_\Gamma H^2 - 2K \mathrm{d}\mathcal{H}^{n-1},$$

instead of

$$\int_\Gamma H^2 \mathrm{d}\mathcal{H}^{n-1}.$$

As a result we can say, that the numerical approximation of the Willmore flow is still an open problem, especially the level-set formulation even without any anisotropy.

8. Conclusion

The thesis deals with one of challenging fourth-order problems – with the Willmore flow. For this purpose, physical background was presented. Chapter 4 summarises tools of differential geometry needed for understanding of this problem. Chapter 5 deals with corresponding mathematical formulation using variational methods In this part there are two contributions by the author – definition of the anisotropic Willmore flow (5.2.6), (5.2.8) and an extension of the energy equality (5.2.10) to anisotropic problems – see the Theorem 5.2.11.

Main contributions concern numerical approximation of the Willmore flow. In Chapter 6 we present three classes of numerical schemes - numerical schemes based on one-sided finite differences, schemes based on central finite differences and schemes based on complementary finite volumes. We demonstrate that the first class is sufficient only for the reference problem of mean-curvature flow. The second class suffers from possible appearance of oscillations in case of discontinuous initial conditions. We obtained the best results using the complementary finite-volume schemes. We reformulate them in terms of finite differences and we apply simple mathematical background for the finite difference method to prove discrete energy equality (5.2.11) and its anisotropic counterpart.

One of main goals of this thesis is a comparison of numerical schemes for the geometric partial differential equations from different points of view. We find experimental order of convergence for all isotropic numerical schemes. For graphs, it was done with additional forcing term which allowed us to find analytical solution. When it comes to the level-set method, we know analytical solution when the initial curve is a circle. Except of the level-set formulation of the Willmore flow (see. Table 7.1.11) we obtained sufficient results.

We have performed many qualitative numerical experiments. We have tested the Willmore flow on many different initial conditions and compared its evolution with the mean-curvature flow. This holds for both - the graph formulation and the level-set formulation. The reader can see differences in evolutions of both flows. We set the same initial conditions even for the anisotropic problems. One can easily see even the differences between several anisotropies. In case of the isotropic level-set method we also give comparison with the parametric approach. This is an important test of reliability of proposed numerical schemes. We have achieved a good agreement.

Unfortunately, there was no space left in the thesis for studying topological changes of curves modelled by the level-set method. For the Willmore flow, it is non-trivial problem which we do not consider as solved yet. In the future we would like to extend the theory of moving hypersurfaces to anisotropic ones. It would allow us to derive a parametric model for the anisotropic Willmore flow. We also would like to study the Willmore flow (even anisotropic one) in context of edge detection and image inpainting. As we already mentioned in the text, a fully implicit numerical scheme based on the Newton solver might be a promising approach to get an efficient algorithm for the level-set formulation of the Willmore flow.

A. Theoretical toolbox

In this chapter we summarise some neccesary theorems from calculus, measure theory and functional analysis.

Definition A.0.1. Diffeomorphism [38]: *Let Γ_1 and Γ_2 be differentiable manifolds. A mapping $\varphi : \Gamma_1 \to \Gamma_2$ is a diffeomorphism if it is differentiable, bijective, ans its inverse φ^{-1} is also differentiable.*

Theorem A.0.2. Implicit function theorem [47]: *Assume $\mathbf{f} = \left(f^1, \cdots f^m\right) \in C^k\left(\Omega; \mathbb{R}^m\right)$, $\Omega \subset \mathbb{R}^{n+m}$ and*

$$\det \left| \frac{\partial\left(f^1, \cdots f^m\right)}{\partial\left(y_1, \cdots y_m\right)}\left(\mathbf{x}_0, \mathbf{y}_0\right) \right| \neq 0,$$

where we denote $(\mathbf{x}, \mathbf{y}) = (x_1, \cdots, x_n, y_1, \cdots y_m) \in \mathbb{R}^{m+n}$. Then there exists an open set $\Psi \subset \Omega$ with $(\mathbf{x}_0, \mathbf{y}_0) \in \Psi$, an open set $\Upsilon \subset \mathbb{R}^n$, with $\mathbf{x}_0 \in \Upsilon$ and a C^k mapping $\mathbf{g} : \Upsilon \to \mathbb{R}^m$ such that

1. $\mathbf{g}\left(\mathbf{x}_0\right) = \mathbf{y}_0$
2. $\mathbf{f}\left(\mathbf{x}, \mathbf{g}\left(\mathbf{x}\right)\right) = \mathbf{z}_0, \ \left(\mathbf{x} \in \Upsilon\right)$

and if $(\mathbf{x}, \mathbf{y}) \in \Psi$ and $\mathbf{f}(\mathbf{x}, \mathbf{y}) = \mathbf{z}_0$, then $\mathbf{y} = \mathbf{g}(\mathbf{x})$. The function $\mathbf{g}$ is implicitly defined near $\mathbf{x}_0$ by the equation $\mathbf{f}(\mathbf{x}, \mathbf{y}) = \mathbf{z}_0$.

Theorem A.0.3. Arzela-Ascoli compactness criterion [47]: *Suppose that $\{f_k\}_{k=1}^{\infty}$ is a sequence of real-valued functions defined on $\mathbb{R}^n$, such that*

$$\left|f_k\left(\mathbf{x}\right)\right| \leq C \text{ for } k = 1, \cdots \text{ and } \mathbf{x} \in \mathbb{R}^n,$$

for some constant C, and the sequence $\{f_k\}_{k=1}^{\infty}$ are uniformly equicontinuous. Then there exists a subsequence $\left\{f_{k_j}\right\}_{j=1}^{\infty} \subset \{f_k\}_{k=1}^{\infty}$ and a continuous function f, such that

$$f_{k_j} \to f \text{ uniformly on compact subset of } \mathbb{R}^n.$$

Definition A.0.4. Hausdorff Measure [48]: *Let $\Gamma \subset \mathbb{R}^n$, $0 \leq s < \infty$, $0 < \delta \leq \infty$. We define*

$$\mathcal{H}_\delta^s\left(\Gamma\right) = \inf \left\{ \sum_{j=1}^{\infty} \alpha\left(s\right) \left(\frac{\text{diam } \Omega_j}{2}\right)^s \mid A \subset \bigcup_{j=1}^{\infty} \Omega_j, \text{diam } \Omega_j \leq \delta \right\},$$

where Ω_j is a system of closed sets in $\mathbb{R}^n$ and

$$\alpha\left(s\right) = \frac{\pi^{\frac{s}{2}}}{\mathbf{\Gamma}\left(\frac{s}{2}+1\right)}.$$

Here $\mathbf{\Gamma}(s) = \int_0^\infty e^{-x}x^{s-1}\mathrm{d}x$, $(0 < s < \infty)$, is the usual gamma function. We denote

$$\mathcal{H}^s\left(\Gamma\right) = \lim_{\delta \to 0} \mathcal{H}_\delta^s\left(\Gamma\right) = \sup_{\delta > 0} \mathcal{H}_\delta^d\left(\Gamma\right),$$

*and we call $\mathcal{H}^s$ **s-dimensional Hausdorff measure** on $\mathbb{R}^n$.*

Theorem A.0.5. Co-area formula [47]: *Let $u : \mathbb{R}^n \to \mathbb{R}$ be Lipschitz continuous and assume that for a.e $r \in \mathbb{R}$ the level-set*

$$\{\mathbf{x} \in \mathbb{R}^n \mid u(x) = r\}$$

is a smooth, $(n-1)$-dimensional hypersurface in $\mathbb{R}^n$. Suppose also $f : \mathbb{R}^n \to \mathbb{R}$ is continous and summable. Then

$$\int_{\mathbb{R}^n} f \left|\nabla u\right| \mathrm{d}x = \int_{-\infty}^{+\infty} \left(\int_{u=r} f \mathrm{d}\mathcal{H}^{n-1} \right) \mathrm{d}r.$$

Theorem A.0.6. Gauss-Green Theorem [47]: *Let Ω be a domain in $\mathbb{R}^n$. Suppose $u \in C^1\left(\overline{\Omega}\right)$. Then*

$$\int_{\Omega} u_{x_i} \mathrm{d}\mathbf{x} = \int_{\partial\Omega} u \nu_i \mathrm{d}S, \text{ for } i = 1, \cdots n.$$

Let $u, v \in C^1\left(\overline{\Omega}\right)$. Then

$$\int_{\Omega} u_{x_i} v \mathrm{d}\mathbf{x} = -\int_{\Omega} u v_{x_i} \mathrm{d}\mathbf{x} + \int_{\partial\Omega} u \nu_i \mathrm{d}S, \text{ for } i = 1, \cdots n.$$

Theorem A.0.7. Stokes theorem: *Let Ω be a domain in $\mathbb{R}^n$. Let $\mathbf{u} \in C^1\left(\overline{\Omega}; \mathbb{R}^n\right)$. Then*

$$\int_{\Omega} \nabla \cdot \mathbf{u} = \int_{\partial\Omega} \mathbf{u} \cdot \nu \mathrm{d}S.$$

Theorem A.0.8. Gauss-Green Theorem for hypersurfaces [56]: *Let Γ be a manifold (or C^1-hypersurface for purposes of this text) in $\mathbb{R}^n$. Let $\mathbf{f} \in C^1(\Gamma, \mathbb{R}^n)$, $g \in C^1(\Gamma)$ and* $\operatorname{supp}(\mathbf{f}g)$ *is compact. Then we have*

$$\int_{\Gamma} \mathbf{f} \cdot \nabla_{\Gamma} g \mathrm{d}\mathcal{H}^{n-1} = -\int_{\Gamma} \left(\nabla_{\Gamma} \cdot \mathbf{f} + H \mathbf{n} \cdot \mathbf{f}\right) g \mathrm{d}\mathcal{H}^{n-1}.$$

Theorem A.0.9. Lax-Milgram [15]: *Given a Hilbert space X, a continuous, coercive bilinear form $a(\cdot,\cdot)$ and a continuous linear functional $F \in X'$ (here X' denotes dual space to X), there exists a unique $u \in X$ such that*

$$a(u, v) = F(v) \text{ for all } v \in X. \tag{A.1}$$

Definition A.0.10. Bounded and coercive bilinear form [15]: *A bilinear form $a(\cdot,\cdot)$ on a normed linear space X is said to be* **bounded** *(or* **continuous***) if there exists $C_1 < \infty$ such that*

$$|a(v, w)| \leq C_1 \|v\|_X \|w\|_X \text{ for all } v, w \in X,$$

and **coercive on $Y \subset X$ if there exists $C_2 > 0$ sucht that**

$$a(v, v) \geq C_2 \|v\|_Y^2 \text{ for all } v \in Y.$$

Theorem A.0.11. Poincaré inequality on Riemannian manifold [56]: *Let $\Gamma \subset \mathbb{R}^n$ be a compact Riemannian manifold of dimension n, and let $1 \leq q < n$ be a real number. There exists a positive constant $C = C(\Gamma, q)$ such that for any $u \in W_q^1(\Gamma)$,*

$$\left(\int_{\Gamma} |u - \bar{u}|^q \mathrm{d}\mathcal{H}^n \right)^{\frac{1}{q}} \leq C \left(\int_{\Gamma} |\nabla_{\Gamma} u|^q \mathrm{d}\mathcal{H}^n \right)^{\frac{1}{q}},$$

where $\bar{u} = \frac{1}{|\Gamma|} \int_{\Gamma} u \mathrm{d}\mathcal{H}^n$.

Theorem A.0.12. Global Gauss-Bonnet theorem [100]: *Let* Γ *be a compact two-dimensional orientable Riemannian manifold without boundary. Then*

$$\int_{\Gamma} K \mathrm{d}\mathcal{H}^{n-1} = 2\pi\chi\left(\Gamma\right),$$

where $\chi\left(\Gamma\right)$ *is the* **Euler-Poincaré characteristic** *of* Γ*.*

Theorem A.0.13. Jacobi's formula [65]: *Let* $A \in C^1\left(\mathcal{I}, \mathbb{R}^{n\times n}\right)$ *for* $\mathcal{I} \subset \mathbb{R}$*. Then*

$$\frac{\mathrm{d}}{\mathrm{d}t} \det A\left(t\right) = \det A\left(t\right) \mathrm{Tr}\Big(A\left(t\right)^{-1} A'\left(t\right)\Big)$$

for $t \in \mathcal{I}$ *provided* $\det A\left(t\right) \neq 0$ *on* $\mathcal{I}$*.*

Bibliography

A

[1] D. Adalsteinsson and J. A. Sethian, *The fast construction of extension velocities in level set methods*, Journal of Computational Physics, 148 (1999), pp. 2–22.

[2] M. Allen, S. and W. Cahn, J., *A microscopic theory for antiphase boundary motion and its application to antiphase domain coarsening*, Acta Metallurgica, 27 (1979), pp. 1085–1095.

B

[3] E. Bänsch, P. Morin, and R. Nochetto, *Surface diffusion of graphs: variational formulation, error analysis and simulation*, SIAM J. Numer. Anal., 42 (2004), pp. 773–799.

[4] M. Bardi and S. Osher, *The nonconvex multi-dimensional Riemann problem for Hamilton-Jacobi equations*, SIAM Journal of Mathematical Analysis, 22 (1991), pp. 344–351.

[5] P. Beck, *Interface migration in recrystallization*, Metal Interfaces, (1952), pp. 208–247.

[6] G. Bellettini and M. Paolini, *Anisotropic motion by mean curvature in the context of Finsler geometry*, Hokkaido mathematical journal, 25 (1996), pp. 537–566.

[7] M. Beneš, *Phase field model of microstructure growth in solidification of pure substances*, PhD dissertation, Faculty of Nuclear Sciences and Physical Engineering,Czech Technical University in Prague, FNSPE, Department of Mathematics, Břehová 7, Prague 1, 110 00, Czech Republic, 1997.

[8] M. Beneš and K. Mikula, *Simulation of anisotropic motion by mean curvature - comparison of phase field and sharp interface approaches*, Acta Mathematica Universitatis Comenianae, 67 (1998), pp. 17–42.

[9] M. Beneš, *Mathematical and computational aspects of solidification of pure substances*, Acta Mathematica Universitatis Comenianae, 70 (2000), pp. 123–151.

[10] ——, *Mathematical analysis of phase-field equations with numerically efficient coupling terms*, Interfaces and Free Boundaries, 3 (2001), pp. 201–221.

[11] ——, *Diffuse-interface treatment of the anisotropic mean-curvature flow*, Applications of Mathematics, 48, No. 6 (2003), pp. 437–453.

[12] ——, *Numerical solution for surface diffusion on graphs*, in Proceedings of Czech Japanese Seminar in Applied Mathematics 2005, M. Beneš, M. Kimura, and T. Nakaki, eds., vol. 3 of COE Lecture Note, Kyushu University Fukuoka, 2006, pp. 9–25.

[13] M. Beneš, K. Mikula, T. Oberhuber, and D. Ševčovič, *Comparison study for level set and direct Lagrangian methods for computing Willmore flow of closed plannar curves*, Computing and Visualizayion in Science, (2008).

[14] M. Brdička, L. Samek, and B. Sopko, *Mechanika kontinua*, Academia, Praha, 2000.

[15] S. C. Brenner and L. R. Scott, *The mathematical theory of finite element methods*, Springer-Verlag, 1994.

[16] A. Briggs, *Numerical solutions of Hamilton-Jacobi equations*, PhD thesis, University of Sussex, 1999.

C

[17] J. W. Cahn, C. M. Elliott, and A. Novick-Cohen, *The Cahn-Hilliard equation with a concentration dependent mobility: motion by minus the Laplacian of the mean curvature*, Euro Journal of Applied Mathematics, 7 (1996), pp. 287–301.

[18] P. Canham, *The minimum energy of bending as a possible explanation of biconcave shape of the human red blood cell*, J.Theoret.Biol., 26 (1970), pp. 61–81.

[19] T. Chen, M.-S. Chiu, and C.-N. Weng, *Derivation of the generalized Young-Laplace equation of curve interfaces in nanoscaled solids*, Journal of Applied Physics, 100 (2006), pp. 074308:1–5.

[20] J. Claisse, *Vortex Density Motion in a Cylindrical Type 2 Superconductor Subject to a Transverse Applied Magnetic Field*, PhD dissertation, University of Sussex, Department of Mathematics, Mantell Building, University of Sussex, Falmer, Brighton, BN1 9RF, UK, 2000.

[21] U. Clarenz, *The Wulff shape minimizes an anisotropic Willmore functional*, Interfaces and free boundaries, 6 (2004), pp. 351–360.

[22] U. Clarenz, U. Diewald, G. Dziuk, M. Rumpf, and R. Rusu, *A finite element method for surface restoration with smooth boundary conditions*, Computer Aided Geometric Design, (2004), pp. 427–445.

[23] U. Clarenz, F. Hausser, M. Rumpf, A. Voigt, and U. Weikard, *Multiscale modeling of epitaxial growth*, vol. 149, Birkhäuser, Basel, 2005, ch. On level set formulations for anisotropic mean curvature ow and surface diusion, pp. 227–237.

[24] M. G. Crandal, H. Ishii, and P.-L. Lions, *User's guide to viscosity solutions of second order partial differential equations*, Bull. Amer. Math. Soc., 27 (1992), pp. 1–67.

[25] M. Crandall and P.-L. Lions, *Viscosity solution of Hamilton-Jacobi equations*, Trans. American Mathematical Society, 277 (1983), pp. 1–41.

[26] M. G. Crandall, *Viscosity solutions: a primer*, in Viscosity solutions and applications (Montecatini Terme, 1995), vol. 1660 of Lecture Notes in Math., Springer, 1997, pp. 1–43.

D

[27] K. Deckelnick, *Error bounds for a difference scheme approximating viscosity solutions of mean curvature flow*, Interfaces and Free Boundaries, (2000), pp. 117–142.

[28] K. Deckelnick and G. Dziuk, *Convergence of a finite element method for non-parametric mean curvature flow*, Numerische Mathematik, 72 (1995), pp. 197–222.

[29] ——, *Error estimates for a semi implicit fully discrete finite element scheme for the mean curvature flow of graphs*, Interfaces and Free Boundaries, 2 (2000), pp. 341–359.

[30] ——, *Numerical Methods for Viscosity Solutions and Applications*, vol. 59 of Adv. Math. Appl. Sciences, World Scientific Publishing Company, 2001, ch. Convergence of numerical schemes for the approximation of level set solutions to mean curvature flow, pp. 77–93.

[31] ——, *A fully discrete numerical scheme for weighted mean curvature flow*, Numerische Mathematik, 91 (2002), pp. 423–452.

[32] ——, *Geometric analysis and nonlinear partial differential equations*, Springer-Verlag Berlin Heidelberg New York, 2003, ch. A finite element level set method for anisotropic mean curvature flow with space dependent weight, pp. 249–264.

[33] ——, *Mathematical aspects of evolving interfaces*, vol. 1812 of Lecture Notes in Mathematics, Springer-Verlag Berlin Heidelberg, 2003, ch. Numerical approximation of mean curvature flow of graphs and level sets, pp. 53–87.

[34] ——, *Error estimates for the Willmore flow of graphs*, Interfaces Free Bound., 8 (2006), pp. 21–46.

[35] K. Deckelnick, G. Dziuk, and C. Elliott, *Computation of geometric partial differential equations and mean curvature ow*, Acta Numer., (2005), pp. 139–232.

[36] K. Deckelnick, G. Dziuk, and C. Elliott, *Fully discrete finite element approximation for anisotropic surface diffusion of graphs*, SIAM J. Numer. Anal., (2005), pp. 1112–1138.

[37] K. Deckelnick and C. M. Elliott, *Uniqueness and error analysis for Hamilton-Jacobi equations with discontinuities*, Interfaces and free boundaries, 6 (2004), pp. 329–350.

[38] M. P. do Carmo, *Riemannian Geometry*, Birkhauser Boston, 1992.

[39] M. Droske, *On variational problems and gradient flows in image processing*, PhD thesis, Universit at Duisburg-Essen, 2005.

[40] M. Droske and M. Rumpf, *A level set formulation for Willmore flow*, Interfaces Free Bound., 6 (2004), pp. 361–378.

[41] Q. Du, C. Liu, R. Ryham, and X. Wang, *A phase field formulation of the Willmore problem*, Nonlinearity, (2005), pp. 1249–1267.

[42] Q. Du, C. Liu, and X. Wang, *A phase field approach in the numerical study of the elastic bending energy for vesicle membranes*, Journal of Computational Physics, (2004), pp. 450–468.

[43] G. Dziuk, *Discrete anisotropic curve shortening flow*, SIAM J. Math. Anal. J. Numer. Anal., 36 (1999), pp. 1808–1830.

[44] G. Dziuk, E. Kuwert, and R. Schätzle, *Evolution of elastic curves in $\mathbb{R}^n$: Existence and computation*, SIAM J. Math. Anal., 41 (2003), pp. 2161–2179.

E

[45] C. M. Elliott, *Approximations of curvature dependent motion*, in State of the Art in Numerical Analysis, G. W. I.S. Duff, ed., Clarendon Press, Oxford, 1997, pp. 407–440.

[46] C. M. Elliott and V. Styles, *Computations of bidirectional grain boundary dynamics in thin metallic films*, Journal of Computational Physics, 187 (2003), pp. 524–543.

[47] L. C. Evans, *Partial differential equations*, Graduate Studies in Mathematics, American Mathematical Society, American Mathematical Society, P. O. Box 6248, Providence, Rhode Island 02940-6248, USA, 1998.

[48] L. C. Evans and R. F. Gariepy, *Measure theory and fine properties of functions*, CRC Press, Boca Raton, 1992.

[49] L. C. Evans and J. Spruck, *Motion of level sets by mean curvature II*, Trans. American Mathematical Society, 330 (1992), pp. 321–332.

F

[50] M. Feistauer, J. Felcman, and I. Straškraba, *Mathematical and Computational Methods for Compressible Flow*, Oxford University Press, 2003.

[51] R. Finn, *Capillary surface interfaces*, Notices of the AMS, 46 (1999), pp. 770–781.

[52] S. Fučík and A. Kufner, *Nelineární diferenciální rovnice*, SNTL, Nakladatelství technické literatury, 1978.

G

[53] Y. Giga, *Surface evolution equations: A level set approach*, Birkhauser Verlag, Switzerland, 2006.

[54] M. E. Gurtin, *On the two-phase stefan problem with interfacial energy and entropy*, Archive for Rational Mechanics and Analysis, 96 (1986), pp. 200–240.

H

[55] A. Handlovičová, K. Mikula, and F. Sgallari, *Semi-implicit complementary volume scheme for solving level set like equations in image processing and curve evolution*, Numerische Mathematik, 93 (2003), pp. 675–695.

[56] E. Hebey, *Sobolev spaces on Riemannian manifolds*, Springer, Berlin, 1996.

[57] W. Helfrich, *Elastic properties of lipid bilayers: theory and possible experiments*, Zeitschrift für Naturforschung, 28 (1973), pp. 693–703.

[58] H.K.Zhao, *Fast sweeping method for eikonal equations*, Mathematics of Computation, 74 (2005), pp. 603–627.

[59] G. Huisken, *Flow by mean curvature of convex surfaces into spheres*, J. Differential Geometry, 20 (1984), pp. 237–266.

[60] ——, *Non-parametric mean curvature evolution with boudary conditions*, J. Differential Geometry, 77 (1988), pp. 369–379.

J

[61] J.A.Sethian, *A fast marching level set method for monotonical advancing fronts*, in Proceedings of the National Academy of Sciences, vol. 93, National Academy of Sciences, 1996, pp. 1591–1595.

[62] C. Johnson and V. Thomeé, *Error estimates for a finite element approximation of a minimal surface*, Mathematics of Computations, 29 (1975), pp. 343–349.

[63] J. Jost, *Riemannian Geometry and Geometric Analysis*, Springer, 3rd ed., 2002.

[64] ——, *Postmodern Analysis*, Springer, Springer-Verlag, Heidleberg, Germany, 2nd ed., 2003.

K

[65] M. Kimura, *Topics in mathematical modeling*, vol. 4 of Jindřich Nečas Center for Mathematical Modelling, Lecture notes, Matfyzpress, Publishing House of the Faculty of Mathematics and Physics, Charles University in Prague, Prague, Czech Republic, 2008, ch. Geometry of hypersurfaces and moving hypersurfaces in R^m for the study of moving boundary problems, pp. 39–94. ISBN 978-80-7378-060-9.

[66] E. Kuwert and R. Schätzle, *The Willmore flow with small initial energy*, Journal of Differential Geometry, 57 (2001), pp. 409–441.

[67] E. Kuwert and R. Schätzle, *Gradient flow for the Willmore functional*, Comm. in anal. and geom., 10 (2002), pp. 307–340.

L

[68] L. Lomtatidze, *Historický vývoj pojmu křivka*, Nadace Universitas, Brno, Czech Republic, 2006.

M

[69] P. S. M. Sussman, E. Fatemi and S. Osher, *An improved level set method for incompressible two-phase flows*, Computers and Fluids, 27 (1998), pp. 663–680.

[70] S. O. M. Sussman, P. Smereka, *A level set approach for computing solutions to incompressible 2-phase flow*, Journal of Computational Physics, 114 (1994), pp. 146–159.

[71] U. F. Mayer and G. Simonett, *A numerical scheme for axisymmetric solutions of curvature-driven free boundary problems, with applications to the Willmore flow*, Interfaces and Free Boundaries, 4 (2002), pp. 89–109.

[72] ——, *Evolution equations: Applications to physics, industry, life scienses economics*, Progress in nonlinear differential equations and their applications, Birkhäuser Verlag Basel/Switzerland, 2003, ch. Self-intersections for Willmore flow, pp. 341–348.

[73] T. McInerney and D. Terzopoulos, *T-snakes: Topology adaptive snakes*, Medical Image Analysis, 4 (2000), pp. 73–91.

[74] K. Mikula, *Numerical methods for viscosity solutions and applications*, vol. 59 of Series on Advances in Mathematics for Applied Sciences, World Scientific, 2001, ch. Solution and application of anisotropic curvature driven evolution of curves (and surfaces), pp. 173–196.

[75] K. Mikula and D. Ševčovič, *Evolution of plane curves driven by a nonlinear function of curvature and anisotropy*, SIAM Journal on Applied Mathematics, 61 (2001), pp. 1473–1501.

[76] ——, *Computational and qualitative aspects of evolution of curves driven by curvature and external force*, Computing and Visualization in Science, 6 (2004), pp. 211–225.

[77] K. Mikula and D. Ševčovič, *Tangentially stabilized Lagrangian algorithm for elastic curve evolution driven by intrinsic Laplacian of curvature*, in Proceedings of ALGORITMY 2005, 2005, pp. 1–10.

[78] W. Mullins, *Two-dimensional motion of idealized grain boundaries*, Journal of Applied Physics, 27 (1956), pp. 900–904.

N

[79] J. C. C. Nitsche, *On new results in the theory of minimal surfaces*, Bull. Amer. Math. Soc., 71 (1965), pp. 195–270.

O

[80] T. Oberhuber, *Numerical recovery of the signed distance function*, in Proceedings of Czech-Japanese Seminar in Applied Mathematics 2004, M. Beneš, J. Mikyška, and T. Oberhuber, eds., 2004, pp. 148–164.

[81] ——, *Numerical solution for the Willmore flow of graphs*, in Proceedings of Czech-Japanese Seminar in Applied Mathematics 2005, M. Beneš, M. Kimura, and T. Nakaki, eds., vol. 3 of COE Lecture Note, 2005, pp. 126–138.

[82] ——, *Finite difference scheme for the Willmore flow of graphs*, Kybernetika, 43 (2007), pp. 855–867.

[83] ——, *Complementary finite volume scheme for the anisotropic surface diffusion flow*, in Proceedings of Algoritmy 2009, A. Handlovičová, P. Frolkovič, K. Mikula, and D. Ševčovič, eds., 2009, pp. 153–164.

[84] J. Oprea, *Differential Geometry and its Applications*, Prentice Hall, 1997.

[85] S. Osher and R. Fedkiw, *Level set methods and dynamic implicit surfaces*, Springer-Verlag, Springer-Verlag New York, Inc., 175 Fifth Avenue, New York, NY 10010, USA, 2003.

[86] D. Ostrov, *Viscosity solutions and convergence of monotone schemes for synthetic aperture radar shape-from-shading equations with discontinous intensities*, SIAM Journal of Applied Mathematics, 59:6 (1999), pp. 2060–2085.

P

[87] L. Pontryagin, *Ordinary Differential Equations*, Elsevier, 1962.

Q

[88] J. Qian, Y. Zhang, and H. Zhao, *Fast sweeping methods for eikonal equations on triangulated meshes*, SIAM Journal on Numerical Analysis, 45 (2007), pp. 83–107.

S

[89] A. A. Samarskij, *Theory of Difference Schemes*, Nauka, Moscow, 1977.

[90] J. A. Sethian, *Level Set Methods, Evolving Interfaces in Geometry, Fluid Mechanics, Computer Vision, and Materials Science*, Cambridge University Press, New York, 1996.

[91] G. Simonett, *The Willmore flow near spheres*, Differential and Integral Equations, 14 (2001), pp. 1005–1014.

[92] P. Smereka, *Semi-implicit level set methods for curvature and surface diffusion motion*, Journal of Scientific Computing, 19 (2003), pp. 439–456.

[93] M. Sussman, A. Almgren, J. Bell, P. Colella, L. Howell, and M. Welcome, *An adaptive level set approach for incompressible two-phase flow*, Journal of Computational Physics, 148 (1999), pp. 81–124.

[94] M. Sussman and E. Fatemi, *An efficient, interface preserving level set re-distancing algorithm and its application to interfacial incompressible fluid flow*, SIAM J. Sci. Comput., 20 (1999), pp. 1165–1191.

[95] S. Svetina and B. Žekš, *Membrane bending energy and shape determination of phospholipid vesicles and red blood cells*, Eur. Biophys. J., 17 (1989), pp. 101–111.

V

[96] A. Visintin, *Models of phase transitions*, Birkhäuser Boston, 1996.

[97] E. Vitásek, *Numerické metody*, SNTL, Nakladatelství technické literatury, 1987.

[98] D. Ševčovič, *Topics on partial differential equations,*, vol. 2 of Jindřich Nečas Center for Mathematical Modeling Lecture notes, MatFyzPress, 2007, ch. Qualitative and quantitative aspects of curvature driven flows of planar curves, pp. 55–119.

W

[99] J. Walkington, N., *Algorithms for computing motion by mean curvature*, SIAM J. Numer. Anal., 33 (1996), pp. 2215–2238.

[100] T. J. Willmore, *Riemannian geometry*, Oxford University Press, 2002.

Y

[101] Y.-G.Chen, Y.Giga, and S.Goto, *Uniqueness and existence of viscosity solutions of generalized mean curvature flow equations*, J. Differential Geometry, 33 (1991), pp. 749–786.

[102] S. O. Y. R. Tsai, L. Cheng and H. Zhao, *Fast sweeping algorithms for a class of Hamilton-Jacobi equations*, SIAM Journal on Numerical Analysis, 41, No. 2 (2003), pp. 673–694.

[103] S. Yazaki, *Topics in mathematical modeling*, vol. 4 of Jindřich Nečas Center for Mathematical Modelling, Lecture Notes, MatFyzPress, Publishing House of the Faculty of Mathematics and Physics, Charles University in Prague, 2008, ch. An area-preserving crystalline curvature ow equation, pp. 169–210. ISBN 978-80-7378-060-9.

[104] T. Young, *An essay on the cohesion of fluids*, Philosophical Transactions of the Royal Society of London, 95 (1805), pp. 65–87.